Classical mechanics

Use momentum and energy to derive constrained motion, solve two-body and rigid-body problems, and explain how forced and nonlinear oscillations differ.

Read the subject in depth

Each volume develops its arguments in sequence, with worked problems and links to experiments.

- ### Analytical mechanics from constraints to invariants

  Recover the dynamics of a body from its constraints, symmetries and measured initial conditions. Follow the argument through rotating bodies, resonances, continuum limits and changes of observer.

- ### Mechanics in the laboratory

  Turn a measured trajectory or force into a test of a mechanical law. Derive the observable, propagate it numerically and determine which parameters the experiment can resolve.

Advanced study across the subject

Each sequence connects the course to detailed chapters in neighbouring subjects. The complete course PDF includes their derivations, examples and exercises.

Parts II–III develop constrained motion and variational principles. Follow parts V–VI for the rotation and vibration strands, then compare the continuum and relativistic descriptions in parts VIII–IX. Torsten Fließbach · Mechanik, 7th edition

1. ### Forces, constraints and a real instrument

   Use virtual work to choose generalised coordinates. Test the predictions for a moving support, a constrained slider and an instrument that exchanges mechanical and electrical energy.

2. ### Rotation and finite-amplitude dynamics

   Translate an angular-momentum balance between laboratory and body frames. Follow it from impact to gyroscopic motion and distinguish driven nonlinear response from a change of stability.

3. ### From discrete coordinates to a continuum

   Follow two coupled coordinates into a chain and a rod. Compare wave and beam dispersion, derive the role of the mass matrix and use an energy quotient to estimate a frequency.

4. ### Hamiltonian motion viewed in other coordinates and frames

   Test phase-space area in a numerical orbit, track an observer change, then compare a relativistic worldline with a semiclassical quantisation condition.

How the course fits together

1. **Chapters 1–4**

Start with a system boundary. An impulse changes its momentum, a force acting through a distance changes its energy, and constraints determine which motions are possible. Linearising the constrained system near equilibrium predicts its normal modes.

2. **Chapters 5–8**

   Change the description while tracking the same motion. Accelerating frames add inertial forces, phase space keeps track of conjugate variables, and a central force reduces a two-body orbit or scattering encounter to radial motion.

3. **Chapters 9–12**

   Let orientation and driving enter the dynamics. A rigid body can exchange rotation among its principal axes. A driven or nonlinear oscillator can change its amplitude, period or even its equilibria as a control parameter varies.

Contents

1. Chapter 1 · Momentum, impulse and collisions
2. Chapter 2 · Potential energy and turning points
3. Problem sheet 1 · Impulses and energy landscapes
4. Chapter 3 · Constraints and Lagrange’s equations
5. Chapter 4 · Normal modes and energy exchange
6. Problem sheet 2 · Constrained motion and modes
7. Chapter 5 · Rotating frames and the Coriolis effect
8. Chapter 6 · Hamiltonian motion in phase space
9. Problem sheet 3 · Moving frames and phase portraits
10. Chapter 7 · Two-body motion and binary masses
11. Chapter 8 · Impact parameters and scattering cross-sections
12. Problem sheet 4 · Orbits and scattering data
13. Chapter 9 · Principal axes and torque-free precession
14. Chapter 10 · Forced, damped vibration
15. Problem sheet 5 · Rotation, damping and frequency measurements
16. Chapter 11 · Nonlinear stiffness and amplitude-dependent period
17. Chapter 12 · Bifurcation of a rotating hoop
18. Problem sheet 6 · Nonlinear frequencies and broken symmetry
19. Chapter 13 · Changing the coordinates of a moving trap
20. Chapter 14 · Recover a trajectory from a family of actions
21. Chapter 15 · Read a period from the area enclosed by an orbit
22. Chapter 16 · From a chain of springs to an elastic field
23. Chapter 17 · Proper time, momentum and a moving clock
24. Chapter 18 · Liouville flow and what an ensemble can remember
25. Chapter 19 · Parametric resonance and Floquet growth
26. Chapter 20 · Reading Earth's rotation from a pendulum trace
27. Problem sheet 7 · Reconstructing an accelerating trap
28. Problem sheet 8 · Can the intermediate axis instability be measured before a body turns over?

29. Analytical mechanics from constraints to invariants
30. Mechanics in the laboratory
31. Forces, constraints and a real instrument
32. Rotation and finite-amplitude dynamics
33. From discrete coordinates to a continuum
34. Hamiltonian motion viewed in other coordinates and frames
35. Applied study
36. Notation and assumptions
37. Further reading

Chapter 1 · Momentum, impulse and collisions

Use the centre-of-mass frame to predict the outcome of a collision and account for the kinetic energy that disappears from the motion of the bodies.

FROM FIRST PRINCIPLES

Construct the centre-of-mass and relative kinetic energies

Take two bodies of constant masses m_1, m_2 moving along one axis. During their brief contact suppose the external impulse is negligible. The mechanical inputs are Newton's momentum balance and equal, opposite contact forces. Add the two balances, then divide the resulting conserved total momentum P by total mass M:

$$\dot{P} = \dot{p}_1 + \dot{p}_2 = 0,$$
$$V = P/M,$$
$$M = m_1 + m_2.$$

Let $u = v_1 - v_2$ be the signed relative speed. Solving this definition together with $m_1 v_1 + m_2 v_2 = MV$ recovers each velocity. These expressions distinguish the common motion shared by both bodies from their approach:

$$v_1 = V + (m_2/M)u,$$
$$v_2 = V - (m_1/M)u.$$

Insert both in the kinetic-energy sum. The terms proportional to Vu cancel, while those in u^2 combine into the reduced mass $\mu = m_1 m_2/M$:

$$K = \tfrac{1}{2} m_1 v_1^2 + \tfrac{1}{2} m_2 v_2^2 = \tfrac{1}{2} M V^2 + \tfrac{1}{2} \mu u^2.$$

No constitutive law for the contact has entered this identity. Since V is fixed, only the second energy term can change during an isolated collision. Restitution or another contact measurement is needed to predict the final relative motion.

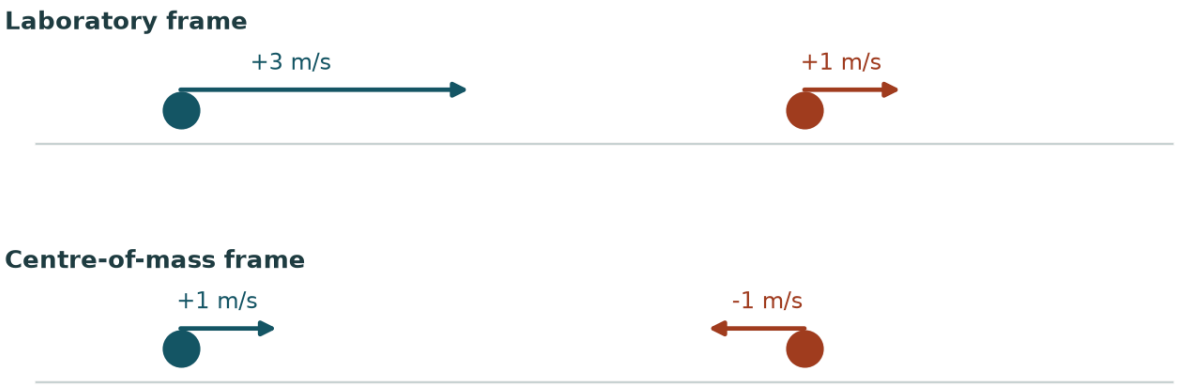

Which portion of the motion can enter a collision?
For equal masses the centre of mass travels at 2 m/s. Subtract this velocity from both arrows. The lower pair now has zero total momentum, but it still has kinetic energy because the two masses approach one another. With 1 kg per mass, 4 J travels with the centre of mass and 1 J belongs to relative motion.

Explore the related parameter study beside the computed figure.

DERIVATION AND APPLICATIONS

Where does kinetic energy go during a finite contact?

A collision record often contains a force trace but no direct measurement of stored deformation energy. Consider two carts moving along the same straight track. Neglect the external impulse during contact, assume that the bodies do not rotate, and define the initial closing speed as $u = v_1 - v_2 > 0$. The common centre-of-mass speed is constant, but the relative speed changes continuously as the contact force grows and subsides.

Let $J(t)$ be the positive impulse applied to cart 2 up to time t. Cart 1 receives the opposite impulse. Subtract the resulting velocities and collect the two inverse masses into the reduced mass μ:

$$
\begin{aligned}
v_1(J) &= v_1 - J/m_1, \\
v_2(J) &= v_2 + J/m_2, \\
u(J) &= u - J/\mu, \\
\mu^{-1} &= m_1^{-1} + m_2^{-1}.
\end{aligned}
$$

For each cart the instantaneous kinetic-energy change is velocity times momentum change. Consequently the sum of both changes measures the relative velocity during contact. Integrating over the measured impulse gives

$$dK = -u(J)\,dJ,$$

$$K(J) - K(0) = -uJ + \frac{J^2}{2\mu}.$$

Maximum compression occurs when the relative velocity first vanishes, at $J_c = \mu u$. At separation let the measured opening speed be eu, where e is the coefficient of restitution. Solving $u(J_f) = -eu$ and inserting the resulting final impulse gives

$$J_f = (1+e)\mu u,$$

$$K(0) - K(J_f) = \tfrac{1}{2}\mu u^2(1-e^2).$$

The two stages need not have the same force histories. The loss is fixed by endpoint data because total momentum was conserved. An elastic contact temporarily removes relative kinetic energy and returns it all. A sticking contact returns none.

WORKED EXAMPLE

Reconstruct the two stages of a cart encounter

Change the inputs and investigate this derivation.

A 0.600 kg cart catches a 0.400 kg cart with $u = 1.50$ m/s. Their force sensor measures $J_f = 0.576$ N s. Here $\mu = 0.240$ kg, so $J_c = 0.360$ N s and $e = 0.576/0.360 - 1 = 0.600$. Compression removes 0.270 J of relative motion. Separation returns $0.270(0.600)^2 = 0.0972$ J; the bodies leave contact with 0.173 J less kinetic energy.

SECOND APPLICATION

Repeat in a moving laboratory

Change the inputs and investigate this derivation.

Suppose the initial cart velocities were 2.00 and 0.500 m/s. The impulses predict final velocities 1.04 and 1.94 m/s. An observer travelling at 1.00 m/s instead obtains 0.040 and 0.940 m/s after contact. In that frame the initial kinetic energy is 0.350 J and the final energy 0.177 J. Their difference again gives 0.173 J: changing the observer changes the centre-of-mass contribution by the same amount at both endpoints.

Try it · Inelastic carts

Vary the physical parameters in the derived relation. Use the units and assumptions in the readout to connect the curves to the two worked examples. A parameter study can test the forward prediction; the same relation can then be inverted to infer a parameter from a measurement.

Open this live calculation

Try the calculation

Target / incident mass	0.7
Restitution coefficient	0.6
Initial relative speed (m/s)	1.5

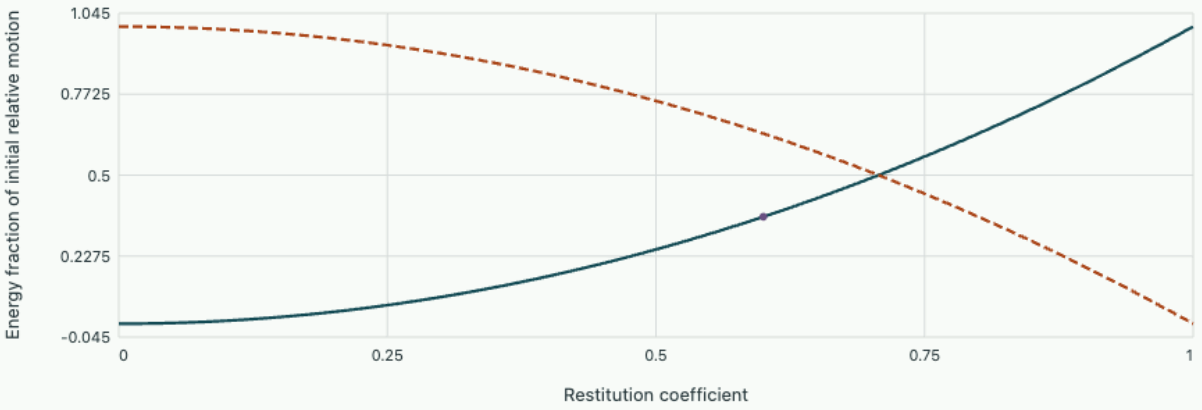

For incident mass 0.6 kg and target mass 0.6r kg, contact impulse = 0.59294 N s. Relative-energy loss fraction 0.64. A common laboratory velocity shift leaves impulse and this loss unchanged.

Select a system and a clock

Two gliders collide on a level air track. A force sensor can display a sharp pulse, while video resolves only the velocities before and after contact. Can the two instruments describe the same event? Begin with Newton's law for a constant-mass particle. Integrating over the contact time gives

$$\mathbf{p}_f - \mathbf{p}_i = \int \mathbf{F}\, dt.$$

The right-hand side is an impulse. It has units of N·s, equal to kg·m/s. A large force acting briefly can produce the same impulse as a smaller force acting for longer.

Draw a boundary around both gliders. The contact forces contribute equal and opposite impulses within that boundary. The change in their total momentum equals the external impulse. Gravity and the track reaction cancel vertically. Provided that horizontal friction supplies little impulse during contact, the horizontal momentum is conserved to the accuracy of that approximation. This reasoning also tells us which claim a measurement can test. Momentum conservation constrains the two final velocities together, but supplies only one scalar equation in a one-dimensional experiment.

Separate translation and approach

Let $M = m_1 + m_2$ be the total mass and $u = v_1 - v_2$ the signed closing velocity. Introduce the centre-of-mass velocity and reduced mass,

$$V = \frac{m_1 v_1 + m_2 v_2}{M},$$
$$\mu = \frac{m_1 m_2}{M}.$$

Solving the two velocity equations for the laboratory measurements gives

$$v_1 = V + \frac{m_2}{M} u,$$
$$v_2 = V - \frac{m_1}{M} u.$$

Substitute both expressions in the kinetic energy. The terms linear in Vu cancel and the squared terms give

$$K = \tfrac{1}{2} M V^2 + \tfrac{1}{2} \mu u^2.$$

The first term translates the centre of mass. A collision with negligible external impulse leaves it fixed. The second term measures the energy available for deformation, heating and relative motion after impact. All observers moving uniformly along the track agree on the relative speed. They assign different values to the first term while agreeing on the kinetic energy lost during this isolated collision.

Supply a material observation

Suppose the gliders approach with $u_i > 0$ and separate afterwards. Define the restitution coefficient along the line of impact as $e = -u_f / u_i$. Elastic rebound gives $e = 1$, and two bodies sticking together have $e = 0$. Substituting the definition into the energy decomposition gives

$$K_i - K_f = \mu (1 - e^2) u_i^2 / 2.$$

A smaller restitution coefficient reduces the energy available for separation. A spring mechanism initially storing energy can instead produce a relative speed larger than its approach speed.

Restitution is an empirical closure. Inferring it from a pair of outgoing velocities is an experimental result. In an oblique impact the normal relative velocity supplies the restitution condition. Tangential motion requires a separate physical assumption about friction and rotation. Applying the one-dimensional formula to the full speed would implicitly impose a tangential contact law as well.

OneSimulation · Two bumpers with the same impulse

A 0.20 kg cart approaches a 0.30 kg cart at a relative speed of 0.50 m/s. Between first touch and separation, an ideal spring bumper exerts the same force magnitude on both carts. Subtract the two acceleration equations. Their relative compression s then obeys the equation for a single oscillator of reduced mass μ.

$$\mu \ddot{s} = -ks,$$

$$\mu = \frac{m_1 m_2}{m_1 + m_2},$$

$$s(0) = 0,$$

$$\dot{s}(0) = v_{\mathrm{rel}}.$$

At the first return to zero compression the spring disengages. The force pulse lasts half a period. Quadrupling the stiffness doubles its peak and halves its duration. OneSimulation integrates the compression in time and checks the area of each pulse against the momentum change $2\mu v_{\mathrm{rel}}$. A momentum measurement alone cannot recover the peak load.

```
"""Elastic collision of two carts with interchangeable spring bumpers."""
import matplotlib.pyplot as plt
import numpy as np
from onesim.numerics.time import ClassicalRungeKutta4TimeIntegrator

mass_left, mass_right = 0.20, 0.30  # kg
closing_speed = 0.50  # m/s
reduced_mass = mass_left * mass_right / (mass_left + mass_right)
stepper = ClassicalRungeKutta4TimeIntegrator()
fig, ax = plt.subplots(figsize=(6.6, 3.5), layout="constrained")

for stiffness in (120.0, 480.0):  # N/m
    omega = np.sqrt(stiffness / reduced_mass)
    times = np.linspace(0, np.pi / omega, 201)
    dt = times[1] - times[0]
    state = (0.0, closing_speed)  # compression and compression rate
    force = [0.0]
    def contact_rate(state, time):
        compression, speed = state
        return speed, -stiffness * compression / reduced_mass
    for time in times[:-1]:
        state = stepper.advance(state, contact_rate, dt, time=time)
        force.append(stiffness * state[0])
    impulse = np.trapezoid(force, times)
    assert np.isclose(impulse, 2 * reduced_mass * closing_speed, rtol=3e-5)
    print(f"{stiffness:g} N/m: {max(force):.3f} N peak, {impulse:.4f} N s")
    ax.plot(1000 * times, force, label=f"{stiffness:g} N/m")
ax.set(xlabel="Time since first contact (ms)", ylabel="Contact force (N)")
ax.grid(alpha=0.2)
```

```
ax.legend(title="Bumper stiffness")
fig.savefig("classical-mechanics.png", dpi=180)
```

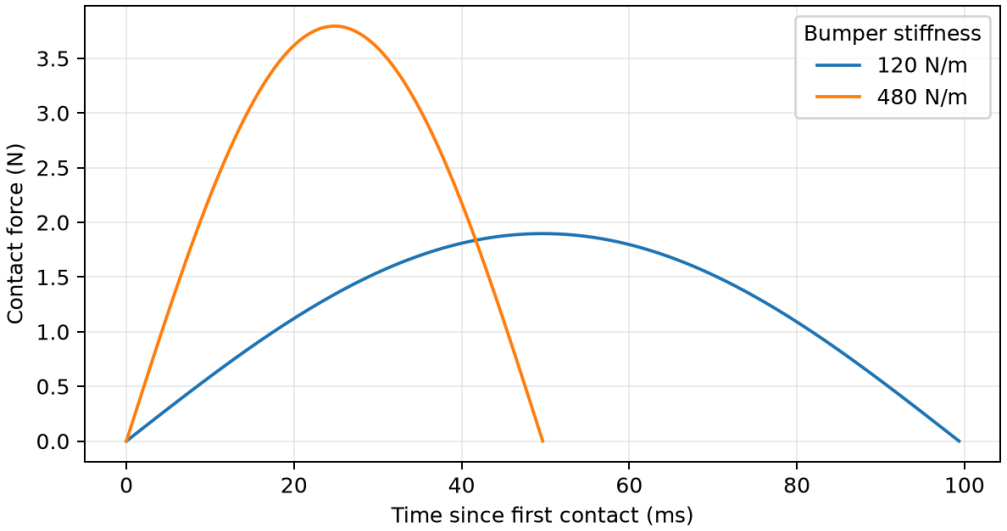

Changing the stiffness from 120 to 480 N/m raises the peak from 1.90 to 3.79 N. Both pulses transfer 0.120 N s.

Try it · Contact pulse

Change the inputs and compare the recalculated curves with the preceding derivation and baseline figure. The axes give the units; the numerical readout states the model assumptions and any limiting cases. Reset the inputs to return to the reference setting.

Open this live calculation

Try the calculation

Contact stiffness (N/m)	120
Reduced mass (kg)	0.03
Approach speed (m/s)	2

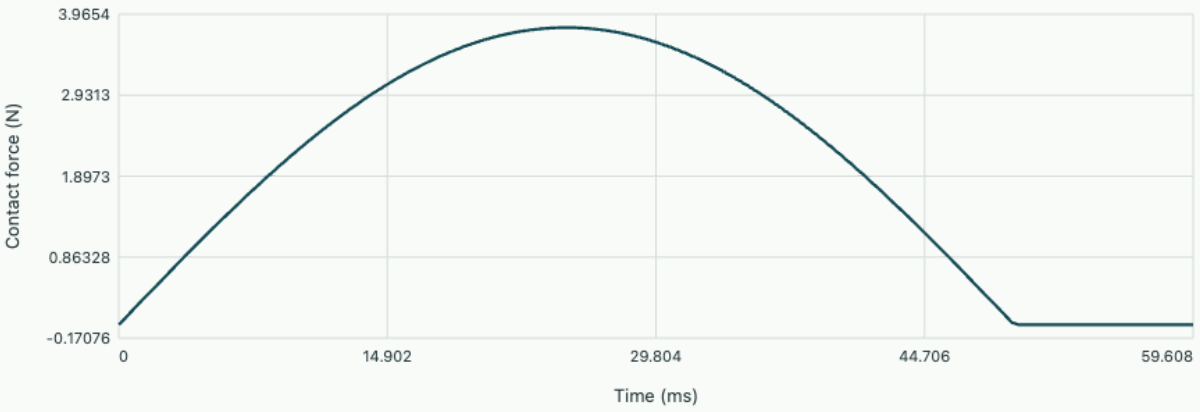

Elastic contact pulse

Contact duration 49.673 ms; maximum force 3.7947 N; impulse 2μv = 0.12 N s. Stiffness changes pulse shape, while impulse stays fixed.

Download the Python example

Reconstruct an air-track event

A 0.60 kg glider moving right at 1.20 m/s strikes a 0.40 kg glider initially at rest. High-speed video gives $e = 0.50$. The centre of mass travels right at 0.72 m/s. The final relative velocity is -0.60 m/s, hence the first glider travels at $0.72 + 0.40(-0.60) = 0.48$ m/s and the second at $0.72 - 0.60(-0.60) = 1.08$ m/s. Both move right, but the smaller glider pulls away.

The impulse on the smaller glider is $0.40(1.08) = 0.432$ N·s. A 12 ms contact would therefore give a mean force of 36 N. The kinetic energy lost is

$$0.5(0.24)(1 - 0.25)(1.20)^2 = 0.130\,\mathrm{J}.$$

Momentum and energy provide independent checks on an instrument record. If both measured impulses agree while the kinetic energy falls by this amount, the missing mechanical energy can reside in the contact material and the sound it emitted.

A different choice of frame changes each cart’s measured kinetic energy but leaves the loss in a collision unchanged if total momentum is conserved. To verify this, subtract a constant velocity U from each velocity before forming the initial and final kinetic sums. In each sum the additional terms are

$-UP + MU^2/2$. The two corrections cancel in the energy difference. This is why a collision film taken by an observer riding beside the track can give the same inferred internal-energy gain.

Resolve an oblique impact along the contact normal

A single restitution coefficient describes the part of relative velocity along the line of impact. A two-dimensional collision needs a geometric measurement as well. Take two smooth disks gliding on a horizontal air table, with negligible external impulse during contact. At first touch draw a unit normal $\mathbf{n}$ from the centre of disk 1 toward disk 2. Let $\mathbf{t}$ be a perpendicular direction in the table. Assume the contact exerts no tangential impulse. The force then passes through the centres and leaves the two spins unchanged, even when the centres approach on intersecting paths.

Call the positive magnitude of contact impulse J. Disk 1 receives $-J\mathbf{n}$ and disk 2 receives $+J\mathbf{n}$. Subtract the individual impulse–momentum equations; if $\mathbf{g} = \mathbf{v}_1 - \mathbf{v}_2$, the relative normal velocity after impact is $g_n' = g_n - J(1/m_1 + 1/m_2)$. Approaching disks have $g_n > 0$ with this choice of normal. Applying $g_n' = -e g_n$ gives

$$J = (1 + e)\mu g_n,$$

$$\mu = \frac{m_1 m_2}{m_1 + m_2}.$$

Both tangential velocities remain individually unchanged. The energy lost is $\mu(1 - e^2)g_n^2/2$, even when tangential motion carries most of the initial relative kinetic energy. A grazing trajectory with g_n tending to zero therefore transfers very little momentum and loses even less energy. If the centres are already moving apart, this instantaneous collision model applies no impulse.

Predict both tracks after an off-centre hit

Take $m_1 = 0.20$ kg, $m_2 = 0.30$ kg, $\mathbf{v}_1 = (1.00, 0)$ m/s and disk 2 initially at rest. A frame taken at contact places $\mathbf{n} = (0.80, 0.60)$, and the normal restitution coefficient is 0.75. Projecting the incoming velocity gives $g_n = 0.80$ m/s. The reduced mass is 0.120 kg, so the impulse magnitude is $(1.75)(0.120)(0.80) = 0.168$ N s. Resolving the changes in the laboratory axes yields

$$\mathbf{v}_1' = (1, 0) - (0.168/0.20)(0.80, 0.60) = (0.328, -0.504)\ \mathrm{m/s},$$

$$\mathbf{v}_2' = (0.168/0.30)(0.80, 0.60) = (0.448, 0.336)\ \mathrm{m/s}.$$

The vertical momenta are equal and opposite. Their horizontal sum is 0.200 kg m/s as before. The final normal relative velocity is -0.600 m/s, and the energy loss is 0.0168 J. Using the full relative speed in the restitution loss formula would give a different result. In the laboratory, fit straight lines to both tracks on either side of contact and compare the inferred impulse vector with the measured centre line. A significant tangential component would motivate adding friction or rotational degrees of freedom to the contact law.

The two-dimensional data also permit a consistency check even when the contact frame is slightly blurred. Subtract disk 2′s incident velocity from its outgoing velocity and normalize that vector. The result estimates the centre line from the observed impulse, given the smooth-disk assumption. Reconstruct the restitution coefficient using this direction and repeat with the direction recorded by the camera. If the inferred coefficient changes significantly between the two choices, possible explanations include a rotational friction impulse or an error in locating the instant of contact. Spin markings on the disks supply an independent discriminator because an off-centre tangential impulse changes their rotation.

How should two colliding carts be mass-matched?

Launch a cart at a stationary target on a horizontal track. Assume a one-dimensional elastic impact. Momentum and relative-speed reversal give $v_2 = 2u_1/(1+r)$ for mass ratio $r = m_2/m_1$. Squaring this speed alone misses the mass factor in the transferred energy.

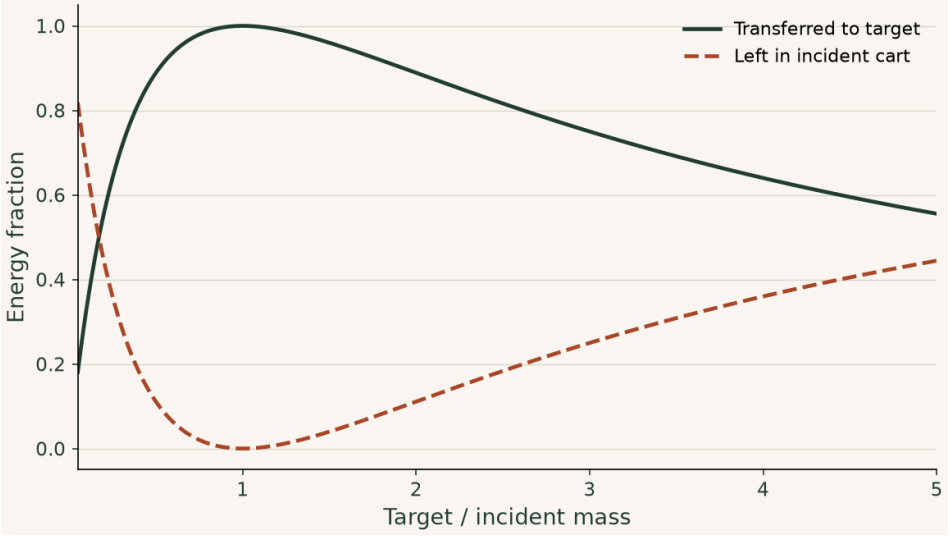

Equal masses transfer all the kinetic energy. Mass ratios 1/4 and 4 each transfer 64%, although the incident cart continues forwards in one case and rebounds in the other. A kinetic-energy measurement alone cannot tell those cases apart.

Try it · Collision

Change the inputs and compare the recalculated curves with the preceding derivation and baseline figure. The axes give the units; the numerical readout states the model assumptions and any limiting cases. Reset the inputs to return to the reference setting.

Open this live calculation

Try the calculation

Target / incident mass 1

Incident speed (m/s) 2

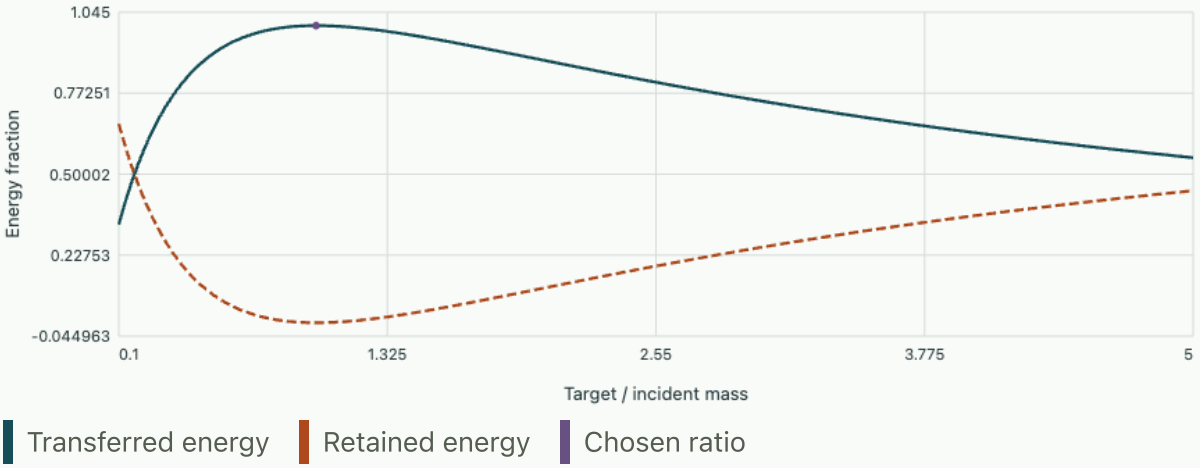

Elastic collision with target initially at rest: outgoing speeds 0 and 2 m/s. Centre-of-mass speed 1 m/s.

▶ **Read values from the plot**

Study the full derivation

Relativistic collisions, centre-of-momentum energy and thresholds · Analytical mechanics from constraints to invariants

Two particles with the same total laboratory energy can have very different energy available for changing their internal state. Determine the energy and motion of the centre-of-momentum system, reconstruct two-body elastic scattering, and follow how a detector threshold transforms between frames.

Chapter 2 · Potential energy and turning points

Use a potential-energy curve to distinguish allowed motion, local stability and escape over a barrier.

FROM FIRST PRINCIPLES

Obtain the energy curve from the measured force

Consider a point mass constrained to a fixed one-dimensional track with no dissipation. Measure the signed force $F(x)$ along the track and suppose it depends only on position. Newton's second law supplies the time evolution. Multiplying by displacement converts it into a statement that can be integrated with respect to position:

$$m\ddot{x}\,dx = m\dot{x}\,d\dot{x} = d\left(\tfrac{1}{2}m\dot{x}^2\right) = F(x)\,dx.$$

Define potential energy relative to an arbitrary reference position x_r by integrating the negative force. The arbitrary additive constant cannot affect any measured speed:

$$U(x) - U(x_r) = -\int_{x_r}^{x} F(s)\,ds,$$

$$\tfrac{1}{2}m\dot{x}^2 + U(x) = E.$$

Thus accessible positions satisfy $U(x) \le E$ and a position reached with zero speed has $U(x) = E$. Whether it is an ordinary turning point or an equilibrium also depends on the slope. Near an equilibrium x_* the linearized force is $-U''(x_*)(x - x_*)$, giving

$$\delta\ddot{x} + \frac{U''(x_*)}{m}\delta x = 0.$$

Positive curvature creates a restoring force and local oscillations; a vanishing slope alone does not establish stability.

DERIVATION AND APPLICATIONS

Why does a trajectory linger near the top of a barrier?

A turning point where the slope of the potential is finite is reached in finite time. A smooth barrier summit presents a different case. Near a nondegenerate maximum at $x = 0$ write $U(x) = U_b - \kappa x^2/2$, with curvature $\kappa > 0$. Take a particle of mass m crossing from $-L$ to $+L$ at energy $E = U_b + \epsilon$. Use a short interval on which the quadratic fit is accurate, and neglect friction. For $\epsilon > 0$ the positive-velocity branch of energy conservation gives

$$\dot{x} = \sqrt{(2\epsilon + \kappa x^2)/m},$$

$$t = \sqrt{m}\int_{-L}^{L} \frac{dx}{\sqrt{2\epsilon + \kappa x^2}}.$$

The scale $x_0 = \sqrt{2\epsilon/\kappa}$ separates a slow central region from faster motion on the sides. To integrate across both without approximating the centre, set $x = x_0 \sinh u$. The factor $\cosh u$ from dx cancels the one from the square root:

$$t = 2\sqrt{m/\kappa}\int_{0}^{\operatorname{arsinh}(L/x_0)} du = 2\sqrt{m/\kappa}\,\operatorname{arsinh}(L/x_0).$$

For an energy excess much smaller than $\kappa L^2/2$, use $\operatorname{arsinh} y = \ln(y + \sqrt{1+y^2})$. This gives the near-threshold dependence

$$t \simeq \sqrt{m/\kappa}\,\ln\!\left(\frac{2\kappa L^2}{\epsilon}\right).$$

Higher-order curvature corrections away from the summit can change a finite offset. The logarithmic growth comes from the increasingly slow passage next to the stationary point. At exactly the barrier energy a trajectory arriving from the left approaches the summit asymptotically.

WORKED EXAMPLE

Time a crossing on a calibrated track

Change the inputs and investigate this derivation.

Let $m = 0.200$ kg, $\kappa = 5.00$ N/m, $L = 0.0400$ m and $\epsilon = 0.100$ mJ. The central speed is

$$\sqrt{2\epsilon/m} = 0.0316\,\mathrm{m/s}.$$

The length $x_0 = 6.32$ mm gives $L/x_0 = 6.32$, so the exact transit time is $0.400\ \operatorname{arsinh}(6.32) = 1.02$ s. Dividing the entire distance by the central speed would give 2.53 s, since it treats the slowest point as representative of the entire track.

SECOND APPLICATION

Infer a curvature from progressively slower crossings

Change the inputs and investigate this derivation.

On another track reducing a sufficiently small energy excess by a factor of four adds 0.416 s to the transit time. Subtracting two logarithms removes the unknown finite offset. Thus

$$\sqrt{m/\kappa} = 0.416/\ln 4 = 0.300\,\mathrm{s}.$$

For a 0.180 kg cart the inferred curvature is 2.00 N/m. As a check, another fourfold reduction should add about the same time, even though its absolute energy change is smaller.

Try it · Saddle transit

Vary the physical parameters in the derived relation. Use the units and assumptions in the readout to connect the curves to the two worked examples. A parameter study can test the forward prediction; the same relation can then be inverted to infer a parameter from a measurement.

Open this live calculation

Try the calculation

Mass (kg)	0.2
Barrier curvature (N/m)	5
Track half-length (mm)	40

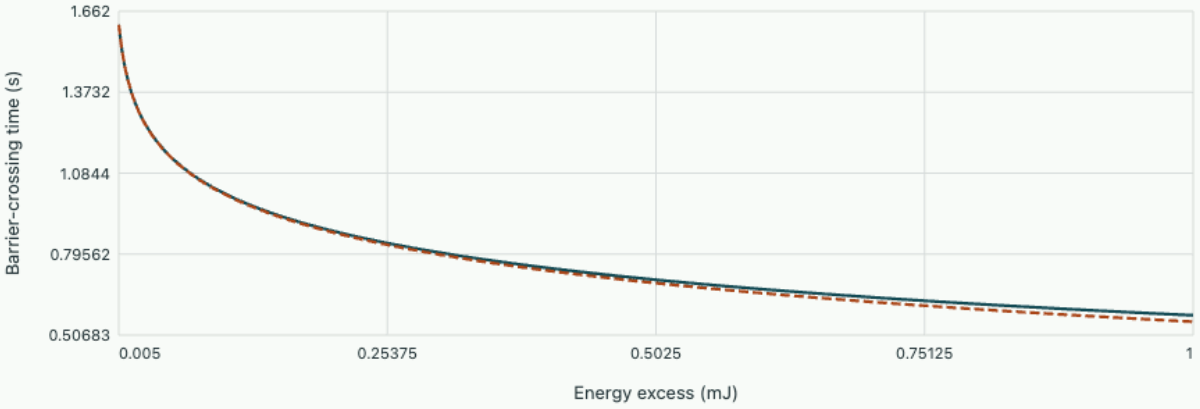

The crossing slows logarithmically as excess energy tends to zero. At 0.1 mJ the exact time is 1.0175 s. The quadratic potential must remain accurate on this interval.

Start from this chapter. At either turning point the radial speed is zero. Use the two radii to determine the semimajor axis. Which change should shorten the time between successive returns?

OneSimulation laboratory · Measure a period from an orbit

Replace time with position

A small cart travels through a shaped track or along a nonlinear spring. Its acceleration changes continuously with position, yet one can often predict where it will reverse direction before solving for its position as a function of time. Consider a single coordinate x in an inertial frame, a constant mass and a force that depends on position alone. Then $F = m\ddot{x}$ times $\dot{x}$ gives

$$F(x)\dot{x} = d(m\dot{x}^2/2)/dt.$$

Define the potential difference by $U(x) - U(x_0) = -\int_{x_0}^{x} F(s)\,ds$. It follows that $E = m\dot{x}^2/2 + U(x)$ is constant.

The zero of U is conventional. Turning points and speed depend on differences, so adding the same constant to E and U has no observable consequence. Allowed positions satisfy

$$U(x) \le E.$$

Where the inequality is strict, two velocities have the same energy, one in each direction. Specifying a position and energy therefore leaves a choice of initial direction.

Examine a pair of wells

Take an illustrative bistable spring with potential $U(x) = A(x^2 - b^2)^2$, where $A > 0$ has units J/m⁴ and b is a length. Differentiation gives

$$F = -4Ax(x^2 - b^2).$$

The equilibrium positions are 0 and $\pm b$. At either outer equilibrium the curvature $U'' = 4A(3x^2 - b^2)$ is $8Ab^2 > 0$. At the origin the curvature is negative. A small displacement from the central equilibrium grows because the force points away from it.

An energy below Ab^4 confines motion to one well, assuming a start there. At higher energy the cart can cross the centre. At exactly the barrier energy, a cart approaching the top from the side slows asymptotically in this frictionless model. Near the top $E - U(x)$ is proportional to x^2, so the time integral $\int dx/\sqrt{2(E-U)/m}$ diverges logarithmically as x approaches zero. A test that checks only $U = E$ misses this distinction between an ordinary reversal and an unstable equilibrium.

Extract the local frequency

Write $x = b + \xi$ and expand the potential about the right-hand minimum. Its constant and linear contributions vanish, leaving $U \simeq (8Ab^2)\xi^2/2$. The equation of motion is harmonic to this order, with $\omega = \sqrt{8Ab^2/m}$. This curvature estimate uses small displacements compared with b. For excursions sampling a significant fraction of the well, the oscillation need not be sinusoidal and its period can differ substantially.

At an arbitrary energy with adjacent turning points x_-, x_+, a full oscillation takes twice the outward transit time. Thus $T = 2\int_{x_-}^{x_+} dx/\sqrt{2(E-U(x))/m}$. For an ordinary turning point with nonzero slope of U, the denominator vanishes as the square root of distance and the integral remains finite. This expression supplies a direct route from a measured force curve to the period without measuring acceleration.

Interpret a threshold experiment

Let $m = 0.200$ kg, $A = 4000$ J/m⁴ and $b = 0.0500$ m. The barrier height is 0.0250 J and the effective spring stiffness at either minimum is 80.0 N/m. A weak disturbance oscillates at 20.0 rad/s, with period 0.314 s. From the minimum an initial speed of 0.400 m/s supplies 0.0160 J, below the crossing threshold. Solving $x^2 = b^2 \pm \sqrt{E/A}$ gives right-well turning points 0.0224 and 0.0671 m. The displacement is asymmetric about the minimum even though the local harmonic approximation is symmetric.

A launch exactly at $\sqrt{2(0.0250)/0.200} = 0.500$ m/s is marginal. Crossing the barrier in finite time requires greater speed in this idealisation. In an experiment, dissipation raises the energy the cart needs at launch. Measuring the speed at several known positions tests conservation along the path and helps distinguish a wrong potential shape from an actual energy loss.

Time measurements give a second access to the shape of the potential. Between ordinary turning points the speed is $\sqrt{2[E-U(x)]/m}$. The half-period is therefore the integral of its reciprocal over the allowed interval. The integrand diverges at a simple turning point, but only as the inverse square root of distance, giving a finite travel time. At an energy that just approaches a smooth unstable maximum, the divergence becomes logarithmic. Extremely slow passage near the barrier can easily be mistaken for a stopped cart.

Design a track whose period is independent of amplitude

The local curvature of a smooth potential fixes a small-oscillation period. An extended track can also be shaped to give exactly harmonic motion over a finite range. Use signed arc length s from the lowest point as coordinate. On a frictionless fixed track kinetic energy is $m\dot{s}^2/2$. In a uniform gravitational field the only configuration-dependent energy is $mgy(s)$. To obtain $\ddot{s} = -\omega^2 s$, require

$$g\,dy/ds = \omega^2 s.$$

Integration sets the necessary height profile $y(s) = \omega^2 s^2/(2g)$, with height zero at the bottom.

A cycloidal arc realizes this condition. With scale a take $x = a(\phi + \sin\phi)$ and $y = a(1-\cos\phi)$ for $-\pi < \phi < \pi$. Differentiate both coordinates. The speed along the parametric curve is

$$ds/d\phi = a\sqrt{(1+\cos\phi)^2 + \sin^2\phi} = 2a\cos(\phi/2).$$

Integrating from the bottom gives $s = 4a\sin(\phi/2)$, retaining the sign of ϕ. Substituting in the height expression eliminates the parameter:

$$y = \frac{s^2}{8a},$$

$$\ddot{s} + \frac{g}{4a} s = 0.$$

The coordinate that executes sinusoidal motion is the path length. Its horizontal projection generally does something different because the track slope changes. A bead released at rest reaches the bottom after one quarter of the period for every nonzero admissible release amplitude. The cancellation between a longer path and a higher typical speed is encoded in the exactly quadratic gravitational potential in s.

Time two different releases

Set $a = 0.250$ m and $g = 9.81$ m/s². The angular frequency is $\sqrt{9.81/(4 \times 0.250)} = 3.13$ rad/s and the predicted time to the bottom is

$$\pi/(2\omega) = 0.502\,\mathrm{s}.$$

Release a bead first from $s = 0.400$ m and then from $s = 0.800$ m. Their initial heights are respectively 0.0800 m and 0.320 m. At the bottom their speeds are $\omega|s_0| = 1.25$ and 2.51 m/s. Doubling arc length quadruples starting potential energy, providing just the required increase in speed to preserve arrival time.

A timing gate near the bottom and an electronic release can measure both quantities independently. A rolling ball has additional rotational inertia and a centre following a curve offset from the track. Treating it as the sliding point mass can bias the comparison even if rolling dissipation is small. Near the bottom the cycloid agrees with a circular arc of its local curvature. Farther away the circular arc develops anharmonic corrections, so comparing equal-time releases at several amplitudes discriminates between two tracks that look almost identical near their lowest point.

There is a useful inverse interpretation of a release series. Suppose the measured bottom speed doubles on doubling signed release distance, but the measured time to the lowest point changes. Correct speed scaling tests only the endpoint height relation. Equal travel times require the integrated speed to have the required dependence throughout the intervening path, and a contact force doing work can spoil that comparison. Measuring several intermediate heights as a function of arc length checks the quadratic law directly. Taking horizontal distance as the release coordinate introduces a purely geometric nonlinearity even for a perfectly machined cycloidal track.

Locate the turning points of a bound orbit

Hold the angular momentum per unit mass fixed at $h^2 = GMr_0$. The radial kinetic energy is the vertical distance from $V_{\mathrm{eff}} = h^2/(2r^2) - GM/r$ up to the total energy. Find both intersections for $E = -3GM/(8r_0)$ before inspecting the curve.

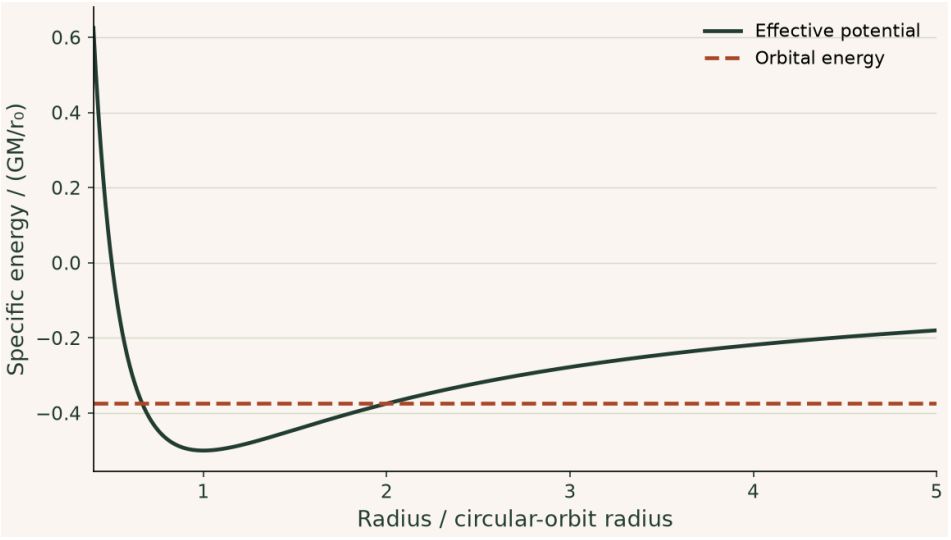

The intersections lie at 2/3 and 2 circular-orbit radii. At radius one the radial kinetic energy is 1/8 in plotted units. The minimum at one is a stable circular orbit only for the lower energy $-1/2$.

Try it · Effective orbit

Change the inputs and compare the recalculated curves with the preceding derivation and baseline figure. The axes give the units; the numerical readout states the model assumptions and any limiting cases. Reset the inputs to return to the reference setting.

Open this live calculation

Try the calculation

Dimensionless energy	-0.37
Angular-momentum scale	1

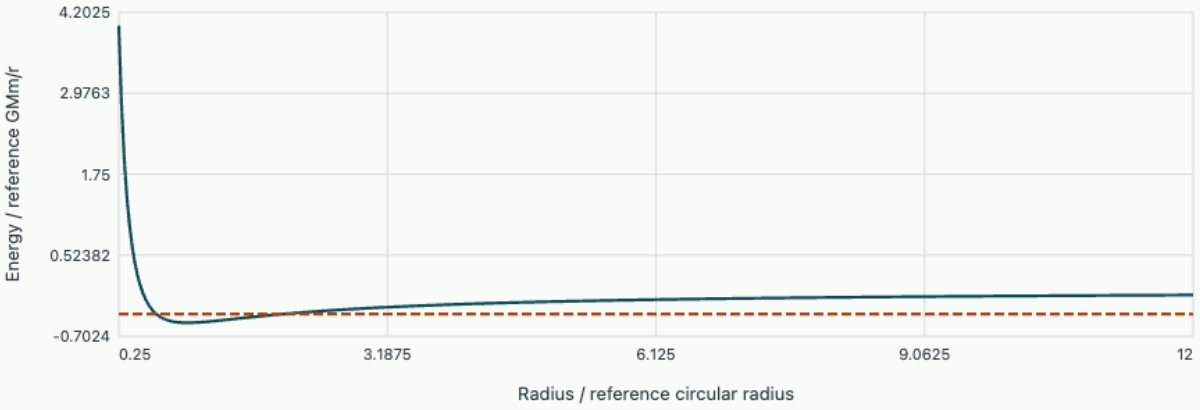

Effective potential | Selected energy

Turning radii 0.66229 and 2.0404. The horizontal energy line bounds the allowed radial motion.

▶ **Read values from the plot**

Problem sheet 1 · Impulses and energy landscapes

Connect the collision measurements of Lecture 1 with the allowed-motion diagrams of Lecture 2.

A triangular force pulse

A 0.40 kg glider travelling right at 1.0 m/s strikes a fixed instrumented wall. The force on the glider points left, rises linearly to a peak of 120 N and falls linearly to zero within 6.0 ms. Calculate the impulse, outgoing velocity and kinetic energy change. Explain which of those results would survive a change in pulse shape at fixed area.

▼ **Integrate the measured force**

The signed area is $-(120)(0.0060)/2 = -0.360$ N·s. The final momentum is $0.400 - 0.360 = 0.040$ kg·m/s and the final velocity is still $+0.100$ m/s. The kinetic energy changes from 0.200 to 0.0020 J, a decrease of 0.198 J. For the stated fixed wall, this time interval cannot describe a completed rebound. The glider is still moving towards it, so the record may cover only part of the contact. For the same initial state any pulse of the same signed area gives the same final velocity and kinetic energy. Its peak force and the maximum deformation can differ.

Compare two frames

A 1.0 kg cart travelling at 3.0 m/s catches a 2.0 kg cart travelling in the same direction at 0.60 m/s. They lock. Calculate the final speed and energy lost in the lab. Repeat using the centre-of-mass frame. Which quantity differs between frames?

▼ **Transform the individual speeds**

Total momentum is 4.2 kg·m/s, total mass is 3.0 kg, and the coupled speed is 1.4 m/s. The energy falls from $4.5 + 0.36 = 4.86$ J to $0.5(3)(1.4)^2 = 2.94$ J, a loss of 1.92 J. Subtracting the centre-of-mass speed from both initial velocities gives $+1.6$ and -0.8 m/s. Their initial energies are then 1.28 and 0.64 J and the final energy is zero. The initial energy differs by the energy of uniform translation. The energy lost and the carts' relative approach speed agree. Momentum has different numerical values in the two frames but is conserved in each.

A vertical spring releases its load

A cart of mass 0.50 kg moves vertically on a linear spring of stiffness 50 N/m, attached at both ends so that compression and extension are possible. Measure y downward from the spring's unstretched position. Write the gravitational and spring potential together, find the stable equilibrium and determine the turning points and period if released from rest at $y = 0$.

▼ **Complete the square**

The potential is $U = ky^2/2 - mgy$. Its derivative vanishes at $y_* = mg/k = 0.0981$ m and its curvature is $k > 0$. Completing the square gives

$$U = k(y - y_*)^2/2 - ky_*^2/2.$$

Release gives total energy zero in the chosen reference. Solving $U = 0$ gives $y = 0$ and $y = 2y_* = 0.1962$ m. Measured from equilibrium the amplitude is 0.0981 m and $T = 2\pi\sqrt{m/k} = 0.628$ s. Gravity shifts the centre of motion and the turning points but leaves the local curvature unchanged.

Explore these relations

- For the frame comparison, inspect the centre-of-mass decomposition and energy loss in a cart collision. Open the live calculation.
- For the force-area argument, compare equal-impulse sinusoidal contact pulses as stiffness changes. Their shape differs from the triangular measured pulse in this sheet. Open the live calculation.

Chapter 3 · Constraints and Lagrange's equations

Eliminate an unknown tension with a generalised coordinate and identify how a pulley's rotational inertia changes an acceleration.

FROM FIRST PRINCIPLES

Derive the one-coordinate Lagrange equation from virtual work

For point masses with fixed, smooth ideal constraints, describe all positions as $\mathbf{r}_i(q)$. An allowed instantaneous virtual displacement is

$$\delta\mathbf{r}_i = (\partial_q \mathbf{r}_i)\delta q.$$

Assume constraint reactions do zero total virtual work. Newton's equations projected along this common displacement therefore eliminate the unmeasured reactions:

$$\sum_i m_i \mathbf{a}_i \cdot \partial_q \mathbf{r}_i = \sum_i \mathbf{F}_i^{\text{applied}} \cdot \partial_q \mathbf{r}_i = Q.$$

Use $K = \sum_i m_i \mathbf{v}_i^2/2$ and $\mathbf{v}_i = (\partial_q \mathbf{r}_i)\dot{q}$. Since $\partial_{\dot{q}} \mathbf{v}_i = \partial_q \mathbf{r}_i$, differentiate $\partial_{\dot{q}} K$ in time. The product term involving $d(\partial_q \mathbf{r}_i)/dt$ equals $\partial_q K$. Subtracting it leaves

$$\sum_i m_i \mathbf{a}_i \cdot \partial_q \mathbf{r}_i = \frac{d}{dt}\frac{\partial K}{\partial \dot{q}} - \frac{\partial K}{\partial q}.$$

If the applied forces derive from a potential $U(q)$ then $Q = -\partial_q U$. Moving the potential term gives the equation for $L = K - U$:

$$\frac{d}{dt}\frac{\partial L}{\partial \dot{q}} - \frac{\partial L}{\partial q} = 0.$$

The coordinate choice can eliminate a tension without assuming that tension vanishes. A rolling constraint requires the virtual displacements to obey its no-slip condition.

Background · Action

$$S = \int_{t_1}^{t_2} L(q, \dot{q}, t)\, dt$$

Compare nearby admissible paths with the specified endpoint data. Stationarity gives a local equation of motion. In SI the action has units of joule seconds.

DERIVATION AND APPLICATIONS

How does a moving pulley change the inertia seen by a load?

A string constraint fixes acceleration ratios before tensions are known. Consider a mass M carried by a light movable pulley. One end of a single inextensible string is fixed to the ceiling. It passes around the movable pulley, over a fixed pulley of radius R and moment of inertia I, and down to a free counterweight m. Use downward coordinate q for the movable assembly and downward coordinate y for the counterweight. The fixed pulley rotates freely about its axle. Assume a massless string, no slip, and constant lengths of the wrapped arcs.

The moving pulley changes the lengths of two vertical segments. Differentiate the length constraint to determine both the counterweight speed and the rim speed of the fixed pulley:

$$2q + y = \text{constant},$$
$$\dot{y} = -2\dot{q},$$
$$|\omega| = 2|\dot{q}|/R.$$

Write all kinetic and potential energies in terms of the single coordinate. Downward displacement reduces gravitational potential, and raising the counterweight contributes with the opposite sign:

$$K = \tfrac{1}{2}\left(M + 4m + 4I/R^2\right)\dot{q}^2,$$
$$U = (-M + 2m)gq + \text{constant}.$$

The Lagrange equation equates the rate of change of generalized momentum to the generalized force. The velocity ratios enter the inertia squared, whereas the displacement ratios enter gravitational work linearly:

$$(M + 4m + 4I/R^2)\ddot{q} = (M - 2m)g.$$

All terms multiplying acceleration have units of mass. An ideal fixed pulley with a heavy rim still slows the motion, even though its centre does not translate. At $M = 2m$ the gravitational driving force vanishes for every value of I.

WORKED EXAMPLE

Predict a descending load and an ascending counterweight

Change the inputs and investigate this derivation.

Set $M = 1.20$ kg, $m = 0.400$ kg, $R = 0.0500$ m and $I = 2.50 \times 10^{-4}$ kg m². The rotational contribution is 0.400 kg and the effective mass is 3.20 kg. The driving force is $0.400g = 3.924$ N, giving $\ddot{q} = 1.23$ m/s² downward and counterweight acceleration 2.45 m/s² upward. A release from rest moves the load 0.153 m in 0.500 s if sufficient travel is available.

SECOND APPLICATION

Measure a pulley inertia from a reversed acceleration

Change the inputs and investigate this derivation.

With the same M and R, change the counterweight to $m = 0.800$ kg. A camera records upward load acceleration 0.8175 m/s². The signed numerator is now -3.924 N, so the measured effective mass is 4.80 kg. Subtracting $M + 4m = 4.40$ kg leaves $4I/R^2 = 0.400$ kg, recovering $I = 2.50 \times 10^{-4}$ kg m² to measurement precision. The reversal tests both the sign of gravitational work and the factor of two in the length constraint.

Try it · Pulley

Vary the physical parameters in the derived relation. Use the units and assumptions in the readout to connect the curves to the two worked examples. A parameter study can test the forward prediction; the same relation can then be inverted to infer a parameter from a measurement.

Open this live calculation

Try the calculation

Descending load M (kg)	**1.2**
Pulley rotational equivalent 4I/R² (kg)	**0.4**

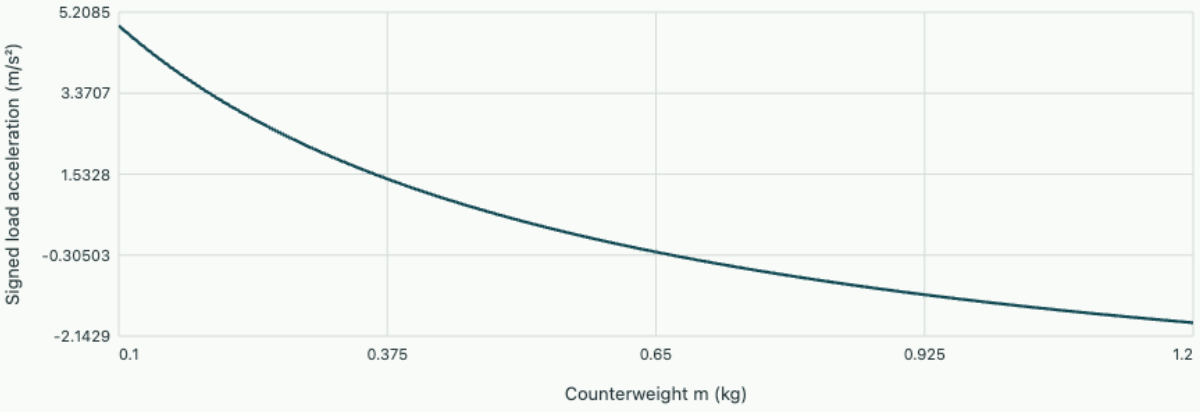

Constrained pulley mechanism

The counterweight moves twice as far with opposite sign. Driving mass M−2m and effective inertia M+4m+4I/R² explain the reversal at m=M/2.

Which parts of a vertical loop need a two-sided constraint?

A bead of mass 100 g moves in a frictionless circular groove of radius R. It starts at the bottom with speed v_0. At angle θ from the downward vertical, energy conservation gives

$$v^2 = v_0^2 - 2gR(1 - \cos\theta).$$

The inward radial equation is

$$N - mg\cos\theta = mv^2/R.$$

The sign of the groove force N is measurable. A two-sided groove can reverse this force; a bead held only against the inside of a smooth rail would lose contact where the required inward force first becomes negative.

Open this experiment online

Try the calculation

Bottom speed (m/s) **4**

Loop radius (m) **0.5**

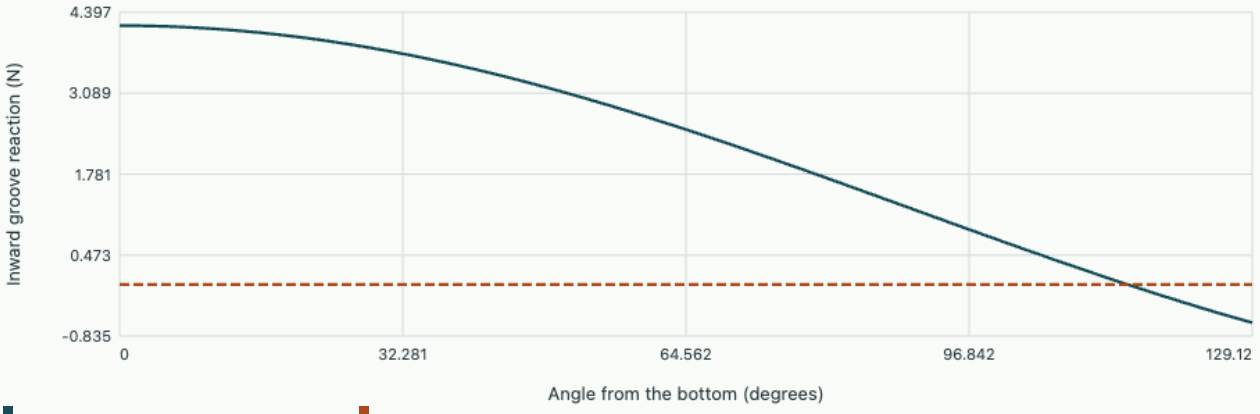

Reachable angle 129.12°. Inward groove reaction there -0.619 N. One-sided loop threshold v_0 = 4.9523 m/s.

The graph ends at the first turning point if the energy cannot reach the top. Compare the speed needed just to reach the height of the top with the speed needed to maintain one-sided contact there. The former has $v_0^2 = 4gR$; setting $N = 0$ at the top gives $v_0^2 = 5gR$ for the latter. A conserved integral of motion and a constraint inequality answer different experimental questions.

Count independent motions

Two hanging masses and a massive pulley appear to introduce two translations, a rotation and several forces. Yet an inextensible taut string and rolling contact without slip leave just one independent motion. Let mass m_2 descend a distance q while mass m_1 rises by the same distance. For a fixed axle and pulley radius R, the rotation is $\theta = q/R$ relative to its initial value. Assume the masses stay clear of the pulley, the string is light, the axle friction is negligible and the pulley's moment of inertia about the axle is I.

A constraint relates permitted displacements before any force balance is written. The fact that both ends move the same distance follows from length conservation. It does not require equal tensions. A massive accelerating pulley needs a net torque, so replacing the tensions by a common value would remove its angular acceleration from the model. This example is a useful test of when a constraint allows us to remove coordinates and when it also allows us to remove forces.

Background · How can an ideal constraint transfer energy?

A bead slides without friction on a rail whose shape and position can change with time. An admissible virtual displacement compares nearby positions at the same time. It is tangent to the rail, so the normal reaction does no virtual work. The actual laboratory velocity also contains the motion of the rail itself. Write a point on the rail as $\mathbf{r}(q,t)$ and take its time derivative.

$$P_{\mathrm{rail}} = \mathbf{N}\cdot\dot{\mathbf{r}} = \mathbf{N}\cdot\left(\frac{\partial \mathbf{r}}{\partial q}\dot{q} + \frac{\partial \mathbf{r}}{\partial t}\right) = \mathbf{N}\cdot\frac{\partial \mathbf{r}}{\partial t}.$$

A horizontal rail lifted vertically at constant speed u gives the simplest check. The bead's vertical acceleration is zero and the normal force is mg. The rail supplies power mgu, exactly the rate at which gravitational potential energy rises. The constraint can be ideal while an external actuator supplies the energy.

Construct the stationarity equation

For ideal time-independent constraints the reaction forces do no total work on allowed virtual displacements. Form the Lagrangian $\mathcal{L} = K - U$ using the independent coordinates. Consider two paths with the same initial and final values of q, differing by a small variation $\delta q(t)$. The first variation of the action is $\int (\partial_q \mathcal{L}\,\delta q + \partial_{\dot q}\mathcal{L}\,\delta\dot q)dt$. Integrate the second term by parts. The endpoint term vanishes and stationarity for arbitrary interior variations requires

$$\frac{d}{dt}\frac{\partial \mathcal{L}}{\partial \dot q} - \frac{\partial \mathcal{L}}{\partial q} = 0.$$

This equation supplies one independent balance for each independent coordinate. If an applied nonconservative force does work $\delta W = Q\,\delta q$, its generalised force Q enters the right-hand side. For an angular coordinate Q has units of torque; for this translational coordinate it has units of force. It must be calculated using the same sign choice as the coordinate.

Find a conserved quantity from a continuous symmetry

Constraints identify which coordinates can vary independently. A symmetry asks a different question: which small change of those coordinates leaves the action unchanged? Let $q_i \mapsto q_i + \varepsilon \xi_i(q,t)$ at fixed time and $p_i = \partial L/\partial \dot q_i$. Along a solution the Euler–Lagrange equations turn the variation into a total derivative,

$$\frac{\delta L}{\varepsilon} = \sum_i \left(\dot p_i \xi_i + p_i \dot \xi_i \right) = \frac{d}{dt} \sum_i p_i \xi_i .$$

If the left side vanishes for every path, $Q = \sum_i p_i \xi_i$ is conserved on solutions. More generally, a change $\delta L = \varepsilon\, dB/dt$ changes only endpoint terms in the action, and $Q = \sum_i p_i \xi_i - B$ is conserved. This is Noether's theorem for this fixed-time transformation. Separate conservation of mechanical energy requires time-translation symmetry.

Consider a bead of mass m on a smooth horizontal table. A light string attached to the bead passes through a central hole. Pulling the string prescribes the radius $r(t)$. Its tension has no azimuthal component. Rotation of the entire trajectory through a constant azimuth leaves $L = m(\dot r^2 + r^2 \dot\phi^2)/2$ unchanged. Therefore $m r^2 \dot\phi$ is constant even when a pulling device supplies work. For $m = 0.250$ kg, $r_i = 0.400$ m and $\dot\phi_i = 3.00$ rad/s, $Q = 0.120$ kg m²/s. Halving the radius raises angular speed to 12.0 rad/s. With zero radial speed at each endpoint, kinetic energy rises from 0.180 to 0.720 J. A central force can do work while exerting no torque about the centre.

Practise on sheet 2 · Recognize translation symmetry on a moving pair. Further reading · University of Cambridge · David Tong, Classical Dynamics · §2.4.1 Noether's Theorem.

Add every energy contribution

Both hanging masses move at speed $|\dot q|$. The pulley contributes rotational kinetic energy $I(\dot q/R)^2/2$. Raising the first mass increases its gravitational potential, while lowering the second decreases it. Omitting an arbitrary constant gives

$$U = (m_1 - m_2) g q .$$

The full kinetic energy is

$$K = (m_1 + m_2 + I/R^2)\dot q^2/2 .$$

Substitution yields

$$(m_1 + m_2 + I/R^2)\ddot q = (m_2 - m_1) g .$$

The quantity I/R^2 enters like an additional translational mass. It stores kinetic energy without changing the gravitational driving force. A constant opposing axle torque of magnitude τ_f would give a generalised

resisting force τ_f/R while the second mass descends. Applying a single constant sign across a reversal would incorrectly model dry friction.

Verify the reactions by restoring the constraints

Take $m_1 = 1.00$ kg, $m_2 = 1.50$ kg, $R = 0.100$ m and $I = 0.0050$ kg·m². The effective mass is 3.00 kg and the unbalanced weight is 4.905 N. Thus $\ddot{q} = 1.635$ m/s². From rest, a descent of 0.300 m produces a speed $\sqrt{2(1.635)(0.300)} = 0.990$ m/s. The drop in potential energy is 1.472 J, equal to the gain in translational and rotational energy together.

Now isolate each hanging body. Upward acceleration on the lighter side requires

$$T_1 = m_1(g + \ddot{q}) = 11.45\,\mathrm{N}.$$

The heavier side gives

$$T_2 = m_2(g - \ddot{q}) = 12.26\,\mathrm{N}.$$

The tension difference times radius is about 0.082 N·m. The pulley independently requires

$$I\ddot{q}/R = 0.0818\,\mathrm{N\,m}.$$

Agreement checks both the direction convention and the contribution of pulley inertia. The energy description solved for observable motion first. The separate body balances recovered forces that a mount or a string must actually withstand.

A useful check is to let one inertia become dominant. If the pulley’s moment of inertia is made very large while its radius and both hanging masses stay fixed, the effective inertia in the denominator grows and acceleration approaches zero. The two string tensions then approach their respective hanging weights, which can remain unequal despite the tiny acceleration. The finite difference supplies torque to a very large rotational inertia. Equality of tension throughout a string that wraps around a massive pulley is therefore an additional physical assumption that must be justified.

Rolling without slipping and the force enforcing it

A constraint can remove an unknown contact force from the equation of motion while leaving a definite physical condition for its realization. Consider a cylinder of mass m, radius R and moment of inertia I about its centre, rolling straight down a plane inclined at angle α. Let x increase down the plane, and take the spin angle θ positive for forward rolling. A stationary contact point on the plane requires

$$\dot{x} = R\dot{\theta}.$$

In this straight-line geometry the velocity constraint integrates directly to $x - R\theta = \text{constant}$. General rolling on a surface with changing direction requires more care because the analogous constraints need not integrate to coordinate relations.

Use x as the sole coordinate. The centre falls through $x\sin\alpha$ and kinetic energy contains both translation and rotation. The reduced Lagrangian is

$$L = \tfrac{1}{2}(m + I/R^2)\dot{x}^2 + mgx\sin\alpha.$$

The Euler–Lagrange equation gives

$$\ddot{x} = g\sin\alpha/(1 + I/(mR^2)).$$

For a body released from rest, the speed follows by integrating $\dot{x}\,d\dot{x}/dx = \ddot{x}$. Different mass distributions at fixed radius and mass therefore arrive at different times even if their initial gravitational energies are equal. Some of that energy appears in spin, whose contribution grows with I.

To determine the unknown friction, return to the original translational and rotational balances. If f points up the plane,

$$m\ddot{x} = mg\sin\alpha - f,$$

$$I\ddot{\theta} = fR.$$

Combining with the rolling constraint gives

$$f = (I/R^2)\ddot{x}.$$

The absence of f from the reduced Lagrangian came from zero virtual work under an admissible rolling displacement. It did not imply zero force.

Decide whether a solid cylinder will actually roll

A uniform solid cylinder has $I = mR^2/2$. Let $m = 2.00$ kg, $R = 0.100$ m and $\alpha = 30.0^\circ$. Predicted acceleration is

$$9.81(0.5)/(1.5) = 3.27\,\mathrm{m/s^2}.$$

The required upward friction is $(m/2)\ddot{x} = 3.27$ N, while the normal force is

$$mg\cos 30^\circ = 17.0\,\mathrm{N}.$$

Static friction can maintain rolling only for $\mu_s \geq f/N = 0.192$. This comparison tests an assumption that could not be checked from the acceleration equation alone.

After travelling 1.00 m from rest a rolling cylinder reaches 2.56 m/s and spins at 25.6 rad/s. Translational energy is 6.54 J and rotational energy is 3.27 J, accounting for the 9.81 J released by gravity. In the limit $I/(mR^2) \to 0$, nearly all energy goes into translation, acceleration tends to $g\sin\alpha$ and the required friction tends to zero. A surface with a measured coefficient below the threshold instead permits slipping. The translation and rotation must then be solved independently using the sliding contact law.

Rolling tests can be run without knowing the cylinder's mass distribution in advance. Obtain acceleration from two light gates at known positions and use $I/(mR^2) = g\sin\alpha/\ddot{x} - 1$ to infer a dimensionless inertia. Repeat at a shallower inclination. A genuine moment of inertia has the same inferred value in both runs, whereas slipping can appear only above a limiting angle. The most direct test tracks a painted mark on the rim as well as the centre. Admissible rolling requires the increase in centre displacement to equal radius times accumulated spin angle in each time interval.

Study the full derivation

Virtual work and the forces hidden by a constraint · Analytical mechanics from constraints to invariants

A bead follows a wire, a pendulum remains the same length, and a rolling wheel obeys a relation between translation and rotation. Their reduced equations describe the motion but can conceal the largest forces in the apparatus. Determine which forces disappear under a virtual displacement, recover their values, and decide when the assumed motion ceases to be physically admissible.

Chapter 4 · Normal modes and energy exchange

Decompose a pair of coupled oscillators into independent motions and predict the envelope of a beat signal.

FROM FIRST PRINCIPLES

Derive the coupled oscillator equations from individual spring extensions

Take identical carts of mass m with outer springs of stiffness k and an interconnecting spring of stiffness k_c. Measure displacements x_1, x_2 rightward from equilibrium. For small motions Hooke's law makes elastic energy quadratic in the extension of each individual spring. The middle one extends only when the positions differ:

$$U = \tfrac{1}{2}kx_1^2 + \tfrac{1}{2}kx_2^2 + \tfrac{1}{2}k_c(x_2 - x_1)^2.$$

The forces are minus the corresponding derivatives of U. Add the two Newton equations to isolate motion that does not stretch the coupling. Subtract them to isolate opposing motion that stretches it twice:

$$m(\ddot{x}_1 + \ddot{x}_2) = -k(x_1 + x_2),$$
$$m(\ddot{x}_1 - \ddot{x}_2) = -(k + 2k_c)(x_1 - x_2).$$

Each new coordinate is a single unforced oscillator; comparing its acceleration with $-\omega^2$ times displacement fixes the two frequencies:

$$\omega_s^2 = k/m,$$
$$\omega_a^2 = (k + 2k_c)/m.$$

For positive coupling the antisymmetric frequency is higher. Releasing only one cart excites both coordinates, so neither measured cart trajectory is generally a single sinusoid. At $k_c = 0$ the frequencies coincide and energy cannot pass through the absent coupling spring.

Background · Normal frequency

$$\det(K - \omega^2 M) = 0$$

Small oscillations around a force-balanced configuration give this generalised eigenproblem. The ordinary frequency in hertz is the angular frequency divided by two pi.

DERIVATION AND APPLICATIONS

What replaces symmetry coordinates when the masses differ?

The symmetric and antisymmetric combinations for identical carts cease to decouple when one cart is loaded. Still, a normal mode has a definite frequency and a fixed ratio of displacements. Take carts of masses m and $2m$, each attached to an outer wall by a spring of stiffness k. Connect them with a third spring, also of stiffness k. Measure both small displacements rightward from equilibrium. The coupling spring extends by $x_2 - x_1$; this determines the signs of its two forces without assuming a mode in advance.

$$m\ddot{x}_1 = -2kx_1 + kx_2,$$
$$2m\ddot{x}_2 = kx_1 - 2kx_2.$$

Seek a sinusoidal solution $x_j = A_j \cos(\omega t + \phi)$. A nonzero pair of amplitudes must solve two homogeneous equations simultaneously. Eliminating A_2 and writing $s = m\omega^2/k$ gives

$$(2 - s)A_1 = A_2, \qquad (2 - 2s)A_2 = A_1, \qquad (2 - s)(2 - 2s) = 1.$$

The last equation is quadratic in squared frequency. Its roots and their displacement ratios are

$$s_\pm = (3 \pm \sqrt{3})/2,$$
$$\omega_\pm = \sqrt{k s_\pm / m}, \qquad (A_2/A_1)_\pm = 2 - s_\pm.$$

The low mode has the carts moving in the same direction, while the high mode stretches their connecting spring by moving them oppositely. The amplitude ratios no longer equal one in magnitude. Ordinary dot products do not describe the kinetic energy of unequal masses. Weighting the second component by two gives $1 + 2(2 - s_+)(2 - s_-) = 0$, the mass-weighted orthogonality that allows arbitrary initial conditions to be decomposed.

WORKED EXAMPLE

Separate measured spectral peaks

Change the inputs and investigate this derivation.

For $m = 0.250$ kg and $k = 25.0$ N/m, $k/m = 100$ s⁻². The predicted modal frequencies are 7.96 and 15.38 rad/s, or 1.27 and 2.45 Hz. The ratios A_2/A_1 are 1.366 and -0.366. A measured 3.00 mm amplitude of the lighter cart in the high mode therefore accompanies a 1.10 mm amplitude of the heavier cart in the opposite phase.

SECOND APPLICATION

Prepare motion in only one mode

Change the inputs and investigate this derivation.

Displace the lighter cart 4.00 mm rightward. To excite the low mode alone, move the heavier cart 5.46 mm rightward and release both from rest. If instead the heavy cart starts at zero, write the initial light-cart displacement as $a_- + a_+ = 4.00$ mm. The second component requires

$$1.366a_- - 0.366a_+ = 0.$$

Solving gives $a_- = 0.845$ mm and $a_+ = 3.15$ mm. Both frequencies now appear even though the same lighter cart was released from the same place.

Try it · Two cart modes

Vary the physical parameters in the derived relation. Use the units and assumptions in the readout to connect the curves to the two worked examples. A parameter study can test the forward prediction; the same relation can then be inverted to infer a parameter from a measurement.

Open this live calculation

Try the calculation

Light cart mass (kg)	0.25
Spring stiffness (N/m)	25
Heavy/light initial displacement ratio	0

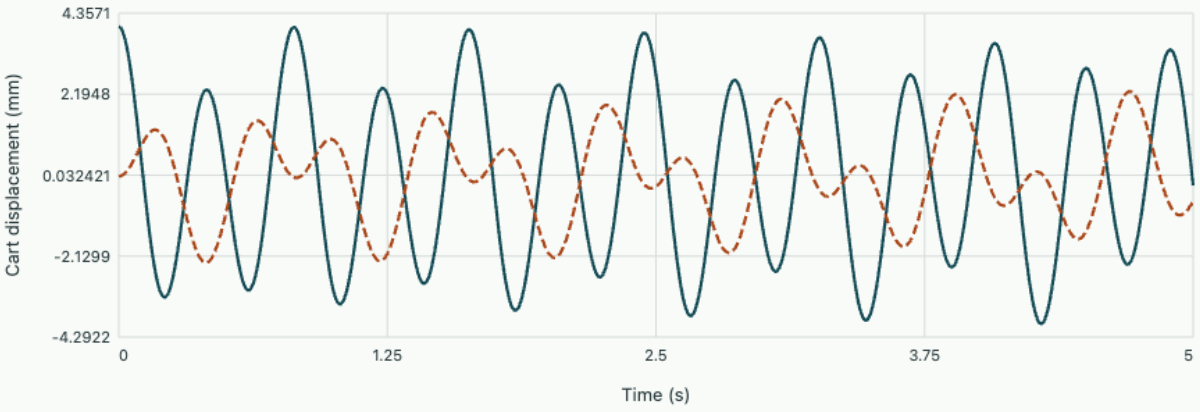

Modal frequencies 7.9623 and 15.382 rad/s. Pure-mode displacement ratios 1.366 and -0.36603. Released from rest; equal adjacent springs and fixed outer ends.

Start with two measurable coordinates

Fix two identical carts of mass m to opposite ends of a track using identical springs of stiffness k, and join the carts to each other with a third spring of stiffness k_c. The equilibrium lengths have already been set. Let x_1 and x_2 be small displacements from equilibrium, both positive to the right. The coupling spring extends by $x_2 - x_1$. Both coordinates contribute independently to the kinetic energy, but their potential energies are linked through this difference.

From $U = k(x_1^2 + x_2^2)/2 + k_c(x_2 - x_1)^2/2$, the equations are

$$m\ddot{x}_1 = -(k + k_c)x_1 + k_c x_2,$$

$$m\ddot{x}_2 = k_c x_1 - (k + k_c)x_2.$$

One moving cart thus exerts a force on its neighbour. Release a single displaced cart and both generally move even though only one carried potential energy in its end spring at the start. The task is to predict that exchange without assuming that either cart alone executes a single harmonic oscillation.

Use symmetry to choose coordinates

Interchanging the two labels leaves the equations invariant. Their sum contains only $x_1 + x_2$ and their difference contains only $x_1 - x_2$. Define $q_s = (x_1 + x_2)/2$ and $q_a = (x_1 - x_2)/2$. Adding then subtracting the equations yields

$$\ddot{q}_s + (k/m)q_s = 0,$$

$$\ddot{q}_a + [(k + 2k_c)/m]q_a = 0.$$

The symmetric mode moves both carts together so that the central spring keeps its length. The antisymmetric mode moves them oppositely and stretches that spring by twice either displacement. These patterns determine the frequencies before an amplitude is chosen. Initial conditions select the weights and phases of the modes. For unequal masses symmetry is lost, but substituting $\mathbf{x} = \boldsymbol{\phi}\cos\omega t$ in $\mathbf{M}\ddot{\mathbf{x}} + \mathbf{K}\mathbf{x} = 0$ still gives the generalised eigenproblem $\mathbf{K}\boldsymbol{\phi} = \omega^2\mathbf{M}\boldsymbol{\phi}$.

Follow a release from one side

Displace cart 1 by A and leave cart 2 at its equilibrium position, both initially at rest. Each normal coordinate starts at $A/2$ with zero velocity. Recombining gives

$$x_1 = A(\cos\omega_s t + \cos\omega_a t)/2,$$

$$x_2 = A(\cos\omega_s t - \cos\omega_a t)/2.$$

With $\bar{\omega} = (\omega_s + \omega_a)/2$ and $\Delta\omega = \omega_a - \omega_s$, the first expression is $A\cos(\bar{\omega}t)\cos(\Delta\omega t/2)$. The rapid motion and the slow envelope arise from the same two undamped modes. A fading displacement over a few cycles need not indicate dissipated energy.

The second cart has a complementary envelope. When the cosine envelope of cart 1 first vanishes, the sine envelope of cart 2 has unit magnitude. Its instantaneous displacement depends on the fast phase. The coupling spring also stores energy, so attributing all system energy to individual carts from their instantaneous displacements can misidentify the time of energy transfer. Modal energies remain constant for a linear undamped system.

Interpret a pair of peaks

Use $m = 1.00$ kg, $k = 100$ N/m, $k_c = 10.5$ N/m and $A = 0.030$ m. The angular frequencies are exactly 10.0 and 11.0 rad/s. A spectrum of the motion of cart 1 contains peaks at 1.592 and 1.751 Hz. The envelope first vanishes after $\pi/\Delta\omega = 3.142$ s and first regains unit magnitude after $2\pi/\Delta\omega = 6.283$ s. This is about ten rapid cycles. From the two measured frequencies and the known cart mass one can estimate the coupling because $k_c = m(\omega_a^2 - \omega_s^2)/2$.

Repeat the release with both carts displaced by the same amount. Only the lower-frequency mode should survive. A remaining upper peak would be evidence to look for unequal initial positions, mass mismatch or spring asymmetry. Comparing the peaks under two physically different preparations gives a sharper model check than a single time trace.

Symmetry gives the shapes directly for identical carts. With unequal carts, multiply the eigenvalue equation for mode i from the left by the transpose of mode j, then subtract the reverse relation. Symmetry of the mass and stiffness matrices leaves $(\omega_i^2 - \omega_j^2)\boldsymbol{\phi}_j^T \mathbf{M} \boldsymbol{\phi}_i = 0$. Distinct modes are orthogonal under the mass-weighted product. This states exactly how to project a measured initial displacement onto unequal-mass modes. An ordinary unweighted average of the two cart displacements would generally mix them. Simultaneous recordings then test predicted mode shapes as well as their frequencies.

A tuned auxiliary mass can suppress the driven motion

Normal modes can be used to alter which coordinate moves under a repeated force. Attach a primary mass m to ground with a spring k and connect an auxiliary mass m_a to the primary with another spring k_a. Both move along one line. Ignore damping for the ideal design and drive only the primary mass with $F_0 \cos \omega t$. Let X, Y denote signed steady harmonic displacement amplitudes. The equilibrium equations at the drive frequency are

$$(k + k_a - m\omega^2)X - k_a Y = F_0,$$

$$-k_a X + (k_a - m_a\omega^2)Y = 0.$$

At $\omega^2 = k_a/m_a$, the coefficient multiplying Y in the second equation vanishes. It then requires $X = 0$. The primary equation fixes $Y = -F_0/k_a$: the auxiliary spring force cancels the external drive on the primary. This is an antiresonance of the primary coordinate. A system with more than one coordinate can have a deep minimum between two resonance peaks because the measured coordinate combines both modal responses with opposing signs.

To distinguish this cancellation from a normal mode, set the right-hand side to zero. Nonzero free motion demands a zero determinant, $(k + k_a - m\omega^2)(k_a - m_a\omega^2) - k_a^2 = 0$. At the proposed cancellation frequency that determinant is $-k_a^2$, strictly nonzero, so the forced solution there is unique. On initial start-up a real experiment also excites transients at both natural frequencies. Weak damping or carefully chosen initial conditions is needed before the pure harmonic response can be observed.

Tune an instrument support

A 2.00 kg instrument sits on a 200 N/m mount and experiences a 1.00 N harmonic force at 10.0 rad/s, exactly its original undamped natural frequency. Add $m_a = 0.200$ kg and choose $k_a = m_a\omega^2 = 20.0$ N/m. The ideal primary coordinate remains stationary at the drive frequency, while the auxiliary mass requires amplitude $1.00/20.0 = 0.0500$ m. A design can therefore predict excellent isolation and still fail a travel constraint.

Set $s = \omega^2$ in the free-motion determinant. With these values it becomes $0.4s^2 - 84s + 4000 = 0$, with roots near 73.0 and 137.0 s⁻². The new natural frequencies are 8.54 and 11.7 rad/s, bracketing the designed minimum. The primary response is therefore vulnerable to detuning in either direction. As auxiliary mass tends to zero at fixed tuning, its spring stiffness tends to zero as well and the required auxiliary travel diverges. Monitoring auxiliary displacement while sweeping the forcing frequency gives a stronger design test than looking only for a minimum in the instrument record.

It is worth distinguishing force cancellation from motion cancellation when interpreting a measured antiresonance. At the designed frequency the primary mass has negligible absolute acceleration, so the summed spring forces and external force must cancel on it. The attachment still experiences a finite cyclic force, equal to its stiffness times relative motion. A load cell in that small spring can therefore record a pronounced signal while the primary displacement sensor records its minimum. The two readings together check that suppression comes from the auxiliary degree of freedom, rather than from a drop in the drive force at that frequency.

Find how much mistuning the absorber tolerates

Return to the mounted instrument and suppose the operating frequency drifts. Eliminate the auxiliary displacement from the two harmonic equations without setting it to resonance first. Cramer's rule gives primary compliance

$$\frac{X}{F_0} = \frac{k_a - m_a\omega^2}{(k + k_a - m\omega^2)(k_a - m_a\omega^2) - k_a^2}.$$

The numerator determines a zero and the denominator determines the two poles. At zero frequency the ratio is $1/k$, since the free auxiliary mass offers no static restoring force. At very high frequency the ratio tends to $-1/(m\omega^2)$ because the primary inertia dominates. Both limits are useful for checking the absolute phase and calibration of a measured response.

Set the drive to 9.80 rad/s, only two percent below design. The auxiliary dynamic stiffness is

$$20.0 - 0.200(9.80)^2 = 0.792\,\mathrm{N/m}.$$

The primary diagonal term is

$$220 - 2.00(9.80)^2 = 27.9\,\mathrm{N/m}.$$

With the original 1.00 N drive the predicted primary amplitude is

$$0.792/|27.9(0.792) - 400| = 2.10\,\mathrm{mm}.$$

The auxiliary amplitude from the second equation is about 53.0 mm. At 10.2 rad/s the corresponding primary amplitude is about 1.98 mm and changes sign relative to the force. Thus a two-percent frequency drift already matters if the instrument's allowed motion is one millimetre.

A small damper between the two masses limits the two resonant peaks but removes exact cancellation at the tuned frequency. The spring's dynamic stiffness is then replaced by $k_a + i\omega c_a$ in both coupling terms. With real drive frequency and positive damping the numerator no longer vanishes exactly. The engineering choice can now be stated quantitatively: hold zero response at one precisely controlled frequency, or allow a finite minimum in order to improve nearby peak response when operating frequency varies.

Distinguish two resonances near a crossing

Two unit masses have squared-frequency matrix with diagonal entries $1, d^2$ and off-diagonal entries 0.12. Sweep the second stiffness while keeping the coupling fixed. Diagonalise the symmetric matrix before taking square roots.

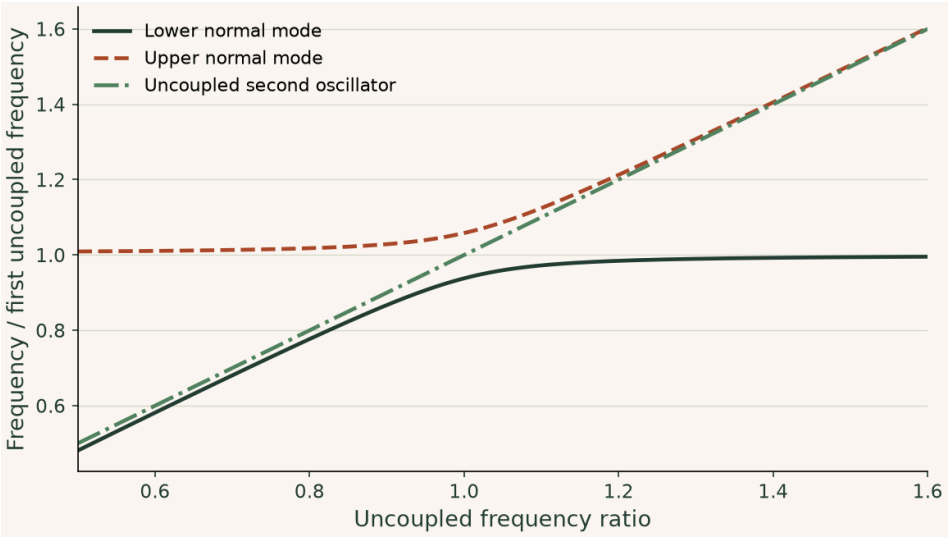

At d = 1 the squared frequencies split to 0.88 and 1.12. The measured frequencies are approximately 0.938 and 1.058. The closest branches mix motion of both masses, so assigning a peak permanently to a single mass fails.

Try it · Mode split

Change the inputs and compare the recalculated curves with the preceding derivation and baseline figure. The axes give the units; the numerical readout states the model assumptions and any limiting cases. Reset the inputs to return to the reference setting.

Open this live calculation

Try the calculation

Coupling of squared frequencies **0.12**

Bare squared-frequency ratio **1**

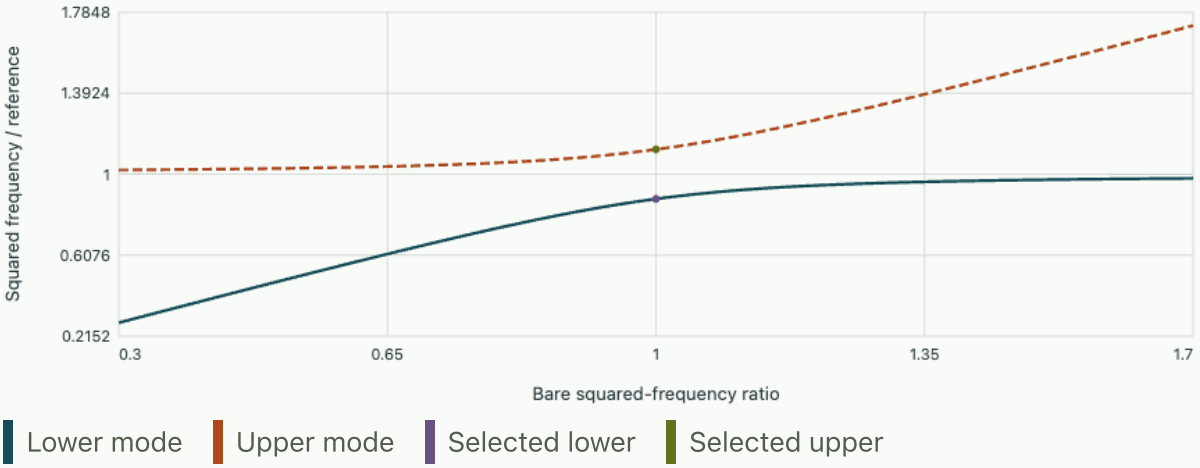

Squared eigenvalues 0.88 and 1.12. Both modes are stable.

▶ **Read values from the plot**

Problem sheet 2 · Constrained motion and modes

Translate the energy method of Lecture 3 into the normal-coordinate calculations of Lecture 4.

Measure the inertia of a pulley

With string radius 80 mm, hanging masses of 1.20 kg and 0.80 kg accelerate at 1.40 m/s², heavier side down. Neglect friction. Infer the pulley inertia, calculate the tension difference and predict the acceleration if the same inertia is used at a winding radius of 40 mm.

▼ **Recover the hidden rotational energy**

The mass difference supplies 3.924 N, requiring an effective total mass $3.924/1.40 = 2.803$ kg. Subtract the hanging mass sum of 2.00 kg to get $I/R^2 = 0.803$ kg, hence $I = 0.00514$ kg·m². Torque balance gives

$$T_h - T_l = I\ddot{q}/R^2 = 1.124\,\mathrm{N}.$$

Halving the radius quadruples the effective rotational mass. The new acceleration is

$$3.924/(2.00 + 4 \times 0.803) = 0.753\,\mathrm{m/s^2}.$$

This test could help separate a radius-dependent inertia effect from an incorrectly weighed hanging mass.

Identify the springs from soundings

Two identical carts of mass 0.50 kg have measured angular frequencies 8.0 and 12.0 rad/s. Identical end springs and a connecting spring are assumed. Determine both stiffnesses. Prescribe a release that isolates the higher mode and predict the time of the first return to the initial configuration.

▼ **Invert the two modal equations**

The symmetric motion uses only the end springs, so

$$k = m\omega_s^2 = 32\,\mathrm{N/m}.$$

The antisymmetric equation gives

$$k_c = m(\omega_a^2 - \omega_s^2)/2 = 20\,\mathrm{N/m}.$$

Displace the carts equally in opposite directions and release together from rest. Their centre stays fixed and the first full return occurs after $2\pi/12 = 0.524$ s. After half that interval the displacements are interchanged, which is distinguishable if the carts are marked.

Find a frequency from a bead’s constraint

A bead of mass m slides without friction in a vertical plane on a wire of shape $z = \alpha x^2$ with $\alpha = 2.0$ m^{-1}, where z increases upwards. Derive the one-coordinate Lagrangian. Find the small-amplitude frequency and estimate how good the kinetic-energy approximation is at $x = 0.10$ m.

▼ **Include the vertical velocity**

The constraint gives

$$\dot{z} = 2\alpha x \dot{x}.$$

Thus $K = m(1 + 4\alpha^2 x^2)\dot{x}^2/2$ and $U = mg\alpha x^2$. The exact Euler–Lagrange equation is

$$(1 + 4\alpha^2 x^2)\ddot{x} + 4\alpha^2 x \dot{x}^2 + 2g\alpha x = 0.$$

Keeping terms first order in the small motion gives $\omega = \sqrt{2g\alpha} = 6.26$ rad/s or 0.997 Hz. At 0.10 m the kinetic-energy factor is 1.16. Treating the bead as moving horizontally undercounts the exact kinetic energy at the same horizontal speed by $0.16/1.16 = 13.8\%$. The small-amplitude frequency is a local prediction near the bottom.

Recognize translation symmetry on a moving pair

Two free carts of masses 0.40 and 0.60 kg interact through a spring whose relaxed length is controlled as a function of time. Initially their speeds are +0.90 and −0.10 m/s. Derive the conserved quantity from a simultaneous translation and find the second cart's speed when the first stops. Can total kinetic plus spring energy change?

▼ **Derive the invariant and use it**

The potential depends on $x_2 - x_1 - \ell(t)$, so equal translations give $\xi_1 = \xi_2 = 1$ and $\delta L = 0$. Noether's charge is $m_1\dot{x}_1 + m_2\dot{x}_2 = 0.300$ kg m/s. When $\dot{x}_1 = 0$, $\dot{x}_2 = 0.300/0.60 = 0.500$ m/s. Changing the prescribed relaxed length introduces explicit time dependence and can transfer energy to the spring even with no net external translational impulse.

Revisit chapter 3 · Find a conserved quantity from a continuous symmetry.

Explore these relations

- For the pulley inference, vary rotational inertia and winding radius and inspect the acceleration. Open the live calculation.

- For the spring inference, vary the coupling and compare the two normal frequencies. Open the live calculation.

Chapter 5 · Rotating frames and the Coriolis effect

Transform a measured trajectory between an inertial laboratory and a rotating observer, and quantify the first sideways deflection.

FROM FIRST PRINCIPLES

Differentiate a vector whose coordinate axes are turning

Let a moving observer have origin $\mathbf{R}_O$ and an orthonormal basis $\mathbf{e}_i(t)$ rotating with angular velocity $\boldsymbol{\Omega}$. Write relative position as $\mathbf{r} = \sum_i r_i \mathbf{e}_i$. A small rigid rotation $d\boldsymbol{\theta}$ moves a unit vector perpendicular to itself through $d\mathbf{e}_i = d\boldsymbol{\theta} \times \mathbf{e}_i$. Hence differentiating both coordinates and basis gives the transport identity

$$\left(\frac{d\mathbf{r}}{dt}\right)_{\text{lab}} = \left(\frac{d\mathbf{r}}{dt}\right)_{\text{rot}} + \boldsymbol{\Omega} \times \mathbf{r}.$$

The absolute velocity is therefore the sum of origin motion, observed relative motion and transport around the origin. Differentiate those three contributions again. In particular, differentiating relative velocity in the lab adds one $\boldsymbol{\Omega} \times \mathbf{v}_{\text{rot}}$, and differentiating the transport velocity adds a second:

$$\mathbf{a}_{\text{lab}} = \mathbf{a}_O + \mathbf{a}_{\text{rot}} + 2\boldsymbol{\Omega} \times \mathbf{v}_{\text{rot}} + \dot{\boldsymbol{\Omega}} \times \mathbf{r} + \boldsymbol{\Omega} \times (\boldsymbol{\Omega} \times \mathbf{r}).$$

Newton’s law applies with the laboratory acceleration if that frame is inertial. Moving the extra accelerations to the force side predicts the rotating observer’s trajectory. A marker fixed to the rotating frame has zero relative velocity, yet its laboratory acceleration can remain nonzero.

DERIVATION AND APPLICATIONS

Why does a dropped object land east of the plumb line?

A release from rest beside a tower initially shares the ground's rotation. It starts with zero velocity in the local rotating frame, yet acquires a horizontal deflection as it falls. Use local axes east, north and up, and let φ denote latitude. Over a short fall treat effective gravitational acceleration g and Earth's angular velocity Ω as constant. The plumb line defines local vertical and already incorporates the static centrifugal acceleration. Neglect air resistance, gravity gradients and corrections of second order in Ωt.

The zeroth-order motion is vertical. Express the rotation vector in the local axes and place that vertical velocity in the Coriolis acceleration:

$$\boldsymbol{\Omega} = (0, \Omega\cos\varphi, \Omega\sin\varphi),$$
$$\mathbf{v}_0 = (0, 0, -gt),$$
$$\mathbf{a}_C = -2\boldsymbol{\Omega} \times \mathbf{v}_0.$$

The east component is positive and grows linearly in time because the fall speed is increasing. Integrating once from zero horizontal velocity gives

$$a_E(t) = 2\Omega g t \cos\varphi,$$
$$v_E(t) = \Omega g t^2 \cos\varphi.$$

Integrate again and eliminate the flight time using the vertical drop h. The horizontal displacement at first contact with the ground is

$$x_E = \tfrac{1}{3}\Omega g \cos\varphi \,(2h/g)^{3/2}.$$

Using the final acceleration for the entire fall would overestimate the result. Only the horizontal component of Earth's rotation couples directly to vertical velocity. At the poles this contribution vanishes. Changing from northern to southern latitudes of equal magnitude leaves the eastward sign unchanged.

WORKED EXAMPLE

Estimate the offset below a tower

Change the inputs and investigate this derivation.

Drop a compact test mass through $h = 45.0$ m in an evacuated shaft at latitude 48.0°. With $g = 9.81$ m/s² and $\Omega = 7.292 \times 10^{-5}$ rad/s, flight time is 3.03 s. Substitution gives $x_E = 4.43$ mm. The final eastward velocity is 4.39 mm/s. Millimetre accuracy makes control of sideways launch velocities essential: an initial eastward drift of 1.00 mm/s would add another 3.03 mm to the measured offset.

SECOND APPLICATION

Compare two release heights without knowing latitude

Change the inputs and investigate this derivation.

At one location, two careful drops from 20.0 and 80.0 m give eastward residuals after a constant launch drift has been removed. The formula predicts

$$x_E(80)/x_E(20) = 4^{3/2} = 8.$$

A 1.40 mm residual in the shorter drop predicts 11.2 mm in the longer drop. A residual caused by a fixed unremoved sideways speed would instead scale with flight time, giving a factor of two. Varying height thus separates two effects that can look identical in one photograph.

Try it · Coriolis drop

Vary the physical parameters in the derived relation. Use the units and assumptions in the readout to connect the curves to the two worked examples. A parameter study can test the forward prediction; the same relation can then be inverted to infer a parameter from a measurement.

Open this live calculation

Try the calculation

Latitude (degrees) **48**

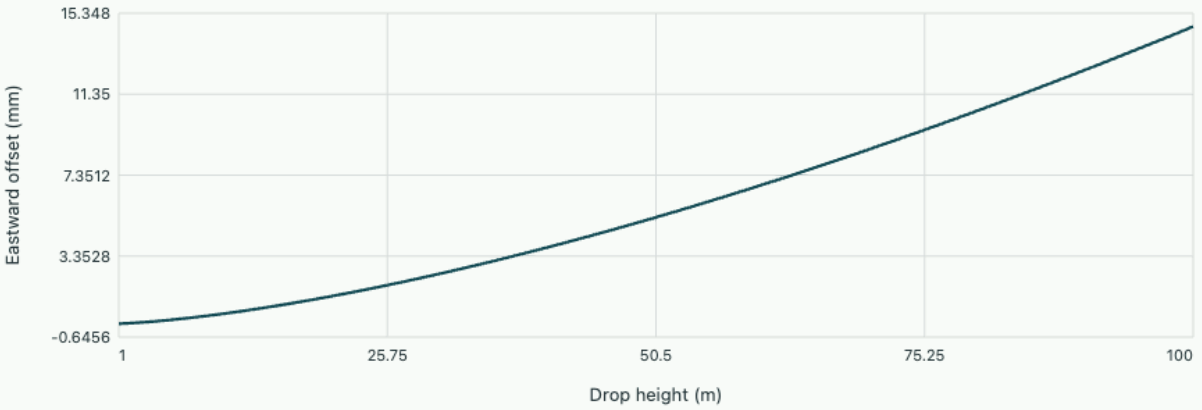

Leading Coriolis offset

Flight time is √(2h/g). The offset scales as h^(3/2), assumes release from rest relative to the tower, and neglects drag and higher rotation orders.

The observer changes the acceleration

Imagine a puck launched directly outwards from the centre of a horizontal rotating table. The nearly frictionless puck moves in a straight line in the laboratory after release. To a camera fixed to the table, it moves sideways. The two descriptions refer to the same sequence of points in space and time, but their coordinate axes evolve differently. A discrepancy in reported acceleration alone does not imply that a new physical interaction acted on the puck.

Let the table rotate with angular velocity $\boldsymbol{\Omega}$. During a small time dt, a vector fixed to the table changes by $\boldsymbol{\Omega} \times \mathbf{A}\, dt$ as seen from the laboratory. If a vector also changes its components relative to the table, the two contributions add. Thus

$$(d\mathbf{A}/dt)_{\mathrm{lab}} = (d\mathbf{A}/dt)_{\mathrm{rot}} + \boldsymbol{\Omega} \times \mathbf{A}.$$

The rule applies to any vector, including the velocity measured with the rotating basis.

Differentiate twice

Permit the rotating origin to translate with acceleration $\mathbf{a}_O$. Write $\mathbf{r}$ for the position relative to that origin. Differentiating the position once adds the frame velocity $\boldsymbol{\Omega} \times \mathbf{r}$. Differentiating a second time and collecting the contributions yields

$$\mathbf{a}_{\mathrm{lab}} = \mathbf{a}_O + \mathbf{a}_{\mathrm{rot}} + 2\boldsymbol{\Omega} \times \mathbf{v}_{\mathrm{rot}} + \dot{\boldsymbol{\Omega}} \times \mathbf{r} + \boldsymbol{\Omega} \times (\boldsymbol{\Omega} \times \mathbf{r}).$$

The two equal contributions to the velocity-dependent term arise from differentiating the moving basis of $\mathbf{v}_{\mathrm{rot}}$ and from the rotating-frame derivative of $\boldsymbol{\Omega} \times \mathbf{r}$. Dropping either loses a factor of two. To solve Newton’s equation for the rotating acceleration, transfer all frame terms to the force side with their signs reversed. For steady rotation at a fixed origin the remaining extra terms are the Coriolis and centrifugal forces.

Distinguish velocity-dependent deflection from a static load

For vertical rotation, the centrifugal force points horizontally away from the axis and has magnitude $m\Omega^2 r_\perp$. An object at rest on the rotating table experiences this term in its rotating-frame balance. In the laboratory a force directed towards the axis supplies its centripetal acceleration. Both descriptions predict the same required friction or tension. By contrast, the Coriolis force vanishes when the rotating-frame velocity is zero. When present it is perpendicular to that velocity, so its instantaneous power in the rotating frame is zero.

A static rotating liquid displays the centrifugal term directly. With gravity downwards and angular speed constant, equilibrium gives

$$\partial_r p = \rho \Omega^2 r,$$
$$\partial_z p = -\rho g.$$

On the free surface the pressure is constant, hence

$$dz/dr = \Omega^2 r / g.$$

Integration gives a parabolic surface with rise $\Omega^2 R^2/(2g)$ from centre to container radius R. With $\Omega = 3.0$ rad/s and $R = 0.20$ m the rise is 18.3 mm. If the container stops suddenly, the preceding static argument ceases to describe the transient flow.

Reconstruct the camera image

Let the puck leave the common origin at speed $u = 0.80$ m/s along the positive laboratory x axis when the two frames coincide. If the table turns counterclockwise at $\Omega = 0.50$ rad/s, transforming the laboratory position $(ut, 0)$ gives

$$x' = ut\cos(\Omega t),$$
$$y' = -ut\sin(\Omega t).$$

After 0.40 s the rotating camera sees $x' = 0.314$ m and $y' = -0.0636$ m. The puck lags behind the rotating radial line.

For $\Omega t \ll 1$ the transverse displacement is

$$y' \simeq -u\Omega t^2.$$

Its initial acceleration is therefore $-2u\Omega = -0.80$ m/s², just the Coriolis term. At launch the centrifugal term is zero because the puck sits at the axis. Later both frame terms contribute. Extrapolating the initial acceleration indefinitely would give a parabola, whereas the exact coordinate transformation yields the rotating trace for any elapsed time that the puck stays on the table.

A further check follows from work. The Coriolis term is perpendicular to instantaneous relative velocity, since $(\boldsymbol{\Omega} \times \mathbf{v}') \cdot \mathbf{v}' = 0$. It can turn a track without directly changing speed in the rotating frame. For constant angular velocity the centrifugal term can be derived from the potential $-m|\boldsymbol{\Omega} \times \mathbf{r}|^2/2$. A time-dependent rotation also introduces the Euler term, whose work generally cannot be folded into that same static potential. This explains why an experiment on a spinning-up table differs from one performed at the same instantaneous angular speed after settling.

Let a pendulum carry a direction across a rotating Earth

A laboratory pendulum can reveal a slow rotation too small to see during one swing. Consider a long pendulum of small amplitude at latitude φ. Use laboratory axes east x, north y and vertically upward. The vertical component of Earth's angular velocity is $\Omega_v = \Omega_\oplus \sin\varphi$. To first order in rotation, the horizontal Coriolis acceleration from horizontal motion involves only this component. The neglected vertical response contributes at higher order to the horizontal swing. Include the nearly constant local centrifugal contribution in the measured gravitational acceleration g.

For length ℓ, ordinary horizontal restoring acceleration is $-\omega_0^2(x, y)$ with $\omega_0 = \sqrt{g/\ell}$. Resolving $-2\boldsymbol{\Omega} \times \dot{\mathbf{r}}$ yields

$$\ddot{x} + \omega_0^2 x = 2\Omega_v \dot{y},$$
$$\ddot{y} + \omega_0^2 y = -2\Omega_v \dot{x}.$$

The coupling turns velocity through a right angle. Combining the coordinates into $z = x + iy$ converts the pair into one equation,

$$\ddot{z} + 2i\Omega_v \dot{z} + \omega_0^2 z = 0.$$

Substitute $z = we^{-i\Omega_v t}$. The terms proportional to $\dot{w}$ cancel, leaving $\ddot{w} + (\omega_0^2 + \Omega_v^2)w = 0$ within the horizontal model. To first order the motion in w is the ordinary swing. The prefactor rotates its axes in the laboratory at $-\Omega_v$. This predicts clockwise precession when viewed from above in the northern

hemisphere. The small second-order shift of swing frequency should not be extracted from this reduced model without restoring the other omitted effects of comparable order.

Plan an observation at midlatitudes

Set $\ell = 10.0$ m and $\varphi = 48.0^\circ$. A swing period is approximately $2\pi\sqrt{10.0/9.81} = 6.34$ s. In the same interval Earth turns only a small fraction of a degree. Using $\Omega_\oplus = 7.292 \times 10^{-5}$ rad/s gives $\Omega_v = 5.42 \times 10^{-5}$ rad/s. The swing axis rotates by 0.195 rad, or 11.2°, in one hour. A complete precession takes about 32.2 hours. Changing the pendulum length changes the number of swings counted during that hour while leaving the ideal precession angle unchanged.

At the equator the vertical component vanishes and the first-order horizontal precession disappears. At the pole its period is one sidereal day. These limits help separate the effect from anisotropic support stiffness, which can also rotate or distort an observed swing ellipse yet has no required latitude dependence. A reproducible procedure fits the major axis over successive groups of several swings, records its slow orientation change and repeats the launch along another initial azimuth to expose a fixed preferred direction in the mount.

The sign prediction can also be checked geometrically. At the north pole the suspension point rotates with Earth beneath an almost fixed inertial oscillation axis. An observer attached to the floor sees the opposite rotation. At the south pole the local upward direction reverses relative to Earth's rotation vector, so the observed precession reverses. At a midlatitude a camera pointed down from above reads the sign used in the equations; a camera looking upward through a transparent floor records the opposite visual sense. Stating the viewing direction prevents a purely optical reversal from appearing to contradict the mechanics.

Study the full derivation

Moving constraints, boundary work and a changing energy · Analytical mechanics from constraints to invariants

A pendulum with a reeled string can gain energy while its support force does no virtual work. A bead on a spinning guide can accelerate without gravity. Follow the work done by the apparatus, derive the relation between a reduced energy and laboratory energy, and identify which quantity a measurement tests.

Chapter 6 · Hamiltonian motion in phase space

Construct a Hamiltonian, read a phase portrait and distinguish bounded motion from rotation at a separatrix.

FROM FIRST PRINCIPLES

Construct Hamilton’s equations by exchanging velocity for momentum

Begin with a smooth Lagrangian $L(q, \dot{q}, t)$ for a conservative mechanical system. Assume the momentum definition $p = \partial_{\dot{q}} L$ can locally be inverted to give $\dot{q}$ as a function of (q, p, t). This regularity is what lets position and momentum serve as independent state coordinates. Define the Hamiltonian and differentiate the product before substituting any equations of motion:

$$H = p\dot{q} - L,$$
$$dH = \dot{q}\, dp + p\, d\dot{q} - L_q\, dq - L_{\dot{q}}\, d\dot{q} - L_t\, dt.$$

The two $d\dot{q}$ terms cancel by the momentum definition. Comparing the coefficients of the independent differentials gives

$$H_p = \dot{q},$$
$$H_q = -L_q.$$

Hamilton's principle previously gave the Lagrange equation $\dot{p} = L_q$, so

$$\dot{q} = \partial_p H,$$
$$\dot{p} = -\partial_q H,$$
$$\partial_t H = -\partial_t L.$$

Along a solution the q and p contributions to dH/dt cancel. For a time-independent Hamiltonian H is constant, so planar trajectories lie on its level sets. In the elementary case $L = m\dot{q}^2/2 - U(q)$, the transformation yields

$$H = p^2/(2m) + U(q).$$

Background · Generalised momentum

$$p_i = \partial L / \partial \dot{q}_i$$

Its units depend on the coordinate. Conjugacy to an angle gives an angular momentum. Conservation requires the associated coordinate to be cyclic in the chosen Lagrangian.

DERIVATION AND APPLICATIONS

How Hamiltonian flow preserves phase-space area

An energy contour shows where a single trajectory may lie. To learn what the dynamics does to nearby initial conditions, follow a small patch of the canonical (q, p) plane. Consider one degree of freedom and a twice continuously differentiable Hamiltonian. Let the system advance by a short time δt. To first order the coordinate map is a displacement along the Hamiltonian velocity field:

$$q' = q + H_p\,\delta t,$$
$$p' = p - H_q\,\delta t.$$

The area of a sufficiently small parallelogram changes by the determinant of this map's derivative. Differentiate with respect to both initial coordinates. The product of off-diagonal elements enters only at second order:

$$\det \frac{\partial(q', p')}{\partial(q, p)} = (1 + H_{pq}\delta t)(1 - H_{qp}\delta t) + H_{pp}H_{qq}\delta t^2 = 1 + O(\delta t^2).$$

For the exact continuous map its area rate is the divergence of the phase velocity. Equality of the mixed second derivatives gives

$$\frac{1}{A}\frac{dA}{dt} = \partial_q \dot{q} + \partial_p \dot{p} = H_{pq} - H_{qp} = 0$$

for an infinitesimal material area A. Integrating adjacent patches gives the same conclusion for a finite region. The outline can stretch and rotate. Even explicit time dependence of H does not change this volume result. A friction force imposed independently of the Hamiltonian can change it. The second-order remainder above belongs to a short expansion; repeatedly taking finite steps with an approximate rule can accumulate a spurious change.

WORKED EXAMPLE

Track a cloud in a harmonic trap

Change the inputs and investigate this derivation.

Prepare a small rectangular set of initial states, 2.00 mm wide in position and 0.0100 kg m/s wide in momentum. Its area is 2.00×10^{-5} J s. In a trap of mass 0.500 kg and frequency $\omega = 4.00$ rad/s, the exact quarter-period map is $q' = p/(m\omega)$, $p' = -m\omega q$. The new widths are 5.00 mm and 0.00400 kg m/s. Their product retains the original area even though neither width is conserved.

SECOND APPLICATION

Diagnose a numerical phase portrait

Change the inputs and investigate this derivation.

An explicit Euler step in the same trap uses $q' = q + p\delta t/m$ and $p' = p - m\omega^2 q\delta t$. Its determinant is exactly $1 + \omega^2\delta t^2$. At $\delta t = 0.0500$ s it expands area by 1.04 per step, giving $1.04^{50} = 7.11$ times the initial area after 50 steps. A graph of the growing cloud could look like physical heating. The determinant exposes a discretization error without requiring an exact trajectory for each point.

Try it · Phase area

Vary the physical parameters in the derived relation. Use the units and assumptions in the readout to connect the curves to the two worked examples. A parameter study can test the forward prediction; the same relation can then be inverted to infer a parameter from a measurement.

Open this live calculation

Try the calculation

Scaled step ωΔt **0.2**

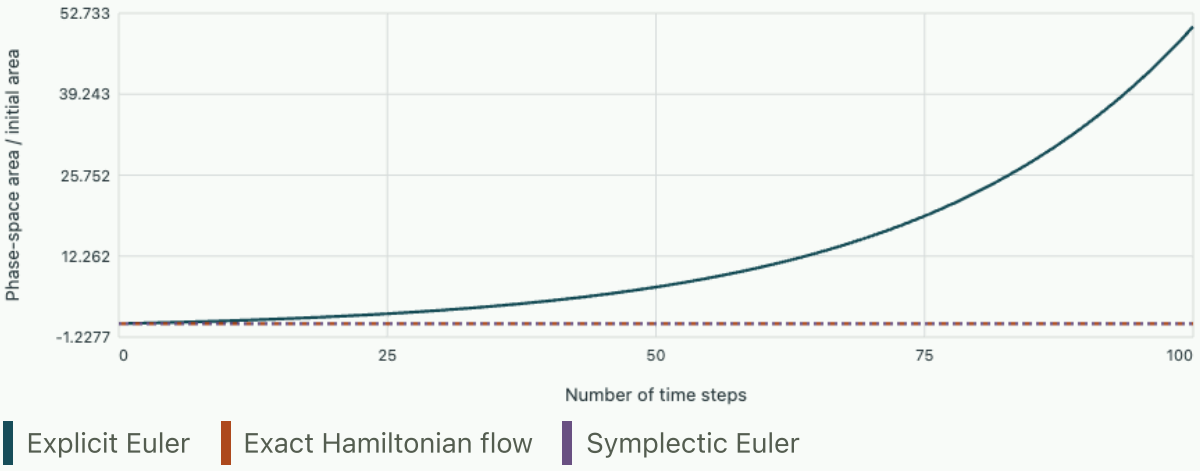

Euler determinant 1+(ωΔt)² = 1.04. A symplectic scheme preserves area but still needs a step-convergence check for phase accuracy.

Position needs a conjugate momentum

The position of a pendulum at one instant does not say which way it will swing. A state needs both a configuration coordinate and a momentum. In Lagrangian mechanics define the canonical momentum by $p = \partial\mathcal{L}/\partial\dot{q}$. It can have different physical dimensions depending on the coordinate. For a particle on a line it has units of linear momentum. For a pendulum angle it has units of angular momentum. The pair (q, p) forms a two-dimensional phase space for one degree of freedom.

Provided the relation between p and $\dot{q}$ can be inverted, define $H(q, p, t) = p\dot{q} - \mathcal{L}(q, \dot{q}, t)$ with the velocity expressed in terms of q, p. Take a differential. The terms proportional to $d\dot{q}$ cancel by the definition of p. Using Lagrange's equation $\partial_q\mathcal{L} = \dot{p}$ gives

$$dH = \dot{q}\,dp - \dot{p}\,dq - \partial_t\mathcal{L}\,dt.$$

Matching the coefficients produces Hamilton's equations

$$\dot{q} = \partial_p H,$$
$$\dot{p} = -\partial_q H.$$

For a system with ordinary quadratic kinetic energy, a velocity-independent potential and fixed constraints, $H = K + U$. Its change along a solution is $dH/dt = \partial_t H$ because the two terms containing the derivatives with respect to q, p cancel. A time-independent Hamiltonian confines the trajectory to a level set.

Use Poisson brackets to test conservation

Hamilton's two equations specify how q_i and p_i change. To follow an observable $A(q, p, t)$, apply the chain rule and substitute $\dot{q}_i = \partial H/\partial p_i$ and $\dot{p}_i = -\partial H/\partial q_i$. This defines the Poisson bracket,

$$\frac{dA}{dt} = \frac{\partial A}{\partial t} + \{A, H\},$$
$$\{A, B\} = \sum_i \left(\frac{\partial A}{\partial q_i}\frac{\partial B}{\partial p_i} - \frac{\partial A}{\partial p_i}\frac{\partial B}{\partial q_i} \right).$$

Since $\{q_i, p_j\} = \delta_{ij}$, a candidate change of phase-space coordinates must preserve these brackets to be canonical. A vanishing bracket with H certifies conservation for an observable having no explicit time dependence. It is a local calculation and does not require solving an orbit.

For a particle in a two-dimensional trap set $H = (p_x^2 + p_y^2)/(2m) + (k_x x^2 + k_y y^2)/2$ and $L_z = x p_y - y p_x$. The momentum derivatives in the bracket cancel the two kinetic contributions. The remaining coordinate terms give $\dot{L}_z = (k_x - k_y) x y$, exactly the torque $x F_y - y F_x$. With $k_x = 4.00$ N/m, $k_y = 6.00$ N/m and instantaneous position $(0.030, 0.040)$ m, angular momentum decreases at 2.40×10^{-3} N m. At a point on either axis the instantaneous derivative vanishes even for the anisotropic trap. For a conservation law holding on every trajectory the expression must vanish throughout phase space, as it does when $k_x = k_y$.

Practise on sheet 3 · Which rescaling preserves Hamilton’s equations?. Further reading · University of Cambridge · David Tong, Classical Dynamics · §4.3 Poisson Brackets.

Draw energy contours before integrating

A rigid pendulum of mass m and length ℓ has $p = m\ell^2\dot{q}$ and $H = p^2/(2m\ell^2) + mg\ell(1 - \cos q)$. At the bottom $q = 0, p = 0$ is a stable equilibrium. Low-energy contours are ellipses to leading order because the cosine potential is quadratic there. Each closed contour returns to its original phase point after one full oscillation. Points of greatest $|p|$ are fastest and occur at the bottom.

The top $q = \pi, p = 0$ has energy $2mg\ell$. Its contour separates swinging trajectories from trajectories that keep rotating in one direction. This separating curve is the separatrix. Since angles differing by 2π label the same physical position, the full portrait lives on a cylinder. A rotation winds around that cylinder. As a

trajectory approaches the separatrix, it spends a long time near the unstable top, so the small-angle period no longer estimates its return time accurately.

Compare thresholds and phase velocities

For $m = 0.50$ kg, $\ell = 0.80$ m and $g = 9.81$ m/s², the potential barrier is 7.85 J. A start from the bottom at 5.0 rad/s supplies kinetic energy $0.5(0.50)(0.80)^2(5.0)^2 = 4.00$ J. At the turning point $\cos q = 1 - 4.00/(0.50 \times 9.81 \times 0.80) = -0.0194$. The maximum angle is about 91.1°. Energy classifies this as a swing even though a small-angle expansion would be inaccurate at the turning point.

Continuous rotation requires bottom speed above $\sqrt{4g/\ell} = 7.00$ rad/s for this ideal pendulum. At precisely that value the system approaches the upper equilibrium asymptotically. This statement assumes a rigid link that can sustain compression. A pendulum made from a flexible string may lose tension before reaching the top, in which case the assumed circular constraint fails.

Check a numerical phase portrait

For any smooth one-degree Hamiltonian the divergence of the phase velocity is

$$\partial_q \dot{q} + \partial_p \dot{p} = H_{pq} - H_{qp} = 0.$$

A small patch of initial states can shear and stretch while preserving its phase-space area. Viscous damping would instead contract the patch. Numerical time integration can also produce apparent contraction or growth, so refining the step is essential before interpreting a spiral as evidence of friction.

For the harmonic oscillator, ordinary forward Euler gives

$$q' = q + \Delta t\, p/m,$$
$$p' = p - \Delta t\, kq.$$

The determinant of this linear update is $1 + \Delta t^2 k/m$, larger than one at every step. The spurious outward spiral follows from the numerical map alone. Updating momentum first and then using the new momentum for the position gives determinant one. That area property preserves the geometric structure, though it does not by itself guarantee accurate phase for a coarse step. Keep both geometry and timing in view when judging numerical trajectories.

The area inside a closed harmonic-oscillator contour provides another numerical test. Its semiaxes are $\sqrt{2E/k}$ in position and $\sqrt{2mE}$ in momentum. Their product times π gives $2\pi E/\omega$. Increasing oscillator energy therefore expands the area in direct proportion. A phase portrait plotted using velocity replaces every momentum value by its value divided by mass, changing numerical areas and their units. Specify the vertical coordinate before comparing this diagnostic between models with different masses.

A slowly changing spring transports a phase-space area

Suppose an oscillator's spring stiffness can be varied externally during the motion. Its Hamiltonian $H = p^2/(2m) + m\omega(t)^2 q^2/2$ now depends explicitly on time, so ordinary energy conservation does not apply. At an instantaneous point on a trajectory Hamilton's equations make the terms involving $\dot{p}$ and $\dot{q}$ cancel in dH/dt. The remaining change is

$$dE/dt = \partial H/\partial t = m\omega\dot{\omega}q^2.$$

Energy is supplied when the imposed parameter raises the potential at the current displacement.

Take $|\dot{\omega}| \ll \omega^2$ so that many cycles occur while the frequency changes by an appreciable fraction. Over one cycle ω and E may then be treated as nearly fixed. Because average potential and kinetic energies of a harmonic oscillator are equal,

$$\langle q^2 \rangle = E/(m\omega^2).$$

Inserting this mean into the work rate gives the averaged relation

$$\frac{dE}{dt} \simeq \frac{E}{\omega}\dot{\omega}, \qquad \frac{d}{dt}\left(\frac{E}{\omega}\right) \simeq 0.$$

The quantity $J = E/\omega$ is the area enclosed by the instantaneous constant-energy ellipse divided by 2π. Calling it an adiabatic invariant states both the approximation and the observable. A slowly changing system migrates between contours of different energies in a way that preserves this action to leading order. This mechanical meaning of adiabatic concerns a timescale ratio. The derivation does not assume heat exchange, dissipation or a thermodynamic temperature.

Compare a slow compression with a sudden change

A 0.500 kg oscillator has initial angular frequency 20.0 rad/s and amplitude 0.0400 m. Its energy is $m\omega_i^2 A_i^2/2 = 0.160$ J and initial action is 0.00800 J s. Raise the frequency smoothly to 40.0 rad/s over many periods. Action conservation predicts $E_f = 0.320$ J and final amplitude $\sqrt{2E_f/(m\omega_f^2)} = 0.0283$ m. The external control supplies work even as the maximum displacement decreases.

For comparison, change the stiffness instantaneously at a turning point, retaining the same initial and final frequencies. Position and momentum are continuous, but the potential energy at that position quadruples immediately. The new energy is 0.640 J and the amplitude remains 0.0400 m. Make the same switch at the zero crossing instead and the energy initially remains 0.160 J because the potential vanishes there. These two outcomes distinguish a rapid change tied to an oscillator phase from the nearly phase-independent slow ramp. Recording both position and velocity after the ramp allows energy, action and phase to be assessed separately.

A time-dependent Hamiltonian still carries each small phase-space area element into one of equal area, even during a sudden change of curvature. This exact conservation for an ensemble is distinct from slow conservation of the contour area assigned to a single orbit. A group of uniformly distributed initial phases

illustrates the difference: immediately after a sudden spring switch all points occupy the same locations and enclose their original region, but their new energies depend on phase. The switch maps the original single-energy contour onto points that subsequently occupy many different energy contours of the new Hamiltonian.

Problem sheet 3 · Moving frames and phase portraits

Apply Lectures 5 and 6 to distinguish real forces, phase-space geometry and numerical drift.

Test the surface of a rotating liquid

A bucket rotates about a vertical axis. At radius 0.15 m the free surface is 12 mm higher than at the centre. Calculate the angular speed, the period and the predicted rise at radius 0.075 m. Specify a condition under which these measurements would no longer fit one parabola.

▼ **Integrate the equilibrium pressure**

Steady rotation gives $\partial_r p = \rho \Omega^2 r$ and vertical hydrostatics gives

$$\partial_z p = -\rho g.$$

Along a constant-pressure free surface these imply $\Delta z = \Omega^2 r^2/(2g)$. Therefore $\Omega = \sqrt{2(9.81)(0.012)}/0.15 = 3.23$ rad/s and the period is 1.94 s. At half radius the rise is one quarter, 3.0 mm. Measurements during spin-up need the transient fluid velocity. Capillary menisci close to the wall can also bias the height used for the fit.

Classify pendulum preparations

A 0.25 kg mass on a rigid 0.60 m link starts at 60° from the downward vertical. Its canonical momentum is initially either 0.12 or 0.25 kg·m²/s. Calculate the energy for each and the positive momentum required for continuous rotation at that starting angle.

▼ **Locate the two phase points**

The inertia is $m\ell^2 = 0.090$ kg·m², potential energy at 60° is $mg\ell/2 = 0.736$ J and the top lies at $2mg\ell = 2.943$ J. Adding $p^2/(2m\ell^2)$ gives 0.816 and 1.083 J. Both states swing; different initial angular momenta need not change the class of motion. At threshold $p = \sqrt{2(0.090)(2.943 - 0.736)} = 0.630$ kg·m²/s. A larger value is needed to pass the top in finite time. Reversing the sign reverses the initial direction while preserving the energy.

Follow a numerical patch of phase space

For $m = 1$ kg and $k = 25$ N/m compare a 0.10 s forward Euler step with an update that first changes momentum using the old position and then changes position using the new momentum. Derive the area factor for each and find the area ratio after ten identical steps.

▼ **Take the determinant of each map**

In the order (q, p) the forward Euler matrix has rows $(1, 0.10)$ and $(-2.50, 1)$ in consistent SI units, so its determinant is 1.25. A patch therefore expands by $1.25^{10} = 9.31$ after ten steps. For the second scheme $p' = p - 2.50q$ and $q' = q + 0.10p' = 0.75q + 0.10p$. Its determinant is $0.75 + 0.25 = 1$ and the area is unchanged. Neither determinant measures phase error. For a timing test, compare the interval between same-direction zero crossings with the analytic period $2\pi/5 = 1.257$ s.

Which rescaling preserves Hamilton's equations?

An oscillator has mass 0.500 kg and spring constant 8.00 N/m. Set $Q = 2q$. Compare $P = 2p$ and $P = p/2$, construct the Hamiltonian in the canonical choice, and calculate the frequency from the transformed equations.

▼ **Evaluate the bracket before transforming the energy**

The brackets are 4 and 1 respectively, so $P = p/2$ is canonical. Then $q = Q/2$, $p = 2P$ and $H = 2P^2/m + kQ^2/8$. Consequently $\dot{Q} = 4P/m$ and $\dot{P} = -kQ/4$, giving $\ddot{Q} = -(k/m)Q$. The physical angular frequency is 4.00 rad/s. Multiplying both coordinates by two would enlarge phase-space area by four and would not preserve the standard bracket.

Revisit chapter 6 · Use Poisson brackets to test conservation.

Explore these relations

- For the numerical phase-space patch, compare the area changes of the update maps. Open the live calculation.
- For the phase-space argument, follow a sheared distribution under Hamiltonian flow. Open the live calculation.

Chapter 7 · Two-body motion and binary masses

Use the motion of both members of a binary to recover the total mass and distinguish the relative orbit from the two individual orbits.

FROM FIRST PRINCIPLES

Reduce two gravitational accelerations to one observed orbit

Consider two point masses that interact only through Newtonian gravity. The measured relative separation vector is $\mathbf{r} = \mathbf{r}_2 - \mathbf{r}_1$ with magnitude r. Newton's gravitational force law is the model input; division by each body's own inertial mass gives opposite accelerations of generally different magnitudes:

$$\ddot{\mathbf{r}}_1 = Gm_2\mathbf{r}/r^3,$$
$$\ddot{\mathbf{r}}_2 = -Gm_1\mathbf{r}/r^3.$$

Subtract these equations to find the relative acceleration and add the mass-weighted equations to establish uniform centre-of-mass motion:

$$\ddot{\mathbf{r}} = -\frac{G(m_1+m_2)}{r^3}\mathbf{r}, \qquad (m_1+m_2)\ddot{\mathbf{R}}_{\mathrm{cm}} = 0.$$

The axial torque about the focus is zero, so $\mathbf{r}\times\dot{\mathbf{r}}$ is constant. For a circular relative orbit of radius a, the inward acceleration has magnitude $a(2\pi/P)^2$. Equality with gravity yields

$$P^2 = \frac{4\pi^2 a^3}{G(m_1+m_2)}.$$

For elliptic motion the same result uses the relative semimajor axis; it follows by combining constant areal speed with the ellipse's area and angular momentum. Observing only one component's orbit gives its distance from the centre of mass, which is generally smaller than the required relative orbit.

Background · Reduced mass

$$\mu = m_1m_2/(m_1+m_2)$$

The relative coordinate of an isolated two-body system carries this inertia. The centre-of-mass motion remains a separate degree of freedom.

DERIVATION AND APPLICATIONS

Convert an orbital position into a clock reading

The conic equation tells us where the companion can be seen, but not when it passes a particular position. Work in the relative orbit of an isolated Newtonian binary. Let a denote its semimajor axis, $e < 1$ its eccentricity, and $b = a\sqrt{1 - e^2}$ its semiminor axis. Fix the origin at the occupied focus and the positive x axis toward pericentre. Parametrize the ellipse by eccentric anomaly u using a circle stretched along one axis:

$$x = a(\cos u - e),$$
$$y = b \sin u,$$
$$r = a(1 - e \cos u).$$

The parameter u is measured on the auxiliary circle; it usually differs from the observed direction $\operatorname{atan2}(y, x)$. A short sector about the focus has oriented area $(x\,dy - y\,dx)/2$. Differentiating the parametrization gives the area swept since pericentre:

$$dA = \tfrac{1}{2} ab(1 - e \cos u)\, du,$$
$$A(u) = \tfrac{1}{2} ab(u - e \sin u).$$

The central gravitational force produces zero torque, so area is swept at a constant rate. A full period P sweeps the entire ellipse πab. The fraction of a period elapsed since pericentre is therefore $A(u)/(\pi ab)$:

$$\frac{2\pi(t - t_p)}{P} = u - e \sin u.$$

This is Kepler's equation, where t_p is the time of pericentre. Its derivative with respect to u is $1 - e \cos u > 0$, so there is a unique position within one revolution for every time. The circular limit $e = 0$ makes anomaly grow uniformly; the distinction between an auxiliary-circle angle and the observed bearing then disappears.

WORKED EXAMPLE

Time the crossing of the semiminor-axis endpoint

Change the inputs and investigate this derivation.

Take a visual binary with $P = 8.00$ yr and $e = 0.600$. At the upper endpoint of the minor axis, $u = \pi/2$, and $t - t_p = 8(\pi/2 - 0.600)/(2\pi) = 1.24$ yr. Exactly one quarter of the geometric parameter range has passed, but the time is considerably shorter than two years. Relative to the focus this endpoint has coordinates $(-0.600a, 0.800a)$ and distance a.

SECOND APPLICATION

Recover an orbital eccentricity from timed astrometry

Change the inputs and investigate this derivation.

A second binary reaches the same geometric point 2.10 yr after pericentre in a 10.0 yr orbit. Using $u = \pi/2$ gives

$$e = \pi/2 - 2\pi(2.10/10.0) = 0.251.$$

The implied ratio of apocentre distance to pericentre distance is

$$(1 + e)/(1 - e) = 1.67.$$

A resolved relative orbit with that ratio gives an independent geometric test of the timing determination.

Try it · Kepler timing

Vary the physical parameters in the derived relation. Use the units and assumptions in the readout to connect the curves to the two worked examples. A parameter study can test the forward prediction; the same relation can then be inverted to infer a parameter from a measurement.

Open this live calculation

Try the calculation

Orbital eccentricity **0.6**

Orbital period (years) **8**

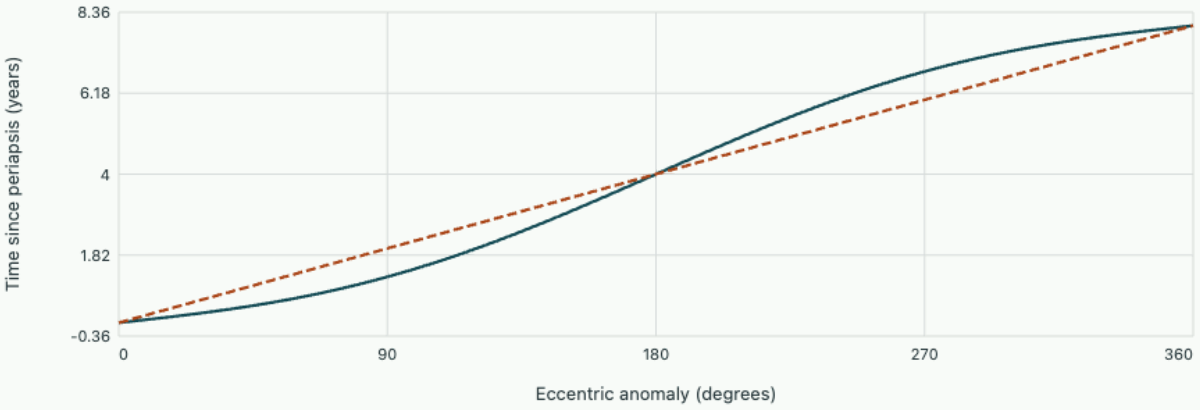

Kepler clock Uniform geometric parameter

At the upper semiminor-axis endpoint: 1.2361 years. Geometry and elapsed time are related by M=E−e sin E.

Start from this chapter. Use the sum of the masses in Kepler's period law. The supplied Earth orbit is the small-secondary-mass limit. Compare its predicted period with upward crossings of the computed trajectory.

OneSimulation laboratory · Measure a period from an orbit

When the moving centre of light hides a binary orbit

A telescope can detect motion without resolving the two stars separately. The reported position is then the centre of their light, whereas Newton's laws evolve the centre of their mass. The difference changes both the inferred scale and the interpretation of a missing astrometric signal.

Derive the observable before fitting a gravitational orbit

Let $\mathbf{r} = \mathbf{r}_2 - \mathbf{r}_1$ be the companion's position relative to the primary and let $B = M_2/(M_1 + M_2)$. In the centre-of-mass frame the condition $M_1\mathbf{r}_1 + M_2\mathbf{r}_2 = 0$ gives

$$\mathbf{r}_1 = -B\mathbf{r},$$

$$\mathbf{r}_2 = (1 - B)\mathbf{r}.$$

For a linear detector and overlapping symmetric images, their combined intensity centroid is the flux-weighted mean. Denoting by $\beta = L_2/(L_1 + L_2)$ the fraction of light in the instrument's particular wavelength band, substitute the two barycentric positions to obtain

$$\mathbf{r}_{\text{light}} = (1 - \beta)\mathbf{r}_1 + \beta\mathbf{r}_2 = (\beta - B)\mathbf{r}.$$

For a circular relative orbit of radius a viewed at inclination i, choose the line of nodes as the sky x axis. Projection makes the apparent relative coordinates proportional to $(\cos\theta, \cos i \sin\theta)$. Its major semiaxis stays a; its minor semiaxis becomes $a|\cos i|$. An unresolved instrument measures the same ellipse scaled by $|\beta - B|$. Its apparent angular major semiaxis in milliarcseconds is $1000|\beta - B|a_{\text{AU}}/D_{\text{pc}}$. A sign change makes the observed motion shift by half a cycle relative to a phase reference.

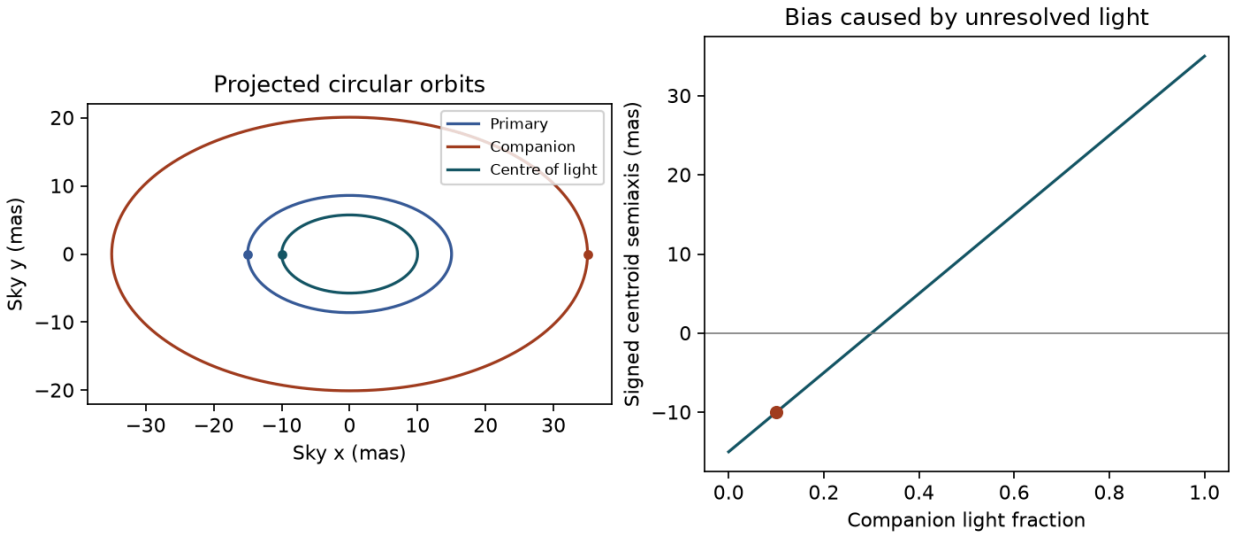

The dots mark one common orbital phase. At equal mass and light fractions the photocentre stays at the origin even though both stars move.

Try it · Photocentre

Change the inputs and compare the recalculated curves with the preceding derivation and baseline figure. The axes give the units; the numerical readout states the model assumptions and any limiting cases. Reset the inputs to return to the reference setting.

Open this live calculation

Try the calculation

Companion mass fraction	0.4
Companion light fraction	0.2
Orbit inclination (degrees)	60

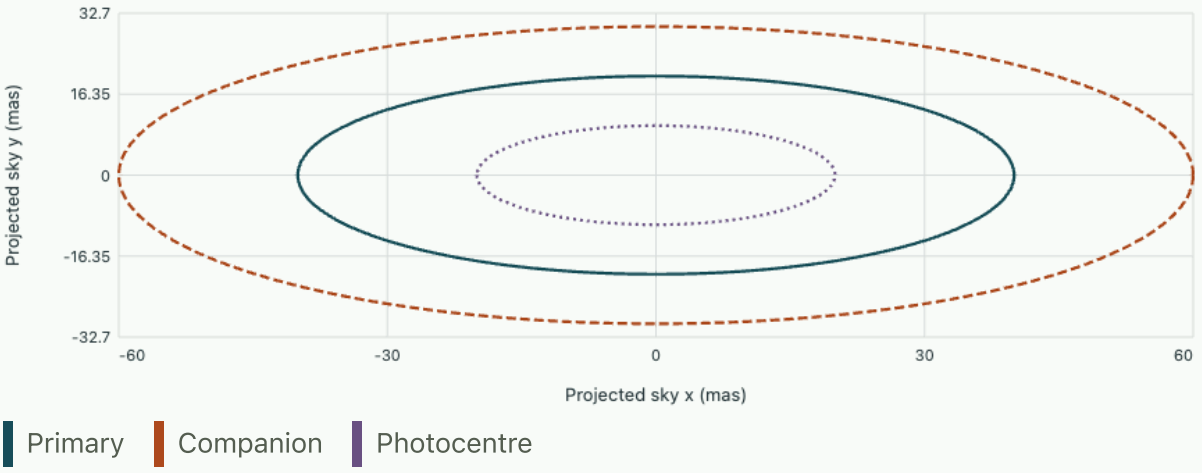

A 1 au relative orbit at 10 pc spans 100 mas. Photocentre semimajor axis 20 mas; it vanishes when mass and light fractions agree.

Download the corresponding editable notebook. The browser recalculates the reduced equations directly; the notebook exposes the full calculation and its checks.

Take $a = 1$ AU and distance 20 pc. A resolved relative orbit would span 50 mas in semimajor axis. If the companion carries 30 per cent of the mass but only 10 per cent of the light, the measured centroid semiaxis is 10 mas. The primary alone would instead travel with a 15 mas semimajor axis. Treating the centroid as the primary underestimates its displacement in this observation. If $\beta = B$, the centroid remains at the barycentre for every orbital phase. Better positional precision alone cannot recover an orbit from that observable in the ideal model.

Try changing the light fraction in the notebook while keeping the masses fixed. A hotter companion may contribute a larger fraction in a bluer band, changing the inferred orbit from one filter to another without changing any gravitational force. A variable or eclipsed light source makes β time dependent; the centroid no longer traces a simple uniformly scaled Kepler orbit. Changes of brightness and orbital acceleration then need to be fitted together.

Two filters measure centroid semiaxes of 10 and 5 mas for the same 1 AU, 20 pc binary. If the second filter has $\beta = 0.20$, can its astrometry alone fix the companion mass fraction?

▼ **Work through the solution**

The second amplitude fixes $|0.20 - B| = 5/50 = 0.10$, giving $B = 0.10$ or 0.30. Its unsigned amplitude loses the sign of the orbital phase. With the first filter's known $\beta = 0.10$ and nonzero 10 mas amplitude only $B = 0.30$ survives. A signed velocity or resolved orbital phase could also discriminate between the two branches.

Open editable notebook Download .ipynb

Recover both turning radii from a single position and velocity

Choose length and time units so that the measured initial separation and the gravitational parameter are both one. Resolve the measured velocity into its radial component v_r and its tangential component v_t. The specific angular momentum is $h = v_t$, and specific energy is

$$E = (v_r^2 + v_t^2)/2 - 1.$$

Working in the plane with the initial separation along $+x$, the eccentricity vector is $(h^2 - 1, -hv_r)$ and has magnitude e. Its direction is the direction of closest approach. The entire ellipse follows from $r(\phi) = h^2/[1 + e_x \cos\phi + e_y \sin\phi]$.

Open this experiment online

Try the calculation

Initial radial velocity **0.1**

Initial tangential velocity **0.9**

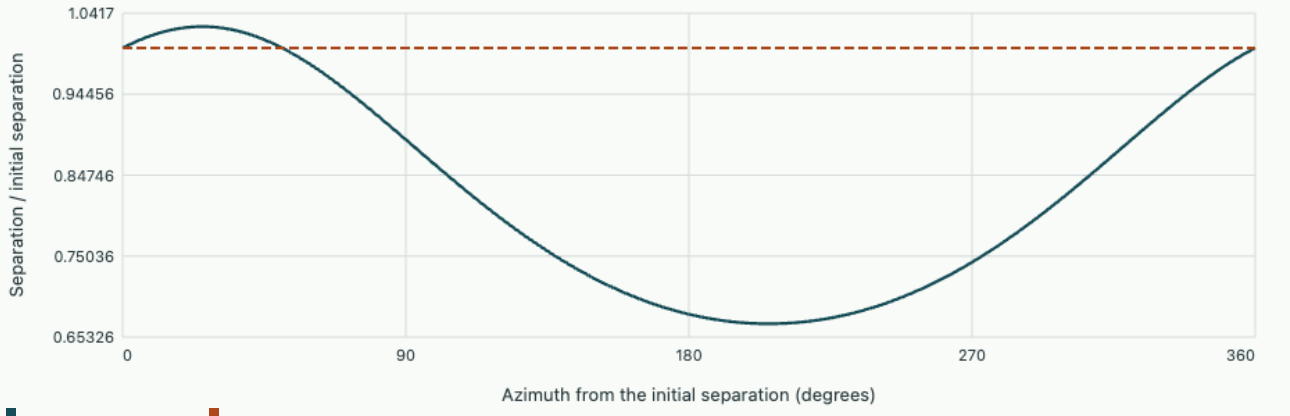

Eccentricity 0.21024. Closest approach 0.66929; largest separation 1.0256.

Try $v_t = 1,\ v_r = 0$, then change only the radial velocity. The first case is a circle with no distinct pericentre direction. Reversing the radial velocity in the second case reflects the direction of the apses but leaves their radii unchanged. Confirm both turning radii independently by setting radial velocity to zero in the energy equation.

Remove the motion of the whole system

Two stars pull on each other. Fixing one star at the origin would be a poor approximation for comparable masses, but the central-force calculation can still be made exact within Newtonian gravity. Take masses m_1, m_2, inertial positions $\mathbf{r}_1, \mathbf{r}_2$ and relative vector $\mathbf{r} = \mathbf{r}_2 - \mathbf{r}_1$. Assume spherical bodies or sufficiently large separation that departures from point-mass gravity can be neglected. Internal forces cancel when the equations of motion are added. With no external forces, the centre of mass moves uniformly.

Subtract the two accelerations instead. The relative coordinate obeys $\ddot{\mathbf{r}} = -G(m_1 + m_2)\mathbf{r}/r^3$. The familiar one-centre orbit therefore applies to the separation vector if the gravitational parameter uses the total mass. In the centre-of-mass frame the individual positions are $\mathbf{r}_1 = -(m_2/M)\mathbf{r}$ and $\mathbf{r}_2 = (m_1/M)\mathbf{r}$, with $M = m_1 + m_2$. The bodies reach closest approach together while each describes its own scaled ellipse. Confusing either individual semimajor axis with the relative semimajor axis changes the mass inferred from timing.

Account for the relative energy

Write each velocity in terms of the centre-of-mass velocity and $\dot{\mathbf{r}}$. Their kinetic energies separate into $MV^2/2 + \mu_r|\dot{\mathbf{r}}|^2/2$, where $\mu_r = m_1 m_2/M$ and the squared speed is the full squared relative velocity. The interaction energy is $-Gm_1m_2/r$. Dividing the relative energy by μ_r recovers the specific potential $-GM/r$. For a bound relative ellipse, its semimajor axis a fixes the relative orbital energy at $-Gm_1m_2/(2a)$. The energy of the centre of mass can be changed by a uniform frame change without changing any internal separation or phase.

A complete relative orbit sweeps area $\pi a^2\sqrt{1-e^2}$. With constant areal rate and the inverse-square conic relation this gives

$$P^2 = 4\pi^2 a^3/(GM).$$

Two independent measurements, physical semimajor axis and period, determine the sum of the masses. A third measurement, such as the two individual orbit sizes or speeds in the centre-of-mass frame, determines their ratio.

Read a visual binary

Suppose the relative orbit is circular with radius 2.00 astronomical units and period 2.00 years. In units where a one-year circular orbit at one astronomical unit corresponds approximately to one solar mass, the total mass is $2^3/2^2 = 2.00$ solar masses. If the more massive component moves on a circle of radius

0.50 astronomical units, the other radius is 1.50 astronomical units. The mass ratio is inverse to the radii, so the components have masses 1.50 and 0.50 solar masses.

A telescope measures an angular separation on the sky; obtaining lengths requires a distance and an orbital inclination model. In a spectroscopic binary each Doppler amplitude measures a projected speed, so their ratio can reveal the mass ratio even before the inclination is known. An independent inclination is needed to turn those projected speeds into absolute masses. This illustrates why a clean period estimate can coexist with a substantial mass uncertainty. For a nearly negligible secondary mass the same relative equation underlies the orbit experiment.

Derive the shape from angular momentum and the force

The period–mass law uses a bound orbit's overall dimensions. A central-force observation can also recover the shape locally. In the relative two-body problem write $h = r^2\dot{\theta}$ for the specific angular momentum and $\mu_g = G(m_1 + m_2)$. The radial equation is

$$\ddot{r} - r\dot{\theta}^2 = -\mu_g / r^2.$$

Introduce the reciprocal radius $u = 1/r$ and differentiate with respect to the polar angle instead of time. Because $\dot{\theta} = hu^2$, the radial velocity becomes

$$\dot{r} = -h\, du/d\theta.$$

Differentiating once more gives

$$\ddot{r} = -h^2 u^2 d^2u/d\theta^2.$$

The geometric acceleration term is $r\dot{\theta}^2 = h^2u^3$. Combining the terms leaves a linear equation despite the nonlinear time evolution,

$$\frac{d^2u}{d\theta^2} + u = \frac{\mu_g}{h^2},$$

$$r = \frac{p}{1 + e\cos(\theta - \theta_p)},$$

$$p = \frac{h^2}{\mu_g}.$$

Two integration constants determine the eccentricity and the direction of closest approach. Choose that direction as zero angle. In a bound ellipse the minimum and maximum radii are $r_p = p/(1+e)$ and $r_a = p/(1-e)$. Solving these two geometric equations gives

$$e = (r_a - r_p)/(r_a + r_p),$$

$$p = 2r_a r_p/(r_a + r_p).$$

Their arithmetic mean is the semimajor axis. This construction separates what can be inferred from images alone from what requires a gravitational mass or a time measurement.

Reconstruct speed away from either turning point

Suppose a resolved relative orbit has nearest separation 2.00 AU and farthest 6.00 AU. Use an independently known $\mu_g = 4\pi^2$ AU³/yr². The semimajor axis is 4.00 AU, eccentricity 0.500 and semilatus rectum 3.00 AU. Specific angular momentum is $\sqrt{\mu_g p} = 10.88$ AU²/yr, so at right angles to periapsis the separation is 3.00 AU and transverse velocity is $h/r = 3.63$ AU/yr.

The orbit is still moving outward there. Differentiating the reciprocal-radius solution gives $\dot{r} = (\mu_g/h)e\sin\theta = 1.81$ AU/yr. Its total relative speed is $\sqrt{3.63^2 + 1.81^2} = 4.06$ AU/yr, about 19.2 km/s. Independently the energy relation predicts $v^2 = \mu_g(2/r - 1/a) = 16.45$ AU²/yr², consistent to rounding. An image sequence can test the transverse speed and the outward sign separately. If the two measured turning radii coincide the eccentricity vanishes, the reconstructed radial velocity is zero at every angle and the orientation θ_p becomes unobservable. Nearly circular orbit fits therefore determine a radius more reliably than a direction of periapsis.

The time information missing from a still image can be recovered by integrating the areal law. An area element swept from the focus is $dA = r^2 d\theta/2$; its rate is therefore $h/2$. The total ellipse area is $\pi a b$, with semiminor axis $b = a\sqrt{1-e^2}$. For the reconstructed orbit $b = 3.46$ AU and the swept area is 43.5 AU² each revolution. Dividing by $h/2 = 5.44$ AU²/yr yields a period of 8.00 years, independently matching the orbital-period relation from the semimajor axis. Equal angle intervals around the orbit generally correspond to very unequal time intervals because swept areas also depend on separation.

If only projected separations on the sky are available, this reconstruction needs an inclination or a full orbital fit first. Projecting an inclined ellipse does not in general preserve its true periapsis and apoapsis distances from the focus.

Where does an eccentric binary spend its time?

Observe binaries with the same semimajor axis and total mass at uniformly spaced times. The area law gives

$$dt/d\nu = r^2/h.$$

Divide by $T/(2\pi)$ so the average over one revolution is one for every curve.

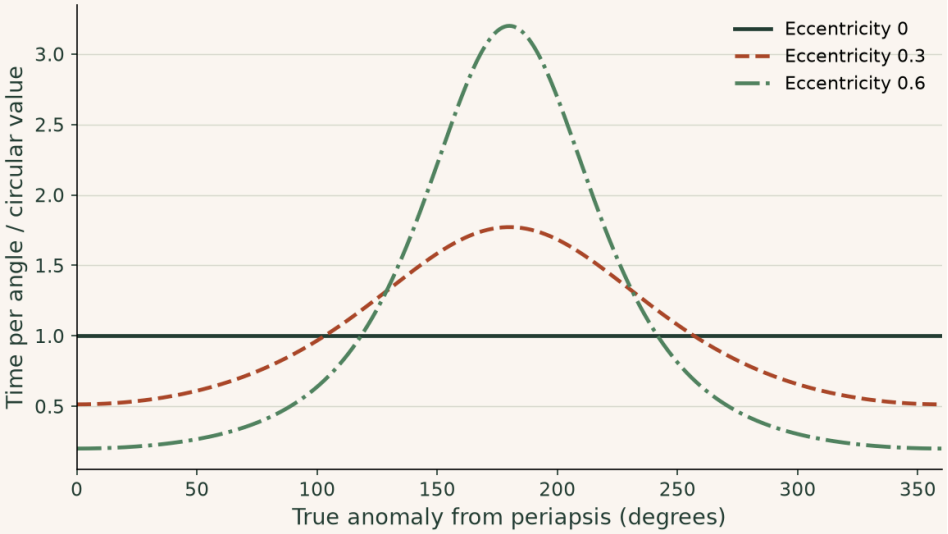

At eccentricity 0.6 the density of observations per degree is sixteen times larger at apoapsis than at periapsis. A histogram heavily weighted toward one end of an ellipse can therefore be consistent with a constant observation cadence.

Try it · Orbital dwell

Change the inputs and compare the recalculated curves with the preceding derivation and baseline figure. The axes give the units; the numerical readout states the model assumptions and any limiting cases. Reset the inputs to return to the reference setting.

Open this live calculation

Try the calculation

Orbital eccentricity **0.6**

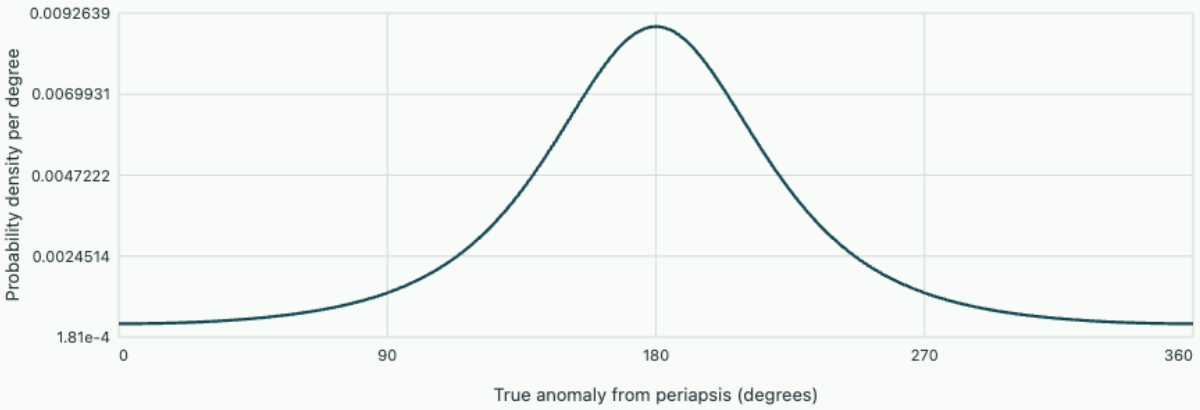

Uniform sampling in time

Apoapsis/periapsis sampling-density ratio 16. A time histogram is not uniform in orbital angle.

▶ **Read values from the plot**

Study the full derivation

Kepler orbits, the eccentricity vector and the loss of apsidal closure · Analytical mechanics from constraints to invariants

An orbit can conserve energy and angular momentum yet gradually rotate its periapsis. The inverse-square problem possesses one more conserved vector that fixes the direction of closest approach. Derive it, turn a single position and velocity measurement into a conic, and measure what a weak perturbation does to the inferred apsidal direction.

Chapter 8 · Impact parameters and scattering cross-sections

Use flux conservation to turn a classical deflection law into an angular distribution observed by a detector.

FROM FIRST PRINCIPLES

Turn an incident annulus into a measured angular distribution

Assume a uniform incident number flux $\mathcal{F}$ on one central scatterer. The trajectories vary only by azimuth and by their initial perpendicular offset b. A ring of incoming impact parameters between b and $b + db$ has area $2\pi b\,db$. Thus the number of events entering that interval per time is

$$d\dot{N} = \mathcal{F}\,2\pi b\,|db|.$$

For an axisymmetric interaction the corresponding polar exit angles θ to $\theta + d\theta$ fill an angular band of solid angle $d\Omega = 2\pi \sin\theta\,|d\theta|$. Equate the rate from the entrance to the rate reported by a detector normalized to flux and solid angle:

$$\mathcal{F}\,\frac{d\sigma}{d\Omega}2\pi\sin\theta\,|d\theta| = \mathcal{F}\,2\pi b\,|db|,$$

$$\frac{d\sigma}{d\Omega} = \frac{b}{\sin\theta}\left|\frac{db}{d\theta}\right|.$$

This is a change of variables based on flux conservation, not a force law. The actual interaction supplies $b(\theta)$. If multiple impact parameters map into one angular band, add their positive contributions. A finite detector averages this distribution over its acceptance, which matters near a sharp angular feature.

Background · Differential cross-section

$$d\sigma/d\Omega = (b/\sin\theta)|db/d\theta|$$

For an axially symmetric single-valued scattering branch this converts incoming area to outgoing solid angle. Sum contributions if more than one impact parameter gives the same angle.

DERIVATION AND APPLICATIONS

Which scattering cross section measures a loss of directed momentum?

A detector counting encounters adds one event in every accepted direction. A force measurement weights the same encounters according to how much directed momentum each removes. Consider a dilute parallel stream of identical particles of speed v and mass m scattered elastically by isolated,

stationary, much heavier centres. The incoming direction defines z. The outgoing speed is unchanged, and assume axial symmetry so that transverse recoils cancel in the ensemble. Let $\mathcal{F}$ be the incident number per area per time.

The outgoing momentum projection is $mv\cos\theta$ for deflection angle θ. Multiply the lost projection by the differential encounter rate in the detector's solid angle:

$$\Delta p_z = mv(1-\cos\theta),$$
$$d\dot{N} = \mathcal{F}\,\frac{d\sigma}{d\Omega}\,d\Omega.$$

Summing over all azimuths, with $d\Omega = 2\pi\sin\theta\,d\theta$, defines the momentum-transfer cross section σ_{tr} and the longitudinal force on one centre:

$$F_z = \mathcal{F}\,mv\,\sigma_{\mathrm{tr}},$$
$$\sigma_{\mathrm{tr}} = \int (1-\cos\theta)\,\frac{d\sigma}{d\Omega}\,d\Omega.$$

For a smooth monotone deflection function $\theta(b)$, the annular area of incident trajectories is $2\pi b\,db$. Changing variables back to impact parameter b shows exactly which trajectories contribute:

$$\sigma_{\mathrm{tr}} = 2\pi\int b\,[1-\cos\theta(b)]\,db.$$

Use the sum of all annuli if the same angle is reached from several impact parameters. Forward scattering transfers almost no longitudinal momentum. Exact backscattering transfers twice the incident longitudinal momentum, even though it still counts as a single encounter.

WORKED EXAMPLE

Compute the momentum flux for elastic spheres

Change the inputs and investigate this derivation.

For a hard sphere of effective contact radius R, specular reflection gives $\cos\theta = 2(b/R)^2 - 1$ for $0 \le b \le R$. The integral is

$$4\pi\int_0^R [b - b^3/R^2]db = \pi R^2.$$

For $R = 1.00$ mm, $\mathcal{F} = 2.00\times10^{7}$ m⁻²s⁻¹, $m = 1.00\times10^{-9}$ kg and $v = 2.00$ m/s, the encounter rate is 62.8 s⁻¹ and the mean force is 1.26×10^{-7} N.

SECOND APPLICATION

Compare two angular distributions with identical event counts

Change the inputs and investigate this derivation.

Suppose an angular histogram is fitted by $d\sigma/d\Omega = C(1 + \alpha \cos\theta)$, with $|\alpha| \leq 1$. Its integrated count is $4\pi C$ for every α. Averaging the momentum factor uses $\langle \cos^2\theta \rangle = 1/3$ on a sphere, giving $\sigma_{\mathrm{tr}} = 4\pi C(1 - \alpha/3)$. For $\alpha = 0.900$, the same count produces only 0.700 of the force for an isotropic distribution. An encounter count alone cannot determine a transport coefficient.

Try it · Momentum cross section

Vary the physical parameters in the derived relation. Use the units and assumptions in the readout to connect the curves to the two worked examples. A parameter study can test the forward prediction; the same relation can then be inverted to infer a parameter from a measurement.

Open this live calculation

Try the calculation

Angular asymmetry α **0.6**

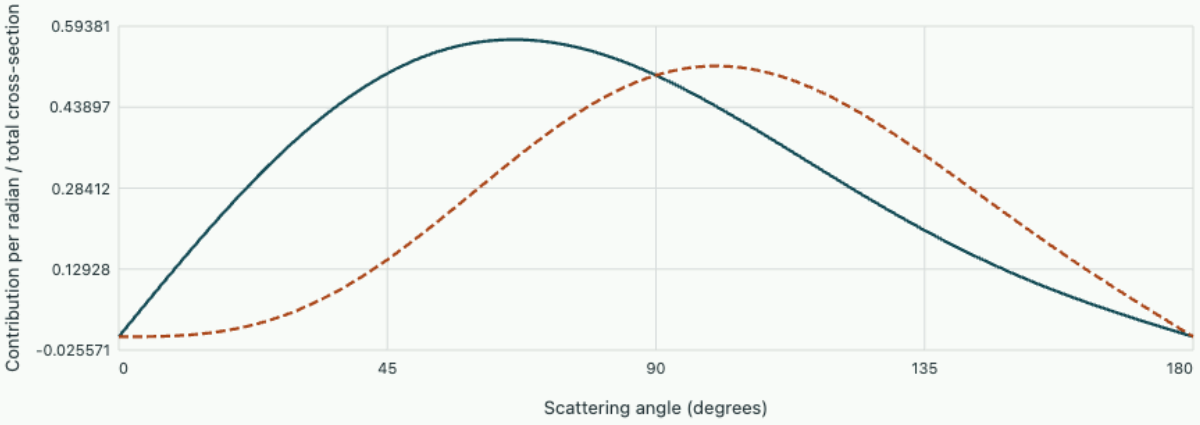

Transport / total cross-section = 1−α/3 = 0.8. Equal event counts can transfer unequal momentum.

What does a detector with equal angular bins count?

A stream of dilute neutral beads meets a much heavier fixed hard sphere with effective contact radius R. For specular elastic reflection the impact parameter and polar deflection angle satisfy

$$b = R\cos(\theta/2).$$

The incoming annulus has area $2\pi b\,|db|$, while an outgoing ring subtends $2\pi \sin\theta\, d\theta$. Dividing gives the constant differential cross-section $R^2/4$ per steradian. A detector with equal polar-angle bins sees a changing count because those bins have unequal solid angle.

Open this experiment online

Try the calculation

Polar detector bins 8

Effective radius (cm) 1

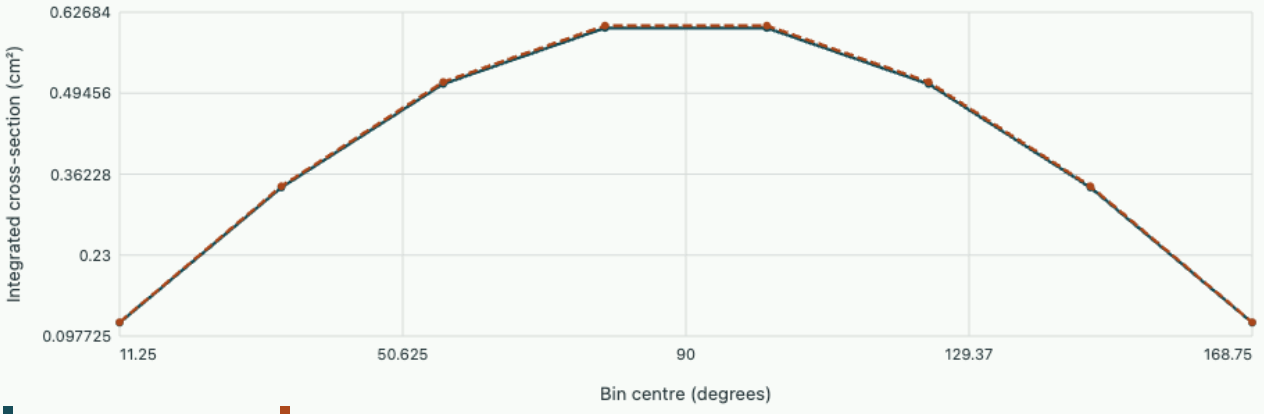

Exact sum 3.1416 cm². Midpoint sum 3.1619 cm². Differential cross-section 0.25 cm²/sr.

Predict which ring receives the largest incoming area. Sum the exact bin cross-sections and compare with πR^2. The second curve uses the midpoint approximation to each bin's solid angle. Narrow the bins and test how that approximation approaches the same total. A plot that makes all counts equal in equal polar-angle bins would not represent isotropic scattering per steradian.

Specify an ensemble of trajectories

A beam of dilute particles approaches a stationary scattering centre. Particles enter parallel to one another with the same speed, but at different perpendicular offsets from the centre. This offset b, measured on the incoming asymptotic straight line, is the impact parameter. For a central potential each trajectory remains in one plane; axial symmetry makes its polar deflection angle depend on b rather than on the azimuth of the initial offset. Neglect collisions between incoming particles and assume a sufficiently heavy centre that recoil can be ignored.

The cross-section has dimensions of area. It quantifies how a known incident flux becomes counts in a detector. If an incoming beam supplies j particles per unit area per second, an annulus of impact parameters from b to $b + db$ contributes $j\,2\pi b\,db$ particles per second to the corresponding outgoing angles. A large response can arise either from a large interval of impact parameters or from trajectories compressed into a narrow angular interval.

Derive the transformation to detector angles

For a single monotonic deflection branch, a ring of outgoing directions between θ and $\theta + d\theta$ subtends $d\Omega = 2\pi \sin\theta \, d\theta$. Equating the incoming count and the outgoing count yields

$$\frac{d\sigma}{d\Omega} = \frac{b}{\sin\theta} \left| \frac{db}{d\theta} \right|.$$

The absolute value matters because stronger deflections often correspond to smaller impact parameters. If several distinct impact parameters produce the same angle, their contributions must be added. Multiplying by a detector's solid angle is justified when its angular aperture is small enough that the differential cross-section is nearly constant across it.

Test the construction on a hard sphere

Take an impenetrable smooth sphere of radius R that reflects incident point particles elastically. At a surface hit the normal component of velocity reverses while the tangential component stays fixed. A central hit returns straight back and a grazing hit barely deflects. The geometry of the contact normal gives

$$b = R\cos(\theta/2).$$

Differentiation and $\sin\theta = 2\sin(\theta/2)\cos(\theta/2)$ give

$$d\sigma/d\Omega = R^2/4.$$

Integrating over all 4π steradians recovers πR^2, the area presented to the incoming parallel beam.

Although the angular density is isotropic in this classical example, the trajectories are deterministic. Isotropy results from the area-to-angle map. A detector covering a fixed span of polar angle but all azimuths receives different counts near the pole and near the equator because its solid angle changes.

Calculate detector counts

Let $R = 2.0$ mm, $j = 1.0 \times 10^{9}$ m⁻²s⁻¹ and a small detector subtend 0.020 sr in a clear outgoing direction. The differential cross-section is 1.0×10^{-6} m²/sr. The expected rate is $j(d\sigma/d\Omega)\Delta\Omega = 20$ s⁻¹. Integrating over angles beyond 90° gives half the total count, or $j\pi R^2/2 = 6.28 \times 10^{3}$ s⁻¹. Only incoming offsets below $R/\sqrt{2}$ enter this backward hemisphere.

Soft interactions can produce very different distributions. In particular, a force reaching far outside any material body can scatter particles arriving at offsets larger than the body radius. The hard-sphere area no longer supplies a universal total cross-section. Detector acceptance and the minimum observable angle then become part of the measurement definition.

Attraction enlarges the area that meets a body

An astronomical body can collect small incoming particles from a larger area than its apparent disk. Consider a stationary spherical body of mass M and radius R with vacuum outside. Small particles arrive from far away with common speed v_∞ and an approximately uniform distribution across their beam. Assume negligible particle mass, no drag, no interactions among particles and an absorbing surface. Gravity changes which incident trajectories reach the surface while conserving each particle's energy and angular momentum until its first contact.

At infinity the specific angular momentum is $h = bv_\infty$ for impact parameter b. The trajectory that just grazes the surface is tangent there, so $h = Rv_p$, where v_p is its speed at closest approach. Energy conservation between infinity and the grazing point gives

$$v_p^2 = v_\infty^2 + 2GM/R.$$

Eliminating v_p supplies the critical impact parameter and capture cross section

$$b_{\max}^2 = R^2\left(1 + \frac{v_{\mathrm{esc}}^2}{v_\infty^2}\right),$$

$$\sigma_{\mathrm{hit}} = \pi b_{\max}^2,$$

$$v_{\mathrm{esc}} = \sqrt{2GM/R}.$$

The incident area element is measured in the undisturbed beam at infinity. Particles with $b < R$ obviously hit; some initially farther from the centre do as well. Very fast particles hardly change direction before passing the body, giving the geometric area in that limit. Very slow incident particles experience strong focusing, and the idealized cross section grows as v_∞^{-2}. For extremely small speeds the assumed uniform, isolated far-field beam can cease to be physically meaningful because other gravitating masses perturb it.

Compare two incoming populations

A spherical minor body has radius $R = 100$ km and escape speed $v_{\mathrm{esc}} = 100$ m/s. Its implied gravitational parameter is $GM = v_{\mathrm{esc}}^2 R/2 = 5.00 \times 10^8$ m³/s². A population approaching at 50.0 m/s has $b_{\max} = R\sqrt{1+4} = 224$ km. The collection area is 1.57×10^{11} m², five times the projected solid disk. The speed at grazing contact is $\sqrt{50^2 + 100^2} = 112$ m/s, and the angular momenta on the two sides agree.

For a second population at 200 m/s the enhancement is only 1.25, giving 3.93×10^{10} m². At equal incident particle flux per square metre the slower population therefore supplies four times as many impacts. At equal far-field number density, however, flux itself is proportional to speed: multiplying each cross section by its own speed makes the two collection rates equal for these particular values. This distinction matters when comparing an instrument that measures incident counts per unit area with a model that reports only a space density.

This collection calculation can be recast as a minimum-angle criterion in a numerical trajectory experiment. Launch particles far upstream at specified offsets and find which trajectories reach the radius of the body before turning away. To estimate a cross section with equally weighted trajectories, sample radius with cumulative probability proportional to its square. Uniform sampling of the impact parameter instead overrepresents rays near the axis. If that sampling is used, weight each ray by the area of its annulus. Convergence of the measured grazing offset and convergence of the weighted hit fraction test distinct aspects of the calculation.

Study the full derivation

Scattering from a central potential and what angular data can recover · Analytical mechanics from constraints to invariants

A detector records angles, whereas the force law refers to separations that were never directly observed. Derive the forward map from incoming impact parameter to angle, distinguish the several trajectories a detector may count in one angular bin, and invert sufficiently complete signed deflection data under stated hypotheses.

Problem sheet 4 · Orbits and scattering data

Infer a binary mass, reconstruct a shielding cross section, and translate between impact parameters and detector counts.

An unresolved binary

Spectroscopy and an eclipsing geometry give circular orbital speeds of 40 and 60 km/s. The period is 20.0 days. Find the separation, total mass and individual masses. What goes wrong for an unknown inclination? Use $G = 6.674 \times 10^{-11}$ SI and $M_\odot = 1.989 \times 10^{30}$ kg.

▼ **Show the orbital reconstruction**

In the centre-of-mass frame the bodies are on opposite sides, so their relative speed is 100 km/s. One relative circular path in 1.728×10^{6} s gives

$$a = v_{\mathrm{rel}} P/(2\pi) = 2.75 \times 10^{10}\,\mathrm{m}.$$

Centripetal acceleration requires $GM/a^2 = v_{\mathrm{rel}}^2/a$ and gives $M = 4.12 \times 10^{30}$ kg or $2.07 M_\odot$. Centre-of-mass momentum balance gives

$$m_{40}/m_{60} = 60/40.$$

The masses are $1.24 M_\odot$ and $0.83 M_\odot$. Spectroscopic velocities alone measure $v \sin i$ for inclination i from face-on. The mass inferred this way would be $M \sin^3 i$.

A shadow in a beam

A collimated beam crosses a dilute slab with 2.0×10^{17} scatterers per square metre of projected area. Its undeflected fraction is 0.960. Determine the scattering cross section and the equivalent hard-sphere radius for point incident particles. Predict transmission for twice the slab thickness.

▼ **Show the attenuation calculation**

For independent scatterers the fractional loss from the original beam in a small areal-density interval is

$$dI/I = -\sigma\, dN_A.$$

Hence

$$\sigma = -\ln(0.960)/N_A = 2.04 \times 10^{-19}\,\mathrm{m}^2.$$

For a hard sphere the intercepted area is πR^2, giving $R = 2.55 \times 10^{-10}$ m. Doubling thickness multiplies survival probabilities, giving $0.960^2 = 0.9216$. A finite detector aperture accepting slightly scattered particles would make the measured loss smaller and bias this estimate downward.

Which impacts populate a detector ring?

For repulsive inverse-square scattering write $b = C\cot(\theta/2)$ with $C = 0.50$ nm. Find the impact-parameter interval and cross section for scattering into all azimuths between 60° and 120°. Compare the result when incident speed doubles at fixed interaction strength.

▼ **Show the annular area**

The smaller deflection comes from the larger impact parameter. The radii are

$$0.50\cot 60^\circ = 0.289\,\mathrm{nm},$$

$$0.50\cot 30^\circ = 0.866\,\mathrm{nm}.$$

Integration of the beam annulus gives $\pi(b_{\max}^2 - b_{\min}^2) = 2.09$ nm². This procedure includes all azimuths, so there is no additional solid-angle factor. Since C is proportional to inverse kinetic energy, doubling speed divides each radius by four and the cross section by sixteen, to 0.131 nm².

Explore these relations

- For the unresolved binary, explore how the orbit period and projected observations constrain the orbital scale. Open the live calculation.
- For detector-ring counts, vary the scattering parameters and compare equal angular bins with equal solid angles. Open the live calculation.

Reconstruct an orbit from its clock

The orbit laboratory reports a crossing period of 21 273.57 s. Take the gravitational parameter to be $398600\ \mathrm{km}^3/\mathrm{s}^2$ and the perigee radius to be 6628.14 km. Recover the apogee radius without using a trajectory plot. A second observer reports only a 0.3% uncertainty in period. Estimate the resulting fractional uncertainty in semimajor axis.

▼ **Work through the solution**

Squaring the areal-law prediction gives

$$a^3 = \mu (T/2\pi)^2.$$

Substitution gives $a \simeq 16\,594$ km and $r_a = 2a - r_p \simeq 26\,560$ km, in agreement with the low-apogee run. At fixed gravitational parameter, logarithmic differentiation gives $da/a = (2/3)dT/T$, hence 0.2% in the semimajor axis. Apogee inferred by subtraction has an absolute timing uncertainty twice that of a, assuming the perigee is independently known.

Use the OneSimulation laboratory to check your answer

Set the perigee altitude to 250 km and apogee radius to 26560 km to recover the measured clock period, then perturb the radius and compare the sensitivity. Open the corresponding live laboratory reference.

Notebook practice · When the moving centre of light hides a binary orbit

Chapter 9 · Principal axes and torque-free precession

Use the inertia tensor to distinguish rotation about a principal axis from the precession of a freely rotating symmetric body.

FROM FIRST PRINCIPLES

Build the inertia tensor from the momenta of particles in a rigid body

Choose the centre of mass as origin and consider a rigid body of fixed mass distribution. Its instantaneous internal velocity field is

$$\mathbf{v} = \boldsymbol{\omega} \times \mathbf{r}.$$

Starting from angular momentum as the moment of linear momentum, integrate over small masses. The vector triple-product identity separates the part parallel to $\boldsymbol{\omega}$ from a direction-dependent subtraction:

$$\mathbf{L} = \int \mathbf{r} \times (\boldsymbol{\omega} \times \mathbf{r})\, dm = \int [r^2 \boldsymbol{\omega} - (\mathbf{r} \cdot \boldsymbol{\omega})\mathbf{r}]\, dm.$$

Reading off coefficients of the components of $\boldsymbol{\omega}$ defines the symmetric inertia tensor. It is diagonal only in appropriately chosen principal axes:

$$L_i = \sum_j I_{ij} \omega_j,$$

$$I_{ij} = \int (r^2 \delta_{ij} - r_i r_j)\, dm.$$

Torque gives the laboratory time derivative of angular momentum. In a body-fixed principal basis the tensor components are constant but the basis rotates. Applying the rotating-vector derivative yields, for the first component,

$$\tau_1 = I_1 \dot{\omega}_1 + (I_3 - I_2)\omega_2 \omega_3.$$

Cyclic permutation gives the others. Even zero torque can change the body-frame components of angular velocity. Alignment of angular velocity and angular momentum holds about a principal direction, or about every direction for spherical inertia.

DERIVATION AND APPLICATIONS

Find a pivot that gives a specified physical-pendulum period

An extended body hanging from a pivot rarely oscillates like a point at its centre of mass. Take a rigid body of mass M with centre of mass a distance d below a horizontal, frictionless axis. Let I_C be its moment of inertia about the parallel axis through the centre of mass. Measure angle θ from vertically downward. For each mass element, decompose its perpendicular displacement from the pivot into the centre-of-mass offset and a displacement relative to the centre. The cross term integrates to zero by definition of the centre:

$$I_O = \int r_\perp^2 \, dm = I_C + M d^2.$$

Gravity is equivalent to a force Mg at the centre, so its torque depends only on d. Angular momentum about the fixed pivot is $I_O \dot{\theta}$ along the rotation axis. The angular equation, followed by its small-angle limit, is

$$(I_C + M d^2)\ddot{\theta} = -M g d \sin\theta,$$
$$\omega^2 = \frac{M g d}{I_C + M d^2}.$$

Define the radius of gyration $k_C = \sqrt{I_C / M}$. A simple pendulum with the same period has effective length $\ell_{\mathrm{eff}} = g/\omega^2$. Unlike the actual distance d, this length includes the cost of rotating the mass distribution about its centre:

$$T = 2\pi \sqrt{\frac{\ell_{\mathrm{eff}}}{g}},$$
$$\ell_{\mathrm{eff}} = d + \frac{k_C^2}{d}.$$

Moving the pivot toward the centre eventually increases the period because the torque vanishes faster than the inertia. Differentiating the effective length gives $d\ell_{\mathrm{eff}}/dd = 1 - k_C^2/d^2$, so the shortest period occurs at $d = k_C$ if the apparatus admits that pivot.

WORKED EXAMPLE

Compare two pivot positions on a uniform bar

Change the inputs and investigate this derivation.

A thin 0.900 m uniform bar oscillates in a vertical plane. Integration of $x^2\,dm$ along its length gives

$$k_C^2 = L^2/12 = 0.0675\,\mathrm{m}^2.$$

Pivoting at the end gives $d = 0.450$ m and $\ell_{\mathrm{eff}} = 0.600$ m, hence $T = 1.55$ s for $g = 9.81$ m/s². Pivoting 0.150 m from the centre also gives

$$0.150 + 0.0675/0.150 = 0.600\,\mathrm{m}.$$

The two periods agree even though the gravitational torque coefficients differ by a factor of three.

SECOND APPLICATION

Infer an unknown inertia from equal periods

Change the inputs and investigate this derivation.

Two distinct pivot distances $d_1 = 0.0800$ m and $d_2 = 0.180$ m give the same measured period for a 0.500 kg body. Equating the effective lengths and canceling $d_1 - d_2$ yields

$$k_C^2 = d_1 d_2 = 0.0144\,\mathrm{m}^2.$$

Thus $I_C = 0.00720$ kg m², and the common effective length is

$$d_1 + d_2 = 0.260\,\mathrm{m}.$$

A predicted period of 1.02 s checks the inference independently of the inertia measurement.

Try it · Physics lab reversible pendulum

Vary the physical parameters in the derived relation. Use the units and assumptions in the readout to connect the curves to the two worked examples. A parameter study can test the forward prediction; the same relation can then be inverted to infer a parameter from a measurement.

Open this live calculation

Try the calculation

Radius of gyration (m) **0.3**

Second pivot distance (m) **0.45**

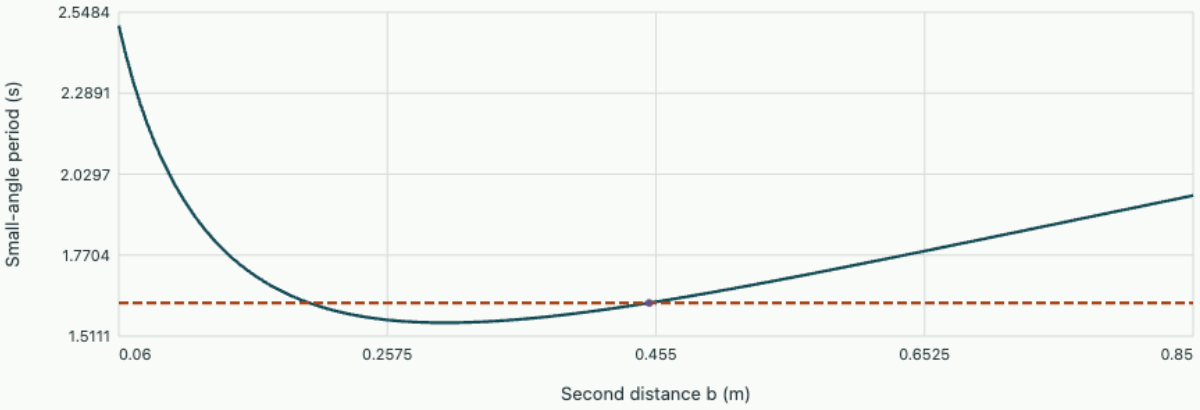

First period 1.6173 s; second 1.6173 s. The other matching distance is 0.45 m.

Distinguish loss of orientation from loss of angular momentum

Release a body spinning almost about its intermediate principal axis, with moments $0.030,\ 0.040,\ 0.050\,\mathrm{kg\,m^2}$. The first transverse angular velocity component can grow while both energy and angular momentum magnitude stay constant. The experiment compares all three torque-free Euler equations with the growing and decaying modes of their linearisation. Vary the spin and the initial departure from the middle axis. The downloadable OneSimulation run includes both conserved quantities alongside the three components.

Open this experiment online

Try the calculation

Nominal middle-axis speed (rad/s) **12**

Initial transverse speed (rad/s) **0.1**

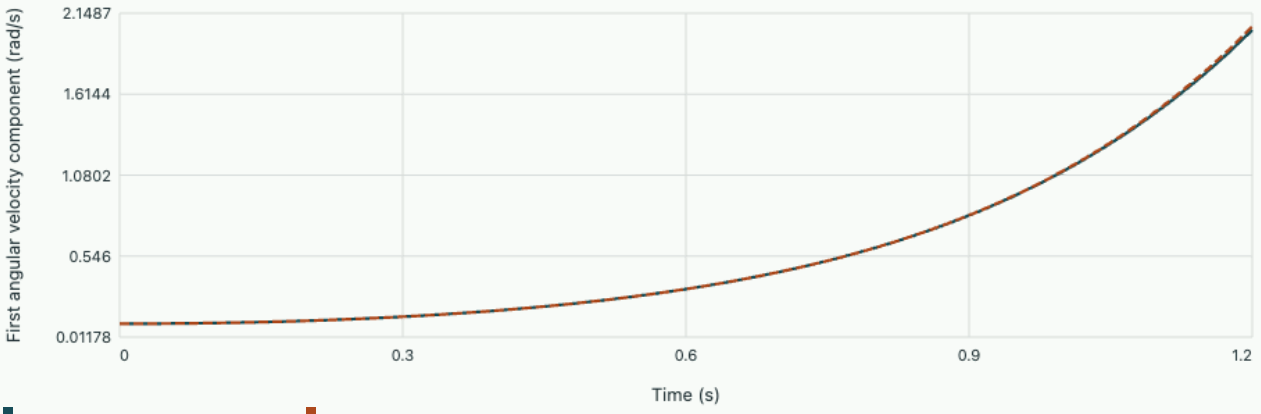

Initial linear growth rate 3.0984 s⁻¹. With zero initial transverse slope the predicted first doubling time is 0.42505 s.

Download the OneSimulation model

In your OneSimulation environment, run the model with these inputs.

```
python spectra-and-orbits.py rotor --spin 12 --seed 0.1
```

Use the worked instrument problem to derive the doubling time for two different preparations. A single image showing a complete flip is a much less precise rate measurement than the early time series.

Describe rotation around a moving centre

Take a rigid body with a freely moving centre of mass and no applied torque about that centre. Remove the uniform translation and label material positions $\mathbf{r}$ relative to the centre. Each material point has velocity $\boldsymbol{\omega} \times \mathbf{r}$. Integrating $\mathbf{r} \times (\boldsymbol{\omega} \times \mathbf{r})\, dm$ gives

$$\mathbf{L} = \mathbf{I}\boldsymbol{\omega},$$

where $I_{ij} = \int (r^2 \delta_{ij} - r_i r_j) dm$. The inertia tensor is symmetric, so a set of orthogonal body axes diagonalises it.

In its principal axes the rotational kinetic energy is $\sum_i I_i \omega_i^2 / 2$. This expression follows by integrating the kinetic energy of individual mass elements. A body containing mass far from an axis usually has large moment of inertia about that axis. Unless the components seeing different moments vanish, angular momentum and angular velocity point in different directions. A body can therefore rotate freely even when the angular velocity changes direction relative to painted marks on its surface.

Background · Where does the parallel-axis term come from?

Compare the kinetic energies for rotation about two parallel axes, one through the centre of mass and one displaced a perpendicular distance d. For a mass element write the perpendicular position about the second axis as $\boldsymbol{\rho} + \mathbf{d}$, where $\boldsymbol{\rho}$ is measured from the centre of mass. Expanding its squared distance produces a mixed term. The mass-weighted mean of $\boldsymbol{\rho}$ vanishes by the definition of the centre.

$$I_{\text{shifted}} = \int |\boldsymbol{\rho} + \mathbf{d}|^2 \, dm = I_{\text{CM}} + Md^2.$$

For a uniform thin rod of length L rotating about a transverse axis through an end, the shift adds $ML^2/4$ to $ML^2/12$. The result is $ML^2/3$. If instead the new axis tilts, each mass element has a different perpendicular projection. Then apply the inertia tensor to the new axis direction before making a parallel shift.

Apply the moving-frame derivative

The laboratory angular momentum is constant in the absence of torque. Its components in the body basis satisfy $(d\mathbf{L}/dt)_{\text{body}} + \boldsymbol{\omega} \times \mathbf{L} = 0$. For axial symmetry put $I_1 = I_2 = I_\perp$ and call I_3 the moment about the symmetry axis. Then $\dot{\omega}_3 = 0$,

$$\dot{\omega}_1 = -(I_3 - I_\perp)\omega_2\omega_3/I_\perp,$$
$$\dot{\omega}_2 = (I_3 - I_\perp)\omega_1\omega_3/I_\perp.$$

These last two equations describe uniform rotation of the pair of transverse components in body coordinates.

The signed angular rate of that rotation is $\Omega_b = (I_3 - I_\perp)\omega_3/I_\perp$. A body-mounted sensor sees its transverse spin vector execute a circle, even though a laboratory observer sees a constant angular-momentum vector. For a spherical inertia tensor the transverse components also become constant. The possible motion then simplifies because $\mathbf{L}$ is parallel to $\boldsymbol{\omega}$ for any spin direction.

Predict what two observers see

The symmetry-axis unit vector $\mathbf{e}_3$ has laboratory derivative $\dot{\mathbf{e}}_3 = \boldsymbol{\omega} \times \mathbf{e}_3$. Express the angular velocity as $\mathbf{L}/I_\perp$ plus a term parallel to $\mathbf{e}_3$, which drops out of the cross product. The result is

$$\dot{\mathbf{e}}_3 = (\mathbf{L}/I_\perp) \times \mathbf{e}_3.$$

Thus in the laboratory the symmetry axis sweeps around fixed $\mathbf{L}$ at rate $L/I_\perp$ and constant tilt. This rate differs from the spin-vector rotation observed in body coordinates because the two measurements track different vectors relative to different frames.

Let $I_\perp = 0.020$ kg·m², $I_3 = 0.030$ kg·m², $\omega_3 = 40$ rad/s and initial transverse angular speed 6.0 rad/s. The body-frame rate is 20 rad/s. The magnitude of momentum is $\sqrt{(0.020\times 6)^2 + (0.030\times 40)^2} = 1.206$ kg·m²/s. Laboratory precession is about 60.3 rad/s. The tilt obeys $\tan\theta = 0.120/1.20 = 0.10$, giving 5.71°. Two cameras recording these distinct angular rates need not disagree on the mechanics.

For three distinct moments the two transverse equations no longer form this simple uniform circle. The stability of individual principal-axis spins then becomes an additional question. Recording both energy and angular momentum helps discriminate conservative tumbling from external bearing drag.

One can also infer a moment of inertia without opening the rotor. Measure angular momentum by applying a calibrated torque for a known duration and integrating the torque impulse. During free motion, track the body axis with an external camera and find its precession frequency about the fixed angular momentum. For the symmetric rotor their ratio estimates the transverse moment I_1. A second measurement of the axial component of angular momentum and spin gives I_3.

Balance torque and angular momentum in a heavy top

Support a symmetric top at one fixed point on its symmetry axis, a distance ℓ below its centre of mass when upright. Unlike free rotation about the centre, gravity now exerts a torque about the pivot. Use principal moments about the pivot, $I_1 = I_2$ and I_3, and let θ be the tilt from upward vertical. In steady precession θ is constant, the azimuth increases at rate Ω, and the body's total angular-velocity component along its symmetry axis is $\omega_3 = \dot\psi + \Omega\cos\theta$.

The rotational kinetic energy in Euler angles is $I_1(\dot\theta^2 + \dot\phi^2\sin^2\theta)/2 + I_3(\dot\psi + \dot\phi\cos\theta)^2/2$. Insert $U = mg\ell\cos\theta$ into the θ equation, differentiating before imposing constant tilt. For $\sin\theta \neq 0$ this yields

$$I_1\cos\theta\,\Omega^2 - I_3\omega_3\Omega + mg\ell = 0.$$

The slower root for rapid spin tends to $mg\ell/(I_3\omega_3)$. This is the rate required for gravity to turn the nearly axial angular momentum. The full quadratic distinguishes that rate from a second, fast precession and gives the spin threshold for a tilted steady solution when $\cos\theta > 0$. Initial conditions outside such a solution produce a varying tilt, called nutation.

For $m = 0.200$ kg, $\ell = 0.0450$ m, $I_1 = 0.00180$ kg m², $I_3 = 0.000800$ kg m², $\omega_3 = 200$ rad/s and $\theta = 30^\circ$, the slow-root approximation is

$$0.0883/0.160 = 0.552\,\mathrm{rad/s}.$$

Substituting the quadratic coefficients gives 0.555 rad/s, a precession period of about 11.3 s. The other root is about 102 rad/s. A camera measuring only rotation of a mark painted on the body cannot generally separate axial spin, precession and nutation without also tracking the axis.

Practise on sheet 5 · Test whether a steady precession exists. Further reading · University of Cambridge · David Tong, Classical Dynamics · §3.6 The Heavy Symmetric Top.

Stability of rotation about a principal axis

A symmetric rotor can precess steadily. A body with three different principal moments has a striking additional possibility. Suppose $I_1 < I_2 < I_3$ and no torque acts about the centre of mass. In body coordinates Euler's equations can be written $I_1\dot{\omega}_1 = (I_2 - I_3)\omega_2\omega_3$, with cyclic permutations for the other components. A pure rotation about any one principal axis is an exact solution. Stability asks what happens to a small transverse disturbance of that solution, a question about neighbouring trajectories rather than the exact rotation itself.

Consider nominal rotation about axis 2 at rate Ω. Write $\omega_1 = u$ and $\omega_3 = w$, both initially small. The change of ω_2 is a product of two small quantities and can be discarded to first order. The first and third equations give

$$\dot{u} = -(I_3 - I_2)\Omega w / I_1,$$
$$\dot{w} = -(I_2 - I_1)\Omega u / I_3.$$

Differentiating the first and substituting the second produces

$$\ddot{u} = \Omega^2 \frac{(I_3 - I_2)(I_2 - I_1)}{I_1 I_3}\, u.$$

A positive coefficient gives hyperbolic solutions with an exponentially growing component for a generic disturbance. Repeating the calculation about the smallest or the largest moment reverses the sign of the product, giving bounded oscillatory disturbances. Energy and angular momentum remain conserved throughout. A nearby angular-velocity direction can change substantially while moving along the intersection of the two invariant surfaces.

Estimate the onset of a visible tumble

Take moments $I_1 = 0.020$, $I_2 = 0.030$ and $I_3 = 0.040$ kg m² and a nominal intermediate-axis rotation $\Omega = 20.0$ rad/s. The small-perturbation growth rate is $20.0\sqrt{0.010 \times 0.010 / (0.020 \times 0.040)} = 7.07$ s⁻¹. Prepare an initial transverse component of 0.020 rad/s in the growing eigenmode. Reaching 0.200 rad/s then takes $\ln(10)/7.07 = 0.326$ s, still within the small-angle range. A perturbation prepared with zero initial derivative instead contains both growing and decaying contributions and follows a hyperbolic cosine initially.

These estimates predict the early departure, not the duration of a full flip. When transverse components approach the nominal spin, the nonlinear terms that preserved the dominant spin to first order can no longer be dropped. As two adjacent moments approach equality the growth rate tends to zero, recovering the absence of this isolated intermediate-axis instability in a symmetric rotor. A motion-capture experiment that records all three body components can test the exponential interval and independently check whether external torques or aerodynamic drag have changed the conserved angular momentum.

There is also a camera-independent prediction for the orientation of the early disturbance in body coordinates. A growing solution has $\dot{u} = \lambda u$. From the first linearized equation this requires

$$w/u = -I_1\lambda/[(I_3 - I_2)\Omega].$$

In the numerical example that ratio is -0.707: the small components point in opposite signed directions. A disturbance with the reverse sign projects partly onto the decaying solution. The eventual growth rate can be the same while the visibility of the first few cycles differs greatly. Recording both components avoids assigning a disagreement in initial conditions to the underlying instability rate.

Study the full derivation

Euler–Poinsot motion, torque-free nutation and the intermediate axis · Analytical mechanics from constraints to invariants

A freely rotating body has fixed angular momentum in space, yet the components recorded by three body-mounted gyroscopes can vary periodically or linger near an unstable rotation. Solve the nonsymmetric top from its invariants, distinguish its body-component period from its spatial orientation, and extract a stability time scale from a measured inertia tensor.

Chapter 10 · Forced, damped vibration

Use amplitude, phase and power together to estimate the mechanical properties of an oscillator from a sinusoidal drive.

FROM FIRST PRINCIPLES

Derive the steady amplitude and its phase lag

The force laws for a simple vibration test are an elastic restoring force $-kx$, a viscous force $-c\dot{x}$ and a prescribed drive $F_0 \cos \omega t$. Newton's law gives

$$m\ddot{x} + c\dot{x} + kx = F_0 \cos \omega t.$$

Assume linear coefficients, positive damping and enough time for the free transient to decay. Seek the response at the measured drive frequency by setting $x = \mathrm{Re}(Xe^{i\omega t})$. Each differentiation multiplies the complex amplitude by $i\omega$, so

$$(k - m\omega^2 + ic\omega)X = F_0.$$

The magnitude of the complex denominator fixes the measured displacement amplitude; its argument gives the lag of the response relative to the applied force:

$$|X| = \frac{F_0}{\sqrt{(k - m\omega^2)^2 + c^2\omega^2}},$$

$$\delta = \operatorname{atan2}(c\omega, k - m\omega^2).$$

At low frequency the spring supports nearly the entire force and the displacement approaches F_0/k. At $\omega = \sqrt{k/m}$ the spring and inertia terms cancel, leaving a quarter-period displacement lag. Multiplying velocity by force and averaging distinguishes this condition of maximum absorbed power from the maximum displacement amplitude.

DERIVATION AND APPLICATIONS

Read the exact mechanical bandwidth from absorbed power

A measured displacement peak need not occur at the frequency of maximum energy absorption. Consider a linear oscillator of mass m, stiffness k and viscous damping coefficient $c > 0$, driven steadily by $F_0 \cos \omega t$. Let X denote the complex displacement amplitude. Work over a complete period supplies the energy dissipated by the damper, whose instantaneous loss is $c\dot{x}^2$. Since the velocity amplitude is $\omega|X|$, averaging its square gives

$$\overline{P} = \tfrac{1}{2}c\omega^2|X|^2 = \frac{cF_0^2\omega^2/2}{(k - m\omega^2)^2 + c^2\omega^2}.$$

Divide numerator and denominator by ω^2. The frequency-dependent term in the denominator becomes $(k/\omega - m\omega)^2$, which vanishes exactly at $\omega_0 = \sqrt{k/m}$. Hence $\overline{P}_{\max} = F_0^2/(2c)$. The half-power condition is particularly simple:

$$|k - m\omega^2| = c\omega.$$

There are two positive roots, one on each side of ω_0. Solving the two quadratics separately yields

$$\omega_\pm = \frac{\sqrt{c^2 + 4mk} \pm c}{2m},$$

$$\omega_+ - \omega_- = \frac{c}{m},$$

$$\omega_+ \omega_- = \frac{k}{m}.$$

The half-power bandwidth in angular-frequency units is exactly c/m for this viscously damped, constant-force experiment. For weak damping the frequencies become nearly symmetric around ω_0. In stronger damping the geometric mean still gives ω_0. The frequencies correspond to half the peak power, equivalently to the velocity amplitude falling to $1/\sqrt{2}$ of its maximum.

WORKED EXAMPLE

Plan the frequency sweep for a test fixture

Change the inputs and investigate this derivation.

For $m = 0.400$ kg, $k = 160$ N/m and $c = 4.00$ N s/m, the peak lies at 20.0 rad/s. The half-power edges are 15.62 and 25.62 rad/s, about 2.49 and 4.08 Hz. A force amplitude $F_0 = 2.00$ N produces 0.500 W at resonance and 0.250 W at either edge. The peak displacement occurs at a slightly lower frequency, so a displacement maximum alone would give a different estimate.

SECOND APPLICATION

Recover a stiffness without measuring the peak height

Change the inputs and investigate this derivation.

A 0.250 kg resonator has measured half-power edges at 3.00 and 4.00 Hz. Convert to radians per second before using the formulas. The damping is $m\,2\pi(4-3) = 1.57$ N s/m; the stiffness is

$$m(2\pi)^2(3)(4) = 118\,\mathrm{N/m}.$$

The peak-power frequency predicted from the product is

$$\sqrt{12} = 3.46\,\mathrm{Hz}.$$

These estimates do not require calibrating the force amplitude, provided it was constant across the sweep.

Try it · Power bandwidth

Vary the physical parameters in the derived relation. Use the units and assumptions in the readout to connect the curves to the two worked examples. A parameter study can test the forward prediction; the same relation can then be inverted to infer a parameter from a measurement.

Open this live calculation

Try the calculation

Mass (kg)	0.4
Stiffness (N/m)	160
Damping (N s/m)	4

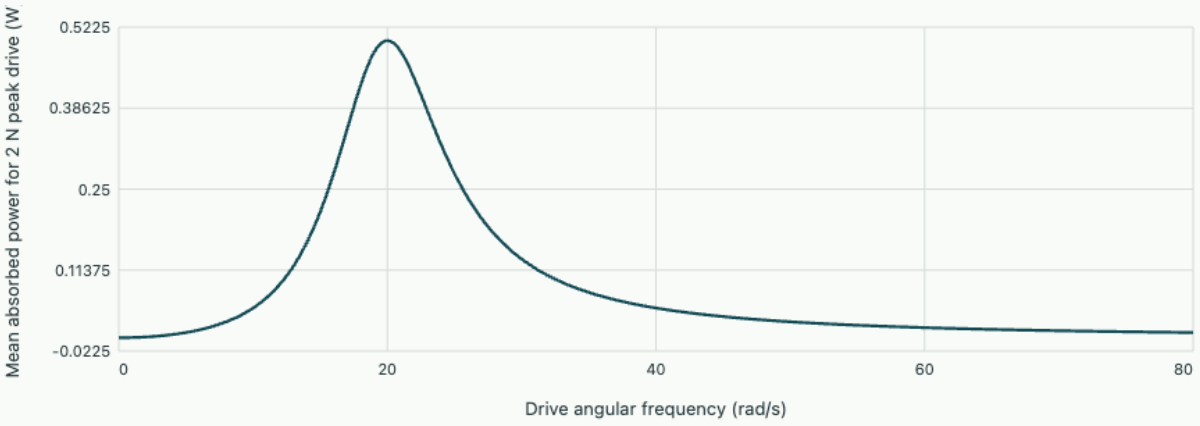

Absorbed power

Half-power edges 15.616 and 25.616 rad/s; bandwidth c/m = 10. Peak power 2/c = 0.5 W.

ONESIMULATION LABORATORY

When does a released mass cross equilibrium?

Release a 1 kg mass from rest 10 mm to the right of equilibrium on a spring of stiffness 4 N/m. A viscous damper exerts a force opposite to the velocity. In a driven machine this free response is the transient left by the initial displacement. Here the external drive is zero, so the transient can be measured on its own.

Predict a crossing. With displacement measured from static equilibrium, the weight has already been balanced. Newton's second law gives one restoring term for displacement and one for velocity. Write the

trial motion as an exponential. Dividing the resulting equation by the nonzero exponential leaves a quadratic:

$$m\ddot{x} = -kx - c\dot{x},$$

$$x = Ae^{st} \quad \Longrightarrow \quad s^2 + 2\zeta\omega_n s + \omega_n^2 = 0,$$

$$\omega_n = \sqrt{k/m},$$

$$\zeta = \frac{c}{2\sqrt{mk}}.$$

Here $\omega_n = 2$ rad/s. At $\zeta = 0.2$ the roots are $-0.4 \pm 1.960i$ s⁻¹. The imaginary part permits a zero crossing. At critical damping the double root is -2 s⁻¹. Applying the initial conditions to the two independent solutions gives $x = 10(1 + 2t)e^{-2t}$ mm. At $\zeta = 2$ the slowest root is about -0.536 s⁻¹. Which of the last two releases is closer to equilibrium at three seconds?

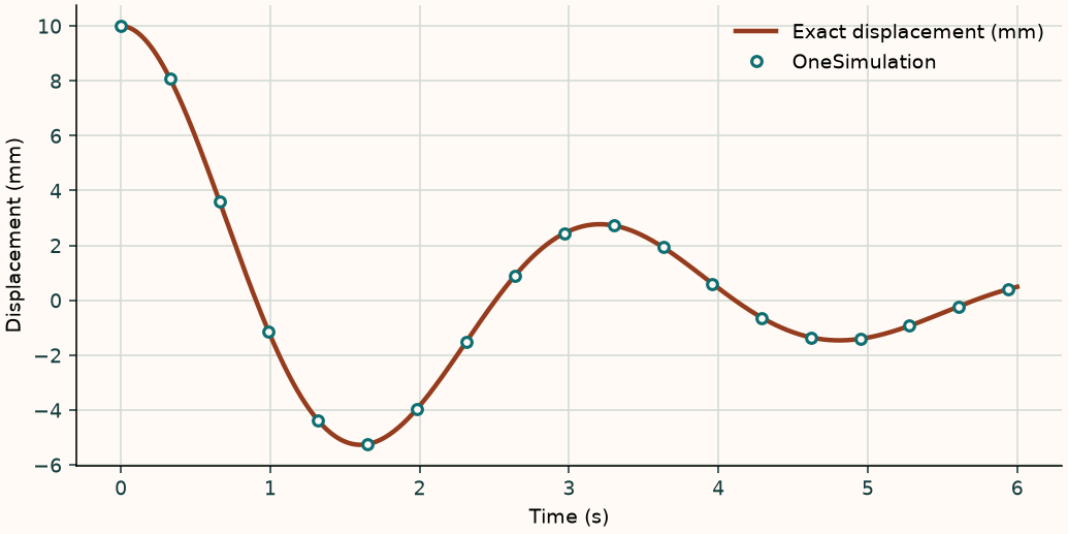

Displacement versus time for a mass released from rest, with the exact solution and sampled numerical displacements. Damping ratio = **0.2**.

Download this run (CSV)

Read the comparison. At three seconds the critical solution is about 0.174 mm from equilibrium. Increasing damping again leaves about 2.16 mm. The slower real root explains the long tail. The underdamped trajectory has already crossed the equilibrium. The points come from integrating the two first-order equations for displacement and velocity. The line comes from their characteristic roots.

Try a fourth case. Change the damping ratio to 0.7. Predict the first zero from the damped frequency and the phase fixed by release from rest, then find the first sign change in the output CSV.

Further reading · MIT 18.03, Natural frequency and damping ratio.

Download the OneSimulation model (Python). Set up the local runtime, then run the downloaded file:

```
python oscillator.py --ratio 0.7
```

Separate the transient from the driven motion

A shaker applies a sinusoidal force to a mass on a spring and viscous damper. Its displacement can lag the force and can remain large even when the applied force is small. Assume motion about a stable equilibrium, constant stiffness k, positive damping coefficient c and drive $F_0 \cos \omega t$. Newton's equation is

$$m\ddot{x} + c\dot{x} + kx = F_0 \cos \omega t.$$

The solution contains a homogeneous contribution set by preparation and a particular response set by the continuing drive.

Positive damping makes the homogeneous part decay. To estimate the steady frequency response, measurements must last several decay times at each frequency. Measurements taken immediately after the drive changes include residual free motion. Close to weakly damped resonance that settling time can span many oscillations, so sweeping too rapidly can shift the apparent location of a peak.

Solve for amplitude and lag

Write the steady displacement as the real part of $Xe^{i\omega t}$ and take F_0 real. Substituting gives

$$X = F_0/(k - m\omega^2 + ic\omega).$$

The denominator groups the elastic and inertial contributions along the real axis and viscous loading in quadrature. Its magnitude gives

$$|X| = \frac{F_0}{\sqrt{(k - m\omega^2)^2 + c^2\omega^2}}.$$

The lag angle is the argument of the denominator, evaluated in the appropriate quadrant. At low frequency $X \simeq F_0/k$, in phase with force. At high frequency $X \simeq -F_0/(m\omega^2)$, nearly opposite in phase. At $\omega_n = \sqrt{k/m}$ the reactive terms cancel and the displacement lags by a quarter cycle. This phase condition identifies the undamped natural frequency even when the amplitude maximum lies slightly lower.

Connect absorbed power to damping

Multiply the equation by $\dot{x}$ and average over one settled cycle. Both stored kinetic and elastic energies return to their initial values, so the mean input power is dissipated by the damper. For peak displacement,

$$\langle P \rangle = c\omega^2 |X|^2/2.$$

At ω_n, the velocity is in phase with force, giving $\langle P \rangle = F_0^2/(2c)$. Minimising the denominator of the displacement response gives a different frequency, $\omega_{\text{peak}}^2 = k/m - c^2/(2m^2)$, if this is positive. A reported "resonance frequency" should identify the measured observable.

A power scan near a lightly damped resonance has a narrow peak whose half-power bandwidth is approximately c/m in rad/s. The damping estimate obtained from that width can be compared with an independent ring-down estimate. Significant disagreement could indicate an amplitude-dependent damper or loss in the drive system.

Read a frequency-response experiment

Take $m = 2.0$ kg, $k = 800$ N/m, $c = 8.0$ N·s/m and $F_0 = 4.0$ N. The low-frequency displacement is 5.0 mm. At 20 rad/s the displacement is 25 mm, the velocity amplitude is 0.50 m/s and the mean power is 1.0 W. The displacement maximum occurs near $\sqrt{400 - 8} = 19.8$ rad/s. A run at a single frequency near the peak cannot identify all three parameters. A low-frequency measurement constrains stiffness, the quarter-cycle lag constrains mass relative to stiffness and the absorbed power at that frequency constrains damping independently.

Motion imposed at the support

A vibration mount is often driven through a moving base rather than by a calibrated force on the mass. Let $y(t)$ be the prescribed absolute displacement of the support and $x(t)$ the absolute displacement of a supported mass m. A spring and a viscous damper both connect mass to base, so they respond to $x - y$ and $\dot{x} - \dot{y}$. Newton's equation is

$$m\ddot{x} + c(\dot{x} - \dot{y}) + k(x - y) = 0.$$

The same mass and stiffness as in a force-driven oscillator can therefore produce a different transfer function because the input enters both elastic and dissipative forces.

For harmonic motion proportional to $e^{i\omega t}$ rearrange the amplitude equation to give

$$(k - m\omega^2 + ic\omega)X = (k + ic\omega)Y.$$

Set $r = \omega/\omega_n$, $\omega_n = \sqrt{k/m}$ and $\zeta = c/(2m\omega_n)$. The ratio of absolute displacement amplitudes is

$$\left|\frac{X}{Y}\right|^2 = \frac{1 + (2\zeta r)^2}{(1 - r^2)^2 + (2\zeta r)^2}.$$

At very low frequencies the mass follows the support almost rigidly. To have $|X| < |Y|$ requires $(1 - r^2)^2 > 1$, which for positive frequency means $r > \sqrt{2}$. Increasing damping reduces the resonant peak but increases the high-frequency path through which the moving support can exert a force. Damping is therefore a design variable with different consequences in different frequency bands.

Check both isolation and suspension travel

A 5.00 kg optical instrument sits on springs with total stiffness 2000 N/m and damping ratio 0.10. Its natural angular frequency is 20.0 rad/s and viscous coefficient $c = 2\zeta m\omega_n = 20.0$ N s/m. A nearby machine imposes a sinusoidal base motion of amplitude 0.800 mm at 60.0 rad/s. Here $r = 3.00$ and $2\zeta r = 0.600$, giving $|X/Y| = \sqrt{1.36/64.36} = 0.145$. The instrument moves through an absolute amplitude of 0.116 mm.

The suspension itself accommodates relative displacement. Subtract Y from X in the complex equation before taking a magnitude. This gives

$$|(X - Y)/Y| = r^2/\sqrt{(1 - r^2)^2 + (2\zeta r)^2} = 1.12.$$

The spring travel is therefore about 0.898 mm, exceeding the base amplitude despite successful instrument isolation. Subtracting the two absolute amplitudes directly would ignore phase and underpredict travel. At twice the damping ratio the same calculation gives $|X/Y| = 0.193$, so high-frequency isolation degrades even as resonance becomes less dangerous. Two simultaneous position sensors, on base and instrument, allow both absolute response and relative travel to be assessed.

A common practical constraint is allowable acceleration rather than displacement. In a sinusoidal test absolute acceleration has amplitude $\omega^2|X|$. For the stated 60 rad/s motion the mount gives an instrument acceleration of $3600 \times 0.000116 = 0.418$ m/s². The bare base acceleration is 2.88 m/s², so the ratio is the same as the displacement ratio at that particular frequency. Across a sweep the factor ω^2 changes. A decreasing displacement curve therefore does not guarantee a decreasing absolute acceleration, especially if the operational environment has a roughly constant displacement excitation over its upper frequency band.

Mechanical stops add a further check on the model. Once the relative travel reaches a stop, the constraint changes within each cycle, producing harmonics absent from the linear solution. A distorted accelerometer trace can therefore identify a travel problem before mean isolation performance is assessed.

Try it · Case oscillator

Explore the same physical relation with adjustable inputs. This independent parameter study has its own displayed reference settings; compare its assumptions and units before matching the static example.

Open this live calculation

Try the calculation

Damping / critical damping **0.2**

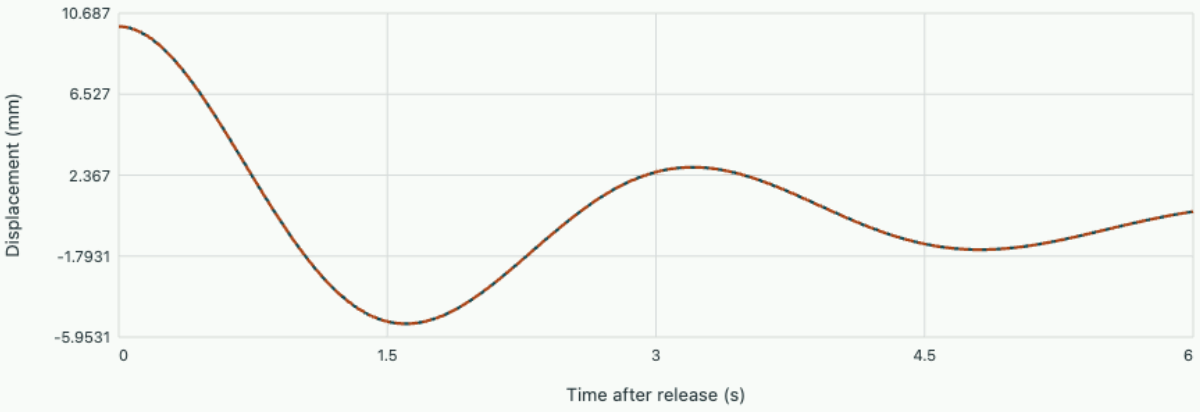

Fourth-order Runge–Kutta Characteristic-root solution

At 6 s the displacement is 0.49230 mm. Largest difference from the exact response on 600 steps: 2.46e-8 mm.

Download the OneSimulation model

In your OneSimulation environment, run the model with these inputs.

```
python oscillator.py --ratio 0.2
```

Which frequency does a phase measurement identify?

Drive a viscously damped oscillator with a sinusoidal force, measure displacement and retain its phase relative to the force. The complex compliance is proportional to $1/(1 - r^2 + 2i\zeta r)$. Use the quadrant-aware argument near and above resonance.

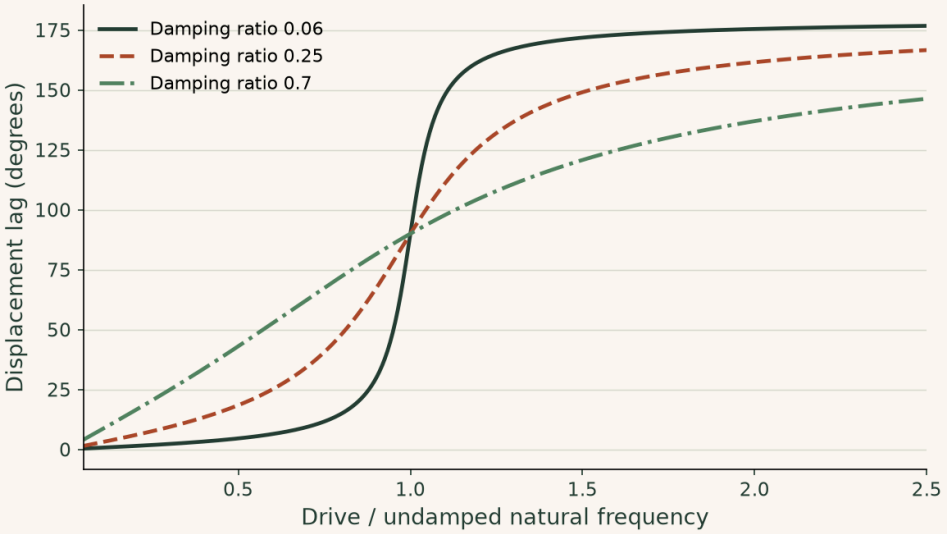

Every curve passes through 90° at r = 1. The amplitude maximum of the displacement, when it exists, is at a damping-dependent lower frequency. This makes a phase crossing an alternative way to identify the undamped frequency.

Try it · Oscillator phase

Change the inputs and compare the recalculated curves with the preceding derivation and baseline figure. The axes give the units; the numerical readout states the model assumptions and any limiting cases. Reset the inputs to return to the reference setting.

Open this live calculation

Try the calculation

Damping ratio ζ **0.2**

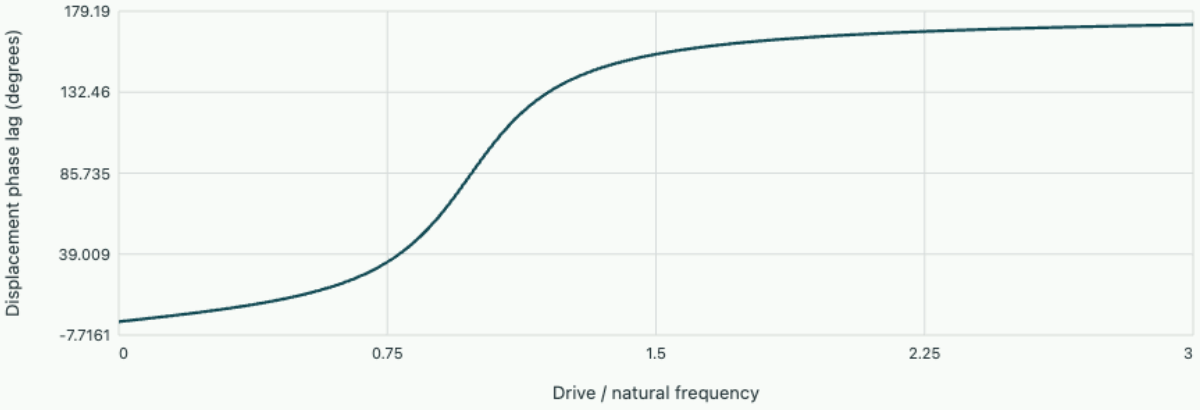

Selected damping

Phase crosses 90° at frequency ratio 1. Displacement amplitude peaks at 0.95917.

▶ **Read values from the plot**

Problem sheet 5 · Rotation, damping and frequency measurements

Use frequency and phase measurements to separate moments of inertia, damping, and static stiffness.

The wobble seen from a rotor

A torque-free symmetric rotor has $I_1 = I_2 = 0.024$ kg m², $I_3 = 0.030$ kg m² and axial angular velocity 100 rad/s. Find the frequency of the transverse angular-velocity components in body coordinates. For an instantaneous transverse speed of 4 rad/s, find the angle between the symmetry axis and angular momentum and the inertial precession rate.

▼ **Show both frame calculations**

Euler's transverse equations give $\Omega_b = (I_3 - I_1)\omega_3 / I_1 = 25$ rad/s or 3.98 Hz. Angular momentum has transverse and axial components 0.096 and 3.00 kg m²/s. Therefore

$$\theta = \arctan(0.096/3) = 1.83^\circ.$$

The body axis follows $\dot{\mathbf{e}}_3 = (\mathbf{L}/I_1) \times \mathbf{e}_3$, so its azimuth about fixed angular momentum advances at $|\mathbf{L}|/I_1 = 125.1$ rad/s. A body-mounted sensor and an external camera measure different rotations.

Read damping from the ring-down

A 0.50 kg oscillator completes ten free cycles in 2.00 s. Its peak displacement decreases from 8.0 to 4.0 mm. Infer the viscous damping coefficient and the spring stiffness. Predict the displacement amplitude under a sinusoidal force of 0.080 N at the undamped natural frequency.

▼ **Show the ring-down and driven response**

Write the envelope as $A_0 e^{-\gamma t}$. Then $\gamma = \ln 2 / 2 = 0.3466$ s⁻¹ and $c = 2m\gamma = 0.3466$ N s/m. The damped frequency is $\omega_d = 2\pi(10/2) = 31.416$ rad/s, so

$$k = m(\omega_d^2 + \gamma^2) = 493.5\,\mathrm{N/m}.$$

At $\omega_0 = \sqrt{k/m}$ the elastic and inertial terms cancel in the complex response. The amplitude is $F_0/(c\omega_0) = 7.35$ mm and the force leads displacement by a quarter cycle.

Distinguish two mechanical faults

A driven instrument has calibrated mass 1.0 kg and static deflection 1.0 mm under a 1.0 N load. During operation the displacement lags the drive by 45° at 5.0 Hz. Infer viscous damping and predict what changes in static deflection and quadrature frequency if damping doubles.

▼ **Show the inference and diagnosis**

Static response gives $k = 1000$ N/m. On the low-frequency side $\tan\delta = c\omega/(k - m\omega^2)$. At 31.416 rad/s the elastic excess is 13.04 N/m, giving $c = 0.415$ N s/m. At exact quadrature $k = m\omega^2$, so $f = 5.033$ Hz for both damping values. Static deflection is also unchanged, since the damper exerts no force at rest. Doubling damping halves the displacement at quadrature and widens the response. A stiffness change would instead shift both independent calibration observables.

Test whether a steady precession exists

At tilt 60° a top has $m = 0.300$ kg, $\ell = 0.0400$ m, $I_1 = 0.00200$ kg m² and $I_3 = 0.00100$ kg m². Find the minimum axial spin for a tilted steady precession. At axial spin 60.0 rad/s estimate the slow rate and compare it with the full solution.

▼ **Inspect the discriminant and select the slow root**

Real roots require $I_3^2\omega_3^2 \geq 4I_1 mg\ell\cos\theta$. With $mg\ell = 0.11772$ N m the threshold is 21.7 rad/s. Rapid-spin balance gives

$$0.11772/0.0600 = 1.96\,\mathrm{rad/s}.$$

The lower root of $0.00100\Omega^2 - 0.0600\Omega + 0.11772 = 0$ is 2.03 rad/s. Below threshold the equations exclude steady rotation at the stipulated tilt. They still allow motion with changing tilt.

Revisit chapter 9 · Balance torque and angular momentum in a heavy top.

Explore these relations

- For the frequency measurements, compare damping, absorbed-power width and the displacement resonance. Open the live calculation.
- For ring-down and fault diagnosis, vary oscillator mass, stiffness and damping and compare the transient response. Open the live calculation.

Chapter 11 · Nonlinear stiffness and amplitude-dependent period

Derive the leading frequency shift of a symmetric nonlinear oscillator and test whether a measured amplitude shift is consistent with a cubic spring.

FROM FIRST PRINCIPLES

Derive the first amplitude correction to a spring's frequency

A symmetric elastic restoring force has no quadratic displacement term; the first correction to a linear spring can therefore be cubic. Suppose a conservative oscillator satisfies $m\ddot{x} + kx + \alpha x^3 = 0$ with $k > 0$ and $|\alpha A^2/k| \ll 1$ at measured peak amplitude A. Leading motion is approximately $A\cos\Omega t$. Cube this motion to find which frequencies enter the perturbing force:

$$x^3 \simeq A^3[\tfrac{3}{4}\cos\Omega t + \tfrac{1}{4}\cos 3\Omega t].$$

To maintain a bounded periodic solution, its fundamental component must balance at first order. Otherwise the remaining fundamental force would resonantly grow the correction. Combine the inertia and restoring-force coefficients at $\cos\Omega t$:

$$-m\Omega^2 A + kA + \tfrac{3}{4}\alpha A^3 \simeq 0, \qquad \Omega \simeq \sqrt{k/m}\left(1 + \frac{3\alpha A^2}{8k}\right).$$

The third-harmonic component also distorts the waveform, but reinserting that order-α distortion into the cubic force affects the fundamental only at the next perturbative order. Positive α raises frequency with amplitude; negative α lowers it within the local range where the stable weakly nonlinear model applies.

DERIVATION AND APPLICATIONS

Find the third harmonic generated by a weak cubic spring

A change in oscillation period is one signature of a nonlinear restoring force. The same nonlinearity also changes the shape of the recorded motion. Let an undamped mass obey $m\ddot{x} + kx + \alpha x^3 = 0$, with $k > 0$. Release it from rest at the measured peak displacement A. Define $\omega_0 = \sqrt{k/m}$, the small signed parameter $\epsilon = \alpha A^2/k$, and a stretched time $\tau = \Omega t$. Write $x/A = \cos\tau + \epsilon u(\tau)$ with $u(0) = u'(0) = 0$ so that A remains the physical turning point.

Allow the frequency to shift as $\Omega = \omega_0(1 + \epsilon\nu)$. Substitute the expansion into the equation and retain terms only to first order in ϵ. Primes below denote differentiation with respect to τ:

$$u'' + u = 2\nu\cos\tau - \cos^3\tau = (2\nu - 3/4)\cos\tau - \tfrac{1}{4}\cos 3\tau.$$

A term driven at the unit frequency would grow proportionally to $\tau \sin \tau$, contradicting a bounded, periodic correction. Choose $\nu = 3/8$ to remove it. The remaining forcing is at three times the fundamental. A trial $C \cos 3\tau$ has $u'' + u = -8C \cos 3\tau$. Add the required homogeneous term to satisfy the turning-point conditions:

$$u(\tau) = \frac{\cos 3\tau - \cos \tau}{32}.$$

The predicted displacement therefore contains two lines with linked amplitudes and a shifted fundamental:

$$x(t) \simeq A[(1 - \epsilon/32)\cos \Omega t + (\epsilon/32)\cos 3\Omega t], \qquad \Omega/\omega_0 \simeq 1 + 3\epsilon/8.$$

The coefficient sign gives the third harmonic relative to the phase of a release at positive displacement. Squaring an amplitude to obtain a power spectrum erases that sign. The approximation assumes $|\epsilon| \ll 1$ and excludes appreciable dissipation during the observation.

WORKED EXAMPLE

Estimate a micrometre-scale distortion

Change the inputs and investigate this derivation.

Take $A = 12.0$ mm, $k = 20.0$ N/m and $\alpha = 1.00 \times 10^{4}$ N/m³. Then $\epsilon = 0.0720$, so the third-harmonic displacement amplitude is

$$12.0(0.0720)/32 = 0.0270\,\mathrm{mm}.$$

The fundamental frequency should increase by 2.70%. With $\omega_0 = 10.0$ rad/s, the third-harmonic line lies close to 30.8 rad/s.

SECOND APPLICATION

Test whether a measured line comes from the spring

Change the inputs and investigate this derivation.

At $A = 6.00$ mm on the same apparatus, ϵ falls by four and the third-harmonic amplitude falls by eight to 3.38 micrometres. The fractional frequency shift becomes 0.675%. A third-harmonic signal that instead halves with amplitude could arise from an already distorted input or readout. The two amplitude scalings plus an independent frequency measurement test the cubic model more strongly than observing a line at three times the frequency.

Try it · Duffing harmonic

Vary the physical parameters in the derived relation. Use the units and assumptions in the readout to connect the curves to the two worked examples. A parameter study can test the forward prediction; the same relation can then be inverted to infer a parameter from a measurement.

Open this live calculation

Try the calculation

Amplitude (mm) **12**

Cubic stiffness (N/m³) **10000**

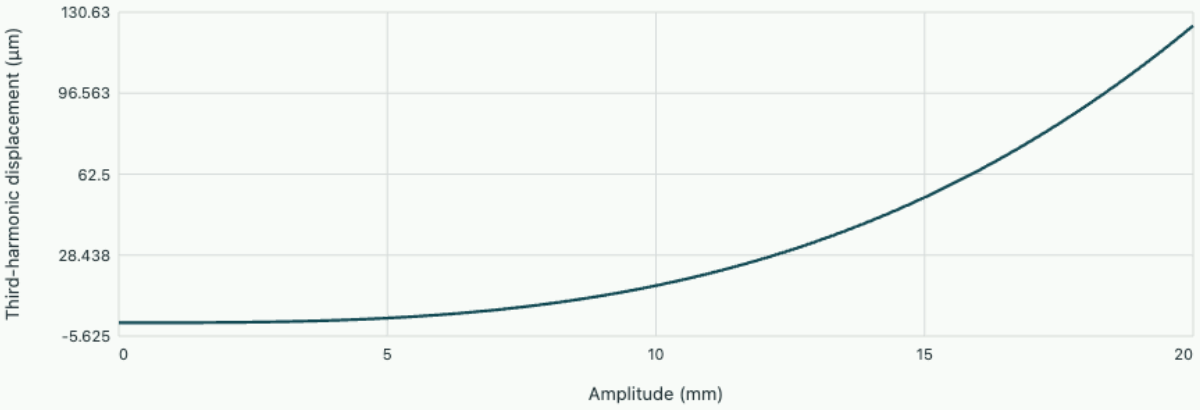

First perturbative harmonic

Linear stiffness 20 N/m. At chosen amplitude ε=0.072, third harmonic 27 µm; first frequency shift 2.7%. Requires ε≪1.

Start from a reversible force law

A spring that looks linear under small deflection can stiffen as it is displaced further. For an oscillator symmetric under $x \mapsto -x$, the restoring force expanded about equilibrium has no even powers. Keep the leading correction and write $m\ddot{x} + kx + \alpha x^3 = 0$, with $k > 0$ and α measured in N/m³. Assume the displacement is small enough that neglected fifth-order terms remain unimportant. Positive α gives a hardening spring. A negative cubic coefficient describes local softening and may need higher-order terms to represent large displacements safely within the model.

The potential is $kx^2/2 + \alpha x^4/4$. Without damping the total energy is conserved and a release at amplitude A fixes that energy. Unlike a harmonic oscillator, the quadratic curvature at the origin no longer fixes the period for every possible energy. We want a quantitative connection between the amplitude of the motion and its zero-crossing interval.

Obtain the first frequency correction

Try $x \simeq A\cos\Omega t$ and substitute it into the cubic equation. The identity $\cos^3 u = (3\cos u + \cos 3u)/4$ shows that the nonlinearity introduces a component at the original frequency and a third harmonic. Balance the fundamental coefficient to get $-m\Omega^2 + k + 3\alpha A^2/4 \simeq 0$. Expanding the square root gives

$$\Omega \simeq \omega_0 \left(1 + \frac{3\alpha A^2}{8k}\right),$$

$$\omega_0 = \sqrt{k/m}.$$

The control parameter is $|\alpha|A^2/k$, the ratio of cubic to linear force at maximum displacement. The small additional third harmonic changes the waveform at first order but only feeds back into this leading frequency result at higher order. Fitting a perfect sinusoid to a high-precision trace may therefore show a residual even when the measured average period follows this formula.

Check the result using the conserved energy

The quarter-period is the time to move from equilibrium to A. Substitution of the energy at the turning point gives an integral over $dx/\sqrt{2[E - U(x)]/m}$. Let $x = A\sin u$ to remove the square-root endpoint. The remaining integrand is proportional to $\{1 + [\alpha A^2/(2k)](1 + \sin^2 u)\}^{-1/2}$. Expanding and averaging over the interval from zero to $\pi/2$ uses mean $\sin^2 u = 1/2$, yielding $T \simeq (2\pi/\omega_0)[1 - 3\alpha A^2/(8k)]$. This agrees with the reciprocal of the harmonic-balance result.

The integral approach generalises to experimentally tabulated conservative forces by integrating them first to obtain a potential. It would need modification for strong damping, where energy varies significantly between the two turning points of one cycle.

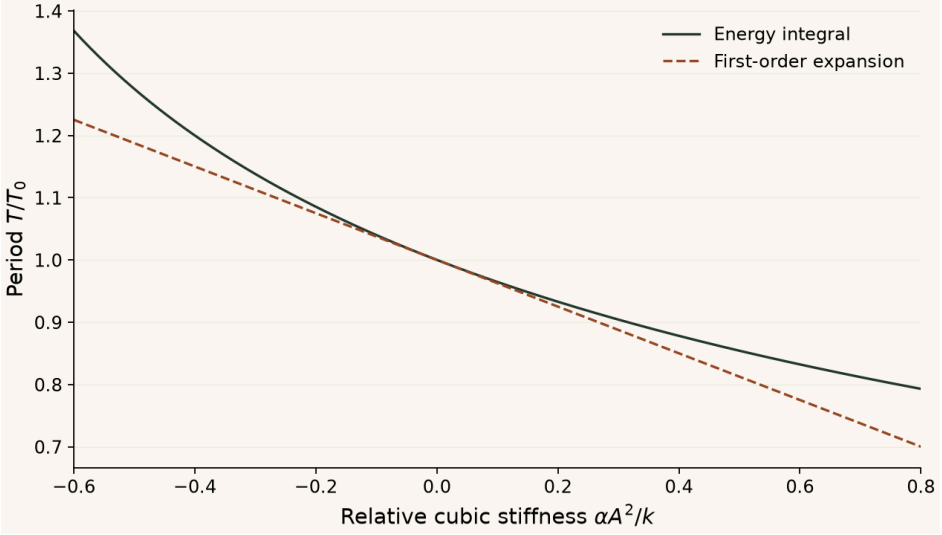

A positive cubic stiffness shortens the period. The first-order expansion is tangent to the energy-integral curve at zero and gradually loses accuracy away from that limit.

Try it · Duffing

Change the inputs and compare the recalculated curves with the preceding derivation and baseline figure. The axes give the units; the numerical readout states the model assumptions and any limiting cases. Reset the inputs to return to the reference setting.

Open this live calculation

Try the calculation

Cubic stiffness × amplitude² / linear stiffness **0.5**

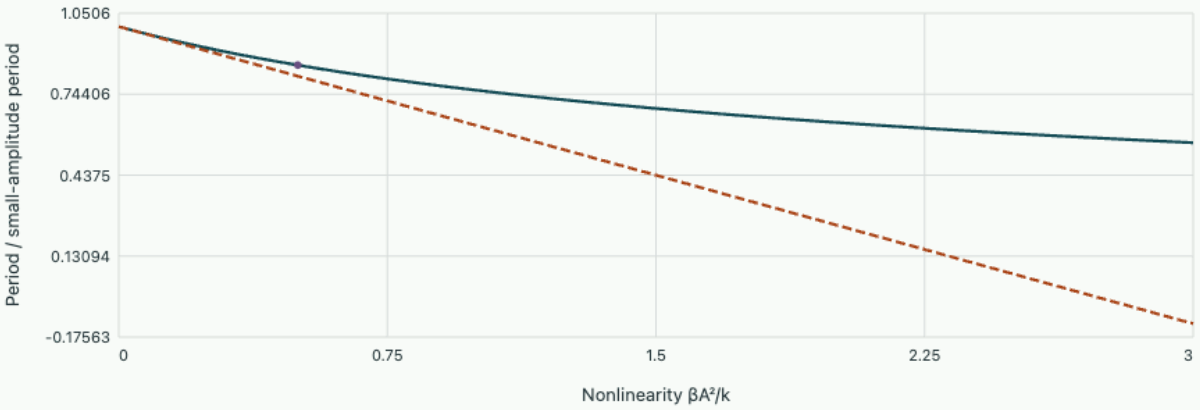

Energy integral | First-order expansion | Selected amplitude

Exact period ratio 0.85413. The expansion is local to βA²/k ≪ 1; it becomes negative if extrapolated far enough.

Infer stiffness from period data

For $m = 0.50$ kg, $k = 200$ N/m and $\alpha = 4.0 \times 10^4$ N/m³, $\omega_0 = 20.0$ rad/s. At $A = 0.020$ m the force ratio is 0.080, giving a leading frequency increase of 3.0% to 20.6 rad/s. At half this amplitude the predicted increase is 0.75%. Measure the period over several cycles at each amplitude, keeping the amplitude change due to loss small. A plot of frequency against the square of amplitude should be approximately straight near the origin. A nonzero intercept shift under a change of temperature could indicate a change in ordinary linear stiffness instead of a new nonlinear coefficient.

Compute the entire amplitude dependence of a pendulum

A cubic expansion is useful near equilibrium. For a pendulum it is possible to carry the energy calculation beyond every finite Taylor approximation. Take a point mass with fixed length ℓ, no friction and a release from rest at angle $0 < \theta_0 < \pi$. Its conserved energy gives

$$\dot\theta^2 = (2g/\ell)(\cos\theta - \cos\theta_0).$$

Use $\cos\theta = 1 - 2\sin^2(\theta/2)$. Defining $k = \sin(\theta_0/2)$ reduces the speed magnitude to $2\sqrt{g/\ell}\sqrt{k^2 - \sin^2(\theta/2)}$.

One quarter period is the time to travel between zero angle and the turning point. The reciprocal speed appears to diverge at the latter, but it has an integrable square-root singularity for every ordinary turning angle. To evaluate it stably, set $\sin(\theta/2) = k\sin u$. The factor $\cos u$ from differentiating cancels the same factor inside the square root. Four equivalent quarters give

$$T = 4\sqrt{\ell/g}\int_0^{\pi/2} \frac{du}{\sqrt{1 - k^2\sin^2 u}} = 4\sqrt{\ell/g}\,K(k).$$

Here K denotes the complete elliptic integral with modulus k. Expanding the integrand at small k and integrating the first correction gives

$$T/T_0 = 1 + k^2/4 + \cdots = 1 + \theta_0^2/16 + \cdots,$$

where $T_0 = 2\pi\sqrt{\ell/g}$. The positive correction is the familiar softening: increasing amplitude lengthens the period because the restoring torque grows more slowly than its linear extrapolation.

Decide when a small-angle clock loses accuracy

A pendulum of length 0.800 m has $T_0 = 1.794$ s at $g = 9.81$ m/s². At a release of 60.0°,

$$k = \sin 30^\circ = 0.500.$$

Evaluating the integral gives $K(0.500) = 1.68575$ and $T/T_0 = 2K/\pi = 1.0732$, hence $T = 1.926$ s. The weak-angle approximation gives

$$1 + (\pi/3)^2/16 = 1.0685.$$

It misses the exact period by roughly 0.008 s per cycle; a many-cycle timing record resolves the accumulated discrepancy.

As θ_0 tends to π, the integrand near $u = \pi/2$ approaches the reciprocal of a vanishing cosine. The integral diverges logarithmically, expressing the long time spent close to the unstable upper equilibrium. No finite polynomial in amplitude can reproduce that divergence. A numerical timing experiment should therefore locate regular zero crossings rather than demand a turning-point velocity of exactly zero in sampled data. Comparing the crossing intervals with the regularized integral distinguishes numerical resolution error from the genuine increase in physical period.

A way to evaluate the elliptic integral without a special-function library is to form the arithmetic–geometric mean. Begin with $a_0 = 1$ and $b_0 = \sqrt{1 - k^2}$, then replace the pair by their arithmetic and

geometric means. Both converge rapidly to a common M, and $K(k) = \pi/(2M)$. For the 60° release the first pair is 1 and 0.86603, the next pair is approximately 0.93301 and 0.93060, and the subsequent pair agrees near 0.93181. Taking the reciprocal of the common value directly gives the period ratio. This procedure supplies an accurate independent benchmark even when the small-amplitude expansion ceases to converge quickly.

Numerical quadrature and the arithmetic–geometric mean should agree at a fixed amplitude. If a period extracted from actual trajectories differs while these two evaluations agree, examine the dynamical time step, how release angle is measured, and whether the observed oscillations have suffered appreciable damping.

Chapter 12 · Bifurcation of a rotating hoop

Use an effective potential to locate competing equilibria and predict the frequency of small oscillations on either side of a stability change.

FROM FIRST PRINCIPLES

Find the instability threshold of the rotating hoop

Assume a frictionless bead constrained to a vertical circular hoop of radius R. The hoop rotates at prescribed constant angular speed Ω about its vertical diameter. With angle θ measured upward from the bottom, the bead moves along the hoop at speed $R\dot{\theta}$ and around the axis at speed $\Omega R\sin\theta$. These directions are perpendicular, and its gravitational height above the bottom is $R(1-\cos\theta)$. Thus its Lagrangian is

$$L = \tfrac{1}{2}mR^2(\dot{\theta}^2 + \Omega^2\sin^2\theta) - mgR(1-\cos\theta).$$

Apply the one-coordinate Lagrange equation. The rotation term tends to move the bead outward while gravity acts toward the bottom:

$$\ddot{\theta} = \sin\theta(\Omega^2\cos\theta - g/R).$$

Linearizing about the bottom gives

$$\ddot{\theta} \simeq (\Omega^2 - g/R)\theta.$$

For $\Omega^2 < g/R$ the coefficient restores a small displacement; above threshold the bottom has growing small disturbances. Setting the exact right side to zero gives the additional equilibrium and its range:

$$\Omega_c = \sqrt{g/R},$$

$$\cos\theta_* = g/(R\Omega^2) \quad (\Omega \geq \Omega_c).$$

The two nonzero angles are related by reflection. Their existence follows from the prescribed rotation, so a freely slowing hoop would require an additional dynamical coordinate.

DERIVATION AND APPLICATIONS

How high is the barrier between the two tilted equilibria?

In the rotating hoop, a new pair of stable angles appears where the bottom loses stability. Its curvature predicts a small-oscillation frequency; its depth determines whether a larger disturbance can carry the bead across the bottom. Consider a bead of mass m on a circular hoop of radius R spinning at

prescribed constant angular speed Ω about its vertical diameter. Ignore friction. Measure θ upward along the hoop from the bottom. The vertical height change is $R(1-\cos\theta)$ and the distance to the rotation axis is $R\sin\theta$.

The constrained bead has kinetic energy $mR^2(\dot\theta^2+\Omega^2\sin^2\theta)/2$. Collect the terms independent of $\dot\theta$ as the potential governing motion in the rotating coordinate:

$$U_{\text{eff}}(\theta)=mgR(1-\cos\theta)-\tfrac{1}{2}mR^2\Omega^2\sin^2\theta.$$

Write $s=\Omega^2R/g$ and differentiate. A tilted equilibrium exists only for $s>1$. At either stable angle θ_* substitute $\cos\theta_*=1/s$ into the potential and factor the result:

$$U'_{\text{eff}}=mgR\sin\theta(1-s\cos\theta),$$
$$U_{\text{eff}}(\theta_*)=-mgR\,\frac{(s-1)^2}{2s}.$$

The bottom has $U_{\text{eff}}(0)=0$. Subtracting the energies gives the barrier and the threshold angular speed for a bead launched from a tilted minimum toward the bottom:

$$\Delta U=mgR\,\frac{(s-1)^2}{2s},$$
$$|\dot\theta|_{\text{th}}=\sqrt{2\Delta U/(mR^2)}.$$

The velocity here is angular speed relative to the hoop. At threshold the trajectory approaches the unstable bottom asymptotically; crossing takes slightly more initial energy. Near $s=1$ the barrier collapses quadratically even though two distinct equilibria already exist. The externally maintained rotation can exchange ordinary laboratory energy with the bead, while the effective one-coordinate energy is conserved.

WORKED EXAMPLE

Estimate the speed needed to change branches

Change the inputs and investigate this derivation.

Take $m=0.0500$ kg, $R=0.200$ m and choose Ω so that $s=2.00$. The two minima then occur at $\pm60.0^\circ$ and the barrier is

$$mgR/4=0.0245\,\text{J}.$$

The tangential threshold speed is $\sqrt{2\Delta U/m}=0.990$ m/s, or 4.95 rad/s along the hoop. A launch at 0.800 m/s has only 0.0160 J and returns to its original branch.

SECOND APPLICATION

Use two measured angles to compare barrier depths

Change the inputs and investigate this derivation.

On the same hoop reduce the rotation until the two minima are at $\pm 36.9^\circ$. Their cosine is about 0.800, giving $s = 1.25$. The new barrier is $mgR(0.25)^2/2.50 = 0.00245$ J, a tenth of the previous value. The new threshold tangential speed is 0.313 m/s. A smaller change in angle than this tenfold energy reduction might suggest is a measurable feature of a shallow double well.

Locate the bifurcation by measuring curvature

A vertical hoop rotates about its vertical diameter at a prescribed angular speed Ω. A frictionless bead can move along the hoop. Measure θ from the bottom. The laboratory kinetic energy is $mR^2(\dot{\theta}^2 + \Omega^2 \sin^2\theta)/2$. In the equation for the bead the effective potential per unit mgR is $-\cos\theta - (\Omega^2 R/2g)\sin^2\theta$. Its derivative factors as $\sin\theta[1 - (\Omega^2 R/g)\cos\theta]$.

Open this experiment online

Try the calculation

Hoop radius (m) **0.3**

Imposed rotation (rad/s) **6**

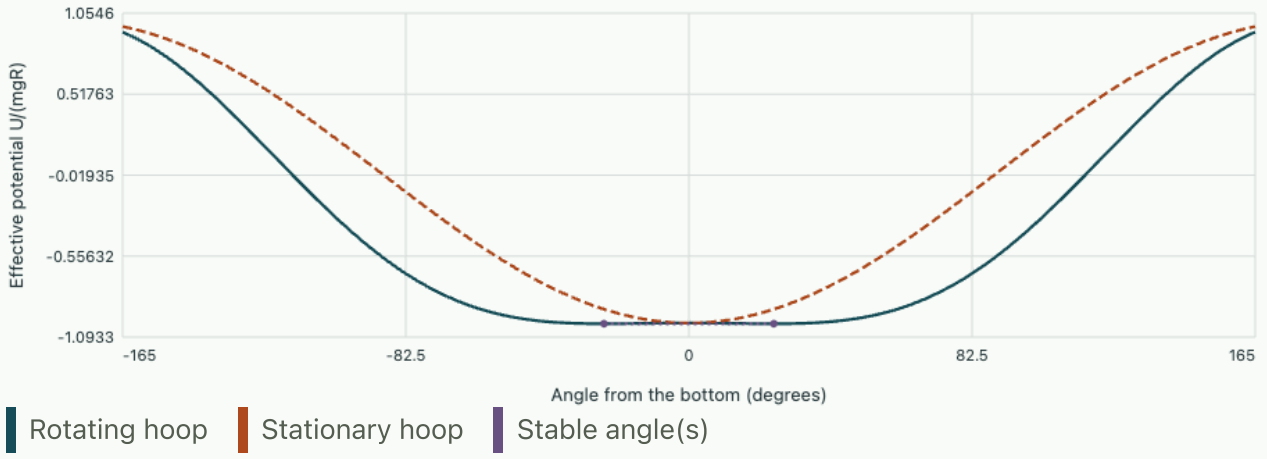

Critical speed 5.7184 rad/s. Bottom curvature in units of mgR is -0.10092. Stable angular magnitude 24.724°.

Plot the potential before and after crossing $\Omega_c = \sqrt{g/R}$. At a stable equilibrium the slope vanishes and the curvature is positive. Above the critical speed the bottom loses positive curvature and two stable angles appear. The motor holding Ω fixed exchanges angular momentum with the system. A freely rotating hoop with fixed total angular momentum describes a different experiment.

Reduce the constraint to one coordinate

A bead slides on a vertical circular hoop of radius R. An external motor rotates the hoop at prescribed constant angular velocity Ω about its vertical diameter. Let θ be the angle from the lowest point. The bead's height relative to that point is $R(1-\cos\theta)$ and its distance from the rotation axis is $R\sin\theta$. Assume negligible friction and a rigid constraint. The bead moves both along the hoop and azimuthally with it, even if θ is momentarily stationary.

In laboratory coordinates its speed squared is $R^2\dot\theta^2 + \Omega^2 R^2 \sin^2\theta$. Subtract gravitational potential energy from this kinetic energy to construct a one-coordinate Lagrangian. Lagrange's equation gives

$$\ddot\theta = \sin\theta(\Omega^2\cos\theta - g/R).$$

Although motion in the laboratory is constrained by a driven apparatus, the reduced equation is autonomous for constant Ω.

Track equilibria as the rotation rate changes

The torque vanishes at the bottom and the top because $\sin\theta = 0$. Off-axis equilibria also appear when $\cos\theta = g/(\Omega^2 R)$. They are possible only if the rotation exceeds $\Omega_c = \sqrt{g/R}$. Each positive-angle equilibrium then has a negative-angle partner. The two have equal energies because the apparatus is symmetric.

For small displacement from the bottom,

$$\ddot\theta \simeq -(g/R - \Omega^2)\theta.$$

Below threshold the bottom is stable with angular frequency $\sqrt{g/R - \Omega^2}$. As the threshold is approached this frequency tends to zero; the potential flattens. Above threshold the sign reverses and a small perturbation grows. Linearising about either displaced equilibrium instead gives a positive frequency squared $\Omega^2\sin^2\theta_{\mathrm{eq}}$. Measuring this small-amplitude response distinguishes two predictions: where the bead rests and how steeply it is restored when disturbed.

Interpret the effective energy

The reduced motion admits the effective potential $U_{\mathrm{eff}} = mgR(1-\cos\theta) - m\Omega^2R^2\sin^2\theta/2$. Its derivative predicts the reduced equation. Its negative centrifugal term differs in sign from the positive laboratory azimuthal kinetic energy. The motor supplies or absorbs work as the bead's distance from the rotation axis changes. Treating the bead's laboratory mechanical energy alone as conserved would therefore lead to the wrong equilibrium.

At exactly the critical rate, the quadratic terms in a small-angle expansion cancel and the first restoring term in U_{eff} is positive and quartic. A finite disturbance can still oscillate there, but its period depends on its amplitude. An arbitrarily small oscillation cannot be assigned a finite harmonic frequency at that point.

Estimate the transition in a real apparatus

With $R = 0.250$ m and $g = 9.81$ m/s² the critical rate is 6.26 rad/s, or about 59.8 rpm. At 5.0 rad/s the bead returns to the bottom with small-oscillation frequency $\sqrt{39.24 - 25} = 3.77$ rad/s. At 8.0 rad/s the two new equilibria satisfy $\cos\theta = 39.24/64 = 0.613$, or $\theta = \pm 52.2^\circ$. Small oscillations about either have angular frequency $8\sqrt{1 - 0.613^2} = 6.32$ rad/s.

When observing the transition, tilt of the axis or a small asymmetry of the hoop can favour one side. Hysteresis-like delays during a fast sweep can also arise from finite settling time in weak damping. Recording both equilibrium angles on slow sweeps and the independently measured oscillation frequency supplies a more discriminating test of the symmetric bifurcation than simply noting which side the bead occupies.

Break the symmetry with a weak bias

The two off-centre positions of the ideal rotating bead have equal energy. A small constant generalized torque τ_b favouring positive θ breaks that symmetry. Over a small working angular range it adds a term $-\tau_b\theta$ to the effective potential. Write the original potential relative to its value at the bottom as $mgR(1-\cos\theta) - m\Omega^2R^2\sin^2\theta/2$. Expanding near the critical rate $\Omega_c^2 = g/R$ gives quadratic coefficient $mR^2(\Omega_c^2 - \Omega^2)/2$. The quartic coefficient evaluated at threshold is $mR^2\Omega_c^2/8$.

On the high-speed side define $a = \Omega^2 - \Omega_c^2 > 0$, $b = \Omega_c^2/2$, and $h = \tau_b/(mR^2)$. To leading order stationarity and local stability become

$$b\theta^3 - a\theta - h = 0, \qquad 3b\theta^2 - a > 0.$$

With zero bias there are two symmetric minima and an unstable central position. Increasing positive bias deepens the positive minimum and eventually destroys the negative one. At the point where the negative minimum meets the adjacent maximum, both the stationarity equation and its derivative in θ vanish. Thus

$$\theta_* = -\sqrt{a/(3b)},$$

$$h_* = (2a/3)\sqrt{a/(3b)}.$$

The critical bias scales as $a^{3/2}$. Near the threshold a surprisingly small imperfection can remove one of the two resting positions entirely.

Estimate the bias needed to select a branch

Use a bead of mass 0.0500 kg on a hoop of radius 0.250 m. Then $\Omega_c^2 = 39.24$ s⁻². Set $\Omega^2 = \Omega_c^2 + 0.600$ s⁻², making $b = 19.62$ s⁻². The unbiased displaced equilibrium angles are approximately $\pm\sqrt{0.600/19.62} = \pm 0.175$ rad. As positive bias is increased, the negative branch disappears near $\theta_* = -0.101$ rad. The corresponding generalized acceleration is $h_* = 0.0404$ s⁻², giving $\tau_b = mR^2h_* = 1.26 \times 10^{-4}$ N m. A tangential force with moment arm R would supply about 0.505 mN.

This estimate uses both small angles and operation close enough to the critical speed that quartic truncation is accurate. An exact calculation differentiates the full trigonometric potential twice and solves the two equations simultaneously. In a slow sweep with weak damping, a bead initially on the unfavoured branch can remain there until its minimum disappears. Vibration or thermal agitation may make it switch earlier by crossing the remaining barrier. Repeating the sweep in both directions and at several bias amplitudes helps distinguish an imperfect constraint from random switching in a nearly symmetric system.

The same model predicts increasing sensitivity before an actual switch. Differentiate the cubic stationarity condition with respect to bias while following a particular equilibrium branch:

$$d\theta/dh = 1/(3b\theta^2 - a).$$

Its denominator is the local dimensionless restoring curvature. Thus a branch nearing disappearance both moves a large angular distance under a small bias increment and shows a very low small-oscillation frequency. Measuring those two effects on the same branch tests the local shape of the potential without requiring a precise measurement of the noisy switching moment. Away from a minimum the static slope can instead be negative, describing an unstable mathematical solution.

The sharp loss of a branch is best resolved with bias steps small compared with the measured interval between its creation and disappearance.

Where will a bead settle on a rotating hoop?

Choose zero potential at the bottom. Gravity contributes $mgR(1-\cos\theta)$; the rotating-frame centrifugal term contributes $-m\Omega^2R^2\sin^2\theta/2$. Inspect both the slope and the curvature at the bottom while increasing speed.

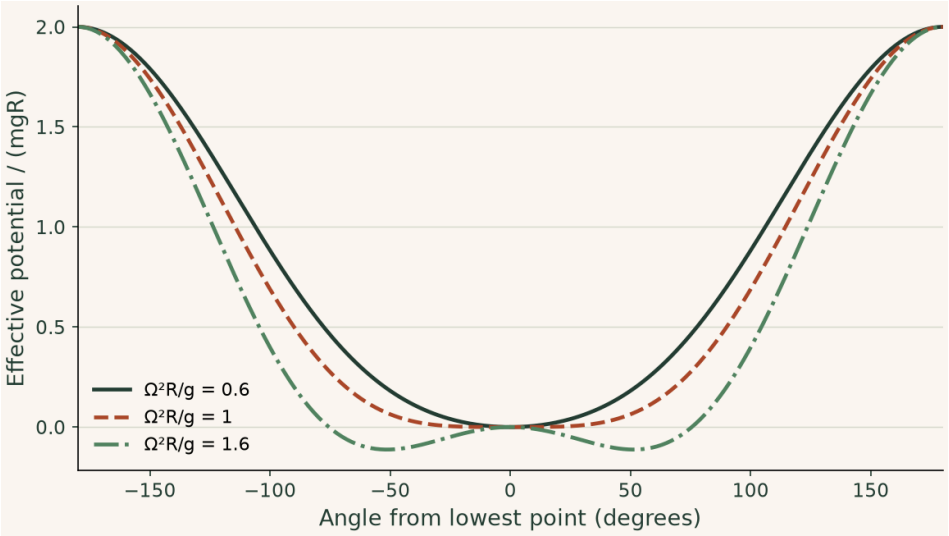

At $\Omega^2R/g = 1.6$ the two minima satisfy $\cos\theta = 0.625$, at approximately $\pm 51.3°$. At the critical value the quadratic term vanishes; the bottom is much flatter than an ordinary harmonic minimum.

▶ **Read values from the plot**

Problem sheet 6 · Nonlinear frequencies and broken symmetry

Identify nonlinear stiffness and track equilibria as a rotating constraint changes stability.

Fit a weak cubic spring

A mass of 0.20 kg has a natural frequency of 10.00 Hz at negligible amplitude. At 10.0 mm amplitude it oscillates at 10.03 Hz. Assume a restoring force $-kx - \beta x^3$. Estimate k and β, predict the shift at 5.0 mm and test the perturbation assumption.

▼ **Show the stiffness estimates**

The linear coefficient is

$$k = m(2\pi f_0)^2 = 790\,\mathrm{N/m}.$$

Retaining the fundamental of $\cos^3 \omega t$ gives $\Delta f / f_0 \simeq 3\beta A^2/(8k)$. Hence $\beta = 8k(0.0030)/(3\times10^{-4}) = 6.32\times10^{4}$ N/m³. The positive sign describes hardening. At half amplitude the shift falls by four, to 0.0075 Hz. The maximum cubic-to-linear force ratio at 10 mm is $\beta A^2/k = 0.0080$, compatible with a first-order estimate.

Which equilibria can hold a bead?

A bead slides without friction on a vertical hoop of radius 0.400 m rotating about its vertical diameter. Find the critical angular speed and stable positions at 6.00 rad/s. Determine the small oscillation frequency about either tilted position and compare with operation at 4.00 rad/s.

▼ **Show the stability calculation**

With angle measured from the bottom the effective potential per unit mass is $-gR\cos\theta - \Omega^2 R^2 \sin^2\theta/2$. Its derivative is $R\sin\theta(g - \Omega^2 R\cos\theta)$. The critical speed is

$$\sqrt{g/R} = 4.95\,\mathrm{rad/s}.$$

At 6.00 rad/s the tilted minima have $\cos\theta = 9.81/(36\times0.4) = 0.6813$, hence $\theta = \pm 47.1^\circ$. Curvature divided by R^2 gives $\omega^2 = \Omega^2\sin^2\theta$, or $\omega = 4.39$ rad/s. At 4.00 rad/s only the bottom is stable and $\omega = \sqrt{g/R - \Omega^2} = 2.92$ rad/s.

Tilt a symmetric double well

For dimensionless displacement x, a potential is $V/E_0 = x^4/4 - a x^2/2 - h x$ with $a = 0.12$. Find equilibria and barrier height at $h = 0$. Determine the magnitude of bias where one metastable well

disappears and explain why the transition can depend on sweep history.

▼ **Show the barrier and the loss of stability**

At zero bias stationary points solve $x(x^2 - a) = 0$. Curvature $3x^2 - a$ gives minima at $\pm\sqrt{a} = \pm 0.346$ and a maximum at zero. The energy barrier is

$$a^2 E_0/4 = 0.00360 E_0.$$

A minimum and adjacent maximum merge when $3x^2 = a$ and $h = x^3 - ax$. Thus

$$|h| = 2(a/3)^{3/2} = 0.0160.$$

A weakly damped or cold system initially captured in the unfavoured well can remain there as the bias crosses zero. In a slowly driven, damped experiment without appreciable fluctuations it switches near the disappearance of that minimum; noise can trigger earlier switching.

Reconstruct a binary orbit from a spectrum

Two spectral lines trace a circular binary with a period of 20.0 days. Their radial-velocity semi-amplitudes are 30.0 and 60.0 km/s. Take the orbit to be edge-on. Find the stellar separation, both masses and the orbital energy. How would the mass estimate change at an inclination of 60°? Use G = 6.6743 × 10^{-11} in SI units and one solar mass = 1.9885 × 10^{30} kg.

▼ **Worked solution**

The two stars orbit their common centre of mass with the same angular frequency. Their speeds add to give a relative circular speed of 90,000 m/s. Over 1,728,000 s the relative separation vector describes a circle of circumference 2πa, hence a = 2.475 × 10^{10} m. The speed ratio gives the inverse mass ratio. The star moving at 30 km/s is twice as massive as the other star.

The relative acceleration is v^2/a and the two-body attraction gives $G(M_1+M_2)/a^2$. Equating the expressions gives 3.00 × 10^{30} kg in total, about 1.51 solar masses. The individual masses are approximately 1.01 and 0.50 solar masses. The reduced mass is two ninths of the total. Its kinetic energy is $\tfrac{1}{2}\mu v^2$, and the total orbital energy is its negative, approximately −2.70 × 10^{39} J.

If the inclination falls to 60°, the observed speeds are projections of the larger orbital speeds. The separation scales as 1/sin i, and the inferred mass as 1/$\sin^3$ i. The total rises by a factor of 1.54. Spectroscopy alone fixes the mass ratio and a projected mass. An independent inclination from an eclipse or astrometric orbit breaks the degeneracy.

Explore these relations

- For the cubic spring, vary its dimensionless nonlinearity and compare the frequency correction and third harmonic. Open the live calculation.
- For the rotating bead, sweep the speed through the stability threshold and locate the equilibria. Open the live calculation.

Chapter 13 · Changing the coordinates of a moving trap

A translating trap looks stationary in its own coordinates. Derive the Hamiltonian measured by that observer, including the term that accounts for motion of the coordinate system.

What does a change of coordinates have to preserve?

A counter moving along a rail reports the bead position relative to the counter. Its reading alone does not transform the bead momentum or tell us how energy changes in the moving frame. Let the laboratory Hamiltonian be $H(q,p,t)$. The phase-space action integrates $p\dot{q} - H$ between specified configurations. Adding a total time derivative changes that integral only at the ends. It therefore provides a way to construct new coordinates in which the same interior trajectories make the action stationary.

Demand that the old and new action forms differ by an exact differential. A convenient function uses the old position and the new momentum as arguments. Subtract QP from it to convert the independent end variables. The product rule gives

$$p\,dq - H\,dt = P\,dQ - K\,dt + d(F_2 - QP) = dF_2 - Q\,dP - K\,dt.$$

Now compare the coefficients of the independent differentials separately. The new energy has an extra term whenever the coordinate map depends explicitly on time.

$$p = \partial_q F_2,$$

$$Q = \partial_P F_2,$$

$$K = H + \partial_t F_2.$$

For a simple test take $F_2 = \lambda q P$ with constant positive λ. Then $Q = \lambda q$ and $P = p/\lambda$. A position interval stretches while the conjugate momentum interval shrinks by the reciprocal factor. The product $dq\,dp$ stays fixed. This checks the derivative rules without using a particular force law.

Move the origin and then move the momentum

Take the trap centre to be $a(t)$ and the laboratory potential to be $k(q-a)^2/2$. Choosing $F_2 = (q-a)P$ gives

$$Q = q - a,\; p = P.$$

Thus the coordinate is relative position, but its conjugate momentum still equals the laboratory momentum. Hamilton's velocity equation reads $\dot{Q} = P/m - \dot{a}$, exactly the velocity seen by the moving counter.

To obtain a momentum equal to $m\dot{Q}$, choose $F_2 = (q-a)(P + m\dot{a}) + g(t)$. This produces $p = P + m\dot{a}$. Substitute it into the kinetic energy and the explicit time derivative of the generator. The cross terms $\dot{a}P$ cancel. The remaining terms depending on time alone can be removed by choosing $\dot{g} = m\dot{a}^2/2$. The result is

$$K = \frac{P^2}{2m} + \frac{kQ^2}{2} + m\ddot{a}\,Q,$$

$$m\ddot{Q} = -kQ - m\ddot{a}.$$

The apparent force comes from the acceleration of the reference point. A constant translation speed drops out of this final equation. A time-dependent acceleration can do work on the relative motion, so the bead's relative mechanical energy need not be conserved.

Predict a displaced equilibrium

Use a 0.50 kg bead and a spring with $k = 8.0$ N/m. Accelerate the support uniformly at 1.6 m/s² in the positive direction. A stationary bead in the accelerating frame has $Q_* = -m\ddot{a}/k = -0.100$ m. Relative oscillations about this new centre have the original angular frequency 4.0 rad/s. The curvature of the potential sets the frequency and the added linear term changes its minimum.

If the bead is initially at $Q = 0$ with zero relative velocity when acceleration starts, its subsequent displacement is

$$Q = Q_*[1 - \cos(\omega t)].$$

At $t = \pi/\omega = 0.7854$ s it reaches -0.200 m, twice the static shift. It then returns. An overdamped measuring device would instead approach the static reading without that overshoot. Damping has been omitted here.

Set the support acceleration

Predict the sign of the first turning point when the acceleration reverses. Change the acceleration, then change the spring stiffness. Track separately the position of the equilibrium and the time between successive extrema.

Open this experiment online

Try the calculation

Support acceleration (m/s²) **1.6**

Spring stiffness (N/m) **8**

The equilibrium is at -0.1 m. The first turning point is -0.2 m at 0.7854 s.

Tutorial on reconstructing the motion

A bead released from the old equilibrium reaches its first relative extremum at –0.060 m after 0.50 s. Find its angular frequency and the support acceleration.

▼ **Work through the solution**

The first extremum occurs after half a cycle, giving $\omega = \pi/0.50 = 6.283$ rad/s. The equilibrium shift is half the extremum, $Q_* = -0.030$ m. The equation for that shift gives

$$\ddot{a} = -\omega^2 Q_* = 1.18\,\mathrm{m/s^2}.$$

Both quantities follow from the trajectory without a separate mass measurement.

Check the momentum transformation directly by measuring kinetic energy. In a frame attached to a support moving at constant $0.30\,\mathrm{m/s}$, a 0.50 kg bead has $P = 0.20\,\mathrm{kg\,m/s}$ along the support velocity. What laboratory momentum and kinetic energy should an observer assign?

▼ **Work through the solution**

The moving-frame kinetic momentum is $m(\dot{q} - \dot{a})$. Thus $p = P + m\dot{a} = 0.35\,\mathrm{kg\,m/s}$, the relative kinetic energy is $P^2/(2m) = 0.0400\,\mathrm{J}$ and the laboratory kinetic energy is

$$p^2/(2m) = 0.1225\,\mathrm{J}.$$

Expanding the square gives the missing cross term $P\dot{a} = 0.0600\,\mathrm{J}$ and offset $m\dot{a}^2/2 = 0.0225\,\mathrm{J}$.

A support acceleration varies with time. How could you reconstruct it from a measured relative trajectory, and which measurements become unreliable first in the presence of position noise?

▼ **Work through the solution**

Rearranging the equation gives

$$\ddot{a} = -\ddot{Q} - kQ/m.$$

A static deflection measures only constant acceleration after transients are controlled. In a time-dependent experiment a second time derivative is unavoidable for this inversion. It amplifies short-time position noise, so fitted trajectories or independent acceleration data can test the reconstruction.

Further reading · Fließbach, Mechanik, Hamiltonformalismus · Tong, Classical Dynamics, canonical transformations.

Study the full derivation

Noether's theorem, boundary terms and measurable constants · Analytical mechanics from constraints to invariants

A constant of motion can survive when neither laboratory energy nor angular momentum is separately conserved. Construct the conserved quantity from an infinitesimal transformation of the action. Then use boosts, a screw symmetry, and a rotating potential to determine what measured combinations should stay fixed.

Chapter 14 · Recover a trajectory from a family of actions

In Hamilton–Jacobi theory a partial differential equation for one function replaces several trajectory equations. A falling bead makes the different roles of position, energy and arrival time explicit.

Use the end of the path as a variable

Let a bead move between a fixed initial event and an adjustable final event. Denote by $S(q,t)$ the action evaluated on the actual trajectory ending at (q,t). For a small change in the endpoint, the interior variation cancels by the Euler–Lagrange equation. If time stays fixed the boundary term is $p\,\delta q$. If time changes, part of the endpoint displacement comes from continuing along the existing path by $\dot q\,\delta t$. The remaining independent displacement is $\delta q - \dot q\,\delta t$. Thus

$$\delta S = p(\delta q - \dot q\,\delta t) + L\,\delta t = p\,\delta q - H\,\delta t.$$

It follows that $p = \partial_q S$ and $-H = \partial_t S$. Eliminate p to obtain

$$\partial_t S + H(q, \partial_q S, t) = 0.$$

The equation involves partial derivatives because it describes an entire family of possible endpoints. By contrast, $dS/dt = L$ along a single trajectory. A useful dimensional check is that a derivative of action with respect to length is momentum, whereas a derivative with respect to time is energy.

Separate time and build a clock from energy

For a time-independent Hamiltonian try $S = W(q;E) - Et$. With $H = p^2/(2m) + U(q)$, this gives

$$(\partial_q W)^2 = 2m(E - U).$$

A trajectory on the increasing-position branch has positive momentum, so an integral from a fixed reference position q_0 supplies W. Differentiate at fixed final position with respect to the family parameter E:

$$W = \int_{q_0}^{q} \sqrt{2m(E-U(s))}\,ds,$$

$$\partial_E W = \int_{q_0}^{q} \frac{m\,ds}{\sqrt{2m(E-U(s))}}.$$

The integrand of the second integral is $1/v$. Hence $\partial_E W$ is the travel time from the reference point. Setting $\partial_E S = 0$ chooses a departure time of zero with this lower integration limit. A different constant amounts to shifting the clock. At a turning point $p = 0$, the one-way branch must be changed to continue the motion.

Work two arrival-time problems

Let $q = x$ point downwards, $U = -mgx$, and release the bead through $x = 0$ with speed u. Its energy is

$$E = mu^2/2.$$

The integral yields

$$t = (\sqrt{u^2 + 2gx} - u)/g.$$

Squaring the relation after isolating the square root gives $x = ut + gt^2/2$, the same trajectory as Newton's equation. For $u = 2.0$ m/s, $g = 9.81$ m/s² and $x = 3.0$ m the arrival time is about 0.604 s. The endpoint momentum uses the final speed, about 7.93 m/s, rather than the average over the fall.

Reverse the experiment by pointing x upward in the same field. If $u = 4.0$ m/s, the maximum height is 0.815 m. A gate 0.50 m above launch is crossed twice. From $x = ut - gt^2/2$ the two times are 0.154 s and 0.661 s. The need for two branches of W is experimentally visible in those two timestamps. A calculation that takes the positive square root everywhere loses the return journey.

Compare two launch speeds

The plot shows upward trajectories and their common observation height. Lower the launch speed towards the value that barely reaches the gate. Watch what happens to the separation between the two arrival times.

Open this experiment online

Try the calculation

Upward launch speed (m/s) **4**

Gate height (m) **0.5**

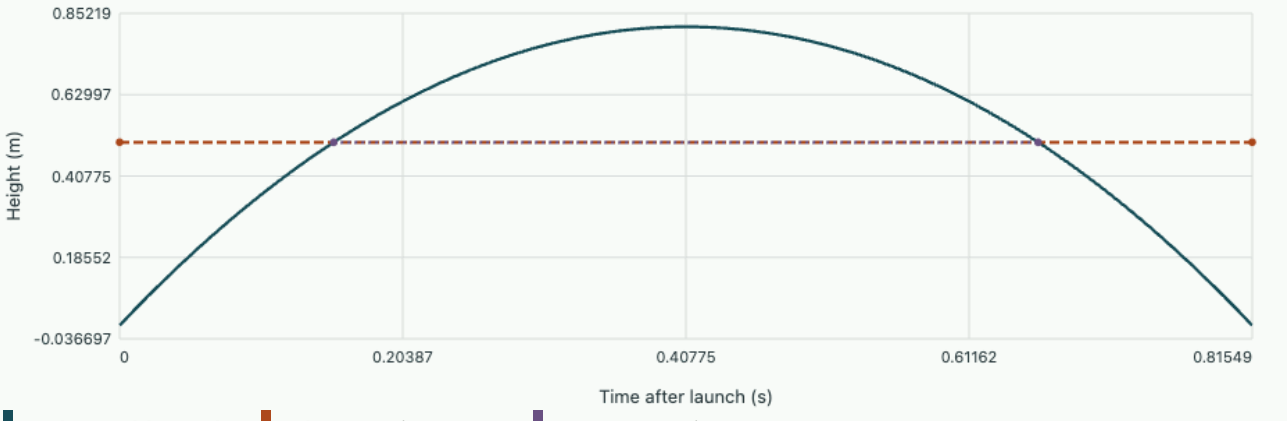

Peak height 0.8155 m. Ascending crossing at 0.1541 s and descending crossing at 0.6614 s.

Tutorial on the double root

A gate records two crossings 0.40 s apart in a uniform field of 9.81 m/s². How high does the trajectory rise above that gate?

▼ **Work through the solution**

The two crossings are symmetric about the maximum. The fall from the maximum takes 0.20 s, giving $g(0.20)^2/2 = 0.1962$ m. Equivalently the speed at the gate is $g(0.40)/2 = 1.962$ m/s and its kinetic energy per unit mass gives the same height.

Estimate the arrival-time sensitivity of a gate on the rising branch. At $u = 4.0\,\mathrm{m/s}$ compare $h = 0.50$ m with $h = 0.80$ m.

▼ **Work through the solution**

Implicit differentiation of $h = ut - gt^2/2$ at fixed launch speed gives

$$dt/dh = 1/(u - gt).$$

On ascent this is $1/\sqrt{u^2 - 2gh}$. Its value grows from $0.402\,\mathrm{s/m}$ at 0.50 m to $1.81\,\mathrm{s/m}$ at 0.80 m. Close to the top a small height error produces much larger timing uncertainty because the trajectory crosses slowly.

Does adding a constant C to a potential alter the predicted arrival times from Hamilton–Jacobi theory when the initial position and speed are unchanged?

▼ **Work through the solution**

Both the total energy label and potential shift by C. Hence $p = \sqrt{2m(E - U)}$ and the abbreviated action as a path integral of p are unchanged for that orbit. The full action acquires $-Ct$. Its spatial derivative and the time crossing predictions remain the same. Comparing the same numerical energy before and after the shift would specify different trajectories.

Further reading · Fließbach, Hamiltonformalismus · Tong, Hamilton–Jacobi theory.

Study the full derivation

Symplectic transformations, Poisson brackets and the geometry of measurements · Analytical mechanics from constraints to invariants

Two phase-space plots can enclose the same volume while predicting different responses to an impulse. Derive the stronger condition that makes a change of variables canonical, test it on measured linear maps and use Poisson brackets to propagate observables without solving separately for every coordinate.

Chapter 15 · Read a period from the area enclosed by an orbit

A track with a V-shaped potential has straight force segments but a strongly amplitude-dependent period. Its area in phase space gives a useful way to predict both the period and a slow change of the track.

Construct the closed area

For one bound degree of freedom at energy E, position runs between two turning points. In a mechanical Hamiltonian $p^2/(2m) + U(q)$, the upper branch of the phase portrait has positive momentum and the lower branch has its negative. The directed integral around one full orbit counts the enclosed area. Define the action J using the area divided by 2π. This choice makes its conjugate phase an angle measured in radians:

$$J(E) = \frac{1}{2\pi} \oint p\, dq = \frac{1}{\pi} \int_{q_-}^{q_+} \sqrt{2m(E - U(q))}\, dq.$$

Now change the energy slightly. The integrand vanishes at each regular endpoint, so the moving-endpoint contributions to the derivative vanish. In the interior $\partial p/\partial E = m/p = 1/v$. The derivative of the upper-branch area therefore measures the time to reach the opposite turning point.

$$\frac{dJ}{dE} = \frac{T(E)}{2\pi},$$

$$\omega(E) = \frac{dE}{dJ}.$$

This argument also explains why the construction becomes delicate near a separatrix. A trajectory can spend an arbitrarily long time near an unstable equilibrium, and T can diverge even though the enclosed area stays finite.

Background · Action variable

$$J = (2\pi)^{-1} \oint p\, dq$$

This area measure is defined for a closed cycle. It can change strongly near a separatrix even under a slow parameter variation.

Carry out the integral for a constant restoring force

Use $U(q) = F|q|$ with $F > 0$. The turning amplitude is $A = E/F$. Integrate the positive branch from 0 to A and use reflection symmetry. Substitution $s = E - Fq$ gives

$$J = \frac{4\sqrt{2m}}{3\pi F} E^{3/2},$$

$$T = \frac{4\sqrt{2mE}}{F} = 4\sqrt{\frac{2mA}{F}}.$$

The answer has an independent mechanical check. From a turning point the bead accelerates uniformly with magnitude F/m until the centre. Covering a distance A from rest takes $\sqrt{2mA/F}$, a quarter period. Doubling the amplitude increases the full period by $\sqrt{2}$. The abrupt change of force direction at the centre leaves the velocity continuous.

Slowly steepen the track

A slowly adjusted parameter can preserve the orbit action to leading order when the motion remains periodic and many cycles fit inside the adjustment time. For this trap m stays constant, so constant J requires $E^{3/2}/F$ to stay fixed. Therefore $E \propto F^{2/3}$,

$$A = E/F \propto F^{-1/3},$$

$$T \propto F^{-2/3}.$$

Work done by adjusting the slope changes the energy despite the approximate conservation of action.

Start with $m = 0.25$ kg, $F = 2.0$ N and $A = 0.080$ m. The initial energy is 0.160 J and the period 0.566 s. A slow eightfold increase of F makes the energy four times larger, 0.640 J, and the amplitude half as large, 0.040 m. The period becomes 0.141 s. In contrast, switching slopes instantaneously at the centre leaves the kinetic energy and position unchanged at that instant. The same final slope would then give amplitude 0.010 m. The route by which a parameter changes matters.

Compare closed orbits at constant action

The axes are position and momentum. Change the slope ratio. Predict how the turning positions and the central momentum move in opposite directions. Their changes balance in the enclosed area.

Open this experiment online

Try the calculation

Final to initial force ratio 2

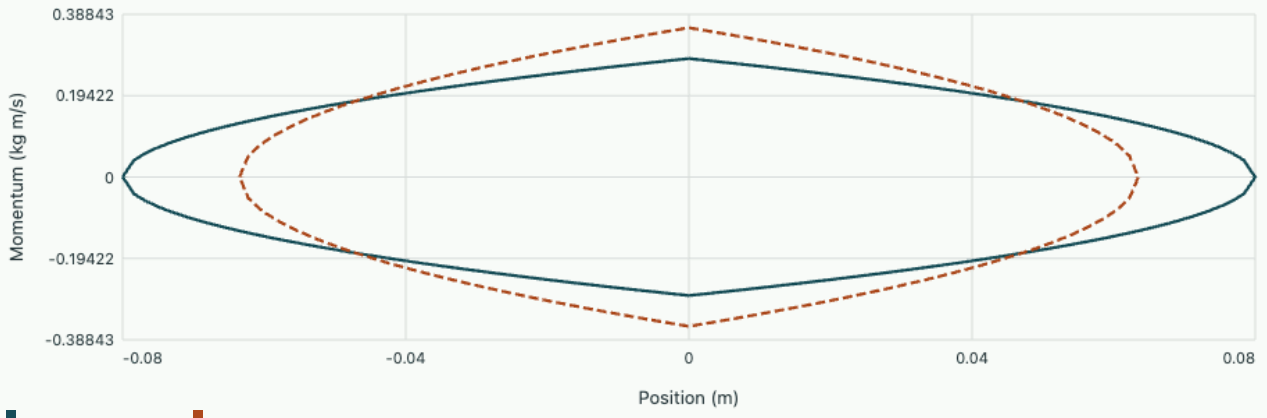

Final amplitude 0.0635 m, energy 0.254 J and period 0.3564 s.

Tutorial on inferring a change

After a slow adjustment the period is 64% of its original value. Find the force and amplitude ratios.

▼ **Work through the solution**

From $T_f/T_i = (F_f/F_i)^{-2/3}$, the force ratio is

$$0.64^{-3/2} = 1.953125.$$

The amplitude ratio is its inverse cube root, 0.800. Squaring the period formula with these values provides an independent check.

Derive a relation between the area action and the product of energy and period in the V trap. What fraction of the total energy is kinetic on a time average over one orbit?

▼ **Work through the solution**

The explicit formulas give $J = ET/(3\pi)$, a quantity with units of action. Along the orbit $p\,dq = p\dot{q}\,dt = 2K\,dt$. Hence $2\pi J = 2T\langle K\rangle$ and $\langle K\rangle = E/3$, leaving $2E/3$ in potential energy. This is an independent check using a measurable time average.

A trap is weakened gradually until the amplitude doubles. Find the predicted changes in energy and period, and state when the slow-ramp argument is most vulnerable.

▼ **Work through the solution**

The amplitude varies as $F^{-1/3}$, so doubling it requires reducing F to one eighth. The energy then falls to one quarter and the period increases fourfold. A ramp duration adequate initially can become too short compared to the final period. Checking the endpoint period alone is insufficient if the control has sharp changes during the ramp.

Further reading · Tong, action–angle coordinates and adiabatic invariants.

Study the full derivation

Action, angle and the slowing clock at a separatrix · Analytical mechanics from constraints to invariants

A phase portrait contains enough information to extract a period by differentiating an area. Use that fact to build a clock for finite-amplitude pendulum motion, determine precisely where slow-parameter invariance fails, and distinguish a librating trajectory from one that makes complete rotations.

Chapter 16 · From a chain of springs to an elastic field

A rod ringing after a small axial displacement can be described by one differential equation at every point. Derive that field equation, its boundary conditions and the range of wavelengths for which it represents a discrete chain.

Take a limit that represents the same rod

Divide a rod of cross-sectional area A, mass density ρ, length L and Young modulus Y into segments of length a. Let $u_j(t)$ be the axial displacement at a site. Each segment carries mass $\rho A a$. Under a small relative displacement Δu the strain is $\Delta u / a$. Hooke's law gives force $Y A \Delta u / a$, hence the segment spring constant is $Y A / a$. Refining the chain must change both its masses and its springs by these rules to preserve the material.

$$\rho A a \, \ddot{u}_j = \frac{Y A}{a} (u_{j+1} - 2u_j + u_{j-1}).$$

For a smooth displacement the second difference is $a^2 u_{xx} + a^4 u_{xxxx}/12 + \cdots$. Cancel a common factor of $A a$. The leading continuum equation is $\rho u_{tt} = Y u_{xx}$ with wave speed $c = \sqrt{Y/\rho}$. The next term already shows why sharp disturbances with wavelengths close to a require the discrete chain.

Vary the field and keep the endpoint term

Alternatively add the kinetic and elastic energy densities using u_x for strain. The action per unit length integrated over time is

$$S = \int dt \int_0^L dx \, \left(\frac{\rho A}{2} u_t^2 - \frac{Y A}{2} u_x^2 \right).$$

Vary u by any smooth small displacement that vanishes at the initial and final times. Integrating its time derivative by parts returns $-\rho A u_{tt}$. Integrating the space derivative by parts returns $+\partial_x (Y A u_x)$ together with an endpoint term $-[Y A u_x \, \delta u]_0^L$. The interior coefficient must vanish independently. A clamped end fixes $\delta u = 0$ there. A free end permits arbitrary virtual displacement and thus requires zero axial traction $Y A u_x = 0$. An externally applied force would contribute boundary work to the action. This reasoning keeps the correct equation even when stiffness and cross section vary with position.

Measure the first resonance

For a uniform rod clamped at zero, $u = X(x)\cos(\omega t)$ gives

$$X = C \sin(k x),$$

with $\omega = c k$. A free end at L requires $\cos(kL) = 0$, so $k_n = (n + 1/2)\pi / L$. With $L = 0.80$ m, $Y = 70.0$ GPa and $\rho = 2700$ kg/m³, $c = 5092$ m/s and the first axial resonance is

$$c/(4L) = 1591 \, \mathrm{Hz}.$$

Clamping both ends requires $X(L) = 0$, changing that first frequency to 3183 Hz. The material has stayed the same while the measured spectrum has changed.

For the infinite chain substitute $u_j = e^{i(kja - \omega t)}$ directly into the second difference. The factors sum to $2\cos(ka) - 2 = -4\sin^2(ka/2)$. Hence $\omega = 2c|\sin(ka/2)|/a$. At $ka = \pi/2$ the ratio to the continuum frequency is

$$2\sqrt{2}/\pi = 0.9003.$$

Shorter wavelength changes the phase advance between neighbouring sites more strongly, making the smooth-gradient approximation less accurate.

Test wavelength resolution

Change the number of sites per wavelength and read the discrete frequency relative to the continuum prediction. Compare the phase speed with the group speed $d\omega/dk$, which controls a narrow packet of modes.

Open this experiment online

Try the calculation

Sites per wavelength **10**

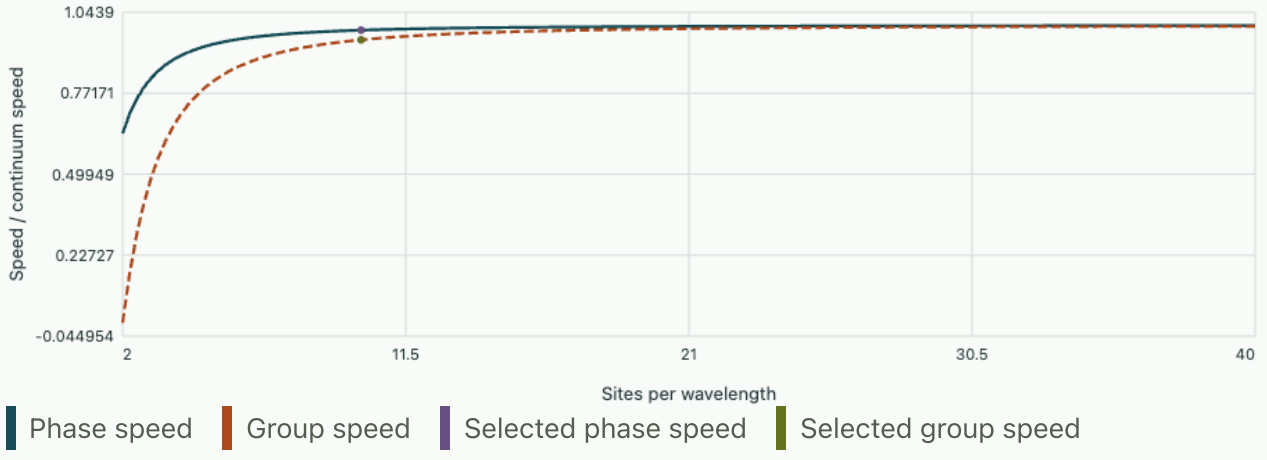

Frequency and phase speed are 98.36% of the continuum prediction. Group speed is 95.11%.

Tutorial on the continuum error

A mesh has ten sites per wavelength. Estimate its fractional phase-speed error first by series expansion, then with the sine formula.

▼ **Work through the solution**

With $x = ka/2 = \pi/10$, the ratio is $\sin x/x$. Keeping $1 - x^2/6$ predicts a deficit of 0.01645. Direct evaluation gives 0.01637, about 1.64%. Doubling the sites per wavelength reduces the leading error by a factor of four.

A frequency scan of the same rod finds equally spaced resonances from 1.59 kHz onwards at 3.18 kHz intervals. Predict the axial displacement at the support and the stress at the opposite end. Which observation distinguishes a clamped–free from a free–free rod?

▼ Work through the solution

The sequence $f_n = (2n+1)c/(4L)$ agrees with the clamped–free case. At the clamp displacement vanishes, while at the opposite end the axial derivative and therefore stress vanish. A free–free rod also has zero stress at both ends, but its nonzero resonances are integer multiples of $c/(2L)$; it also permits a zero-frequency rigid translation.

For a narrow wave packet at four sites per central wavelength, use the dispersion relation to compare the arrival of the centre of the packet with a single crest.

▼ Work through the solution

Here $ka/2 = \pi/4$. The phase travels at $c\sin(\pi/4)/(\pi/4) = 0.9003c$, whereas the envelope moves at $c\cos(\pi/4) = 0.7071c$. Over a fixed distance the packet centre arrives about $0.9003/0.7071 = 1.27$ times as late as a crest with that phase speed. A broadband pulse need not have one well-defined group speed.

Further reading · Fließbach, Kontinuumsmechanik · Tong, Phonons.

Study the full derivation

Action density, stress waves and the boundary that reflects them · Analytical mechanics from constraints to invariants

A chain of coupled masses becomes an elastic field when the wavelength is long compared with the spacing. Derive the field equation and its boundary traction from the same variation, follow energy and stress across a junction, and decide whether a measured pulse is limited by material waves or by numerical dispersion.

Chapter 17 · Proper time, momentum and a moving clock

A pair of light pulses lets observers compare clocks without assuming a universal time. Build the invariant interval and use it to calculate transit times and the energy exchanged by moving material.

Identify what every inertial observer can agree on

Assign coordinates x, t to events using rulers and synchronized clocks in an inertial laboratory. A light ray moving along the positive or negative axis obeys $x = \pm ct$. A linear transformation between two inertial laboratories must take each family of light rays into itself if both measure the same c. Introduce $u = ct - x$ and $w = ct + x$, coordinates constant on the two families. A boost rescales them. Reciprocity between inertial frames and spatial reflection give opposite rescalings,

$$u' = e^{\eta} u,\ w' = e^{-\eta} w.$$

Here the additive parameter η is called rapidity.

$$c^2 t'^2 - x'^2 = u'w' = uw = c^2 t^2 - x^2.$$

Adding and subtracting the transformed coordinates gives

$$ct' = ct \cosh \eta - x \sinh \eta,$$
$$x' = x \cosh \eta - ct \sinh \eta.$$

The moving origin obeys $x' = 0$, so

$$v/c = \tanh \eta,$$
$$\cosh \eta = \gamma = 1/\sqrt{1 - v^2/c^2}.$$

These statements concern pairs of events. An experiment involving a rod must separately specify which endpoint events are simultaneous in the observer's frame.

Follow one clock along its trajectory

Events on the same material clock have $dx' = 0$ instantaneously in its rest frame. The invariant interval then gives

$$d\tau = dt \sqrt{1 - v(t)^2/c^2}.$$

Over a curved path integrate this local relation. Two synchronized clocks reunited at the same event can have accumulated different proper times because their intervening paths differ.

Consider an inertially moving clock passing two fixed laboratory gates 12 light-microseconds apart. With $v = 0.80c$ the lab crossing interval is 15 µs. The travelling clock accumulates $15/1.6667 = 9.0$ µs. It measures the simultaneous distance between gates in its own frame as 7.2 light-microseconds. Dividing

that distance by $0.80c$ gives the same 9.0 µs. Combining a laboratory distance with a clock time from another frame would obscure this check.

From a clock to energy and momentum

Differentiate the spacetime position with respect to the invariant proper time. The resulting four-velocity transforms as a four-vector. For a particle of constant rest mass m, multiply by that mass to obtain the four-momentum $p^\mu = (E/c, \mathbf{p}) = m\gamma(c, \mathbf{v})$. The invariant norm is obtained in the rest frame and gives

$$E^2 - p^2c^2 = m^2c^4,$$

$$K = E - mc^2.$$

For low speed, expanding γ returns $K = mv^2/2$ to lowest order. For light, the massless relation $E = pc$ holds without defining a rest frame. These elementary cases are useful checks when adding the four-momenta of a system.

Imagine two identical material samples with equal and opposite speeds $0.60c$ close into a sealed calorimeter at rest in their centre-of-momentum frame. Ignoring the original container mass and any energy escaping, the total momentum vanishes and the invariant mass of the combined contents is $2\gamma m = 2.50m$. The excess $0.50mc^2$ over the original rest energies is internal energy in this frame. Energy conservation applies throughout the process.

Vary the gate experiment

Increase speed at fixed laboratory gate separation. Predict both the coordinate time and the travelling clock's proper time. At a fixed speed, doubling the distance doubles both readings.

Open this experiment online

Try the calculation

Speed / speed of light **0.8**

Gate separation (light-µs) **12**

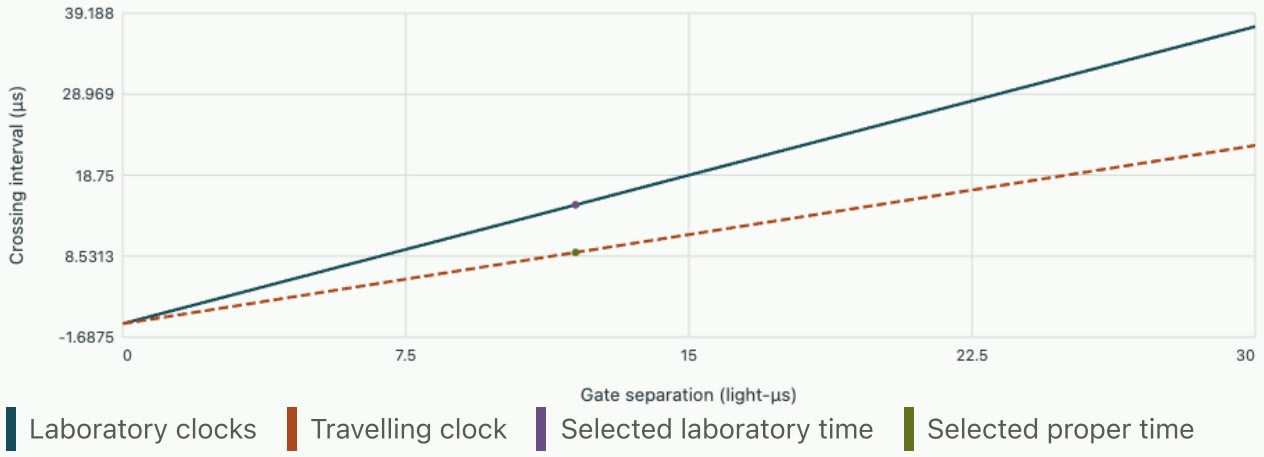

The laboratory records 15 µs. The travelling clock records 9 µs.

Tutorial on identifying the frame

A laboratory separates two gates by 24 light-microseconds. A travelling clock measures 18 µs between crossings. Determine the speed.

▼ **Work through the solution**

In units with distance in light-microseconds, the lab time is $24/\beta$ µs. The interval gives $18^2 = (24/\beta)^2 - 24^2$, so

$$\beta = 24/30 = 0.800.$$

The laboratory time is 30 µs. This inversion uses one distance and two events without assuming the clocks display the same elapsed time.

An emission and reception have laboratory separation 6 light-microseconds and time difference $10\,\mu s$. Could one inertial clock record both, and which speed would it need?

▼ **Work through the solution**

The interval is timelike because $10^2 - 6^2 = 64 > 0$. The unique inertial path between the two events has speed $0.6c$. Its measured time is $8\,\mu s$, consistent with $10/\gamma$ and $\gamma = 1.25$. A laboratory separation of 12 light-microseconds at the same time difference would be spacelike and could not be joined by such a clock.

In the laboratory a single light pulse has energy E and momentum E/c. Compare its invariant mass with that of two pulses of energy E travelling in opposite directions together as a system.

▼ **Work through the solution**

For one pulse $E^2 - p^2c^2 = 0$. For the pair the energies add to $2E$ and the vector momenta cancel. The system therefore has invariant mass $2E/c^2$. The invariant mass of a composite system depends on total four-momentum. Individual invariant masses alone do not specify it.

Further reading · Fließbach, Relativistische Mechanik · Tong, Dynamics and Relativity, chapter 7.

Study the full derivation

Relativistic collisions, centre-of-momentum energy and thresholds · Analytical mechanics from constraints to invariants

Two particles with the same total laboratory energy can have very different energy available for changing their internal state. Determine the energy and motion of the centre-of-momentum system, reconstruct two-body elastic scattering, and follow how a detector threshold transforms between frames.

Chapter 18 · Liouville flow and what an ensemble can remember

A cloud of identical noninteracting beads is released with slightly different initial positions and momenta. Its position distribution widens. Does the system occupy more phase space, or has its uncertainty merely changed shape?

Follow a small phase-space element

For one canonical degree of freedom the velocity of a point (q, p) is $(\partial_p H, -\partial_q H)$. A short-time map takes $\boldsymbol{z}$ to $\boldsymbol{z} + \boldsymbol{v}(\boldsymbol{z}, t)\, dt$. Its Jacobian matrix is $I + (\partial \boldsymbol{v}/\partial \boldsymbol{z})dt$; expanding the determinant gives $1 + (\nabla_z \cdot \boldsymbol{v})dt + O(dt^2)$. Hamilton's equations make the divergence zero because the two mixed second derivatives of a smooth Hamiltonian cancel. Each additional canonical pair contributes a similar cancellation. A time-dependent Hamiltonian may change energy but still preserve the instantaneous phase-space volume along the flow.

Conservation of the number of ensemble members in a moving phase-space box also gives the continuity equation $\partial_t f + \nabla_z \cdot (f\boldsymbol{v}) = 0$. The vanishing divergence leaves $df/dt = 0$ on each trajectory. A stationary mechanical system can admit $f = F(H)$ as a stationary distribution because trajectories stay on energy surfaces. Such stationarity alone does not imply that one trajectory explores an entire energy surface. For example, further integrals of motion restrict regular multidimensional trajectories.

Propagate a cloud released into free flight

For mass m, the exact map is $p = p_0,\ q = q_0 + t p_0/m$. Its determinant is one regardless of time. An initially uncorrelated cloud with variances s_q^2, s_p^2 has evolved covariance $C_{qp} = t s_p^2/m$. The new position variance is $s_q^2 + (t s_p/m)^2$, while the momentum variance stays fixed. Compute the determinant of this covariance matrix:

$$\sigma_q^2 \sigma_p^2 - C_{qp}^2 = s_q^2 s_p^2.$$

For a Gaussian the ellipse at a fixed multiple of the covariance radius thus retains its area while it shears. With $m = 1\,\mathrm{kg}$, $s_q = 1\,\mathrm{m}$, $s_p = 0.5\,\mathrm{kg\,m/s}$, and $t = 4\,\mathrm{s}$, the observed position standard deviation is $\sqrt{5} = 2.236\,\mathrm{m}$. The momentum standard deviation remains 0.5 and the covariance becomes $1.0\,\mathrm{kg\,m^2/s}$. Their uncorrected width product is 1.118 in action units. The square root of the covariance determinant is still 0.5. Multiplication of measured marginal widths alone falsely suggests an area increase.

Compare reversible shear and real drag

Now apply a linear drag $\dot{p} = -\gamma p$ to each bead with constant $\gamma > 0$. Its phase-space divergence is $-\gamma$, hence the map determinant after time t is $e^{-\gamma t}$. Direct integration gives

$$p = e^{-\gamma t} p_0,\ q = q_0 + (1 - e^{-\gamma t}) p_0/(m\gamma).$$

The cloud now genuinely loses area in the reduced bead description. A larger Hamiltonian model of bead plus environment can remain volume preserving. Choose a drag rate in the graph and compare the original, freely sheared and damped ellipses for the same observation time. Check there is a smooth zero-drag limit rather than substituting zero into a quotient.

Open this experiment online

Try the calculation

Time after release (s) **4**

Drag rate γ (1/s) **0.2**

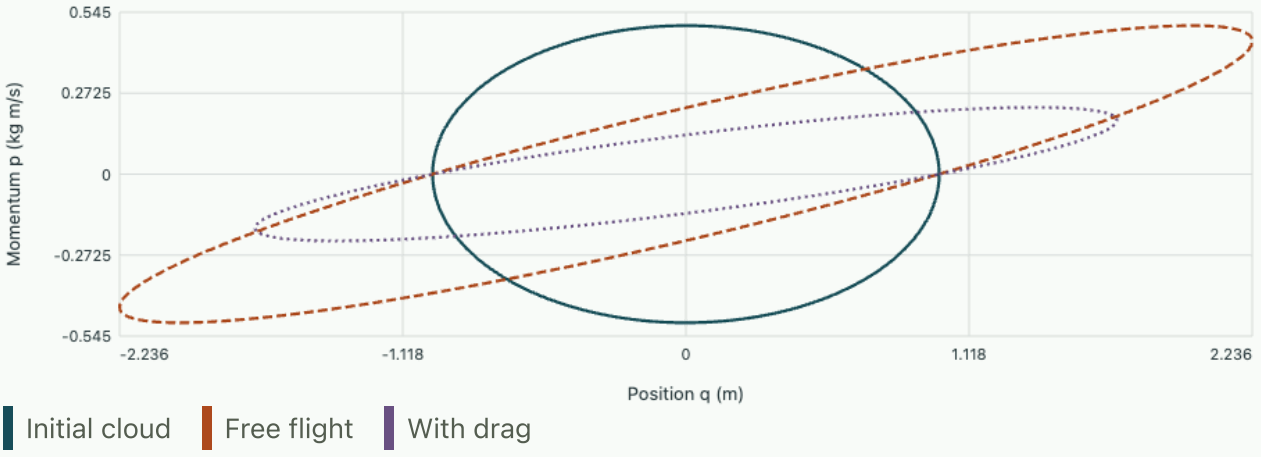

Free position spread 2.236 m. The damped ellipse retains 44.93% of its initial area and has position spread 1.702 m.

Tutorial on distinguishing a shear from dissipation

A harmonic oscillator maps its scaled quadratures by a rotation. Show why an initially anisotropic cloud can periodically sharpen in position without phase-space cooling.

▼ **Work through the solution**

Write its covariance as $R\Sigma_0 R^T$. Since $\det R = 1$, its determinant is unchanged. A rotation of one quarter turn exchanges the original widths, so position can sharpen when the original momentum width in scaled units was smaller. Energy extraction is unnecessary.

At $t = 3\,\mathrm{s}$ the measured ellipse area is 55 percent of the initial area in the linear-drag model. Infer γ. Which independent observable checks the inference?

▼ **Work through the solution**

$$\gamma = -\ln(0.55)/3 = 0.199\,\mathrm{s}^{-1}.$$

The ratio of final to initial momentum standard deviations should also be 0.55 for drag without random forcing. Added environmental fluctuations would modify that prediction.

Further reading · Cambridge classical dynamics, Hamiltonian flow and Liouville's theorem.

Chapter 19 · Parametric resonance and Floquet growth

A pendulum can gain energy when its length varies periodically even if no additive force acts on it. A modulation near twice a natural frequency amplifies one phase of the oscillation and attenuates another. The stability test concerns the growth of a perturbation over a complete modulation period.

Linearise the timing mechanism

Consider $\ddot{x} + 2\gamma\dot{x} + \omega_0^2[1 + h\cos(\Omega t)]x = 0$. Here h is the fractional modulation of the stiffness and γ is the amplitude damping rate. If $x = \dot{x} = 0$ exactly, the solution stays zero. Small fluctuations or an initial condition provide the seed. Direct differentiation of $E = [\dot{x}^2 + \omega_0^2(1 + h\cos\Omega t)x^2]/2$ yields

$$\dot{E} = -2\gamma\dot{x}^2 - h\omega_0^2\Omega x^2\sin(\Omega t)/2.$$

Energy transfer depends on the phase of x^2, which naturally contains a component at twice the oscillation frequency.

Near $\nu = \Omega/2 \simeq \omega_0$, write $x = A(t)e^{i\nu t} + A^*(t)e^{-i\nu t}$ with slowly varying A. Multiplication by $\cos(2\nu t)$ mixes the negative-frequency term back into the positive-frequency term with coefficient $h\omega_0^2/2$. There is also a component at 3ν, rapidly oscillating in this first-resonance approximation. Retain terms proportional to $e^{i\nu t}$, neglect $\ddot{A}$ and products of small damping with $\dot{A}$. This gives

$$2i\nu\dot{A} + (\omega_0^2 - \nu^2 + 2i\gamma\nu)A + (h\omega_0^2/2)A^* = 0.$$

Find the first instability tongue

Set $\Delta = \nu - \omega_0$ and keep leading terms in the small ratios $h, \gamma/\omega_0, |\Delta|/\omega_0$. The slow equations are $\dot{A} = (-\gamma - i\Delta)A + igA^*$ and their conjugate, where $g = h\omega_0/4$. The two-by-two characteristic equation is

$$(s + \gamma)^2 = g^2 - \Delta^2.$$

The faster exponent is

$$\operatorname{Re} s_+ = -\gamma + \operatorname{Re}\sqrt{(h\omega_0/4)^2 - \Delta^2}.$$

The oscillation grows when $g^2 > \gamma^2 + \Delta^2$. Exactly on resonance this gives $h > 4\gamma/\omega_0$. With $\omega_0 = 10\,\mathrm{s}^{-1}$, $\gamma = 0.10\,\mathrm{s}^{-1}$ and $h = 0.08$, $g = 0.20\,\mathrm{s}^{-1}$, giving an on-resonance doubling time $\ln 2/0.10 = 6.93\,\mathrm{s}$. The approximate growing interval in drive angular frequency is $20 \pm 0.346\,\mathrm{s}^{-1}$. A large-amplitude real oscillator can saturate as its natural frequency changes with amplitude, a mechanism absent from this linear equation.

Compute the period map without averaging

Integrate the original linear equation over one drive period from two independent initial states $(1, 0)$ and $(0, 1)$. Their final columns form a matrix M, which maps every initial perturbation over the same period T. After j periods the map is M^j; the maximum asymptotic amplitude exponent is $\ln \max |\lambda_i(M)|/T$. Its determinant also has an exact check $e^{-2\gamma T}$ from the divergence in the $(x, \dot{x})$ plane. The calculation below integrates both columns by fourth-order Runge–Kutta. Compare the numerical Floquet exponent with the averaged prediction as the modulation depth increases. Both curves describe growth rates, including negative rates for decay.

Open this experiment online

Try the calculation

Fractional stiffness modulation	**0.08**
Damping γ (1/s)	**0.1**
Drive frequency Ω (rad/s)	**20**

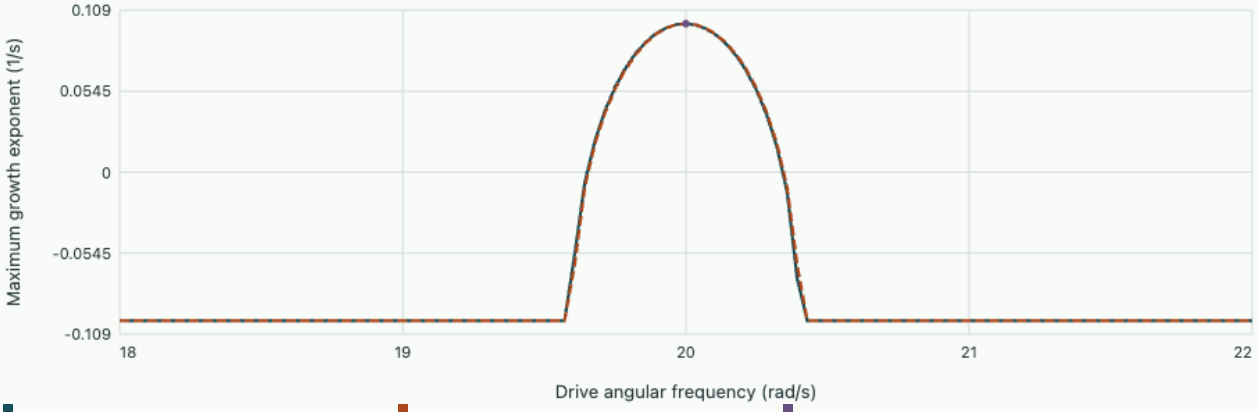

At Ω = 20 rad/s, numerical exponent 0.09997 s⁻¹ and averaged exponent 0.1 s⁻¹. Amplitude doubling time 6.934 s.

Tutorial on phase-sensitive amplification

At exact resonance and zero loss, substitute $A = X + iY$ into $\dot{A} = igA^*$. Identify the two special quadrature directions.

▼ **Work through the solution**

Equating real and imaginary parts yields

$$\dot{X} = gY,\ \dot{Y} = gX.$$

Along $Y = X$ both grow at g, whereas along $Y = -X$ they decay at g. These directions reflect how timing the stiffness change can add or remove work on each cycle.

On resonance an oscillator with $\omega_0 = 40\,\mathrm{s}^{-1}$ first grows near $h = 0.03$. Estimate its small-signal damping and its free amplitude e-folding time.

▼ **Work through the solution**

From the weak-modulation threshold $\gamma = h\omega_0/4 = 0.30\,\mathrm{s}^{-1}$. Without modulation the underdamped free amplitude falls as $e^{-\gamma t}$, giving $3.33\,\mathrm{s}$. Threshold uncertainty or nonlinear frequency shifts propagate into this inference.

Further reading · Verhulst, Utrecht University, perturbation analysis of parametric resonance.

Study the full derivation

Canonical perturbations, small denominators and resonant capture · Analytical mechanics from constraints to invariants

A weak periodic force can produce a bounded ripple on most trajectories and a large change on a narrow band of initial conditions. Derive the averaging transformation away from resonance, construct the slow resonant dynamics where that transformation fails, and estimate the physically observable width and time scale of a resonance.

Chapter 20 · Reading Earth's rotation from a pendulum trace

A free pendulum supplies two clocks. The bob returns in seconds, while the axis traced on the floor takes hours to rotate. Derive both rates from the tension and gravity, then work out what a camera actually measures and how a slightly imperfect suspension can imitate part of the signal.

A clock in a room that is itself rotating

Hang a bob from a long, flexible thread. Mark an east–west line on the floor, pull the bob a little way east of its resting point and release it without a push. Watching a few passages through the centre usually suggests a fixed swing plane. Compare photographs taken hours apart, however, and the line traced in the room may point somewhere else. To describe that observation we need the acceleration relative to the room. A distant inertial observer and a camera attached to the building do not use the same time derivative of a rotating vector.

For a vector expressed in axes rotating with angular velocity $\boldsymbol{\Omega}$, its inertial derivative is its rotating-frame derivative plus $\boldsymbol{\Omega} \times \mathbf{A}$. Apply this rule twice to position. For steady rotation the acceleration contains the local acceleration, twice the cross product of rotation rate with relative velocity, and the centrifugal contribution with the opposite apparent force when moved to the equation for relative acceleration. The motion of the support and the steady centrifugal force are already included when a plumb line defines local vertical and a gravimeter supplies g. Using that measured g a second time as a purely gravitational inertial acceleration would double-count part of the effect.

Choose x east, y north and z up. At latitude λ the vertical component of Earth's angular velocity is $f = \Omega \sin \lambda$. For a nearly horizontal bob velocity the product of the horizontal rotation component with that velocity is vertical. It therefore changes the tension to first order but makes no leading horizontal Coriolis force. Small horizontal displacements tilt the thread by approximately x/L and y/L; multiplying by the equilibrium tension mg gives the linear restoring components. Ignoring damping and spatial changes of effective gravity across the apparatus, the result is

$$\ddot{x} = -\omega_0^2 x + 2 f \dot{y},$$

$$\ddot{y} = -\omega_0^2 y - 2 f \dot{x},$$

$$\omega_0^2 = g/L.$$

A positive eastward velocity thus produces a southward sideways acceleration at positive latitude. Checking this sign using an actual right-handed east–north–up triad prevents a correct rate from being reported in the wrong direction. The Coriolis force has zero dot product with the horizontal velocity. It can change the trace while doing no work, so constant mechanical energy is consistent with a slowly turning pattern.

How two nearby circular modes make a turning line

Put $u = x + iy$. Multiplication by i turns a horizontal vector to the left through a right angle. The coupled real equations become

$$\ddot{u} + 2if\dot{u} + \omega_0^2 u = 0.$$

Seek a rotating coordinate $u = e^{-ift}v$. The two terms proportional to $\dot{v}$ cancel and the equation for v is a harmonic oscillator with $\nu^2 = \omega_0^2 + f^2$. This is an exact solution of the linear model with the stated effective local gravity. Terms of order Ω^2 omitted in constructing an ideal local apparatus would matter if one tried to measure the tiny quadratic correction to the swing period itself.

The release specifies both a position and a velocity in the room. For $u(0) = A$ and $\dot{u}(0) = 0$ the initial conditions for v are A and ifA. Hence

$$u(t) = Ae^{-ift}\left[\cos(\nu t) + i\frac{f}{\nu}\sin(\nu t)\right].$$

In the second set of axes the point traces an ellipse with semiaxis ratio $|f|/\nu$. Its long axis rotates in the floor frame at signed rate $-f$. Omitting the small sine term gives an attractive sketch, but that approximation gives the bob the initial sideways velocity $-ifA$. The experiment genuinely released from rest discriminates between these initial conditions even though the ellipse width is too small for many classroom measurements.

Equivalently expand the sine and cosine into circular exponentials. The two counter-rotating circular motions have positive angular-speed magnitudes $\nu - f$ and $\nu + f$. Their splitting is $2f$, whereas the line azimuth drifts at one half of that splitting with the sign set by the floor axes. A frequency spectrum with inadequate resolution may see a single broad swing peak. The orientation of many short traces measures the beat without requiring a direct observation of two separate spectral peaks.

Open editable notebook Download .ipynb

A numerical prediction for a camera in the hall

Take $L = 10.0$ m, $g = 9.81$ m/s² and $\lambda = 48^\circ$. Earth turns through 2π radians in a sidereal day, approximately 86,164 s. This gives $f = 5.42 \times 10^{-5}$ rad/s. The swing period is 6.34 s; the clockwise azimuth change is about 11.18° in one hour. A measurement three hours after release should therefore rotate the trace through 33.5°. At a 15 cm release amplitude the off-axis semiaxis predicted in rotating swing axes is only about eight micrometres. A visually broad ellipse has another cause worth investigating.

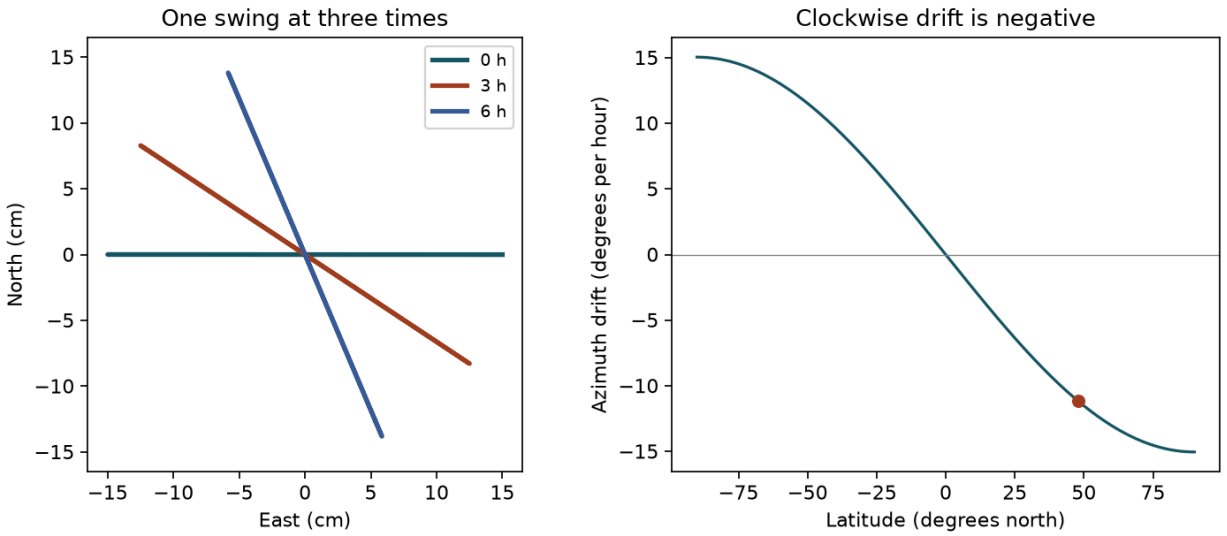

Each coloured line on the left covers one complete oscillation at the indicated time. Their directions change even though the support imposes no preferred horizontal direction. The point on the right uses the same latitude.

Try it · Foucault

Change the inputs and compare the recalculated curves with the preceding derivation and baseline figure. The axes give the units; the numerical readout states the model assumptions and any limiting cases. Reset the inputs to return to the reference setting.

Open this live calculation

Try the calculation

Latitude (degrees north) 48

Hours after release 3

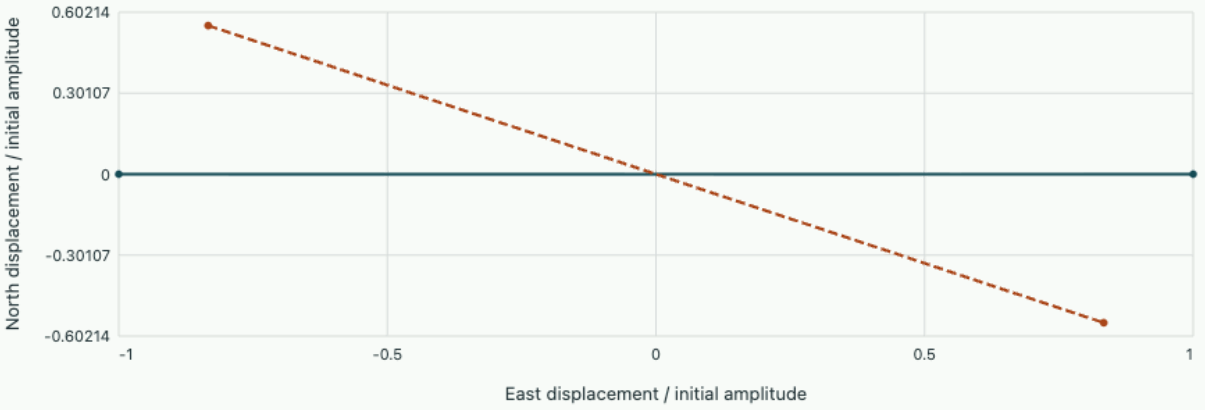

Initial swing axis Swing axis at chosen time

Leading-order Foucault azimuth drift -11.178 degrees/hour. Directed axis rotates by -33.533 degrees. Small swing amplitude and Earth rate much smaller than the pendulum frequency are assumed.

Download the corresponding editable notebook. The browser recalculates the reduced equations directly; the notebook exposes the full calculation and its checks.

The notebook draws each short trace by evaluating the coupled solution at actual laboratory times, allowing the bob to complete many oscillations between windows. A second panel holds Earth fixed and varies the observer's latitude instead. Try reversing the latitude before running the cells. The direction of rotation should reverse; the fast period and magnitudes of the two horizontal extents should agree after the reflection of the north coordinate. The optional OneSimulation run integrates the two real second-order balances written as four first-order equations. The numerical endpoint is compared with the complex solution, which tests signs and time step independently of the plot.

There are two meanings of a return. A directed arrow attached to the long positive axis turns through 360° in about 32.2 hours here. A painted line on the floor has no arrow. Its geometrical orientation repeats after 180°, or around 16.1 hours. Neither interval promises that the bob will occupy exactly its

starting position with exactly its original velocity then. That stronger recurrence would require the fast and slow phases to line up simultaneously.

Extract azimuth from positions with no marked turning point

A practical measurement records pairs of east and north coordinates at evenly spaced times. Subtract the local mean to remove the camera origin and form the two-by-two covariance matrix of positions in a time window. For a fixed straight swing along a unit vector $\mathbf{e}$, the position is $A\mathbf{e}\cos\nu t$. Averaging over complete cycles gives $A^2\mathbf{e}\mathbf{e}^{\mathsf{T}}/2$; its larger-eigenvalue eigenvector therefore estimates the swing direction. The smaller eigenvalue measures transverse spread, which can include noise, optical distortion or a real elliptical orbit. Fitting a slope y/x would instead be singular just when the line passes the north axis.

The principal direction is defined modulo π. A robust way to unwrap it is to double its angle, unwrap the result as a usual full-circle angle, and then divide by two. Choose a window containing many fast cycles but little slow rotation. If consecutive windows are separated by a day, the smaller principal-angle change can have the wrong sign after unwrapping. Predict the largest plausible rotation before choosing a sampling interval. A useful comparison is to fit the same drift with several window lengths and check whether the result stays within the uncertainty due to noisy coordinates.

A suspension with unequal horizontal stiffnesses produces different natural frequencies even in a laboratory with $f = 0$. Release away from its principal axes and the two linear oscillations accumulate relative phase, turning an initially straight trace into an appreciably open ellipse. At the north pole an ideal device has maximal Coriolis rotation; at the equator the linear vertical-component model has none. A nonzero equatorial drift is thus a reason to inspect the suspension, ellipticity, air currents or camera geometry. Rotating the release direction relative to the support is a further discrimination because a true latitude dependence does not select a preferred horizontal spring direction.

Tutorial on phase, latitude and identifiable quantities

A camera sees the line turn clockwise by 42.0 degrees in four solar hours. Estimate the latitude. How does a two-degree uncertainty in the measured angle propagate?

▼ **Work through the solution**

The rate is 10.5 degrees per hour, while Earth's sidereal angular speed is 15.041 degrees per solar hour. The sine of latitude is their ratio, approximately 0.698, giving about 44.3 degrees north. A two-degree angle uncertainty means 0.5 degree per hour in the rate. Dividing by the equatorial rate and by the cosine of 44.3 degrees gives about 0.046 rad, or 2.7 degrees, of local latitude uncertainty. The same inference becomes ill-conditioned close to a pole.

Double the thread length but keep the release angle small. Which observable changes by a factor of the square root of two and which one stays fixed?

▼ **Work through the solution**

The fast period grows approximately as the square root of length, so a 10 m bob's 6.34 s becomes about 8.97 s at 20 m. The slow angular rate still equals minus the local vertical component of Earth's rotation. At fixed linear amplitude the fractional transverse width grows because the fast angular frequency drops. The dependence of the width does not imply that the slow rotation accelerates.

A 120 s camera window is used at 48 degrees north. Estimate its number of fast cycles and drift within the window. Would a 3 h window make a better single direction estimate?

▼ **Work through the solution**

At 10 m there are about 18.9 cycles in 120 s, and the swing plane turns only 0.37 degree. Endpoint weighting or an integer number of cycles can improve the covariance estimate. Over three hours the true azimuth changes about 33.5 degrees. Averaging all of those samples gives an orientation intermediate between the endpoints and appreciable transverse variance even for a perfect apparatus. Several shorter windows resolve the secular rotation.

Further reading · Tevian Dray, Oregon State University · The Foucault Pendulum (PDF)

Problem sheet 7 · Reconstructing an accelerating trap

An optical stage can produce either a harmonic potential or a triangular one. Use a harmonic trap to calibrate the stage acceleration, then predict the motion in a different trap whose orbit area can be integrated analytically. Record each prediction before changing a control.

Calibrate the acceleration from the trace

A 0.50 kg test carriage in a spring of stiffness $8.0\,\mathrm{N/m}$ starts at rest relative to the support. After a sudden change to constant support acceleration, its first relative turning point lies at $-0.20\,\mathrm{m}$ at $0.785\,\mathrm{s}$. Infer the acceleration using the signed displacement. Use the time independently to check the assumed stiffness.

▼ **Work through the solution**

In the support frame the equilibrium is $Q_* = -ma/k$, and a carriage starting at the old centre reaches $2Q_*$ at its first turning point. Thus $Q_* = -0.10\,\mathrm{m}$ and $a = 1.60\,\mathrm{m/s^2}$. The half-period is

$$\pi\sqrt{m/k} = 0.7854\,\mathrm{s}.$$

The time tests k/m without requiring the displacement calibration.

Reproduce the displacement and turning time in the accelerating harmonic trap

Check an independent calibration with a slow change of slope

Return the support to inertial motion and fit a 0.25 kg test mass in $U = F|Q|$. Begin at $F = 2.0$ N, amplitude 0.080 m. Increase the slope slowly by a factor of eight. Predict the final energy, turning amplitude and period. Which combination of measured turning amplitude and slope would test preservation of orbit area?

▼ **Work through the solution**

The orbit action is proportional to $E^{3/2}/F$ at fixed mass. Hence $E_f = 0.160 \times 8^{2/3} = 0.640\,\mathrm{J}$,

$$A_f = E_f/16 = 0.040\,\mathrm{m},$$

$$T_f = 4\sqrt{2mA_f/F_f} = 0.1414\,\mathrm{s}.$$

Substitution of $E = FA$ gives $J^2 \propto FA^3$, so the measured product FA^3 should stay fixed in the slow limit. Check this product as well as the period.

Compare the two measured phase-space areas

Combine the two experiments

Restore the initial triangular slope. Ramp the calibrated stage acceleration $a = 1.60\,\mathrm{m/s^2}$ from zero over many periods, smoothly at each endpoint. Derive the new right and left turning distances relative to the support. Predict whether the orbit area changes at leading order.

▼ **Work through the solution**

The inertial contribution to potential energy is maQ. The two positive slope magnitudes are $F + ma$ on the right and $F - ma$ on the left. Both must remain positive for confinement. Integrating each half of the triangular orbit separately gives

$$J \propto E^{3/2}[1/(F + ma) + 1/(F - ma)].$$

Set this equal to the original value $2E_0^{3/2}/F$. Writing $s = ma/F = 0.20$ gives

$$E = E_0(1 - s^2)^{2/3} = 0.1557\,\mathrm{J}.$$

The right distance is $E/2.4 = 0.0649\,\mathrm{m}$, and the left distance $E/1.6 = 0.0973\,\mathrm{m}$. The orbit becomes asymmetric while its area is conserved to leading adiabatic order.

Design a falsification test

If both turning positions have a common, unknown camera magnification, which quantity still tests the calibrated acceleration? What limit makes the assumption of a slowly adjusted bound orbit fail?

▼ **Work through the solution**

Divide the left distance by the right. The common energy and camera scale cancel, leaving $(F + ma)/(F - ma) = 1.50$. As $|ma|$ approaches F, one confining slope approaches zero and the period grows. A ramp slow at zero acceleration may then fail the separation-of-time-scales condition. At $|ma| \geq F$ the potential no longer confines both sides.

Problem sheet 8 · Can the intermediate axis instability be measured before a body turns over?

A marked rigid body rotates in free flight. A camera sees an apparently steady rotation followed by a rapid change of orientation. Obtain a growth rate from torque balance, identify the invariant deciding the local geometry and design a measurement that separates exponential growth from a bad estimate of the initial alignment.

Obtain the equations in the frame that moves with the body

Let $I_1 < I_2 < I_3$ be distinct principal moments. Express angular momentum in body components. If there is no applied torque, explain why the time derivatives of those three components do not all vanish. Derive the equation for each angular velocity before considering any equilibrium.

▼ Work through the solution

A body basis vector has inertial derivative $\boldsymbol{\omega} \times \mathbf{e}_i$. Differentiating the expansion of angular momentum in that basis gives

$$(d\mathbf{L}/dt)_{\text{inertial}} = (d\mathbf{L}/dt)_{\text{body}} + \boldsymbol{\omega} \times \mathbf{L}.$$

In principal axes the inertia tensor is constant and diagonal, so $L_i = I_i \omega_i$. Setting the left hand side to zero gives

$$I_1 \dot{\omega}_1 = (I_2 - I_3)\omega_2 \omega_3,$$
$$I_2 \dot{\omega}_2 = (I_3 - I_1)\omega_3 \omega_1,$$
$$I_3 \dot{\omega}_3 = (I_1 - I_2)\omega_1 \omega_2.$$

Multiply the equations by their respective ω_i and add. The coefficients sum to zero and the kinetic energy is constant. Dot the vector equation with $\mathbf{L}$ and the cross product drops out, proving conservation of its norm. These are two independent checks on a numerical trace.

Identify the instability from two conserved quantities

Set the nominal spin to $\omega_2 = \Omega$. Linearise in the two transverse components and find the characteristic exponents. Then explain the same phenomenon without differentiating a perturbation a second time.

▼ Work through the solution

The equation for $\dot{\omega}_2$ contains only the product of the small perturbations. To first order Ω stays fixed. Put $a = (I_3 - I_2)\Omega / I_1$,

$$b = (I_2 - I_1)\Omega / I_3.$$

The remaining equations are

$$\dot{\omega}_1 = -a\omega_3,$$
$$\dot{\omega}_3 = -b\omega_1.$$

Both a and b are positive for positive spin, so $\ddot{\omega}_1 = ab\omega_1$. The eigenvalues are $\pm\sqrt{ab}$. Changing the sense of rotation exchanges the directions that grow and decay.

At fixed angular momentum magnitude, $\mathbf{L}$ lies on a sphere. Eliminate L_2^2 from the energy using that sphere. The resulting difference from steady intermediate-axis energy is exact.

$$2T - |\mathbf{L}|^2/I_2 = (1/I_1 - 1/I_2)L_1^2 + (1/I_3 - 1/I_2)L_3^2.$$

One coefficient is positive and the other negative. Energy has a saddle at the intermediate orientation. At the minimum or maximum inertia axis those two coefficients have the same sign. The nearby energy contours close around those two spins. Conservation of energy alone does not select stability until one states which other invariant restricts the motion.

Read a doubling time without knowing the original tilt

Take principal moments $0.030, 0.040, 0.050\,\mathrm{kg\,m^2}$, spin $12\,\mathrm{rad\,s^{-1}}$, and $\omega_1(0) = 0.10\,\mathrm{rad\,s^{-1}}$, $\omega_3(0) = 0$. Estimate when the first component reaches 0.20. Compare with a fit that assumes an exponential from the first frame.

▼ **Work through the solution**

The rates are $a = 4.0\,\mathrm{s^{-1}}$,

$$b = 2.4\,\mathrm{s^{-1}},$$
$$\sigma = \sqrt{9.6} = 3.0984\,\mathrm{s^{-1}}.$$

The zero initial slope places equal weight on the increasing and decreasing solutions. Thus $\omega_1(t) = 0.10\cosh(\sigma t)$. It first doubles at $\operatorname{arcosh}(2)/\sigma = 0.425\,\mathrm{s}$. A pure growing mode doubles in $\ln(2)/\sigma = 0.224\,\mathrm{s}$. An initially horizontal tangent is compatible with linear instability.

To excite the growing mode alone, prepare $\omega_3(0) = -\sigma\omega_1(0)/a$. The relevant marker here reads the body components of angular velocity. Projecting a fixed line of sight onto a body mark introduces a separate kinematic modulation. A vector gyroscope or a reconstruction using multiple marks separates orientation from angular velocity.

Compare a perturbation calculation with all three Euler equations

The downloadable OneSimulation run uses the four-stage Runge–Kutta integrator on these three Euler equations. Its CSV includes kinetic energy and angular momentum magnitude at each output time.

Compare the first component against the browser curve and both invariants against their first-row values. A physical flip can occur while both diagnostics stay constant.

The graph integrates the full equations with the initial transverse velocity along the first axis. Predict which portion agrees with a hyperbolic cosine. Vary the initial perturbation and spin independently. At the same time compare two initially distinct motions that both stay near the middle axis for several frames.

Open this experiment online

Try the calculation

Nominal middle-axis speed (rad/s) **12**

Initial transverse speed (rad/s) **0.1**

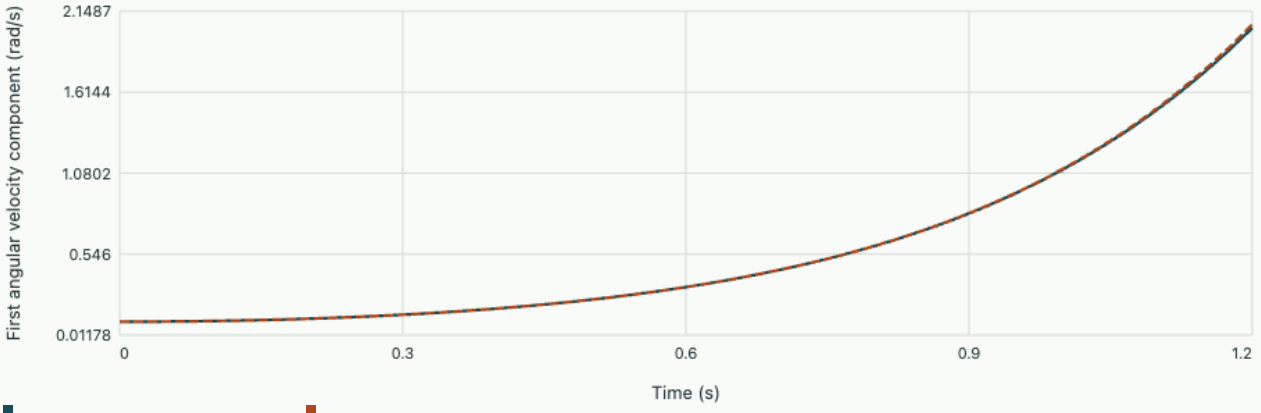

Initial linear growth rate 3.0984 s^{-1}. With zero initial transverse slope the predicted first doubling time is 0.42505 s.

Download the OneSimulation model

In your OneSimulation environment, run the model with these inputs.

```
python spectra-and-orbits.py rotor --spin 12 --seed 0.1
```

▼ Work through the solution

For small initial amplitude the neglected correction to $\dot{\omega}_2$ is quadratic. A smaller seed leaves a longer interval before the linear approximation loses accuracy. Doubling the spin doubles the local growth rate. A perfectly aligned spin is an exact solution with an unstable neighbourhood. Numerical or experimental perturbations need a finite time to grow. Once a transverse component approaches the nominal spin, the hyperbolic cosine can grow without bound while the true components are restricted by the angular momentum sphere. That separation diagnoses a depleted range of validity even in an accurate integration.

For a second treatment of rigid-body motion and the body frame, work through the rigid bodies chapter and second problem sheet in David Tong's Cambridge course.

Notebook practice · Reading Earth's rotation from a pendulum trace

Analytical mechanics from constraints to invariants

Recover the dynamics of a body from its constraints, symmetries and measured initial conditions. Follow the argument through rotating bodies, resonances, continuum limits and changes of observer.

1. ## Virtual work and the forces hidden by a constraint

   A bead follows a wire, a pendulum remains the same length, and a rolling wheel obeys a relation between translation and rotation. Their reduced equations describe the motion but can conceal the largest forces in the apparatus. Determine which forces disappear under a virtual displacement, recover their values, and decide when the assumed motion ceases to be physically admissible.

2. ## Moving constraints, boundary work and a changing energy

   A pendulum with a reeled string can gain energy while its support force does no virtual work. A bead on a spinning guide can accelerate without gravity. Follow the work done by the apparatus, derive the relation between a reduced energy and laboratory energy, and identify which quantity a measurement tests.

3. ## Noether's theorem, boundary terms and measurable constants

   A constant of motion can survive when neither laboratory energy nor angular momentum is separately conserved. Construct the conserved quantity from an infinitesimal transformation of the action. Then use boosts, a screw symmetry, and a rotating potential to determine what measured combinations should stay fixed.

4. ## Kepler orbits, the eccentricity vector and the loss of apsidal closure

   An orbit can conserve energy and angular momentum yet gradually rotate its periapsis. The inverse-square problem possesses one more conserved vector that fixes the direction of closest approach. Derive it, turn a single position and velocity measurement into a conic, and measure what a weak perturbation does to the inferred apsidal direction.

5. ## Scattering from a central potential and what angular data can recover

   A detector records angles, whereas the force law refers to separations that were never directly observed. Derive the forward map from incoming impact parameter to angle, distinguish the several trajectories a detector may count in one angular bin, and invert sufficiently complete signed deflection data under stated hypotheses.

6. ## Euler–Poinsot motion, torque-free nutation and the intermediate axis

   A freely rotating body has fixed angular momentum in space, yet the components recorded by three body-mounted gyroscopes can vary periodically or linger near an unstable rotation. Solve the

nonsymmetric top from its invariants, distinguish its body-component period from its spatial orientation, and extract a stability time scale from a measured inertia tensor.

7. The heavy symmetric top, precession branches and the sleeping state

Gravity supplies a torque to a top pivoted away from its centre of mass. Its axis may precess steadily, nutate between two turning angles, or trace loops. Derive all three from the same angular kinetic energy and determine when an upright spinning top can remain stable.

8. Symplectic transformations, Poisson brackets and the geometry of measurements

Two phase-space plots can enclose the same volume while predicting different responses to an impulse. Derive the stronger condition that makes a change of variables canonical, test it on measured linear maps and use Poisson brackets to propagate observables without solving separately for every coordinate.

9. Action, angle and the slowing clock at a separatrix

A phase portrait contains enough information to extract a period by differentiating an area. Use that fact to build a clock for finite-amplitude pendulum motion, determine precisely where slow-parameter invariance fails, and distinguish a librating trajectory from one that makes complete rotations.

10. Canonical perturbations, small denominators and resonant capture

A weak periodic force can produce a bounded ripple on most trajectories and a large change on a narrow band of initial conditions. Derive the averaging transformation away from resonance, construct the slow resonant dynamics where that transformation fails, and estimate the physically observable width and time scale of a resonance.

11. Action density, stress waves and the boundary that reflects them

A chain of coupled masses becomes an elastic field when the wavelength is long compared with the spacing. Derive the field equation and its boundary traction from the same variation, follow energy and stress across a junction, and decide whether a measured pulse is limited by material waves or by numerical dispersion.

12. Relativistic collisions, centre-of-momentum energy and thresholds

Two particles with the same total laboratory energy can have very different energy available for changing their internal state. Determine the energy and motion of the centre-of-momentum system, reconstruct two-body elastic scattering, and follow how a detector threshold transforms between frames.

13. Which path is shortest across the surface of a cone?

A point can move along a conical surface while its azimuth and height both change. Unroll the geometry and predict the shortest path between two marked points. The measurable minimum radius distinguishes the geodesic from a line drawn along a horizontal circle.

14. Motion in a medium and momentum carried across a boundary

Two beads can approach exactly the same terminal speed with recognisably different histories. A sand cart can slow down while the total horizontal momentum of sand and cart stays fixed. Both observations begin by specifying which material the equation of motion follows.

15. From a repeating trajectory to a chaotic attractor

A damped pendulum under a periodic drive can settle into the same orbit on each run yet visit a different point on successive drive periods. A return map supplies the right clock for distinguishing a new period from a slowly decaying transient.

16. From differential acceleration to three-dimensional strain and stress

An accelerometer in a falling laboratory can read zero while a pair of falling test masses moves apart. A crystal can support different longitudinal and transverse speeds in the same direction. Both measurements require the spatial variation of a vector field, represented by a tensor.

Analytical mechanics from constraints to invariants · 1. Virtual work and the forces hidden by a constraint

A bead follows a wire, a pendulum remains the same length, and a rolling wheel obeys a relation between translation and rotation. Their reduced equations describe the motion but can conceal the largest forces in the apparatus. Determine which forces disappear under a virtual displacement, recover their values, and decide when the assumed motion ceases to be physically admissible.

Hold the clock fixed when defining a virtual displacement

A system of particles has Cartesian positions $\mathbf{r}_i$ and applied forces $\mathbf{F}_i$. A holonomic constraint is an equation $g_\alpha(\mathbf{r}_1, \dots, \mathbf{r}_N, t) = 0$. At a fixed instant an admissible infinitesimal change of configuration obeys $\sum_i \nabla_i g_\alpha \cdot \delta\mathbf{r}_i = 0$. The physical velocities obey a different relation, $\sum_i \nabla_i g_\alpha \cdot \dot{\mathbf{r}}_i + \partial_t g_\alpha = 0$. A virtual displacement compares geometrically allowed configurations at the same time. It has no prescribed duration and makes no claim that the system's momentum actually points along it.

The distinction becomes measurable for a bead on a moving horizontal table. Every allowed virtual displacement has zero vertical component, so the table's upward normal force gives zero virtual work. An upward-moving table can nevertheless raise the bead and perform positive ordinary work. Ordinary power involves the actual velocity, which includes the table motion. A careless statement that constraint forces do no work confuses two different operations. For a fixed ideal frictionless surface the real velocity is tangent as well, and vanishing virtual work then does imply vanishing ordinary power.

Let $\mathbf{R}_i$ be the reaction forces and use $m_i\ddot{\mathbf{r}}_i = \mathbf{F}_i + \mathbf{R}_i$. Multiply by an admissible $\delta\mathbf{r}_i$ and sum over particles. We call the constraints ideal when $\sum_i \mathbf{R}_i \cdot \delta\mathbf{r}_i = 0$ for every allowed virtual displacement. Eliminating those reactions gives d'Alembert's principle,

$$\sum_i (\mathbf{F}_i - m_i\ddot{\mathbf{r}}_i) \cdot \delta\mathbf{r}_i = 0.$$

This is a dynamical equation expressed through a static-looking virtual-work test. It applies instantaneously along the motion. It does not assert that the total force vanishes or that the acceleration is an independent virtual displacement. One advantage is that the detailed construction of a rigid support need not be known to determine the admissible tangential acceleration; its force can be calculated afterwards when designing the support.

Pass from virtual work to equations for coordinates

Choose independent coordinates q_a with $\mathbf{r}_i = \mathbf{r}_i(q, t)$ and independent virtual increments δq_a. The velocity is $\sum_a \partial_{q_a}\mathbf{r}_i\, \dot{q}_a + \partial_t \mathbf{r}_i$. With kinetic energy $T = \sum_i m_i \dot{\mathbf{r}}_i^2/2$, differentiation at fixed q, t gives

$$\partial_{\dot{q}_a} T = \sum_i m_i \dot{\mathbf{r}}_i \cdot \partial_{q_a}\mathbf{r}_i.$$

Differentiate in time. The product rule produces an acceleration term and a second term involving $d(\partial_{q_a}\mathbf{r}_i)/dt$. The latter equals $\partial_{q_a}\dot{\mathbf{r}}_i$, with the generalised velocities held fixed, and supplies $\partial_{q_a} T$. Hence

$$\frac{d}{dt}\frac{\partial T}{\partial \dot{q}_a} - \frac{\partial T}{\partial q_a} = \sum_i m_i \ddot{\mathbf{r}}_i \cdot \frac{\partial \mathbf{r}_i}{\partial q_a}.$$

The projected applied force is

$$Q_a = \sum_i \mathbf{F}_i \cdot \partial_{q_a} \mathbf{r}_i.$$

Independence of the coordinate variations in d'Alembert's principle gives one equation $d(\partial_{\dot{q}_a} T)/dt - \partial_{q_a} T = Q_a$ per coordinate. When $\mathbf{F}_i$ comes from a potential $V(q,t)$, the conservative contribution is $-\partial_{q_a} V$. Other contributions such as a measured resisting torque remain explicit. A coordinate expressed as an angle has a generalised force in joules per radian; a coordinate expressed as a length has one in newtons. Checking $Q_a\, dq_a$ as work avoids mistaking a generalised force for a Cartesian component.

For a simple pendulum of length l and mass m, choose θ measured from downward vertical. Then $T = ml^2\dot{\theta}^2/2$ and $V = mgl(1-\cos\theta)$. The equation $ml^2\ddot{\theta} = -mgl\sin\theta$ follows at once. The string tension vanished under the angular displacement. It has not been shown to vanish physically. Projecting Newton's equation onto the direction from the bead toward the pivot gives

$$T_{\text{string}} = mg\cos\theta + ml\dot{\theta}^2.$$

This second observable is sensitive to speed even when the reduced angular acceleration depends only on angle.

Recover multipliers before choosing coordinates

Cartesian coordinates keep reaction directions explicit. Put all coordinates into a vector x, let M be the mass matrix and let G contain the rows ∇g_α. The tangent virtual displacements are precisely those satisfying $G\delta x = 0$. A reaction doing zero virtual work must be a linear combination of the normal covectors, $R = G^T\lambda$, when the constraints are independent. Newton's equation becomes

$$M\ddot{x} = F + G^T\lambda.$$

Differentiate the constraints twice along the trajectory: $G\ddot{x} + \gamma = 0$, where γ includes the known velocity, curvature and explicit time terms. Substituting for $\ddot{x}$ determines reactions from a much smaller system,

$$(GM^{-1}G^T)\lambda = -\gamma - GM^{-1}F.$$

For any vector c, $c^T GM^{-1}G^T c = (G^T c)^T M^{-1}(G^T c)$ is positive if G has independent rows and particle masses are positive. Dependent constraint equations make the individual multipliers ambiguous. For instance writing both $g = 0$ and $2g = 0$ declares the same geometrical restriction twice. Only the combined reaction is then determined. The magnitude of a raw multiplier also depends on the units and

normalisation of g. Reporting the force $G^T\lambda$ makes comparisons between alternative constraint descriptions meaningful.

Use $g = (x^2 + y^2 - l^2)/2 = 0$ for a planar pendulum, with y upward, so the gradient is the radius vector $\mathbf{r}$. Newton's equation reads $m\ddot{\mathbf{r}} = -mg\hat{y} + \lambda\mathbf{r}$, where the symbol g in the gravitational term denotes the acceleration magnitude. The acceleration constraint $\mathbf{r}\cdot\ddot{\mathbf{r}} = -v^2$ gives

$$\lambda = (mgy - mv^2)/l^2.$$

The inward tension is $-\lambda l = mv^2/l - mgy/l$. Since $y = -l\cos\theta$, this is the radial-force result already obtained. The multiplier in this convention has units of force per length. Using the radial-distance constraint instead would make its magnitude a force.

Background · What if the support can push but cannot pull?

Replacing a surface by an equality constraint assumes the object stays in contact. A particle sliding along the inside of a smooth vertical circular track illustrates the additional physical test. At the top, gravity and the inward normal reaction together must supply the centripetal acceleration.

$$N = \frac{mv^2}{R} - mg, \qquad N \geq 0.$$

At a top speed below $\sqrt{gR}$ the equality-constrained solution requires negative N. An ordinary track cannot exert that pull. Its normal force then falls to zero and the particle must follow free flight until it meets the track again. A bead threaded on a wire could receive the oppositely directed force and would follow a different trajectory. Both models have the same geometrical path during contact.

Recognise an inequality at a contact

A bead threaded on a stiff loop can experience reaction in either direction, whereas a string can pull only. A surface without adhesion can push only. Derive the constrained motion, calculate its reaction, and compare the required sign with the physical mechanism. When a calculated tension turns negative, replace the constrained trajectory by free flight until a new contact event. Continuing to integrate the pendulum equation would retain a mathematically valid circle and a physically unavailable pushing string.

A mass starts at the bottom of a frictionless vertical loop with speed v_b. Energy conservation gives $v_{\text{top}}^2 = v_b^2 - 4gl$, since the top is $2l$ higher. A string just remaining taut at the top requires $T_{\text{top}} = mv_{\text{top}}^2/l - mg \geq 0$, giving $v_b^2 \geq 5gl$. The energy-only criterion for reaching the elevation is $v_b^2 \geq 4gl$; the interval between these two values illustrates why a trajectory test must include reactions. With $l = 0.80\,\text{m}$, the threshold bottom speed is $6.26\,\text{m/s}$. At this threshold the bottom tension is $6mg$, six times the weight, even though the tension is about to vanish at the top.

Recover the forces on a wedge that is free to slide

Place a wedge of mass M on a smooth horizontal floor and a block of mass m on its smooth upper face. Let the slope descend to the right at angle α. Choose X as the wedge's horizontal position and s as distance down the face. The block's coordinates apart from fixed offsets are $x = X + s\cos\alpha,\ y = -s\sin\alpha$. Its relative velocity points down the slope but its absolute acceleration need not. The kinetic energy contains a mixed term $m\dot{X}\dot{s}\cos\alpha$. Dropping that term is equivalent to holding the wedge stationary while allowing it to recoil, two incompatible mechanical models.

The reduced equations are $(M+m)\ddot{X} + m\ddot{s}\cos\alpha = 0$ and $\ddot{s} + \ddot{X}\cos\alpha = g\sin\alpha$. The first is conservation of total horizontal momentum, since the block–wedge normal force is internal and the floor is frictionless. Elimination gives

$$\ddot{s} = (M+m)g\sin\alpha/(M + m\sin^2\alpha),$$

$$\ddot{X} = -mg\sin\alpha\cos\alpha/(M + m\sin^2\alpha).$$

The acceleration down the moving face exceeds $g\sin\alpha$ because the wedge moves left as the block slides right. Nevertheless the absolute vertical acceleration of the block remains less than or equal to free fall because the upper face pushes upward.

To find the block's normal force, project its absolute acceleration onto the outward unit normal $(\sin\alpha, \cos\alpha)$. The part proportional to $\ddot{s}$ cancels, leaving $\ddot{X}\sin\alpha$. Newton's equation along that direction gives

$$N = m(g\cos\alpha + \ddot{X}\sin\alpha) = mMg\cos\alpha/(M + m\sin^2\alpha).$$

With $M = 3.0\,\mathrm{kg}$, $m = 1.0\,\mathrm{kg}$, $\alpha = 30^\circ$, one finds $\ddot{s} = 6.04\,\mathrm{m/s^2}$,

$$\ddot{X} = -1.31\,\mathrm{m/s^2},$$

$$N = 7.84\,\mathrm{N}.$$

The normal based on a stationary wedge would be $8.50\,\mathrm{N}$. A force sensor under the moving face could distinguish the two models even when a short record of relative slope displacement cannot resolve the difference.

Which reaction does no virtual work here? The normal force on the block has virtual work $N\hat{n}\cdot(\delta X\hat{x} + \delta s\hat{t}) = N\sin\alpha\,\delta X$. The opposite normal force on the wedge gives $-N\sin\alpha\,\delta X$, so the sum cancels. Considering only the block and asserting zero work from the normal for arbitrary δX would be incorrect. At the real velocities the same reaction transfers energy between the bodies even though its net internal power on their pair is zero. The floor's normal reaction balances the vertical momentum change of the whole system. During the slide it is $(M+m)g - m\ddot{s}\sin\alpha$, less than total weight while the block accelerates downwards.

Take the limits as an additional test. At fixed m, α, increasing M to infinity returns the familiar fixed-wedge results. At a nearly horizontal face, downslope acceleration and wedge recoil vanish, restoring the full block weight as normal force. At a vertical face the normal vanishes and the block falls. These limits hold because the contact has no friction and can be maintained with a nonnegative normal. A moving

wedge of independently prescribed acceleration would replace the horizontal momentum equation by a control input, changing both the relative acceleration and the support force.

Distinguish rolling constraints from purely geometric restrictions

A cylinder of radius R, mass m and axial inertia I rolls without slip down a fixed rough incline. Choose coordinate s down the incline and spin angle ϕ in the corresponding sense. The constraint $\dot{s} = R\dot{\phi}$ is integrable in this one-dimensional motion, so it can be inserted as $s - R\phi = \text{constant}$. The resulting kinetic energy is $(m + I/R^2)\dot{s}^2/2$. The reduced equation gives

$$\ddot{s} = g\sin\alpha/[1 + I/(mR^2)].$$

Reconstruct the static friction from translation, $f = gm\sin\alpha - m\ddot{s}$, directed up the slope, and compare it with the available maximum $\mu_s mg\cos\alpha$.

For a homogeneous solid cylinder $I = mR^2/2$, the speed-up is $2g\sin\alpha/3$ and friction magnitude $mg\sin\alpha/3$. A ring of the same mass and radius has $I = mR^2$, half the gravitational downslope acceleration and half the downslope weight component as friction. At 30° the minimum static friction coefficients are respectively $\tan 30^\circ/3 = 0.192$ and $\tan 30^\circ/2 = 0.289$. Two objects on the same surface can therefore diverge qualitatively because the ring slips while the cylinder still rolls. Treating an assumed no-slip relation as exact without testing that inequality can produce an unphysical result despite apparently consistent energy conservation.

The friction on a rigid body rolling without slip on a fixed surface has zero power because its instantaneous point of contact is stationary. The force still changes both linear and angular momentum. On a moving conveyor the contact velocity is no longer zero in the laboratory; friction can supply mechanical energy even while the relative contact velocity vanishes. For a wheel steering on a plane the restrictions $\dot{x} = R\dot{\phi}\cos\psi,\ \dot{y} = R\dot{\phi}\sin\psi$ depend on heading ψ. In general they cannot be integrated into two configuration equations relating x, y, ϕ, ψ globally. d'Alembert's fixed-time allowed variations still project out ideal rolling reactions, but replacing those velocity constraints by invented holonomic coordinates gives the wrong dynamics. The distinction can be seen geometrically by rolling and steering through a closed sequence of steering operations that leaves a net displacement.

Find loads on two supports of a suspended bar

A rigid horizontal bar of mass m and length $2a$ is supported at its ends by two vertical inextensible light cords. At one instant both cords are vertical and the bar is horizontal. An extra downward load of magnitude F is applied at horizontal coordinate s relative to the centre. Ask first for a static experiment. The two vertical reaction forces T_L, T_R obey force balance $T_L + T_R = mg + F$ and moment balance $a(T_R - T_L) = sF$. This gives

$$T_R = (mg + F + sF/a)/2,$$

$$T_L = (mg + F - sF/a)/2.$$

The lever arms encode geometry that the vertical balance alone cannot provide.

The same result can be obtained from virtual variations if the reactions are kept as multipliers until the end. For small vertical translation y of the centre and small tilt θ, the endpoint vertical displacements are $\delta y - a\delta\theta$ on the left and $\delta y + a\delta\theta$ on the right. The load point displacement is $\delta y + s\delta\theta$. Before eliminating the endpoint constraints, project all applied and reaction forces against arbitrary independent $\delta y, \delta\theta$; vanishing of both coefficients gives the preceding balances. After imposing both endpoint constraints directly, these two variations vanish and the reduced model for vertical motion contains no equation from which the support loads can be read. Removing a degree of freedom can remove precisely the observable of interest unless reactions are reconstructed.

For $m = 2.0\,\mathrm{kg}$, $a = 0.40\,\mathrm{m}$, $F = 12\,\mathrm{N}$ and $s = 0.25\,\mathrm{m}$, the total load is $31.62\,\mathrm{N}$ and the load difference $7.50\,\mathrm{N}$. Hence $T_R = 19.56\,\mathrm{N}$, $T_L = 12.06\,\mathrm{N}$. Exchanging the load from right to left reverses the difference while preserving the sum. This symmetry is a calibrating manoeuvre for two load cells with different offsets: subtract readings from mirrored configurations to isolate the lever-arm response, and compare their sum to the known total weight and applied force.

Now imagine three vertical supports at $-a, 0, +a$. Their three tensions enter only two independent balances. Perfectly rigid constraints determine no unique allocation to the centre support. The ambiguity is physical; the stiffnesses, preloads and small height differences of real supports decide the result. With three identical unstrained linear springs and a centred load F, each spring extends equally if the bar stays level, so each carries one third of the total weight. If the middle spring is twice as stiff and all have the same unloaded height, it carries one half and each outer spring one quarter. Both answers satisfy exactly the same force and moment balances. Reporting a unique value from a singular ideal multiplier system would manufacture an unmeasured constitutive assumption.

Test an acceleration constraint against drift of the position itself

Solving $G\ddot{x} + \gamma = 0$ guarantees the correct instantaneous normal acceleration at a state lying on the constraint manifold with tangent velocity. It does not magically repair earlier position or velocity errors in approximate time integration. For a particle constrained to a circle, monitor $g = (r^2 - l^2)/2$, $\dot{g} = \mathbf{r} \cdot \mathbf{v}$, and the computed force. A small tangential displacement can give tiny instantaneous force error while the radius gradually drifts. Integrating an acceleration-level constraint twice without a position or velocity correction can cause substantial mismatch over many revolutions.

A simple projection illustrates what each correction does. Normalise an approximate position vector to length l, then remove the radial component of velocity by $\mathbf{v} \leftarrow \mathbf{v} - \hat{r}(\hat{r} \cdot \mathbf{v})$. The corrected point and tangent satisfy the constraints, but the velocity correction removes kinetic energy $m(\hat{r} \cdot \mathbf{v})^2/2$, and the position change can alter potential energy. Projection is therefore a numerical operation whose physical invariant errors must be measured. A structure-preserving constrained integrator builds the position and momentum conditions into the step and often gives better long-time behaviour. Compare convergence of reaction, constraint residual and energy separately instead of treating a rounded radius as proof of a correct force.

A pendulum on a free cart tests the complete mass matrix

Mount a pendulum pivot on a cart of mass M moving horizontally on a smooth track. The bob has mass m, length l and downward angle θ. Choose the cart position X and use bob coordinates $X + l\sin\theta$, $-l\cos\theta$. The kinetic energy is $(M+m)\dot{X}^2/2 + ml\dot{X}\dot{\theta}\cos\theta + ml^2\dot{\theta}^2/2$. Two different off-diagonal mass terms would contradict its origin as a quadratic form; the same factor $ml\cos\theta$ multiplies the companion acceleration in each equation. This is a useful check on a manually assembled multibody model.

The equations are

$$(M+m)\ddot{X} + ml(\ddot{\theta}\cos\theta - \dot{\theta}^2\sin\theta) = 0,$$

$$l\ddot{\theta} + \ddot{X}\cos\theta + g\sin\theta = 0.$$

In the small-angle regime the horizontal centre of mass moves uniformly. Choosing zero total momentum gives

$$\dot{X} \simeq -ml\dot{\theta}/(M+m).$$

Substitute its derivative into the angular equation to obtain

$$\ddot{\theta} + [(M+m)g/(Ml)]\theta = 0.$$

Releasing the support raises the oscillation frequency because the effective angular inertia falls while the gravitational stiffness stays the same. The result is a statement about the relative pendulum angle, measured from an inertial vertical, with an unforced horizontally moving support.

For $M = 0.60\,\mathrm{kg}$, $m = 0.20\,\mathrm{kg}$ and $l = 0.50\,\mathrm{m}$, the small-angle period is

$$2\pi\sqrt{Ml/[(M+m)g]} = 1.229\,\mathrm{s}.$$

Fixing the cart with a clamp gives $1.419\,\mathrm{s}$ instead. At zero total horizontal momentum the cart displacement from its equilibrium is approximately $-0.125\,\theta$ metres, so a $0.10\,\mathrm{rad}$ angle corresponds to $12.5\,\mathrm{mm}$ of recoil. Simultaneous position measurements on cart and bob should reconstruct a horizontal centre of mass that is stationary to within tracking uncertainty. A missing cart inertia or a wrongly filled cross term can alter both period and recoil; checking just one number may not identify which error occurred.

The reaction on the moving bob can again be recovered. Its radial acceleration along the outward string direction is $\ddot{X}\sin\theta - l\dot{\theta}^2$. Thus the tension is $T = m[g\cos\theta - \ddot{X}\sin\theta + l\dot{\theta}^2]$. The acceleration of the support appears explicitly. Reusing the fixed-pivot formula at all angles would omit a term that vanishes accidentally at the bottom. To test the sign, observe a rightward tilted pendulum whose pivot accelerates right: the support's acceleration has an outward projection along the tilted string, reducing the inward tension needed for the same relative motion. Substituting a directly measured cart acceleration provides an independent load-cell prediction.

Follow a force eliminated by a constraint

Predict when a two-sided circular groove must reverse its normal force. Check the prediction against the exact energy and radial balances.

Open this experiment online

Try the calculation

Bottom speed (m/s) **4**

Loop radius (m) **0.5**

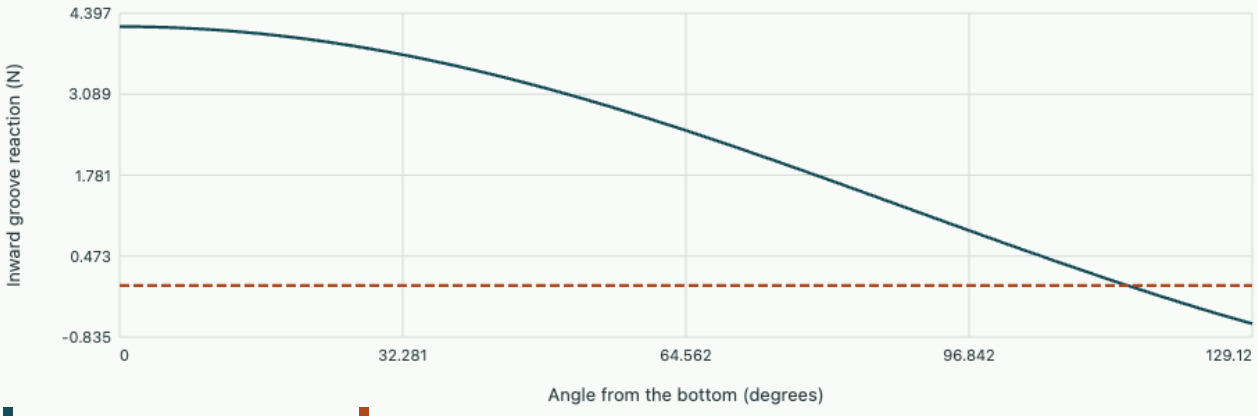

Reachable angle 129.12°. Inward groove reaction there -0.619 N. One-sided loop threshold v_0 = 4.9523 m/s.

Decide which force a sensor actually reports

Reaction forces can be reported as tension along a member, normal traction at a contact, total support load on a floor, or a single Cartesian component read by a load cell. A rigid-body idealisation alone does not specify a sensor's orientation or the weight of its housing. For a fixed pendulum, for example, the string carries tension T, while a vertical force channel at its pivot reads the vertical string contribution $T\cos\theta$. A horizontal channel reads $T\sin\theta$. The force on the pivot is opposite the force exerted on the bob. Selecting the wrong sign or leaving out the fixture's own weight can create a discrepancy even when the dynamical calculation is correct.

Suppose an ideal load cell with its sensitive axis vertical is tared with the fixture installed but the $0.40\,\mathrm{kg}$ bob removed. When the bob is held at 60° by a separate purely tangential actuator and is otherwise stationary, the radial balance gives

$$T = mg\cos 60^\circ = 1.96\,\mathrm{N}.$$

The pivot's vertical reading attributable to the string is $0.981\,\mathrm{N}$. The tangential actuator supplies the remaining vertical support as well as a horizontal component. Once the actuator releases,

instantaneously the same tension and reading hold because radial speed is still zero. At the bottom of the subsequent swing the load jumps to the dynamical value obtained earlier, even though no upper fixture mass has changed.

A student hangs the bob at the same 60° angle using a separate horizontal cord instead of a tangential actuator. Should the pivot cell read the preceding $0.981\,\mathrm{N}$?

▼ **Work through the solution**

The horizontal cord contributes no vertical support. Static balance now requires $T\cos 60^\circ = mg$, giving $T = 7.85\,\mathrm{N}$ and vertical pivot contribution $3.92\,\mathrm{N}$. The horizontal holding force has a nonzero radial projection and changes the radial-force balance. After the horizontal cord is removed the tension immediately changes to $mg\cos 60^\circ$ because no momentum impulse is required for a finite jump in force. A schematic that shows only the bob angle is insufficient to infer the support load without saying how the angle is maintained.

In the free cart experiment bearing drag is weak but measurable. Can an observed frequency shift distinguish it from a wrongly assumed cart mass?

▼ **Work through the solution**

A viscous drag changes the horizontal momentum balance and allows the formerly stationary centre of mass to move as momentum leaks to the track. A mass error in a drag-free model changes the relative period and recoil ratio without supplying an actual external impulse. Track the complete centre of mass using independently weighed masses, compare its momentum change with the integrated bearing force, and measure the decay envelope. The frequency alone is a single scalar and can often be fitted by several combinations of missing mass, spring compliance and drag.

Locate contact loss on a smooth convex surface

A small block starts sliding from near rest just to one side of the top of a smooth fixed sphere of radius R. Measure angle θ from upward vertical. Energy gives $v^2 = 2gR(1-\cos\theta)$ during contact, while the inward radial equation reads $mg\cos\theta - N = mv^2/R$. Thus $N = mg(3\cos\theta - 2)$. Contact first vanishes at $\cos\theta = 2/3$, or 48.2°. For a sphere of radius $0.50\,\mathrm{m}$, this occurs after a vertical drop $R/3 = 0.167\,\mathrm{m}$ and at speed $1.81\,\mathrm{m/s}$. A block balanced exactly at the top at exact rest is an unstable equilibrium in the ideal model; a small initial displacement or speed initiates the measured trajectory.

Once the block leaves, the same spherical coordinates can still be used to describe position, but $r = R$ is no longer an equation of motion. Continue with the measured tangential velocity and free gravitational acceleration. Enforcing the sphere condition beyond release would make the computed normal negative and predict a surface that pulls on the block. The zero normal, the geometric release angle and the subsequent ballistic arc provide three independent observables for the same force reconstruction.

Tutorial on measuring reactions

A $0.40\,\mathrm{kg}$ pendulum of length $0.75\,\mathrm{m}$ is released from rest at 60° from downward vertical. Predict the load-cell reading at the pivot when it passes the bottom. What part does the reduced equation alone omit?

▼ **Work through the solution**

The height change is

$$l(1-\cos 60^\circ) = 0.375\,\mathrm{m}.$$

Energy conservation gives

$$v^2 = 2g(0.375) = 7.36\,\mathrm{m}^2/\mathrm{s}^2.$$

At the bottom the tension is $mg + mv^2/l = 7.85\,\mathrm{N}$, twice the weight. The tangential acceleration there vanishes because gravity points along the string, but the radial acceleration remains nonzero. A sensor measuring the string force sees this centripetal contribution directly.

A bead lies on a smooth moving plane with upwards acceleration a_z. Which acceleration first makes a passive contact impossible if the bead initially shares the plane's motion?

▼ **Work through the solution**

Vertical Newton balance requires $N - mg = ma_z$, or $N = m(g + a_z)$. At $a_z = -g$ the reaction vanishes. A more negative plane acceleration would require the plane to pull the bead down, so contact is lost and the bead follows free fall until the separation closes. For upward acceleration the normal exceeds weight. In all these cases a virtual displacement tangent to the plane produces zero virtual normal work.

Two code implementations use $(x^2 + y^2 - l^2)/2$ and $x^2 + y^2 - l^2$ as constraints for the same state. Their multipliers differ by a factor two. How can the physical result be tested?

▼ **Work through the solution**

The second gradient is twice the first at the same point. Its multiplier must be half the first multiplier for $G^T\lambda$ to coincide. Compare the reaction vector in newtons, its dot product with an independently chosen tangent direction, and the normal acceleration required by the geometry. A comparison of raw multiplier values alone would flag a difference that is entirely due to normalisation.

Compare a constrained trajectory with the motion and force calculations above.

David Tong develops virtual work and constrained coordinates in his classical dynamics course.

Analytical mechanics from constraints to invariants · 2. Moving constraints, boundary work and a changing energy

A pendulum with a reeled string can gain energy while its support force does no virtual work. A bead on a spinning guide can accelerate without gravity. Follow the work done by the apparatus, derive the relation between a reduced energy and laboratory energy, and identify which quantity a measurement tests.

Parameterise the motion of a guide as well as the bead

Let a prescribed moving guide define positions $\mathbf{r}(q,t)$. Its relative velocity along the guide is $\mathbf{r}_q\dot q$ and its imposed local velocity is $\mathbf{r}_t$, where t is differentiated at fixed coordinate. The kinetic energy $T=m|\mathbf{r}_q\dot q+\mathbf{r}_t|^2/2$ includes a quadratic term in $\dot q$, a mixed term linear in $\dot q$, and a term independent of $\dot q$. Dropping the last two merely because the guide motion is prescribed generally changes the bead equation. A term independent of $\dot q$ may still depend on its position q.

For $L=T-V$ define $p=\partial_{\dot q}L$ and $\mathcal{E}=p\dot q-L$. Differentiating along a solution of the Euler–Lagrange equation gives $d\mathcal{E}/dt=-\partial_t L$ in the absence of extra nonconservative generalised forces. This identity involves the partial time derivative at fixed $q,\dot q$. The laboratory energy is

$$E_{\mathrm{lab}}=m|\dot{\mathbf{r}}|^2/2+V.$$

Direct substitution gives $\mathcal{E}=E_{\mathrm{lab}}-m\dot{\mathbf{r}}\cdot\mathbf{r}_t$ for a single particle and ordinary position potential. Thus a time-independent reduced Lagrangian can conserve a quantity different from the laboratory mechanical energy. Which observer supplies a force, and which independent variables are held fixed, determine the energy being tracked.

Work supplied by a steadily rotating straight slot

A smooth horizontal guide turns about its inner end with prescribed angle $\varphi=\Omega t$. Let r be the bead's distance from the pivot. The velocity is $\dot r\hat r+r\Omega\hat\varphi$, and the reduced Lagrangian is $m(\dot r^2+\Omega^2r^2)/2$. Its Euler–Lagrange equation is

$$\ddot r=\Omega^2 r.$$

With $r(0)=r_0,\dot r(0)=0$ the solution is $r_0\cosh\Omega t$ until the bead leaves the slot. In the laboratory no force acts along the radial tangent of the slot, yet radial acceleration in polar coordinates is $\ddot r-r\Omega^2$, precisely zero. The tangential acceleration $2\Omega\dot r$ is provided by the slot wall.

The wall reaction $R_\varphi=2m\Omega\dot r$ exerts a torque rR_φ on the bead. The driving motor balances the opposite reaction on the slot and supplies power $\Omega rR_\varphi=2m\Omega^2r\dot r$. Differentiating $E_{\mathrm{lab}}=m(\dot r^2+\Omega^2r^2)/2$ and using the radial equation gives the same power. The reduced energy $m(\dot r^2-\Omega^2r^2)/2$ is constant. Its difference from E_{lab} equals $-\Omega L_z$, with $L_z=mr^2\Omega$. This is a consequence of uniform imposed rotation, not a negative physical rotational kinetic energy.

For $m=0.10\,\mathrm{kg}$, $r_0=0.050\,\mathrm{m}$ and $\Omega=4.0\,\mathrm{rad/s}$, consider $t=0.25\,\mathrm{s}$. The radial position is $77.2\,\mathrm{mm}$, radial speed $0.235\,\mathrm{m/s}$, and wall reaction $0.188\,\mathrm{N}$. The motor supplies about $0.0580\,\mathrm{W}$ at that instant. Laboratory energy has risen from $0.00200\,\mathrm{J}$ to approximately $0.00752\,\mathrm{J}$. Measuring only the angular

motor speed would miss the incoming mechanical work. The torque on the drive shaft or the changing moment of inertia supplies the other observable required for an energy budget.

A pendulum with prescribed length

Let a point pendulum have length $l(t) > 0$ and angle θ from downward vertical. Using $x = l\sin\theta$, $y = -l\cos\theta$ gives $T = m(\dot{l}^2 + l^2\dot{\theta}^2)/2$ and $V = -mgl\cos\theta$ for a fixed gravitational datum. The angular Euler–Lagrange equation becomes

$$\frac{d}{dt}(ml^2\dot{\theta}) = -mgl\sin\theta,$$

$$\ddot{\theta} + 2\frac{\dot{l}}{l}\dot{\theta} + \frac{g}{l}\sin\theta = 0.$$

The term proportional to $\dot{l}\dot{\theta}$ comes directly from differentiating angular momentum about the pivot. With increasing length the angular speed at fixed angular momentum decreases; reeling in has the opposite effect. It can look like damping or amplification in the angular equation even with no friction. A mechanical energy balance distinguishes the reversible exchange with a reel from energy lost as heat.

The radial Newton equation, taking outward as positive, is $m(\ddot{l} - l\dot{\theta}^2) = mg\cos\theta - T_{\text{string}}$. Hence $T_{\text{string}} = m(g\cos\theta + l\dot{\theta}^2 - \ddot{l})$. The tension power on the bob is $-T_{\text{string}}\dot{l}$. This has the correct sign when a heavy nearly vertical bob is lowered slowly: $\dot{l} > 0$ and the gravitational potential decreases as the string takes energy out. At the bottom of a swing the tension is larger, so a reel shortening the string there does more positive work per unit length than it would at a turning point. Timing a cyclic length change can pump an oscillation while the guide returns to precisely its initial length.

With $m = 0.50\,\text{kg}$, $l = 1.0\,\text{m}$, $\dot{\theta} = 2.0\,\text{rad/s}$, and the bob at the bottom, a short interval of constant-rate shortening at $\dot{l} = -0.030\,\text{m/s}$ has tension $6.91\,\text{N}$ and delivers $0.207\,\text{W}$. When the bob is momentarily at rest at 30°, the tension for the same length and zero radial acceleration is $4.25\,\text{N}$. Reversing the reel rate there would remove only $0.127\,\text{W}$. A complete finite cycle requires integrating the time-varying tensions and checking the acceleration during each reel reversal.

Translate a pivot and separate real forcing from a coordinate choice

For a pivot translating horizontally at prescribed $X(t)$ and constant string length l, write $x = X + l\sin\theta$, $y = -l\cos\theta$. The kinetic energy includes $ml\dot{X}\dot{\theta}\cos\theta$. In the angular Euler–Lagrange equation the terms proportional to $\dot{X}\dot{\theta}\sin\theta$ cancel, leaving $l\ddot{\theta} = -g\sin\theta - \ddot{X}\cos\theta$. A constant pivot velocity therefore does not force the relative angle. Replacing the pivot velocity by its magnitude as a driving force would wrongly violate Galilean invariance. A horizontal pivot acceleration does force the angle; it appears as the opposite inertial acceleration in the translating frame.

For $|\theta| \ll 1$ and $X = X_0\cos\omega t$, the equation becomes

$$\ddot{\theta} + \omega_0^2 \theta = (X_0 \omega^2 / l) \cos \omega t,$$

$$\omega_0^2 = g/l.$$

At drive frequencies well below ω_0,

$$\theta \simeq -\ddot{X}/g.$$

The bob nearly aligns with the effective gravity in the moving frame. Far above ω_0, the particular solution is approximately $-X/l$; then the bob's absolute horizontal coordinate $X + l\theta$ changes little even while the pivot moves. Near resonance the undamped steady particular amplitude is inappropriate, and the initial transient or a physical damping model matters.

Calculate work done by a moving wall in an elastic collision

A particle of mass m moves along a line and collides elastically with a wall whose prescribed laboratory velocity is U during the short contact. In the instantaneous wall frame the incoming relative velocity $v^- - U$ reverses, so

$$v^+ = 2U - v^-.$$

In the laboratory the impulse is $J = m(v^+ - v^-) = 2m(U - v^-)$ and the kinetic energy change is $\Delta K = m[(v^+)^2 - (v^-)^2]/2 = UJ$. The energy gained by the particle equals wall velocity times the impulse delivered by the wall. A perfectly elastic contact still changes laboratory kinetic energy when the wall moves, since elasticity was defined for the relative normal velocity.

Suppose a particle of mass $0.20\,\mathrm{kg}$ moves right at $3.0\,\mathrm{m/s}$ into a right wall moving left at $0.50\,\mathrm{m/s}$. Its final velocity is $-4.0\,\mathrm{m/s}$, and the impulse on the particle is $-1.40\,\mathrm{N\,s}$. The particle's kinetic energy rises from 0.90 to $1.60\,\mathrm{J}$, exactly $UJ = 0.70\,\mathrm{J}$. The actuator keeping the wall on schedule supplies the energy. When the same wall recedes to the right at $0.50\,\mathrm{m/s}$, the outgoing velocity is $-2.0\,\mathrm{m/s}$ and kinetic energy falls by $0.50\,\mathrm{J}$. The difference is not symmetric under reversal of wall speed at fixed incoming particle velocity, because that reversal also changes the relative approach speed.

Now trap a particle between a fixed wall and a length $l(t)$ varying slowly compared with the collision period. To leading order a right-wall collision changes the particle's speed by $-2\dot{l}$, and such collisions occur about once in $2l/v$. Hence $dv/dt \simeq -(v/l)\dot{l}$, so vl is approximately constant. The one-dimensional action around a full bounce cycle is

$$J_{\mathrm{act}} = (2\pi)^{-1}(2mvl) = mvl/\pi.$$

This elementary wall argument explains the adiabatic action without requiring the smooth-force approximation at the instantaneous collision. If the wall speed varies quickly within a round trip, the collision phases matter and the averaged invariant can fail.

Starting with $l_0 = 0.40\,\mathrm{m}$ and speed $4.0\,\mathrm{m/s}$, slow compression to $0.30\,\mathrm{m}$ predicts $v \simeq 5.33\,\mathrm{m/s}$. Its kinetic energy increases by a factor $16/9$, supplied through the moving boundary. A pressure sensor at

the wall measures impulse per time, $2mv$ times the collision frequency $v/(2l)$, giving average force mv^2/l at leading order. Multiplying this force by the inward speed gives the power required by the predicted energy law. An instantaneous compression while the particle is elsewhere would instead change no kinetic energy until a later collision. The final length alone does not determine the energy unless the rate protocol is specified.

Follow a string through a moving boundary in configuration and time

For a vertical moving pivot with height $Y(t)$, coordinates $x = l\sin\theta$, $y = Y - l\cos\theta$ give kinetic energy $m[\dot{Y}^2 + 2l\dot{Y}\dot{\theta}\sin\theta + l^2\dot{\theta}^2]/2$. Derive the angular equation by differentiating $p_\theta = ml^2\dot{\theta} + ml\dot{Y}\sin\theta$. The terms containing $\dot{Y}\dot{\theta}\cos\theta$ cancel as in horizontal translation; the remaining equation is

$$l\ddot{\theta} = -(g + \ddot{Y})\sin\theta.$$

A vertical acceleration changes the restoring coefficient multiplicatively, unlike a horizontal displacement whose small-angle effect is an additive forcing term. The distinction is visible even when the two pivot motions have identical amplitudes and frequencies.

For $Y = A\cos\Omega t$, the effective gravity oscillates as $g - A\Omega^2\cos\Omega t$. The perfectly vertical solution remains an exact solution at any drive amplitude. A small deviation need not remain small, because its linear equation has a periodic coefficient. An observed growth of swing from a tiny initial disturbance near twice the natural frequency is a parametric effect. A camera viewing the pivot and bob together can separate relative angle from large imposed vertical displacement. Estimating angular amplitude from absolute bob height alone introduces a component at the drive frequency unrelated to the swing.

At modest drive $A = 1.0\,\mathrm{mm}$, $\Omega = 20\,\mathrm{rad/s}$, the pivot acceleration amplitude is $0.40\,\mathrm{m/s^2}$, about four percent of gravity. A pendulum of length $0.10\,\mathrm{m}$ has small-angle frequency $9.90\,\mathrm{rad/s}$, putting this drive near twice its natural frequency despite the small displacement. For an exactly stationary vertical bob relative to the pivot, the string tension is $m(g + \ddot{Y})$ as long as that value is positive. A force measurement thus contains a direct drive-frequency signal even before transverse oscillation develops. Combining an angle sensor with a load cell helps distinguish contact loss from growth of parametric oscillation.

A fast vertical drive can also modify the slow stability of the inverted position. A quantitative treatment requires separating a fast small angular ripple from the slow tilt and averaging its feedback, with the support acceleration and frequency satisfying the relevant ordering. The instantaneous sign of $g + \ddot{Y}$ alone is insufficient to establish the stability of the inverted solution. An upright motion that briefly samples a favourable sign each cycle may still drift away over many cycles. Compare initial perturbations at several drive phases and fit the envelope over complete periods before drawing a stability conclusion.

Treat the drive itself as a degree of freedom

A prescribed rotating slot conceals the energy source behind a fixed pattern speed. Replace the motor by a free rotating turntable with moment of inertia I_0, and let its angle φ evolve dynamically. In the horizontal frictionless problem the total kinetic energy is $m\dot{r}^2/2 + (I_0 + mr^2)\dot{\varphi}^2/2$. The angle is cyclic, so the total angular momentum $P = (I_0 + mr^2)\dot{\varphi}$ is constant. As the bead moves out, the turntable slows. The radial equation remains $\ddot{r} = r\dot{\varphi}^2$, but its coefficient now decreases according to the total angular momentum instead of remaining externally fixed.

Eliminate $\dot{\varphi}$ from the total energy to find

$$E = m\dot{r}^2/2 + P^2/[2(I_0 + mr^2)].$$

The reduced radial potential decreases outwards and feeds radial kinetic energy, but the total energy available is finite. Differentiating the potential gives a radial acceleration $P^2 r/(I_0 + mr^2)^2$, consistent with the original radial equation. One should not simply insert $\dot{\varphi} = P/(I_0 + mr^2)$ into the original kinetic Lagrangian before varying r; the correct fixed-momentum Routh reduction subtracts $P\dot{\varphi}$, reversing the sign of the eliminated rotational term. The energy and Lagrangian methods agree once their controlled quantities are distinguished.

With $I_0 = 0.020\,\mathrm{kg\,m^2}$, $m = 0.10\,\mathrm{kg}$, $r_0 = 0.10\,\mathrm{m}$, initial angular speed $4.0\,\mathrm{rad/s}$ and zero radial speed, total momentum is $0.084\,\mathrm{kg\,m^2/s}$ and energy $0.168\,\mathrm{J}$. At $r = 0.30\,\mathrm{m}$ the rotation rate has fallen to $0.084/0.029 = 2.90\,\mathrm{rad/s}$. The remaining radial kinetic energy is $0.168 - 0.084^2/(2 \cdot 0.029) = 0.0463\,\mathrm{J}$, giving radial speed $0.962\,\mathrm{m/s}$. Under a prescribed constant angular speed of four, the radial first integral instead gives $\dot{r} = 4\sqrt{r^2 - r_0^2} = 1.13\,\mathrm{m/s}$ there. The two runs started with identical positions and velocities but have different power connections.

The drive can also be modelled between those limits. Let a servo apply torque $\tau_{\mathrm{drive}} = K_{\mathrm{s}}(\Omega_{\mathrm{command}} - \dot{\varphi})$. Then $d[(I_0 + mr^2)\dot{\varphi}]/dt = \tau_{\mathrm{drive}}$, and the rate of increase of total mechanical energy is $\tau_{\mathrm{drive}}\dot{\varphi}$. A high control gain with finite response time can approximate the prescribed-speed case over part of a trajectory, yet a rapid radial change can cause a measurable speed sag. Recording shaft torque and speed together tests the drive rather than attributing its lag to a fictitious radial friction on the bead.

Infer drive work from a closed loop of length and measured tension

The reel-pendulum experiment produces synchronised records of string force and length. Over a period in which the length returns to its original value, the work on the bob from the reel is $-\oint T\,dl$. A graph of tension against length can enclose a signed area although the string force at each instant is perpendicular to the bob's allowed virtual angular displacement. That loop area measures energy transferred by the imposed control. If the bob returns to its full mechanical state and there are no other energy sources, any net positive reel work must go into losses. If only the string length returns, the bob's energy can increase cycle after cycle.

Suppose the reel shortens by $20\,\mathrm{mm}$ during a high-tension interval averaging $7.0\,\mathrm{N}$, then pays out the same length while the mean tension is $4.5\,\mathrm{N}$. The net mechanical work on the bob is $0.020(7.0-4.5)=0.050\,\mathrm{J}$ for that cycle. A torque sensor on a reel of changing winding radius must convert torque to tension with the actual instantaneous radius. A force signal delayed relative to the length encoder can create a spurious enclosed area, especially when tension changes rapidly near a turning point. Repeating the measurement slowly with a known hanging calibration weight provides a direct check of polarity and timing.

Derive rapid-pivot stabilisation rather than replacing gravity by its mean

The vertical-pivot equation can be written $\ddot{\theta}+[g/l-(A\Omega^2/l)\cos\Omega t]\sin\theta=0$. The time average of the oscillatory coefficient is zero. Nevertheless a high-frequency pivot can alter slow stability because the small fast ripple in θ correlates with the fast acceleration. Let $\theta=\Theta+\xi$, where Θ varies little in a drive period and ξ is small. Keeping the leading rapidly oscillating term gives $\ddot{\xi}\simeq(A\Omega^2/l)\sin\Theta\cos\Omega t$, hence $\xi\simeq-(A/l)\sin\Theta\cos\Omega t$. Its amplitude scales with displacement ratio A/l, so large acceleration and small angular ripple can coexist.

Expand $\sin(\Theta+\xi)\simeq\sin\Theta+\xi\cos\Theta$, insert the fast solution, and average. Terms linear in the cosine average to zero but the product of ripple and imposed acceleration gives a mean cosine square of one half. To leading order the slow equation is

$$\ddot{\Theta}+\frac{g}{l}\sin\Theta+\frac{A^2\Omega^2}{2l^2}\sin\Theta\cos\Theta=0.$$

It derives from an effective potential per angular inertia $U_{\mathrm{eff}}/(ml^2)=-(g/l)\cos\Theta+[A^2\Omega^2/(4l^2)]\sin^2\Theta$, up to a constant. Linearising near $\Theta=\pi+\eta$ gives

$$\ddot{\eta}+[A^2\Omega^2/(2l^2)-g/l]\eta=0.$$

The inverted state is stable within the averaged approximation if $A^2\Omega^2>2gl$. The restoring contribution depends on squared pivot speed amplitude. Replacing effective gravity by its simple time average would miss it entirely.

Choose a rigid pendulum arm with $l=0.20\,\mathrm{m}$, drive amplitude $A=0.0040\,\mathrm{m}$, and $\Omega=600\,\mathrm{s}^{-1}$. The small displacement ratio is 0.020, the pivot speed amplitude is $2.4\,\mathrm{m/s}$, and $A^2\Omega^2=5.76\,\mathrm{m}^2/\mathrm{s}^2$, above $2gl=3.92\,\mathrm{m}^2/\mathrm{s}^2$. The predicted slow angular frequency about the inverted state is $\sqrt{5.76/(2\cdot0.20^2)-9.81/0.20}=4.79\,\mathrm{s}^{-1}$, far below the drive frequency. A slow ripple of tilt $0.10\,\mathrm{rad}$ has a leading drive-frequency micromotion of roughly $0.0020\,\mathrm{rad}$. A camera sampling at an unfortunate phase can hide this micromotion or alias it into apparent slow drift.

The rigid arm in this example is essential. An ordinary string cannot push its bob when an averaged upright configuration requires alternating compression and tension throughout a fast cycle. Check the actual instantaneous radial reaction and the physical actuator's ability to deliver the large acceleration. Also check drive-period, arm elasticity and support resonance before identifying an observed stable

wobble with the averaged rigid-arm prediction. The leading formula assumes small ripple and a clear separation between Ω and all slow angular frequencies; near threshold the slow restoring coefficient is a small difference and higher-order effects or friction become relatively important.

Separate support work from energy in a moving coordinate

Prescribe an accelerating support. Compare the relative response with what a laboratory observer sees and identify how the drive supplies energy.

Open this experiment online

Try the calculation

Support acceleration (m/s²) **1.6**

Spring stiffness (N/m) **8**

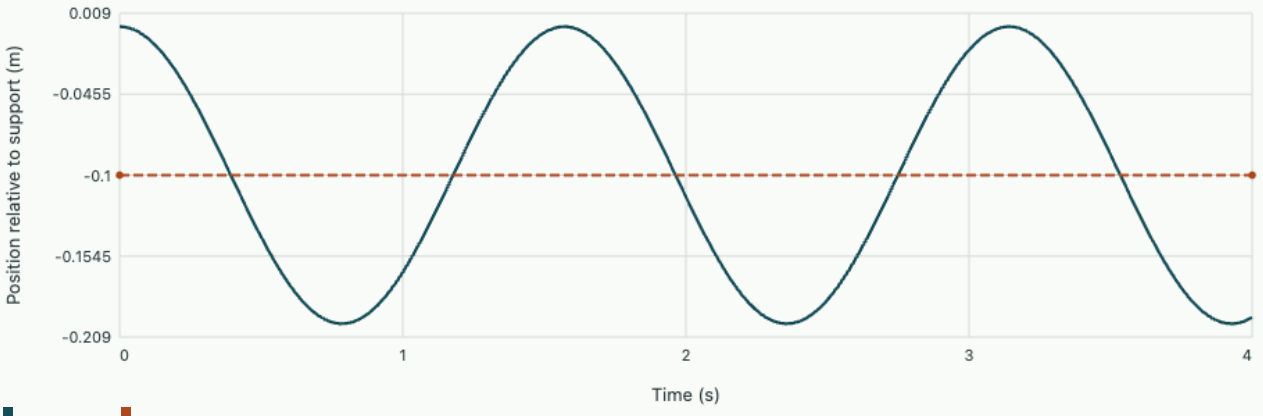

The equilibrium is at -0.1 m. The first turning point is -0.2 m at 0.7854 s.

Distinguish two ways of moving an endpoint in Hamilton's principle

When a constraint itself is explicitly time dependent, the identity $\delta g = \nabla g \cdot \delta x = 0$ describes a virtual change at fixed time on the moving surface. A variational problem may instead allow the endpoint time to change. If a terminal point moves along a prescribed spacetime curve $q_b(t)$, the endpoint variation includes $dq_b = \dot{q}_b\, dt$; it is not an arbitrary tangent displacement at fixed laboratory clock. The boundary term in the on-shell action is $p\, dq - H\, dt$. Reading these two terms separately tells which physical terminal conditions a derivation has assumed.

For a free particle of mass m moving in one dimension from the origin at time zero to q at time T, the extremal action is $S = mq^2/(2T)$. Its derivatives are $S_q = mq/T = p$ and $S_T = -mq^2/(2T^2) = -H$. If the terminal marker moves as $q_b(T) = uT$, the action of the connecting extremal is $mu^2T/2$. Its derivative along that endpoint line is $pu - H = mu^2/2$, exactly the direct derivative. Holding the

endpoint position fixed while differentiating instead gives $-mu^2/2$. Both derivative experiments are legitimate, but the different signs demonstrate why one must state what is fixed.

Can a numerical action fit identify momentum and energy from a single sequence of terminal markers all moving at speed u?

▼ **Work through the solution**

Along that one curve it returns the combination $pu - H$. Separating momentum and energy requires independent endpoint variations in position and time, or another dynamical relation. For the free-particle model the known quadratic Hamiltonian supplies such a relation. For an unknown effective system a single endpoint track can leave different combinations indistinguishable. A grid of nearby fixed-time endpoints estimates p, and a separate grid of terminal times at fixed place estimates $-H$. This measurement interpretation is the finite-dimensional counterpart of separating virtual reaction work from actual boundary power.

Infer whether a moving wall may be treated as prescribed

In an actual impact apparatus the wall has finite effective mass M. For a one-dimensional elastic impact with an initially moving wall, conservation of total momentum and reversal of relative velocity give

$$v^+ = [(m - M)v^- + 2MU]/(m + M),$$
$$U^+ = [2mv^- + (M - m)U]/(m + M).$$

Only the limit $M/m \to \infty$, or active feedback able to enforce the schedule on the collision time scale, gives the prescribed-wall expression used earlier. A motor that restores its target speed a second later may still behave as a finite inertia during the collision itself.

Take $m = 0.20\,\mathrm{kg}$, $M = 2.0\,\mathrm{kg}$, $v^- = 3.0\,\mathrm{m/s}$ and $U = -0.50\,\mathrm{m/s}$. The finite wall sends the particle back at approximately $-3.36\,\mathrm{m/s}$ and recoils to $+0.136\,\mathrm{m/s}$, compared with the prescribed-wall prediction of $-4.0\,\mathrm{m/s}$. Check that the initial and final total momenta both equal about $-0.40\,\mathrm{kg\,m/s}$. Measuring wall speed immediately before and after contact separates an imperfectly enforced boundary from an inelastic impact; both can reduce the magnitude of particle rebound relative to an ideal prescribed boundary.

Tutorial on a prescribed moving apparatus

The rotating slot is held at fixed Ω, but the bead is initially given inward speed $-\Omega r_0$. Predict its subsequent motion and whether the motor delivers or receives power.

▼ **Work through the solution**

The general solution is a combination of growing and decaying exponentials. These initial conditions select $r = r_0 e^{-\Omega t}$. The wall reaction $2m\Omega\dot{r}$ is negative, and its power $2m\Omega^2 r\dot{r}$ is also negative. The

motor receives energy from the bead while maintaining its speed. The same geometric constraint can therefore inject or absorb energy depending on the actual trajectory. The origin is approached only asymptotically in the ideal solution.

At $l = 0.80\,\mathrm{m}$ and $\theta = 0$, a bob has zero angular speed and the prescribed reel tries to accelerate the length outward at $12\,\mathrm{m/s^2}$. Can a string enforce this motion?

▼ **Work through the solution**

The radial-force equation gives $T = m(g - 12)$, a negative tension. A string cannot push the bob outward. The reel pays out slack and the bob initially accelerates under gravity, so treating $l(t)$ as its exact radius becomes inadmissible. A rigid telescopic arm capable of compression would impose a different physical constraint and could enforce the same geometrical schedule.

A pivot is displaced sinusoidally by $2.0\,\mathrm{mm}$ at $1.0\,\mathrm{Hz}$ with $l = 0.25\,\mathrm{m}$. Is the low-frequency tilt formula suitable?

▼ **Work through the solution**

The natural angular frequency is $\sqrt{9.81/0.25} = 6.26\,\mathrm{rad/s}$, almost equal to the drive angular frequency $2\pi = 6.28\,\mathrm{rad/s}$. The low-frequency expansion requires a frequency much smaller than the natural one and fails here. Measure damping and initial conditions, or model a finite-time drive. A steady frictionless amplitude calculated from the small difference of squared frequencies is extremely sensitive to uncertainties in the length and drive frequency.

Compare a second rotating constraint and identify what the motor holds fixed.

David Tong's Lagrangian dynamics chapter develops explicitly time-dependent coordinate changes.

Analytical mechanics from constraints to invariants · 3. Noether's theorem, boundary terms and measurable constants

A constant of motion can survive when neither laboratory energy nor angular momentum is separately conserved. Construct the conserved quantity from an infinitesimal transformation of the action. Then use boosts, a screw symmetry, and a rotating potential to determine what measured combinations should stay fixed.

Vary a path and its time labels

Let $q_i(t)$ be a path for $L(q, \dot{q}, t)$. Consider a continuous family of transformations $t' = t + \varepsilon\tau(q, t)$, $q_i'(t') = q_i(t) + \varepsilon\xi_i(q, t)$, to first order in a constant parameter. The transformation at the corresponding new time has displacement ξ_i; at the original time the path perturbation is $\eta_i = \xi_i - \dot{q}_i\tau$. Distinguishing these variations prevents a time translation from being mistaken for a vertical displacement in a configuration-versus-time plot. Differentiating the transformed coordinates gives

$$\delta\dot{q}_i/\varepsilon = \dot{\xi}_i - \dot{q}_i\dot{\tau},$$

with dots on the generator functions meaning derivatives along the path.

The transformed integration element is $dt' = (1 + \varepsilon\dot{\tau})dt$. A variational symmetry need only preserve the action up to an endpoint term. If its first-order change in the Lagrangian times the time element is $\varepsilon\, dF/dt\, dt$, the equations of motion with fixed endpoints are unchanged. Substitute the variations to write

$$\sum_i \left(L_{q_i}\xi_i + p_i\dot{\xi}_i - p_i\dot{q}_i\dot{\tau}\right) + L_t\tau + L\dot{\tau} = \frac{dF}{dt},$$

$$p_i = L_{\dot{q}_i}.$$

On a physical path $L_{q_i} = \dot{p}_i$. Combine the first two terms into $d(\sum p_i\xi_i)/dt$. Define $H = \sum p_i\dot{q}_i - L$; its derivative on a solution is

$$\dot{H} = -L_t.$$

The terms with τ then combine into $-d(H\tau)/dt$. Thus $Q = \sum_i p_i\xi_i - H\tau - F$ is conserved. Reversing the sign of the generator reverses the sign of the charge, which has no bearing on conservation. Scaling the group parameter also rescales the charge, so specifying the transformation matters when reporting its units.

Recover the familiar examples and test broken symmetry

For a common infinitesimal translation along fixed unit vector $\hat{n}$, every particle has $\xi_a = \hat{n}$, $\tau = 0$. A potential depending solely on pair separations is invariant, so $F = 0$. The conserved charge is total momentum along $\hat{n}$. For an infinitesimal rotation about the origin,

$$\xi_a = \hat{n} \times \mathbf{r}_a;$$

the scalar triple product gives $\hat{n} \cdot \sum_a \mathbf{r}_a \times \mathbf{p}_a$, the chosen angular momentum component. For time translation $\tau = 1, \xi = 0$, an explicitly time-independent Lagrangian gives $Q = -H$. In each case the symmetry refers to the system including the prescribed external fields. Internal pair forces may conserve momentum while a fixed trap exerting an external force breaks the translation symmetry of the particles.

The algebra also gives an exact diagnostic for an approximate symmetry. If the variation of $L dt$ differs from the boundary term by $\varepsilon \mathcal{D}\, dt$, the same steps give

$$\dot{Q} = \mathcal{D}.$$

In a weak potential $V(x) = V_0 + \epsilon U(x)$, translation of x gives

$$\dot{p}_x = -\epsilon U'(x).$$

A drifting computed momentum is therefore not automatically a failure of the time integrator. Compare its change with the integrated physical symmetry-breaking force. Reversing the small external bias helps separate the first-order physical drift from a numerical offset that does not reverse.

Derive a boost charge that needs an endpoint term

Consider a free Newtonian particle in one dimension and a small Galilean boost $x' = x + \varepsilon t$. Here $\xi = t$, $\tau = 0$, and $L = m\dot{x}^2/2$ changes to first order by $m\dot{x}\varepsilon = d(mx\varepsilon)/dt$. The Lagrangian is not pointwise invariant, but its change is a total derivative. The charge is $Q = pt - mx$; its constancy is equivalent to $x - (p/m)t$ remaining equal to the initial position. Dropping the endpoint term would give pt, whose derivative is generally the nonzero momentum itself.

For mutually interacting particles with translationally invariant internal forces, summing the argument gives

$$Q = Pt - MR_{\mathrm{cm}}.$$

Constancy of total momentum and boost charge together imply that the centre of mass moves uniformly along a straight line. Take two pucks of masses 0.20 and $0.30\,\mathrm{kg}$ with $x_1(0) = 0$, $x_2(0) = 1.0\,\mathrm{m}$, and velocities 2.0 and $-0.5\,\mathrm{m/s}$. Their total momentum is $0.25\,\mathrm{kg\,m/s}$ and centre of mass starts at $0.60\,\mathrm{m}$. At $t = 0.40\,\mathrm{s}$, including any intervening isolated elastic collision, it must be at $0.80\,\mathrm{m}$. The boost charge $0.25t - 0.50R_{\mathrm{cm}}$ remains $-0.30\,\mathrm{kg\,m}$. Internal impact changes the individual momenta but preserves both total quantities.

Rotate and translate together in a helical landscape

Let a particle move in cylindrical coordinates in a potential $V(r, z - c\varphi)$, with the combination physically interpreted on a helical branch or within a periodic potential compatible with 2π rotation. Rotation

through a small angle ε combined with translation $z \to z + c\varepsilon$ leaves the potential unchanged. The kinetic energy $m(\dot r^2 + r^2\dot\varphi^2 + \dot z^2)/2$ also stays unchanged. The generator has $\xi_\varphi = 1, \xi_z = c$, hence $Q = p_\varphi + c p_z$ is conserved. The constant c has units of length per radian, so both terms have angular-momentum units.

Differentiate directly as a check. Writing $u = z - c\varphi$, Hamilton's equations give

$$\dot p_\varphi = +c\,V_u,$$

$$\dot p_z = -V_u.$$

Each can change, yet the combination has zero derivative. A guided particle receiving a burst of axial momentum can exchange a specific amount of angular momentum with the helical potential. For $c = 0.030\,\mathrm{m}$ and $\Delta p_z = 0.080\,\mathrm{kg\,m/s}$, the relation predicts $\Delta p_\varphi = -0.0024\,\mathrm{kg\,m^2/s}$. A circularly symmetric potential would conserve angular momentum on its own and represents a different field configuration.

Exchange energy and angular momentum in a rotating pattern

A potential $V(r, \varphi - \Omega t)$ with constant pattern speed is unchanged when time increases by ε and the particle coordinates rotate by $\Omega\varepsilon$. Take $\tau = 1, \xi_\varphi = \Omega$. The conserved combination is $H - \Omega p_\varphi$, up to the sign chosen for Q. A torque from the rotating apparatus can change ordinary energy and ordinary angular momentum. Their changes obey $dH = \Omega\, dp_\varphi$ along the trajectory when the Hamiltonian contains only the prescribed rotating potential as explicit time dependence. The external power equals angular speed times the torque acting through that pattern.

Suppose $\Omega = 12\,\mathrm{rad/s}$ and a particle gains $0.015\,\mathrm{kg\,m^2/s}$ in axial angular momentum during a passage past the rotating potential. Its mechanical energy must gain $0.180\,\mathrm{J}$. A numerical run reporting $0.195\,\mathrm{J}$ calls for accounting for other time dependence, sampling uncertainty or integration error. If Ω itself slowly varies, introduce a pattern angle $\alpha(t)$, $\Omega = \dot\alpha$. One still finds $\dot H = \Omega \dot p_\varphi$, but $d(H - \Omega p_\varphi)/dt = -\dot\Omega p_\varphi$. Testing an exact rotating-frame invariant with a ramped motor would therefore diagnose the wrong experiment.

Find the conserved momentum in a magnetic field directly from the action

A charge q of mass m moves in a uniform static field $B\hat z$. Choose vector potential $A_y = Bx$, scalar potential zero. Its Lagrangian in the perpendicular plane is $L = m(\dot x^2 + \dot y^2)/2 + qBx\dot y$. The position y is cyclic, so $p_y = m\dot y + qBx$ is constant. The physical force is also invariant under translations in x, although x appears in this chosen Lagrangian. Under $x \to x + \varepsilon$, its change is $qB\dot y\,\varepsilon = d(qBy\varepsilon)/dt$. The corresponding Noether charge is $p_x - qBy = m\dot x - qBy$. Thus both spatial translation symmetries survive once the endpoint term is included.

Write $\omega_c = qB/m$, which retains the sign of the charge. Rearranging the two constants gives the coordinates of the guiding centre $X_c = x + \dot y/\omega_c$, $Y_c = y - \dot x/\omega_c$. Differentiate using

$m\ddot{x} = qB\dot{y},\ m\ddot{y} = -qB\dot{x}$ to see both are independent of time. A uniform field changes velocity direction but does no work. In a force experiment the centre of the measured circular arc, its radius and its angular orientation can be estimated without measuring any vector potential. The endpoint terms explain why two gauge choices can assign different canonical momenta while predicting the same observed guiding centre.

There is a useful algebraic surprise. Denote the translation charges by $K_x = p_x - qBy$ and $K_y = p_y$ in the chosen gauge. Their canonical bracket is $\{K_x, K_y\} = -qB$. Each is conserved, yet the bracket does not vanish. The result is a constant, so Jacobi's identity is satisfied. The mechanical effect of their infinitesimal flows on positions commutes; a central constant in the charge bracket has zero Hamiltonian vector field. Conservation, commutation of the generated coordinate motions, and zero bracket of the generating functions are related but distinct statements. This example supplies a direct check when applying symmetry counting in phase space.

For an illustrative particle with $q/m = 2.0\,\mathrm{C/kg}$, $B = 0.50\,\mathrm{T}$, initial $(x, y) = (0.20, 0.10)\,\mathrm{m}$ and velocity $(0.30, -0.40)\,\mathrm{m/s}$, the signed cyclotron frequency is $1.0\,\mathrm{s^{-1}}$. The guiding centre is $(-0.20, -0.20)\,\mathrm{m}$, and the radius from that centre is $0.50\,\mathrm{m}$. The speed is $0.50\,\mathrm{m/s}$, consistent with radius $v/|\omega_c|$. Replacing the field by its negative at the same initial state moves the guiding centre to the opposite side of the initial velocity and reverses the sense of rotation. A constant numerical offset in the vector potential should leave both reconstructed centres unchanged.

Use scaling to decide when a formal transformation creates a charge

Many equations of motion have scaling relations. A map taking one solution into another need not preserve the action up to an endpoint term, and therefore need not supply a Noether charge. To test an example, let $L = T - V$ in three dimensions with V homogeneous of degree n, so $V(\lambda \mathbf{r}) = \lambda^n V(\mathbf{r})$. Take $\mathbf{r} \to e^{\varepsilon}\mathbf{r}$, $t \to e^{a\varepsilon}t$. Kinetic energy times dt scales as $e^{(2-a)\varepsilon}$, while potential energy times dt scales as $e^{(n+a)\varepsilon}$. Equating the exponents gives $a = (2 - n)/2$, a map that rescales the entire action by a common factor and preserves stationary paths. Exact invariance of the action additionally requires the common exponent to vanish, giving $a = 2, n = -2$.

For a potential proportional to $1/r^2$, the continuous symmetry has $\xi = \mathbf{r}, \tau = 2t$, $F = 0$, and charge $D = \mathbf{r} \cdot \mathbf{p} - 2tH$. Direct differentiation gives $d(\mathbf{r} \cdot \mathbf{p})/dt = 2T - \mathbf{r} \cdot \nabla V = 2T + 2V = 2H$, verifying conservation. At fixed positive energy this particular scalar product grows linearly in time. This does not require every coordinate to grow linearly; it follows from the scaling structure of the combined kinetic and potential energies. Collision singularities may limit the interval on which a classical solution exists.

For a Newtonian potential $n = -1$, the path scaling gives $a = 3/2$, precisely the scaling of orbital periods with orbital size. The common action exponent is $1/2$, so this scaling does not produce the preceding conserved D. Instead the virial identity $d(\mathbf{r} \cdot \mathbf{p})/dt = 2T + V$ implies $2\langle T \rangle + \langle V \rangle = 0$ on a bounded periodic trajectory after time averaging. This distinction can be checked numerically on one elliptical orbit: the virial combination generally oscillates during a cycle, whereas its integrated full-cycle average vanishes. Mistaking a scaling of solutions for exact invariance of the action would turn that averaged result into a false instantaneous conservation law.

Derive a centre-of-energy statement from a boost charge

For a free relativistic particle in one spatial dimension use $L = -mc^2\sqrt{1 - \dot{x}^2/c^2}$. An infinitesimal Lorentz boost, with a parameter carrying velocity units and the sign convention $x' = x + \varepsilon t$, has generators $\xi = t, \tau = x/c^2$. Proper time is invariant, so $L dt$ is invariant and $F = 0$. The Noether charge is $K = pt - Hx/c^2$, where $H = \gamma mc^2$, $p = \gamma m\dot{x}$. Its derivative vanishes because $p = H\dot{x}/c^2$. At low speed H/c^2 approaches m, and the Newtonian boost charge reappears up to relativistic corrections.

For an isolated set of freely propagating particles away from local collisions, sum the charges to obtain

$$K = Pt - (E_{\mathrm{tot}}/c^2)X_E,$$

where $X_E = \sum E_i x_i / E_{\mathrm{tot}}$ is the centre of energy. If collisions conserve total energy and momentum and occur at the same spacetime point for their participants, the summed charge passes continuously across them. Its constancy implies

$$dX_E/dt = c^2 P / E_{\mathrm{tot}}.$$

In an interacting field problem energy stored between particles also belongs in the weighted centre; assigning every bit of energy to particle positions can violate the balance. A field-carrying interaction illustrates why the Newtonian centre of mass alone is insufficient in a relativistic energy accounting.

Imagine equal positive rest masses at $x = 0$ and $x = 2.0\,\mathrm{m}$. At the observation instant their energies are $2mc^2$ and mc^2, with the more energetic particle moving to the right and the second at rest. Their ordinary mass centre is $1.0\,\mathrm{m}$, while their energy centre is $2/3\,\mathrm{m}$. The total momentum is $\sqrt{3}\,mc$, the total energy $3mc^2$, so the centre of energy moves at $c/\sqrt{3}$. The numerical difference is not a correction to the measured coordinates but a change in the physical quantity whose motion follows a boost symmetry. A centre-of-momentum frame for the pair moves at the same speed.

Diagnose symmetry from noisy finite-time balances

In an experiment one rarely has symbolic access to every component of the Lagrangian. A practical symmetry test measures the candidate charge at two times and independently integrates the physical source expected to change it. For the rotating potential, use $R = \Delta H - \int_{t_1}^{t_2} \Omega(t)\, dL_z$. If Ω is measured on the same clock as the trajectory, the integral can be estimated by summing the mean Ω across each angular-momentum increment. This avoids taking a second time derivative of position merely to reconstruct the torque. An equivalent form obtained by parts is $\Delta(H - \Omega L_z) + \int L_z\, d\Omega$. Both versions should agree if endpoint times and signs are consistent.

Take a short programmed ramp in which Ω increases linearly from 10 to $12\,\mathrm{s^{-1}}$ and L_z from 0.030 to $0.050\,\mathrm{kg\,m^2/s}$ over the same time. If the rotating pattern is the only external work source, the energy change is mean speed times angular-momentum change,

$$11(0.020) = 0.220\,\mathrm{J}.$$

The product ΩL_z changes by $0.600 - 0.300 = 0.300\,\mathrm{J}$, so $H - \Omega L_z$ falls by $0.080\,\mathrm{J}$. The missing amount equals

$$-\int L_z \, d\Omega = -0.040(2) = -0.080\,\mathrm{J}.$$

These two balances provide a nontrivial sign test when the drive speed is varied deliberately.

When measurements are noisy, an observed discrepancy must be compared with the uncertainties of both charge and physical source. An erroneous angular zero in a central problem can affect the torque reconstruction while leaving a scalar speed unchanged; a simple time shift between the motor encoder and position camera can mimic an extra source of work. Change the drive direction, repeat with constant speed, and estimate the effect of clock offsets using resampled records. These experiments test the specific symmetry under investigation. A plot that appears almost flat on an arbitrary vertical scale supplies neither a physical tolerance nor a discrimination among competing error sources.

Derive a conservation law for an elastic field

Noether's argument also applies when the coordinates form a continuous field $u(x, t)$. Consider a uniform string or rod with density per length ρ_l, displacement field u and stiffness coefficient C, so $\mathcal{L} = \rho_l u_t^2/2 - C u_x^2/2$. A constant shift $u \to u + \varepsilon$ changes no strain and leaves the density invariant. The Euler–Lagrange equation becomes $\partial_t(\rho_l u_t) + \partial_x(-C u_x) = 0$, a local conservation law. For an axial rod the density $\rho_l u_t$ is ordinary longitudinal momentum per unit length, and the boundary term is axial traction with its outward sign. A uniform displacement symmetry survives a free translation of the whole rod but is broken if an end displacement is imposed relative to a clamp.

Integrate from $x = 0$ to L. The total physical momentum changes as $dP/dt = C u_x(L) - C u_x(0)$. A fixed end can exert a nonzero reaction and spoil conservation of the rod's momentum even when it does no power because its actual velocity vanishes. The distinction between a momentum source and an energy source is experimental: a rigid wall reflecting a pulse can accept net impulse while taking no mechanical energy. Including the support in the system restores the corresponding balance. Checking only the field density's invariance in the interior neglects boundary conditions, which are part of a physical symmetry.

The uniformity of material parameters also gives an invariance under translations of the material coordinate x in an infinite or periodic homogeneous domain. The associated density is proportional to $-\rho_l u_t u_x$, often called wave pseudomomentum under this convention. Derive its local balance by multiplying $\rho_l u_{tt} = C u_{xx}$ by $-u_x$ and applying the product rule. One obtains

$$\partial_t(-\rho_l u_t u_x) + \partial_x[C u_x^2/2 + \rho_l u_t^2/2] = 0.$$

This conserved quantity differs from the ordinary momentum found from shifting u itself. A small-amplitude sinusoidal travelling wave can have zero mean material velocity over one period yet positive mean transport of this wave quantity.

For $u = A\cos(kx - \omega t)$,

$$u_t = \omega A \sin(kx - \omega t),$$
$$u_x = -kA \sin(kx - \omega t).$$

The cycle-averaged wave density is $\rho_l \omega k A^2/2$ while ordinary momentum density averages to zero. With $\rho_l = 0.20\,\mathrm{kg/m}$, $A = 1.0\,\mathrm{mm}$, $k = 5.0\,\mathrm{m^{-1}}$, and $\omega = 100\,\mathrm{s^{-1}}$, the average wave density is $5.0 \times 10^{-5}\,\mathrm{kg/s}$. Its units are momentum per unit length, but equal dimensions do not make the two conserved charges interchangeable. To identify the charge, specify whether the symmetry shifts every displacement equally or shifts the material-coordinate pattern.

Test the evolution of a phase-space patch

Follow a family of initial conditions in a Hamiltonian flow. Compare changes in its shape with the conservation of its phase-space area.

Open this experiment online

Try the calculation

Time after release (s) **4**

Drag rate γ (1/s) **0.2**

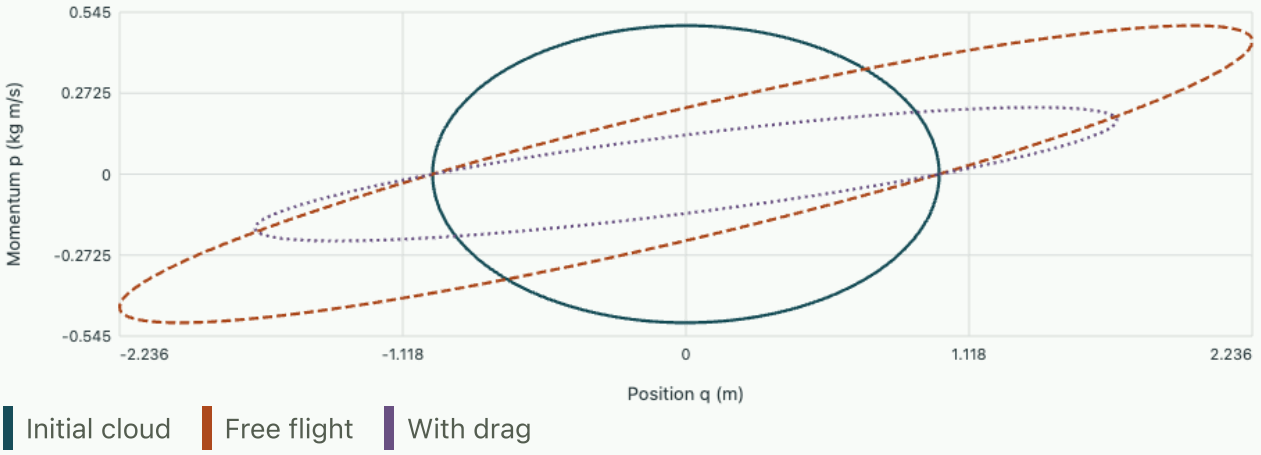

Free position spread 2.236 m. The damped ellipse retains 44.93% of its initial area and has position spread 1.702 m.

Derive an identity without assuming the equations of motion

The usual on-shell proof substitutes the Euler–Lagrange equations just before a total derivative appears. Retaining the difference gives an equally useful off-shell identity. Define the residual $R_i = dp_i/dt - \partial L/\partial q_i$. For a true variational symmetry and any differentiable trial path, repeat the calculation with $\eta_i = \xi_i - \dot{q}_i \tau$. The result is

$$dQ/dt = \sum_i R_i \eta_i.$$

Thus the drift of a Noether charge evaluated on an approximate path is a particular projection of its dynamical residual. A path can have zero drift of one charge while violating equations in directions to which that charge is insensitive.

For a free particle in two dimensions, perfect conservation of p_x enforces zero residual acceleration in the x direction but says nothing about a spurious force in y. Conversely tracking two independent translational charges checks both components. Energy conservation tests a different projection, $dH/dt = \dot{\mathbf{q}} \cdot \mathbf{R}$ for a time-independent Lagrangian. An error force always perpendicular to velocity can leave the speed and energy unchanged while bending an originally straight trajectory. That is one reason an invariant energy graph cannot replace a force residual or a comparison of trajectories.

A numerical planar free particle follows a circle of constant speed even though the programmed potential vanishes. Its energy is conserved exactly. Which Noether quantities expose the problem most directly?

▼ **Work through the solution**

The two laboratory translation momenta should each be constant. On the reported circle their vector changes direction continuously, so their residuals immediately reveal the missing transverse equation. A check of only the magnitude of momentum would also pass because that magnitude is fixed by energy. The angular momentum about the circle centre can remain constant too. Testing a set of charges selected for the actual symmetry and measured geometry identifies information lost by each scalar test on its own.

If the Lagrangian acquires a small explicitly time-dependent conservative potential $V_1(t)q^2$, what quantity should replace a flat-energy test?

▼ **Work through the solution**

The energy change on a physical path is $\Delta H = \int \dot{V}_1(t) q(t)^2 \, dt$. Positive or negative changes are allowed according to how the externally imposed stiffness is varied during the motion. Compare the measured change with this integral while keeping the time dependence inside the Hamiltonian itself. A flat-energy requirement would incorrectly penalise physical work by the control, whereas a residual after the input integral tests the dynamics.

Separate a discrete symmetry from a continuous one

A potential $V(q) = a(q^2 - b^2)^2$ is invariant under the discrete reflection $q \mapsto -q$. Reflecting both position and velocity maps any solution into another solution with equal energy. There is no continuously tunable parameter that takes the identity smoothly to this isolated reflection while preserving the same one-dimensional potential at every intermediate step. No infinitesimal translation generator follows from this symmetry, and the momentum generally changes along either path. A pair of measured trajectories

launched from mirrored initial data should match after reflection, but neither trajectory is required to have zero or constant momentum.

For $a = 1$ and $b = 1$ in consistent scaled units, release particles from $q = 0.50$ and -0.50 at rest. The force is $-4q(q^2 - 1)$, giving initial accelerations $+1.50/m$ and $-1.50/m$. The two accelerations are mirror images, not individually zero. A numerical method that accidentally introduces a constant bias force breaks the reflection comparison and shifts the two turning times in opposite senses. Energy can remain nearly conserved with respect to a slightly tilted effective potential, so trajectory pairing is a complementary diagnostic. Reflection symmetry imposes a relationship between solutions even when Noether's continuous-symmetry construction supplies no new conserved scalar.

Tutorial on identifying symmetries

A Lagrangian is replaced by $L' = L + dG(q,t)/dt$. Does the numerical value of an appropriately derived Noether charge have to change?

▼ Work through the solution

The new momentum is $p'_i = p_i + G_{q_i}$, and $H' = H - G_t$. Under the given symmetry the new boundary term is $F' = F + \sum_i G_{q_i}\xi_i + G_t\tau$. Substitution into $p'\xi - H'\tau - F'$ cancels the extra terms exactly. Charges can still be shifted by a physically irrelevant additive constant through the choice of boundary term. Comparing raw canonical momentum in two such conventions without also transforming F, H confuses intermediate variables with observations.

A central potential is changed into an axisymmetric potential $V(r,\theta)$. Which angular-momentum tests remain exact?

▼ Work through the solution

Rotation about the symmetry axis remains a continuous symmetry, so its angular-momentum component is conserved. Tilt rotations generally change the potential, so the transverse components need not stay constant. The torque may cause the angular momentum direction or magnitude to evolve while maintaining its axial component. A code test that requires all components to remain fixed would reject many legitimate axisymmetric trajectories.

A table exerts an unmodelled approximately constant horizontal drag $0.010\,\mathrm{N}$ opposite the motion of the two pucks for $0.40\,\mathrm{s}$. Estimate how the translation and boost checks change.

▼ Work through the solution

Total momentum changes by $-0.0040\,\mathrm{kg\,m/s}$. The derivative of $Pt - MR_{\mathrm{cm}}$ is $t\dot{P}$, since $P = M\dot{R}_{\mathrm{cm}}$. Its change is therefore $-0.010(0.40)^2/2 = -0.00080\,\mathrm{kg\,m}$ under constant drag. The differing time dependence gives an additional way to distinguish a sustained external force from an initial position calibration error.

Follow the action of an infinitesimal generator on phase space.

David Tong treats continuous symmetries and Noether's theorem in Lagrangian dynamics.

Analytical mechanics from constraints to invariants · 4. Kepler orbits, the eccentricity vector and the loss of apsidal closure

An orbit can conserve energy and angular momentum yet gradually rotate its periapsis. The inverse-square problem possesses one more conserved vector that fixes the direction of closest approach. Derive it, turn a single position and velocity measurement into a conic, and measure what a weak perturbation does to the inferred apsidal direction.

Reduce the two-body system without freezing either mass

Two bodies of masses m_1, m_2 have positions $\mathbf{r}_1, \mathbf{r}_2$. Define total mass $M = m_1 + m_2$, centre $\mathbf{R} = (m_1\mathbf{r}_1 + m_2\mathbf{r}_2)/M$, relative coordinate $\mathbf{r} = \mathbf{r}_1 - \mathbf{r}_2$, and reduced mass $\mu = m_1 m_2 / M$. Substitution into the kinetic energy cancels the cross terms, giving $M\dot{\mathbf{R}}^2/2 + \mu\dot{\mathbf{r}}^2/2$. Newtonian gravitational potential is $-\kappa/r$ with $\kappa = G m_1 m_2$. The centre moves uniformly when isolated, while the relative motion obeys $\mu\ddot{\mathbf{r}} = -\kappa\hat{r}/r^2$. Dividing by the reduced mass gives the acceleration parameter $k = \kappa/\mu = GM$; replacing it by Gm_1 is the test-particle approximation.

Use specific energy $\epsilon = v^2/2 - k/r$ and specific angular momentum $\mathbf{h} = \mathbf{r} \times \mathbf{v}$, both per unit reduced mass. A central force makes $\dot{\mathbf{h}} = 0$, fixing the plane of nonradial motion. The area of the triangle swept in time dt is $r^2 d\varphi/2 = h\,dt/2$, yielding the constant areal rate. The radial energy is $\dot{r}^2/2 + h^2/(2r^2) - k/r$. Its turning points determine the accessible radii, but energy and h alone cannot specify where the major axis lies in the chosen inertial plane.

Construct a vector whose derivative vanishes

The derivative of $\mathbf{v} \times \mathbf{h}$ is $(-k\hat{r}/r^2) \times \mathbf{h}$. Use $\mathbf{h} = r^2\dot{\varphi}\,\hat{z}$ with an oriented plane in which motion is positive. Since $\hat{r} \times \hat{z} = -\hat{\varphi}$, the derivative becomes

$$k\dot{\varphi}\hat{\varphi} = k\,d\hat{r}/dt.$$

Consequently the eccentricity vector

$$\mathbf{e} = \frac{\mathbf{v} \times \mathbf{h}}{k} - \hat{r}$$

is constant. The dimensional Runge–Lenz vector is proportional to this choice: for relative momentum $\mathbf{p} = \mu\mathbf{v}$,

$$\mathbf{A} = \mathbf{p} \times \mathbf{L} - \mu\kappa\hat{r} = \mu\kappa\mathbf{e}.$$

Every term in the specific expression is dimensionless. The step equating the derivative to $k\,d\hat{r}/dt$ uses exactly the inverse-square radial force. General central forces retain areal velocity but lose this cancellation.

Dot $\mathbf{e}$ with $\hat{r}$. The triple product $(\mathbf{v} \times \mathbf{h}) \cdot \hat{r} = h^2/r$ gives

$$e\cos(\varphi-\varpi)=h^2/(kr)-1,$$

where ϖ is the fixed direction of $\mathbf{e}$. Thus $r=p/[1+e\cos(\varphi-\varpi)]$, $p=h^2/k$, the conic in focus-centred polar coordinates. Squaring $\mathbf{e}$ and eliminating v^2 with the energy gives

$$e^2=1+2\epsilon h^2/k^2.$$

Bound ellipses have $\epsilon<0, e<1$, parabolic escape has $\epsilon=0, e=1$, and positive energy gives hyperbolas for nonzero angular momentum. Radial trajectories require separate care because their orbital plane and apsidal angle are degenerate.

Recover the orbit from a single state vector

In units chosen so $k=1$, a measured relative position is $(2,0,0)$ and velocity is $(0.2,0.6,0)$. Compute $h_z=1.2$, $\epsilon=(0.04+0.36)/2-1/2=-0.30$, and $p=1.44$. The cross product $\mathbf{v}\times\mathbf{h}=(0.72,-0.24,0)$ gives $\mathbf{e}=(-0.28,-0.24,0)$, with $e=\sqrt{0.136}\approx 0.369$. The direction of periapsis is about 220.6° from the positive x axis. At the measured point $\dot r>0$, so the body is travelling from periapsis toward apoapsis. Dropping the radial component of velocity would rotate the eccentricity vector and change the inferred shape.

The semimajor axis is

$$a=-k/(2\epsilon)=1.667.$$

Periapsis and apoapsis radii $a(1-e)$ and $a(1+e)$ are approximately 1.05 and 2.28, consistent with the observed radius of two. The orbital period is $2\pi\sqrt{a^3/k}=13.52$ time units. Derive this last result by dividing ellipse area πab by the areal speed $h/2$. Using $b=a\sqrt{1-e^2}$ and $h^2=ka(1-e^2)$ cancels eccentricity exactly. This shows why changing the initial radial velocity can change shape and orientation while the period depends only on binding energy.

Determine time along an ellipse and check limiting cases

Introduce the eccentric anomaly E by $x=a(\cos E-e)$, $y=a\sqrt{1-e^2}\sin E$ in axes centred on the focus, with x pointing toward periapsis. Then $r=a(1-e\cos E)$. Compute $x\,dy-y\,dx=ab(1-e\cos E)\,dE$ and equate it to $h\,dt$. Integrating from periapsis gives

$$n(t-t_p)=E-e\sin E,$$

where $n=\sqrt{k/a^3}$. This relation turns orbital geometry into an observation clock. The true anomaly is generally different from the linearly advancing mean anomaly because the body sweeps angle faster at small radius.

For $e = 0.6$ and the time $t - t_p = T/4$, the mean anomaly is $\pi/2$. Newton iteration for $F(E) = E - 0.6 \sin E - \pi/2$ uses denominator $1 - 0.6 \cos E$, which stays positive. Starting near $E = 2.0$ yields $E \simeq 2.091$ radians and $r \simeq 1.30a$. The orbit has already moved beyond its semimajor radius at a quarter period. At $e = 0$, E equals the mean and true anomalies up to an arbitrary origin, and $\mathbf{e} = 0$ has no definable periapsis direction. Estimating a periapsis angle for a nearly circular noisy orbit is therefore poorly conditioned even when the radius and period are well measured.

Perturb the force and measure apsidal precession

For any central acceleration $f(r)\hat{r}$, put $u = 1/r$. Since $\dot{\varphi} = hu^2$, radial velocity is $-h\,du/d\varphi$. Substituting into the radial acceleration gives Binet's equation $u'' + u = -f(1/u)/(h^2u^2)$, where primes denote angular derivatives. Choose $f(r) = -k/r^2 - \alpha/r^3$. Then $u'' + (1 - \alpha/h^2)u = k/h^2$. If $0 < \alpha < h^2$, a radial oscillation requires angular advance $2\pi/\sqrt{1 - \alpha/h^2}$, greater than one full turn. Successive periapses advance by that value minus 2π, approximately $\pi\alpha/h^2$ for a weak perturbation.

With $\alpha/h^2 = 0.010$, the exact precession per radial cycle is approximately $0.03165\,\mathrm{rad} = 1.81^\circ$. Ordinary energy and angular momentum remain constant in this conservative central potential. The Kepler eccentricity vector evaluated from instantaneous position and velocity now changes. Track periapses using zeros of the radial velocity with positive radial acceleration, then compare their inertial angles. A numerical Kepler integrator can precess even for $\alpha = 0$; refine the time step and repeat the unperturbed control before assigning a small precession to the physical perturbation.

Infer an orbit using quantities that remain well conditioned

Suppose positions and velocities are measured with finite precision. A circular orbit has exact eccentricity vector zero, so even tiny perpendicular perturbations can swing the direction of that vector through large angles. Keep its Cartesian components when computing a fit near circularity. For an initially transverse circular state at radius r and speed $v_c = \sqrt{k/r}$, perturb the velocity by radial δv_r and tangential δv_t. In the local $(\hat{r}, \hat{\varphi})$ basis the eccentricity components are $rv_t^2/k - 1$ and $-rv_rv_t/k$. At first order they become $2\delta v_t/v_c$ and $-\delta v_r/v_c$. This linear response is well behaved even though taking an inverse tangent to quote periapsis longitude can become meaningless.

For a circular speed of $10.0\,\mathrm{m/s}$, radial and tangential measurement errors each of $0.010\,\mathrm{m/s}$ correspond to component uncertainties about 0.0010 and 0.0020. A reported eccentricity of 0.0012 is not accompanied by a precise preferred direction under those uncertainties. Repeated orbital samples reduce independent noise but do not remove a persistent tangential velocity bias. Measuring the radius and period independently supplies an additional constraint on k and the orbital energy. A model that regards the primary as fixed also introduces a systematic mass error when the secondary has non-negligible mass.

At the opposite extreme, a near-parabolic orbit can have a well-defined eccentricity direction but a badly conditioned energy estimate. Its energy is the small difference of $v^2/2$ and k/r. Since $a = -k/(2\epsilon)$, a small energy uncertainty produces a very large uncertainty in semimajor axis and period. Report the measured state vector, eccentricity vector and energy uncertainty before interpreting an enormous best-

fit period. If the energy uncertainty straddles zero, bounded and unbounded conics are both consistent with the measured data. Integrating a single best-fit ellipse for many revolutions does not resolve that ambiguity.

Calculate the velocity impulse to transfer between circular radii

The same two-body invariants reconstruct a transfer between circular trajectories without requiring a time-stepped simulation. Set a lower radius r_1 and an upper radius $r_2 > r_1$. An ellipse tangent to both has periapsis r_1, apoapsis r_2, semimajor axis $a_t = (r_1 + r_2)/2$, and eccentricity $(r_2 - r_1)/(r_2 + r_1)$. At either apsis its speed follows from energy:

$$v_t(r) = \sqrt{k(2/r - 1/a_t)}.$$

A first instantaneous tangential velocity change moves the particle from its lower circular trajectory to the transfer ellipse. A second tangential change at the opposite apsis matches the upper circular speed. These formulas describe impulses idealised as short compared with the orbital period.

Choose normalised $k = r_1 = 1$, $r_2 = 2$. Initial speed is one, transfer semimajor axis 1.5, and periapsis speed $\sqrt{4/3} = 1.1547$. The first change is 0.1547. At the upper radius the transfer speed is $\sqrt{1/3} = 0.57735$, while the circular speed there is

$$1/\sqrt{2} = 0.70711.$$

The second change must also be forward, by 0.12976. The flight time between the two impulses is $\pi\sqrt{1.5^3} = 5.77$ time units, half the transfer period. Simply increasing the initial speed until the path reaches radius two does not make it circular upon arrival. Matching position and angular momentum at the final boundary requires the second change.

Verify the energy increment from an impulse independently. A change $\Delta\mathbf{v}$ at fixed position gives

$$\Delta\epsilon = \mathbf{v} \cdot \Delta\mathbf{v} + |\Delta\mathbf{v}|^2/2.$$

At the lower radius our impulse raises ϵ from -0.5 to $-1/3$, an increase of $1/6$. Substitution of the rounded 0.1547 gives the same value. The same velocity increment generally changes energy more when applied where the initial speed is larger and aligned with the impulse. This is a statement about mechanical work at different initial states, not an exception to conservation between impulses.

A laboratory analogue uses a central potential engineered over a limited radius range. A small finite-duration tangential push changes radius as well as speed during the push. To check the impulse approximation compute the change in angular momentum as $\int \mathbf{r} \times \mathbf{a}_{\text{applied}}\, dt$ and energy as $\int \mathbf{v} \cdot \mathbf{a}_{\text{applied}}\, dt$. Compare these with the instantaneous predictions and shorten the pulse while holding its integrated velocity change fixed. If the return radius still drifts, map the force against radius to distinguish a finite-pulse error from an actual deviation from inverse-square attraction.

Continue the time law across the escape boundary

A hyperbolic Kepler orbit can be described without calling a divergent ellipse period a clock. Define a positive hyperbolic length $a_h = k/(2\epsilon)$ for $\epsilon > 0$, and let $e > 1$. With periapsis on the positive x axis use $x = a_h(e - \cosh H)$,

$$y = a_h\sqrt{e^2 - 1}\sinh H.$$

Then $r = a_h(e\cosh H - 1)$, and the swept-area relation gives

$$t - t_p = \sqrt{a_h^3/k}(e\sinh H - H).$$

The hyperbolic anomaly H increases monotonically from negative to positive along the passage. At large positive H the ratio dr/dt approaches $\sqrt{k/a_h} = \sqrt{2\epsilon}$, the asymptotic speed predicted by the conserved energy.

At the parabolic boundary $e = 1, \epsilon = 0$, put $D = \tan(\varphi/2)$ with φ measured from periapsis. If q_p is the periapsis distance, the semilatus rectum is $p = 2q_p$ and $r = q_p(1 + D^2)$. Since $dt = r^2 d\varphi/h$, $d\varphi = 2dD/(1 + D^2)$ and $h = \sqrt{2kq_p}$, integration gives Barker's relation $t - t_p = \sqrt{2q_p^3/k}(D + D^3/3)$. This expression is finite on either side of the periapsis for finite radius, even as the time to reach infinity diverges. A parabolic passage therefore has an entirely useful local time-of-flight law despite having no period.

For $k = 1$, $q_p = 1$ in scaled units, a parabolic trajectory reaches $\varphi = 90^\circ$ at $D = 1,\ r = 2$. Its elapsed time is

$$4\sqrt{2}/3 = 1.886.$$

Using the instantaneous angular speed at periapsis for the entire quarter turn would predict $(\pi/2)/\sqrt{2} = 1.111$, much too short. The areal speed stays constant, but angular speed decreases by a factor of four by the time radius has doubled. Integrating $r^2 d\varphi/h$ along the conic captures that slowdown directly.

Near zero energy, formulas involving a semimajor axis of enormous magnitude can lose numerical accuracy through cancellation. For example $r = a(1 - e\cos E)$ involves subtracting two near-equal terms near periapsis in a high-eccentricity ellipse. Expressions in $q_p = a(1 - e)$ and half-angle quantities, such as $r = q_p + 2ae\sin^2(E/2)$, avoid one damaging subtraction. A state-based numerical propagation should preserve angular momentum, compare the periapsis passage time with a quadrature, and test both small positive and small negative energies. Agreement only in the well-bound ellipse regime is a weak test of an algorithm used for near-escape trajectories.

Relate the Runge–Lenz direction to a velocity-space circle

The spatial Kepler conic has a simpler partner in velocity space. In the orbital plane,

$$d\mathbf{v}/d\varphi = \mathbf{a}/\dot{\varphi} = (-k\hat{r}/r^2)/(h/r^2) = -(k/h)\hat{r}.$$

Since $d\hat{\varphi}/d\varphi = -\hat{r}$, integration gives

$$\mathbf{v} = (k/h)\hat{\varphi} + \mathbf{v}_c,$$

where $\mathbf{v}_c$ is a constant vector. Thus the velocity vector traces a circle of radius k/h, or part of that circle on an unbound orbit. At periapsis a prograde orbit has speed $(k/h)(1+e)$, so the circle centre is shifted in the prograde tangential direction by ke/h. The offset direction is perpendicular to the eccentricity vector.

One can recover k/h and e from a set of calibrated velocity samples by fitting a circle in the orbital plane and comparing its radius with the offset of its centre from zero velocity. This method still needs the correct inertial frame: adding a constant observer velocity translates every velocity-space point, moving the fitted centre while preserving the circle radius. A time sequence of relative velocities between the two masses removes a common boost. If the force departs from inverse square, the derivative $d\mathbf{v}/d\varphi$ acquires radius dependence and the velocity circle generally distorts. Simultaneously checking the spatial conic and the velocity circle makes a more discriminating test than plotting either shape alone.

Derive which central orbits remain nearly closed

A circular orbit at radius r_c in a smooth potential per mass $U(r)$ has $h^2 = r_c^3 U'(r_c)$. Its angular frequency obeys $\Omega^2 = U'(r_c)/r_c$. Small radial deviations at fixed h see the effective potential $U + h^2/(2r^2)$, so their squared epicyclic frequency is

$$\kappa_r^2 = U''(r_c) + 3U'(r_c)/r_c.$$

During one radial oscillation the orbital angle advances roughly $2\pi\Omega/\kappa_r$. If the two frequencies differ, the apsidal orientation generally rotates, even though energy and angular momentum remain constants. This local result distinguishes near-circular closure from the much stronger claim that all bounded orbits close for a given force law.

For an attractive radial acceleration $-kr^{-s}$, $U' = kr^{-s}$ and $\kappa_r^2 = (3-s)\Omega^2$. A stable circular orbit requires $s < 3$. For inverse square, $s = 2$, radial and angular frequencies agree, so the apsis returns to its starting orientation each revolution. For an isotropic harmonic potential the force is proportional to r, so $s = -1$ and $\kappa_r = 2\Omega$. There are two radial minima per full turn; its closed ellipse is centred on the force centre rather than focused there. A rational near-circular ratio at one energy or radius does not by itself prove global closure for all eccentricities. The Runge–Lenz derivation supplied much stronger information for the inverse-square case.

Suppose a weak field calibration drift changes the local logarithmic force slope from $s = 2$ to $s = 1.98$, approximately constant over a narrow radial range. The near-circular radial frequency is 1.00995Ω. Consecutive closest approaches are separated by $2\pi/\sqrt{1.02} \approx 6.221\,\mathrm{rad}$, giving a retrograde change about $0.062\,\mathrm{rad}$ per radial period. The sign is opposite the advance induced by the additional attractive inverse-cube contribution considered before. Estimating the radial oscillation frequency and orbital

frequency independently can therefore diagnose deviations that an energy test would miss. At larger eccentricity the sampled force covers a broader radial interval and the local-power approximation must be replaced by the full turning-point integral.

Reconstruct a Kepler ellipse from one state

Vary initial radial and tangential velocity separately. Infer the direction of the eccentricity vector and compare both turning radii with the energy equation.

Open this experiment online

Try the calculation

Initial radial velocity **0.1**

Initial tangential velocity **0.9**

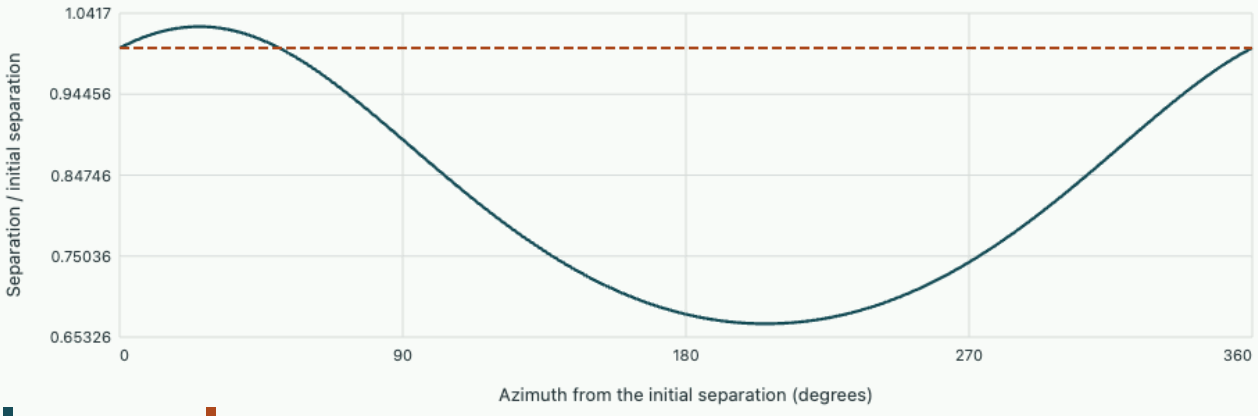

Eccentricity 0.21024. Closest approach 0.66929; largest separation 1.0256.

Use conservation of the eccentricity vector to test an orbital integrator

A code integrating $\ddot{\mathbf{r}} = -k\mathbf{r}/r^3$ can be tested on a moderate ellipse where both apses are well resolved. Choose $k = 1$, semimajor axis $a = 1$, eccentricity $e = 0.6$, and start at periapsis $\mathbf{r} = (0.4, 0)$, $\mathbf{v} = (0, 2.0)$. Then $h = 0.8$, $\epsilon = -0.5$, and the eccentricity vector is exactly $(0.6, 0)$. The apoapsis must lie at $(-1.6, 0)$ with speed 0.5, and the return time is 2π. This one initial condition tests two-dimensional direction, speed, position and clock against independent invariant predictions.

A kick–drift method for a central force can preserve angular momentum exactly at each substep. A radial kick changes velocity along position and gives zero torque; a free drift changes position along velocity and likewise preserves the cross product. Such a method can nevertheless rotate the eccentricity vector slowly or distort the time of periapsis. A symmetric velocity-Verlet step often produces bounded energy errors but still a systematic numerical periapsis shift. Record the eccentricity vector just after each

interpolated periapsis crossing over a fixed number of physical periods and compare its direction as the step is halved. Do not locate a closest approach merely by selecting the nearest stored time sample if that timing error is comparable to the shift under study.

A high-eccentricity orbit requires a smaller near-periapsis time step than its full period alone suggests. At the example periapsis, a local bend time is $r_p/v_p = 0.20$ in the scaled units, about one thirtieth of the period. For $e = 0.95$ at the same semimajor axis it becomes $0.05/\sqrt{39} \approx 0.0080$, almost eight hundred times smaller than the period. A time step that produces a smooth-looking wide ellipse at $e = 0.6$ may skip much of the rapid turning near $e = 0.95$. Refine according to the fastest relevant local dynamics as well as the final integration length.

How could a simulation distinguish a real apsidal advance from an error in fitting the coordinate origin?

▼ **Work through the solution**

Translate the calculated orbit to a candidate force centre and evaluate both the radial force law and the eccentricity vector at many positions. A constant wrong origin changes the measured radius and radial direction in a phase-correlated way even within a single orbit. A physical perturbation about the true centre can preserve zero torque and produce a gradual cycle-to-cycle change. Check angular momentum about the candidate centre, the direction of the measured acceleration, and convergence under grid or time-step refinement. Several diagnostics are needed because a short arc alone may admit many fitted centres and apsidal directions.

Determine the total mass from a visual binary

If the two bodies can both be resolved, measure their relative semimajor axis a and period T. Kepler's area relation gives $M = 4\pi^2 a^3/(GT^2)$, the sum of masses. Motion about the common centre divides the same relative semimajor axis in inverse proportion to the masses: $a_1/a_2 = m_2/m_1$. For a visual orbit with $a_1/a_2 = 0.50$ and a dynamically inferred total of three mass units, the bodies have masses two and one in those units. An orbit of only one luminous body around an unobserved centre normally supplies fewer independent constraints.

A projected semimajor axis and a measured angular period require additional geometric information before applying the mass law. The apparent ellipse on the sky can be shortened by inclination and the focus of the spatial ellipse does not in general map to a focus of the apparent ellipse. Distances converting an angular semimajor axis to metres enter cubed: an independent distance bias of two percent produces approximately a six-percent mass bias at fixed angular scale and period. This makes the gravitational invariant a sensitive quantitative measurement rather than simply a qualitative statement that the relative trajectory looks elliptical.

Tutorial on orbital inference

A body passes periapsis of an ellipse at r_p with purely transverse speed v_p. Express its eccentricity in terms of these measurements. Which ambiguity occurs if the apsis has not been identified?

▼ **Work through the solution**

At an apsis the eccentricity vector is $(rv^2/k - 1)\hat{r}$. At periapsis it points outward along $\hat{r}$, giving $e = r_p v_p^2/k - 1$. At apoapsis the coefficient is negative and its magnitude is the eccentricity. A purely transverse velocity identifies a turning point of radius but does not by itself distinguish which apsis without comparing v with the circular value $\sqrt{k/r}$ or measuring radial acceleration.

At fixed orbital radius the speed is increased tangentially from circular speed to exactly $\sqrt{2}$ times circular speed. What has changed in a, e and the apsidal interpretation?

▼ **Work through the solution**

The specific kinetic energy now equals k/r, giving total energy zero. The resulting orbit is parabolic with $e = 1$ and no finite semimajor axis or orbital period. The launch point is periapsis since radial speed is initially zero and the transverse speed exceeds the circular value. Taking the ellipse period formula with a very large fitted a near this energy boundary makes tiny measurement errors produce enormous period uncertainties.

Two solutions report nearly identical energy histories but their eccentricity vectors rotate in opposite directions as time advances. What can a controlled comparison establish?

▼ **Work through the solution**

Compute angular momentum and eccentricity vector from positions and velocities using one common force parameter and frame. Run both at decreasing time steps over a fixed physical number of orbits, with the same periapsis event interpolation. If the rotation vanishes under refinement in the inverse-square problem, the original precession was a discretisation effect. If a prescribed conservative non-Kepler term remains present, a finite shift can survive with energy conserved. Energy conservation is one scalar condition and cannot determine the apsidal direction.

Test a state vector and compare the predicted turning radii.

Torsten Fließbach's mechanics course includes dynamics in central potentials.

Analytical mechanics from constraints to invariants · 5. Scattering from a central potential and what angular data can recover

A detector records angles, whereas the force law refers to separations that were never directly observed. Derive the forward map from incoming impact parameter to angle, distinguish the several trajectories a detector may count in one angular bin, and invert sufficiently complete signed deflection data under stated hypotheses.

Build the deflection integral from a radial turning point

Use relative mass μ, asymptotic relative speed v_∞, incoming energy $E = \mu v_\infty^2/2 > 0$ and impact parameter $b \geq 0$. With a central interaction that tends to zero at infinity, angular momentum is $\ell = \mu v_\infty b$. For a single repulsive encounter let r_0 be the closest approach. Energy gives

$$\dot{r}^2 = v_\infty^2[1 - U(r)/E - b^2/r^2];$$

r_0 is the outer turning root reached from infinity. Dividing $\dot{\varphi} = \ell/(\mu r^2)$ by the radial speed and integrating over the outgoing half trajectory gives

$$\Phi(b) = \int_{r_0}^{\infty} \frac{b\,dr}{r^2\sqrt{1 - U(r)/E - b^2/r^2}},$$

$$\chi(b) = \pi - 2\Phi(b).$$

The straight, free trajectory sweeps $\Phi = \pi/2$ between closest approach and infinity and gives zero deflection. For repulsive bend away from the centre this sign convention gives positive χ. A weak attraction can give negative signed deflection even though a detector reporting the angle between incoming and outgoing velocities may supply only its magnitude. If the path winds by more than a complete turn, angular data modulo 2π also lose winding information. The square-root singularity in the integral for an ordinary turning point is integrable. A substitution $r = r_0 + s^2$ makes the near-endpoint quadrature regular. A double turning point requires separate analysis because it can make the angular advance diverge.

Incoming trajectories with parameters between b and $b + db$ represent annular area $2\pi b\,db$ for an axially symmetric beam. At a detected polar angle θ the solid angle of a ring is $2\pi \sin\theta\,d\theta$. Conservation of incoming counts gives

$$\frac{d\sigma}{d\Omega} = \sum_j \frac{b_j}{\sin\theta}\left|\frac{db_j}{d\theta}\right|.$$

The sum includes all incoming impact parameters reaching that angular bin. Correcting measured counts requires incident flux, target number, angular acceptance and efficiency. The formula is a density in solid angle. Its apparent divergence at an isolated angle need not imply an infinite number in a finite acceptance bin. Integrate the density against the actual bin solid angle or use the preimage areas of the bin directly.

Solve a hard sphere and an inverse-square repulsion

A hard sphere of effective exclusion radius a specularly reverses the incoming normal velocity at the impact surface. The angle between incoming and outgoing directions is $\theta = 2\arccos(b/a)$ for $b < a$. Therefore $b = a\cos(\theta/2)$,

$$|db/d\theta| = (a/2)\sin(\theta/2).$$

The factors cancel to give $d\sigma/d\Omega = a^2/4$, independent of polar angle, and total cross section πa^2. Equal polar angular bins do not give equal counts: their solid angles differ by $\sin\theta$. This geometric distinction often accounts for a measured histogram that does not look uniform even for a constant differential cross section.

For $U(r) = K/r$ with $K > 0$, the orbit is a repulsive hyperbola. The analytic relation is

$$\tan(\theta/2) = K/(2Eb).$$

It can be derived from the energy and the angle through the deflection integral: put $u = b/r$ so that $\Phi = \int_0^{u_0} du/\sqrt{1 - (K/Eb)u - u^2}$. Complete the square and evaluate the arcsine at the root to get

$$\Phi = \pi/2 - \arctan[K/(2Eb)].$$

Define $d = K/(2E)$; then $b = d\cot(\theta/2)$,

$$d\sigma/d\Omega = d^2/[4\sin^4(\theta/2)].$$

High precision near the forward direction is physically limited by finite beam size, detector acceptance and any screening of the long-range interaction.

For $d = 2.0\,\mathrm{mm}$ in an abstract mechanical analogue, a deflection of 60° corresponds to $b = 3.46\,\mathrm{mm}$, and the differential cross section is $16\,\mathrm{mm}^2/\mathrm{sr}$. The cross section for deflections greater than 60° is the area $\pi b^2 = 37.7\,\mathrm{mm}^2$. The differential value and integrated area answer different laboratory questions. Doubling energy at fixed interaction halves d, quarters the cross section into a fixed angular interval and reduces the deflection at a fixed incoming b. Measuring only a total count without specifying angular threshold is inadequate for a long-range interaction.

Recover impact parameter from angular counting under monotonicity

Suppose the deflection decreases continuously from π at $b = 0$ to zero at large b. Integrating counts for all angles at least θ then gives precisely the incident disk $\pi b(\theta)^2$. The recovered map satisfies

$$b(\theta)^2 = 2\int_\theta^\pi (d\sigma/d\Omega)(\theta')\sin\theta'\,d\theta'.$$

Applying this formula to constant hard-sphere intensity gives $b^2 = a^2(1+\cos\theta)/2$, the geometrical result. It also exposes the information needed from a detector: a finite upper cutoff can leave the reconstruction with an unknown disk-area offset.

Failing monotonicity, the same cumulative counts give the total area of all incoming regions producing deflections above threshold, which can be a collection of annuli. No unique $b(\theta)$ follows from that one number. Near a smooth extremum $\theta(b) = \theta_r + c(b-b_r)^2/2 + \cdots$, two branches contribute inverse square-root factors proportional to $1/\sqrt{|\theta-\theta_r|}$. A finite bin contains finite counts because integrating that singularity gives a square root. Tagging the incoming impact parameter in a controlled beam or measuring trajectory time delay can separate branches invisible in a final-angle histogram.

Invert a signed deflection function at one energy

Assume smooth $U(r)$ with $\rho(r) = r\sqrt{1-U(r)/E}$ strictly increasing on the radial interval sampled by the trajectories. The turning condition is

$$\rho(r_0) = b.$$

Write $W(\rho) = \ln[r(\rho)/\rho]$ and transform the deflection integral to $\Phi = b\int_b^\infty [d\ln r/d\rho]\, d\rho/\sqrt{\rho^2-b^2}$. The term from $d\ln\rho/d\rho$ gives the free angle $\pi/2$; the remainder has $\chi = -2b\int_b^\infty W'(\rho)\, d\rho/\sqrt{\rho^2-b^2}$. This is an Abel-type map. Multiply by $1/\sqrt{b^2-s^2}$ and integrate from $b=s$ to infinity. Interchanging the integrals produces the inner integral

$$\int_s^\rho \frac{b\,db}{\sqrt{b^2-s^2}\sqrt{\rho^2-b^2}} = \frac{\pi}{2}.$$

Substitute $b^2 = s^2 + (\rho^2-s^2)\sin^2\alpha$ to check the identity. With $W(\infty)=0$ the inversion is $W(s) = \pi^{-1}\int_s^\infty \chi(b)\, db/\sqrt{b^2-s^2}$. Recover $r = se^{W(s)}$ and finally $U(r) = E[1-(s/r)^2]$ parametrically. This derivation explains the restrictions. A trajectory only samples radii outside its turning point, the signed angle must retain branch information, and the map to ρ must be single valued. Unknown large-b tails influence the integral even when only comparatively small radii are of interest.

Derive the weak-deflection formula from a straight incoming trajectory

When the deflection is small one can calculate the transverse impulse along the undeflected line before evaluating a nonlinear radial integral. Put the incoming velocity along x and the impact point at $y = b > 0$, so the unperturbed trajectory is $x = v_\infty t$, $r = \sqrt{x^2+b^2}$. The transverse force is $-U'(r)b/r$. Dividing its time integral by the incoming momentum μv_∞ gives the signed leading deflection

$$\chi(b) \simeq -\frac{b}{E}\int_b^\infty \frac{U'(r)\, dr}{\sqrt{r^2-b^2}}.$$

The factor follows from replacing dt by dx/v_∞, using symmetry between positive and negative x, and the identity $dx = r\,dr/\sqrt{r^2 - b^2}$. A decreasing positive potential gives a positive angle, consistent with repulsive scattering in the chapter's convention. The approximation neglects longitudinal momentum change at leading order; a finite speed change far from the interaction would also be inconsistent with elastic energy conservation. Near a turning barrier or for a large angle the original deflection integral must replace this straight path.

An analytically tractable finite-range model is $U(r) = U_0 \exp[-r^2/(2a^2)]$. Along the incoming straight line the transverse force is $(U_0 b/a^2)\exp[-(x^2 + b^2)/(2a^2)]$. The Gaussian x integral gives

$$\chi(b) \simeq \sqrt{\pi/2}(U_0/E)(b/a)\exp[-b^2/(2a^2)].$$

A central hit has zero transverse force by symmetry if the particle crosses through the weak smooth potential rather than being reflected. Distant particles see little interaction, so the deflection must peak at an intermediate impact parameter. Differentiation places the maximum at $b = a$, with height $\sqrt{\pi/(2e)}U_0/E$.

For $U_0/E = 0.10$ the peak is about $0.0760\,\mathrm{rad} = 4.36^\circ$, comfortably small for this leading calculation. Two impact-parameter families can contribute to one smaller nonzero angle. For example $b = 0.50a$ gives $0.0553\,\mathrm{rad}$; a trajectory with b between $1.5a$ and $1.7a$ produces a similar deflection on the declining branch. A detector counting more events near four degrees may be recording the merging of these branches, rather than a particularly large local force at the turning separation. Reconstructing $b(\theta)$ from monotonically accumulated disk areas would be invalid for this smooth repulsive bump even though every encounter is elastic.

Measure the energy dependence to distinguish the weak limit. For fixed b/a the leading angle scales as $1/E$. Doubling energy halves the predicted peak angle. A finite spread of incident energies therefore broadens the observed rainbow before detector angular resolution is considered. A position-tagged incident beam can furnish $\chi(b)$ point by point; a detector measuring final angles alone mixes weakly and more strongly penetrating paths. Adding incoming-position information changes what inverse problem is identifiable, without improving the detector's angular precision.

Limit a scattering inference using finite range and measurement bandwidth

The Abel reconstruction requires data to arbitrarily large b. A finite experiment measures up to $b_{\max}$, and the unmeasured tail contributes an integral to $W(s)$. For the example of a known asymptotic $\chi = C/b$, the tail from $b_{\max}$ to infinity evaluates to $C\,\arcsin(s/b_{\max})/(\pi s)$ for $s < b_{\max}$. Substitute $b = s/\cos\alpha$ to obtain this result. For $s \ll b_{\max}$, it approaches $C/(\pi b_{\max})$. Setting the tail to zero therefore introduces an offset across the reconstructed log-radius even at small s. Bounded angular noise and uncertainty in the tail model should be propagated separately.

As a numerical illustration take $C = 5.0\,\mathrm{mm}$,

$$b_{\max} = 100\,\mathrm{mm},$$
$$s = 20\,\mathrm{mm}.$$

The missing contribution is about 0.0160, corresponding to roughly a 1.6% multiplicative error in reconstructed radius if other terms were exact. At that same s, the leading whole weak-tail value $C/(2s) = 0.125$ would be biased appreciably by this omission. A model with a short exponential tail would give a quite different correction. Adding a physically motivated tail with an uncertainty range is more informative than extending a noisy measured curve by an unrestricted polynomial.

The lower integration endpoint has a square-root weight. Uniform samples in b can be wasteful near a selected reconstruction radius and coarse interpolation there can dominate the result. Substitute $b = s\cosh u$ to obtain

$$db/\sqrt{b^2 - s^2} = du.$$

The Abel integral becomes a straightforward integral of $\chi(s\cosh u)$ over u, with a finite upper limit if the data stop at $b_{\max}$. This substitution removes a numerical singularity but adds no information about missing impact parameters. Validate a reconstruction by inserting its inferred potential back into the original forward integral and predicting angular measurements withheld from the fit. Agreement with the very data used in the inversion alone can conceal an incorrect tail or a misassigned branch.

Convert centre-of-momentum angles into laboratory angles

An ordinary collision experiment often launches a particle of mass m_1 into a stationary particle of mass m_2. In Newtonian elastic scattering the centre-of-mass speed is $V = m_1 v_{\mathrm{in}}/(m_1 + m_2)$, while the projectile's speed in that frame is $u_1 = m_2 v_{\mathrm{in}}/(m_1 + m_2)$. Rotate that velocity by the centre-of-mass angle χ in the scattering plane, then add the centre velocity back. The outgoing laboratory velocity components are $V + u_1\cos\chi$ longitudinally and $u_1\sin\chi$ transversely. Consequently $\theta_{\mathrm{lab}} = \operatorname{atan2}(\sin\chi, m_1/m_2 + \cos\chi)$. The centre-of-mass solid-angle density derived from the impact parameter does not transfer unchanged to a lab angular histogram.

If $m_1 = m_2$, the identity $1 + \cos\chi = 2\cos^2(\chi/2)$ gives $\theta_{\mathrm{lab}} = \chi/2$ except when the projectile stops and loses a well-defined direction. A heavy projectile can be restricted to a narrow forward cone. Let $r = m_1/m_2 > 1$. Differentiating the laboratory angle gives

$$d\theta_{\mathrm{lab}}/d\chi = (1 + r\cos\chi)/(1 + 2r\cos\chi + r^2).$$

It vanishes at $\cos\chi = -1/r$. At that angle $\sin\theta_{\max} = 1/r$; hence $r = 2$ limits the projectile to $\theta_{\max} = 30^\circ$. Two centre-of-mass angles can generate the same nonzero laboratory angle below this maximum. This laboratory-frame fold may appear even for a monotone centre-of-mass repulsive potential.

Energy helps separate the branches. The outgoing laboratory projectile energy divided by its incident energy is $[m_1^2 + m_2^2 + 2m_1m_2\cos\chi]/(m_1 + m_2)^2$. For $m_1 = 2m_2$, head-on reversal in the momentum frame gives energy fraction $1/9$, while forward scattering gives one. Both can land near the

laboratory beam direction. A detector reporting angle only cannot distinguish a barely deflected fast projectile from a strongly deflected slow one emerging along almost the same line. Recording time of flight to a downstream detector or measuring the recoil supplies the missing information. Instrumental and kinematic multiplicity should therefore be addressed before attributing a two-branch angular signal to an exotic force law.

Ask what a flight-time measurement adds to angle data

At a given impact parameter choose a large comparison sphere of radius R enclosing a short-range potential. The transit time from its incoming boundary to the outgoing boundary is $t_U(R,b) = 2v_\infty^{-1}\int_{r_0}^{R} dr/\sqrt{1-U/E-b^2/r^2}$. The free reference at the same b is $t_0 = 2\sqrt{R^2-b^2}/v_\infty$. Their difference is a classical time delay under a precisely specified pair of surfaces. It combines a different path length with the altered speed along the path. A repulsive barrier can cause either a shorter geometrical penetration or longer dwell near a turning point, so the sign cannot be inferred merely from the word repulsive.

For an impenetrable sphere of radius $a > b$, the particle moves at free speed on each straight segment. The radial turning point is replaced by specular contact at a, so $t_{\mathrm{hard}} = 2[\sqrt{R^2-b^2}-\sqrt{a^2-b^2}]/v_\infty$. The delay is $-2\sqrt{a^2-b^2}/v_\infty$. Using $a = 3.0\,\mathrm{mm}$, $b = 1.8\,\mathrm{mm}$, and $v_\infty = 2.0\,\mathrm{m/s}$, one finds $-2.4\,\mathrm{ms}$. The hard sphere takes less transit time between the two points where the respective trajectories cross the large sphere. Those points differ from the endpoints of the free line, so this negative delay implies no acceleration above the fixed free speed.

For a potential with a true long-range $1/r$ tail the simple free-reference difference can acquire a logarithmic dependence on the comparison radius. A reported time delay then needs its reference geometry and tail model, just as a measured forward angle needs its angular acceptance. In the inverse problem, combining deflection and delay can help separate long dwell near a nearly unstable circular orbit from a large geometrical bend at an ordinary turning point. A large angle alone contains insufficient information to assign the time spent close to the scattering centre.

Reconstruct a finite-depth potential well from two deflections

A circularly symmetric square well provides a forward problem in which the trajectory is straight in each region and changes direction at the potential boundary. Let $U(r) = -U_0 < 0$ for $r < a$ and zero outside. A particle with $b < a$ enters with speed v_∞ and travels inside at $v_{\mathrm{in}} = v_\infty\sqrt{1+U_0/E} \equiv n v_\infty$. Angular momentum conservation across the radial impulse gives

$$v_\infty \sin i = v_{\mathrm{in}} \sin r_i,$$

where i and r_i are angles of the velocity to the normal outside and inside. Thus $\sin i = b/a,\ \sin r_i = b/(na)$. At each crossing the direction bends toward the centre. The magnitude of net deflection is $2(i - r_i)$, with negative signed deflection in the convention used for attraction here.

Take $n = 1.25,\ b = 0.60a$. Then $i = 36.87^\circ$, $r_i = 28.69^\circ$, and the total deflection has magnitude 16.35°. As b approaches a from below, the magnitude approaches $2[\pi/2 - \arcsin(1/n)]$, about 73.7°.

For $b > a$ the trajectory does not touch the ideal sharp boundary and is undeflected. A smooth finite-width transition removes the ideal discontinuity at grazing incidence and can generate trajectories that linger near the outer part of the well. Examining a well with measured edge width is therefore different from trying to fit all grazing events with a perfectly sharp step.

If a is known, an incoming position tag and a measured deflection at one b determine $n = \sin i / \sin(i - |\chi|/2)$, hence $U_0/E = n^2 - 1$. The preceding numbers give

$$U_0/E = 0.5625.$$

For an independently known E this determines the well depth. If a is unknown too, one angle supplies only one equation for two parameters. Multiple impact parameters, an independent threshold for entering the well, or a measured time of flight can supply the additional scale. Near $b = 0$ the deflection is approximately $2(b/a)(1 - 1/n)$, so a series of very small impact parameters measures mainly that one combination; broad coverage is needed to resolve a and n individually.

The time inside the well is $2a \cos r_i/(nv_\infty)$, because the interior chord has offset b/n and speed nv_∞. At the same b, the time between intersections of the free path with the circle is $2a \cos i/v_\infty$. For $n = 1.25, b = 0.6a$, their ratio is $\cos 28.69^\circ / [1.25 \cos 36.87^\circ] \approx 0.877$. The faster interior motion crosses a longer chord in less time. For grazing free paths the reference chord becomes very short and the comparison can reverse. Reporting which part of the trajectory the timing equipment resolves is therefore as important as measuring the dwell accurately.

Recover incoming annuli from scattering angles

Bin the exactly solvable hard-sphere reflection in polar angle and compare the integrated cross-section with the incoming geometric area.

Open this experiment online

Try the calculation

Polar detector bins 8

Effective radius (cm) 1

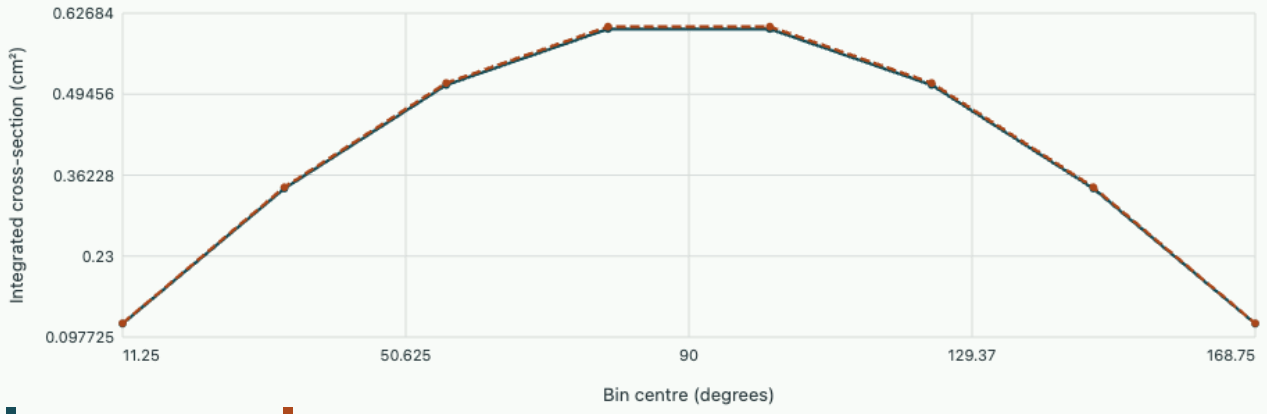

Incoming annulus Midpoint solid angle

Exact sum 3.1416 cm². Midpoint sum 3.1619 cm². Differential cross-section 0.25 cm²/sr.

Propagate uncertainties from a detector ring to an inferred force

Suppose N counts are recorded in an angular ring and the product of incident fluence, target count and calibrated efficiency is C. The estimate of bin-averaged cross section is $N/(C\Delta\Omega)$, with $\Delta\Omega = 2\pi[\cos\theta_{\mathrm{low}} - \cos\theta_{\mathrm{high}}]$ for full azimuth. Approximately independent counting events have fractional standard error $1/\sqrt{N}$, but the fluence and efficiency create correlated scale errors across angular bins. When integrating bins to reconstruct $b^2(\theta)$, a shared five-percent normalisation uncertainty does not shrink just because the number of angular bins grows. It propagates into an approximately 2.5% scale uncertainty in the recovered impact parameter.

For an ideal hard sphere, let an experiment integrate the area feeding angles greater than 90° and find $14.1 \pm 0.7\,\mathrm{mm}^2$. Since this is $\pi b(90^\circ)^2 = \pi a^2/2$, the inferred radius is $\sqrt{2(14.1)/\pi} = 3.00\,\mathrm{mm}$ with uncertainty approximately $0.075\,\mathrm{mm}$ for small errors. If the unobserved backward final ten degrees are simply omitted, an extra solid angle $\Delta\Omega = 2\pi[1 - \cos 10^\circ]$ is missed. Its small size for a smooth hard-sphere law can be estimated, but a general inverse analysis cannot assume that backward intensity is smooth without testing it.

Is multiplying each measured bin centre by the angular density there sufficient for a steep forward-scattering law?

▼ **Work through the solution**

A finite bin measures an integral against solid angle, not the value at its centre. For a rapidly varying $\sin^{-4}(\theta/2)$ density near zero, the lower-angle part of the bin can dominate its count. Use the exact preimage annulus $\pi[b(\theta_{\mathrm{low}})^2 - b(\theta_{\mathrm{high}})^2]$ or integrate the model numerically over the detector's angle-dependent efficiency. Repeat with narrower bins as a check. If the lower acceptance overlaps the direct

beam, separate the unscattered population and account for its instrumental angular spread before assigning a cross section to small deflections.

Work directly in counts for a finite annular detector

For the repulsive inverse-square example take $d = 2.0\,\mathrm{mm}$ and a full-azimuth ring that accepts polar angles from 55° to 65°. The expected incident area is $\pi d^2[\cot^2(27.5^\circ) - \cot^2(32.5^\circ)]$, about $15.4\,\mathrm{mm}^2$. Multiplying by an incident fluence of 100 particles per square millimetre and efficiency 0.80 predicts about 1230 counts. A Poisson fluctuation scale is then roughly 35 counts. The exact integral supplies a meaningful reference even when the plotting software reports a differential value at the centre of the bin.

Moving both angular boundaries one degree outward decreases the count because the repulsion sends fewer particles through larger angles. The change can be calculated by reevaluating the two cotangents, keeping the fluence and efficiency fixed. This sensitivity allows a calibration uncertainty in the angular zero to be propagated into a count prediction without treating it as a force uncertainty. If fluence is independently measured the dependence on d^2 can then estimate the interaction scale. If fluence is itself unknown, a single count measures only their product; independent calibration or measurements across energies are needed to separate them.

Tutorial on inverse scattering

An incoming uniform beam scatters from a hard disk in three-dimensional impact geometry with effective radius $3.0\,\mathrm{mm}$. What area feeds the polar bin from 60° to 90°?

▼ **Work through the solution**

The accepted impact parameters run from $a\cos 45^\circ$ to $a\cos 30^\circ$. The difference of their squared radii is $9(0.75 - 0.50) = 2.25\,\mathrm{mm}^2$, giving area $2.25\pi = 7.07\,\mathrm{mm}^2$. Alternatively the bin has solid angle $2\pi(\cos 60^\circ - \cos 90^\circ) = \pi$ steradians and differential cross section $a^2/4 = 2.25\,\mathrm{mm}^2/\mathrm{sr}$. The agreement checks both the Jacobian and the angular convention.

At large impact parameter a weak repulsion gives $\chi(b) \simeq C/b$ with C a length. Use the inversion to identify the leading tail of the potential.

▼ **Work through the solution**

Substitute $b = s/\cos\alpha$ into the Abel integral. One obtains

$$W(s) \simeq C/(2s).$$

Thus $r \simeq s + C/2$ and $U/E = 1 - e^{-2W} \simeq C/s \simeq C/r$. The potential tail is EC/r. For the exact repulsive Coulomb result $C = K/E$, matching the original K/r. This check uses the weak-tail expansion at large radii only; continuing it to small radii would discard higher deflection terms.

A measured angular bin near a rainbow doubles in width towards its allowed side. By what approximate factor do its counts change if background is negligible?

▼ **Work through the solution**

At a simple fold the angular density grows as the inverse square root of distance from the extremal angle. For a bin of width $\Delta\theta$ starting at the fold, the integral scales as $\sqrt{\Delta\theta}$ provided $\sin\theta_r$ is nonzero and other weights are locally smooth. Doubling the width gives a factor $\sqrt{2}$, unlike the factor two from a smooth background. Finite angular resolution rounds off the divergence and can obscure this scaling in very narrow bins.

Compare angular bins and conserved incoming area.

Fließbach's mechanics text treats trajectories in central fields.

Analytical mechanics from constraints to invariants · 6. Euler–Poinsot motion, torque-free nutation and the intermediate axis

A freely rotating body has fixed angular momentum in space, yet the components recorded by three body-mounted gyroscopes can vary periodically or linger near an unstable rotation. Solve the nonsymmetric top from its invariants, distinguish its body-component period from its spatial orientation, and extract a stability time scale from a measured inertia tensor.

Derive the body equations from a spatial conservation law

Choose principal axes fixed in a rigid body and label its moments $I_1 < I_2 < I_3$. In the co-rotating basis the angular-momentum components are

$$L_i = I_i \omega_i.$$

For any vector expressed in that basis, its inertial derivative is its component derivative plus $\boldsymbol{\omega} \times \mathbf{L}$. With no external torque the inertial derivative is zero. Taking components gives

$$I_1 \dot{\omega}_1 = (I_2 - I_3)\omega_2 \omega_3,$$
$$I_2 \dot{\omega}_2 = (I_3 - I_1)\omega_3 \omega_1,$$
$$I_3 \dot{\omega}_3 = (I_1 - I_2)\omega_1 \omega_2.$$

Multiply these equations by the corresponding ω_i and sum: the coefficients of $\omega_1\omega_2\omega_3$ cancel, giving constant $E = \sum I_i \omega_i^2/2$. Multiplying instead by $I_i\omega_i$ gives constant $L^2 = \sum I_i^2 \omega_i^2$. In body angular-momentum space the motion lies on the intersection of a sphere and an energy ellipsoid. At fixed L, the possible energies range from $L^2/(2I_3)$ to $L^2/(2I_1)$. The intermediate value $L^2/(2I_2)$ divides two families of closed curves and contains the unstable principal-axis orientations.

In Poinsot's construction the inertia ellipsoid in angular-velocity space rolls on an invariable plane normal to the fixed spatial angular momentum. The ellipsoid corresponding to a given energy is

$$\sum I_i \omega_i^2 = 2E.$$

Its normal at the instantaneous angular velocity is proportional to $\mathbf{L}$; the tangent plane obeys $\mathbf{L} \cdot \mathbf{x} = 2E$. In space that plane therefore has fixed distance $2E/L$ from the origin. Its instantaneous point in the body along $\boldsymbol{\omega}$ has zero instantaneous rotational velocity because the vector cross product of angular velocity with itself is zero. These facts underlie the rolling construction. A photographed body axis traces a different curve from the moving contact point or from a body-frame gyro trace.

Test all three principal rotations locally

For rotation $(0, 0, \Omega)$, linearise the first two Euler equations in transverse perturbations. Eliminating one component gives

$$\ddot{\omega}_1 = -\Omega^2[(I_3 - I_2)(I_3 - I_1)/(I_1 I_2)]\omega_1.$$

Small transverse deviations oscillate. Performing the analogous process about I_1 also gives a restoring sign. About $(0, \Omega, 0)$ the sign reverses and the growing exponent is $\lambda = |\Omega|\sqrt{(I_2 - I_1)(I_3 - I_2)/(I_1 I_3)}$. The unstable rotation is still an exact solution when both perturbations vanish identically. Instability describes the evolution of arbitrarily small disturbances, not a spontaneous violation of the torque-free equations.

For moments proportional to $1, 2, 3$ and intermediate-axis rotation $\Omega = 6.0\,\mathrm{rad/s}$, $\lambda = 3.46\,\mathrm{s}^{-1}$ and the linear e-folding time is $0.289\,\mathrm{s}$. A perturbation with a growing-mode component 10^{-3} of the spin reaches roughly 10^{-1} in $\ln(100)/\lambda = 1.33\,\mathrm{s}$. Its nonlinear fate remains bounded by the momentum sphere and energy ellipsoid. An exponential growth fit carried past the first large reorientation would therefore misrepresent the global motion. Initial perturbations projected entirely on the decaying linear eigenvector can delay the first visible flip.

Solve the low-energy family with elliptic functions

For $L^2/(2I_3) < E < L^2/(2I_2)$ the trajectory surrounds the largest-inertia axis. Start at a crossing with $\omega_2 = 0, \omega_1 = A > 0, \omega_3 = C > 0$. Solving the two invariants gives

$$A^2 = (2EI_3 - L^2)/[I_1(I_3 - I_1)],$$
$$C^2 = (L^2 - 2EI_1)/[I_3(I_3 - I_1)].$$

When ω_1 reaches zero the other transverse component has maximum $B^2 = (2EI_3 - L^2)/[I_2(I_3 - I_2)]$. Use $s = \omega_2/B$. Eliminating the other squares with the invariants gives

$$\omega_1^2 = A^2(1 - s^2),$$
$$\omega_3^2 = C^2(1 - k_e^2 s^2).$$

Euler's second equation now reduces to

$$\dot{s}^2 = \nu^2(1 - s^2)(1 - k_e^2 s^2),$$
$$\nu^2 = \frac{(I_3 - I_2)(L^2 - 2EI_1)}{I_1 I_2 I_3},$$
$$k_e^2 = \frac{(I_2 - I_1)(2EI_3 - L^2)}{(I_3 - I_2)(L^2 - 2EI_1)}.$$

Separating variables defines $u = \nu t = \int_0^s dw/\sqrt{(1 - w^2)(1 - k_e^2 w^2)}$. Its inverse is Jacobi's $\mathrm{sn}(u, k_e)$. The continuously signed square roots are cn and dn, giving $(\omega_1, \omega_2, \omega_3) = (A\,\mathrm{cn}, B\,\mathrm{sn}, C\,\mathrm{dn})$. This construction defines the special functions from the mechanical quadrature instead of assuming them as a table of answers. At $k_e = 0$ the inverse is a sine and the stabilising motion is harmonic. As $k_e \to 1$, the integral to $s = 1$ diverges logarithmically and the period grows without bound.

The body-frame period is

$$T_b = 4K(k_e)/\nu,$$

with K the same integral evaluated at one. Some software defines elliptic functions in terms of parameter $m = k_e^2$ rather than modulus k_e. Supplying one to an implementation expecting the other produces a plausible curve with the wrong period. Check the derivative at the zero crossing $\dot{\omega}_2(0) = B\nu$ and the time of its first maximum K/ν before fitting a long trace. The third component dn repeats after half the full period, so a single principal-axis gyro can report a dominant frequency twice that of the full body vector.

Reconstruct the observed nutation angle

Orient the inertial vertical along $\mathbf{L}$. The angle between body axis three and this fixed direction obeys $\cos\theta = L_3/L = I_3\omega_3/L$. For $I_1, I_2, I_3 = (1, 2, 3)\,\mathrm{kg\,m^2}$ and initial $\boldsymbol{\omega} = (0.50, 0, 1.00)\,\mathrm{rad/s}$, the invariants give $L^2 = 9.25$, $2E = 3.25$ in SI, $A = B = 0.50\,\mathrm{rad/s}$, $C = 1.00\,\mathrm{rad/s}$, $\nu = 1.00\,\mathrm{s^{-1}}$, and $k_e^2 = 1/12$. Thus the nutation angle changes from $\arccos(3/\sqrt{9.25}) \approx 9.46^\circ$ to $\arccos[3\sqrt{11/12}/\sqrt{9.25}] \approx 19.2^\circ$. A torque is unnecessary for this change in the angle of a body axis relative to fixed $\mathbf{L}$.

The principal-axis components alone determine body orientation only when supplemented with an initial attitude and the kinematic equation. For the Euler-angle convention with polar axis $\mathbf{L}$, the azimuthal rate of body axis three is $\dot{\phi} = L(L_1^2/I_1 + L_2^2/I_2)/(L_1^2 + L_2^2)$ away from the polar singularity. It follows by differentiating the body-axis unit vector in space and projecting onto its azimuthal direction. A complete period of the body components therefore leaves a finite spatial rotation about fixed $\mathbf{L}$. Return of the three gyro readings does not imply that a painted mark has returned to its starting position in the laboratory.

Solve the high-energy family and join both sides at the separatrix

For $L^2/(2I_2) < E < L^2/(2I_1)$ the closed curves on the angular-momentum sphere surround axis one. The component ω_1 now keeps its sign while ω_3 changes sign through a cycle. As in the first family, choose a phase with $\omega_2 = 0$ and both other components positive. The two invariants give the same initial $A^2 = (2EI_3 - L^2)/[I_1(I_3 - I_1)]$ and $C^2 = (L^2 - 2EI_1)/[I_3(I_3 - I_1)]$. Now the maximum of ω_2 occurs when $\omega_3 = 0$, so

$$B^2 = (L^2 - 2EI_1)/[I_2(I_2 - I_1)].$$

Which component reaches zero is the physical branch choice that determines the arrangement of elliptic functions.

Let $s = \omega_2/B$. The invariant equations give

$$\omega_3^2 = C^2(1 - s^2),$$

$$\omega_1^2 = A^2(1 - k_h^2 s^2).$$

Substitution in the second Euler equation yields the same elliptic quadrature but with $\nu_h^2 = (I_2 - I_1)(2EI_3 - L^2)/(I_1 I_2 I_3)$ and $k_h^2 = (I_3 - I_2)(L^2 - 2EI_1)/[(I_2 - I_1)(2EI_3 - L^2)]$. All components are given by $(A\,\mathrm{dn}, B\,\mathrm{sn}, C\,\mathrm{cn})(\nu_h t, k_h)$, where the notation means each function is

evaluated at the same time and modulus. On this energy side $0 < k_h < 1$. The low-energy modulus formula evaluated here would exceed one, signalling that the original choice of component scaling and physical extrema must be changed.

For the same inertias $1, 2, 3$, choose initial $(1, 0, 0.20)\,\mathrm{rad/s}$. Then $L^2 = 1.36,\ 2E = 1.12$, and the high-energy inequality holds since $2E > L^2/I_2 = 0.68$. The formulas give

$$A = 1,\ B = \sqrt{0.12} = 0.3464,\ C = 0.20,\ \nu_h = \sqrt{1/3} = 0.5774\,\mathrm{s}^{-1},\ k_h^2 = 0.12.$$

The minimum ω_1 is $A\sqrt{1 - k_h^2} = 0.9381\,\mathrm{rad/s}$, so that principal gyro never reverses even though the third one does. A body-marking aligned with axis three can undergo a conspicuous reversal while the dominant axis-one spin changes only modestly. These component predictions are more specific than an energy or angular-speed trace.

At $2E = L^2/I_2$, both moduli approach one. The definitions give

$$\mathrm{sn}(u, 1) = \tanh u,$$
$$\mathrm{cn}(u, 1) = \mathrm{dn}(u, 1) = \operatorname{sech} u.$$

One separatrix solution therefore has $\omega_2 = B\tanh(\nu t)$ with $\omega_1 = A\operatorname{sech}(\nu t)$ and $\omega_3 = C\operatorname{sech}(\nu t)$, up to signs and time shifts consistent with Euler's equations. It connects opposite steady orientations along axis two as t goes from negative to positive infinity. Its asymptotic approach is exponential, with ν equal to the small-disturbance growth exponent at the intermediate-axis equilibrium after inserting $B = L/I_2$. A nearby periodic orbit spends much of its time near the unstable spin and flips more rapidly between those intervals.

Reconstruct spatial attitude without a singular azimuth

Let $R(t)$ map body components into a laboratory basis. For body angular velocity $\boldsymbol{\omega}_b$, its kinematic equation is

$$\dot{R} = R[\boldsymbol{\omega}_b]_\times,$$

where the skew matrix acts by a cross product. Starting from measured $R(0)$, propagate by multiplying by the rotation appropriate to each short time interval. Exponentiating the skew matrix for an interval with constant estimated body angular velocity preserves orthogonality and determinant exactly. Applying a naive forward-Euler matrix addition $R + hR[\omega]_\times$ generally stretches the basis, even if the angular velocity components came from an exact elliptic solution.

For a constant rotation about axis three at one radian per second, a single Euler step of duration $0.10\,\mathrm{s}$ takes a transverse unit vector to one of length $\sqrt{1 + 0.10^2} = 1.00499$. After one hundred such steps the transverse length would grow by $(1.01)^{50} \approx 1.64$. A quaternion or matrix exponential avoids that artificial stretch. Normalising each axis separately is insufficient if the axes lose orthogonality; check $R^T R$ against identity and $\det R$ against one. Also compute $R(I_1\omega_1, I_2\omega_2, I_3\omega_3)^T$ at every time. It should give the same spatial vector in a torque-free run.

A measured attitude time series allows a different inference from fitting Euler angles separately. Use relative rotations between successive images to estimate angular velocity in the correct body or spatial frame. A camera can momentarily lose sensitivity to yaw when a marked axis points towards it; simultaneous orthogonal views or multiple non-collinear marks avoid that degeneracy. The gyro and attitude measurements together distinguish a true physical precession from an Euler-angle wrap by 2π. Synchronise their clocks before comparing the phase of a nutation extremum, since even a small time delay produces a plausible-looking mismatch near a fast flip.

Infer inertia ratios from a free-rotation record

A calibrated triad records $\omega_i(t)$ in axes thought to be principal. Euler's equations predict that $\dot{\omega}_1/(\omega_2\omega_3)$ is the constant $(I_2 - I_3)/I_1$ wherever the denominator is appreciable, and similarly for cyclic indices. Instead of dividing noisy derivatives near zeros, integrate each component over a time interval. For example $\omega_1(t_2) - \omega_1(t_1) = a_1 \int_{t_1}^{t_2} \omega_2\omega_3 \, dt$. Fit a_1 over several intervals and repeat for a_2, a_3. Select intervals with different angular configurations so that products do not all average nearly to zero. The ratios depend on inertia shape; multiplying every moment by a common constant leaves a torque-free angular-velocity record unchanged.

For a record giving $a_1 = -1.0$, $a_2 = 1.0$ and $a_3 = -1/3$, solve the homogeneous equations $I_2 - I_3 = -I_1$, $I_3 - I_1 = I_2$, $I_1 - I_2 = -I_3/3$. They give $I_1 : I_2 : I_3 = 1 : 2 : 3$. An independent angular-momentum or torque calibration is needed to set the absolute scale. A known short applied torque impulse that changes one principal angular velocity by a measured amount can do this, provided the other gyroscopic contributions over that impulse are small or accounted for. A fit that estimates all absolute inertias from angular velocity alone can have an apparently excellent residual and still be structurally underdetermined.

If the sensors are not along principal axes the inertia matrix contains off-diagonal entries. The coordinate-free body equation is

$$I\dot{\boldsymbol{\omega}} + \boldsymbol{\omega} \times (I\boldsymbol{\omega}) = 0.$$

Each measured time sample gives equations linear in the constant entries of the symmetric inertia tensor. With sufficiently rich motion one may estimate these entries up to scale, then diagonalise the fitted tensor to recover principal directions. Pure rotation along one axis gives insufficient excitation to reveal three distinct directions. Comparing a family of initial spins with a single tensor provides a stronger validity test than fitting a different set of effective principal inertias to each record.

Relate a body-frame period to a measured geometric phase

After a closed polhode in body angular-momentum space the laboratory orientation differs by a rotation about the fixed spatial momentum. That phase can be separated into a term accumulated at a dynamical rate and a term depending on the oriented solid angle of the body momentum path. For a fixed L, the angular-velocity component along the momentum is $\boldsymbol{\omega} \cdot \hat{L} = 2E/L$, since $\mathbf{L} \cdot \boldsymbol{\omega} = 2E$. Over one body period it contributes $2ET_b/L$. Parallel transport of a transverse reference direction along the unit

momentum curve contributes minus the oriented solid angle enclosed, up to whole turns and the chosen orientation of the sphere. The resulting net attitude phase is $2ET_b/L - \Omega_{\text{solid}} \pmod{2\pi}$.

The geometric part can be visualised by carrying a local tangent basis along the closed curve. Its two basis vectors are constrained to stay perpendicular to the moving unit momentum and are transported with no imposed twist around that direction. A return to the initial unit momentum need not return that basis to its starting orientation. For a latitude circle on the unit sphere the enclosed cap area is $2\pi(1-\cos\theta)$; shrinking the path to a point makes the geometric phase vanish modulo 2π. This is why comparing a painted mark after a nutation only to an integrated scalar spin speed can give a discrepancy even with exact torque-free motion.

In practice the total phase can be measured without choosing a cap convention. Fit the attitude at two times separated by the full gyro period, form $R(t+T_b)R(t)^T$, and extract the relative rotation around the known fixed spatial momentum. Independently integrate $2E/L$ over that interval and compare the difference modulo 2π with the signed spherical area traced by normalised body momentum. A factor-of-two error in the identified period, common if only ω_3 is recorded in the low-energy family, generally leaves the relative attitude rotation axis different from $\mathbf{L}$. The axis check can reveal the error before assigning a numerical geometric phase.

Identify which inertias can exist in an actual rigid body

Three positive principal moments inserted into Euler's equations define a mathematical top, but the moments of a physical nonnegative mass distribution also satisfy triangle inequalities. In principal coordinates $I_1 = \int (y^2 + z^2)\, dm$,

$$I_2 = \int (z^2 + x^2)\, dm,$$

$$I_3 = \int (x^2 + y^2)\, dm.$$

Therefore $I_1 + I_2 - I_3 = 2\int z^2\, dm \geq 0$, and likewise by cyclic permutation. Equality means all mass is confined to the corresponding coordinate plane. The convenient example $1, 2, 3$ lies on that boundary and can be realised by an ideal planar lamina. A fitted ratio $1, 2, 3.5$ would imply negative mean squared distance along one direction and should prompt a calibration or modelling check.

A uniform thin rectangular plate of mass M and side lengths b along body axis one and a along body axis two has $I_1 = Ma^2/12,\ I_2 = Mb^2/12,\ I_3 = M(a^2+b^2)/12$. Choosing $b = \sqrt{2}\,a$ gives exactly $1:2:3$. For $M = 0.60\,\mathrm{kg}$, $a = 0.20\,\mathrm{m}$, $b = 0.283\,\mathrm{m}$, the moments are approximately $0.0020, 0.0040, 0.0060\,\mathrm{kg\,m^2}$. The component equations for these moments give the same time histories as the scaled numerical example for identical initial angular velocities, while the actual angular momentum and energy are smaller by a factor 500. This gives a physical specimen for checking principal-axis stability without requiring a massive rotor.

Adding a small mass at a known location changes both inertia and possibly the centre of mass. If a symmetric pair of equal small masses is attached at $\pm d\hat{e}_3$, their combined mass m_a adds $m_a d^2$ to I_1 and I_2, nothing to I_3, and leaves the centre fixed. For the plate above and $m_a = 0.10\,\mathrm{kg}, d = 0.10\,\mathrm{m}$,

the new moments are $0.0030, 0.0050, 0.0060\,\mathrm{kg\,m^2}$. The intermediate-axis growth exponent at fixed Ω changes from $|\Omega|/\sqrt{3}$ to $|\Omega|\sqrt{(0.005-0.003)(0.006-0.005)/(0.003\cdot 0.006)} = |\Omega|/3$. A reversible mass-placement experiment tests the inertia dependence of instability, not merely the existence of a visually dramatic flip.

Test intermediate-axis stability with the full body equations

Change the initial tilt and spin. Compare the linear perturbation and the complete torque-free motion while monitoring energy and angular momentum in the OneSimulation output.

Open this experiment online

Try the calculation

Nominal middle-axis speed (rad/s) **12**

Initial transverse speed (rad/s) **0.1**

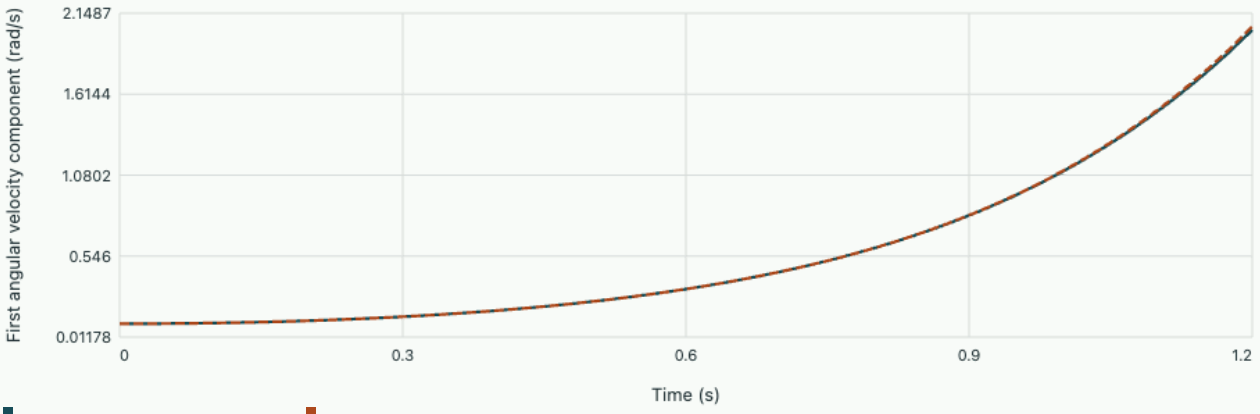

Initial linear growth rate 3.0984 s⁻¹. With zero initial transverse slope the predicted first doubling time is 0.42505 s.

Download the OneSimulation model

In your OneSimulation environment, run the model with these inputs.

```
python spectra-and-orbits.py rotor --spin 12 --seed 0.1
```

Estimate distance from a separatrix using dwell time

Near the intermediate-axis energy, elliptic modulus approaches one on either side. Writing $d = 1 - k_e^2$ on the low-energy family gives $K \sim \ln(4/\sqrt{d})$. Thus $T_b \sim 4\ln(4/\sqrt{d})/\nu$ for a slowly varying scale ν. Changing d by a factor of one hundred increases the expected body period by approximately $4\ln 10/\nu$. A tiny difference in the initial inertia-weighted energy can produce a readily observed increase in the time

between reorientation events while the maximum angular speed scarcely changes. The logarithm follows from passages near a hyperbolic equilibrium, where the signed unstable perturbation grows exponentially.

If $\nu = 3.0\,\mathrm{s}^{-1}$ and $d = 10^{-4}$, the leading estimate is

$$T_b = (4/3)\ln 400 \approx 7.99\,\mathrm{s}.$$

Reducing d to 10^{-6} gives $T_b \approx 11.06\,\mathrm{s}$. Inverting this relation makes estimates of d exponentially sensitive to a period offset. An uncertain start or stop event of a few tenths of a second, or a weak external torque during a long dwell, can affect an inferred separatrix energy considerably. Report the uncertainty of $E - L^2/(2I_2)$ as well as the fitted period when claiming close approach to the unstable family.

One experimental check is to use both the crossing speed of $\omega_2 = 0$ and the time between successive such crossings. At a low-energy upward crossing the slope has magnitude $B\nu$; it remains finite near the separatrix even while the period diverges. A simple global slowdown from increased bearing drag tends to modify the crossing speed as well as the dwell. A correctly prepared near-separatrix torque-free motion has relatively rapid crossings separated by long intervals close to intermediate-axis rotation. The distinction is visible in the time domain and does not depend on estimating a derivative at the slowest, noisiest part of the record.

A fit places a nominally torque-free experiment slightly above the separatrix when E, L are computed from gyros, but below it when inferred from the oscillating component pattern. What should be checked first?

▼ **Work through the solution**

Recalculate both invariants from the same time stamps, calibrated orientation and inertia axes. The energy classification subtracts comparable quantities and can be sensitive to cross-axis bias. The low-energy family keeps its third component's sign, whereas the high-energy family keeps its first component's sign with the stated ordering. Verify that a full body period was actually recorded and that sign changes were resolvable. Persistent disagreement after uncertainty and sampling checks can indicate a slow torque, changing mass distribution or a misspecified principal-axis alignment.

Quantify a small external torque before fitting a free-top period

Suppose the laboratory angular momentum has magnitude $3.0\,\mathrm{kg\,m^2/s}$ and an approximately constant transverse torque $0.010\,\mathrm{N\,m}$ acts for a $6.0\,\mathrm{s}$ body period. The accumulated transverse impulse is $0.060\,\mathrm{kg\,m^2/s}$, enough to tilt the spatial angular-momentum direction by roughly $0.020\,\mathrm{rad}$, or 1.15°. Its magnitude changes only to second order if the torque remains perpendicular to the initial momentum. A check using only L^2 could therefore show a small relative error while the invariable plane has moved perceptibly.

Use two marked inertial reference directions to track the spatial momentum vector and plot its Cartesian increments against the integrated measured torque. When gravity acts about a support whose line

passes through the mass centre, its torque vanishes ideally, but a small offset can supply just such a transverse disturbance. Reversing the initial spin while retaining the support geometry helps distinguish a fixed parasitic torque from gyro bias. If the spatial direction changes appreciably during one long near-separatrix dwell, fitting a torque-free elliptic period to the complete signal becomes inaccurate even if the early, fast gyro crossings agree with the free model.

Tutorial on a torque-free body's time scales

What period should be measured for the transverse gyro in the worked example? Use the small-parameter expansion $K = (\pi/2)[1 + m/4 + 9m^2/64 + \cdots]$ with $m = k_e^2$.

▼ **Work through the solution**

Substitution of $m = 1/12$ gives $K \approx 1.605$ and $T_b \approx 6.42\,\mathrm{s}$. The third-axis component repeats after about $3.21\,\mathrm{s}$, while the second component first reaches its positive maximum at $1.61\,\mathrm{s}$. Checking all three features tests the phase relation among the gyros and helps identify a sensor axis swap.

For a body with $I_1 = I_2 < I_3$, how do Euler's equations simplify and which feature of the asymmetric example disappears?

▼ **Work through the solution**

The third body component remains exactly constant, and the first two rotate sinusoidally at body-frame frequency $(I_3 - I_1)|\omega_3|/I_1$. The polar angle to fixed angular momentum is constant. A body axis can still precess in space, but the varying torque-free polar nutation caused by distinct transverse inertias disappears. Taking this limit in the low-energy solution gives $k_e \to 0$ consistently.

A gyro experiment reports slow amplitude decay along with fixed spatial angular momentum. Can that arise in a strictly rigid, torque-free model conserving kinetic energy?

▼ **Work through the solution**

The two rigid-body invariants fix the allowed intersection curve, so a persistent drift between such curves requires an effect beyond that ideal model or a changing calibration. Internal dissipation in a deformable body can decrease kinetic energy while conserving total spatial angular momentum, favouring rotation about the largest-inertia axis. An external torque could instead change angular momentum. Measuring both invariants helps distinguish the two explanations.

Compare principal-axis stability before fitting an asymmetric-top gyro trace.

David Tong derives the Euler equations, Euler angles and free-top motion.

Analytical mechanics from constraints to invariants · 7. The heavy symmetric top, precession branches and the sleeping state

Gravity supplies a torque to a top pivoted away from its centre of mass. Its axis may precess steadily, nutate between two turning angles, or trace loops. Derive all three from the same angular kinetic energy and determine when an upright spinning top can remain stable.

Project gravity onto a body with one fixed point

Let $I_1 = I_2 = I$ and I_3 be moments about the pivot, with the centre of mass a distance l along the symmetry axis. Use Euler angles θ, ϕ, ψ, where θ measures the tilt from upward laboratory vertical, ϕ measures the azimuth of the symmetry axis, and ψ spins the body about that axis relative to the nodal line. The centre-of-mass height is $l\cos\theta$, so gravity contributes $V = Mgl\cos\theta$. In the body the spin component of angular velocity is $\omega_3 = \dot\psi + \dot\phi\cos\theta$. The squared transverse component is $\dot\theta^2 + \dot\phi^2\sin^2\theta$. Consequently

$$L = \tfrac{1}{2}I(\dot\theta^2 + \dot\phi^2\sin^2\theta) + \tfrac{1}{2}I_3(\dot\psi + \dot\phi\cos\theta)^2 - Mgl\cos\theta.$$

The angles ϕ and ψ are absent themselves. Their momenta $L_z = I\dot\phi\sin^2\theta + L_3\cos\theta$ and $L_3 = I_3\omega_3$ are constants. Gravity torque about the pivot is perpendicular to the vertical and to the body symmetry axis, consistent with these two conservation laws. The entire vector $\mathbf{L}$ need not be constant. Distinguish the axial spin ω_3 measured by a body gyro from the Euler rate $\dot\psi$. A precessing top can have appreciable $\dot\phi\cos\theta$; using the painted-mark rate in a spin estimate without specifying the reference can bias a precession prediction.

Eliminate cyclic velocities to find the nutation potential

Solve $\dot\phi = (L_z - L_3\cos\theta)/(I\sin^2\theta)$ and $\dot\psi = L_3/I_3 - \dot\phi\cos\theta$. The energy can now be written $E = L_3^2/(2I_3) + I\dot\theta^2/2 + V_{\text{eff}}(\theta)$, with

$$V_{\text{eff}}(\theta) = Mgl\cos\theta + \frac{(L_z - L_3\cos\theta)^2}{2I\sin^2\theta}.$$

The second term is not an additional gravitational interaction. It is the transverse rotational energy required by the two fixed angular momenta at each tilt. A root of $E - L_3^2/(2I_3) - V_{\text{eff}} = 0$ is a polar turning angle; a simple root is generally reached and reversed in finite time. A minimum gives stable regular precession under sufficiently small nutations at fixed conserved momenta. The apparent divergence at a pole disappears if the numerator vanishes in the same limit. The possibility of the upright sleeping state therefore requires

$$L_z = L_3.$$

Putting $u = \cos\theta$ gives a polynomial first integral. With $E' = E - L_3^2/(2I_3)$, one obtains

$$I^2\dot{u}^2 = 2I(E' - Mglu)(1-u^2) - (L_z - L_3 u)^2 = P_3(u).$$

The accessible range lies within $[-1, 1]$ where $P_3 \geq 0$. The physical turning points can be found without assigning an Euler azimuth at a pole. A nutation period is $2I\int_{u_{\min}}^{u_{\max}} du/\sqrt{P_3(u)}$. Computing the azimuthal advance over the same cycle requires averaging $\dot{\phi}(u)$ with the same time weight. An arithmetic average of the two turning-point precession rates misses the longer dwell times near the endpoints.

Find slow and fast regular precession

For constant tilt and constant $\dot{\phi} = \Omega$, the θ equation at a nonzero tilt gives

$$I\Omega^2 \cos\theta - L_3\Omega + Mgl = 0.$$

This relation follows directly by differentiating the Lagrangian with respect to θ, using $\partial_\theta[\dot{\psi} + \dot{\phi}\cos\theta] = -\dot{\phi}\sin\theta$. It is quadratic in precession speed, so the often-used $\Omega \simeq Mgl/L_3$ is only one limit. For a top above the horizontal plane and $L_3 > 0$, two positive precession branches exist if $L_3^2 \geq 4IMgl\cos\theta$. Their sum is $L_3/(I\cos\theta)$, and their product is $Mgl/(I\cos\theta)$.

Take $I = 0.020\,\mathrm{kg\,m^2}$, $I_3 = 0.010\,\mathrm{kg\,m^2}$, $Mgl = 0.200\,\mathrm{N\,m}$,

$$L_3 = 0.200\,\mathrm{kg\,m^2/s},$$

$$\theta = 60^\circ.$$

The quadratic is $0.010\Omega^2 - 0.200\Omega + 0.200 = 0$, with roots 1.056 and $18.94\,\mathrm{rad/s}$. Both have the same material spin $\omega_3 = 20\,\mathrm{rad/s}$, but their vertical angular momenta are different. The slow branch has $L_z = 0.020(1.056)(0.75) + 0.200(0.5) = 0.1158\,\mathrm{kg\,m^2/s}$; the fast branch has about $0.384\,\mathrm{kg\,m^2/s}$. Preparing a tilt and a spin alone therefore does not select a unique regular precession. The initial angular velocity of the tilted axis also matters.

Distinguish looping, cusped and monotone azimuth traces

During nutation the sign of $\dot{\phi}$ is the sign of $L_z - L_3 u$. If $u_* = L_z/L_3$ lies strictly between the turning points, the azimuth reverses along each nutation and the axis can trace loops on the unit sphere. If u_* equals a turning point, both $\dot{\theta}$ and $\dot{\phi}$ can vanish together there, producing a cusp in the ideal trace. If the numerator keeps one sign the azimuth advances monotonically even as tilt oscillates. Seeing an apparent loop in a two-dimensional camera projection is insufficient by itself; recover the three-dimensional orientation or check the signed azimuthal rate.

One classic release starts with a tilted axis that initially has no angular velocity except spin about its own direction. Then $L_z = L_3\cos\theta_0$, $\dot{\phi} = 0$, $\dot{\theta} = 0$. The gravitational torque starts tilting the axis down; on returning to that initial turning point the projected angular speed again momentarily vanishes. By contrast, giving the top the correct nonzero precession velocity at release puts it on a regular precession

branch with no initial nutation. Identical tilt and spin measurements can thus yield dramatically different trajectories if the release mechanism imparts a different transverse angular velocity.

Derive the upright stability threshold

At $L_z = L_3$, reduce the ratio $(1-\cos\theta)^2/\sin^2\theta$ to $(1-\cos\theta)/(1+\cos\theta)$. Near zero tilt the effective potential is $Mgl + [L_3^2/(8I) - Mgl/2]\theta^2 + O(\theta^4)$. A positive coefficient gives an energy minimum and requires $L_3^2 > 4IMgl$. For the preceding I, Mgl this critical angular momentum is $0.1265\,\mathrm{kg\,m^2/s}$, or an axial spin speed $12.65\,\mathrm{rad/s}$ for the chosen I_3. A high spin stabilises the upper position by coupling tilt to conservation of angular momentum. The purely gravitational potential by itself has a maximum there.

The fixed-$L_z = L_3$ quadratic energy curvature describes a polar disturbance within that momentum class. Near the axis ϕ, ψ individually become coordinate singularities. To analyse arbitrary small perturbations, use horizontal components of the unit axis and linearise their coupled gyroscopic equations. The two circular precession frequencies at the pole solve $I\Omega^2 - L_3\Omega + Mgl = 0$, giving the same discriminant. Exactly at threshold the linear frequencies coalesce, and nonlinear terms or dissipation can dominate a finite disturbance. Distinguishing a stable ideal top from an experimentally long-lived slowly slowing top requires monitoring spin over the entire observation interval.

Measure the nutation frequency of a regular precession branch

Take any regular precession tilted away from the poles, with prescribed constants L_z, L_3. A small perturbation of the polar angle gives $I\ddot{\eta} + V_{\mathrm{eff}}''(\theta_0)\eta = 0$, so the nutation frequency at fixed momenta follows from the second derivative of the effective potential. Differentiating while holding the instantaneous $\dot{\phi}$ fixed would give a different result, because a displaced top with the same momenta must change its precession rate. This distinction matters when preparing a perturbation: a small tap that adds a transverse angular impulse can change the constants as well as the tilt.

A convenient explicit formula follows by writing $F(\theta) = L_z - L_3\cos\theta$,

$$w(\theta) = F/(I\sin^2\theta).$$

Then $V_{\mathrm{eff}}' = \sin\theta[-Mgl + L_3 w - Iw^2\cos\theta]$. At a regular solution the bracket vanishes. Differentiate w as $w' = (L_3/I - 2w\cos\theta)/\sin\theta$, substitute into the derivative of the bracket, and obtain

$$\omega_{\mathrm{nut}}^2 = \frac{V_{\mathrm{eff}}''(\theta_0)}{I} = \left(\frac{L_3}{I} - 2\Omega\cos\theta_0\right)^2 + \Omega^2\sin^2\theta_0.$$

For the 60° example,

$$L_3/I = 10.0\,\mathrm{s^{-1}}.$$

On the slow branch $\Omega = 1.056\,\mathrm{s}^{-1}$, this gives $\omega_{\mathrm{nut}} \approx 8.99\,\mathrm{s}^{-1}$, or a nutation period of $0.699\,\mathrm{s}$. On the fast branch $\Omega = 18.94\,\mathrm{s}^{-1}$, it gives approximately $18.7\,\mathrm{s}^{-1}$, or $0.336\,\mathrm{s}$. Both tilted regular solutions have positive fixed-momentum curvature in this example. Comparing just the precession rates would miss the different small oscillations around their two reduced equilibria.

Suppose a small angular displacement conserves L_z, L_3 on the slow branch. The correlated rate shift is $w'\delta\theta$. At the example point $w' = (10 - 1.056)/\sin 60^\circ = 10.33\,\mathrm{s}^{-1}/\mathrm{rad}$. A nutation of $0.020\,\mathrm{rad}$ therefore modulates the precession rate by about $0.207\,\mathrm{rad/s}$, a substantial fraction of its slow steady value. A low-resolution video that measures azimuth per frame can show a conspicuous modulation even when the nutation angle itself is visually small. Filtering only one angle and fitting it with constant angular speed would hide this dynamical correlation.

Recover a nutation trajectory from energy and two turn angles

Suppose a measured top has $I = 0.020\,\mathrm{kg\,m^2}$, $Mgl = 0.20\,\mathrm{J}$, $L_3 = 0.20\,\mathrm{kg\,m^2/s}$, and is released without precession or nutation at $\cos\theta_0 = 0.50$. Its constants are $L_z = 0.10\,\mathrm{kg\,m^2/s}$ and $E' = 0.10\,\mathrm{J}$. The polar polynomial becomes

$$P_3(u) = 0.04(0.10 - 0.20u)(1 - u^2) - (0.10 - 0.20u)^2.$$

Factoring out $0.10 - 0.20u$ leaves $0.04(1 - u^2) - (0.10 - 0.20u)$. The other roots satisfy $0.04u^2 - 0.20u + 0.06 = 0$, giving $u \simeq 0.3206$ and $u \simeq 4.68$. Only the first lies within the physical interval. Thus the tilt runs from 60° to about 71.3°, and the unphysical cubic root must be discarded.

At the initial $u = 0.50$, the azimuthal numerator vanishes and the top momentarily has no precession. At the lower turning $u \simeq 0.3206$, the precession rate is $(0.10 - 0.20u)/[0.020(1 - u^2)] \approx 2.0\,\mathrm{rad/s}$. These two measurements together discriminate the cusped release from regular slow precession. A detector reporting only a mean precession rate near one radian per second could confuse them. Timing the first turning angle after release offers an independent check of Mgl/I, while a direct gyro constrains L_3/I_3.

To evaluate the nutation quadrature numerically without endpoint difficulties, substitute $u = u_{\min} + (u_{\max} - u_{\min})\sin^2\alpha$. As α approaches either endpoint, du cancels the simple square-root singularity from P_3. Integrate once with numerator one for time and once with the extra factor $\dot\phi(u)$ for azimuth. Repeat after halving the quadrature spacing. An exactly repeated root signals a limiting regular solution or a separatrix; the simple-turning substitution alone cannot regularise an actual logarithmically divergent period. In the cusped trajectory above the angular trace is continuous at the polar turning, even though the tangent to that trace can vanish.

Use horizontal tilt coordinates at the sleeping pole

Near the upright orientation the separate Euler angles ϕ, ψ are ill conditioned. Instead let the symmetry-axis unit vector be $\mathbf{n} = (x, y, 1) + O(x^2 + y^2)$ in an inertial frame with z upward. Here x, y are small dimensionless tilts, not translations. The instantaneous transverse angular velocity is $\mathbf{n} \times \dot{\mathbf{n}} \approx (-\dot y, \dot x, 0)$

, because $(\mathbf{n}\times\dot{\mathbf{n}})\times\mathbf{n}=\dot{\mathbf{n}}$. The laboratory angular momentum to first order is $I\mathbf{n}\times\dot{\mathbf{n}}+L_3\mathbf{n}$. Its derivative equals the gravitational torque $Mgl\,\hat{z}\times\mathbf{n}$. Equating the two horizontal components yields

$$I\ddot{x}+L_3\dot{y}-Mgl\,x=0,$$

$$I\ddot{y}-L_3\dot{x}-Mgl\,y=0.$$

Let $w=x+iy$. These combine into $I\ddot{w}-iL_3\dot{w}-Mgl\,w=0$. Substituting $w\propto e^{i\Omega t}$ returns $I\Omega^2-L_3\Omega+Mgl=0$ without ever assigning azimuth to the exact pole. For spin strictly above threshold, a general small tilt is a superposition of two circular motions of the two real frequencies. Their vector sum traces a wobble. For spin below threshold, the two frequencies form a complex conjugate pair and one mode grows exponentially. A perfectly vertical initial state can remain exactly vertical in an ideal simulation on either side, so stability requires a nonzero test perturbation.

Take a below-threshold spin $L_3=0.100\,\mathrm{kg\,m^2/s}$ with the earlier $I=0.020$ and $Mgl=0.200$. The real precession rate is $L_3/(2I)=2.50\,\mathrm{s^{-1}}$ and the exponential growth rate is

$$\sqrt{4IMgl-L_3^2}/(2I)=1.94\,\mathrm{s^{-1}}.$$

If the growing-mode component starts at $1\,\mathrm{mrad}$, a $20\,\mathrm{mrad}$ excursion takes about $\ln 20/1.94=1.55\,\mathrm{s}$ within the linear model. Below threshold the top need not collapse immediately after release. A short video can show several degrees of apparently orderly precession before growing tilt becomes unmistakable.

Just above threshold the mode frequencies are nearly degenerate. Decomposing noisy initial conditions into two circular amplitudes then involves division by their small frequency separation. A finite tilt impulse can produce a large beat envelope even though both ideal modes remain bounded. At exactly the repeated root the general linear solution contains $te^{i\Omega t}$ as well as $e^{i\Omega t}$; neutral-looking roots alone do not ensure boundedness. This distinction matters when inferring a critical spin from finite observation windows. Report the initial perturbation and the tilt threshold used to define loss of stability.

Infer the centre-of-mass offset from controlled precession

If regular precession can be prepared at a known tilt, the quadratic balance gives

$$Mgl=L_3\Omega-I\Omega^2\cos\theta.$$

Neglecting the second term is customary only on a sufficiently slow branch. With the slow 60° case the neglected term is about $0.0112\,\mathrm{N\,m}$, or 5.6% of the true gravitational torque scale. Inferring the centre-of-mass offset by using $l=L_3\Omega/(Mg)$ would overestimate l by this fraction. On the fast branch the two terms nearly cancel and a small error in I or Ω can be magnified substantially in the inferred Mgl.

For a top of measured mass $0.50\,\mathrm{kg}$ and $Mgl=0.200\,\mathrm{N\,m}$, the offset is $0.0408\,\mathrm{m}$. An uncertainty of $0.002\,\mathrm{N\,m}$ in gravitational torque corresponds to about $0.41\,\mathrm{mm}$ before mass and local gravity uncertainty. Repeat at several known tilts while measuring body spin and laboratory precession individually. A consistent l across slow and fast branches checks the kinetic-energy model, whereas a

gradual decrease of apparent L_3 during a single run suggests pivot drag or aerodynamic torque. A static suspension measurement of the centre of mass is a useful independent reference when estimating inertias from dynamic data.

Verify the torque law with a horizontal gyroscope

An instructive limiting experiment supports one end of a spinning wheel axle at a pivot, leaving its symmetry axis nearly horizontal. Choose the centre of mass along the free end of the axle and define the wheel's axial angular momentum by the right-hand rule. The gravitational torque is $\boldsymbol{\tau} = Mgl\,\hat{z} \times \mathbf{n}$. If $\mathbf{L}$ is approximately $L_3\mathbf{n}$, a regular precession at laboratory angular speed Ω gives

$$\dot{\mathbf{L}} \approx L_3 \Omega\, \hat{z} \times \mathbf{n}.$$

Equating the torque gives

$$\Omega = Mgl / L_3.$$

At exactly horizontal tilt this agrees with the finite root of the full quadratic; slightly away from horizontal the small transverse angular momentum affects the quantitative result.

For a wheel with $I_3 = 0.012\,\mathrm{kg\,m^2}$, axial spin $40\,\mathrm{rad/s}$, mass $0.40\,\mathrm{kg}$ and pivot offset $0.060\,\mathrm{m}$,

$$L_3 = 0.480\,\mathrm{kg\,m^2/s},$$
$$Mgl = 0.235\,\mathrm{N\,m}.$$

Horizontal precession is $0.490\,\mathrm{rad/s}$, one revolution in $12.8\,\mathrm{s}$. Reversing the spin reverses the precession direction. Moving the pivot to the other side of the centre also reverses the gravitational torque for a fixed axis convention. Testing each reversal separately helps distinguish the true gyroscopic response from a static torque due to a tilted support or a twisting suspension lead.

The phrase that gravity causes the wheel to stay up hides a vertical support force and a changing horizontal angular momentum. The pivot supplies most or all of the vertical force required to support the wheel's weight. With steady horizontal precession, the centre of mass also accelerates horizontally toward the precession axis with magnitude $l\Omega^2$. Thus the pivot must supply a horizontal radial reaction $Ml\Omega^2$. For the numerical wheel this is only $0.0058\,\mathrm{N}$, much smaller than the $3.92\,\mathrm{N}$ vertical support. A torque signal can be easy to see through slow precession while the corresponding horizontal reaction is weak. A load cell measuring only vertical force would not directly measure the gravitational torque acting about the pivot.

Spin friction alters the interpretation of a long run. Suppose the measured axial spin falls from 40 to $35\,\mathrm{rad/s}$ over one minute and the axis remains close to horizontal regular precession. The predicted precession speed rises from 0.490 to $0.561\,\mathrm{rad/s}$, even though mechanical energy is being dissipated. This is not negative damping. Less axial angular momentum must change direction under essentially the same gravitational torque, so its direction turns more rapidly. If the spin-down time becomes comparable with a nutation period, an instantaneous regular-precession approximation is no longer sufficient; include dissipative torques in the full equations and measure both tilt and angular momentum.

Identify the precession branches

Change the angular momentum of a supported top before identifying its steady rotation rates. Check which approximation singles out the slower branch.

Open this experiment online

Try the calculation

Tilt from vertical (°) **60**

Moment arm (mm) **60**

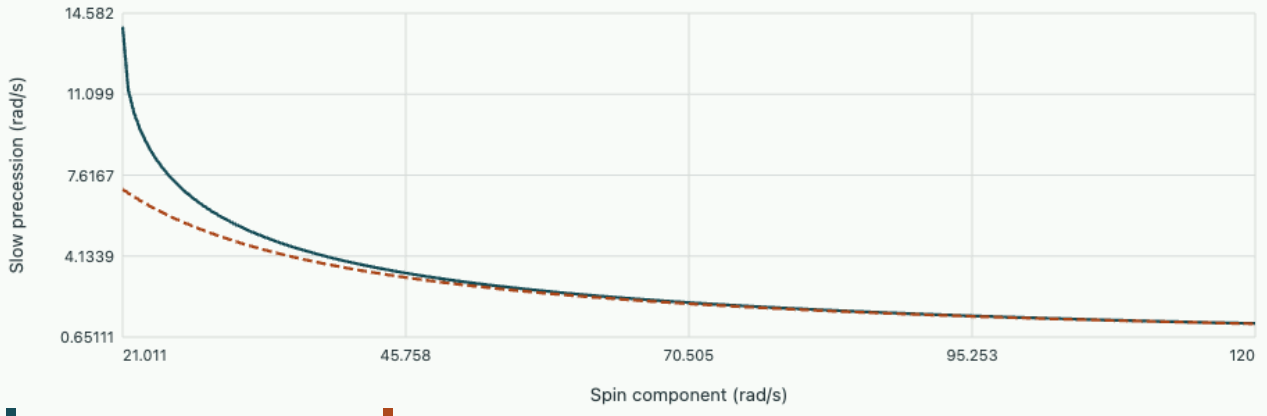

For this tilt the two regular-precession branches first exist at spin 21.0 rad/s. At 100 rad/s the exact slow rate is 1.488 rad/s.

Extract polar turning points from uncertain orientation data

A camera supplies a unit direction $\mathbf{n}(t)$, while body and pivot calibrations supply I, I_3, Mgl. To infer L_3, either measure the gyro component along $\mathbf{n}$ or combine two independent orientation marks so that spin about the axis is observable. A single unmarked axis direction cannot reveal that spin. Vertical angular momentum follows from $L_z = I(\mathbf{n} \times \dot{\mathbf{n}})_z + L_3 n_z$. This expression remains regular at a vertical pose and avoids differentiating an azimuth divided by a small $\sin\theta$. Estimating $\dot{\mathbf{n}}$ still requires timing and finite-difference checks, especially near a fast turn.

The transverse kinetic energy is $I|\dot{\mathbf{n}}|^2/2$, so $E' = I|\dot{\mathbf{n}}|^2/2 + Mgl\,n_z$. These vector formulas allow each time sample to supply independent estimates of the invariants. Compute their median or uncertainty-weighted values over a torque-free-about-vertical segment, then locate the physical roots of $P_3(u)$. Reject roots outside $[-1, 1]$ before converting to angles, and propagate measured parameter ranges into intervals for the roots. Near a repeated root a small coefficient error can split the pair substantially or apparently remove it. A nearly steady precession should therefore be assessed using the dynamic measurement uncertainty, not classified solely by the discriminant of a fitted cubic.

A direction-only camera sees apparently steady 60° precession at $1.0\,\mathrm{rad/s}$. Can it infer the axial spin without measuring a second body mark?

▼ **Work through the solution**

In a precisely known ideal regular state the torque balance gives $L_3 = (I\Omega^2\cos\theta + Mgl)/\Omega$, so one can infer spin from a dynamical model and calibrated inertias. Using $I = 0.020$, $Mgl = 0.200$ gives

$$L_3 = 0.210\,\mathrm{kg\,m^2/s}.$$

That is an indirect inference, sensitive to gravity calibration, pivot torque, and the assumption of exactly regular precession. The orientation of one axis alone supplies no purely kinematic measurement of rotation about itself. A second mark or gyro offers an independent check rather than fitting the same torque law twice.

A numerical implementation rescales $\mathbf{n}$ to unit length at every step and observes bounded plotted angles. Does this establish correct top dynamics?

▼ **Work through the solution**

Unit length is only the configuration constraint. Reconstruct L_z, L_3, E', compare polar turning points with the cubic, and repeat at smaller time step. The vector can stay exactly on the sphere while its azimuth and nutation phase drift, or while a spurious torque transfers axial angular momentum. A support torque and gravitational work budget, with a clear reference for the potential, test complementary aspects that normalisation alone cannot enforce.

Check the fixed-pivot inertia before drawing an instability boundary

A laboratory data sheet may quote the transverse inertia about the centre of mass, whereas the Lagrangian here needs the inertia about the pivot. With a pivot on the symmetry axis a distance l from the centre, the parallel-axis relation gives $I = I_{\mathrm{cm}} + Ml^2$ for each transverse direction, while I_3 remains unchanged. For $M = 0.50\,\mathrm{kg}$, $l = 0.080\,\mathrm{m}$, and $I_{\mathrm{cm}} = 0.010\,\mathrm{kg\,m^2}$, the correct value is $0.0132\,\mathrm{kg\,m^2}$. Neglecting the shift underpredicts the critical spin by a factor $\sqrt{0.010/0.0132} = 0.870$.

Moving the pivot changes both the gravitational torque scale Mgl and the transverse inertia. Doubling l does not merely multiply the stability threshold by $\sqrt{2}$ if Ml^2 is appreciable. Compute the new I and then the product that enters $L_{3,\mathrm{crit}}^2 = 4IMgl$. A two-pivot experiment with one unchanged rotor provides a direct test of the parallel-axis correction and checks why a table of freely rotating principal moments cannot be inserted unaltered into a supported top calculation.

Tutorial on a heavy top

With the same constants, impose a tilt of 90°. Does the regular precession formula become singular when $\cos\theta = 0$?

▼ **Work through the solution**

The unsimplified quadratic becomes $-L_3\Omega + Mgl = 0$, so the finite regular precession is

$$\Omega = Mgl/L_3 = 1.0\,\mathrm{rad/s}.$$

A quadratic formula written with $2I\cos\theta$ in the denominator masks this regular solution. The other branch becomes unbounded as the horizontal configuration is approached from the side with positive cosine at fixed spin. Keep the original equation when taking a degenerate limit.

A top undergoes nutation with u between 0.30 and 0.70, with $L_z = 0.11$ and $L_3 = 0.20$ in consistent angular-momentum units. Does the azimuth reverse?

▼ **Work through the solution**

The numerator of $\dot\phi$ vanishes at $u = 0.55$, inside the allowed interval. For $u < 0.55$ precession is positive in this convention; for $u > 0.55$ it is negative. A camera recording the full axis should therefore find an azimuthal reversal twice per nutation period. The polar velocity need not vanish at those two reversals, so these instants are distinct from the polar turning points.

A frictionless rigid-top simulation reports exact E, L_z, L_3 but returns a nutation frequency differing by ten percent from an independent measurement. Name two checks that use more than the conserved values.

▼ **Work through the solution**

Compute the turning points from the cubic and compare the measured times between them against its quadrature, then reconstruct the azimuthal phase over the same cycle. Check whether the measured spin was ω_3 or a painted-mark Euler rate and whether the inertias include the parallel-axis contribution about the pivot. A numerical method can conserve constants while producing a phase error, and an inconsistent initial state can preserve different constants perfectly.

Compare a free principal-axis rotation with a pivoted top subject to gravity.

David Tong's rigid-body chapter includes the heavy symmetric top.

Analytical mechanics from constraints to invariants · 8. Symplectic transformations, Poisson brackets and the geometry of measurements

Two phase-space plots can enclose the same volume while predicting different responses to an impulse. Derive the stronger condition that makes a change of variables canonical, test it on measured linear maps and use Poisson brackets to propagate observables without solving separately for every coordinate.

Derive the matrix condition from Hamilton's equations

Collect n canonical positions and momenta into $z = (q_1, \dots, q_n, p_1, \dots, p_n)^T$. Write Hamilton's equations as $\dot{z} = J\nabla_z H$, where J has zero diagonal blocks, identity upper right and minus identity lower left. For a time-independent change $Z = f(z)$ with Jacobian $S = \partial Z/\partial z$, the chain rule gives

$$\dot{Z} = SJS^T \nabla_Z H.$$

To preserve the canonical form for every differentiable Hamiltonian require

$$SJS^T = J.$$

For an invertible square matrix this is equivalent to $S^T J S = J$. In geometric terms the bilinear antisymmetric form $\omega(u, v) = u^T J v$ has the same value on any transported pair of tangent vectors.

Taking determinants gives $(\det S)^2 = 1$, and symplectic maps have positive determinant equal to one. One way to see the sign is to take the top exterior power of the preserved two-form: ω^n fixes an oriented volume. In one canonical pair the identity $S^T J S = (\det S) J$ makes determinant one sufficient. In two or more pairs a single volume condition cannot enforce every entry of the matrix condition. For example in ordering (q_1, q_2, p_1, p_2), scaling by diagonal entries $(2, 1, 1, 1/2)$ preserves four-dimensional volume. But $\{Q_1, P_1\} = 2$ and $\{Q_2, P_2\} = 1/2$, so neither conjugate pair has the required bracket. A volume-preserving histogram test alone would miss this failure.

Identify brackets of observables and what they measure

Define $\{A, B\} = (\nabla A)^T J \nabla B = \sum_i (A_{q_i} B_{p_i} - A_{p_i} B_{q_i})$. For any explicitly time-dependent observable $A(z, t)$, differentiation along Hamiltonian trajectories gives

$$\dot{A} = \{A, H\} + \partial_t A.$$

The bracket is antisymmetric and obeys the product rule. Computing it with the chain rule in the new variables proves that canonical transformations preserve brackets, even between nonlinear observables. Conversely the fundamental brackets $\{Q_i, P_j\} = \delta_{ij}$, $\{Q_i, Q_j\} = \{P_i, P_j\} = 0$ are precisely the entries of $SJS^T = J$.

For a particle set $L_z = x p_y - y p_x$. Its Hamiltonian flow as a generator sends x to $x - \varepsilon y$, y to $y + \varepsilon x$ and rotates momenta by the same infinitesimal angle. The angular momentum components satisfy $\{L_x, L_y\} = L_z$ with cyclic permutations. Derive one entry directly for $L_x = y p_z - z p_y$ and

$L_y = zp_x - xp_z$. The z, p_z pair contributes $xp_y - yp_x$, with the other terms zero. Rotations about two different axes generally fail to commute. The resulting commutator has the form of a rotation about the third axis even though each underlying infinitesimal motion preserves every canonical bracket.

Jacobi's identity $\{A, \{B, C\}\} + \{B, \{C, A\}\} + \{C, \{A, B\}\} = 0$ implies that the bracket of two time-independent conserved quantities is conserved under the same Hamiltonian. If the Hamiltonian is invariant under rotations about x and y, its invariance about z follows from this relation and $\{L_x, L_y\} = L_z$. Conservation alone need not make two observables commute. A central force can conserve all three angular momentum components, but their mutual brackets remain nonzero. For independent commuting integrals in an integrability argument one must check the involution condition explicitly.

Construct a canonical map for any smooth point transformation

Suppose new coordinates depend only on old coordinates, $Q = f(q)$. Preserve the canonical one-form exactly,

$$p^T dq = P^T dQ = P^T Df\, dq.$$

Thus $p = (Df)^T P$ and $P = (Df)^{-T} p$. Applying the same coordinate matrix to momenta works only for a restricted case such as an orthogonal change of coordinates. An extension of position must be accompanied by a reciprocal rescaling of its conjugate momentum. For $Q = q^2$ on $q > 0$, for example, $P = p/(2q)$. The free Hamiltonian becomes $2QP^2/m$; even a physically free particle can acquire a coordinate-dependent expression for its kinetic energy.

Polar coordinates demonstrate why a momentum variable need not equal a measured tangential component. In the plane $x = r\cos\varphi, y = r\sin\varphi$. Substituting into $p_x dx + p_y dy$ gives

$$p_r = \mathbf{p} \cdot \hat{r},$$

$$p_\varphi = r\,\mathbf{p} \cdot \hat{\varphi} = L_z.$$

The physical tangential momentum is p_φ / r. At radius $0.40\,\mathrm{m}$ and transverse momentum $0.60\,\mathrm{kg\,m/s}$, the canonical angular momentum is $0.24\,\mathrm{kg\,m^2/s}$. Treating the transverse component itself as conjugate to angle would make $\{\varphi, p_\varphi^{\mathrm{wrong}}\} = 1/r$. The coordinate singularity at $r = 0$ also prevents these canonical polar variables from covering the entire original phase space with one chart.

Generate shears and test a numerical map

A type-two generating function $F_2(q, P, t)$ defines $p = \partial_q F_2$, $Q = \partial_P F_2$, and $K = H + \partial_t F_2$ where the transformation can be locally inverted. The differential $d(F_2 - QP)$ equals $p\,dq - P\,dQ + (K - H)\,dt$. Thus the actions differ only by an endpoint term; taking another exterior derivative at fixed time gives the symplectic form condition. For $F_2 = qP + sP^2/(2m)$, the map is $p = P, Q = q + sp/m$, free drift over time s. For $F_2 = qP + sV(q)$, the map is

$P = p - sV'(q), Q = q$, a potential kick. Their composition is canonical for any step size even though an alternating drift and kick need not give the exact trajectory.

Take a unit-mass, unit-frequency oscillator with $h = 0.5$. A kick followed by drift gives $P = p - hq$, $Q = q + hP = (1 - h^2)q + hp$. Its amplification matrix has determinant one and trace $2 - h^2 = 1.75$, so its eigenvalues form a unit-modulus conjugate pair. The numerical phase per step is $\arccos(1 - h^2/2) = 0.50536$, slightly ahead of the exact phase 0.50000. Starting at $q = 1, p = 0$, the first step gives $Q = 0.75, P = -0.50$, and physical energy becomes 0.40625 instead of 0.5. Exact bracket preservation does not imply exact conservation of the original energy at every point. If $h > 2$ the same matrix remains symplectic but has a real expanding and contracting eigenvalue; geometric preservation is compatible with numerical instability.

For a numerical implementation with analytic equations unavailable, approximate the Jacobian of a one-step map at selected states by perturbing one canonical component at a time. Compute $S^T J S - J$ after nondimensionalising coordinates and momenta in conjugate pairs. Repeat with smaller perturbations and at different integration tolerances. A determinant close to one in four dimensions is insufficient. Testing the transported brackets of one position–momentum pair and one cross-pair can reveal a swapped column or misplaced mass factor before a long simulation exhibits visible energy drift.

Track canonical area for a transported experimental ensemble

A narrow group of trajectories lets an experimenter estimate a tangent map without applying a separate perturbation to each coordinate at the same time. Prepare a small covariance ellipse in one canonical pair $z = (q, p)$, propagate each member through a known linear Hamiltonian device, and compute $\Sigma_{\mathrm{out}} = S \Sigma_{\mathrm{in}} S^T$. The ellipse area is proportional to $\sqrt{\det \Sigma}$, and a symplectic map in one pair preserves that area. Its projections can grow or contract individually: a focusing device can reduce position spread while increasing momentum spread or correlation. Measuring only the two marginal widths ignores their covariance and can falsely suggest area growth.

For a free unit-mass drift of duration two in scaled units,

$$S = \begin{pmatrix} 1 & 2 \\ 0 & 1 \end{pmatrix}.$$

Start with $\Sigma = \mathrm{diag}(1, 1)$. The outgoing covariance has entries $\Sigma_{qq} = 5, \Sigma_{pp} = 1, \Sigma_{qp} = 2$. The apparent rectangle of marginal standard deviations grows by $\sqrt{5}$, yet the determinant remains $5 - 4 = 1$. A plot that suppresses the correlation has discarded exactly the information needed for the area test. Noise in the two channels also contributes to observed covariance, so calibrate sensor variances independently before attributing a small apparent growth to physical dissipation or numerical smoothing.

For two pairs it is possible for a perfectly canonical coupling to exchange projected emittances. Take a uniform rotation of the two positions and the same rotation of their conjugate momenta. It is canonical by construction. If the two incoming pairs have different covariance areas, a ninety-degree rotation swaps them completely; at forty-five degrees each outgoing projected pair contains a mixture. The full four-dimensional symplectic structure remains intact. An experimentally available two-dimensional marginal

then tests only part of the dynamics. Counting phase-space points in a volume and measuring cross-pair brackets answer different questions about a strongly coupled system.

The eigenvalues of $J\Sigma$ are invariant under the linear canonical covariance transport. Indeed $JS = S^{-T}J$ for symplectic S, so $J\Sigma_{\mathrm{out}} = S^{-T}(J\Sigma_{\mathrm{in}})S^{T}$, a similarity transformation. For a positive covariance these eigenvalues occur as conjugate imaginary pairs, and their positive magnitudes give symplectic covariance scales. This algebraic test can distinguish loss of correlations in a fitted transfer matrix from actual exchange between pairs. It assumes linear propagation of the ensemble. A nonlinear canonical map can stretch a finite ellipse into a curved shape whose covariance determinant changes while its exact enclosed area remains preserved.

Use generating functions to find a moving normal-mode basis

Consider a two-dimensional isotropic oscillator and rotate its coordinate axes by a prescribed time-dependent angle $\alpha(t)$. Let $Q = R(\alpha)^{T} q$, $P = R(\alpha)^{T} p$ for a proper planar rotation. At any fixed time the map is orthogonal and symplectic. To derive the Hamiltonian in these moving variables, use $F_2(q, P, t) = q^{T} R(\alpha) P$. Its time derivative at fixed old q and new P is $-\dot{\alpha}(Q_x P_y - Q_y P_x)$, with the sign corresponding to axes rotating counterclockwise in the laboratory. The transformed Hamiltonian is therefore

$$K = H_0(Q, P) - \dot{\alpha} L_z.$$

For constant rotation rate and an isotropic potential the new Hamiltonian has no explicit time dependence. Its value is the combination energy minus rotation rate times angular momentum encountered in the Noether argument. Hamilton's equations now include $-\dot{\alpha}\,\hat{z} \times Q$ in $\dot{Q}$ relative to the rotated physical velocity. Thus the transformed canonical momentum P equals the rotated laboratory momentum rather than $m\dot{Q}$. Confusing the two yields incorrect initial conditions for a rotating-frame simulation even if the transformation matrix at the starting instant is the identity.

Take $m = 1.0\,\mathrm{kg}$, a laboratory point initially at $q = (0.20, 0)\,\mathrm{m}$ with $p = (0, 0.30)\,\mathrm{kg\,m/s}$, and axes initially aligned but rotating at $2.0\,\mathrm{rad/s}$. The canonical P_y is $0.30\,\mathrm{kg\,m/s}$. The derivative of the rotating-frame coordinate is

$$0.30 - 2.0(0.20) = -0.10\,\mathrm{m/s}.$$

It moves in the negative rotating-frame y direction while its laboratory velocity points positive y. The angular momentum is $0.060\,\mathrm{kg\,m^2/s}$, so K lies $0.120\,\mathrm{J}$ below the laboratory Hamiltonian. Both position–momentum transformations preserve brackets; the extra term derives from the moving basis, not a failure of canonical geometry.

An oscillator with two nearly equal natural frequencies provides another reason to track the generating function. If one diagonalises a slowly changing stiffness matrix at each time and keeps only the instantaneous diagonal frequencies, the omitted rotation of the eigenvectors couples the nominal modes through a term of this type. When the eigendirections turn rapidly near a degeneracy, the coupling can be appreciable even if both eigenvalues change little. Measuring the orientation as well as the

eigenfrequencies allows the size of this effect to be estimated before fitting amplitude transfer to a spurious dissipation term.

Compare exact phase transport with a dissipative fit

A damped oscillator with $m\ddot{q} + c\dot{q} + kq = 0$ has equations $\dot{q} = p/m$, $\dot{p} = -kq - cp/m$. In the physical (q, p) plane their divergence is $-c/m$. A small material phase-space area therefore contracts as $A(t) = A(0)e^{-ct/m}$. No time-independent canonical coordinate change on the same two-dimensional isolated phase space can turn that physical contraction into a Hamiltonian flow preserving area. This conclusion concerns the reduced dissipative description. An expanded system including the degrees of freedom that absorb energy can still be Hamiltonian.

For $c/m = 0.40\,\mathrm{s}^{-1}$, a pair of independent initial perturbations spanning area one in calibrated coordinates spans only 0.449 after two seconds. A numerical step of $0.10\,\mathrm{s}$ fitted to that exact map should have determinant $e^{-0.04} = 0.9608$. Forcing its determinant to one during system identification would remove a real dissipative measurement. Conversely a conservative oscillator propagated by forward Euler at matched units and $h = 0.10$ has amplification determinant $1 + h^2 = 1.01$, corresponding to a spurious area growth. A geometric diagnostic is interpretable only after deciding what physical system and coordinate pair were actually observed.

The pair q, v differs from canonical q, p by a constant mass scaling for an ordinary single particle. In one pair with constant mass that scaling does not change a measured same-coordinate before-and-after determinant. For a position-dependent mass, constrained coordinates with a varying metric, or explicit time-dependent changes of measurement scale, volume in raw position–velocity coordinates need not equal canonical volume. For example a free particle expressed in $Q = q^2$ has canonical momentum $P = m\dot{Q}/(4Q)$. A detector estimating phase area in $(Q, \dot{Q})$ without the Q-dependent factor can infer contraction or expansion even when canonical phase area is exactly conserved.

Compute a bracket of mechanical momenta and recover the Lorentz force

For a charge e in a prescribed vector potential write mechanical momentum $\boldsymbol{\pi} = \mathbf{p} - e\mathbf{A}(\mathbf{q}, t)$. The canonical brackets are $\{q_i, p_j\} = \delta_{ij}$, but the measured mechanical components satisfy

$$\{\pi_i, \pi_j\} = e(\partial_i A_j - \partial_j A_i) = e\epsilon_{ijk} B_k.$$

At nonzero magnetic field they are not simultaneously canonical momenta conjugate to the Cartesian positions. This result is gauge invariant because it involves only the curl of the vector potential. It offers a physical example where replacing canonical by measured momenta in a software interface changes the matrix of fundamental brackets.

With $H = \pi^2/(2m) + e\phi$, the time derivative is

$$\dot{\pi}_i = \{\pi_i, H\} + \partial_t \pi_i.$$

The kinetic-energy bracket contributes $(e/m)(\boldsymbol{\pi}\times\mathbf{B})_i$; the scalar potential contributes $-e\partial_i\phi$; and the explicit derivative supplies $-e\partial_t A_i$. Their sum is $e[\mathbf{E}+(\boldsymbol{\pi}/m)\times\mathbf{B}]_i$. Dropping the last term would make time-dependent electric acceleration depend on gauge. In a static uniform B_z, the transverse mechanical momenta rotate although their energy is constant. Canonical bracket structure therefore contains observable information about the force even before integrating a trajectory.

A useful finite-difference test sets $A_y = Bx$ and samples the map from canonical to mechanical variables around one state. The measured bracket $\{\pi_x,\pi_y\} = eB$ should be constant in space. A code that insists on zero will attribute the entire magnetic response to an erroneous Hamiltonian gradient. A code using mechanical variables legitimately can instead use their noncanonical bracket matrix; its equations must then preserve the correct transformed structure, not the original constant J. Testing the resulting acceleration at zero velocity and at a transverse velocity distinguishes electric and magnetic terms and catches sign errors in the antisymmetric entries.

Derive a reversible drift–kick–drift scheme and its measured phase

For $H = p^2/(2m) + V(q)$, exact kinetic flow for a duration t is $D_t : (q,p) \mapsto (q + tp/m, p)$. Exact potential flow is $K_t : (q,p) \mapsto (q, p - tV'(q))$. Each is canonical. Compose $D_{h/2}K_hD_{h/2}$ in chronological order. Applying the same construction with $-h$ undoes each substep in reverse order, so the full map is time reversible. Symmetry eliminates the even local-error powers in the effective generator, giving a second-order method for smooth V. The individual Hamiltonian pieces need not commute; if they did, the split map would be exact at any step.

For a unit oscillator, carrying out the algebra gives

$$Q = (1 - h^2/2)q + h(1 - h^2/4)p,$$

$$P = -hq + (1 - h^2/2)p.$$

Verify directly that the determinant is one. The trace gives the same step angle $2\arcsin(h/2)$ as the first-order kick–drift matrix in its stable range, but the new off-diagonal coefficients make the amplitude errors and time reversal different. Starting from $q = 1, p = 0$ at $h = 0.50$, one gets $Q = 0.875, P = -0.50$, energy 0.5078125. A negative step returns to the initial values apart from roundoff. Passing this one reversal test says nothing about absolute phase accumulated over hundreds of periods.

The map preserves $q^2 + (1 - h^2/4)p^2$ exactly for the harmonic test. At $h = 0.5$ the coefficient of p^2 is 0.9375, so the preserved ellipses differ slightly from the circles of physical energy. Their reversible oscillation in physical energy is bounded for $|h| < 2$. The per-step phase is about 0.50536 at this step, giving a phase gain 0.536 radians after one hundred steps. As h is halved while physical integration time stays fixed, the overall phase error falls approximately by four. Measuring an energy oscillation, a reversal residual and a return time therefore probes three different properties of one apparently simple map.

Compare a symplectic map with the phase of a physical orbit

Change the step of the midpoint update. Distinguish preservation of phase-space structure from agreement of the measured oscillation frequency.

Open this experiment online

Try the calculation

Time step h (ω = 1) **0.5**

Number of forward steps **20**

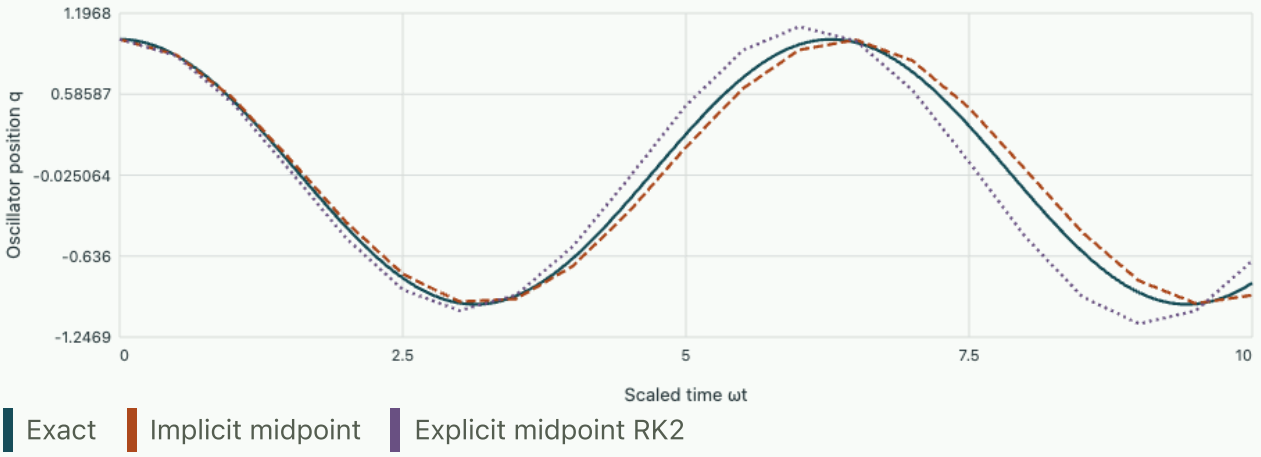

Implicit midpoint phase lag 0.2009 rad. Forward-backward distance from the start is 8.951e-16 for implicit midpoint and 0.3635 for explicit midpoint.

Relate the order of two pulses to their Poisson bracket

A canonical transformation close to identity can be built by applying two brief Hamiltonian operations in different orders. Take one free drift and one potential kick, each of short duration s. A drift then a kick gives

$$q' = q + sp/m,\ p' = p - sV'(q + sp/m).$$

A kick then a drift gives

$$p'' = p - sV'(q),\ q'' = q + s[p - sV'(q)]/m.$$

To second order their coordinate difference is $q' - q'' = s^2V'(q)/m$; their momentum difference is $p' - p'' = -s^2pV''(q)/m + O(s^3)$. The difference vector equals the Hamiltonian vector generated by $G = pV'(q)/m = \{V, T\}$, multiplied by s^2. The bracket sets the leading effect of reversing the operation order.

For the harmonic oscillator at $q = 1, p = 0, m = k = 1$ with $s = 0.10$, a drift then kick gives $(1, -0.10)$; kick then drift gives $(0.99, -0.10)$. The coordinate difference 0.01 equals $s^2 V'/m$, and the leading momentum difference is zero for this initial condition. At $q = 0, p = 1$, the complementary experiment gives a momentum difference of -0.01 and no coordinate difference. Running both initial states tests the two components of the bracket-generated perturbation. A single apparently correct coordinate update would not detect a sign swap in the other component.

An experimental implementation might use a short force pulse as a kick and free propagation between pulses. The pulse must be short enough that motion during the kick is negligible; otherwise its own kinetic drift enters the comparison at the same order as the desired bracket. Extrapolate the measured difference divided by s^2 to small s, and separately measure acquisition noise, which grows in relative importance under that division. Alternating the pulse order cancels many static calibration shifts but does not magically remove timing offsets correlated with the order. Treat the small bracket signal as a physical difference between two specified protocols.

A transformation preserves all coordinate–momentum brackets but a time integration on the transformed variables produces the wrong laboratory trajectory. Can the bracket check alone identify the error?

▼ **Work through the solution**

Canonical coordinates guarantee the form of Hamilton's equations. Their actual trajectories still require the correct transformed Hamiltonian, including explicit time dependence of the generating function, consistent initial momenta and a sufficiently accurate integrator. Transform an independently known initial state, compare the initial velocity and acceleration of a measurable coordinate, and follow both descriptions back to the same laboratory frame. A bracket test can establish that a change of variables is admissible without establishing that the correct energy function or physical input was attached to it.

Set compatible units before inspecting a symplectic residual

Suppose position is recorded in millimetres and momentum in kilogram metres per second. Scaling each numerical coordinate to unit variance is convenient for fitting a matrix, but independent scaling of each coordinate and momentum can change the bracket matrix from its textbook form. If $z' = Dz$ with diagonal D, then $J' = DJD^T$. For one pair this multiplies its bracket by the product of the position and momentum scale factors. In two pairs these factors can differ. A residual computed against the original J can flag a harmless unit change or, conversely, mask an error if scales happen to compensate.

Choose a characteristic length q_0, momentum p_0, and common action scale $q_0 p_0$ for each pair if the dimensionless chart is to have a common symplectic scale. Otherwise carry the transformed bracket explicitly through the test. With two oscillators of different physical units, a canonical nondimensionalisation may balance the dynamics better than using the same numerical length scale for both. Report the dimensional transformation along with any determinant or defect norm so another calculation can reconstruct which tangent vectors and measurement units were actually compared.

Tutorial on canonical tests

In two degrees of freedom try $Q_1 = q_1,\ Q_2 = q_2,\ P_1 = p_1 + \alpha q_2,\ P_2 = p_2$. Is this map canonical? What is the simplest modification that restores the condition?

▼ **Work through the solution**

The fundamental mixed momentum bracket is $\{P_1, P_2\} = \alpha$. Restore zero by also taking $P_2 = p_2 + \alpha q_1$, since then the extra term $\{p_1, \alpha q_1\} = -\alpha$ cancels. The added momentum vector is now the gradient of the scalar $\alpha q_1 q_2$, whose derivative matrix is symmetric. Both candidate maps preserve volume, reinforcing why volume alone cannot decide.

For the unit oscillator kick–drift map find a quadratic quantity it preserves exactly while its physical energy changes.

▼ **Work through the solution**

Direct substitution gives $Q^2 + P^2 - hQP = q^2 + p^2 - hqp$ for the kick–drift convention above. Multiplying by one half gives a positive modified quadratic invariant when $|h| < 2$. The first step at $h = 0.5$ gives $0.75^2 + (-0.50)^2 - 0.5(0.75)(-0.50) = 1.0$, equal to its initial value. At $h = 2$ the quadratic becomes degenerate and beyond it no longer bounds the motion.

A time-dependent momentum shift is generated by $F_2 = qP - a(t)q$. For a free physical particle find the transformed Hamiltonian and verify constant physical momentum.

▼ **Work through the solution**

The transformation gives

$$p = P - a,\ Q = q,$$
$$K = (P - a)^2/(2m) - \dot{a}\,Q.$$

Hamilton's equation gives $\dot{P} = +\dot{a}$, hence $\dot{p} = 0$. Omitting the explicit $\partial_t F_2$ term would predict constant P and a spurious acceleration of the original free particle. This test uses an observable whose physical behaviour is already fixed independently.

Compare generated canonical changes and numerical determinant tests.

David Tong develops canonical transformations and Poisson brackets in Hamiltonian dynamics.

Analytical mechanics from constraints to invariants · 9. Action, angle and the slowing clock at a separatrix

A phase portrait contains enough information to extract a period by differentiating an area. Use that fact to build a clock for finite-amplitude pendulum motion, determine precisely where slow-parameter invariance fails, and distinguish a librating trajectory from one that makes complete rotations.

Turn a closed phase-space loop into an action variable

For a one-degree-of-freedom Hamiltonian $H(q,p;\lambda)$ at fixed parameter λ, take a connected periodic orbit of energy E. Define its action by $J(E,\lambda)=(2\pi)^{-1}\oint p\,dq$, oriented along the actual motion. The units are energy times time. A smooth family of nested librating loops has $2\pi J$ equal to the enclosed canonical phase area. For circulation on a coordinate cylinder, such as an angle increasing through 2π, the integral still defines an action even though the loop winds around the cylinder. Its area interpretation and sign need a reference branch.

At fixed q,λ, differentiating $H(q,p(E,q))=E$ gives

$$\partial_E p = 1/H_p = 1/\dot{q}.$$

Differentiating the action integral yields $\partial_E J = T/(2\pi)$, because $dq/\dot{q}=dt$ around the orbit. At ordinary turning points $\dot{q}=0$, the derivative integrand has an integrable singularity while the two endpoints of the closed loop agree; one can justify the derivative using a local square-root coordinate. Inverting gives

$$\omega(J)=\partial_J E.$$

If θ is the angle conjugate to J, the transformed Hamiltonian is $E(J)$ and $\dot{\theta}=\omega(J)$ is constant. This canonical angle generally differs from the geometric angle reported by a camera.

For a unit-mass harmonic oscillator the energy curve $p^2+\omega_0^2q^2=2E$ is an ellipse. Its area is $2\pi E/\omega_0$, giving $J=E/\omega_0$ and a frequency independent of amplitude. One may take $q=\sqrt{2J/\omega_0}\sin\theta,\ p=\sqrt{2J\omega_0}\cos\theta$, whose bracket is one. The position turns nonuniformly in coordinate space even though the phase angle advances uniformly. Under a slow change in ω_0, constant J predicts $E\propto\omega_0$ and amplitude proportional to $1/\sqrt{\omega_0}$. Constant action does not mean constant mechanical energy while work is performed by a changing spring.

Integrate the finite-amplitude pendulum

Let $I=ml^2$, $\omega_0^2=g/l$, and measure q from downward vertical. The Hamiltonian $H=p^2/(2I)+I\omega_0^2(1-\cos q)$ has separatrix energy $E_s=2I\omega_0^2$. For a libration of turning angle $q_m<\pi$, define $k=\sin(q_m/2)=\sqrt{E/E_s}$. The positive momentum branch is $p=2I\omega_0\sqrt{k^2-\sin^2(q/2)}$. Set $\sin(q/2)=k\sin u$. Evaluating four quarter-arcs of the loop gives

$$J_{\mathrm{lib}} = \frac{8 I \omega_0}{\pi}\left[\mathsf{E}(k) - (1-k^2)\mathsf{K}(k)\right],$$

$$T_{\mathrm{lib}} = \frac{4}{\omega_0}\mathsf{K}(k).$$

Here $\mathsf{K}(k) = \int_0^{\pi/2} (1 - k^2 \sin^2 u)^{-1/2} du$ and $\mathsf{E}(k) = \int_0^{\pi/2} \sqrt{1 - k^2 \sin^2 u}\, du$. To verify the first formula after substitution, note that $k^2 \cos^2 u = (1 - k^2 \sin^2 u) - (1 - k^2)$. The transformed integral of $k^2 \cos^2 u / \sqrt{1 - k^2 \sin^2 u}$ splits exactly into the two quoted complete elliptic integrals. The period follows either by $dq/\dot{q}$ or by differentiating the action. That independent check is useful when numerical differentiation of noisy action estimates amplifies sampling errors.

At small k,

$$\mathsf{K} = (\pi/2)(1 + k^2/4 + \cdots),$$

$$T \approx (2\pi/\omega_0)(1 + q_m^2/16 + \cdots).$$

At $q_m = 60^\circ$, $k = 1/2$ and $\mathsf{K} \simeq 1.68575$, giving $T/T_{\mathrm{small}} = 1.0732$. A pendulum of length $1.00\,\mathrm{m}$ then has period about $2.153\,\mathrm{s}$, where the small-angle answer is $2.006\,\mathrm{s}$. Timing ten periods rather than one helps resolve the accumulated difference. Measuring the arc amplitude from a projected image requires a geometric correction if the swing plane is tilted relative to the camera.

Approach the saddle from either side

At the upright position $q = \pi$, the potential is maximal and the equilibrium is a hyperbolic saddle in phase space. Put $q = \pi + s$ with small s; the energy near the saddle is $H \simeq E_s + p^2/(2I) - I\omega_0^2 s^2/2$. For an orbit at $E_s - \Delta E$, the time spent in a fixed small neighbourhood includes an integral proportional to $\int ds / \sqrt{s^2 - 2\Delta E/(I\omega_0^2)}$. As ΔE decreases, this develops a logarithm. Equivalently $\mathsf{K}(k) \sim \ln[4/\sqrt{1-k^2}]$ as $k \to 1^-$. The separatrix encloses finite canonical area but its period is infinite. Hence $\partial_E J$ diverges although J itself remains finite.

On the positive rotation branch $E > E_s$, set $k_r = \sqrt{E_s/E} < 1$. A period is the time for q to increase through 2π, so there is only one positive branch of momentum in its action integral. Direct integration gives

$$J_{\mathrm{rot}} = (2/\pi)\sqrt{2IE}\,\mathsf{E}(k_r),$$

$$T_{\mathrm{rot}} = 4\sqrt{I/(2E)}\,\mathsf{K}(k_r).$$

At very high energy, the potential is a small modulation and these formulas approach free-rotor values $\sqrt{2IE}$ and $2\pi\sqrt{I/(2E)}$. At the separatrix the positive rotation action approaches $4I\omega_0/\pi$, half the limiting libration action $8I\omega_0/\pi$. The two actions count different closed paths on a cylinder. The factor two is a topological change in the cycle, not a discontinuous jump in the mechanical momentum at a point.

Test slow conservation against the actual orbit period

To treat slowly varying parameters, define instantaneous action–angle coordinates for each fixed λ. The generating function $W(q, J, \lambda)$ acquires explicit time dependence when $\lambda = \lambda(t)$, adding $\dot{\lambda}\,\partial_\lambda W$ to the transformed Hamiltonian. Its angle dependence produces an oscillating $\dot{J} = -\dot{\lambda}\,\partial_\theta \partial_\lambda W$. On a regular periodic orbit, the integral of an angle derivative over a cycle vanishes. If λ changes little during that cycle and there is no resonant complication, this cancellation explains why the action changes little on average. The requirement uses the actual orbit period at the chosen energy. Near a separatrix it cannot be justified merely by comparing a drive rate to the small-amplitude period.

Consider a parameter ramp lasting $20\,\mathrm{s}$ for the one-metre pendulum. Near the bottom this covers about ten periods. For $1 - E/E_s = 10^{-6}$, the asymptotic $\mathsf{K} \simeq \ln 4000 = 8.29$ gives a period of approximately $10.6\,\mathrm{s}$, so the same ramp spans less than two cycles. Even longer ramps fail the scale separation sufficiently close to the saddle. If a varying parameter changes the separatrix area until it meets the trajectory, continued use of a single analytic action branch is especially unreliable. A trajectory can pass into circulation or return to libration depending on its phase and the ramp history.

Compute an action without measuring momentum continuously

Suppose a camera tracks one-dimensional positions over one full cycle, and velocity estimates are noisy. For a known position-dependent potential and calibrated mass, an independent measurement of the turning energy allows phase-area integration without differentiating the camera trace. On a bound orbit $p_\pm(q) = \pm\sqrt{2m[E - V(q)]}$, so $J = \pi^{-1}\int_{q_-}^{q_+} \sqrt{2m[E - V(q)]}\,dq$. One needs a potential calibration, both turning positions and a common energy datum. An additive constant in the potential cancels when E is shifted by the same amount. An unrecognised dissipative force makes the inward and outward energy profiles different and invalidates the assumed single closed energy curve.

Take a particle in the potential $V(q) = a|q|$, $a > 0$, which can approximate opposed constant restoring forces away from a narrow central smoothing zone. Its turning displacements are $\pm E/a$. Integrate on the positive half and use symmetry to find

$$J = 4\sqrt{2m}E^{3/2}/(3\pi a).$$

Differentiating gives

$$T = 2\pi\,dJ/dE = 4\sqrt{2mE}/a.$$

The same period follows by constant acceleration: starting at rest at a positive turning point, the fall to the origin takes $\sqrt{2mE}/a$, one quarter period. Agreement across a nondifferentiable potential cusp is a useful check that the action calculation handles the turning boundaries rather than requiring sinusoidal motion.

For $m = 0.10\,\mathrm{kg}$, $a = 2.0\,\mathrm{N}$, and $E = 0.20\,\mathrm{J}$, the amplitude is $0.10\,\mathrm{m}$, action is $0.00849\,\mathrm{J\,s}$, and period is $0.400\,\mathrm{s}$. If the restoring strength a doubles slowly at fixed action, $E \propto a^{2/3}$ increases by $2^{2/3} = 1.59$, while the turning amplitude shrinks by $2^{-1/3} = 0.794$. A harmonic-oscillator action rule $J = E/\omega$ using

a single measured frequency would be incorrect here: the actual $E/\omega = ET/(2\pi)$ exceeds the action by a factor $3/2$. The equality found for a harmonic oscillator follows from its linear energy–action relation and need not generalise.

Separate the angle accumulated during a cycle from the action it encloses

In a slowly modulated oscillator an almost constant action can coexist with a measurable phase error. Consider $\ddot{q} + \omega(t)^2 q = 0$ with smooth positive ω. An approximate oscillation is $q = A(t)\cos\Phi(t)$. At leading order $\dot{\Phi} = \omega$. Cancelling the first-order sine term gives $2\dot{A}\omega + A\dot{\omega} = 0$, so $A\sqrt{\omega}$ is approximately constant. The amplitude law reproduces conservation of E/ω after averaging. The accumulated phase is $\int \omega(t)\,dt$, which can change by many radians during a slow parameter cycle even if the initial and final frequency and action agree.

For $\omega(t) = 10[1 + 0.10\sin(2\pi t/T_r)]\,\mathrm{s}^{-1}$ and $T_r = 20\,\mathrm{s}$, integration over one full ramp gives $200\,\mathrm{rad}$ of leading phase. The largest value of $|\dot{\omega}|/\omega^2$ is only a few 10^{-3}. To first order the final amplitude returns to its initial value, but the position at the end is set by a phase that is generally not an integer multiple of 2π. A calculation that expects to return to its initial point after the parameter cycle confuses action invariance with angle closure. A small constant frequency calibration error, integrated over a long ramp, can dominate the final phase error while producing little amplitude error.

A sudden frequency switch gives an instructive opposite limit with exact phase dependence. At fixed q, p, changing ω_1 instantly to ω_2 changes the action to $J_2 = p^2/(2m\omega_2) + m\omega_2 q^2/2$. Write the initial state at action J_1 using the harmonic angle. Then

$$J_2/J_1 = (\omega_1/\omega_2)\cos^2\theta + (\omega_2/\omega_1)\sin^2\theta.$$

For a frequency doubling, the ratio ranges from one half at a passage through the centre to two at a turning point. For a uniformly sampled ensemble the average ratio is 1.25, although the pre-switch and post-switch Hamiltonians are both perfectly integrable.

An experiment can therefore test slowness by preparing the same initial action at different phases and comparing the distribution of final actions. A broad phase-dependent distribution for a rapid switch narrows as the ramp becomes slow on a regular family of tori. Near a separatrix a slow external ramp can still yield a broad distribution because the orbital clock itself stalls. The size of the instantaneous energy, measured without phase and the final Hamiltonian, does not distinguish these mechanisms.

Resolve a separatrix in time without integrating arbitrarily close to the saddle

At exactly E_s, energy conservation gives $p = \pm 2I\omega_0\cos(q/2)$ on $-\pi < q < \pi$. Choose the increasing branch passing through $q = 0$ at $t = 0$. Separation of variables in $\dot{q} = 2\omega_0\cos(q/2)$ gives

$$\tan(\pi/4 + q/4) = e^{\omega_0 t}.$$

Therefore $q(t) = 4\arctan(e^{\omega_0 t}) - \pi$,

$$p(t) = 2I\omega_0 \operatorname{sech}(\omega_0 t).$$

This exact orbit approaches the upright saddle exponentially at both infinite endpoints. The two endpoints represent the same physical angle on the cylinder even though they differ by 2π on an unwrapped plot.

The separatrix momentum falls to one tenth of its maximum after $\omega_0 t = \operatorname{arcosh} 10 \approx 2.993$. At $\omega_0 = 3.13\,\mathrm{s^{-1}}$ that takes only $0.956\,\mathrm{s}$. Reaching one hundredth takes $\operatorname{arcosh} 100/\omega_0 \approx 1.69\,\mathrm{s}$. The logarithmic increase in time per retained significant digit explains why an apparently captured upright state can simply be a trajectory very close to the saddle. Measuring angular velocity as well as angular displacement makes the exponential approach easier to distinguish from a truly stationary upright solution.

The phase area enclosed by both separatrix branches can also be recovered directly. Integrating their difference gives

$$\int_{-\pi}^{\pi} 4I\omega_0 \cos(q/2)\,dq = 16I\omega_0.$$

Dividing by 2π yields the libration limit $8I\omega_0/\pi$ obtained using elliptic integrals. By contrast a trajectory winding once on the upper branch integrates only the upper momentum, giving half that value. Testing these two integrals on an unwrapped numerical phase trace can reveal a missing lower turning branch or a routine that silently wraps the angle before accumulating $p\,dq$.

Find a frequency directly from noisy orbital areas

Suppose a calibrated experiment measures the phase areas $A(E) = \oint p\,dq$ at several energies. With $J = A/(2\pi)$, the identity $dA/dE = T$ says that an area-versus-energy slope directly has units of time. Take three close energies $0.09, 0.10, 0.11\,\mathrm{J}$, with measured areas $0.180, 0.202, 0.225\,\mathrm{J\,s}$. A central difference gives $T \simeq (0.225 - 0.180)/0.020 = 2.25\,\mathrm{s}$ at the centre. If each area has an independent uncertainty $0.001\,\mathrm{J\,s}$, the propagated standard uncertainty of that difference is about $0.071\,\mathrm{s}$, before accounting for energy uncertainty and curvature of $A(E)$.

Decreasing the energy spacing would reduce smooth finite-difference bias but amplify the effect of those same area errors. A local fit over several energies can trade variance against the assumption of a smooth slope. Near a separatrix the actual slope varies rapidly, so a wide polynomial fit may smooth away precisely the period increase being sought. Compare with direct return times at selected energies, or fit the logarithmic form justified by the saddle expansion when the orbit is demonstrably in its asymptotic regime. A measured phase area can be highly accurate while an inferred frequency remains poorly constrained because it is a derivative.

A practical area estimate from ordered camera samples uses the polygon formula $\tfrac{1}{2}\sum_i (p_i + p_{i+1})(q_{i+1} - q_i)$, including the return to the initial point with a consistent sign. Very long time sampling can overrepresent the slow turn neighbourhood but need not corrupt a properly oriented

geometric line integral. It can make a uniform-clock finite difference of velocity near a turnaround noisy, however. If a dataset includes several cycles with dissipation, do not simply close the final state back to the beginning of the first cycle. Find individual return events, estimate the action per cycle and test whether its change is consistent with measured losses.

Construct the canonical angle on two sides of a turning point

For a bound one-dimensional potential take a reference crossing at the lower turning point and choose the increasing-q branch. A Hamilton–Jacobi generating integral is

$$W(q, J) = \int_{q_-}^{q} p(q', E(J))\, dq'.$$

Its angle is $\theta = \partial_J W = (dE/dJ) \int_{q_-}^{q} dq'/\dot{q}' = \omega t_{\mathrm{flight}}$ on that branch. At the upper turning point $\theta = \pi$ for a time-reversal-invariant kinetic-plus-potential Hamiltonian. On the return branch the same coordinate q must be assigned the complementary angle $2\pi - \theta_{\mathrm{outgoing}}(q)$, because its momentum has opposite sign. The coordinate alone is insufficient to reconstruct a unique phase.

For a harmonic oscillator beginning at its leftmost position a quarter-amplitude point is crossed at two different times. In coordinates $q = -A\cos\theta$ take $q = -A/2$. The increasing branch gives

$$\theta = \pi/3;$$

the returning branch gives $5\pi/3$. Their velocities have opposite signs. Using the principal arccosine for every time sample forces both branches onto the same interval and makes an apparently discontinuous phase that never completes a cycle. Measuring the sign of velocity or interpolating successive turning events restores the appropriate branch. Near a saddle, tiny velocities make this branch identification particularly sensitive to camera noise.

Once a reliable angle is available, the phase deviation from the uniform prediction $\theta(t_0) + \omega(t - t_0)$ becomes a useful diagnostic. A static potential with a wrongly calibrated shape can cause a phase error periodic in position even when its return time is fitted correctly. Dissipation usually changes the action as well, while a constant clock error causes a steadily accumulating phase drift. Compare the residual over several cycles at different amplitudes and plot it against reconstructed angle as well as laboratory time. These alternate plots test different physical explanations of the same timing mismatch.

Measure the area of a closed orbit

Inspect how deformation of a potential changes an energy contour. Compute its action before using it to infer an adiabatic frequency.

Open this experiment online

Try the calculation

Final to initial force ratio 2

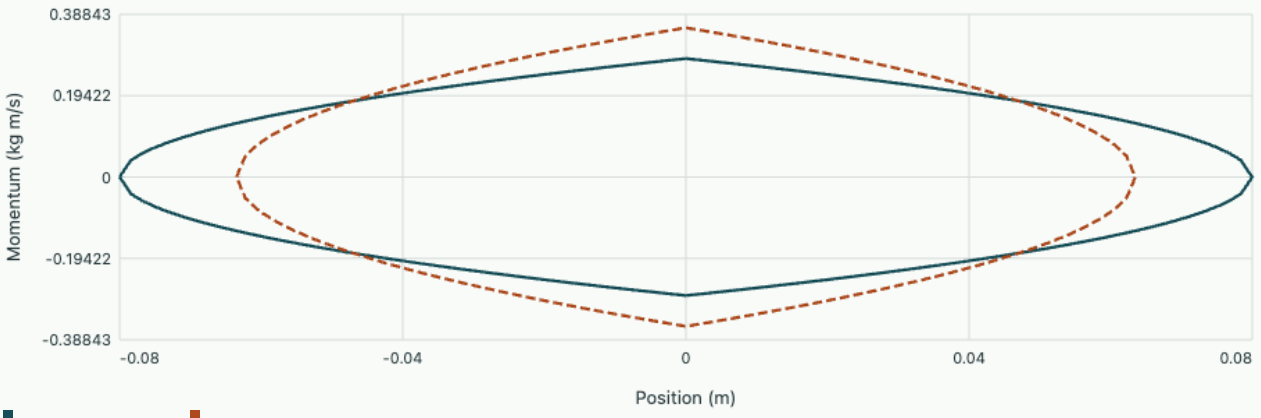

Final amplitude 0.0635 m, energy 0.254 J and period 0.3564 s.

Separate a true separatrix crossing from a change of angle convention

Imagine slowly reducing the pendulum's gravitational strength while a bob initially librates. The separatrix action $J_s = 8I\omega_0/\pi$ decreases with ω_0. Away from the crossing the orbit approximately maintains its own action, so its energy as a fraction of the instantaneous barrier rises. When the shrinking separatrix action reaches that of the orbit, no closed librating torus of that action remains. The system can enter one of the two circulation branches. Its action convention changes because the relevant closed curve on the cylinder now winds rather than traversing two momentum branches. An apparent numerical factor-of-two jump caused by this convention is distinct from the actual dynamics through the slow saddle neighbourhood.

For an initial libration action equal to 0.40 of the original separatrix action at fixed I, a parameter protocol reducing ω_0 to half its original value leaves J/J_s about 0.80, assuming adiabatic tracking remains valid. Reducing it to 0.30 of the initial value would formally give $J/J_s = 1.33$, impossible for a libration. The naive crossing estimate is $\omega_0 = 0.40\omega_{0,\mathrm{initial}}$, but the timing and selected rotation direction require integrating the actual trajectory near the saddle; the adiabatic argument loses uniform accuracy there. A local measure of p and unwrapped q supplies the physical distinction.

A real parameter protocol must specify how gravity strength changes. A pendulum length ramp changes both $I = ml^2$ and $\omega_0 = \sqrt{g/l}$, so its separatrix area scales as $I\omega_0 = m\sqrt{g}\,l^{3/2}$. Reducing length to 0.64 of its starting value reduces the separatrix action by $0.64^{3/2} = 0.512$, whereas replacing only ω_0 in a fixed-I model would predict the opposite trend. A literal change of length also brings radial kinetic energy and actuator work, as derived for the reelled pendulum. Specify the physical control path in parameter space before applying a numerical action law.

An unwrapped angle increases by 2π over a recorded interval but the phase portrait seems to contain a bounded loop. Can both observations be trusted simultaneously?

▼ **Work through the solution**

A true circulation winds around the cylindrical phase space, whereas a libration has zero net unwrapped displacement after a full return. A plot that wraps angles into a fixed interval and draws a line across its boundary can display an artificial closing segment. Conversely, measurement noise near $\pm\pi$ can make a naive unwrapping code insert a spurious 2π jump. Inspect signed momentum and the time-resolved crossing of the angle boundary, then reconstruct the loop in adjacent copies of the coordinate interval. Explicitly identifying the cycle on which the action was integrated resolves the apparent contradiction.

Infer work during an adiabatic change from a phase average

Differentiate the action integral at fixed energy with respect to the external parameter λ. The energy relation gives $\partial_\lambda p|_{E,q} = -H_\lambda/H_p$, so $J_\lambda|_E = -(2\pi)^{-1}\oint H_\lambda\,dt$. Combine this with $J_E = T/(2\pi)$ and differentiate at fixed J. The result is

$$\partial_\lambda E|_J = \langle \partial_\lambda H \rangle_{\text{time}}.$$

A slowly changed parameter therefore does net reversible work at the orbit-averaged rate dictated by its conjugate generalised force. The average must weight time, not distance along the plotted phase curve.

For a harmonic spring with stiffness k, $H_k = q^2/2$ and $\langle q^2\rangle = A^2/2 = E/k$, giving $\partial_k E|_J = E/(2k)$. Integrating yields $E \propto \sqrt{k}$, consistent with $J = E/\omega$. A 4% slow stiffness increase raises energy by about 1.98% exactly under this law. Changing stiffness at a single turning point would instead add 4% to the energy for that sudden change. The difference quantifies why observing only identical start and end stiffnesses does not identify the work protocol.

Tutorial on interpreting an action experiment

A harmonic oscillator has energy $0.030\,\mathrm{J}$ and frequency $5.0\,\mathrm{Hz}$. Its stiffness is increased slowly until the frequency doubles. Determine action, final energy and relative amplitude.

▼ **Work through the solution**

The action is

$$0.030/(2\pi\cdot 5.0) = 9.55\times10^{-4}\,\mathrm{J\,s}.$$

Approximately constant action gives a final energy of $0.060\,\mathrm{J}$. With fixed mass and $E = m\omega^2A^2/2$, the final amplitude is $1/\sqrt{2}$ times its initial value. A sudden change performed at a particular phase would in general give a different final action.

A simulation estimates pendulum periods by differentiating sampled action values on a coarse uniform energy grid. Why is the last estimated period below the separatrix likely to be inaccurate even if the individual areas are well converged?

▼ **Work through the solution**

A finite difference averages $dJ/dE = T/(2\pi)$ over a finite energy interval. The derivative rises logarithmically near the saddle, so the average can underestimate its endpoint value markedly. Refine adaptively in the distance to E_s, use the elliptic quadrature or measure return times directly. The numerical integrator must also locate the long dwell near the unstable equilibrium without stepping across it artificially.

Two trajectories have energy $E_s + \delta$, one rotating clockwise and one anticlockwise. Can energy and the positive magnitude of rotation action distinguish them?

▼ **Work through the solution**

Both have the same speed at each angle and the same positive action magnitude and period. The sign of momentum or a signed orientation of the fundamental rotational cycle distinguishes the branches. Near the separatrix a numerical classifier looking only at energy and unsigned area can lose track of this information. Count the unwrapped angular change and inspect the sign of p to identify circulation direction.

Measure phase area and compare its change under a parameter ramp.

David Tong develops action–angle variables and adiabatic invariance.

Analytical mechanics from constraints to invariants · 10. Canonical perturbations, small denominators and resonant capture

A weak periodic force can produce a bounded ripple on most trajectories and a large change on a narrow band of initial conditions. Derive the averaging transformation away from resonance, construct the slow resonant dynamics where that transformation fails, and estimate the physically observable width and time scale of a resonance.

Separate the unperturbed clock from a weak correction

Take an integrable Hamiltonian $H(I,\theta,t)=H_0(I)+\epsilon H_1(I,\theta,t)$ in action–angle variables. With $\epsilon=0$, actions are constants and angles advance at $\boldsymbol{\omega}(I)=\partial_I H_0$. A perturbation with Fourier component $h_{\mathbf{n}}(I)\cos(\mathbf{n}\cdot\theta-\Omega t)$ drives action changes proportional to its sine. If the phase sweeps quickly through all angles, positive and negative contributions largely cancel. If $\mathbf{n}\cdot\boldsymbol{\omega}-\Omega$ is small, the perturbation acts with a coherent sign over a long time. We want a transformation that makes both statements quantitative.

Use a near-identity type-two generating function $F_2(\theta,J,t)=\theta\cdot J+\epsilon S_1(\theta,J,t)$. Old actions are $I=J+\epsilon\partial_\theta S_1$, and new angles are $\psi=\theta+\epsilon\partial_J S_1$. Expand $H_0(I)=H_0(J)+\epsilon\boldsymbol{\omega}(J)\cdot\partial_\theta S_1+O(\epsilon^2)$. At first order the new Hamiltonian is $K=H_0(J)+\epsilon[H_1+\partial_t S_1+\boldsymbol{\omega}\cdot\partial_\theta S_1]$. Replacing old by new angles inside that bracket produces only higher-order errors. To leave the averaged part $\langle H_1\rangle$, solve the homological equation

$$(\partial_t+\boldsymbol{\omega}\cdot\partial_\theta)S_1=-\big(H_1-\langle H_1\rangle\big).$$

For an oscillating cosine with detuning $\Delta=\mathbf{n}\cdot\boldsymbol{\omega}-\Omega$, choose $S_1=-h_{\mathbf{n}}\sin(\mathbf{n}\cdot\theta-\Omega t)/\Delta$. The transformation is useful while the resulting action displacement $\epsilon|\partial_\theta S_1|$ is small on the relevant action scale and the derivatives entering the angle transformation remain controlled. Small ϵ alone is insufficient if Δ is even smaller. A singular denominator says that this choice to remove the harmonic is unsuitable, not that the underlying mechanical force becomes infinite.

Obtain a nonlinear frequency shift from the angle average

A free oscillator with mass m, small-amplitude frequency ω_0, and quartic correction $\beta q^4/4$ has unperturbed coordinates $q=\sqrt{2I/(m\omega_0)}\sin\theta$. Substituting gives the correction $\beta I^2\sin^4\theta/(m^2\omega_0^2)$. Since $\langle\sin^4\theta\rangle=3/8$, the first-order averaged Hamiltonian is $K=\omega_0 J+3\beta J^2/(8m^2\omega_0^2)$. Its derivative gives

$$\omega=\omega_0+3\beta J/(4m^2\omega_0^2).$$

Expressing $J\simeq m\omega_0 A^2/2$ in terms of leading oscillation amplitude yields the frequency shift $3\beta A^2/(8m\omega_0)$. Oscillatory harmonics at $2\theta,4\theta$ change the waveform but do not contribute directly to this averaged first-order clock.

For $m = 0.20\,\mathrm{kg}$, $\omega_0 = 10.0\,\mathrm{s}^{-1}$, $\beta = 80\,\mathrm{N/m^3}$, and $A = 0.10\,\mathrm{m}$, the predicted shift is $0.150\,\mathrm{s}^{-1}$, about 1.5%. The nonlinear-to-linear force ratio at maximum displacement is $\beta A^2/(m\omega_0^2) = 0.040$, consistent with the expansion. At twice the amplitude the shift quadruples and the expansion parameter grows to 0.16. Measuring period over several amplitudes and plotting the frequency against A^2 tests both the slope and the onset of curvature from higher orders. A positive β stiffens the spring; a negative quartic term is only a local approximation unless higher powers restore global confinement.

Solve the slow motion in the resonant frame

Consider a rotor $H = I^2/(2\mathcal{I}) - \epsilon V\cos(\theta - \Omega t)$, where $\mathcal{I}$ is moment of inertia and $\epsilon V > 0$ has energy units. Choose $F_2 = (\theta - \Omega t)P$, so $P = I$,

$$\phi = \theta - \Omega t,$$

$$K = P^2/(2\mathcal{I}) - \Omega P - \epsilon V\cos\phi.$$

Completing the square gives $K = (P - P_*)^2/(2\mathcal{I}) - \epsilon V\cos\phi + \text{constant}$ with $P_* = \mathcal{I}\Omega$. This is an exact pendulum in the rotating frame. It retains the resonant cosine instead of attempting to average it away. Phase locking means libration of ϕ around zero; outside its separatrix the relative phase circulates.

The stable fixed point has $P = P_*, \phi = 0$; its small libration frequency is

$$\omega_{\mathrm{lib}} = \sqrt{\epsilon V/\mathcal{I}}.$$

The saddle at $\phi = \pi$ has energy $+\epsilon V$ relative to the same constant. At $\phi = 0$ that energy is reached for $|P - P_*| = 2\sqrt{\mathcal{I}\epsilon V}$, the resonance half-width in action. Its complete width is twice that number. For $\mathcal{I} = 0.050\,\mathrm{kg\,m^2}$, $\Omega = 8.0\,\mathrm{s}^{-1}$ and $\epsilon V = 0.0020\,\mathrm{J}$, the central action is $0.40\,\mathrm{kg\,m^2/s}$; the half-width is $0.020\,\mathrm{kg\,m^2/s}$ and small libration period $31.4\,\mathrm{s}$. The rotor makes many laboratory turns while its slow relative phase completes one libration.

An initial action inside the quoted half-width is necessary but not sufficient for trapping at every phase. At $\phi = \pi$, any nonzero $P - P_*$ is above the saddle energy. Compute the actual rotating-frame energy of the initial state and compare with the saddle. For $\phi = 0, P = 0.415$, the kinetic detuning energy is $0.00225\,\mathrm{J}$; subtracting $0.0020\,\mathrm{J}$ gives $0.00025\,\mathrm{J}$, below the saddle. With the same action at $\phi = \pi$ the value is $0.00425\,\mathrm{J}$, above the saddle. Selecting trajectories by mean frequency alone can therefore mix trapped and circulating populations.

Retain a resonant harmonic in a general integrable system

For one action with $H_0'(I_*) = \Omega$, use the rotating frame and expand $H_0(I) - \Omega I$ about I_*. The linear term vanishes, leaving $H_0''(I_*)(I - I_*)^2/2$. Retain the slowly varying resonant cosine and average the rapidly varying harmonics. When $H_0'' \neq 0$, this gives the same pendulum normal form with an effective inertia and possibly a reversed sign of the stable phase. The action half-width scales as $2\sqrt{\epsilon|V/H_0''|}$. Thus a weak perturbation can influence a band of width proportional to $\sqrt{\epsilon}$, parametrically larger than a typical nonresonant action ripple proportional to ϵ.

For an exactly harmonic oscillator $H_0 = \omega_0 I$ the curvature vanishes. One cannot replace H_0'' with zero in the width formula. An exactly tuned additive drive in a linear oscillator instead produces secular growth until damping, detuning, nonlinearity or a finite drive interval intervenes. In multiple actions, one first transforms to the resonant phase $\mathbf{n} \cdot \theta - \Omega t$ and complementary angles, preserving the canonical one-form. Other near-resonances can prevent isolation of a single pendulum. Apparent chaos inferred from a short irregular time trace alone needs additional tests, including resolved phase portraits, convergence under time refinement and identification of competing resonances.

Calculate a phase-locking threshold for a drive that sweeps in frequency

The exact rotating rotor also allows a tractable time-dependent drive frequency. Write the pattern angle as $\alpha(t)$, with $\Omega(t) = \dot{\alpha}$. In its frame $K = P^2/(2\mathcal{I}) - \Omega(t) P - \epsilon V \cos\phi$. Hamilton's equations give

$$\dot{\phi} = P/\mathcal{I} - \Omega(t),$$

$$\dot{P} = -\epsilon V \sin\phi.$$

Define the detuning momentum $p = P - \mathcal{I}\Omega(t)$. Even when $\dot{\phi} = 0$ at one instant, phase locking throughout a ramp requires $\dot{p} = 0$ and hence $\sin\phi_0 = -\mathcal{I}\dot{\Omega}/(\epsilon V)$. The restoring torque must be sufficient to accelerate the rotor along with the changing pattern.

For constant $\dot{\Omega}$ and $|\mathcal{I}\dot{\Omega}| < \epsilon V$, a stable locked phase with $\cos\phi_0 > 0$ exists. Perturbing the phase by η gives $\ddot{\eta} + (\epsilon V/\mathcal{I})\cos\phi_0\, \eta = 0$, so the libration softens as the required torque approaches its maximum. At threshold the stable and unstable stationary phases meet. Above it no fixed phase can provide the torque needed by the ramp. The mere existence of a stable locked solution still does not imply that an arbitrary initial phase and momentum will be captured in it. In a conservative system initial phase-space location and separatrix crossing are essential.

With the previous $\mathcal{I} = 0.050\,\mathrm{kg\,m^2}$ and $\epsilon V = 0.0020\,\mathrm{J}$, the largest trackable constant acceleration in this model is $0.040\,\mathrm{rad/s^2}$. At half that value the stable phase lags by $\pi/6$, and the small relative-phase frequency is

$$0.20\sqrt{\cos(\pi/6)} = 0.186\,\mathrm{s^{-1}}.$$

Increasing the drive frequency by $1.0\,\mathrm{rad/s}$ at this rate takes $50\,\mathrm{s}$, only about one and a half libration periods. Adiabatic capture estimates that additionally require many libration periods may therefore be unconvincing even though the elementary torque threshold is satisfied. A measured lag versus sweep rate assesses the static torque condition, while a full phase trajectory tests dynamic capture.

The same equations admit a tilted effective washboard potential in the accelerating frame, $U_{\mathrm{rel}} = -\epsilon V\cos\phi + \mathcal{I}\dot{\Omega}\,\phi$, as long as $\dot{\Omega}$ is constant. Its potential difference over a whole 2π turn is nonzero, so unwrap the relative phase before using its energy. Mapping every phase back to $[-\pi, \pi)$ hides this difference and produces artificial jumps in the inferred energy. In the original variables the

physical motor does work. There is no contradiction between a conserved local accelerating-frame energy for a constant ramp and the changing laboratory kinetic energy of a locked rotor.

Derive secular energy exchange in a pair of weakly coupled oscillators

Take two equal masses m with individual natural frequency ω_0 and potential coupling $k_c(q_1 - q_2)^2/2$. The normal coordinates $Q_\pm = (q_1 \pm q_2)/\sqrt{2}$ have frequencies $\omega_+ = \omega_0$,

$$\omega_- = \sqrt{\omega_0^2 + 2k_c/m}.$$

Release mass one at displacement A with both velocities and q_2 initially zero. Superposition gives

$$q_1 = A[\cos\omega_+ t + \cos\omega_- t]/2,$$
$$q_2 = A[\cos\omega_+ t - \cos\omega_- t]/2.$$

The slowly varying difference phase transfers oscillation amplitude between the masses over a time much longer than their rapid periods.

For $\omega_0 = 10\,\mathrm{s}^{-1}$ and $k_c/m = 1.0\,\mathrm{s}^{-2}$, the exact separation is

$$\sqrt{102} - 10 = 0.0995\,\mathrm{s}^{-1}.$$

The first near-complete exchange occurs at $t = \pi/|\omega_- - \omega_+| \approx 31.6\,\mathrm{s}$. Over a single fast period the displacements can look almost like uncoupled oscillations, despite large later energy redistribution. Perturbing two isolated oscillators while trying to average the coupling over both independent fast angles would discard a term depending on their slow difference phase. Retaining the resonant combination predicts the exchange; diagonalising the linear model supplies a reference solution for that approximation.

Detune the uncoupled springs so their natural frequencies have a separation large compared with $k_c/(m\omega_0)$. The coupled normal modes then align more closely with the original oscillators, and the energy exchange cannot reach its former depth. In a nonlinear problem the individual frequencies also depend on action, so the energy transfer can detune itself. To interpret an observed beating envelope, measure both normal frequencies and relative phases. An apparent loss of amplitude in oscillator one can be energy stored in oscillator two, distinguishable from damping through recovery at later times and a balance of the total Hamiltonian.

Estimate the accuracy of averaging over a finite observation time

For a nonresonant perturbation with initially slow action change, one can integrate the first-order drive along the unperturbed trajectory over the actual observation window instead of assuming an infinite-time average. For $H_1 = A\cos(\theta - \Omega t)$, $\dot{I} = A\sin(\Delta t + \phi_0)$ to leading order with $\Delta = \omega_0 - \Omega$. Thus $\Delta I(T) = A[\cos\phi_0 - \cos(\Delta T + \phi_0)]/\Delta$. For $\Delta \neq 0$ its absolute value remains at most $2|A/\Delta|$, and

its largest possible value over initial phase is $2|A\sin(\Delta T/2)/\Delta|$. For $\Delta \to 0$ the phase-dependent result tends to $AT\sin\phi_0$. The finite-time expression is regular right at resonance and shows exactly when a secular term emerges.

For $A = 0.001\,\mathrm{J}$, $T = 10\,\mathrm{s}$ and $\Delta = 0.20\,\mathrm{s}^{-1}$, the maximum-amplitude change in action over initial phase is $0.00841\,\mathrm{J\,s}$. At zero detuning the leading largest change is $0.0100\,\mathrm{J\,s}$, only modestly larger because this observation window resolves a frequency band of order $1/T$. For $\Delta = 2\pi/T$ the change after exactly T vanishes, although the action swung during the interval. A final-minus-initial measurement alone can mistake a completed nonresonant excursion for an entirely unperturbed trajectory. Recording at an additional end time tests that cancellation.

At leading order a force of finite duration produces this sine-over-detuning envelope even in a linear system. It is an observation-time bandwidth, distinct from the dynamical resonance width proportional to $\sqrt{\epsilon}$ in the nonlinear rotor. Repeat the experiment with doubled drive duration at fixed amplitude. Features that narrow inversely with the duration are evidence of finite-time spectral selection. A persistent bounded island in a stroboscopic phase portrait, with the predicted amplitude-dependent width and libration frequency, is evidence of the phase-locking dynamics. If drive amplitude is large enough to change the natural frequency appreciably over the interval, the unperturbed phase-integration formula ceases to describe the trajectory.

Construct a stroboscopic section with the right clock

For a time-periodic Hamiltonian sample (I, θ) every period of the external drive at a fixed drive phase. This creates a two-dimensional area-preserving map for one periodically forced degree of freedom. A phase-locked solution can become a fixed point of this map, and librating trajectories around it can form an island. Sampling at each crossing of a moving coordinate threshold instead can produce a different return map and a different phase weight. A return plot can look irregular simply because the drive phase was not held fixed at the samples.

Consider a rigid rotor commanded at $\Omega = 8\,\mathrm{s}^{-1}$. Its drive period is

$$2\pi/8 = 0.7854\,\mathrm{s}.$$

An acquisition system sampling nominally every $0.7900\,\mathrm{s}$ accumulates approximately $8(0.7900 - 0.7854) = 0.0368\,\mathrm{rad}$ of phase error per sample. After one hundred samples the sampling phase has moved about $3.68\,\mathrm{rad}$, enough to smear a narrow island across a substantial fraction of the plot. Interpolating trajectories to timestamps from a synchronised drive encoder controls that effect. Keep unwrapped relative phase as a separate channel to count actual slips.

A numerical area test on the stroboscopic map should use canonical action and angle or an equivalent canonical coordinate pair. A scatter plot of polar angle against angular velocity for a state-dependent inertia can distort area. Changes of pixel density, trajectory dwell time and resolution near the separatrix further affect visual appearance. To identify a resonance quantitatively, measure the action extent at the stable phase, the local libration period and the saddle crossing energy on independently prepared trajectories. Agreement among those three observations is less easily mimicked by a sampling artefact than the existence of a visually closed loop alone.

Recover a frequency shift by removing a secular term

Canonical averaging yields a frequency correction for the quartic oscillator. An independent derivation makes clear why a small difference in frequency can become a large trajectory error at long times. Write the equation as $\ddot{q} + \omega_0^2 q + (\beta/m) q^3 = 0$. Put $q = Ax$, $\tau = \omega t$, $\lambda = \beta A^2/(m\omega_0^2)$ and seek $\omega = \omega_0(1 + c\lambda + \cdots)$,

$$x = x_0 + \lambda x_1 + \cdots .$$

Leading initial conditions $x(0) = 1, x'(0) = 0$ give

$$x_0 = \cos\tau .$$

At first order one finds

$$x_1'' + x_1 = 2c\cos\tau - \cos^3\tau .$$

Using $\cos^3\tau = (3\cos\tau + \cos 3\tau)/4$, the right-hand side contains a term $(2c - 3/4)\cos\tau$ resonant with the leading motion. Choosing $c = 3/8$ removes the forcing that would otherwise generate a term proportional to $\tau\sin\tau$. The frequency then agrees with the action-angle calculation. The remaining particular solution is $\cos 3\tau/32$. Including the homogeneous term required by $x_1(0) = x_1'(0) = 0$ gives

$$x_1 = (\cos 3\tau - \cos\tau)/32 .$$

This separates the leading frequency shift from an actual third-harmonic distortion of the orbit. Fitting only frequency and overlooking the small third harmonic cannot generally reproduce a precise waveform.

In the earlier example $\lambda = 0.040$, so the displacement amplitude at the third harmonic is $A\lambda/32 = 0.125\,\mathrm{mm}$ at $A = 0.10\,\mathrm{m}$. The frequency shift is about $0.15\,\mathrm{s}^{-1}$. After twenty seconds the uncorrected harmonic prediction is nearly three radians out of phase, far larger than the instantaneous third-harmonic displacement. A small-amplitude correction to the right-hand side can therefore cause an order-one error in the long-time phase. Measuring both the third harmonic and frequency gives two independent checks of the same inferred quartic stiffness. A drive electronics harmonic can mimic the former without producing the amplitude-dependent free-oscillation frequency.

Inspect growth on a parametrically driven orbit

Move the drive away from resonance and examine stroboscopic growth. Determine whether changing phase, amplitude or forcing frequency is responsible.

Open this experiment online

Try the calculation

Fractional stiffness modulation	0.08
Damping γ (1/s)	0.1
Drive frequency Ω (rad/s)	20

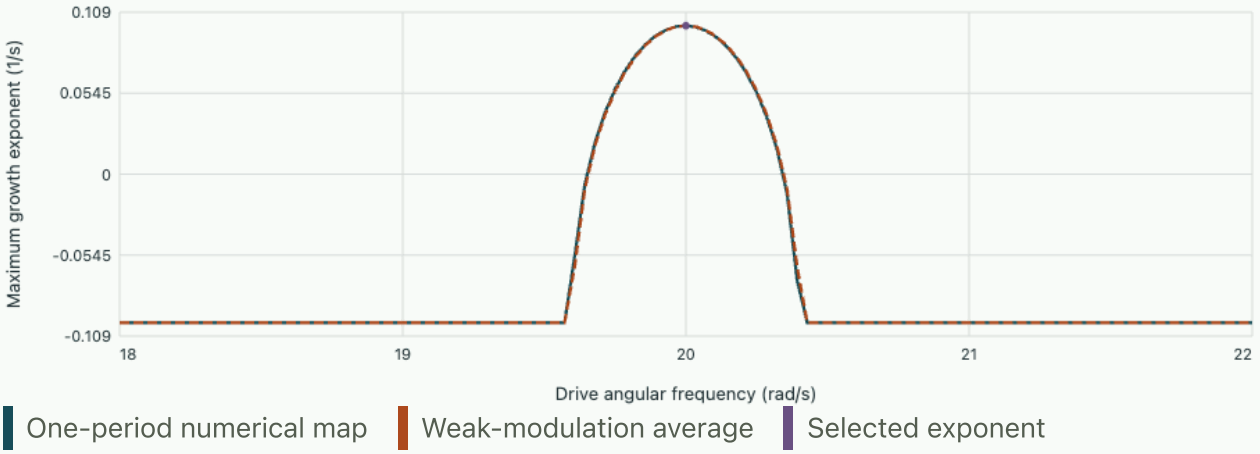

At Ω = 20 rad/s, numerical exponent 0.09997 s⁻¹ and averaged exponent 0.1 s⁻¹. Amplitude doubling time 6.934 s.

Test overlap of nearby resonances without declaring chaos from one curve

Take a rotor driven by two weak periodic patterns with distinct angular speeds Ω_1, Ω_2. For an isolated pattern j, the earlier calculation gives a resonant centre $P_j = \mathcal{I}\Omega_j$ and half-width $\Delta P_j = 2\sqrt{\mathcal{I}\epsilon V_j}$. Comparing the sum of estimated half-widths with the separation $|P_2 - P_1|$ is a practical indication of when the isolated-island approximation may fail. It does not by itself prove every trajectory between the resonances is chaotic. The relative phases, other harmonics and the actual time dependence determine the global structure.

For the same inertia $0.050\,\mathrm{kg\,m^2}$, choose $\Omega_1 = 8.0\,\mathrm{s^{-1}}$, $\Omega_2 = 8.6\,\mathrm{s^{-1}}$, and forcing energies 0.0020 and $0.00050\,\mathrm{J}$. The centres differ by $0.030\,\mathrm{kg\,m^2/s}$; the individual half-widths are 0.020 and $0.010\,\mathrm{kg\,m^2/s}$. Their nominal intervals just touch. Halving both forcing energies shrinks both widths by $1/\sqrt{2}$, leaving a gap. Doubling both makes the estimated intervals overlap. The speed difference corresponds to a beat period $2\pi/0.6 = 10.47\,\mathrm{s}$, another clock that must be resolved when recording nearby motion.

Transforming into the first rotating frame makes the first perturbation stationary and leaves the second with time dependence proportional to $\cos[\phi - (\Omega_2 - \Omega_1)t]$. A stroboscopic map sampled at the beat period is therefore more informative than a map with unsynchronised lab sampling. Prepare nearby initial conditions, compare their separation over multiple beat periods, and repeat with a refined symplectic time step and a modestly varied observation interval. Short-term stretching near an ordinary hyperbolic fixed point is possible even in a fully integrable pendulum. Evidence for widespread chaotic transport requires more than the growth of one separation during one saddle passage.

A student finds an apparent threshold by plotting whether the momentum ever crosses the midpoint between the two resonant centres. What additional evidence distinguishes irregular transport from a single large regular libration?

▼ **Work through the solution**

A regular libration may cross that midpoint repeatedly inside one island, especially near its separatrix. Plot return pairs at a fixed beat phase, check for closed invariant curves or broader area filling, and track unwrapped relative phase to see whether it slips irregularly between the two patterns. Vary initial conditions and compare the statistical trend with the isolated-width estimate. Confirm that energy balance in the driven system includes explicit work by both patterns; a drift of the autonomous single-pattern energy is expected once the second drive is present.

Use phase reversal to isolate the resonant action transfer

For an initially weak sinusoidal drive, prepare two otherwise identical trajectories with initial relative phases differing by π. Their leading changes of action during a short resonant pulse have opposite signs, since $\dot{I}$ is proportional to $\sin\phi_0$. Half the difference isolates that phase-sensitive term, whereas half the sum can reveal phase-independent heating or higher-order effects. With drive coefficient $A = 0.001\,\mathrm{J}$, duration $2.0\,\mathrm{s}$ and initial phases $\pm\pi/2$, short-pulse first-order predictions differ by $0.0040\,\mathrm{J\,s}$. The test requires that detuning and nonlinear phase drift over the pulse remain small.

Perform the comparison at several durations. A linear growth of the early phase-sensitive difference is compatible with coherent transfer. Subsequent saturation, reversal or a slow oscillation can reflect the resonant pendulum dynamics once the action shift changes the phase. Friction can also saturate a response, but it produces mechanical energy loss and typically modifies the two phase preparations in different ways from conservative trapping. Measuring work from the applied torque and the full phase history adds the independent information needed to separate those explanations. A final amplitude alone gives neither the sign of the action transfer nor its phase dependence.

Tutorial on weak forcing

Far from resonance let a one-mode perturbation be $A\cos(\theta - \Omega t)$ with $A = 0.001\,\mathrm{J}$ and detuning $0.50\,\mathrm{s}^{-1}$. What first-order ripple scale should appear in the old action?

▼ **Work through the solution**

The generating function has amplitude $A/|\Delta| = 0.002\,\mathrm{J\,s}$. For harmonic number one its angle derivative has the same amplitude, so the old action oscillates about the averaged action on that scale. At detuning $0.01\,\mathrm{s}^{-1}$ the nominal ripple would be fifty times larger. Check its size against the action scale and the change of detuning across the ripple before trusting that continuation.

In the rotor example the forcing energy is multiplied by four. What happens to the resonant action, action width and small-amplitude libration period?

▼ **Work through the solution**

The central action is set by $H_0' = \Omega$ and stays $0.40\,\mathrm{kg\,m^2/s}$. The half-width doubles to $0.040\,\mathrm{kg\,m^2/s}$. The libration frequency doubles, so the period halves to $15.7\,\mathrm{s}$. These predictions apply to the exact sinusoidal rotor model; other harmonics of a physical drive may also change as its amplitude increases.

A slowly swept drive seems to carry a phase-locked rotor beyond its original resonance band. Is this inconsistent with the static separatrix estimate?

▼ **Work through the solution**

A varying $\Omega(t)$ moves the resonance centre $\mathcal{I}\Omega(t)$. In coordinates measured from that moving centre the equation for detuning momentum has an additional torque-like term $-\mathcal{I}\dot{\Omega}$. Locking can persist if the available restoring torque can track the ramp and the initial motion stays inside the evolving island. The static width describes a fixed-frequency section. Comparing a captured trajectory to its initial centre after the sweep tests the wrong phase portrait.

Compare a resonance driven by a varying stiffness with a rotating additive potential.

David Tong's Hamiltonian course develops canonical variables and adiabatic invariants.

Analytical mechanics from constraints to invariants · 11. Action density, stress waves and the boundary that reflects them

A chain of coupled masses becomes an elastic field when the wavelength is long compared with the spacing. Derive the field equation and its boundary traction from the same variation, follow energy and stress across a junction, and decide whether a measured pulse is limited by material waves or by numerical dispersion.

Pass from a discrete rod to an action density

Let equal masses of spacing a move longitudinally by $u_j(t)$, with nearest-neighbour spring constant k_s and mass m_s per site. Their Lagrangian is $\sum_j [m_s \dot{u}_j^2/2 - k_s(u_{j+1}-u_j)^2/2]$. For variations smooth on the spacing, $(u_{j+1}-u_j)/a \to u_x$ and $\sum_j a\, f_j \to \int f(x)\,dx$. Hold the line density $\rho A = m_s/a$ and axial rigidity $EA = k_s a$ fixed. The continuum Lagrangian density per unit reference length is

$$\mathcal{L} = \rho A\, u_t^2/2 - EA\, u_x^2/2,$$

with A area, ρ volume density and E Young modulus. Both terms have units of joules per metre. This is a slender-rod model with small strain, primarily uniaxial stress and wavelengths long compared with the cross-sectional dimensions.

Vary the field in the action over $[0,L]\times[t_1,t_2]$. Integration of $\rho A\, u_t \delta u_t$ by parts in time, with fixed endpoint fields, produces $-\rho A\, u_{tt}\delta u$. Integration of $-EA u_x \delta u_x$ by parts in space produces $+\partial_x(EA u_x)\delta u$ and a remaining term $-[EA u_x \delta u]_0^L$. Thus the interior equation is $\rho A u_{tt} = \partial_x(EA u_x)$, and the end force conjugate to displacement is axial force $N = EA u_x$. Adding external work $F_L(t)\delta u(L)$ at the right face yields

$$N(L) = F_L.$$

A prescribed displacement instead imposes $\delta u(L)=0$, leaving its reaction as an output. Keeping this boundary term prevents prescribing displacement and independent traction simultaneously at the same end of a second-order rod.

Determine the energy flux and characteristic impedance

Assume time-independent coefficients. Multiply the field equation by u_t and rearrange to obtain

$$\partial_t[\rho A u_t^2/2 + EA u_x^2/2] + \partial_x[-EA u_x u_t] = 0.$$

The energy flux is $-N u_t$, with positive sign denoting energy moving towards increasing x. The minus sign follows the convention of positive tensile N: positive mechanical power entering through a right face is $N u_t$, which is inward with respect to the rod on its left. This identity controls energy transport across both smooth material changes and sharp joints.

For a homogeneous right-moving wave $u = F(x - ct)$, $c = \sqrt{E/\rho}$, particle velocity $v = u_t = -cF'$ and axial force $N = EAF' = -Zv$, where $Z = \rho A c = EA/c$. A left-moving wave has $N = +Zv$. The impedance is force divided by particle velocity and has units $\mathrm{kg/s}$. If one instead uses stress, impedance is ρc per unit area. Doubling the area of the same material keeps wave speed unchanged but doubles the force–velocity impedance. A transit-time measurement and a reflection measurement therefore provide independent material or geometry information.

For a rod with $E = 70\,\mathrm{GPa}$, $\rho = 2700\,\mathrm{kg/m^3}$ and $A = 1.0 \times 10^{-4}\,\mathrm{m^2}$, $c \approx 5092\,\mathrm{m/s}$ and $Z \approx 1375\,\mathrm{kg/s}$. A right-going compressive pulse with particle speed $0.020\,\mathrm{m/s}$ carries axial force $-27.5\,\mathrm{N}$, compressive stress $0.275\,\mathrm{MPa}$, and instantaneous power $Zv^2 = 0.550\,\mathrm{W}$ across a section. A rectangular approximation lasting $100\,\mu\mathrm{s}$ carries about $55\,\mu\mathrm{J}$ and occupies $0.509\,\mathrm{m}$. The pulse speed is kilometres per second; the material particles move only millimetres per second. Treating these as the same velocity would spoil force, impulse and energy estimates.

Match a bonded interface and distinguish amplitude from power

At a perfect massless bond displacement and axial force are continuous. For an incident right-going velocity amplitude v_i in rod 1, let v_r be reflected left-going velocity and v_t transmitted right-going velocity. Velocity continuity gives

$$v_i + v_r = v_t.$$

Force continuity gives

$$-Z_1 v_i + Z_1 v_r = -Z_2 v_t.$$

Thus

$$r_v = \frac{Z_1 - Z_2}{Z_1 + Z_2},$$

$$t_v = \frac{2Z_1}{Z_1 + Z_2},$$

$$\mathcal{R} = r_v^2,$$

$$\mathcal{T} = \frac{Z_2}{Z_1} t_v^2 = \frac{4Z_1 Z_2}{(Z_1 + Z_2)^2}.$$

The power fractions add to one for real positive impedances. The reflected force coefficient has opposite sign to the reflected velocity coefficient because the wave direction reverses. At a free end $Z_2 \to 0$, reflected velocity equals incident velocity, so end velocity doubles while total force vanishes. At a rigid end $Z_2 \to \infty$, velocity reverses and force doubles. The sign a strain gauge reports can therefore differ from that of a velocity-sensitive optical measurement at the same reflection.

A step from the worked rod into one of the same material with twice the cross-sectional area gives $Z_2 = 2Z_1$, $r_v = -1/3$, $t_v = 2/3$, and power fractions $1/9$ and $8/9$. A reduced transmitted velocity amplitude does not imply that most energy is reflected. If the interface includes a concentrated mass M_b

, force jumps instead obey $N_2 - N_1 = M_b \dot{v}_b$ with signs determined by forces exerted on that mass from either side. At high frequency the reaction of that mass can mimic a much stiffer termination. Frequency-dependent reflection is then an expected boundary effect, rather than evidence that the bulk modulus varies with frequency.

Connect continuum modes to their lattice predecessor

For a periodic chain the exact discrete equation is

$$m_s \ddot{u}_j = k_s(u_{j+1} - 2u_j + u_{j-1}).$$

Substitute $u_j = U e^{i(kja - \omega t)}$ to obtain

$$\omega = 2\sqrt{k_s/m_s}\,|\sin(ka/2)|.$$

In the first positive Brillouin zone, $\omega/(ck) = \sin(ka/2)/(ka/2)$ and group velocity $d\omega/dk = c\cos(ka/2)$, where $c = a\sqrt{k_s/m_s}$. The continuum rod retains only the leading low-ka term. A wave with eight sites per wavelength has phase speed about $0.9745c$ and group speed $0.9239c$. A narrowband packet's peak can arrive later than the continuum prediction even when a single crest is timed fairly accurately.

A finite-difference code approximating the continuum rod can produce the same spatial dispersion with its mesh spacing in place of a physical lattice spacing. Distinguish them experimentally or numerically by changing the computational mesh while holding the physical structure fixed. Lattice effects persist as the numerical grid is refined; artificial spatial dispersion diminishes. A separate time-step study is needed if a time integrator also disperses the wave. Comparing both peak arrival and phase at two frequencies tests more of the dynamics than fitting a single transit time.

Derive transverse beam waves from curvature energy

A slender beam bending laterally is governed by a different elastic energy from the axial rod. Let $w(x,t)$ denote small transverse deflection of its neutral axis. Under the Euler–Bernoulli assumption that cross sections remain plane and normal to that axis, the axial strain a distance z from the neutral axis is approximately $-z w_{xx}$. Integrating the local elastic energy $E\epsilon_{xx}^2/2$ across the section gives $EI_A w_{xx}^2/2$ per unit length, where $I_A = \int z^2\,dA$ is a geometrical second moment of area, with units m^4. It is distinct from a mass moment of inertia. The kinetic contribution uses line density ρA as before.

Varying $\mathcal{L} = \rho A w_t^2/2 - EI_A w_{xx}^2/2$ requires integrating twice by parts in space. With constant coefficients the interior variation gives

$$\rho A w_{tt} + EI_A w_{xxxx} = 0.$$

The boundary terms are $-[EI_A w_{xx}\delta w_x] + [(EI_A w_{xx})_x \delta w]$. Thus slope variations pair with bending moments and displacement variations with shear forces, with signs set by the chosen face orientation. A

clamped end prescribes both deflection and slope; a free end sets moment and shear to zero. A simply supported end prescribes deflection and zero bending moment. Using only one boundary condition per end, as for the axial rod, leaves the fourth-order beam problem underdetermined.

A sinusoid $e^{i(kx-\omega t)}$ gives

$$\omega = \sqrt{EI_A/(\rho A)}\, k^2.$$

Phase speed grows proportionally to wavenumber and group speed is twice phase speed in this model. A narrow transverse pulse in a long beam consequently spreads even in a perfectly homogeneous non-dissipative continuum. By contrast the axial rod was nondispersive in its long-wavelength continuum approximation. At high enough frequency the simple bending model omits rotary inertia, shear deformation and eventually three-dimensional elastic behaviour. Extrapolating its unbounded speed to arbitrary k would use the slender, low-frequency approximation far beyond its derivation.

For a simply supported beam with length L, the sine modes satisfy both end conditions and give

$$\omega_n = (n\pi/L)^2 \sqrt{EI_A/(\rho A)}.$$

For a rectangular section of width w_b and thickness d in the bending direction, $I_A = w_b d^3/12$ and $A = w_b d$. Doubling thickness doubles all the natural angular frequencies at fixed L, E, ρ, whereas doubling width alone leaves the ideal frequencies unchanged. The stiffness increases and so does the inertia. A beam with $L = 0.50\,\mathrm{m}$, $d = 5.0\,\mathrm{mm}$ and the earlier aluminium properties has $\sqrt{EI_A/(\rho A)} \approx 7.35\,\mathrm{m^2/s}$, giving fundamental $46.2\,\mathrm{Hz}$. The second bending mode is near four times that frequency, a clear difference from the approximately harmonic axial mode sequence.

Match a force pulse to a support spring and dashpot

A right termination exerts force on the rod through a dashpot with mechanical impedance Z_L. For a real positive dashpot impedance the reflected velocity fraction is $r = (Z - Z_L)/(Z + Z_L)$. Taking $Z_L = Z$ gives zero reflection at the termination even though energy leaves a finite rod: the dashpot dissipates the arriving power. With $Z_L = 3Z$ one obtains a reflected velocity of $-1/2$ of the incident value, a reflected energy fraction one quarter and absorbed power fraction three quarters. A free or rigid end also reflects energy, but it absorbs no net power in the ideal limit. A measured weak reflection alone is therefore not proof of weak damping inside the rod.

For a pure end spring of stiffness k_L attached to a rigid support, the velocity impedance is $Z_L = k_L/(i\omega)$ under $e^{i\omega t}$. It is imaginary, so the reflection coefficient has unit magnitude at every frequency and a frequency-dependent phase. At low frequency the spring impedance is large and the end looks nearly fixed. At high frequency its impedance is small and the end looks nearly free within the lumped approximation. An impulsive signal contains many frequencies and can return with a changed waveform even without any transmitted or dissipated energy. A support combining a resistor-like dashpot and a spring gives both amplitude loss and phase variation.

A measurement with strain gauges at two positions can separate forward and backward waves if their path delays are resolved. In a narrow frequency band the two records are linear combinations of advancing and returning phase factors. If the gauge spacing corresponds to an integer number of half wavelengths, these combinations become linearly dependent and the separation is ill-conditioned. Change the spacing, use a broadband pulse, or combine a velocity measurement with a strain measurement at one station so that the two characteristic directions enter with opposite signs. The relation $v = (v_+ + v_-)$, $N = Z(-v_+ + v_-)$ then gives a direct local decomposition.

Derive sound propagation from mass and momentum conservation

The displacement-action argument has a fluid analogue. Take an initially uniform fluid of density ρ_0 and pressure p_0, moving little from equilibrium in one spatial dimension. Write small perturbations ρ', p', v. Linearised mass conservation is

$$\partial_t \rho' + \rho_0 \partial_x v = 0.$$

Momentum balance for a short fluid parcel is $\rho_0 \partial_t v = -\partial_x p'$. If compression over an acoustic cycle is approximately isentropic, $p' = c_s^2 \rho'$ with $c_s^2 = (\partial p/\partial \rho)_s$. Differentiate the first equation in time, eliminate the velocity derivative with momentum balance, and obtain $\partial_t^2 p' = c_s^2 \partial_x^2 p'$.

The thermodynamic derivative matters because pressure can respond differently when compression is slow enough for heat exchange. For a perfect gas with ratio of specific heats γ, isentropic perturbations give

$$c_s^2 = \gamma p_0 / \rho_0.$$

Taking an isothermal derivative would give p_0/ρ_0 instead. For $p_0 = 101\,\mathrm{kPa}$, $\rho_0 = 1.20\,\mathrm{kg/m^3}$, and $\gamma = 1.40$, the isentropic speed is about $343\,\mathrm{m/s}$, while the isothermal calculation gives $290\,\mathrm{m/s}$. A measured transit time can discriminate between these constitutive conditions. Wall heat exchange in a very narrow tube can alter which approximation is appropriate over a chosen frequency band.

For a right-moving sound wave $p' = \rho_0 c_s v$, with the pressure positive in compression. This differs in sign from the tensile-positive axial force used for the rod, so match physical force conventions before borrowing formulas across the two examples. The acoustic power per area is $p' v$. For sinusoidal pressure with rms amplitude $1.0\,\mathrm{Pa}$ in the stated gas, the mean intensity is

$$p_{\mathrm{rms}}^2 / (\rho_0 c_s) = 2.43 \times 10^{-3}\,\mathrm{W/m^2}.$$

A peak amplitude of $1.0\,\mathrm{Pa}$ would yield half this number. Writing rms or peak explicitly prevents a routine factor-of-two error when comparing a microphone measurement with an energy flux.

Determine whether a measured transit reveals a modulus or a

geometry

Suppose two axially loaded slender rods have measured wave speeds agreeing within their uncertainties. That alone determines only the ratio E/ρ under the slender-rod assumptions. Measuring force–velocity impedance $Z = \rho A c$ and cross section as well gives $\rho = Z/(Ac)$ and $E = Zc/A$. With $Z = 1375\,\mathrm{kg/s}$, $c = 5092\,\mathrm{m/s}$ and $A = 1.0 \times 10^{-4}\,\mathrm{m^2}$, the inversion gives

$$\rho = 2700\,\mathrm{kg/m^3},$$

$$E = 70.0\,\mathrm{GPa}.$$

If area were overestimated by five percent, both inferred quantities would be underestimated by almost five percent while their ratio remained correct.

Now examine a thick elastic solid under a narrow compressional disturbance with wavelengths short compared with its transverse dimensions. Lateral deformation can be constrained by surrounding material. In an isotropic three-dimensional continuum the longitudinal plane-wave modulus is $\lambda + 2\mu_s$, where λ, μ_s are Lamé coefficients, rather than the uniaxial-stress Young modulus of a slender rod. The shear-wave speed satisfies $c_T^2 = \mu_s/\rho$ and longitudinal speed $c_L^2 = (\lambda + 2\mu_s)/\rho$. Measuring both, together with density, can recover the two independent elastic moduli. Using only one longitudinal speed to infer Young modulus without specifying the deformation geometry can give a physically incorrect value.

For $\rho = 2500\,\mathrm{kg/m^3}$, $c_L = 5000\,\mathrm{m/s}$ and $c_T = 3000\,\mathrm{m/s}$, these relations give

$$\mu_s = 22.5\,\mathrm{GPa},$$

$$\lambda = 17.5\,\mathrm{GPa}.$$

The implied Young modulus $E = \mu_s(3\lambda + 2\mu_s)/(\lambda + \mu_s) = 54.8\,\mathrm{GPa}$, while $\rho c_L^2 = 62.5\,\mathrm{GPa}$. Both numbers represent material stiffness, but they enter different mechanical boundary conditions. A long thin specimen of the same material should have an axial speed closer to $\sqrt{E/\rho} = 4680\,\mathrm{m/s}$. Comparing the bulk and rod experiments tests the constitutive and geometrical assumptions behind the measured speed.

Derive orthogonality when a rod changes material along its length

For a rod with positive varying density $\rho(x)$, area $A(x)$ and modulus $E(x)$, a separated free oscillation $u(x,t) = \phi(x)\cos \omega t$ satisfies

$$-[EA\phi']' = \omega^2 \rho A \phi.$$

Suppose two modes ϕ_n, ϕ_m satisfy the same homogeneous fixed or free boundary conditions and the correct continuity of displacement and axial force across every perfectly bonded interface. Multiply the first equation by ϕ_m, the second by ϕ_n, subtract and integrate. Interior terms produced by integration by parts cancel pairwise, including the interface flux terms, and the endpoint terms vanish. Thus

$$(\omega_n^2 - \omega_m^2) \int \rho A \phi_n \phi_m \, dx = 0.$$

Mode shapes with distinct frequencies are orthogonal under the mass-weighted inner product, not generally under a simple average of displacements measured at uniformly spaced stations. An initial velocity distribution $v_0(x)$ projects onto mode n with coefficient $\int \rho A v_0 \phi_n \, dx / \int \rho A \phi_n^2 \, dx$. In a rod with a heavy section, the same imposed velocity there stores more energy and carries more modal weight. An experiment interpreting raw camera amplitudes without line-density weighting can misassign energy among modes. Normalising each measured mode shape to unit maximum does not fix the mass weighting needed for energies.

Multiplying one eigenvalue equation by its own shape gives

$$\omega_n^2 = \int EA(\phi_n')^2 dx / \int \rho A \phi_n^2 dx.$$

For an admissible trial function satisfying prescribed displacement conditions, the same quotient bounds the fundamental squared frequency from above when rigid translations are excluded. Consider a uniform fixed–free rod and trial $\phi = x/L$. The numerator is EA/L and denominator $\rho A L/3$, giving $\omega_{\mathrm{trial}} = \sqrt{3}\, c/L$. The exact fundamental is $\pi c/(2L)$, so this one-parameter shape overestimates frequency by about 10.3%. It need not satisfy the free-end traction condition itself because that is a natural condition of the variational minimiser; it does need to satisfy the essential fixed-end displacement.

For a free–free rod the constant displacement mode has zero frequency. Using an arbitrary positive trial function without removing its mass-weighted mean can drive a quotient towards zero by adding a large constant. To estimate the first deforming mode impose orthogonality to the rigid translation, $\int \rho A \phi \, dx = 0$. This has an immediate mechanical interpretation: the deformation mode should not translate the centre of mass of an isolated rod. The null mode and its mass-weighted constraint reappear in numerical eigenproblems built from discretised stiffness and mass matrices.

Find where a discrete elastic chain ceases to look continuous

Shorten the wavelength relative to the lattice spacing. Compare the phase and group velocities with those inferred from a continuum action.

Open this experiment online

Try the calculation

Sites per wavelength 10

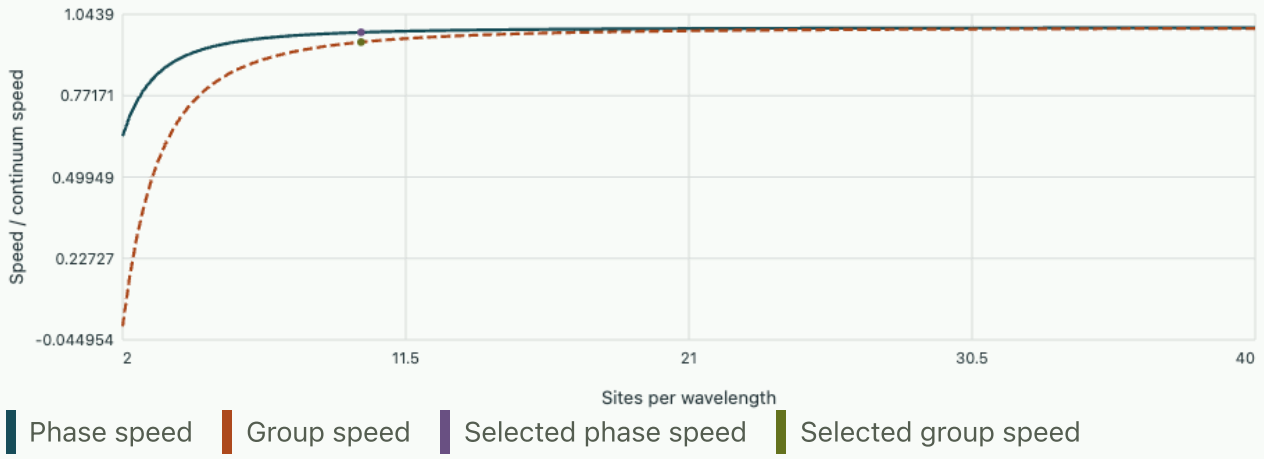

Frequency and phase speed are 98.36% of the continuum prediction. Group speed is 95.11%.

Track work and impulse in a one-dimensional pulse experiment

A finite displacement pulse provides a useful warning about integrating strain and velocity records. A right-going strain pulse of one sign can carry net momentum $\int \rho A v \, dx$. Because $v = -c u_x$, its integrated material momentum is $-\rho A c[u(+\infty) - u(-\infty)]$ at a fixed time. A localised displacement bump that returns to the same displacement on both sides has zero net ordinary material momentum, even though its energy is positive and travels to the right. Its strain and particle-velocity records contain positive and negative parts. A unipolar velocity pulse leaves behind a displacement step, produced by a source that has supplied net impulse.

For a right-moving rectangular velocity pulse of amplitude $0.020\,\mathrm{m/s}$, duration $100\,\mu\mathrm{s}$ in the worked rod, the local displacement jump measured in time is $2.0\,\mu\mathrm{m}$. Its impulse magnitude across a section is $Z v \Delta t = 2.75 \times 10^{-3}\,\mathrm{N\,s}$, while its transmitted energy is

$$Z v^2 \Delta t = 55.0\,\mu\mathrm{J}.$$

A second equal pulse of opposite velocity sign launched later cancels the net displacement and material momentum but doubles the transmitted energy. Thus integrating a signed velocity signal and integrating its square distinguish different properties of the same experimental record.

A displacement sensor has a small linear drift during a burst. Which inferred observables are particularly sensitive?

▼ **Work through the solution**

Differentiating adds a constant offset to particle velocity. Integrating that apparent velocity over a long window produces a growing spurious displacement jump and momentum estimate. Squaring it adds both

a cross term with the physical velocity and a positive baseline energy. Measure a pre-pulse baseline, choose an integration interval covering the physical pulse, and test that the result is stable when the window is moderately extended. An independent strain gauge gives another characteristic combination; comparison with $N = -Zv$ can expose drift or an overlapping reflection.

Can a finite-element rod model with a plausible first eigenfrequency still fail an impulse test?

▼ Work through the solution

The first frequency mostly probes a long-wavelength weighted stiffness-to-mass ratio. A brief pulse contains higher modes and is sensitive to temporal resolution, dispersion, boundary tractions and the way discrete source work enters. Verify modal frequencies at several wavelengths, check the pulse's positive energy and signed impulse separately, and compare the measured incoming and reflected characteristic fluxes. A single standing-wave eigenvalue cannot validate all of those physically independent balances.

Recover a jump condition at an interface with a point mass

For a concentrated mass M_b joining two rods include $M_b u_t(x_b)^2/2$ as a separate contribution to the Lagrangian. Its time variation contributes $-M_b u_{tt}\delta u$ at the joint. The left and right rod boundary terms contribute respectively $-N_1\delta u$ and $+N_2\delta u$. Requiring stationarity for an independently varying shared displacement gives exactly $N_2 - N_1 = M_b u_{tt}$. This derivation identifies both the sign and the constitutive assumption of a perfectly bonded, nonslipping joint.

For identical rods and a sinusoidal drive at angular frequency ω, the reflected velocity coefficient becomes $r = -i\omega M_b/(2Z + i\omega M_b)$ under the stated phasor convention. At $\omega M_b = 2Z$ it reflects half the power and transmits half. The mass itself absorbs no cycle-averaged energy, though it stores kinetic energy during a cycle. For $Z = 100\,\mathrm{kg/s}$ and $M_b = 0.10\,\mathrm{kg}$, the equal-power frequency is about $318\,\mathrm{Hz}$. A real joint that loses appreciable power at that frequency needs a damping or radiation term in addition to its measured mass.

Tutorial on stress waves

A gauge $0.80\,\mathrm{m}$ from a free end records the echo of a sharp disturbance in the worked rod. What echo delay and strain sign should it expect?

▼ Work through the solution

The extra path from gauge to end and back is $1.60\,\mathrm{m}$, giving $1.60/5092 = 0.314\,\mathrm{ms}$. A free end has zero net axial force, so the reflected force and strain have opposite signs to the incident ones. The velocity reflection keeps its sign. Finite pulse width and any change of material between gauge and end can obscure that simple result.

A bonded step has measured reflected velocity coefficient -0.20 and no detectable dissipation. Infer its impedance ratio and transmitted energy fraction.

▼ **Work through the solution**

Rearranging $r_v = (1 - r)/(1 + r)$ gives

$$r = Z_2/Z_1 = (1 - r_v)/(1 + r_v) = 1.50.$$

The energy reflection is 0.04 and transmission 0.96. The velocity transmission is 0.80, whose square alone is only 0.64. Multiplying by the transmitted-to-incident impedance ratio recovers the correct energy fraction.

A rod model with a prescribed displacement at its right end reports nonzero work there, even though the variational boundary term vanished in deriving its equation. Is there a contradiction?

▼ **Work through the solution**

Vanishing of $N\delta u$ follows because the allowed virtual displacement at a prescribed boundary is zero. Actual boundary velocity can be nonzero when the prescribed displacement varies in time. The actuator supplies power Nu_t at the right boundary. Compare the time-integrated input with the change of stored energy plus any losses or outgoing energy rather than identifying an admissible variation with actual displacement.

Compare a finite chain with its long-wavelength continuum.

Fließbach includes string vibrations, beam bending and sound in his continuum mechanics treatment.

Analytical mechanics from constraints to invariants · 12. Relativistic collisions, centre-of-momentum energy and thresholds

Two particles with the same total laboratory energy can have very different energy available for changing their internal state. Determine the energy and motion of the centre-of-momentum system, reconstruct two-body elastic scattering, and follow how a detector threshold transforms between frames.

Form the conserved total four-momentum

For a particle with rest mass m, energy E and momentum $\mathbf{p}$, write $p^\mu = (E/c, \mathbf{p})$ with metric signature $+---$. The on-shell condition $E^2 - c^2 p^2 = m^2 c^4$ holds for each freely propagating particle. In an isolated collision sum the incoming four-momenta and equate them to the outgoing sum. A frame-independent measure of the total is $s = (E_1 + E_2)^2 - c^2 |\mathbf{p}_1 + \mathbf{p}_2|^2$, defined here with units of energy squared. Some books assign momentum-squared units to s instead; stating this convention fixes all factors of c. The centre-of-momentum energy is $\sqrt{s}$.

A boost along the total momentum brings it to zero if the total four-vector is timelike. Its velocity is $\mathbf{V}_{\mathrm{cm}} = c^2(\mathbf{p}_1 + \mathbf{p}_2)/(E_1 + E_2)$. Individual particles can approach the speed of light while this frame is slow or even stationary in the laboratory when their momenta cancel. A pair of perfectly parallel massless rays gives a null total and has no rest frame. For massive particles the positive total rest energy generally ensures a timelike total. Knowing $\sqrt{s}$ determines the internal energy available, while $\mathbf{V}_{\mathrm{cm}}$ determines how the final directions and energies are seen by a laboratory camera.

Expand the square using the two on-shell conditions to obtain

$$s = m_1^2 c^4 + m_2^2 c^4 + 2(E_1 E_2 - c^2 \mathbf{p}_1 \cdot \mathbf{p}_2).$$

At fixed energies the dot product shows why head-on motion gives more centre-of-momentum energy than parallel motion. This relation also applies when one participant is a photon by setting its rest mass to zero. A familiar Newtonian analogy separates centre-of-mass translational kinetic energy from relative kinetic energy. In relativity the exact separation is carried by the invariant mass of the total four-vector and the boost of that total.

Compare a fixed target with two opposing beams

Let both incoming particles have rest energy $mc^2 = \mathcal{M}$. With one initially stationary and the other carrying kinetic energy K, the invariant is $s = 4\mathcal{M}^2 + 2\mathcal{M}K$. By contrast, two identical beams carrying kinetic energy K_b each and meeting with opposite momenta give

$$\sqrt{s} = 2(\mathcal{M} + K_b).$$

If a specified final channel has minimum sum of rest energies $\mathcal{W}$, the massive products at threshold have zero relative momentum in their common centre-of-momentum frame. The fixed-target threshold is $K_{\mathrm{th}} = (\mathcal{W}^2 - 4\mathcal{M}^2)/(2\mathcal{M})$ when positive. A symmetric collider needs $K_b = (\mathcal{W} - 2\mathcal{M})/2$ in each beam. The channel must also satisfy other conservation laws; these equations give kinematic conditions.

For an abstract excitation channel with $\mathcal{M} = 1.00\,\mathrm{GeV}$ and $\mathcal{W} = 3.00\,\mathrm{GeV}$, the fixed-target projectile needs $K = 2.50\,\mathrm{GeV}$, whereas each symmetric beam needs $0.50\,\mathrm{GeV}$. At the fixed-target threshold the total lab energy is $4.50\,\mathrm{GeV}$ and the total momentum times c is

$$\sqrt{3.50^2 - 1.00^2} = 3.354\,\mathrm{GeV}.$$

Hence $V_{\mathrm{cm}}/c = 0.7454$ and $\gamma_{\mathrm{cm}} = 1.50$. The final system has centre-of-momentum energy $3.00\,\mathrm{GeV}$ but still carries substantial bulk motion in the laboratory. Equating an energy deficit directly to projectile kinetic energy would ignore its conserved momentum.

Solve any two-body final state in its momentum frame

Let the two final particles have rest energies $\mathcal{M}_3, \mathcal{M}_4$. In the centre-of-momentum frame their spatial momenta have equal magnitudes p_* and opposite directions. Energy conservation gives

$$E_3^* + E_4^* = \sqrt{s}.$$

Subtract their squared mass-shell relations to obtain

$$(E_3^*)^2 - (E_4^*)^2 = \mathcal{M}_3^2 - \mathcal{M}_4^2.$$

Factoring this difference gives

$$E_3^* = \frac{s + \mathcal{M}_3^2 - \mathcal{M}_4^2}{2\sqrt{s}},$$

$$cp_* = \frac{\sqrt{[s - (\mathcal{M}_3 + \mathcal{M}_4)^2][s - (\mathcal{M}_3 - \mathcal{M}_4)^2]}}{2\sqrt{s}}.$$

The square root exposes the threshold and is symmetric under interchanging the products. When the masses are equal, each receives exactly $\sqrt{s}/2$. When they differ, equal momenta do not mean equal energies or velocities. At threshold the momentum vanishes, so an angular distribution there becomes a delicate concept; a boost can send both products in the same lab direction even when they move apart appreciably above threshold.

For $\sqrt{s} = 5.0\,\mathrm{GeV}$, $\mathcal{M}_3 = 2.0\,\mathrm{GeV}$ and $\mathcal{M}_4 = 1.0\,\mathrm{GeV}$, the energies are 2.80 and $2.20\,\mathrm{GeV}$. Each gives

$$cp_* = \sqrt{2.8^2 - 2.0^2} = \sqrt{2.2^2 - 1.0^2} = 1.960\,\mathrm{GeV}.$$

Their speed ratios cp_*/E^* are 0.700 and 0.891. Summing these two speeds would exceed c as a numerical closing rate in that frame, but the speed of either particle measured from the other's rest frame follows relativistic velocity addition and remains below c.

Transform a centre-of-momentum angular pattern to a detector

Choose the laboratory boost along z with parameters β, γ. A product emitted at polar angle θ_* has $p_{z,*} = p_* \cos\theta_*$,

$$p_{\perp,*} = p_* \sin\theta_*.$$

A Lorentz boost to the laboratory gives $E = \gamma(E^* + \beta c p_* \cos\theta_*)$,

$$c p_z = \gamma(c p_* \cos\theta_* + \beta E^*),$$

$$p_\perp = p_{\perp,*}.$$

Use a quadrant-aware angle from the resulting longitudinal and transverse components. A tangent formula alone loses the distinction between a particle moving backward and one moving nearly forward when its denominator changes sign.

For particle 3 in the preceding example take $\beta = 0.60, \gamma = 1.25$ and emission at 90° in the centre-of-momentum frame. The laboratory energy is $3.50\,\mathrm{GeV}$, axial momentum times c is $2.10\,\mathrm{GeV}$, and transverse momentum times c remains $1.960\,\mathrm{GeV}$. The polar angle is 43.0°. A detector that accepts only angles above 60° would miss this event despite its centre-of-momentum emission being transverse. To convert an angular density, transform the solid-angle Jacobian or count the preimage of each finite acceptance bin; matching angles by name between frames is insufficient.

If the detector instead accepts a product only above lab energy $E_{\min}$, the inequality becomes $\cos\theta_* \geq [E_{\min}/\gamma - E^*]/(\beta c p_*)$ for positive β, p_*. With $E_{\min} = 4.0\,\mathrm{GeV}$ this gives $\cos\theta_* \geq 0.340$. For an isotropic distribution in its own momentum frame that detector accepts fraction $(1 - 0.340)/2 \simeq 0.330$, assuming full azimuth and no other losses. At $\beta = 0$ energy selection becomes independent of angle, so the divided expression must be replaced by its original inequality.

Follow an elastic collision of equal masses all the way to the laboratory

In a Newtonian elastic collision of equal masses with one initially at rest, the two nonzero outgoing velocities are perpendicular. At relativistic energies that rule changes even when the collision remains exactly elastic. For equal final masses in the centre-of-momentum frame the two outgoing energies and momentum magnitudes are equal. In the laboratory where target 2 was initially at rest, the boost speed of the centre equals the speed of each particle in the momentum frame: boosting initially stationary particle 2 into that frame supplies the equality. Write this common dimensionless speed as β, and let particle 1 scatter through angle θ_* to the positive boost axis. Particle 2 leaves with opposite momentum.

With $p_* c = \beta E^*$, the laboratory longitudinal components are $p_{1z} = \gamma p_*(1 + \cos\theta_*)$ and $p_{2z} = \gamma p_*(1 - \cos\theta_*)$, and their transverse components are opposite with magnitude $p_* \sin\theta_*$. The two lab polar angles therefore obey $\tan\theta_1 = \tan(\theta_*/2)/\gamma$ and $\tan\theta_2 = \cot(\theta_*/2)/\gamma$. Multiplying gives

$$\tan\theta_1 \tan\theta_2 = 1/\gamma^2.$$

At low speed $\gamma \to 1$, so $\theta_1 + \theta_2 \to 90^\circ$. For finite boost the opening angle becomes smaller. Endpoint cases where one outgoing particle is stationary leave its direction undefined and must be handled separately.

Take rest energy $\mathcal{M}$ and projectile kinetic energy $K = 2\mathcal{M}$ against an identical stationary target. The invariant energy is $\sqrt{8}\mathcal{M}$ and the laboratory total energy is $4\mathcal{M}$, giving $\gamma_{\mathrm{cm}} = \sqrt{2}$. For a transverse centre-of-momentum collision, both products have laboratory angle $\arctan(1/\sqrt{2}) = 35.26^\circ$ on opposite sides of the beam, so the opening is 70.53°. Both laboratory energies are $2\mathcal{M}$; their kinetic energies are each $\mathcal{M}$, sharing the incident kinetic energy equally. Angular data and energy partition together offer an overdetermined test of elastic equal-mass kinematics.

For a general θ_*, the lab kinetic-energy fractions are $[1 + \cos\theta_*]/2$ and $[1 - \cos\theta_*]/2$ of the incoming kinetic energy in this equal-mass geometry. This follows by inserting $E^* = \gamma_{\mathrm{cm}}\mathcal{M}$ in the boost and using $K = 2\mathcal{M}(\gamma_{\mathrm{cm}}^2 - 1)$. Equal masses do not imply equal final energies in the laboratory; that occurs for the transverse centre-of-momentum geometry. A detector threshold of $0.25K$ on both products selects $|\cos\theta_*| \le 0.50$. For an isotropic momentum-frame distribution that condition accepts half the events irrespective of the azimuth, provided the lab apparatus covers both directions.

Compare two methods of estimating missing invariant mass

Suppose a known laboratory total has energy $5.0\,\mathrm{GeV}$ and axial momentum times c of $3.0\,\mathrm{GeV}$. One registered product has energy $2.0\,\mathrm{GeV}$, longitudinal momentum times c of $1.0\,\mathrm{GeV}$, and transverse momentum times c of $0.60\,\mathrm{GeV}$. Subtracting vectors gives missing energy $3.0\,\mathrm{GeV}$, axial momentum times c of $2.0\,\mathrm{GeV}$, and transverse momentum times c of $-0.60\,\mathrm{GeV}$. Its invariant mass energy is

$$\sqrt{9 - 4 - 0.36} = 2.154\,\mathrm{GeV}.$$

Dropping the transverse measurement would give $2.236\,\mathrm{GeV}$, an error of about 3.8%. Subtracting reported kinetic energies instead of total energies would introduce an uncontrolled rest-energy offset.

The same result can be reconstructed in the initial centre-of-momentum frame. The total invariant energy is $4.0\,\mathrm{GeV}$, so the laboratory boost is

$$\beta = 0.60, \gamma = 1.25.$$

Transforming the observed product back gives $E^* = 1.25(2.0 - 0.60 \times 1.0) = 1.75\,\mathrm{GeV}$ and $cp_z^* = 1.25(1.0 - 0.60 \times 2.0) = -0.25\,\mathrm{GeV}$, while its transverse component stays $0.60\,\mathrm{GeV}$. Missing energy is $2.25\,\mathrm{GeV}$, and missing squared momentum times c^2 is $0.25^2 + 0.60^2$. The invariant is again $4.64\,\mathrm{GeV}^2$. Repeating the computation in two frames checks signs and coordinate components without adding independent experimental information.

To propagate uncertainty use the squared quantity before taking its square root. With $c = 1$ for numerical units, perturbations satisfy

$$\delta M_{\mathrm{miss}}^2 = 2E_{\mathrm{miss}}\delta E_{\mathrm{miss}} - 2\mathbf{p}_{\mathrm{miss}} \cdot \delta\mathbf{p}_{\mathrm{miss}}.$$

If the energy and momentum of one detected particle come from the same calibrated tracking measurement they may be strongly correlated. Treating those uncertainties as independent can seriously misestimate the spread, especially near a missing-mass threshold where M^2 is close to zero. Retain the full covariance and report a distribution in mass squared near that boundary. Mapping negative noisy values to zero before averaging biases the result upward and erases information about detector resolution.

Recover a recoil energy from photon scattering

Consider an incoming photon of energy E colliding with a free particle of rest energy $\mathcal{M}$ initially at rest. The outgoing photon has energy E' and turns through angle θ in the original laboratory. Four-momentum conservation gives the final target energy $\mathcal{M} + E - E'$ and its squared momentum times c^2 is $E^2 + E'^2 - 2EE'\cos\theta$. Imposing the final target mass-shell condition and cancelling equal squares yields

$$\mathcal{M}(E - E') = EE'(1 - \cos\theta).$$

Therefore

$$E' = \frac{E}{1 + (E/\mathcal{M})(1 - \cos\theta)}.$$

The scattered energy equals the incident energy for perfect forward scattering, whereas backscattering transfers most energy at fixed incident E. Rearrangement gives

$$1/E' - 1/E = (1 - \cos\theta)/\mathcal{M}.$$

Multiplying by hc gives the usual wavelength shift with scale $h/(mc)$. The argument uses only four-momentum conservation and the initial target mass to determine kinematics. It does not give the probability of any scattering angle, which requires an interaction model. Bound target motion or initially moving scatterers change the measured line shape even when the elementary free-particle kinematics is understood.

Take $E = \mathcal{M}/2$. At $\theta = 90^\circ$ the outgoing photon energy is $\mathcal{M}/3$; at $\theta = \pi$ it is $\mathcal{M}/4$. In the right-angle event the target kinetic energy is

$$E - E' = \mathcal{M}/6.$$

Its final momentum magnitude times c can be computed from its energy as $\sqrt{(7\mathcal{M}/6)^2 - \mathcal{M}^2} = \sqrt{13}\mathcal{M}/6$, or from the photon momentum triangle as $\sqrt{(\mathcal{M}/2)^2 + (\mathcal{M}/3)^2}$. These two values agree. A detector that measures only target kinetic energy can infer the photon angle if the initial photon energy was known and the free stationary target assumptions hold.

The maximum possible target kinetic energy is $2E^2/(\mathcal{M} + 2E)$. For $E \ll \mathcal{M}$ this is approximately $2E^2/\mathcal{M}$, much smaller than the incident energy. At $E \gg \mathcal{M}$ the recoiling target can receive most of the photon energy. Scanning incident energy therefore changes both the absolute and fractional accessible

recoil range. If an observed event falls beyond that kinematic edge, changing only the angular cross section cannot explain it; examine energy calibration, initial target motion, coincidence assignment or overlapping events.

Identify what two unknown detector scales can be calibrated together

A two-body decay at rest into two photons yields equal energies and an opening angle of 180°. In any frame its invariant parent rest energy is

$$Mc^2 = \sqrt{2E_1E_2(1-\cos\alpha)}.$$

This formula remains valid when the parent moves and the detected photon energies differ. A common multiplicative energy calibration factor multiplies the reconstructed mass by that factor. An angular bias also changes the inferred mass, with fractional derivative $\frac{1}{2}\sin\alpha/(1-\cos\alpha) = \frac{1}{2}\cot(\alpha/2)$. Nearly collinear photon pairs are therefore particularly sensitive to angular uncertainties, even when their individual energy measurements are accurate.

For $E_1 = 2.0\,\mathrm{GeV}$, $E_2 = 1.0\,\mathrm{GeV}$, $\alpha = 60^\circ$, the reconstructed rest energy is $\sqrt{2}\,\mathrm{GeV}$, although the lab energy sum is $3.0\,\mathrm{GeV}$. A one-degree positive error in the opening angle changes the inferred mass by approximately $0.5\cot 30^\circ(\pi/180) = 1.51\%$. Measuring events with a range of opening angles can distinguish an angular offset from a common energy-scale factor, since the latter has no such angular amplification. A calibration performed only on back-to-back pairs is weakly sensitive to opening-angle errors to first order.

Invariant reconstruction is especially valuable when different observers disagree on which laboratory particle appears fast or forward. Agreement requires the entire event be expressed in one frame, with coincident incoming and outgoing measurements and a consistent sign convention for momentum. A Lorentz transformation cannot repair a mispaired event. Estimate statistical backgrounds and detector resolution independently before interpreting a narrow or displaced mass feature. The invariant provides a kinematic check; it gains physical meaning from the measurement model used to construct it.

Reconstruct a two-body decay with a nonzero boost

A parent with known rest energy W decays into one massive daughter of rest energy m_dc^2 and one photon. In the parent rest frame the common momentum magnitude follows from the two-body formula, so photon energy is

$$E_\gamma^* = [W^2 - (m_dc^2)^2]/(2W).$$

For a moving parent, the lab photon energy spans a range depending on the emission angle:

$$E_\gamma = \gamma E_\gamma^*(1+\beta\cos\theta_*).$$

The end energies $E_{\max}, E_{\min}$ for emission forward and backward have product $(E_\gamma^*)^2$ and ratio $(1+\beta)/(1-\beta)$. Thus a measured energy band can give both the rest-frame line energy and the parent speed if its full angular range is observed and all parents share a common boost.

Take $W = 3.0\,\mathrm{GeV}$,

$$m_d c^2 = 1.0\,\mathrm{GeV}.$$

The rest-frame photon energy is $4/3\,\mathrm{GeV}$. With $\beta = 0.60, \gamma = 1.25$, the accessible lab endpoints are 2.667 and $0.667\,\mathrm{GeV}$. Their geometric mean recovers $1.333\,\mathrm{GeV}$, and $(E_{\max} - E_{\min})/(E_{\max} + E_{\min}) = 0.600$ recovers the boost. The total energy released as rest energy difference is $2.0\,\mathrm{GeV}$, larger than the photon energy in the rest frame because the massive daughter must recoil. Assigning all the rest-energy difference to radiation ignores that conserved momentum even before any laboratory transformation.

If the parent decays isotropically in its rest frame, $\cos\theta_*$ is uniformly distributed. The linear photon-energy relation then gives a flat lab energy density between the endpoints when every direction is detected with equal efficiency and the parent boost is fixed. A laboratory detector covering only a forward cone selects part of the interval and can produce an apparently shifted line or a nonuniform spectrum. A spread of parent speeds superposes intervals with different endpoints. Before interpreting spectral width as an intrinsic lifetime or a spread in masses, separate angular acceptance, boost distribution and instrumental resolution.

The lab photon angle obeys $\cos\theta_{\mathrm{lab}} = (\cos\theta_* + \beta)/(1 + \beta\cos\theta_*)$. At transverse rest-frame emission $\cos\theta_* = 0$, the lab photon points at about 53.1° for the stated boost. Its energy is $1.667\,\mathrm{GeV}$. The corresponding massive daughter has a different aberration relation because its rest-frame speed is below c. A photon angle formula should not be reused for a massive track. Transform its actual four-vector to draw the two lab directions and compare them with the expected missing momentum of the unobserved partner.

Compare elapsed times along different trajectories

Study proper time and laboratory coordinate time for the same motion. Identify the invariant clock interval before comparing a measurement between frames.

Open this experiment online

Try the calculation

Speed / speed of light **0.8**

Gate separation (light-μs) **12**

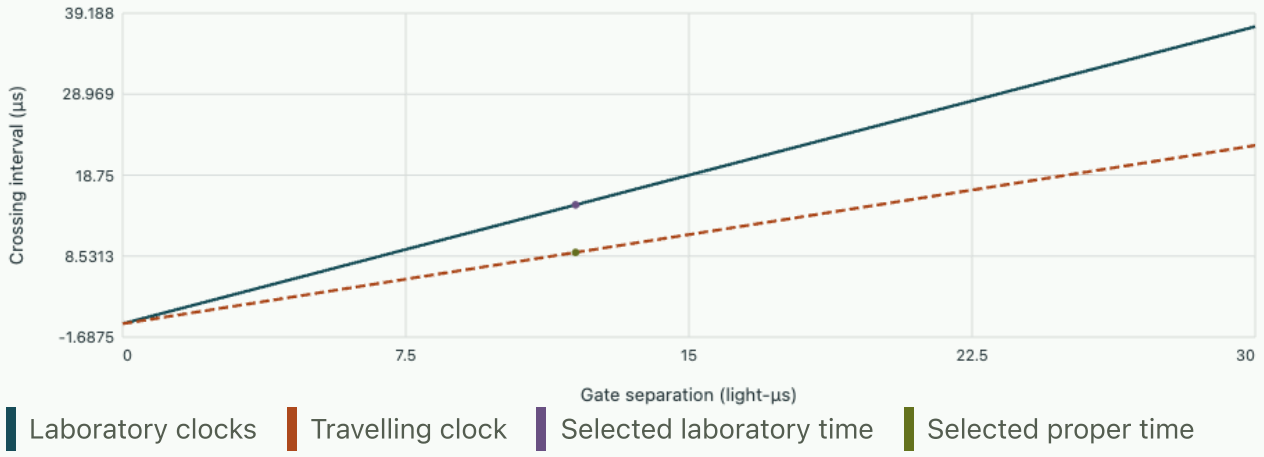

The laboratory records 15 μs. The travelling clock records 9 μs.

Audit a relativistic event using dimensionless rapidity

For one-dimensional motion define rapidity y by $E = mc^2 \cosh y,\ cp = mc^2 \sinh y$. Then $v/c = \tanh y$ and collinear boosts add or subtract rapidities. The invariant for two collinear massive particles becomes

$$s = \mathcal{M}_1^2 + \mathcal{M}_2^2 + 2\mathcal{M}_1\mathcal{M}_2 \cosh(y_1 - y_2).$$

The available energy depends on their relative rapidity, not on their common boost. At very high same-direction energies, constructing $E_{\text{total}}^2 - (cp_{\text{total}})^2$ can lose floating-point precision through subtraction. Expressing the input with known rest energies and relative rapidity can be numerically better conditioned.

For two equal masses at rapidities 3.0 and 2.0,

$$\sqrt{s} = 2\mathcal{M}\cosh(0.5) = 2.2553\mathcal{M}.$$

A common boost adding ten to both leaves this value unchanged even though each lab energy grows by orders of magnitude. Their centre-of-momentum rapidity is 2.5 in the initial frame because equal masses at rapidities ± 0.5 have opposite momenta. A particle starting at rapidity three appears to move only at $\tanh(0.5) = 0.462c$ in that frame. This separates a very large laboratory kinetic energy from a modest relative collision energy.

A computation obtains slightly negative s for two very energetic nearly parallel massive tracks, even though both individual four-vectors were formed from positive masses. What calculation can distinguish rounding from a physical inconsistency?

▼ **Work through the solution**

Recalculate using independently measured directions and rest masses. For a track of known momentum magnitude, evaluate $E - cp = \mathcal{M}^2/(E + cp)$ so that a small positive difference is recovered without subtracting nearly equal large numbers. In a collinear test use the rapidity expression; at nonzero angle separate the positive angular term $c^2 p_1 p_2 (1 - \cos\alpha)$, with $1 - \cos\alpha = 2\sin^2(\alpha/2)$. Compare with higher precision and propagated measurement covariance. For ideal future-directed massive four-vectors their total cannot be spacelike, so a stable negative value would indicate inconsistent measured inputs or a reconstruction error rather than a new kinematic channel.

Choose a laboratory energy convention for published event tables

An event table may label one column beam energy while another experiment quotes beam kinetic energy for the same particle. The distinction is a full rest energy. For a stationary equal-mass target, inserting total projectile energy E_{proj} gives

$$s = 2\mathcal{M}^2 + 2\mathcal{M}E_{\mathrm{proj}};$$

inserting kinetic energy K requires

$$s = 4\mathcal{M}^2 + 2\mathcal{M}K.$$

At a quoted numerical beam value $2\mathcal{M}$ the two interpretations yield centre-of-momentum energies $\sqrt{6}\,\mathcal{M}$ and $\sqrt{8}\,\mathcal{M}$, distinct enough to change whether a final channel is kinematically open.

Before comparing two angular or energy spectra, record which particle was initially at rest, the energy convention, whether angles refer to the momentum frame or laboratory, and which particles passed the selection. Each changes an equation already derived above. A sample with a laboratory energy cut can acquire a forward asymmetry even if the underlying centre-of-momentum scattering is perfectly isotropic. Mapping every selected event back to the momentum frame without also correcting the angle-dependent acceptance will preserve that selection bias. The conserved invariant determines the accessible final kinematics; the detector determines which part of that set becomes visible.

Tutorial on collision measurements

At fixed-target energy $K = 0.020\mathcal{M}$, compare the available kinetic energy above the two incoming rest energies in the momentum frame with the Newtonian reduced-mass prediction.

▼ **Work through the solution**

Expansion gives

$$\sqrt{s} = 2\mathcal{M}\sqrt{1 + K/(2\mathcal{M})} \simeq 2\mathcal{M} + K/2 - K^2/(16\mathcal{M}).$$

The leading available energy is half the lab projectile kinetic energy, as for two equal Newtonian masses with one at rest. The correction here is $0.000025\mathcal{M}$, about one quarter percent of the leading available kinetic energy. An energy expansion must subtract the rest-energy offset before calculating a relative error.

Two photons of equal energy E_γ intersect at angle α. Derive the total centre-of-momentum energy, including the parallel and antiparallel limits.

▼ **Work through the solution**

The mass-shell terms vanish and the spatial momenta have magnitude E_γ/c. Thus

$$s = 2E_\gamma^2(1-\cos\alpha) = 4E_\gamma^2\sin^2(\alpha/2).$$

Parallel rays have a null total and zero invariant energy, although laboratory energy is $2E_\gamma$. Opposing rays have zero net momentum and centre-of-momentum energy $2E_\gamma$. A relative closing rate is not the invariant energy.

An unknown neutral product escapes an otherwise recorded two-body event. Which four-vector combination should a detector reconstruct, and what does a negative inferred mass squared suggest?

▼ **Work through the solution**

Subtract the measured final four-momenta from the known incoming total and square the missing four-vector with the stated metric. A single missing physical massive product gives its positive rest mass squared after the appropriate powers of c; a massless one gives zero. A significantly negative result indicates an inconsistent reconstruction, an unaccounted incoming momentum, event mismatch or measurement bias. Multiple escaping products generally yield their combined invariant mass and cannot be identified uniquely from that scalar alone.

Compare velocity and momentum transformations across reference frames.

Fließbach's mechanics text includes a full final treatment of special relativity.

Analytical mechanics from constraints to invariants · 13. Which path is shortest across the surface of a cone?

A point can move along a conical surface while its azimuth and height both change. Unroll the geometry and predict the shortest path between two marked points. The measurable minimum radius distinguishes the geodesic from a line drawn along a horizontal circle.

Turn the constraint into a distance measurement

Let r denote the slant distance from the apex and α the angle between the cone's side and its central axis. A point at r lies on a horizontal circle of radius $r \sin\alpha$. Small radial and azimuthal displacements on the surface meet at right angles. Their squared distance adds to $ds^2 = dr^2 + r^2 \sin^2\alpha \, d\phi^2$. The change of variable $\psi = \phi \sin\alpha$ turns this into the polar metric of a plane. Cutting the cone along a generator and flattening it produces a sector of opening angle $2\pi \sin\alpha$.

Without a tangential force a particle follows a straight line in the unrolled sector. Its coordinates need not evolve linearly in the original azimuth. For two positions at equal slant distance R separated by physical azimuth $\Delta\phi$ of magnitude at most π, the shortest branch uses a straight chord spanning $\Delta\psi = \sin\alpha \, \Delta\phi$. Bisecting the isosceles triangle gives

$$L = 2R \sin(|\Delta\psi|/2),$$

$$r_{\min} = R \cos(\Delta\psi/2).$$

The other copies of the endpoint correspond to winding around the cone on different branches. The chord formula uses a branch reached without passing through the apex. When the physical endpoints are diametrically opposite, clockwise and anticlockwise branches have equal shortest length. A laboratory string stretched across the interior would use the three-dimensional chord, which need not stay on the surface.

Detect the departure from the horizontal ring

For a cone of half-angle 30 degrees, two marks 120 degrees apart at slant distance 5 cm appear only 60 degrees apart in the plane. Their shortest surface path is 5.00 cm long and passes through radius 4.33 cm. Staying on the horizontal ring would require $R\Delta\psi = 5.24$ cm. The straight three-dimensional chord between the same marks is only 4.33 cm long but cuts through the cone. Comparing those three lengths distinguishes a free-space displacement from two distinct constrained motions.

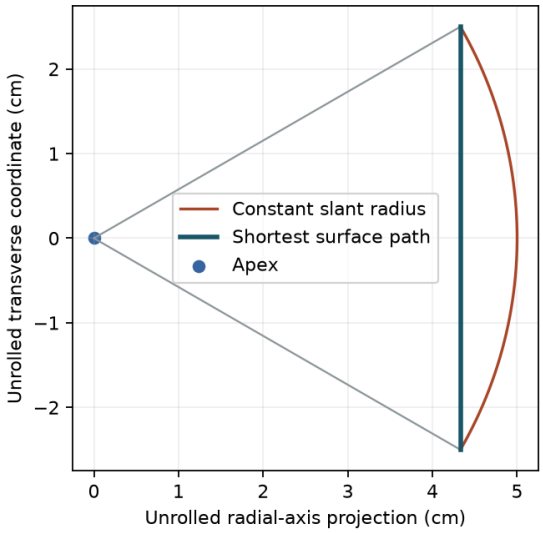

The endpoints share a radius while the middle of the geodesic lies closer to the apex. Both axes measure lengths intrinsic to the surface.

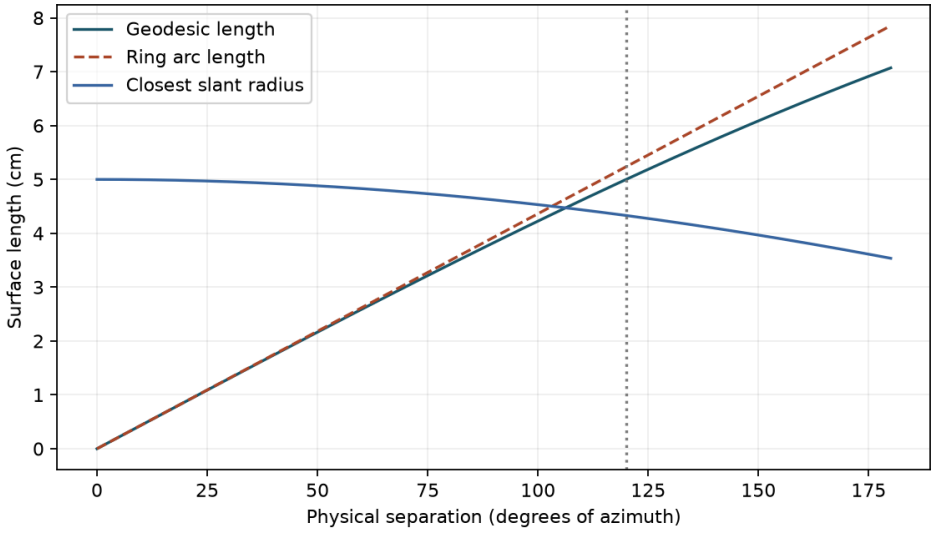

Changing only the endpoint separation alters the sag towards the apex. At small separation the geodesic length approaches the circular arc.

Exercise · infer the slope

Two marks at slant distance 10 cm and azimuth separation 120 degrees have a geodesic of length 10 cm. What is the cone half-angle?

▼ Work through the solution

The measured chord gives

$$\sin(\Delta\psi/2) = 10/(2 \cdot 10) = 1/2.$$

The shortest branch has $\Delta\psi = 60^\circ$, hence $\sin\alpha = 60/120 = 1/2$ and $\alpha = 30^\circ$. Use the same angular units in the ratio.

Exercise · compare with a weakly curved path

Find the relative excess of ring length over geodesic for a small unrolled separation δ. Why does a very small patch look flat?

▼ **Work through the solution**

Expanding $2\sin(\delta/2) = \delta - \delta^3/24 + \cdots$ gives

$$(R\delta - L)/(R\delta) = \delta^2/24 + O(\delta^4).$$

Both paths have the same tangent at leading order. The cone away from its apex is intrinsically developable; the small difference here measures the curvature of the chosen ring inside that developed plane.

Try it · Cone

Change the inputs and compare the recalculated curves with the preceding derivation and baseline figure. The axes give the units; the numerical readout states the model assumptions and any limiting cases. Reset the inputs to return to the reference setting.

Open this live calculation

Try the calculation

Cone half-angle (degrees)	30
Endpoint azimuth separation (degrees)	120
Slant radius (cm)	5

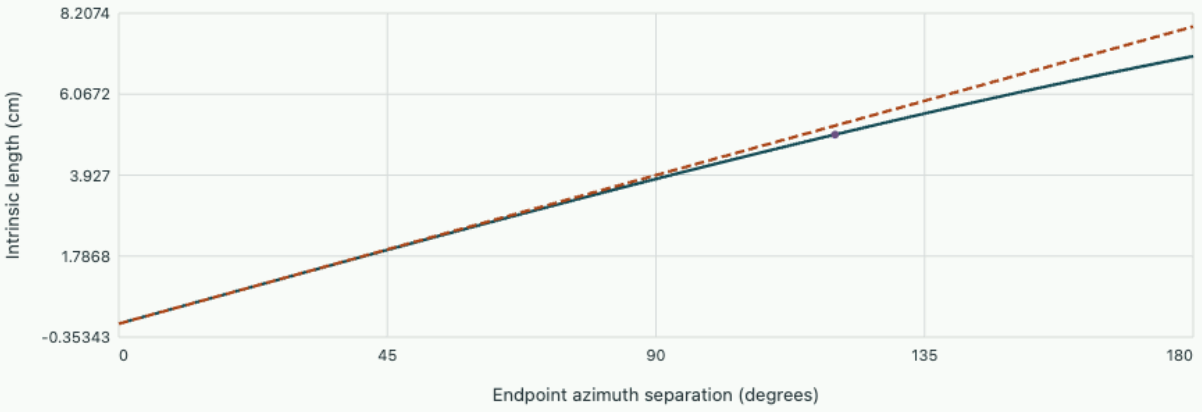

Geodesic chord on unrolled cone | Constant-radius arc | Selected separation

Closest slant radius 4.3301 cm. Cut and unroll the cone to obtain the straight chord; the planar distance is the intrinsic surface distance.

Download the corresponding editable notebook. The browser recalculates the reduced equations directly; the notebook exposes the full calculation and its checks.

Open editable notebook Download .ipynb

Analytical mechanics from constraints to invariants · 14. Motion in a medium and momentum carried across a boundary

Two beads can approach exactly the same terminal speed with recognisably different histories. A sand cart can slow down while the total horizontal momentum of sand and cart stays fixed. Both observations begin by specifying which material the equation of motion follows.

Infer the force law from a falling bead

Choose downward displacement as positive. A submerged bead of volume V, density ρ_b and mass m displaces fluid of density ρ_f. In a fluid initially at rest the static pressure gradient supplies buoyancy $\rho_f V g$. Combine the two constant forces into $m g_e = (\rho_b - \rho_f) V g$. Assume a heavy bead, negligible wall effects and sufficiently slow changes to neglect added mass and viscous memory. A drag law must reverse sign when the velocity changes sign.

$$m\dot{v} = m g_e - b v,$$

$$m\dot{v} = m g_e - c|v|v.$$

In the first model b has units kg/s, in the second c has units kg/m. Equating drag to the effective weight gives $v_\infty = m g_e / b$ or $v_\infty = \sqrt{m g_e / c}$. Near zero speed both models give initial acceleration g_e. Equal initial slope and equal terminal speed therefore leave the force law undetermined.

Solve both initial-value problems

Choose the characteristic time $\tau = v_\infty / g_e$ and write $u = v/v_\infty$, $s = t/\tau$. Starting from rest the positive-speed branches obey $du/ds = 1 - u$ and $du/ds = 1 - u^2$. Separation and integration from zero give $-\ln(1-u) = s$ and $\operatorname{artanh} u = s$. A second integration supplies displacements that a camera can measure directly.

$$u_{\mathrm{lin}} = 1 - e^{-s},$$

$$z_{\mathrm{lin}} = v_\infty \tau (s - 1 + e^{-s}).$$

$$u_{\mathrm{quad}} = \tanh s,$$

$$z_{\mathrm{quad}} = v_\infty \tau \ln(\cosh s).$$

To start a data analysis, fit the early displacement to $g_e t^2/2$ and determine the late speed independently. After this scaling, each curve is a prediction with no free fitting amplitude. With $g_e = 9.81$ m/s² and $v_\infty = 3.0$ m/s the time scale is 0.306 s. The competing predictions already differ by about 0.39 m/s at 0.30 s.

Recall · Which drag law has a mechanical basis here?

For a rigid sphere of radius a moving slowly in a Newtonian fluid the creeping-flow result is $b = 6\pi\eta a$. Check $\mathrm{Re} = 2a\rho_f|v|/\eta$ throughout the run. When inertia matters a pressure-drag model uses $c = \rho_f C_D A/2$ with frontal area A. Treating C_D as constant requires a range in which it varies slowly.

OneSimulation experiment · Two trajectories with the same terminal speed

Try the force laws in your browser

Adjust the common terminal speed, effective gravity and RK4 step. The curves are recomputed from the two equations of motion above. Keep the physical parameters fixed while reducing the step to distinguish integration error from a different drag law. Then compare the time needed to reach 90% of the terminal speed.

This browser calculation implements RK4 directly. The notebook below runs the same initial-value problem with OneSimulation; set its `terminal`, `g` and `step` to the displayed values to reproduce the comparison. The constant-coefficient drag assumptions still apply.

Open this experiment online

Try the calculation

Terminal speed (m/s)	**3**
Effective gravity (m/s²)	**9.81**
RK4 time step (s)	**0.01**

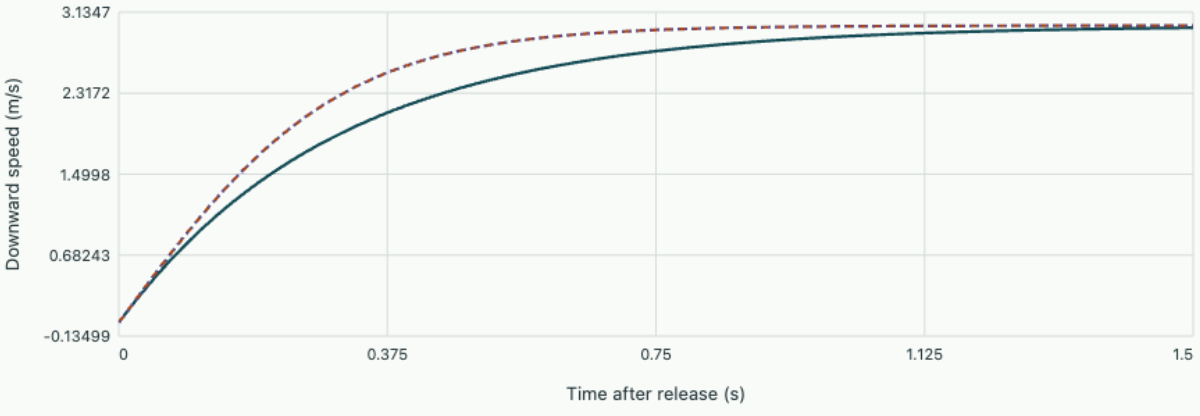

Characteristic time = 0.30581 s. Maximum quadratic-drag integration error = 5.18e-8 m/s. At 0.30 s the exact speeds are 1.87519 and 2.2605 m/s. Actual step = 0.01 s.

Reproduce with OneSimulation

Change the terminal speed and the time step. Compare the entire computed trace with the exact quadratic result, then identify where the two force models separate most visibly.

Run the downloaded notebook with OneSimulation, NumPy and Matplotlib installed. The output below was recorded with the displayed calculation.

```
"""Drop a bead from rest in two media with equal terminal speeds."""
import numpy as np
import matplotlib.pyplot as plt
from onesim.numerics.time import ClassicalRungeKutta4TimeIntegrator

g, terminal = 9.81, 3.0  # effective downward acceleration and terminal speed
step = 0.01
time = np.arange(151) * step
method = ClassicalRungeKutta4TimeIntegrator()

def rates(speed, t):
    linear, quadratic = speed
    return (g * (1 - linear / terminal),
            g * (1 - quadratic * abs(quadratic) / terminal**2))

speeds = [(0.0, 0.0)]
for t in time[:-1]:
    speeds.append(method.advance(speeds[-1], rates, step, time=t))
linear, quadratic = np.array(speeds).T
exact = terminal * np.tanh(g * time / terminal)
print(f"At 0.30 s: linear {linear[30]:.4f} m/s, quadratic {quadratic[30]:.4f} m/s")
print(f"Largest RK4 discrepancy for quadratic drag: {max(abs(exact-quadratic)):.2e} m/s")
plt.plot(time, linear, label="Linear drag")
plt.plot(time, quadratic, label="Quadratic drag")
plt.axhline(terminal, linestyle=":", color="grey", label="Terminal speed")
plt.xlabel("Time after release (s)")
plt.ylabel("Downward speed (m/s)")
plt.legend()
plt.tight_layout()
plt.savefig("physics-drag-laws.png", dpi=160)
```

Computed output

```
At 0.30 s: linear 1.8752 m/s, quadratic 2.2605 m/s
Largest RK4 discrepancy for quadratic drag: 5.18e-08 m/s
```

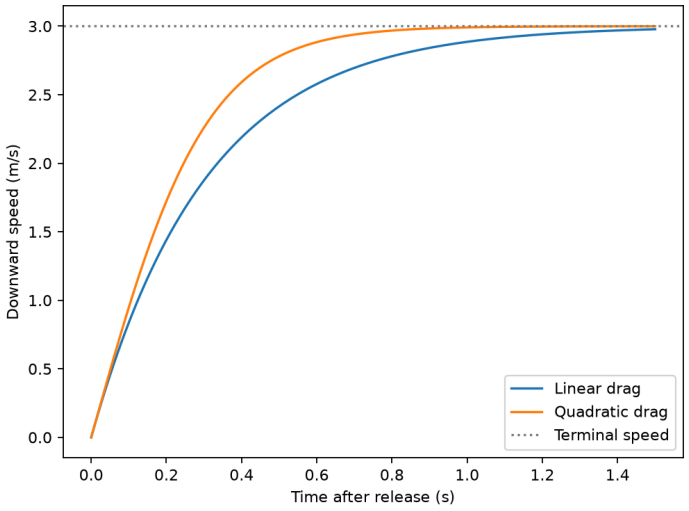

Two trajectories with the same terminal speed.

Download editable notebook · Download Python script

Derive the equation for a changing collection of matter

Let a horizontal cart of instantaneous mass M and speed v collect grains at rate $\dot{M} > 0$. Just before collection a small parcel dM has horizontal laboratory velocity w. Over dt the momentum of cart plus parcel changes by the external impulse. The incoming parcel is included on the initial side so that the comparison follows the same matter.

$$Mv + w\,dM + F_{\text{ext}}\,dt = (M + dM)(v + dv).$$

Drop the product $dM\,dv$, divide by time and keep the finite acceleration. The relative speed determines how strongly the intake changes the cart velocity.

$$M\dot{v} = F_{\text{ext}} + (w - v)\dot{M},$$

$$\frac{d(Mv)}{dt} = F_{\text{ext}} + w\dot{M}.$$

Take a 20 kg cart rolling at 3 m/s on a level frictionless track. Grains falling vertically carry zero horizontal momentum. After collecting 10 kg, the common speed is 2 m/s. The horizontal kinetic energy falls from 90 J to 60 J. The collisions can dissipate energy even though the horizontal external impulse vanishes. The vertical momentum and gravitational energy belong to a separate balance.

Recall · Moving boundaries and signs

The formula uses laboratory-frame w immediately outside the cart and signed mass rate into the cart. For outflow use the velocity of matter as it leaves. A leaking cart with material departing at the cart's horizontal speed has no resulting horizontal acceleration.

Tutorial on identifying a mechanical system

1 · When do the two beads reach 90% of the terminal speed?

▼ **Work through the solution**

The dimensionless times are $\ln 10 = 2.303$ and $\operatorname{artanh}(0.9) = 1.472$. At the stated parameters these are 0.704 s and 0.450 s. An early-velocity measurement distinguishes the laws more efficiently than another terminal-speed estimate.

---

2 · Infer an intake speed from a measured acceleration

▼ **Work through the solution**

A 12 kg cart moving at 1.5 m/s gains 0.40 kg/s and accelerates at 0.020 m/s² along a level frictionless track. From $w = v + M\dot{v}/\dot{M}$ the grains enter at 2.10 m/s. Using $F = d(Mv)/dt$ without an inlet flux would falsely infer an external force.

---

3 · Test a radius scaling before fitting a drag coefficient

▼ **Work through the solution**

For spheres of the same density, effective weight scales as a^3. Stokes drag then predicts $v_\infty \propto a^2$. At fixed C_D, quadratic drag gives $v_\infty \propto a^{1/2}$. Doubling radius gives speed ratios 4 and $\sqrt{2}$. Check Reynolds numbers, wall clearances and bead density before inferring a force law.

For further study see Taylor, Classical Mechanics, chapters 1–4 on force laws, dissipative motion and momentum transport.

Analytical mechanics from constraints to invariants · 15. From a repeating trajectory to a chaotic attractor

A damped pendulum under a periodic drive can settle into the same orbit on each run yet visit a different point on successive drive periods. A return map supplies the right clock for distinguishing a new period from a slowly decaying transient.

Build a map from a continuous mechanical experiment

Consider a pendulum with dimensionless time in units of its small-angle period divided by 2π. Let q be the positive damping rate, A the drive amplitude and ω the drive frequency.

$$\dot{\theta} = p,$$

$$\dot{p} = -qp - \sin\theta + A\cos(\omega t).$$

Prepare all observations at drive phase zero and evolve for $T = 2\pi/\omega$. The stroboscopic map takes (θ_n, p_n) to (θ_{n+1}, p_{n+1}). Complete rotations can be plotted modulo 2π while the unwrapped angle tracks transport. An attracting period-one orbit appears as one point after transients. A period-two orbit alternates between two points and returns after $2T$.

For a small patch in the state plane the instantaneous fractional area growth is the divergence $\partial_\theta p + \partial_p \dot{p} = -q$. Integration over a period gives a Jacobian determinant e^{-qT}. Phase-area contraction allows an attractor. A periodically driven Hamiltonian system at $q = 0$ instead has a unit determinant.

> **Recall · Why use a section at fixed drive phase?**
>
> Two trajectories with identical angle and speed can accelerate differently at different phases of an external drive. Sampling once per drive period compares equal external conditions. Recording at a nearby period can turn a perfectly regular response into an apparent cloud of points.

Calculate a period doubling in a solvable map

Near a flip bifurcation with only one slow direction, a one-dimensional map helps explain stability changes. The logistic map $f(x) = rx(1-x)$ on $0 \le x \le 1$ for $0 < r \le 4$ is an illustrative return law. Its r is not a calibrated pendulum torque. An interior fixed point is $x_* = 1 - 1/r$. For a small displacement $\delta_{n+1} \simeq f'(x_*)\delta_n$, giving a multiplier $2 - r$. Its magnitude crosses one at $r = 3$ with negative sign.

To find the new orbit, solve $f(f(x)) - x = 0$ and remove the two fixed-point factors x and $x - x_*$. The remaining quadratic has roots

$$x_\pm = \frac{r + 1 \pm \sqrt{(r-3)(r+1)}}{2r}.$$

Its two-step multiplier is $f'(x_+)f'(x_-) = -r^2 + 2r + 4$. At $r = 3.2$ it is 0.16 and deviations fall by that factor every two observations. At $r = 1 + \sqrt{6}$ it reaches -1, so that orbit loses stability. Additional

doublings create intervals of higher-period motion. Periodic windows interrupt the chaotic parameter range.

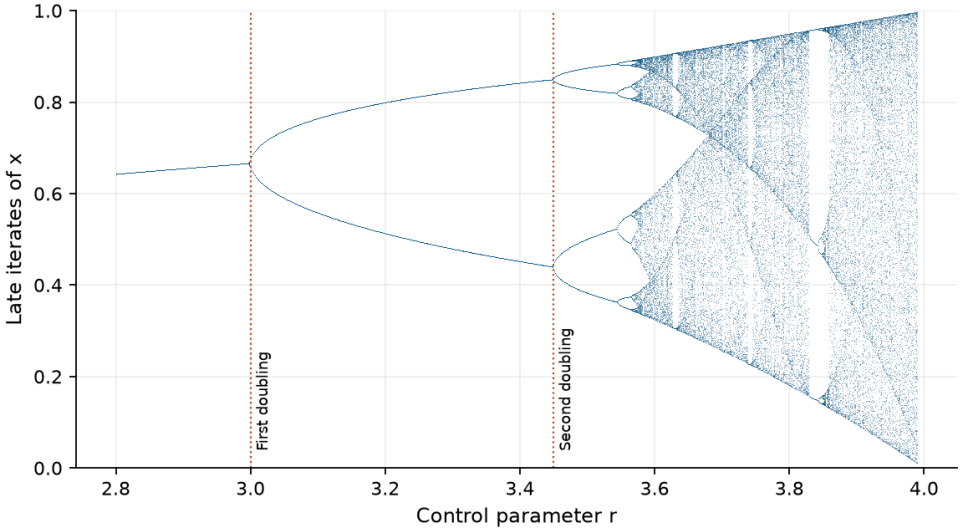

Each column records 120 late iterates at one setting after discarding 850 returns. First one branch splits, then each of its daughters splits. Narrow periodic windows remain visible among broader bands.

Try it · Logistic

Change the inputs and compare the recalculated curves with the preceding derivation and baseline figure. The axes give the units; the numerical readout states the model assumptions and any limiting cases. Reset the inputs to return to the reference setting.

Open this live calculation

Try the calculation

Return-map parameter r **3.6**

Initial state **0.2**

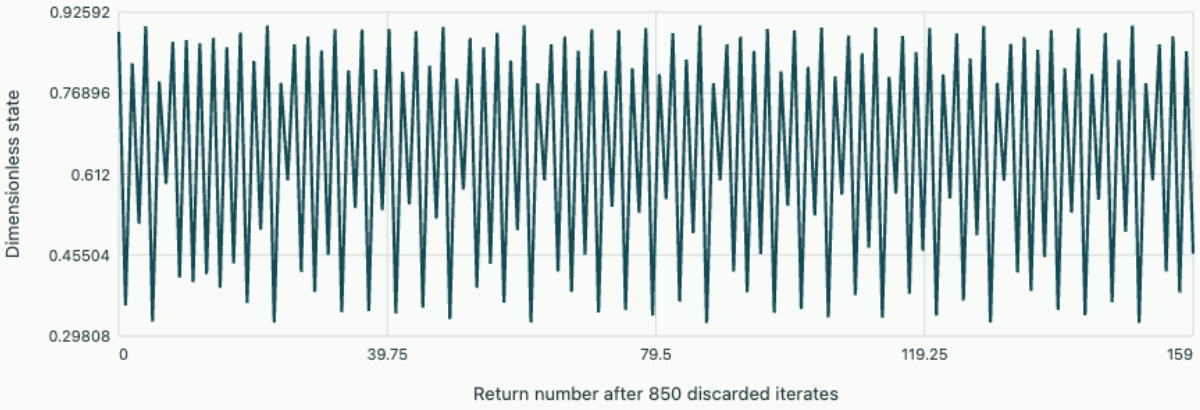

Late return sequence

Finite-window Lyapunov estimate 0.13665 per return. Positive values suggest sensitive dependence; repeat with nearby initial states and longer notebooks before identifying an attractor.

Estimate a growth rate while keeping the observations bounded

A separation eventually saturates at the attractor size. To estimate growth over many periods, multiply the local tangent factors and take a logarithm before averaging. Along a sampled orbit the largest exponent of the scalar map is

$$\lambda_N = \frac{1}{N}\sum_{j=0}^{N-1} \ln\left|r(1-2x_j)\right|.$$

For $r = 4$ the substitution $x = \sin^2\phi$ maps an iteration to angle doubling modulo the symmetries of the sine. Typical invariant-measure trajectories have $\lambda = \ln 2$ per iteration. Exceptional exact initial

conditions, including a critical point that maps onto zero, do not estimate that typical value. Finite precision eventually creates repetitions. Report the sampling window and discard transient returns.

For a mechanical test, integrate two nearby pendulum trajectories, sample at T, rescale the difference back to its small original norm and accumulate its log growth. Repeat with smaller time step and different starting points in the same basin. A positive long-time exponent and recurrent bounded motion are distinct pieces of evidence. Slow beats and noisy sensors can broaden a spectrum without deterministic chaos.

Tutorial on return maps

1 · Predict the number of observed return points

▼ **Work through the solution**

For $r = 3.2$, the roots of the two-cycle are about 0.5130 and 0.7995. Check directly that the first maps near 0.7995. Two sensor samples cannot distinguish a two-cycle from a transient. Repeated pairs should approach these values with the calculated two-step multiplier.

---

2 · Separate dissipation from instability

▼ **Work through the solution**

For $qT = 0.4$ the area factor is 0.6703. If one real multiplier of a period-one orbit is -1.2, its partner is $0.6703/(-1.2) = -0.559$. The orbit expands along one direction despite contracting area in total.

---

3 · Design a finite-time comparison

▼ **Work through the solution**

An apparent doubling every three drive periods corresponds to $\ln 2/3 = 0.231$ per return. Repeat the estimate with several initial separations above roundoff and below the nonlinear scale, increase the observation window and verify persistence when the numerical step is halved.

For further study see Taylor, Classical Mechanics, chapters 11–12 on nonlinear oscillations, the driven pendulum and chaos.

Analytical mechanics from constraints to invariants · 16. From differential acceleration to three-dimensional strain and stress

An accelerometer in a falling laboratory can read zero while a pair of falling test masses moves apart. A crystal can support different longitudinal and transverse speeds in the same direction. Both measurements require the spatial variation of a vector field, represented by a tensor.

Derive the relative acceleration in a falling frame

Let a laboratory origin fall freely at position $\mathbf{R}$ in the field $\mathbf{g}(\mathbf{R}) = -GM\mathbf{R}/R^3$ of a spherical source. Over a small separation $\boldsymbol{\xi}$ choose parallel nonrotating axes. Subtract the origin's acceleration and expand to first order:

$$\ddot{\xi}_i = g_i(\mathbf{R}+\boldsymbol{\xi}) - g_i(\mathbf{R}) \simeq T_{ij}\xi_j,$$

$$T_{ij} = \frac{GM}{R^3}(3n_in_j - \delta_{ij}),$$

$$\mathbf{n} = \mathbf{R}/R.$$

The radial eigenvalue is $2GM/R^3$. Both transverse eigenvalues are $-GM/R^3$. Outside the source the sum vanishes as required by $\nabla\cdot\mathbf{g} = 0$. Over a short time the fractional change of an initially stationary separation along an eigenvector is $T_it^2/2$. Near Earth's surface $g/R \simeq 1.54\times10^{-6}$ s⁻². Free masses initially separated by 2 m radially acquire a relative acceleration near 6.2 μm/s².

Recall · Which frame cancels gravity?

The origin's uniform acceleration cancels at all test masses when forming the difference. A rotating frame contributes centrifugal and Coriolis terms as well. For a small free-fall experiment state how axes are maintained and which relative velocities were initially present.

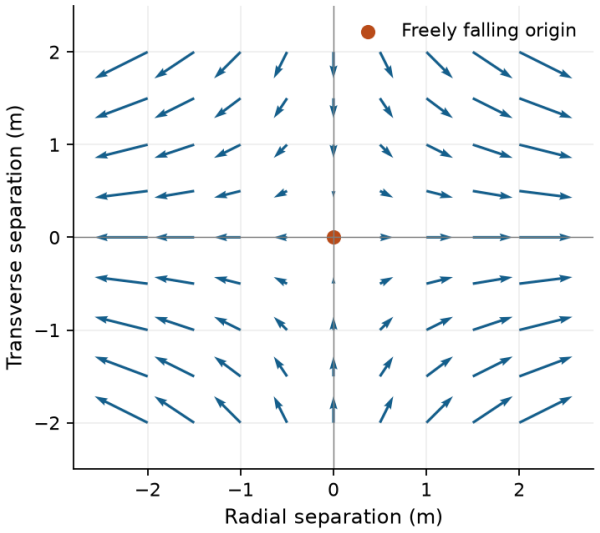

Relative acceleration in the freely falling laboratory. Two neighbours separated radially pull apart, while a transverse pair draws together. The common acceleration of the origin has been subtracted.

Try it · Tidal

Change the inputs and compare the recalculated curves with the preceding derivation and baseline figure. The axes give the units; the numerical readout states the model assumptions and any limiting cases. Reset the inputs to return to the reference setting.

Open this live calculation

Try the calculation

Central mass / Earth mass 1

Laboratory radius / Earth radius 1

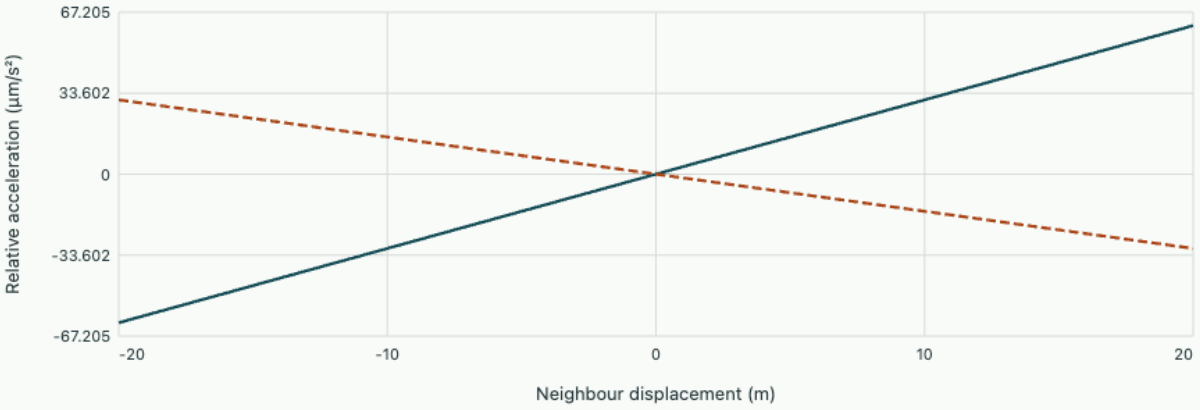

Tidal eigenvalues (2,−1,−1) × 1.541e-6 s⁻²; their sum is zero outside the source. Displacements must remain small compared with the laboratory radius.

Compare nearby material points before and after a displacement

Label a reference point by $\mathbf{X}$ and let its displacement be $\mathbf{u}(\mathbf{X})$. An initial segment $d\mathbf{X}$ becomes $(I + \nabla \mathbf{u}) d\mathbf{X}$. Expand its squared length, retaining the first-order terms. The antisymmetric part drops out of the quadratic form for length change.

$$d\ell'^2 - d\ell^2 = 2\, dX_i\, \varepsilon_{ij}\, dX_j,$$

$$\varepsilon_{ij} = \tfrac{1}{2}(\partial_i u_j + \partial_j u_i).$$

The trace gives fractional volume change. A rigid translation has zero displacement gradient. An infinitesimal rotation has an antisymmetric gradient, so it has zero linear strain as well. For simple shear $u_x = \gamma y$ the component $\varepsilon_{xy} = \gamma/2$ explains the factor of two between tensor and engineering shear strain.

Build Hooke's law from symmetries and an energy

On a cut normal to $\mathbf{n}$, force per area is the traction $t_i = \sigma_{ij} n_j$. Balancing moments in a continuum without intrinsic body couples gives symmetric Cauchy stress. In an initially unstressed isotropic linear solid a quadratic elastic energy can depend only on the two independent rotationally invariant quadratic forms of the strain.

$$W = \tfrac{1}{2}\lambda (\operatorname{tr}\varepsilon)^2 + \mu\, \varepsilon_{ij}\varepsilon_{ij},$$

$$\sigma_{ij} = \partial W / \partial \varepsilon_{ij} = \lambda \operatorname{tr}\varepsilon\, \delta_{ij} + 2\mu \varepsilon_{ij}.$$

Under uniform dilation $\varepsilon = \eta I$ the bulk modulus is $K = \lambda + 2\mu/3$. Pure shear isolates μ. Stability requires $K > 0$ and $\mu > 0$. The general anisotropic relation $\sigma_{ij} = C_{ijkl}\varepsilon_{kl}$ need not reduce to two constants. Crystal symmetry decides which entries can be determined by rotating a sound measurement.

Recover both moduli from two arrival times

Balance of linear momentum gives $\rho \ddot{u}_i = \partial_j \sigma_{ij}$ in a homogeneous body with no body force. A plane longitudinal displacement has nonzero divergence. A transverse displacement has zero divergence. Substitution gives their phase speeds:

$$c_L^2 = (K + 4\mu/3)/\rho,$$

$$c_T^2 = \mu/\rho.$$

For a solid of density 2500 kg/m³ with $c_L = 5000$ m/s and $c_T = 3000$ m/s the two moduli are $\mu = 22.5$ GPa and $K = 32.5$ GPa. One longitudinal speed would determine only their combination. Short wavelengths comparable with the lattice spacing, or waves in a thin guide, require dispersion or geometric corrections before using these bulk equations.

Tutorial on differential measurements

1 · Recover a missing tidal eigenvalue

▼ Work through the solution

Two transverse values measured outside a spherical source are each -1.5×10^{-6} s⁻². Zero trace implies a radial value $+3.0 \times 10^{-6}$ s⁻². A positive radial gradient means the higher test mass falls slightly less quickly.

---

2 · A diagonal cut through a sheared specimen

▼ Work through the solution

Let only $\sigma_{xy} = \sigma_{yx} = 4$ MPa be nonzero. With $\mathbf{n} = (1, 1, 0)/\sqrt{2}$, traction is $4\mathbf{n}$ MPa. The same stress state that is pure shear on coordinate planes becomes a purely normal traction on this cut.

---

3 · Test isotropic elasticity using an additional wave

▼ **Work through the solution**

If c_T differs systematically for two orthogonal transverse polarisations at the same direction and frequency, a homogeneous isotropic bulk model predicts the wrong degeneracy. Check the sample dimensions and alignment first, then measure crystal orientation before assigning a distinct shear modulus.

For further study see Taylor, Classical Mechanics, chapters 9 and 16 on noninertial observers and elastic continua.

Mechanics in the laboratory

Turn a measured trajectory or force into a test of a mechanical law. Derive the observable, propagate it numerically and determine which parameters the experiment can resolve.

1. Measure gravity with a pendulum of finite amplitude

A metre-long pendulum is an appealing clock because its small-angle period depends only on length and gravity. A precise clock can nevertheless give a precisely wrong value of gravity. Derive the full period, trace the systematic error to an identifiable approximation and design a measurement that distinguishes a length error from a release-angle error.

2. Measure inertia and gravity with two suspension axes

A rigid pendulum can oscillate from either of two knife edges. If the periods agree at distinct distances from the centre of mass, the spacing of the edges determines gravity. Derive the cancellation, identify a second way equal periods can arise and find why a poorly chosen geometry magnifies timing errors.

3. Distinguish a physical precession from numerical drift

A bound orbit circulates many times about its centre. A small change in the angle of successive closest approaches could be physical or could be accumulated phase error. Construct an exactly solvable family of precessing orbits that lets the two effects be compared without assuming a reference trajectory from another code.

4. Which track reaches a lower point first?

A bead is released from rest and slides without friction along a track between two points. A straight track is shortest, yet another path can deliver the bead sooner. Derive the travel-time functional, solve its boundary problem and compare actual times while changing the horizontal distance independently of the vertical drop.

5. When can shaking a support stabilise an upside-down pendulum?

A rapidly oscillating pivot can stabilise a pendulum near its normally unstable upright orientation. Develop the slowly varying effective potential, test its assumptions with the full time-dependent equation and compare the observable that each calculation predicts.

6. When does a smooth circular guide lose contact?

A bead moves inside a vertical circular guide after receiving a known speed at the bottom. Predict whether it turns around, separates from the guide or completes the circle. A normal-force measurement can distinguish these outcomes before a simple top-height energy test can.

Mechanics in the laboratory · 1. Measure gravity with a pendulum of finite amplitude

A metre-long pendulum is an appealing clock because its small-angle period depends only on length and gravity. A precise clock can nevertheless give a precisely wrong value of gravity. Derive the full period, trace the systematic error to an identifiable approximation and design a measurement that distinguishes a length error from a release-angle error.

Define the measured length and time

Use a point bob on a massless, inextensible string attached to a fixed pivot. Let L be the distance from pivot to the bob's centre of mass, and θ the signed departure from the downward vertical. For a rigid extended bob, rotational inertia about its own centre adds to mL^2; a length measured to the bottom of the bob is neither of these dynamical lengths. Measure the elapsed time between successive crossings of a photogate in the same direction. Crossings in opposite directions give half of the period in a symmetric oscillation. A stationary turning point is a poor timing marker because the position error there produces a large time error.

At rest at the release angle θ_0, the energy is $mgL(1-\cos\theta_0)$. At a later angle the speed is $L|\dot\theta|$. Equating kinetic plus potential energy to the release value gives

$$\dot\theta^2 = (2g/L)(\cos\theta - \cos\theta_0).$$

Only a quarter cycle is needed. Inverting the angular speed and integrating from zero to θ_0 produces a square-root singularity at release. The period is finite since integrating the inverse square root over a small interval gives a square root.

Resolve the turning point before approximating

Write $k = \sin(\theta_0/2)$ and substitute $\sin(\theta/2) = k\sin u$. The vanishing square root cancels a factor $\cos u$ from the differential. One obtains the complete elliptic integral of the first kind with modulus k.

$$T = 4\sqrt{\frac{L}{g}}\,K(k),$$

$$K(k) = \int_0^{\pi/2} \frac{du}{\sqrt{1-k^2\sin^2 u}}.$$

Expanding its integrand yields

$$K(k) = (\pi/2)(1 + k^2/4 + 9k^4/64 + \cdots).$$

Since $k \simeq \theta_0/2$ at small amplitude, the first fractional period correction is $\theta_0^2/16$ with angle in radians. It is positive. At larger amplitude the tangential component of gravity rises more slowly with angle than the linear restoring law predicts. The pendulum spends longer near the turns. Passing degrees directly into the quadratic correction would give nonsense even if the timer and recorded angle were perfect.

Infer the bias in gravity

Suppose the true acceleration is $9.81\,\mathrm{m\,s^{-2}}$, the length is 1.000 m and the release angle is 30 degrees. The small-angle period is about 2.0061 s and the finite-amplitude period about 2.0410 s. Interpreting the longer measured period by the linear formula would give about $9.48\,\mathrm{m\,s^{-2}}$. The fractional gravity error is about twice the fractional period error with opposite sign because gravity is inferred from T^{-2}. Timing a hundred periods reduces random timing error but leaves this systematic shift.

The numerical curve evaluates the complete elliptic integral. It uses the arithmetic–geometric mean identity $K(k) = \pi/[2\,\mathrm{AGM}(1, \sqrt{1-k^2})]$, so no sampled point sits on the turning point. The single-correction curve truncates the amplitude series after its first nonconstant term. Vary angle and length, comparing both the predicted period and the result a linear analysis would infer. Which change rescales both period curves together? Which changes their relative discrepancy?

Open this experiment online

Try the calculation

Release angle (degrees) 30

Pendulum length (m) 1

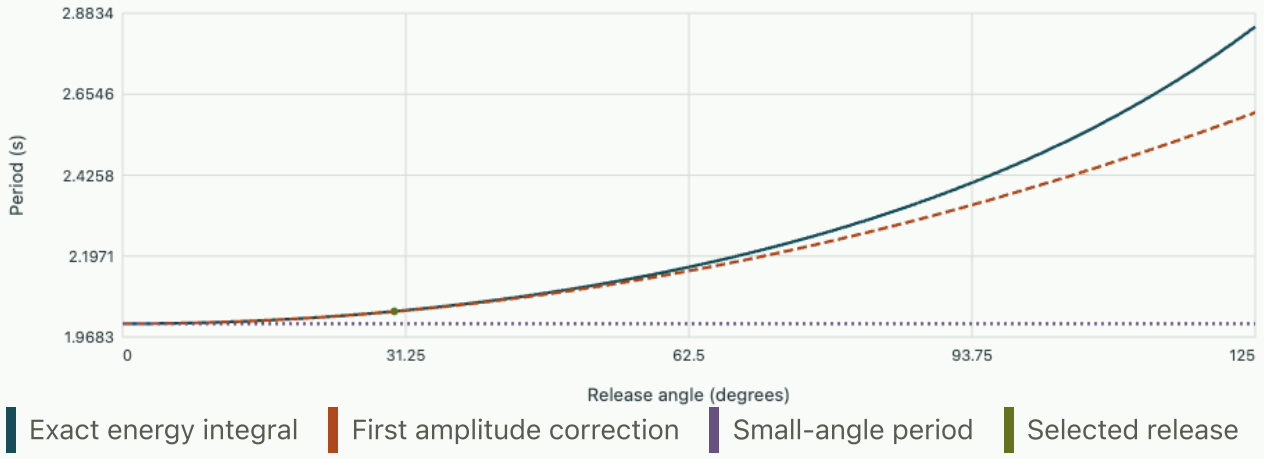

Period 2.041 s. Small-angle analysis would infer g = 9.4772 m/s².

Design a two-release check

For the same pendulum the ratio $T(\theta_a)/T(\theta_b) = K(k_a)/K(k_b)$ cancels the unknown length and local gravity. Measure at two amplitudes before deciding whether to recalibrate the length. If the ratio agrees but both absolute times differ from prediction, check the effective length, clock rate and model of the bob. If the ratio changes during a decaying swing, record initial and final amplitudes for the timed sequence. The period associated with a long sequence is an average over its slowly changing amplitude. Substituting the initial angle throughout would overcorrect the measurement.

Tutorial

At small amplitude, what release angle gives a fractional period bias of approximately one part in a thousand?

▼ **Work through the solution**

Set $\theta_0^2/16 = 0.001$. This gives 0.1265 rad, about 7.25 degrees. The gravity bias from an uncorrected measurement would be approximately two parts in a thousand. A tolerance on one quantity is not automatically the same tolerance on the other.

A photogate records successive interruptions every 1.02 seconds for the metre pendulum. A calculation gives nearly four times local gravity. Identify one possible error in the observable.

▼ **Work through the solution**

The gate may have counted both directions and returned a half period. Doubling that interval gives about 2.04 s. Because the inferred acceleration is inversely proportional to the square of the period, the missing factor of two gives a factor of four.

Why does reducing the grid spacing in an integration of the linear equation fail to recover the finite-amplitude curve?

▼ **Work through the solution**

Integration error vanishes as the step is refined, but the restoring torque in that equation is $mgL\theta$. The true torque is $mgL\sin\theta$. A converged numerical solution can therefore provide independent evidence of an inadequate physical approximation.

For the equation of motion, phase portrait and dissipation, see the MIT treatment of the simple pendulum.

Mechanics in the laboratory · 2. Measure inertia and gravity with two suspension axes

A rigid pendulum can oscillate from either of two knife edges. If the periods agree at distinct distances from the centre of mass, the spacing of the edges determines gravity. Derive the cancellation, identify a second way equal periods can arise and find why a poorly chosen geometry magnifies timing errors.

Torque about an offset pivot

Take a rigid body of mass m with parallel suspension axes perpendicular to its plane of oscillation. Its moment of inertia about the centre of mass is $I_C = m\rho^2$; ρ is the radius of gyration. For a pivot a distance $a > 0$ from the centre, the parallel-axis theorem gives

$$I_a = m(\rho^2 + a^2).$$

Gravity exerts torque $-mga\sin\theta$. In the small-angle limit,

$$T_a^2 = \frac{4\pi^2}{g}\,\frac{\rho^2 + a^2}{a},$$

$$L_a = a + \frac{\rho^2}{a}.$$

Here L_a is the length of a point pendulum with the same period. It can lie beyond the physical centre of mass. A tap applied at this distance from a pivot gives the centre of percussion when the ideal instantaneous pivot reaction is to vanish. The same combination of mass distribution and geometry appears in an impulsive and in an oscillatory measurement because both depend on angular momentum about that pivot.

Match the periods and keep both algebraic branches

Put the second knife edge on the opposite side of the centre at distance b. Equal periods require

$$a + \rho^2/a = b + \rho^2/b.$$

Rearrange before dividing by $a - b$:

$$(a - b)\left(1 - \frac{\rho^2}{ab}\right) = 0.$$

Two equal distances always give equal periods. That branch provides no information about ρ. If the distances are distinct, equality implies

$$\rho^2 = ab.$$

Both equivalent lengths then equal $a + b$, the directly measurable edge separation. For $a = 0.200\,\mathrm{m},\ b = 0.450\,\mathrm{m},\ \rho = 0.300\,\mathrm{m}$, the equivalent length is 0.650 m and both periods at

standard laboratory gravity are about 1.62 s. A small value of $a - b$ is an experimental warning sign, even if the observed equality is exceptionally clean.

Background · Can unequal release amplitudes imitate a mismatch between pivots?

A rigid pendulum about either knife edge obeys the same sine nonlinearity as a simple pendulum. To leading order in its release angle θ in radians, the measured period exceeds the small-amplitude period by the fraction $\theta^2/16$. At matched small-amplitude periods, measurements with amplitudes θ_a, θ_b therefore give

$$\frac{T_a - T_b}{T_0} \simeq \frac{\theta_a^2 - \theta_b^2}{16}.$$

Releasing at 6° about the first edge and 2° about the other creates a fractional mismatch of about 6.1×10^{-4}. For a two-second period this is 1.2 ms. Record the two amplitudes along with the timing data and reduce both periods to the same limit before moving the trim mass. Otherwise the trim can compensate a preparation error.

Extract gravity when the two measured periods differ

Multiply the first period equation by a and the second by b. Subtract to eliminate ρ^2. The exact small-angle result for unequal distances is

$$g = 4\pi^2 \, \frac{a^2 - b^2}{a T_a^2 - b T_b^2}.$$

At matched periods this reduces to the simple expression in terms of the edge spacing. The general formula involves a difference in its denominator. If a and b nearly coincide, the denominator is small and two independent timing errors subtract with poor relative precision. This is a property of the inverse measurement, even if computing each individual period is perfectly well conditioned.

Once g is known, use $\rho^2 = g a T_a^2/(4\pi^2) - a^2$ to recover the body inertia per unit mass. A negative value may indicate a wrong distance measured to the centre or a timing observable that is actually a half period. Verify the result using the second pivot and recover a separately predicted period after shifting a suspension point. A single successful cancellation is weaker than reproducing an additional measurement.

Move one knife edge in the experiment

Hold $a = 0.200\,\mathrm{m}$ fixed and vary both the radius of gyration and the second distance. The graph plots the period against the possible second distance. Before inspecting intersections, predict where the second match should lie as ρ grows. The dependence on distance has a minimum at $b = \rho$ because effective length comprises a growing and a decreasing term.

Open this experiment online

Try the calculation

Radius of gyration (m) **0.3**

Second pivot distance (m) **0.45**

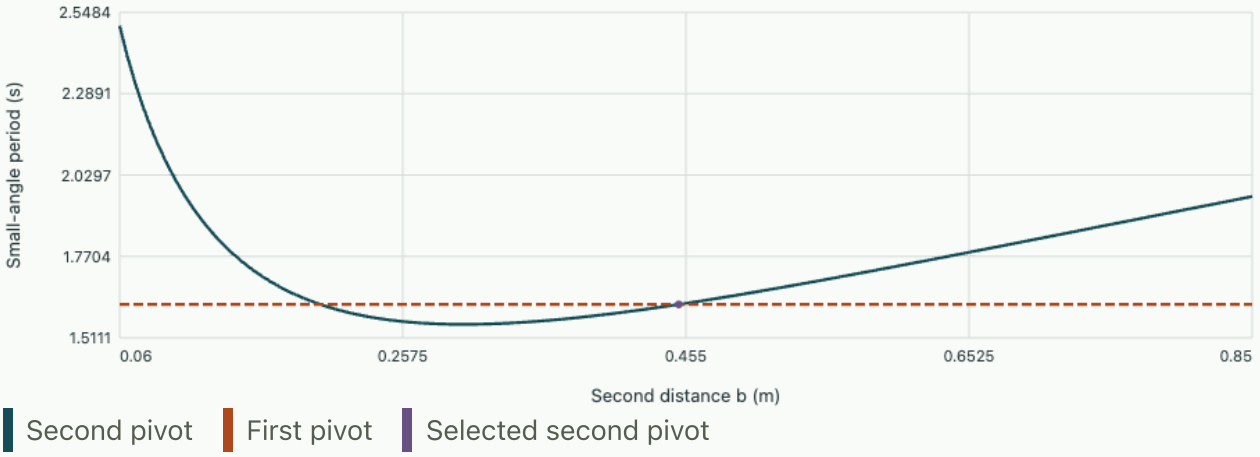

First period 1.6173 s; second 1.6173 s. The other matching distance is 0.45 m.

With a finite oscillation amplitude, the physical pendulum has the same elliptic correction as a point pendulum of length L_a, provided the body is rigid and the frictionless pivot stays fixed. Matching different amplitudes can bias the cancellation. Measuring both at the same small angle removes the leading difference, and extrapolating both to zero amplitude provides a check. Rotational compliance of the knife edge and a shifting centre of mass require a different model.

Tutorial

For $a = 0.240$ m and $\rho = 0.300$ m, where should the second distinct match occur and what length should be used in $g = 4\pi^2 L/T^2$?

▼ **Work through the solution**

The second branch gives

$$b = 0.0900/0.240 = 0.375\,\mathrm{m}.$$

Because the pivots straddle the centre of mass the equivalent length is 0.615 m.

Both pivots lie on the same side of the centre, at the same distances a, b as in the previous question. What changes in the cancellation?

▼ **Work through the solution**

The periods depend on the magnitudes of the offsets, so equal periods still imply $\rho^2 = ab$ on the distinct branch. The sum $a + b$ still gives the equivalent length, but the physical ruler distance between pivots is $|a - b|$. The direct measurement shortcut relies on the chosen geometry.

Why does setting both axes exactly at the same distance make even noise-free measurements insufficient to determine both g and ρ?

▼ **Work through the solution**

The two equations are then identical. For every positive choice of inertia radius the first period determines a corresponding value of gravity. Improving timing precision cannot provide the missing independent equation.

Connect the offset-pivot calculation to the rigid-body inertia chapter.

Mechanics in the laboratory · 3. Distinguish a physical precession from numerical drift

A bound orbit circulates many times about its centre. A small change in the angle of successive closest approaches could be physical or could be accumulated phase error. Construct an exactly solvable family of precessing orbits that lets the two effects be compared without assuming a reference trajectory from another code.

Replace time by the measured polar angle

A particle of mass m moves in a static central potential $V(r) = -k/r + \alpha/(2r^2)$ with $k > 0$. The radial force is $-k/r^2 + \alpha/r^3$. Angular momentum $L = mr^2\dot{\phi}$ is constant. Put $u = 1/r$ and differentiate with respect to ϕ, denoting this derivative by a prime. The identities $\dot{r} = -(L/m)u'$ and $\ddot{r} = -(L^2/m^2)u^2u''$ follow by the chain rule. Subtracting the centripetal term $r\dot{\phi}^2 = (L^2/m^2)u^3$ from radial acceleration gives Binet's equation.

$$u'' + (1+\delta)u = \frac{mk}{L^2},$$

$$\delta = \frac{m\alpha}{L^2}.$$

The sign of the perturbation matters. Positive α gives a repulsive short-range correction, increasing radial frequency per unit angle. A mildly negative correction decreases it. This family is a test potential; a measured nonzero advance in nature need not have this particular cause.

Read apses from a harmonic equation

For $1 + \delta > 0$, write $\nu = \sqrt{1+\delta}$, $u_c = mk/[L^2(1+\delta)]$ and impose $u(0) = u_c(1+e)$, $u'(0) = 0$ with $0 < e < 1$. Then $u = u_c[1 + e\cos(\nu\phi)]$. The radial minimum corresponds to a maximum of u. Its next occurrence is at angle $2\pi/\nu$, so the change of line of apsides per radial period is

$$\Delta\omega = 2\pi\left(\frac{1}{\sqrt{1+\delta}} - 1\right).$$

For $\delta = 0.04$, successive pericentres rotate backwards by approximately 7.0 degrees. At $\delta = 0$ the Kepler ellipse closes. For a strictly circular orbit the algebraic radial frequency has a well-defined small-oscillation limit, but the direction of pericentre of the observed circle has no unique value. A nearly circular orbit therefore has a genuine experimental difficulty even when the integration is accurate.

Compute the bias of a discrete orbit exactly

Shift $v = u - u_c$. On a uniform angular grid of spacing h, the centred second difference gives

$$v_{j+1} = 2v_j - v_{j-1} - (h\nu)^2 v_j.$$

Insert the trial $v_j = e^{ij\psi}$ and simplify:

$$\cos\psi = 1 - \tfrac{1}{2}(h\nu)^2,$$

$$\nu_h = \frac{2}{h}\arcsin(h\nu/2).$$

The numerical mode oscillates if $h\nu < 2$. Inside that range it is too fast, since the arcsine exceeds its argument. A bounded orbit can thus accumulate a negative apsidal error. For an unperturbed Kepler case and a 30-degree grid, the numerical angular frequency is roughly 1.012. Treating this as a physical result would infer a retrograde precession of roughly four degrees per revolution. Refining h halves the angular step and quarters the leading error, because $\nu_h = \nu + \nu^3 h^2/24 + \cdots$.

The experiment plots radial phase after multiple nominal revolutions and reports the implied apsidal angles. Vary the perturbation at fixed step first, then halve the step at fixed perturbation. Distinguish the discrepancy that persists in the continuum from the discrepancy that can be extrapolated away. Starting all curves at pericentre makes the phase convention identical.

Hold the force exactly Newtonian. Compare the accumulated numerical phase on a 30° grid and 6° grid. The exact radial phase stays at zero in both runs. Use the exported values to estimate how the phase error scales when the angular step is divided by five.

Open this experiment online

Try the calculation

Relative force correction δ **0.04**

Angular grid step (degrees) **24**

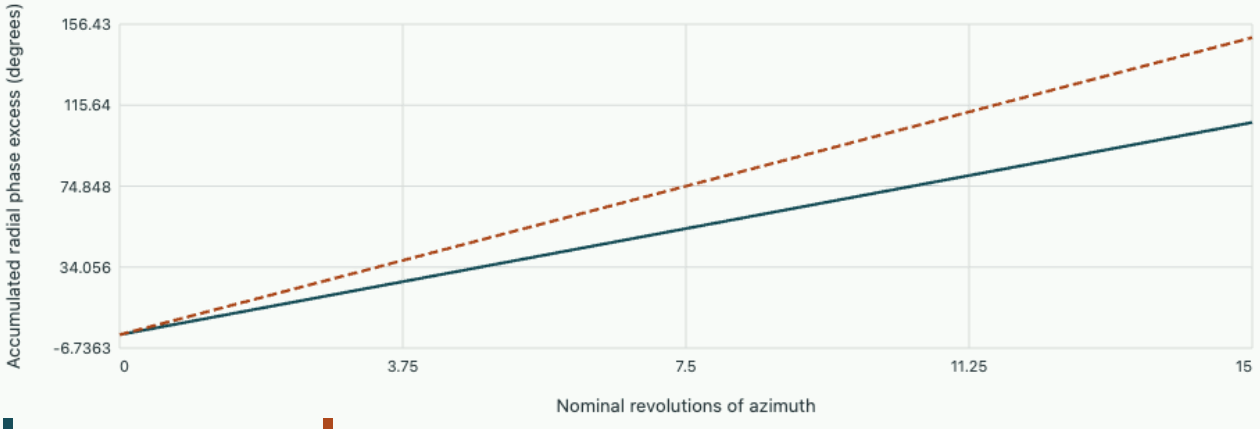

Apsidal advance per radial period: exact -6.991°, numerical -9.7105°.

Tutorial

A measured radial period is 364 degrees of azimuthal advance. In this family, which sign of α is indicated and what is δ?

▼ Work through the solution

The radial cycle takes more than 360 degrees, so the radial frequency per unit angle is below one. The inferred correction is attractive,

$$\delta = (360/364)^2 - 1 \simeq -0.02186.$$

A simulation reports advances of −1.20, −0.60 and −0.45 degrees at successive halvings of the angular step. What leading continuum estimate follows?

▼ Work through the solution

With second-order phase bias, the final difference 0.15 equals three times the remaining magnitude of that bias. Adding 0.05 to −0.45 gives −0.40 degrees. The earlier pair gives the same estimate. An additional refinement tests the assumed scaling.

Can a long observation of a closed numerically integrated orbit rule out a time-step error in the orbital period?

▼ Work through the solution

No. Closure depends on a ratio of radial to azimuthal phase advances. Both may be biased in the same proportion. Independently time successive crossings and compare with an analytic period or a finer integration. Different observables can hide different errors.

The midpoint experiment shows the converse sign of phase error for another bounded integrator.

Mechanics in the laboratory · 4. Which track reaches a lower point first?

A bead is released from rest and slides without friction along a track between two points. A straight track is shortest, yet another path can deliver the bead sooner. Derive the travel-time functional, solve its boundary problem and compare actual times while changing the horizontal distance independently of the vertical drop.

Choose the coordinate appearing in the speed law

Let y increase downwards from the release point, x increase along the horizontal and g be uniform. A small frictionless bead conserves mechanical energy, so its speed at depth y is $\sqrt{2gy}$. For a track expressed as $y(x)$ the time element is line element divided by speed. Hence

$$T[y] = \frac{1}{\sqrt{2g}} \int_0^X \sqrt{\frac{1+y'^2}{y}}\, dx,$$

$$y(0) = 0,$$

$$y(X) = Y.$$

A straight line has distance $\sqrt{X^2+Y^2}$ and component of acceleration $gY/\sqrt{X^2+Y^2}$, giving $T_{\text{line}} = \sqrt{2(X^2+Y^2)/(gY)}$. The advantage of a steeper early path is to build speed at the part of the trajectory where the bead would otherwise remain slow. A path with a longer distance can take less time because distances at different depths cost different amounts of time.

Use a first integral to remove a differential equation

Write the integrand excluding its constant multiplier as $F = \sqrt{1+y'^2}/\sqrt{y}$. Since it contains no explicit x, the Euler–Lagrange equation implies $F - y'F_{y'} =$ constant. Differentiating this expression with respect to x shows the cancellation explicitly:

$$dF/dx = F_y y' + F_{y'} y'';$$

the derivative of the second term removes $F_{y'}y''$ and leaves $y'(F_y - dF_{y'}/dx) = 0$. Substituting the integrand gives $y(1+y'^2) = 2a$ for some positive length a.

Set $y = a(1-\cos u)$. On the descending part $y' = \cot(u/2)$. Integrating $dx = \tan(u/2)dy$ yields

$$x = a(u - \sin u).$$

The signed derivative continues through zero at $u = \pi$ and produces an ascending segment for $\pi < u < 2\pi$. A track may pass below the final point, then climb towards it while spending speed acquired earlier.

Solve for the actual endpoint and clock reading

Divide the endpoint coordinates to eliminate a. The angle u_f solves $(u_f - \sin u_f)/(1 - \cos u_f) = X/Y$ on the first arch. The ratio starts at zero and increases without bound; bisection gives a robust root for positive finite X/Y. Recover $a = Y/(1 - \cos u_f)$. Along the cycloid $ds = 2a \sin(u/2) du$, while $v = 2\sqrt{ga}\sin(u/2)$. Their ratio is finite even at the cusp where both vanish:

$$T_{\text{cyc}} = u_f \sqrt{a/g}.$$

For $Y = 1$ m and $X = \pi/2$ m, $u_f = \pi$ and $a = 0.5$ m. The cycloid time is approximately 0.709 s and the straight track needs about 0.841 s. The endpoint is the bottom of this particular cycloid. Increasing the horizontal offset beyond $\pi Y/2$ makes the first-arch solution turn upwards before it arrives.

Compare two feasible experiments

The graph plots downward depth against horizontal position. Vary endpoint distance and depth, then predict whether the fastest path has an ascending segment. Read the two calculated times. A physical rolling sphere differs from the sliding particle: rotational kinetic energy multiplies the time by a constant factor if the body rolls without slipping with fixed inertia ratio, whereas frictional loss can alter the optimum shape itself. A track with a prescribed minimum bend radius would also define a different variational problem.

Open this experiment online

Try the calculation

Horizontal distance X (m) **1.58**

Vertical drop Y (m) **1**

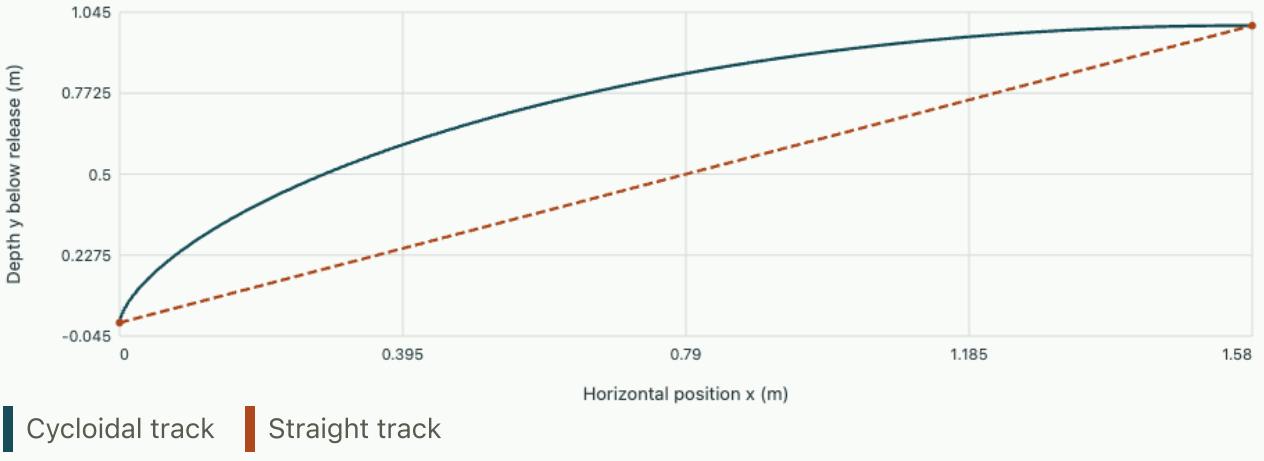

Travel time: cycloid 0.71133 s, straight 0.84429 s. Final cycloid parameter 3.1508 rad.

Tutorial

Keep track shape geometrically similar and double every length. By which factor does the travel time change?

▼ **Work through the solution**

The parameter angle is fixed by a length ratio and a doubles. The time grows by $\sqrt{2}$. The straight track time obeys the same scaling. A measured different exponent would suggest another dimensional scale in the apparatus.

Why might a numerical quadrature applied directly in x at the first sample point report infinite time?

▼ **Work through the solution**

The release speed vanishes and the track has a vertical tangent. The local time integral remains finite. The cycloid parametrisation cancels both vanishing factors analytically. Evaluating a singular endpoint as an ordinary sample in a trapezoidal rule is an integration error.

How can two paths be compared if a common release mechanism imparts a small initial speed v_0?

▼ **Work through the solution**

Energy now gives

$$v(y) = \sqrt{v_0^2 + 2gy}.$$

Recompute the time functional using that speed and the actual initial condition. Subtracting an arbitrary time offset from both runs cannot undo a depth-dependent modification of travel speed.

Revisit the origin of stationary action and essential boundary data in the moving-constraint chapter.

Mechanics in the laboratory · 5. When can shaking a support stabilise an upside-down pendulum?

A rapidly oscillating pivot can stabilise a pendulum near its normally unstable upright orientation. Develop the slowly varying effective potential, test its assumptions with the full time-dependent equation and compare the observable that each calculation predicts.

Start in the moving frame

Measure angle θ from the downward vertical. Let the upward support displacement be $y_p = a\cos\Omega t$. The effective downward acceleration in the translating frame is $g + \ddot{y}_p = g - a\Omega^2\cos\Omega t$. The exact angular equation under these assumptions is

$$\ddot{\theta} + \left(\frac{g}{L} - \frac{a\Omega^2}{L}\cos\Omega t\right)\sin\theta = 0.$$

A simple time average of the coefficient would leave the ordinary pendulum. That would miss the correlation between the rapidly oscillating force and the rapidly oscillating part of the angle. The pivot can do work even though its mean position is fixed. The energy of the pendulum alone is therefore not generally conserved.

Eliminate the fast motion

Write $\theta = \Theta + \xi$, with slowly varying Θ and a small fast correction ξ. In one forcing cycle treat $\sin\Theta$ as constant. Integrating $\ddot{\xi} = (a\Omega^2/L)\sin\Theta\cos\Omega t$ twice for its oscillatory part gives

$$\xi = -(a/L)\sin\Theta\cos\Omega t.$$

Inserting $\sin(\Theta+\xi) \simeq \sin\Theta + \xi\cos\Theta$ into the exact equation creates a product of two cosines with nonzero mean. Retaining the leading averaged terms yields

$$\ddot{\Theta} = -\frac{g}{L}\sin\Theta - \frac{a^2\Omega^2}{2L^2}\sin\Theta\cos\Theta,$$

$$\frac{U_{\mathrm{eff}}}{mL^2} = -\frac{g}{L}\cos\Theta + \frac{a^2\Omega^2}{4L^2}\sin^2\Theta.$$

Two approximations entered. The displacement ratio a/L must keep micromotion small and the drive must be fast compared with the slow angular motion. A large acceleration $a\Omega^2$ can coexist with a small displacement a; acceleration alone is not the stability criterion.

An observable threshold

Expand about $\Theta = \pi + \eta$. The averaged restoring coefficient is

$$\omega_{\mathrm{up}}^2 = a^2\Omega^2/(2L^2) - g/L.$$

A local minimum appears if $a\Omega > \sqrt{2gL}$. For $L = 0.15$ m and a 60 Hz vertical vibration the threshold amplitude is approximately 4.55 mm. At 6 mm the averaged small-oscillation frequency is about 1.11 Hz. A motion sensor attached to the bob will also see the 60 Hz micromotion. Comparing an unfiltered peak with the slow prediction can make the theory seem wrong even when the averaged phase portrait is accurate.

Test the slow approximation against a full integration

Release the bob slightly off the top and change the drive frequency or amplitude. The plot samples the exact forced equation once per forcing period at a fixed phase and compares it with the averaged equation evaluated on the same time grid. The observable is angular deviation from the top, with full turns retained. Small bounded oscillations depend on initial displacement as well as the local curvature; outside the linear range a pendulum can leave the top even when the curvature is positive. Very near the threshold a short record is poor evidence for stability because both a small growth rate and a small oscillation frequency produce slow motion.

Open this experiment online

Try the calculation

Vertical amplitude (mm) **6**

Drive frequency (Hz) **60**

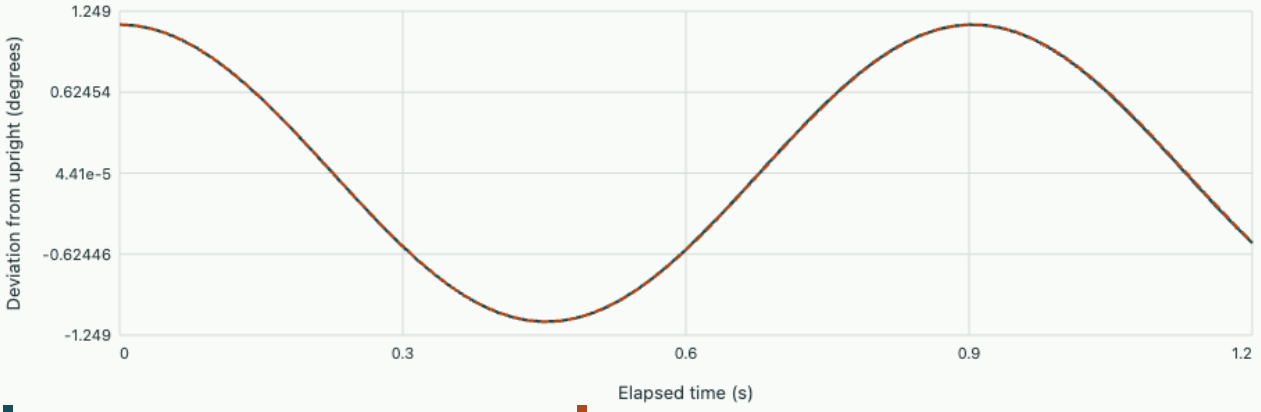

Threshold amplitude 4.5506 mm. Averaged upright curvature 48.298 s⁻²; oscillation frequency 1.1061 Hz.

Tutorial

Two drives have the same product $a\Omega$ but one uses twice the frequency. What is identical in the averaged model and what differs in the full motion?

▼ **Work through the solution**

The leading effective potential is unchanged. The higher-frequency drive has half the displacement amplitude and therefore smaller leading angular micromotion. Its separation of time scales is typically better.

Is exactly upright motion evidence that the drive has stabilised the pendulum?

▼ **Work through the solution**

At $\theta = \pi, \dot{\theta} = 0$ the sine vanishes for all time. This exact trajectory exists even below threshold. Release with controlled positive and negative tilts and assess whether nearby trajectories remain close.

If the drive is switched off after one second, can the effective potential still be used to predict a permanently stable upright position?

▼ **Work through the solution**

Once the pivot stops, only the ordinary gravitational potential remains. Integrate the undriven equation using the angle and angular velocity at switch-off. The phase of the rapid motion can affect that initial state.

Compare slow stabilisation here with parametric growth near twice a mode frequency.

Mechanics in the laboratory · 6. When does a smooth circular guide lose contact?

A bead moves inside a vertical circular guide after receiving a known speed at the bottom. Predict whether it turns around, separates from the guide or completes the circle. A normal-force measurement can distinguish these outcomes before a simple top-height energy test can.

Check the constraint force after solving for speed

Use $\theta = 0$ at the bottom, increasing along the rising side. Let R be the radius of the bead centre's path, v_0 its bottom speed and $u = v_0^2/(gR)$. The smooth guide does no work. The rise in gravitational energy $mgR(1 - \cos\theta)$ therefore gives

$$v^2/(gR) = u - 2 + 2\cos\theta.$$

This relation applies only while the bead follows the circle and the computed speed is real.

With inward radial direction positive, force balance is

$$N - mg\cos\theta = mv^2/R.$$

Substitution gives

$$\frac{N}{mg} = u - 2 + 3\cos\theta.$$

A guide underneath the bead can push but cannot pull. For $u < 2$ the speed first reaches zero while the contact force is still positive. For $2 < u < 5$ the force reaches zero with positive speed at $\cos\theta = (2 - u)/3$. Above that point circular motion would require a negative normal force. For $u > 5$ the bead can remain in contact throughout the circle. At the boundaries $u = 2$ gives a zero-speed, zero-normal grazing turn at the side and $u = 5$ gives marginal contact at the top. A captive slotted carriage or a bead threaded onto a wire has a different constraint and can transmit force of either sign.

Distinguish an energetically accessible top from a feasible trajectory

Let $R = 0.25$ m and choose $v_0 = \sqrt{3gR} = 2.71$ m/s. The guide loses contact when $\cos\theta = -1/3$, or at 109.5 degrees from the bottom. The remaining speed there is $\sqrt{gR/3} = 0.904$ m/s. Raising the initial energy so that $u = 4$ pays the gravitational energy cost to reach the top, but a continuously guided motion still fails the nonnegative force condition earlier. The mechanical-energy and force-balance tests answer different questions.

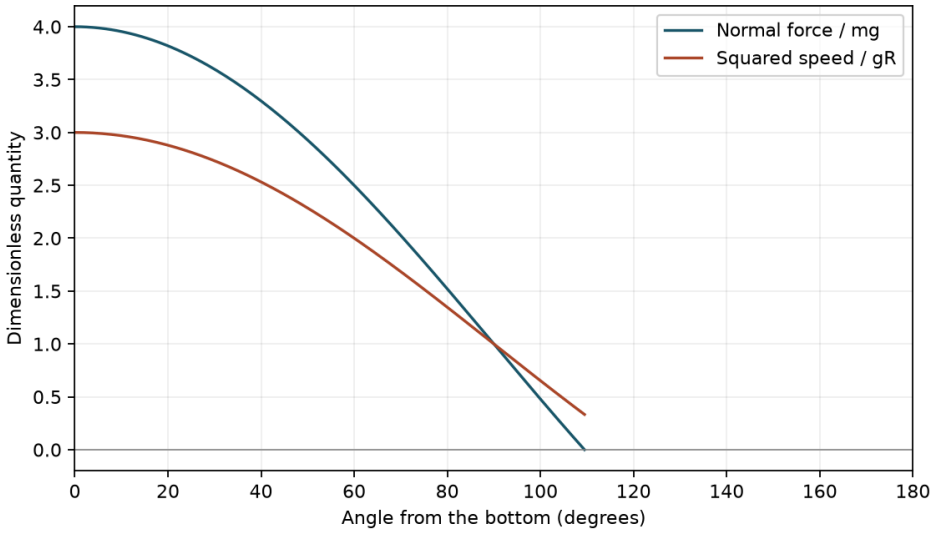

The first quantity to reach zero determines which constraint fails. The part after contact loss requires a different trajectory.

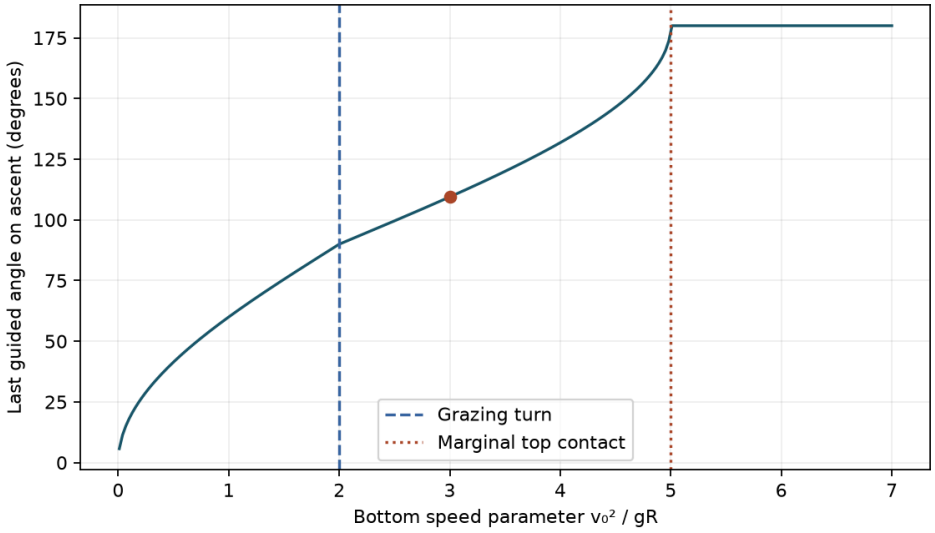

The horizontal branch records completion of the ascent, including marginal contact at its threshold. It does not mean that the bead stops at the top.

Exercise · find the lower turning point

For $u = 1$, determine the turning angle and force there.

▼ Work through the solution

Zero speed requires $\cos\theta = 1 - u/2 = 1/2$, hence $\theta = 60^\circ$. The contact force then balances the outward radial component of gravity, $N = mg\cos\theta = mg/2$. It remains compressive through the turn.

Exercise · size a classroom loop

A bottom speed of 2.0 m/s is available. What is the largest ideal path radius for continuous contact through the top?

▼ **Work through the solution**

The limiting condition is $v_0^2 = 5gR$, so $R = 4/(5 \cdot 9.81) = 0.0815$ m. This is the radius of the bead centre. Rolling friction, rotational kinetic energy or a different channel radius would alter this calculation.

Try it · Guide contact

Change the inputs and compare the recalculated curves with the preceding derivation and baseline figure. The axes give the units; the numerical readout states the model assumptions and any limiting cases. Reset the inputs to return to the reference setting.

Open this live calculation

Try the calculation

Bottom speed squared / gR 3

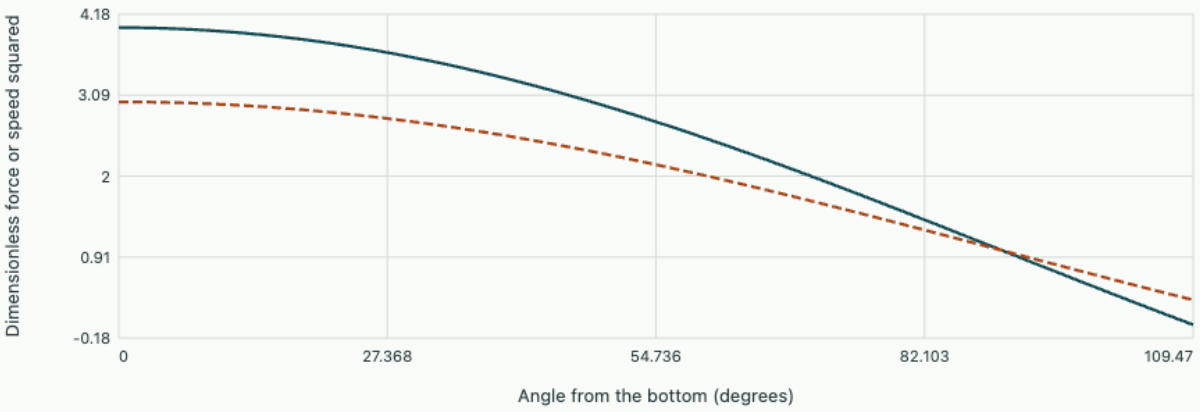

Loses contact at 109.47°. Curves stop at the first physical limit of the unilateral guide.

Download the corresponding editable notebook. The browser recalculates the reduced equations directly; the notebook exposes the full calculation and its checks.

Open editable notebook Download .ipynb

Forces, constraints and a real instrument

Use virtual work to choose generalised coordinates. Test the predictions for a moving support, a constrained slider and an instrument that exchanges mechanical and electrical energy.

1. From cut forces to local equilibrium
2. How a continuum balance becomes a finite-element stiffness matrix
3. Finding a displacement when no load acts in its direction
4. Coordinates, energy and equivalent inertia
5. Energy coordinates and Lagrange’s equation
6. Why a radial slide presses sideways on a rotating guide
7. When a suspended capacitor loses its stable equilibrium
8. A moving-coil galvanometer as an electrical and mechanical system
9. Why an oscillator can move without its packet spreading

From cut forces to local equilibrium

Engineering mechanics

A support reaction tells you the total force entering a part. To predict what an inclined internal surface carries, keep track of both the orientation of the cut and the direction of the force across it.

A force that depends on the surface you choose

Imagine a small triangular wedge cut out of a thin, slowly loaded plate. Its sloping face has unit outward normal $\mathbf{n} = (n_x, n_y)$ and area A. The two faces normal to the coordinate axes have areas An_x and An_y when both components are positive. Name the internal force per unit area on a face its traction. Opposite faces of the same cut carry equal and opposite tractions. Gravity and acceleration act on volume, which shrinks faster than area as the wedge shrinks. Dividing its force balance by A therefore gives a relation that no longer contains its size.

$$\mathbf{t}(\mathbf{n}) = n_x \mathbf{t}(\mathbf{e}_x) + n_y \mathbf{t}(\mathbf{e}_y) = \boldsymbol{\sigma}\mathbf{n}.$$

The columns of the stress matrix are the two coordinate-face tractions. Their linear combination supplies the force on any inclined face. A small square additionally needs zero net moment. To leading order, the shear forces on opposite faces form two couples of opposite sign and equal lever arm. Their balance requires $\sigma_{xy} = \sigma_{yx}$ for an ordinary material without internal body couples.

> **Background · Traction**
>
> $$\mathbf{t}(\mathbf{n}) = \boldsymbol{\sigma}\mathbf{n}$$
>
> Specify the plane normal before projecting the force per area into normal and shear parts. A stress component is not a net force until integrated over an area.

Why a gradient of stress carries a body force

Now use a tiny rectangular element of side lengths dx, dy and unit thickness. The right-face contribution to horizontal force is $\sigma_{xx}(x + dx, y)dy$; the left face contributes its negative evaluated at x. Their difference is $\partial_x \sigma_{xx}\, dx\, dy$ to leading order. Resolve the upper and lower shear tractions in the same way. Add a prescribed horizontal force per volume b_x and divide by volume. Repeating in the vertical direction produces two independent equations.

$$\partial_x \sigma_{xx} + \partial_y \sigma_{xy} + b_x = 0,$$
$$\partial_x \sigma_{xy} + \partial_y \sigma_{yy} + b_y = 0.$$

These equations say nothing yet about how much the material stretches. They can test an assumed stress field before the elastic modulus has even been measured. A candidate must also reproduce the applied boundary tractions. Satisfying the interior equations alone leaves many possible stresses.

Worked example · the grip on a diagonal bonding plane

At a measurement point let $\sigma_{xx} = 60, \sigma_{yy} = 20, \sigma_{xy} = 10$ MPa. The outward normal is $(0.6, 0.8)$. Matrix multiplication gives $\mathbf{t} = (44, 22)$ MPa. Projection along the normal gives $0.6(44) + 0.8(22) = 44.0$ MPa tension. Projection on the unit tangent $(-0.8, 0.6)$ gives -22.0 MPa. Reversing the tangent changes the sign of reported shear. Reversing the surface normal reverses the traction vector itself. For a uniform 100 mm² patch the force has components 4.40 and 2.20 kN. Using only normal stress would miss the tangential load that the adhesive must transmit.

Worked example · a specimen with a known stress gradient

Stand a bar upright, support it at its bottom and leave the top free. Use upward y, length L, constant density ρ, and tension positive. The vertical equation reads $d\sigma_{yy}/dy - \rho g = 0$. Integrating from the free top gives

$$\sigma_{yy} = \rho g (y - L).$$

For a 3.0 m aluminium bar of density 2700 kg/m³ the base stress is −79.5 kPa. Its upward support traction is positive because the bottom face has downward outward normal. A uniform cross-sectional area of 200 mm² gives a base reaction of 15.9 N, equal to the weight. The local and global checks involve different quantities but must agree.

Find the angles where the shear traction passes through zero. Compare each with an extremum of the normal traction. Change the sign of the imposed xy shear, sketch the new angles before moving the slider, and check whether the two extreme normal stresses change.

Open this experiment online

Try the calculation

Normal stress xx (MPa) **60**

Shear stress xy (MPa) **10**

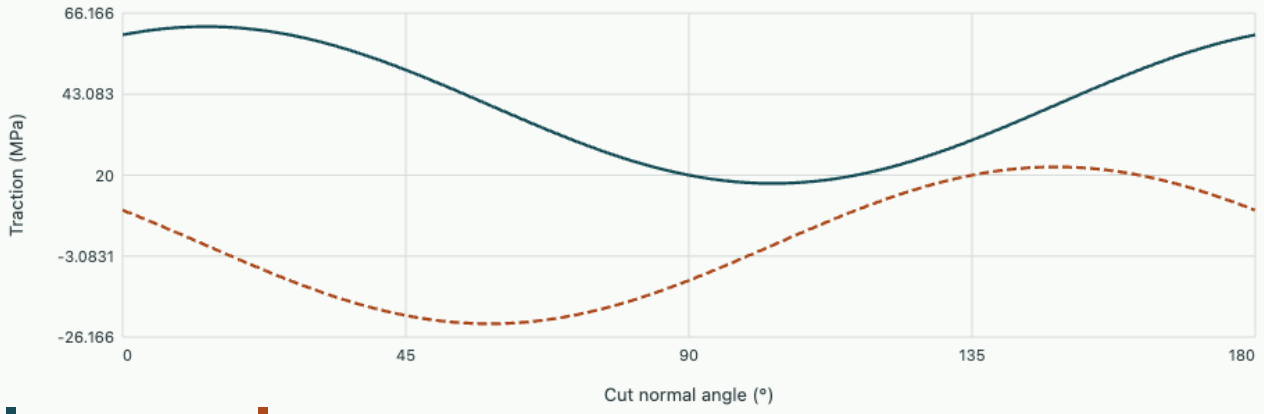

On the cut with normal (0.6, 0.8), the normal traction is 44.00 MPa and the signed shear is -22.00 MPa.

Tutorial · test a candidate before using a material law

In a region with x, y in metres, propose $\sigma_{xx} = ax,\ \sigma_{xy} = -ay,\ \sigma_{yy} = 0$, where $a = 2.0$ MPa/m. Does the field need a body force? Find the traction at $x = 0.30,\ y = 0.20$ m on a face normal to positive x.

▼ **Check the balance and the boundary reading**

The horizontal divergence is $a - a = 0$. The vertical divergence is zero because the shear has no x variation. No body force is needed. The face sees the first column of the matrix, $(0.60, -0.40)$ MPa. A traction-free exterior at that location would reject this field even though it satisfies both interior equations.

Further reading · A. F. Bower, Applied Mechanics of Solids, §2.3, internal forces and stress

How a continuum balance becomes a finite-element stiffness matrix

Engineering mechanics

A single bar element can predict an end displacement exactly and still miss the stress field inside. The difference follows directly from the balance it is asked to satisfy.

Turn a differential balance into work against a test displacement

Let a straight small-strain bar of length L have area A, Young's modulus E, displacement $u(x)$ and distributed axial load $q(x)$ in N/m. Tensile axial resultant is $N = EAu'$. Force balance on a slice gives $N' + q = 0$. Clamp the left end and prescribe a right-end force P. Multiply the balance by any smooth virtual displacement v satisfying $v(0) = 0$, integrate along the bar, and integrate the derivative of N by parts.

$$\int_0^L EA\,u'v'\,dx = P\,v(L) + \int_0^L qv\,dx.$$

The boundary term at the clamp disappears because that displacement is prescribed. The unknown reaction can later be recovered by equilibrium. This formulation requires only first derivatives of trial displacements. Piecewise linear displacements are therefore admissible even though their slopes may jump at internal nodes.

Compute the stiffness rather than memorising it

On an element from $x = 0$ to h, interpolate the two nodal displacements linearly:

$$u = (1 - x/h)u_1 + (x/h)u_2.$$

Let the test displacement have the same two basis functions. A virtual change of the first or second node gives the corresponding row of the balance. Both derivatives are constant with opposite signs.

$$B = [-1/h \quad 1/h], \qquad K_e = \int_0^h B^T EAB\,dx = \frac{EA}{h}\begin{bmatrix} 1 & -1 \\ -1 & 1 \end{bmatrix}.$$

For a constant distributed load, each basis function integrates to $h/2$, so each node receives equivalent load $qh/2$. The two rows of stiffness sum to zero. A uniform translation stores no strain energy. At a shared node the neighbouring virtual-work contributions add because both elements refer to the same unknown displacement.

Worked example · compare a nodal value with the stress in a cell

Take a 1 m bar with $EA = 2.0$ MN, uniform $q = 1200$ N/m and free right end. Exact balance integrated from $N(L) = 0$ gives

$$N = q(L - x).$$

Integrating strain from the clamp produces $u = q(Lx - x^2/2)/(EA)$. The free-end displacement is 0.300 mm. With a single element the free row of the discrete system has stiffness EA/L and load $qL/2$, giving the same displacement. Yet its piecewise constant axial force is

$$EAu(L)/L = 600\,\mathrm{N}.$$

The exact force ranges from 1200 N at the clamp to zero at the free end. The numerical force represents the mean over the cell.

Worked example · see what doubling resolution changes

Divide the bar into two equal elements. The middle node receives 600 N from both halves together, while the free node receives 300 N. The right element carries 300 N. Equilibrium of the middle node then puts 900 N in the left element. Their extensions are $900(0.5)/(2 \times 10^6) = 0.225$ mm and 0.075 mm. Nodal displacements agree with the exact quadratic at both nodes. The largest one-sided stress-resultant error within either element is now 300 N instead of 600 N. Comparing only tip displacements would hide this improvement.

Double the number of cells until the force error is below 100 N for the baseline load. Inspect the values on both sides of an element boundary and explain why agreement in tip displacement alone could have ended this refinement study too early.

Open this experiment online

Try the calculation

Number of elements 2

Distributed load (N/m) 1200

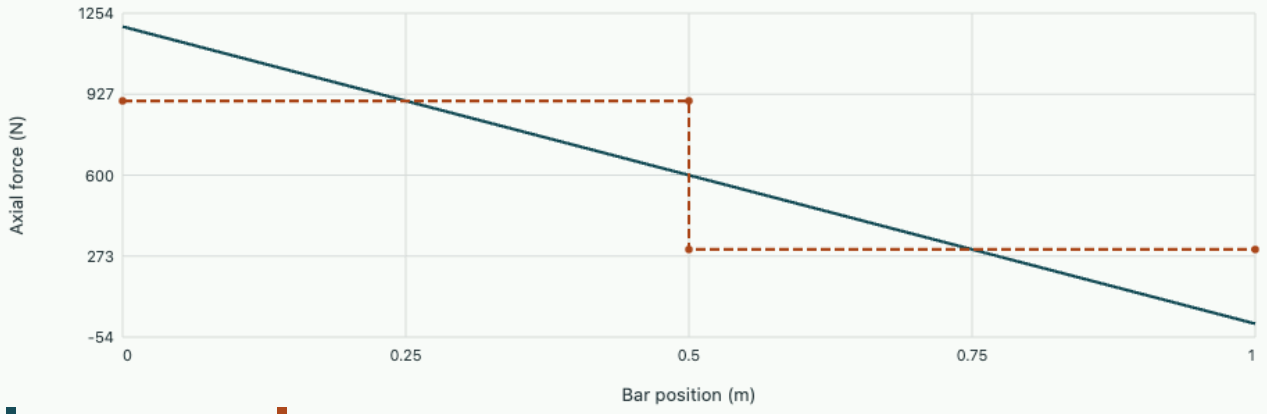

The tip displacement is 0.300 mm on every mesh here. Maximum axial-force error is 300.0 N with 2 elements.

A related OneSimulation calculation

Compare the bar's nodal displacement with a OneSimulation truss assembled from axial members. Run the area-doubling case and check the predicted inverse-area change in displacement.

Run the truss stiffness comparison in OneSimulation

Tutorial · find the support reaction from the discarded row

For the two-element calculation, recover the left reaction using the assembled loads and displacement. Then derive an expression for the maximum axial-force error with n equal elements. Why can two different mesh studies give two different conclusions?

▼ **Evaluate the clamp row and the local profile**

The left internal nodal force is -900 N. The left external distributed-load share is $+300$ N. Equilibrium requires an additional reaction -1200 N. On an element of width L/n the exact linearly varying force changes by qL/n; its constant midpoint approximation misses an endpoint by $qL/(2n)$. Tip displacement and maximum local force answer different engineering questions. Mesh convergence must therefore name its measured quantity.

Further reading · A. F. Bower, Applied Mechanics of Solids, §8.1, finite-element equations for elastic solids

Finding a displacement when no load acts in its direction

Engineering mechanics

A displacement gauge measures the lateral travel of a truss joint under a vertical load. A force balance determines the bar forces, but cannot directly give the sideways motion. Introduce a dummy load, differentiate the stored energy and recover the gauge reading with its sign.

Link an external force coordinate to stored strain energy

For a linear elastic pin-jointed truss, neglect support movement and temperature changes and assume small displacements. Bar i has constant axial force N_i, length L_i, modulus E_i and area A_i. Integrating its force against its extension gives

$$U_i = N_i^2 L_i/(2E_i A_i).$$

Superposition makes each force linear in the external loads. A small increment of load changes the equilibrium configuration. For a linear elastic conservative system the complementary energy equals U and its derivative with respect to an independent applied force gives displacement along that force.

$$U = \sum_i \frac{N_i^2 L_i}{2E_i A_i},$$

$$\delta_Q = \frac{\partial U}{\partial Q} = \sum_i \frac{N_i n_i L_i}{E_i A_i},$$

$$n_i = \frac{\partial N_i}{\partial Q}.$$

The derivative n_i is the member force produced per unit trial load in the requested direction, with all other independent loads held fixed. Solve this trial equilibrium even if $Q = 0$ physically. Setting $Q = 0$ before differentiating erases its entire contribution. As a dimensional check, n_i is dimensionless when Q and N_i both use newtons, and the sum has dimensions of length.

Compute the two-bar flexibility matrix

A joint hangs from two overhead pins by straight bars slanting up-left and up-right, each at 45° to horizontal. Positive joint coordinates are rightward and downward. Let V be the applied downward force and H the rightward force; bars carry tension positive. Equilibrium gives

$$N_L = (V + H)/\sqrt{2},\ N_R = (V - H)/\sqrt{2}.$$

Define bar axial compliances $c_i = L_i/(E_i A_i)$. Insert the forces into the energy and differentiate with respect to H and V independently:

$$\begin{bmatrix} \delta_H \\ \delta_V \end{bmatrix} = \frac{1}{2} \begin{bmatrix} c_L + c_R & c_L - c_R \\ c_L - c_R & c_L + c_R \end{bmatrix} \begin{bmatrix} H \\ V \end{bmatrix}.$$

The cross coefficients are equal because the mixed derivatives of the stored energy commute. This is Maxwell–Betti reciprocity. A cross displacement can be negative even though both direct compliances and stored energy are positive. The eigenvalues of this particular flexibility matrix are c_L, c_R, corresponding to the two independent bar-extension directions.

Predict a sideways gauge reading and reverse the test

Take $c_L = 0.0020,\ c_R = 0.0040$ mm/N. At $V = 100$ N and $H = 0$, both members carry 70.71 N. The vertical displacement is 0.300 mm, and the horizontal displacement is −0.100 mm. The more compliant right bar stretches farther; the joint moves left and down to accommodate both bar extensions. Half the vertical load times its displacement gives 15 N mm of strain energy. Summing the two bar energies independently gives the same result.

Apply instead $H = 100$ N and $V = 0$, assuming the slender right bar remains stable under compression. The vertical reading is −0.100 mm and horizontal motion is +0.300 mm. Thus the lateral response to the vertical test predicts the vertical response to a lateral test of equal magnitude. Equalizing bar areas would remove the cross response if the lengths and moduli matched. In practice a pin with clearance or a cable that goes slack can break the assumed linear bilateral response.

Exchange the left and right compliances. Before looking at the new graph, mark which readout should reverse sign and which should remain equal. Then set the two values alike and identify the symmetry that removes cross-coupling.

Open this experiment online

Try the calculation

Left bar compliance (µm/N) 2

Right bar compliance (µm/N) 4

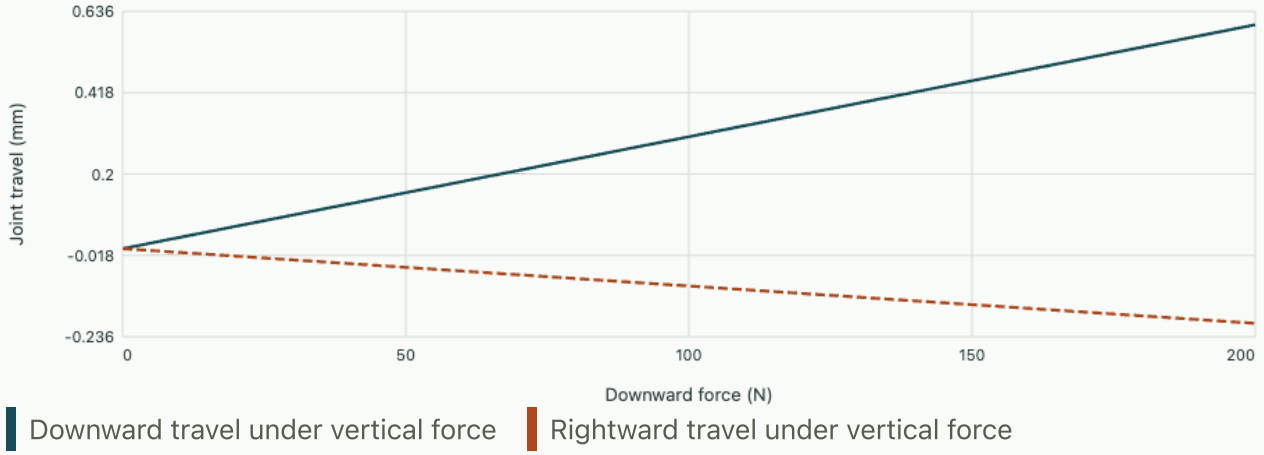

At 100 N down the joint travels 0.300 mm down and -0.100 mm right. By reciprocity the latter also gives downward travel under 100 N right.

A related OneSimulation calculation

Use the course truss to test the same flexibility scaling on a larger assembly. Double every member area at fixed loads and geometry, then compare the joint displacement with the separately calculated chord force.

Run the OneSimulation truss experiment

Tutorial · identify the two member compliances from one load case

A 200 N vertical test gives +0.50 mm down and +0.10 mm right. Estimate each compliance and predict horizontal travel under simultaneous 60 N rightward and 100 N downward loading. How can one additional gauge reading test reciprocity?

▼ **Show the identification and loading prediction**

Direct compliance is $0.50/200 = 0.0025$ mm/N and cross compliance is $0.10/200 = 0.0005$ mm/N. Adding and subtracting gives $c_L = 0.0030,\ c_R = 0.0020$ mm/N. The predicted horizontal motion is

$$0.0025(60) + 0.0005(100) = 0.200\,\mathrm{mm}.$$

A 200 N rightward test should give +0.10 mm down. A disagreement after changing load direction suggests checking seating and the linear-elastic domain before assigning a single compliance to each bar.

Further reading · David Roylance, MIT 3.11 · truss displacements, strain energy and Castigliano's theorem

Coordinates, energy and equivalent inertia

Machine dynamics

Reduce a constrained drive to one coordinate and use a power balance to check its equation of motion.
FROM FIRST PRINCIPLES

Refer moving masses to one shaft by matching kinetic energy

Choose shaft angle θ as the independent coordinate of a rigid mechanism. Suppose the angular speeds of its rotating components and the linear speeds of its translating components are fixed multiples of $\dot{\theta}$. Assume ideal constraints with no slip, so specifying θ and $\dot{\theta}$ fixes the motion. Total kinetic energy is the sum of the individual translational and rotational energies.

$$T = \sum_i \tfrac{1}{2} m_i v_i^2 + \sum_j \tfrac{1}{2} J_j \omega_j^2 = \tfrac{1}{2} J_{\mathrm{eq}} \dot{\theta}^2.$$

Here rotational inertias are about the component centres or fixed rotation axes as appropriate, with no motion counted twice. Dividing by $\dot{\theta}^2/2$ gives the inertia seen at the chosen shaft.

$$J_{\mathrm{eq}} = \sum_i m_i \left(\frac{v_i}{\dot{\theta}} \right)^2 + \sum_j J_j \left(\frac{\omega_j}{\dot{\theta}} \right)^2.$$

A force on a translating part contributes the shaft torque that gives the same instantaneous power,

$$T_i \dot{\theta} = F_i v_i.$$

For constant speed ratios and constant equivalent inertia, energy balance then gives

$$\sum T_i = J_{\mathrm{eq}} \ddot{\theta}.$$

The square on the speed ratio in inertia reflection follows from energy and is essential when changing the reference shaft.

Background · Generalised inertia

$$M(q) = 2T/\dot{q}^2$$

This scalar definition applies to one independent moving coordinate with purely quadratic kinetic energy. Changing the coordinate changes the numerical inertia.

DERIVATION AND APPLICATIONS

Derive the extra drive term for position-dependent inertia

A motor can require a torque at constant angular speed if a mechanism changes the linear speed of its payload during a revolution. Use a single angular coordinate θ, input inertia J_0, and a guided mass m with position $x = f(\theta)$. Assume a rigid lossless linkage and a horizontal guide, so gravity does no work. The kinematic constraint sets the payload velocity and fixes the instantaneous reflected inertia by equating the total kinetic energy to that of one shaft.

$$\dot{x} = f'(\theta)\dot{\theta},$$
$$T = \tfrac{1}{2}[J_0 + m(f')^2]\dot{\theta}^2 = \tfrac{1}{2}J(\theta)\dot{\theta}^2.$$

Differentiate the energy with respect to time. The shaft input supplies the full change in kinetic energy through its power $\tau\dot{\theta}$. Equating the two and cancelling speed gives the required drive torque. At a turning point the same equation follows directly from Lagrange's equation.

$$\tau = J(\theta)\ddot{\theta} + \tfrac{1}{2}J'(\theta)\dot{\theta}^2.$$

For an ideal sinusoidal guide $x = a\sin\theta$, substitution makes the speed-squared contribution explicit. It changes sign within each turn because the translating payload first absorbs and then releases kinetic energy.

$$J = J_0 + ma^2\cos^2\theta,$$
$$\tau = J\ddot{\theta} - ma^2\sin\theta\cos\theta\,\dot{\theta}^2.$$

A constant-inertia approximation omits this alternating torque even if it predicts the total energy averaged over a turn. Its integral over a full constant-speed revolution vanishes as the payload returns to its initial speed.

WORKED EXAMPLE

Predict a constant-speed torque measurement

A 2.00 kg carriage follows $x = 0.0500\sin\theta$ metres with shaft speed 20.0 rad/s. At $\theta = 45^\circ$ its required torque is $-2.00(0.0500)^2(0.5)(20.0)^2 = -1.00$ N m. The motor absorbs 20.0 W at that instant. At 135° the required torque is $+1.00$ N m. Both readings occur at the same shaft speed and the same reflected inertia.

Change the inputs and inspect this calculation below

SECOND APPLICATION

Identify a payload from the torque harmonic

A separate horizontal mechanism has stroke parameter $a = 40.0$ mm and runs at 30.0 rad/s. After removing its empty-linkage trace, the measured second-harmonic torque amplitude is 0.720 N m. Since $|\sin\theta\cos\theta|_{\max} = 1/2$, the fitted mass is

$$2(0.720)/[(0.0400)^2(30.0)^2] = 1.00\,\mathrm{kg}.$$

A run at half speed should show 0.180 N m amplitude if the measured harmonic is inertial.

Interactive calculation · Change the inputs of this example

Use the adjustable quantities to test the two worked calculations above. The plot recomputes this derivation's balance or constitutive relation; its numerical readout reports the quantities needed for the forward calculation and the inverse or design question. Keep the fixed assumptions stated in the readout when comparing with the example values.

Open this live calculation

Try the calculation

Carriage mass (kg)	2
Motion amplitude (mm)	50
Constant shaft speed (rad/s)	20

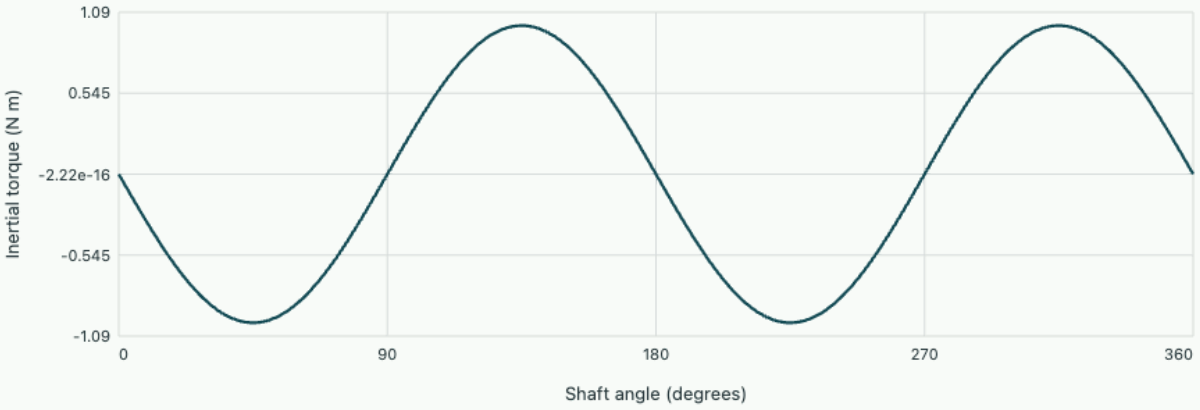

Constant-speed carriage torque

Torque-harmonic amplitude 1.000 N m. Energy is exchanged despite zero shaft acceleration.

Follow the motion through a mechanism

A motor accelerating a load feels inertia from components that turn at different speeds. Simply adding their physical moments of inertia would treat all of those speeds as equal. Instead, choose one independent coordinate and express every kinetic energy in terms of it. No-slip belts, rigid gears and inextensible cables give useful constraints when their compliance and backlash are negligible over the motion of interest.

Consider a drum of radius R winding a cable carrying a vertically guided mass m. Choose the drum angle θ positive when the mass rises. If the effective winding radius is constant, displacement, velocity and acceleration satisfy $x = R\theta$, $\dot{x} = R\dot{\theta}$ and $\ddot{x} = R\ddot{\theta}$. These equalities are kinematic. A torque relation requires force balance or work in addition. When the cable builds successive layers on a spool, the effective radius varies with angle and the constant-ratio assumption must be revisited.

Background · What changes when the reflected inertia depends on position?

For a piston linkage let the piston position be $x(q)$, where q is shaft angle. Its kinetic energy contributes $m(dx/dq)^2$ to the shaft inertia. As the linkage moves through a stroke this contribution varies, even for a piston of constant mass. Use the energy derivative to find the generalised inertial torque.

$$\frac{d}{dt}\frac{\partial T}{\partial \dot{q}} - \frac{\partial T}{\partial q} = J(q)\ddot{q} + \tfrac{1}{2}J'(q)\dot{q}^2,$$

$$T = \tfrac{1}{2}J(q)\dot{q}^2.$$

Uniform shaft speed sets the first term to zero. The second term represents kinetic energy flowing into and out of the accelerating piston. Its shaft work over a complete cycle vanishes when the mechanism returns to the same angle and speed. An average torque meter can consequently miss a substantial alternating torque.

Reflect mass and forces to a common shaft

Let J_d be the drum inertia. Add the rotational energy of the drum to the translational energy of the load, then express both in terms of the drum speed.

$$\begin{aligned} K &= \tfrac{1}{2}J_d\dot{\theta}^2 + \tfrac{1}{2}m\dot{x}^2 \\ &= \tfrac{1}{2}\left(J_d + mR^2\right)\dot{\theta}^2, \\ J_{\mathrm{eq}} &= J_d + mR^2. \end{aligned}$$

A small positive angle raises the mass through $R\,d\theta$, increasing its potential energy by $mgR\,d\theta$. Thus gravity contributes a resisting torque mgR. A positive applied torque T_d supplies power $T_d\dot{\theta}$. Applying the energy balance gives the equation of motion.

$$\frac{d}{dt}\left(\tfrac{1}{2}J_{\mathrm{eq}}\dot{\theta}^2 + mgR\theta\right) = T_d\dot{\theta},$$
$$J_{\mathrm{eq}}\ddot{\theta} = T_d - mgR.$$

The second expression also holds at zero speed by force balance. It separates steady effort, needed to hold or raise the load against gravity, from the extra effort needed to accelerate the two inertias. With the motor disconnected, an ideal light cable does not make the mass accelerate quite at g, since the drum must gain rotational kinetic energy too.

Calculate a motor torque

A drum with $R = 0.10$ m and $J_d = 0.15\,\mathrm{kg\,m^2}$ lifts 25 kg. A reduction gear gives

$$\dot{\theta}_m = 4\dot{\theta}.$$

The rotor has inertia $J_m = 0.020\,\mathrm{kg\,m^2}$. Refer the train to the motor coordinate. The drum-plus-load inertia becomes $(0.15 + 25(0.10)^2)/4^2 = 0.025\,\mathrm{kg\,m^2}$, so the total at the motor is 0.045 kg·m². Gravity contributes $25(9.81)(0.10)/4 = 6.13$ N·m at that shaft.

Demand upward acceleration 0.80 m/s². The drum must accelerate at 8.0 rad/s² and the motor at 32 rad/s². The motor supplies

$$6.13 + 0.045(32) = 7.57\,\mathrm{N\,m}.$$

A separate check at load speed 1.0 m/s gives motor speed 40 rad/s. Its 303 W then divide into about 245 W raising the weight and 57.6 W increasing kinetic energy. Ideal gearing changes torque and angular speed inversely while preserving transmitted power.

Identify which approximation controls the answer

At constant lifting speed the inertial torque vanishes. At constant angular acceleration, doubling the transmission ratio decreases reflected load inertia by four but also doubles the motor acceleration for the same load motion. The rotor’s own inertia remains at the motor and eventually dominates. A gear ratio therefore cannot reduce every part of acceleration torque indefinitely. Bearings, cables and gears also dissipate energy or store it elastically. Include their effects when a measured transient shows a repeatable lag, oscillation or loss that an ideal rigid constraint cannot explain.

Is the largest reduction always preferable?

For a prescribed drum acceleration α_d and reduction $n = \omega_m/\omega_d$, collect gravity and load-side acceleration into the drum demand $T_d = mgR + (J_d + mR^2)\alpha_d$. The motor torque becomes

$$T_m = T_d/n + J_m n\alpha_d.$$

The first term falls as reduction rises, while rotor acceleration grows. Differentiating with respect to n gives an ideal minimum at $n = \sqrt{T_d/(J_m \alpha_d)}$. For the stated lift $T_d = 27.73$ N m and $\alpha_d = 8$ rad/s², giving $n = 13.2$ approximately. This torque minimum assumes the motor can achieve the associated speed. At a drum speed of 10 rad/s it would turn at 132 rad/s, over three times its speed with the original reduction. Shaft-speed and voltage limits can therefore select a different practical ratio.

Derive speed ripple from a torque diagram

A crank-driven machine can require very different torque at different angles even when the average load is constant. A flywheel stores kinetic energy when driving torque exceeds resisting torque, then releases it when the load peaks. Refer all inertias and torques to the same shaft and suppose the equivalent inertia J is constant. The signed difference $M(\theta) = T_{\mathrm{drive}} - T_{\mathrm{load}}$ gives

$$J\dot{\omega} = M.$$

For continuous positive rotation write $\dot{\omega} = \omega\, d\omega/d\theta$. Integration between two angular positions gives an exact work–energy relation.

$$\tfrac{1}{2} J[\omega_b^2 - \omega_a^2] = \int_{\theta_a}^{\theta_b} M(\theta)\, d\theta.$$

A periodic steady sequence requires zero net area under the torque-difference curve over a whole revolution. Its cumulative area nevertheless has a maximum and a minimum. Their difference ΔE is the energy that must swing into and out of the rotating inertia. Define mean speed in the ripple specification as the arithmetic mean of the two extreme speeds $\bar{\omega} = (\omega_{\max} + \omega_{\min})/2$ and fluctuation coefficient $C_s = (\omega_{\max} - \omega_{\min})/\bar{\omega}$. Factoring the difference of squared speeds gives

$$J = \Delta E/(\bar{\omega}^2 C_s).$$

A time-average tachometer reading approximates this mean for small ripple, but the definitions are distinct for a strongly pulsating shaft.

Size a flywheel for a repeating work demand

A laboratory indexing machine runs at a nominal 300 rpm. A motor supplies approximately constant 30 N m. The resisting torque is 70 N m for the first quarter revolution and a lower constant value for the remaining three quarters. Equate total input and output work over each revolution: $30(2\pi) = 70(\pi/2) + T_l(3\pi/2)$, giving $T_l = 16.67\,\mathrm{N\,m}$. The first quarter produces a 40 N m deficit, so the cumulative energy falls by $40(\pi/2) = 62.83\,\mathrm{J}$. The remaining 13.33 N m surplus restores exactly that energy.

For a maximum peak-to-peak speed variation of 2% and $\bar{\omega} = 31.42\,\mathrm{rad/s}$, total inertia required is

$$62.83/[31.42^2(0.02)] = 3.18\,\mathrm{kg\,m^2}.$$

If the machine already has 1.00 kg m² on this shaft, an extra 2.18 kg m² is required. A thin-ring estimate at mean radius 0.30 m gives mass $2.18/0.30^2 = 24.2\,\mathrm{kg}$. A solid disc of the same radius needs twice the mass because its material lies closer to the shaft. At half speed the same torque-versus-angle work deficit requires four times the total inertia for the same fractional ripple. Startup torque or bearing load may therefore limit an inertia-based solution even when steady motor power suffices.

The torque balance also predicts where a shaft encoder should record the two speed extremes. The energy derivative with respect to angle equals the torque difference, so the maximum occurs just before the high resisting plateau begins and the minimum where that plateau ends. The maximum torque itself persists over a finite angular interval, while minimum speed occurs only at its end. This distinction matters when timing a torque pulse from a speed record: the sign of the speed derivative, rather than the absolute value of speed, identifies when the flywheel is discharging.

Energy coordinates and Lagrange's equation

Machine dynamics

Derive a coupled translation–rotation equation with a rolling constraint and identify which reaction disappears from the energy balance.

FROM FIRST PRINCIPLES

Derive the equation of motion using one independent coordinate

An ideal geometric constraint ties several motions together. Choose an independent coordinate q that automatically satisfies it and express kinetic energy $T(q,\dot q)$ and potential energy $V(q)$ in that coordinate. In the principle of virtual work, ideal constraint reactions do no work along admissible small motions. The balance of inertial, conservative and applied virtual work gives Lagrange's equation

$$\frac{d}{dt}\frac{\partial T}{\partial \dot q}-\frac{\partial T}{\partial q}+\frac{\partial V}{\partial q}=Q_{\mathrm{nc}},$$

$$\delta W_{\mathrm{nc}}=Q_{\mathrm{nc}}\,\delta q.$$

For a rigid cylinder rolling on a stationary surface without slip, take centre displacement $q=x$ and angular speed $\dot x/R$. Its translation and rotation contribute to kinetic energy; a horizontal spring attached at the centre supplies the potential.

$$T=\tfrac12(m+I_G/R^2)\dot x^2,$$

$$V=\tfrac12 kx^2,\qquad (m+I_G/R^2)\ddot x+kx=Q_{\mathrm{nc}}.$$

Static friction supplies the contact reaction required for rolling. The contact point has zero instantaneous velocity, so that reaction contributes zero power here. The solution must still demand no more friction than the surface can supply.

DERIVATION AND APPLICATIONS

Derive the effective stiffness of a pendulum on an accelerating cart

A continuously accelerating support changes both the equilibrium direction and the small-oscillation frequency of a hanging load. Model a point mass m on a massless rigid link of length ℓ with an ideal hinge. Let the support move horizontally with imposed coordinate $X(t)$ and measure angle θ from the downward vertical towards positive horizontal displacement. Ignore drag. With mass coordinates $x=X+\ell\sin\theta$ and $y=-\ell\cos\theta$, the kinetic and potential energies are

$$T=\tfrac12 m[\dot X^2+2\dot X\ell\dot\theta\cos\theta+\ell^2\dot\theta^2],$$

$$V=-mg\ell\cos\theta.$$

Differentiate $\partial T/\partial\dot\theta$ with respect to time and subtract $\partial T/\partial\theta$. The velocity cross terms involving $\dot X\dot\theta$ cancel, leaving a forcing term set by support acceleration, independent of support speed.

$$\ell\ddot\theta + g\sin\theta + \ddot X\cos\theta = 0.$$

For constant support acceleration a, a stationary angle obeys $\tan\theta_0 = -a/g$. Choose the hanging equilibrium. Expanding the restoring term about θ_0 gives the effective gravitational acceleration along this new direction and the frequency of small oscillations.

$$\theta = \theta_0 + \eta,$$

$$\ddot\eta + \frac{\sqrt{g^2+a^2}}{\ell}\eta = 0,$$

$$\omega_n = \sqrt{\frac{\sqrt{g^2+a^2}}{\ell}}.$$

A positive cart acceleration tips the pendulum backwards. The first correction to angle is linear in a/g, while the first relative correction to frequency is quadratic. The exact equilibrium result holds at finite a; the frequency expression requires small oscillations about it.

WORKED EXAMPLE

Predict a suspended sensor's direction

A cart accelerates at 3.00 m/s² carrying a pendulum of length 0.600 m. Its steady angle is

$$-\arctan(3.00/9.81) = -17.0^\circ.$$

The effective acceleration is 10.26 m/s², giving $\omega_n = 4.13$ rad/s and period 1.52 s. A sensor that treats the pendulum direction as vertical during this manoeuvre would carry the full angular bias.

Change the inputs and inspect this calculation below

SECOND APPLICATION

Infer acceleration from a steady deflection

In another rig a 0.400 m pendulum settles 8.00° backwards after weak damping removes its initial swing. Constant acceleration is

$$9.81\tan 8.00^\circ = 1.38\,\mathrm{m/s^2}.$$

The effective gravity is $9.81/\cos 8.00^\circ = 9.91$ m/s², predicting a small-oscillation period $2\pi\sqrt{0.400/9.91} = 1.26$ s for weak damping. The angle is much more sensitive to modest acceleration than the period.

Interactive calculation · Change the inputs of this example

Use the adjustable quantities to test the two worked calculations above. The plot recomputes this derivation's balance or constitutive relation; its numerical readout reports the quantities needed for the forward calculation and the inverse or design question. Keep the fixed assumptions stated in the readout when comparing with the example values.

Open this live calculation

Try the calculation

Cart acceleration (m/s²) **3**

Pendulum length (m) **0.6**

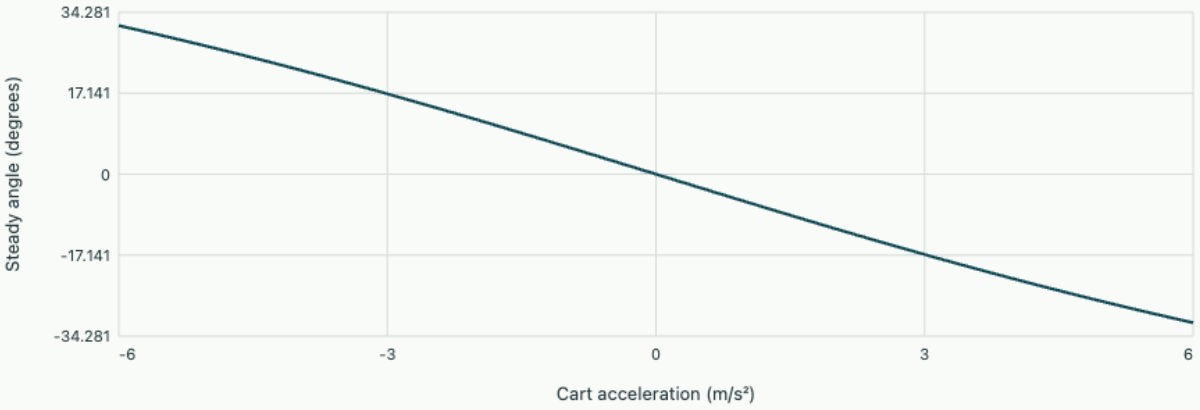

Effective-gravity alignment

Selected equilibrium angle -17.004°; small oscillation frequency 4.135 rad/s.

Let geometry remove a reaction

A cylinder rolls along a horizontal rail while a spring attached at its centre pulls it towards equilibrium. The rail friction is essential for rolling, but an ideal contact point is instantaneously at rest and the friction force does no work. One can write separate translational and rotational equations with an unknown friction force. Alternatively choose a coordinate that satisfies rolling from the beginning. The reduced energy then contains the rotational inertia without introducing a contact reaction.

Take the rightward displacement x of the cylinder centre as independent coordinate and clockwise angle as positive. On the fixed surface the no-slip condition gives $x = R\theta$, up to a reference offset. A body of total mass m and centre inertia I_G has kinetic energy from both translation and rotation. A centre spring with stiffness k has elastic potential $kx^2/2$.

$$T = \tfrac{1}{2}(m + I_G/R^2)\dot{x}^2,$$
$$V = \tfrac{1}{2}kx^2.$$

Connect energy to a dynamical equation

The virtual work of a horizontal force F applied at the centre is $F\delta x$. In this coordinate its generalised force is simply F. A torque M acting clockwise would do $M\delta\theta = (M/R)\delta x$ and would enter as a force M/R. With a centre damper c, the dissipative force is $-c\dot{x}$. Lagrange's equation for this system becomes

$$\frac{d}{dt}\frac{\partial T}{\partial \dot{x}} - \frac{\partial T}{\partial x} + \frac{\partial V}{\partial x} = F - c\dot{x}, \qquad (m + I_G/R^2)\ddot{x} + c\dot{x} + kx = F.$$

For coordinates whose inertia depends on position, retain both derivatives involving T. The differentiation of $\partial T/\partial \dot{x}$ then generates a term proportional to $\dot{x}^2$, part of which cancels $\partial T/\partial x$. Simply multiplying a configuration-dependent effective mass by acceleration would miss the remaining term.

Predict a frequency and check rolling

A solid cylinder has $m = 8.0\,\mathrm{kg}$, $R = 0.10\,\mathrm{m}$, and $I_G = mR^2/2 = 0.040\,\mathrm{kg\,m^2}$. The effective mass seen by the spring is

$$8 + 0.040/0.10^2 = 12.0\,\mathrm{kg}.$$

With $k = 480\,\mathrm{N/m}$ and negligible damping the natural frequency is

$$\sqrt{480/12}/(2\pi) = 1.007\,\mathrm{Hz}.$$

Release it from rest at $x = +0.060\,\mathrm{m}$. Its initial acceleration is

$$-480(0.060)/12 = -2.40\,\mathrm{m/s^2}.$$

Writing only the centre's translation and ignoring rotation would overpredict the acceleration magnitude.

Reconstruct the previously eliminated contact force from translation. The spring pulls leftwards with 28.8 N and the centre accelerates leftwards with $m\ddot{x} = -19.2\,\mathrm{N}$. Friction must therefore point rightwards with 9.6 N to supply the appropriate angular acceleration. The coefficient of static friction must be at least $9.6/(8 \times 9.81) = 0.122$ at release. For a smaller coefficient, the assumed rolling constraint fails and the model needs separate rotational and translational coordinates together with a slipping contact law.

Compare two cylinders with identical mass

A thin-walled hoop of the same mass and rolling radius has $I_G = mR^2$. With the original spring its effective mass doubles the translational mass, giving natural frequency $\sqrt{480/16}/(2\pi) = 0.872\,\mathrm{Hz}$. A no-slip ring-down can therefore distinguish two bodies whose masses and outer dimensions are identical but whose internal mass distributions differ.

Use a cyclic coordinate to reduce coupled motion

Mount a pendulum on a cart that can roll horizontally on a level frictionless guide. Let cart displacement be x, bob angle θ from downward vertical, length l, bob mass m and remaining cart mass M. The bob position is $(x + l\sin\theta, -l\cos\theta)$. Differentiating and squaring its speed gives a cross term $2l\dot{x}\dot{\theta}\cos\theta$ because cart and pendulum velocities need not be perpendicular. The full energy terms are

$$T = \tfrac{1}{2}(M+m)\dot{x}^2 + ml\cos\theta\,\dot{x}\dot{\theta} + \tfrac{1}{2}ml^2\dot{\theta}^2,$$

$$V = mgl(1-\cos\theta).$$

Horizontal position itself does not occur in either expression. It is a cyclic coordinate, so $\partial T/\partial\dot{x} = (M+m)\dot{x} + ml\cos\theta\,\dot{\theta}$ is conserved if no external horizontal force acts. This is horizontal momentum written in generalised coordinates. The pendulum equation from Lagrange's equation is

$$l\ddot{\theta} + \ddot{x}\cos\theta + g\sin\theta = 0.$$

For small swings from rest, differentiate the momentum relation and linearise to obtain

$$\ddot{x} = -ml\ddot{\theta}/(M+m).$$

Substituting gives

$$[lM/(M+m)]\ddot{\theta} + g\theta = 0.$$

Free horizontal motion makes the small-swing frequency larger than for a clamped cart, by $\sqrt{(M+m)/M}$. This result reflects motion about the system's horizontally constrained centre of mass. The extra degree of freedom also permits uniform horizontal translation at zero frequency. Its presence does not imply an additional oscillatory mode.

Predict opposing cart travel in a release test

Let $M = 3.0$ kg, $m = 1.0$ kg and $l = 0.60$ m. Clamp the cart: the oscillation period would be $2\pi\sqrt{0.60/9.81} = 1.55\,\mathrm{s}$. Release its horizontal guide and the period becomes

$$2\pi\sqrt{0.60(3)/(9.81\times 4)} = 1.35\,\mathrm{s}.$$

At release the bob is at $\theta_0 = 10^\circ$ and both bodies are at rest. Because horizontal momentum remains zero, integrate the exact relation to obtain

$$(M+m)x + ml\sin\theta = \text{constant}.$$

As the bob first crosses the vertical, the cart has shifted $ml\sin 10^\circ/(M+m) = 0.0260\,\text{m}$ to the right from its starting point.

At the vertical the potential-energy decrease is

$$mgl(1-\cos 10^\circ) = 0.0894\,\text{J}.$$

Substituting $\dot{x} = -ml\dot{\theta}/(M+m)$ into the kinetic energy at this instant gives effective angular inertia $ml^2M/(M+m) = 0.270\,\text{kg}\,\text{m}^2$. Thus the angular speed magnitude is $\sqrt{2(0.0894)/0.270} = 0.814\,\text{rad/s}$, and the cart speed magnitude is $0.15(0.814) = 0.122\,\text{m/s}$. The frequency estimate used a small-angle approximation; the centre-of-mass and energy results at the vertical used the actual release angle. A horizontal cable pulling on the cart or measurable wheel friction would change the conserved momentum and should be measured before attributing deviations solely to pendulum nonlinearity.

The two-sensor experiment can measure conservation without estimating acceleration. Track the cart position and bob angle from video, then plot $x + [ml/(M+m)]\sin\theta$. For the chosen masses its value should stay constant at the initial offset despite the cart and pendulum both moving. A steadily sloping line indicates nonzero initial horizontal momentum; a curved departure suggests an external force or tracking bias. This separation is useful because rolling resistance can be weak enough to leave the first measured period nearly unchanged while producing visible drift over several cycles. The conserved combination is specific to the inertial laboratory coordinate, so a camera fixed on the moving cart needs a separate record of cart displacement.

Why a radial slide presses sideways on a rotating guide

Machine dynamics

A low-friction carriage moves along a radial slot in a horizontal turntable. It can move at constant speed relative to the guide and still require a changing force. Keeping track of the moving basis exposes both acceleration components.

Differentiate the direction vectors

Let $r(t)$ be displacement from the turntable centre along the guide and $\theta(t)$ the angle of the guide. In fixed Cartesian components the radial unit vector is $(\cos\theta, \sin\theta)$ and the tangential vector is $(-\sin\theta, \cos\theta)$. Differentiating shows $\dot{\mathbf{e}}_r = \dot\theta \mathbf{e}_\theta$ and $\dot{\mathbf{e}}_\theta = -\dot\theta \mathbf{e}_r$. Apply the product rule to the position $r\mathbf{e}_r$ to obtain the velocity and then differentiate both terms.

$$\mathbf{v} = \dot r \mathbf{e}_r + r\dot\theta \mathbf{e}_\theta,$$

$$\mathbf{a} = (\ddot r - r\dot\theta^2)\mathbf{e}_r + (r\ddot\theta + 2\dot r\dot\theta)\mathbf{e}_\theta.$$

One contribution to $2\dot r\dot\theta$ comes from differentiating the radially directed velocity as its basis turns. The other comes from differentiating the magnitude of the tangential velocity $r\dot\theta$. For positive rotation and outward travel, both point in the positive tangential direction. The expression already gives the acceleration in an inertial frame. Multiplying by mass gives the net real force required on the carriage.

Check sideways force with angular momentum and energy

Hold the angular speed at Ω, and drive the radial position as $r = r_0 + ut$ with constant u. Gravity and support cancel vertically. The net radial drive force is $-mr\Omega^2$ and the guide must exert a side force $2mu\Omega$. The resulting torque about the axis is $2mru\Omega$. This equals the derivative of the angular momentum $mr^2\Omega$, providing an independent sign and factor-of-two check.

$$P_r + P_\theta = (-mr\Omega^2)u + (2mu\Omega)(r\Omega) = mru\Omega^2 = \frac{d}{dt}\left[\frac{m}{2}(u^2 + r^2\Omega^2)\right].$$

The side force does work in the laboratory since its contact point moves tangentially. Describing a smooth slot as doing zero work without specifying the frame would lose this energy transfer. The radial actuator absorbs power during outward constant-speed travel.

Forces and power on two passes

A 0.40 kg carriage moves from $r = 0.10$ m outwards at 0.20 m/s, with $\Omega = 5$ rad/s. At $t = 0.50$ s it reaches 0.20 m. Its radial force is −2.0 N, tangential force is +0.80 N and net mechanical power is

$$-2(0.20) + 0.80(1) = 0.40\,\mathrm{W}.$$

Setting u to zero removes the side force, while the guide still requires a radial restraint to maintain circular travel.

On an inward pass at −0.20 m/s, evaluated at the same radius, the radial force remains −2.0 N. The side force reverses and the turntable now receives angular momentum from the carriage. The magnitude of each force depends on a different combination of radius, radial speed and angular speed. Use the trace to distinguish the constant side load from the changing inward force.

Set radial speed to zero before changing angular speed. Restore outward motion and predict how doubling angular speed changes the two force components at the same radius. Use mechanical power as a separate sign check.

Open this experiment online

Try the calculation

Angular speed (rad/s) **5**

Outward speed (m/s) **0.2**

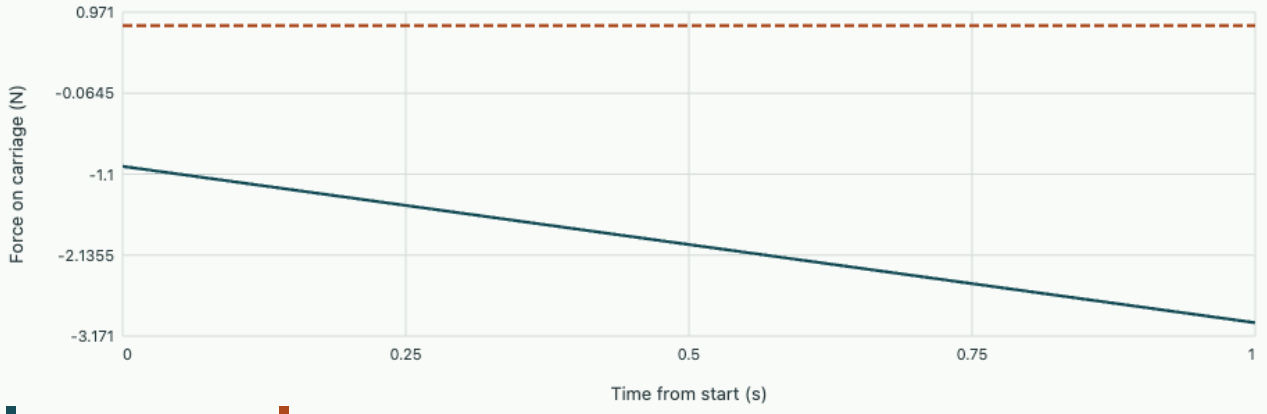

At 0.50 s the radial and tangential forces are -2.00 N and 0.80 N. The net mechanical power is 0.40 W.

Tutorial · reconstruct angular acceleration from a side load

At one instant the carriage is at 0.20 m, with mass 0.40 kg, $\dot{r} = 0.10$ m/s and $\dot{\theta} = 4$ rad/s. A tangential force transducer measures +0.48 N. Estimate $\ddot{\theta}$ and explain what a rigidly fixed carriage would read at the same instant.

▼ **Show the reconstruction**

The tangential acceleration is

$$0.48/0.40 = 1.20\,\mathrm{m/s^2}.$$

Subtract $2(0.10)(4) = 0.80$ m/s² to isolate $r\ddot{\theta} = 0.40$ m/s². Thus $\ddot{\theta} = 2.0$ rad/s². With no radial sliding the second term disappears and the side load falls to $0.40(0.20)(2.0) = 0.16$ N. The radial centripetal component points along the guide and does not enter this reading.

Further reading · MIT 2.003SC · velocity, acceleration and rotational motion

When a suspended capacitor loses its stable equilibrium

Electromechanics, optics and measurement

An electrode suspended on a spring can remain motionless at a bias that makes the calculated electrostatic force grow as it moves. Static force balance alone misses the voltage at which that equilibrium disappears. Deriving the small-signal frequency gives an independent measurement of the same instability.

Start with the electrical and mechanical control variables

A movable conducting plate of area A faces a fixed electrode. Its unstressed gap is g. Define positive displacement x toward the fixed plate, with spring force $-kx$, mass m and viscous damping coefficient b. For $0 \le x < g$ assume ideal parallel plates, negligible tilt and fringing, constant ϵ, and a linear elastic spring. The capacitance is $C(x) = \epsilon A/(g-x)$. The model ends when the plates approach contact or when the suspending structure departs from its specified elastic law. It cannot by itself calculate adhesion, contact resistance or post-contact motion.

Before differentiating electrical energy specify whether the source holds voltage or charge. At fixed charge Q, electrical energy is $Q^2/[2C(x)]$, and its negative displacement derivative gives the force toward increasing x. At fixed voltage V, a source supplies $V\,dQ$ as the plates move. The appropriate potential for mechanical equilibrium is the spring energy plus the field energy minus QV, which here is $\mathcal{U}_V = kx^2/2 - C(x)V^2/2$. Differentiating gives the outward spring reaction and the attractive electrical force $F_e = V^2 C'(x)/2 = \epsilon A V^2/[2(g-x)^2]$. An independent derivation multiplies the conductor pressure $\epsilon E^2/2$ by area with $E = V/(g-x)$. Both give a positive force. Replacing the source potential with the stored energy at fixed voltage would reverse its sign.

Locate all equilibria before choosing a branch

Define $s = x/g$ and $\Lambda = \epsilon A V^2/(2kg^3)$. The static force equation reduces to

$$\Lambda = s(1-s)^2.$$

At a specified voltage one can find s by scanning the curve $s \mapsto s(1-s)^2$ over the physically admissible interval $0 \le s < 1$. Its derivative is $(1-s)(1-3s)$, giving an interior maximum $4/27$ at $s = 1/3$. For $0 < \Lambda < 4/27$ there are two physical roots. The smaller is a local minimum of $\mathcal{U}_V$ while the larger is a local maximum. Their merger is a fold of the static equilibrium branch:

$$x_{\mathrm{pi}} = g/3,$$

$$V_{\mathrm{pi}} = \sqrt{\frac{8kg^3}{27\epsilon A}}.$$

The often-quoted one-third displacement is the result for a linear spring, ideal voltage drive and this capacitance geometry. It is not a universal travel limit determined by the gap alone. Additional mechanical restoring forces or a different electrical boundary condition change the fold. Neither positive net electrical force nor the mere existence of a real solution is evidence of stable operation. A root finder

started near the almost closed gap can converge to the unstable large-displacement root with an extremely small static residual.

The two branches can be distinguished experimentally without deliberately reaching contact. At static equilibrium $kx = F_e$. Linearise the total force about x_0 while maintaining voltage at its prescribed value. The incremental restoring stiffness and corresponding weak-damping natural frequency are

$$k_{\text{eff}} = k - \frac{\epsilon A V^2}{(g - x_0)^3} = k\,\frac{1 - 3s_0}{1 - s_0},$$

$$f_{\text{small}} = \frac{1}{2\pi}\sqrt{\frac{k_{\text{eff}}}{m}}.$$

A small push toward the fixed electrode is restored only when $k_{\text{eff}} > 0$. The familiar electrostatic softening is the reason the smaller equilibrium is stable. The small-signal frequency tends to zero as the fold is approached. With appreciable damping the observed amplitude resonance and ringdown oscillation have slightly different frequencies; fit the full mechanical response rather than identifying an arbitrary peak with the undamped f_{small}.

Background · Can a sudden step pull in a statically stable actuator?

An ideal voltage step applied to a plate initially at rest can push it past the unstable equilibrium. During the motion at fixed voltage the effective potential per kg^2 is $u(s) = s^2/2 - b/[2(1 - s)]$, where $s = x/g$ and $b = \epsilon A V^2/(kg^3)$. Neglect damping and begin at $s = 0$. At the dynamical threshold the initial energy equals the saddle energy and the slope vanishes at that saddle.

$$u(s) = u(0) \implies b = s(1 - s),$$

$$u'(s) = 0 \implies b = 2s(1 - s)^2.$$

The two equations meet at $s = 1/2$, $b = 1/4$. The quasistatic fold gives $b = 8/27$. Consequently the undamped step threshold is only $\sqrt{27/32} \simeq 0.919$ times the slow-ramp pull-in voltage. A device operated between the two voltages can survive a ramp but collapse after an abrupt step. Dissipation and the actual rise time change this prediction.

Reconstruct the prepared state from a frequency measurement

Take a 100 µm square electrode in vacuum, $g = 2.00$ µm, $k = 2.00$ N/m and $m = 5.00 \times 10^{-10}$ kg. The predicted pull-in voltage is 7.32 V, the zero-bias capacitance 44.3 fF and the zero-bias natural frequency 10.07 kHz. On the low branch $s_0 = 0.20$ gives $x_0 = 0.400$ µm and voltage 6.80 V. Then $k_{\text{eff}} = 1.00$ N/m and the small-signal frequency is 7.12 kHz. A measured frequency ratio f/f_0 can be inverted via $s = (1 - r)/(3 - r)$, where $r = (f/f_0)^2$. The result is independent of absolute optical displacement calibration if the mass and underlying spring stiffness have not changed during the bias sweep.

At the same voltage the other physical root is $s = 0.48769$. A numerical force balance at this root would give the same supply reading but a negative tangent stiffness. The ideal voltage-controlled potential in

units kg^2 is $u(s) = s^2/2 - \Lambda/(1-s)$. The barrier height $kg^2[u(0.48769) - u(0.20)]$ for this example is 7.26×10^{-14} J. A sufficiently energetic disturbance can carry the plate out of the stable basin even below static pull-in. This is different from loss of the static equilibrium itself. A quasistatic model predicts the existence and local stiffness of the equilibrium; a transient simulation must additionally specify initial displacement, velocity, drive ramp and damping.

Change the preparation to fixed charge

Disconnect a perfect isolated capacitor after placing a known charge Q on it, neglecting leakage and parasitic capacitance. Then $F_Q = Q^2/(2\epsilon A)$ is independent of the remaining gap, because $D = Q/A$ is fixed. Static equilibrium is $x_0 = Q^2/(2\epsilon A k)$, with incremental stiffness exactly k. At the same initial voltage and gap the instantaneous force agrees with the voltage-controlled value, since $Q = C(x_0)V$. The derivatives governing subsequent motion differ. At $x_0 = 0.400$ µm the required charge in the numerical example is 0.376 pC. After ideal electrical isolation the small-signal frequency returns to the underlying elastic value even though the loaded static position stays the same.

Ideal charge isolation is delicate in a small device. A fixed parasitic capacitance C_p from the isolated node to a reference means the conserved charge belongs to $C(x) + C_p$. Motion changes the fraction of total charge residing on the actuator. The electrical energy becomes $Q_{\text{total}}^2/[2(C + C_p)]$, so the force is $Q_{\text{total}}^2 C'/[2(C + C_p)^2]$, generally displacement dependent. If $C_p \gg C$, the node voltage changes little with a small displacement and behavior is closer to voltage control. Interpreting an observed softening after disconnecting the supply as evidence against electromagnetic force balance would overlook this boundary change.

A different practical preparation puts an intentional series capacitor C_s between a fixed voltage supply and the actuator. Its series combination is $C_{\text{ser}} = \epsilon A/[g - x + \epsilon A/C_s]$. For static mechanical work at fixed supply voltage use $F = V_s^2 C'_{\text{ser}}/2$. Defining an effective electrical spacing $g_e = g + \epsilon A/C_s$, the static fold occurs at $x = g_e/3$ if this lies within the open physical gap. If $\epsilon A/C_s \geq 2g$, contact would occur before any such static fold in the ideal model. This calculation shows a direct connection between passive circuit design and allowed mechanical travel, while making clear that the maximum actuator voltage can differ from the voltage printed on the supply.

Why a sudden voltage change can reach contact below static pull-in

For a rapid electrical step the plate has a position and velocity inherited from the previous preparation. Suppose it starts at rest at its zero-bias position, the supply steps to a constant V much faster than a mechanical period, and mechanical damping is initially negligible. Immediately after the step, energy in the mechanical potential $u(s) = s^2/2 - \Lambda/(1-s)$ is $u(0) = -\Lambda$ in units of kg^2. Motion under this constant voltage can reach the force barrier if the initial value exceeds the potential at the unstable stationary point. This question can be solved by comparing two energies without integrating an entire time history.

Let s_b be the unstable root of $\Lambda = s_b(1-s_b)^2$. At threshold the initial state is on the separatrix, the trajectory separating oscillations in the well from excursions to the closing gap. Set $u(0) = u(s_b)$, subtract the two expressions and cancel s_b from the nontrivial solution. The two conditions become

$$\Lambda = \frac{s_b(1-s_b)}{2},$$

$$\Lambda = s_b(1-s_b)^2.$$

Thus $s_b = 1/2$, $\Lambda = 1/8$, and the ideal undamped step threshold is

$$V_{\mathrm{step}}/V_{\mathrm{pi}} = \sqrt{27/32} = 0.919.$$

In our example this is 6.72 V. A slow increase to 6.80 V leads to the observed stable 0.40 µm deflection, whereas a sudden ideal voltage step to the same value from rest at the origin contains enough energy to escape the well. Starting on the biased equilibrium before applying a small perturbation is a different experiment. The direction of the threshold shift makes physical sense: damping removes mechanical energy during the first excursion, and a slow ramp allows the equilibrium to move with the plate. The undamped value specifies a particular ideal initial-value experiment, rather than a voltage rating for an unspecified drive waveform.

One can check a simulated step by monitoring $m\dot{x}^2/2 + \mathcal{U}_V$ after the supply settles. With viscous damping its derivative is $-b\dot{x}^2$, so any sustained increase during a constant-voltage segment points to a numerical or modelling error. Before the step ends there is an explicit drive term $-CV\dot{V}$ in this energy balance. The mechanical potential already includes the source work. Adding $V\dot{Q}$ to the same balance a second time gives an artificial energy imbalance. A transient solver should stop at a physically specified minimum gap instead of marching across the singularity; a statement about contact time depends on what counts as contact.

A finite source resistance changes what a ringdown measures

A dc supply with series resistance R can maintain the static voltage accurately while failing to hold the actuator voltage fixed over a mechanical cycle. Let its steady node voltage be V, with equilibrium capacitance $C = C(x_0)$. A small sinusoidal displacement δx causes current $i\omega(C\,\delta v + VC'\delta x)$ into the actuator. The small-signal supply voltage is zero, so $\delta v = -Ri$. Eliminating current gives

$$\delta v = -\frac{VC'}{C}\frac{i\omega\tau}{1+i\omega\tau}\delta x,$$

$$\tau = RC.$$

Linearise $F_e = V^2C'/2$ allowing both voltage and position to vary. The direct derivative is $K_{e0} = V^2C''/2$, while the change from node voltage is $VC'\,\delta v$. For an ideal parallel plate $C''/2 = (C')^2/C$, so the two terms combine to the simple complex relation $\delta F_e = K_{e0}\delta x/(1+i\omega\tau)$. At low frequency the electrical force follows displacement with its fixed-voltage slope. At high frequency the slope vanishes, as it must for an isolated ideal plate carrying fixed charge over one oscillation. At intermediate frequency a motion-induced current dissipates heat in the resistor.

Bring δF_e to the left side of the mechanical equation. Its real part subtracts $K_{e0}/[1+(\omega\tau)^2]$ from the mechanical stiffness; its imaginary part adds $K_{e0}\tau/[1+(\omega\tau)^2]$ to the viscous damping coefficient. This damping is positive for a passive resistor. At $s = 0.20$ the static electrical stiffness is 1.00 N/m, the operating capacitance is 55.3 fF and $R = 400$ MΩ gives

$$\tau = 22.1\,\mu\mathrm{s}.$$

A 7.2 kHz interrogation has $\omega\tau \simeq 1$. Only about half the static electrical slope survives and the added damping is roughly $11\,\mu\mathrm{N\,s/m}$. Treat these as frequency-dependent coefficients in the driven susceptibility. Substituting the low-frequency stiffness into a ringdown fit at this frequency would give the wrong displacement when the fitted frequency is inverted. Fitting the complex response at several frequencies avoids that ambiguity.

An experiment can separate the circuit effect from mechanical nonlinearity. Keep the same static bias and displacement, insert two known series resistances, then measure both in-phase and quadrature response to a small sinusoidal force. The displaced equilibrium should remain essentially unchanged at dc if leakage stays small. A stiffness dispersion and dissipative peak that shift in proportion to $1/R$ support an electrical cause. Then repeat at a smaller oscillation amplitude. Amplitude-dependent frequency shift that survives the change in resistance can arise from nonlinear spring or force curvature, which the first-order susceptibility leaves out. A simple change to the external circuit has turned the slope of an energy curve into a prediction for a measured phase lag.

Compare force intersections for voltage and charge control

The initial gap is 2.00 µm, the area is a 100 µm square and the mass is 0.50 µg. Use the voltage ratio to move the force curve through the fold. At 93% of pull-in the low-displacement fixed-voltage intersection has a positive restoring slope. The high-displacement intersection has a negative slope. The charge-controlled line is prepared at the selected voltage at the original open gap. It gives the same initial force but a different subsequent curve. The readout reports both open-gap roots even if the upper root lies beyond the plotted interval. At the baseline stiffness, static pull-in is 7.32 V.

Change the spring stiffness while holding the voltage ratio fixed. The dimensionless locations of the roots stay in place, but their dimensional force and small-signal frequency change. This checks the scaling that eliminated the physical dimensions in the fold equation. Then set the ratio between the dynamic step threshold and unity. Use the force intersections to locate the potential maximum and sketch the area between attraction and spring reaction from the initial position. Its signed integral supplies the work which distinguishes a bounded excursion from crossing the maximum. The displayed curves predict initial-value behaviour only when combined with a choice of initial kinetic energy and damping.

Open this experiment online

Try the calculation

Bias as fraction of static pull-in **0.93**

Spring stiffness (N/m) **2**

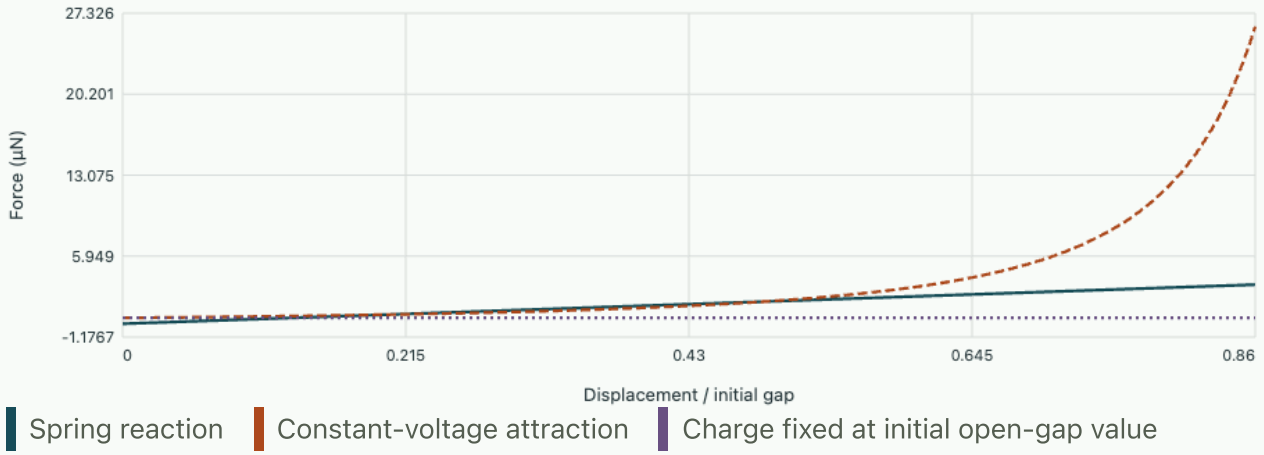

Bias 6.805 V; static pull-in 7.317 V. Stable x/g = 0.200, unstable x/g = 0.487, small-signal frequency 7.11 kHz.

Tutorial · distinguish stability from force balance

Infer a gap fraction and a bias from a resonance

An otherwise identical actuator shows $f/f_0 = 0.80$ at a stable fixed voltage. Find the deflection as a fraction of gap, the voltage relative to pull-in, and the independent capacitance change. What could spoil this comparison?

▼ Work through the solution

Here $r = 0.64$ and $s = (1 - 0.64)/(3 - 0.64) = 0.1525$. The bias ratio is $\sqrt{(27/4)s(1-s)^2} = 0.860$ approximately. The parallel-plate capacitance should rise by $1/(1-s) - 1 = 18.0\%$. Measure the change relative to the active capacitance after removing any constant wiring capacitance. Disagreement can come from changing mode shape, a nonlinear spring, a tilted plate, a measurement frequency above the electrical equilibration bandwidth, or an incorrect extraction of mechanical stiffness from a strongly damped resonance. With a measured gap and mode shape these explanations yield different quantitative corrections.

Choose a series capacitor to move the static fold

The original 44.3 fF zero-bias actuator should remain on its stable slope as far as $x = 0.60g$, ignoring contact and other limits. Find the series capacitance whose fold falls exactly at this displacement. How much supply voltage appears across the actuator at that point?

▼ **Work through the solution**

Set $g_e/3 = 0.60g$, giving $\epsilon A/C_s = 0.80g$ and $C_s = C(0)/0.80 = 55.4$ fF. At $0.60g$ the actuator capacitance is $C(0)/0.40 = 110.7$ fF. Series charge is identical in both capacitors, so

$$V_{\text{act}}/V_{\text{supply}} = C_s/(C_s + C_{\text{act}}) = 1/3.$$

Choosing exactly this value places operation at vanishing ideal stiffness, so a strictly positive measured restoring slope at that displacement requires a smaller series capacitance or a different margin. The result is sensitive to additional capacitance connected between the series node and ground.

Further reading

- Derive capacitor pressure from field stress and work

A moving-coil galvanometer as an electrical and mechanical system

Electromechanics, optics and measurement

A scale division records an angle, yet the quantity marked on the dial is electric current. A spring, a magnetic field and the resistance of the external measuring circuit connect the two. Derive the calibration, predict how a pointer approaches its reading, and find which experiment measures the charge of a short pulse.

Convert the force on two straight sides into a torque

A light rectangular coil has N turns, active length l, width w, and area per turn $A = lw$. It pivots about an axis parallel to its long sides. Shaped pole pieces confine an approximately radial magnetic field of magnitude B to an air gap. Over the working angular range the magnetic field is perpendicular to the active wire and lies approximately in the plane of the coil. An elementary length carrying conventional current i experiences $d\mathbf{F} = i\,d\mathbf{l} \times \mathbf{B}$. The two long sides carry current in opposite directions and experience forces of equal magnitude $NilB$. Acting with lever arms $w/2$, the forces make a couple whose torque is $NiAB$. Their net force is approximately zero. The short ends supply negligible torque about the pivot under the ideal geometry.

Write $K = NAB$, and choose the positive sense of current to give positive torque. Its units are $\mathrm{N\,m/A}$. In a uniform Cartesian field an ordinary rigid loop instead gives torque $NiAB\sin\alpha$, where α is the angle between its normal and the field. The radial gap maintains the factor equivalent to $\sin\alpha$ close to unity as the pointer turns. This is a design choice that produces a nearly linear scale. If a measured calibration curve flattens at a large angle, field nonuniformity and a nonlinear torsion spring are candidate causes that can be tested separately.

For a soft torsion spring with stiffness κ, the return torque is $-\kappa\theta$ at small deflections from the zero-current setting. At static equilibrium $\theta = Ki/\kappa$. With $N = 200$, $A = 1.00\,\mathrm{cm^2}$, $B = 0.250\,\mathrm{T}$ and $\kappa = 8.0 \times 10^{-4}\,\mathrm{N\,m/rad}$, the torque constant is $0.0050\,\mathrm{N\,m/A}$ and the current sensitivity is $6.25\,\mathrm{rad/A}$. A $5.0\,\mathrm{mA}$ current turns the pointer through $0.03125\,\mathrm{rad}$, about 1.79°. A mirror mounted on the same axle deflects a reflected laser through twice this angle. At a screen distance of $0.50\,\mathrm{m}$ the spot shifts $0.50\tan(2\theta) = 31.3\,\mathrm{mm}$, making the small mechanical rotation easy to resolve.

Recover the reciprocal voltage from work

Now rotate the coil through a small positive angle while it carries positive current. The electromagnetic torque does mechanical work $Ki\,d\theta$. The voltage associated with the motion must therefore draw electrical work $ie_{\mathrm{back}}\,dt$ of equal magnitude when the motor torque assists that motion. This gives the back-emf relation $e_{\mathrm{back}} = K\dot\theta$, measured as a positive drop in the motor sign convention. Its coefficient has units $\mathrm{V\,s/rad}$, numerically the same SI coefficient as the torque constant. One can also derive it from the motional emf on the two active sides. Each moves at speed $(w/2)\dot\theta$, crosses field B, and generates a voltage $Bl(w/2)\dot\theta$ along its wire. The two contributions add over every turn.

Let J denote the rotational inertia, b the mechanical viscous damping coefficient, L the coil inductance and R the sum of winding plus external series resistance seen by a voltage source $v(t)$. The

electromechanical equations are

$$J\ddot{\theta} + b\dot{\theta} + \kappa\theta = Ki,$$

$$L\dot{i} + Ri + K\dot{\theta} = v(t).$$

Multiplying the first equation by $\dot{\theta}$ and the second by i eliminates the coupling power $Ki\dot{\theta}$. The result says that source power vi equals the rate of increase of $J\dot{\theta}^2/2 + \kappa\theta^2/2 + Li^2/2$, plus $b\dot{\theta}^2 + Ri^2$. This identity fixes the relative signs of the torque and back emf. If a sign mistake turns a passive closed coil into a self-accelerating pointer, the same mistake produces a residual coupling term in this power balance. Mechanical friction and winding heat represent distinct sinks even though both can damp the observed displacement.

Predict overshoot and find a critical external resistance

If the electrical relaxation time L/R is short compared with the oscillation time $1/\sqrt{\kappa/J}$, set $i \simeq (v - K\dot{\theta})/R$. Substituting into the mechanical equation increases its effective damping to $b_{\mathrm{eff}} = b + K^2/R$. Set $v = 0$ when discussing free relaxation with the electrical terminals connected through a resistor. A moving shorted coil generates a current that opposes its motion. Opening the circuit instead suppresses that current and leaves the mechanical damping. An ideal current source holding specified current through all pointer motions also changes the back-emf response because its output voltage adjusts to enforce that current.

The undamped angular frequency is $\omega_0 = \sqrt{\kappa/J}$ and the damping ratio is

$$\zeta = b_{\mathrm{eff}}/(2\sqrt{\kappa J}).$$

Take $J = 2.0 \times 10^{-6}\,\mathrm{kg\,m^2}$, $b = 1.6 \times 10^{-5}\,\mathrm{N\,m\,s/rad}$, and the preceding K, κ. Then $\omega_0 = 20.0\,\mathrm{rad/s}$, $2\sqrt{\kappa J} = 8.0 \times 10^{-5}\,\mathrm{N\,m\,s/rad}$, and an open circuit gives $\zeta = 0.20$. With $R = 1.00\,\Omega$ the electric contribution to damping is $2.50 \times 10^{-5}\,\mathrm{N\,m\,s/rad}$, giving $\zeta = 0.5125$. For a voltage step the ideal fractional overshoot in the reduced model is

$$\exp[-\pi\zeta/\sqrt{1-\zeta^2}] = 0.153.$$

The first peak occurs after $\pi/(\omega_0\sqrt{1-\zeta^2}) = 0.183\,\mathrm{s}$.

Critical damping occurs when $b + K^2/R = 2\sqrt{\kappa J}$, which requires a total resistance of about $0.391\,\Omega$. A winding resistance of $0.300\,\Omega$ therefore leaves $0.091\,\Omega$ for external source and leads. If the winding alone exceeds the target resistance, a simple passive external series resistor cannot reach this damping in the reduced model. A finite L must also be checked: with $L = 5.0\,\mathrm{mH}$ and $R = 1.0\,\Omega$, $\omega_0 L/R = 0.10$, so the approximation provides a useful starting estimate. Reducing R indefinitely eventually invalidates the elimination of current. The full pair of equations then predicts the damping and frequency dependence.

Distinguish a charge impulse from a slow current reading

Suppose a brief imposed current pulse ends long before the pointer has turned appreciably. Integrating the torque equation over that interval gives

$$J\Delta\dot{\theta} \simeq K\int i\,dt = Kq.$$

The initial signal is now angular velocity proportional to total transmitted charge. For weak subsequent damping, the first excursion is approximately $Kq/(J\omega_0)$. A dose of $20\,\mu\mathrm{C}$ gives $2.50\,\mathrm{mrad}$ with the instrument above, corresponding to about $2.50\,\mathrm{mm}$ on the mirror scale. Two current pulses of identical charge but different shapes give nearly the same reading if both are short on the mechanical time scale. Their peak currents can be entirely different.

For appreciable damping, use the impulse solution $\theta(t) = Kq\,e^{-\zeta\omega_0 t}\sin(\omega_d t)/(J\omega_d)$, with $\omega_d = \omega_0\sqrt{1-\zeta^2}$ for an underdamped pointer. Its maximum obeys $\tan(\omega_d t_p) = \omega_d/(\zeta\omega_0)$ in the first quarter cycle. Substitution corrects the ballistic calibration instead of treating the damped peak as an undamped amplitude. The state of the external circuit after the pulse matters because it determines ζ during the throw. A calibration pulse should leave the measuring circuit connected in the same way as the unknown pulse.

Measure the torque constant without assuming the magnetic field

The preceding design calculation multiplies turn count, active area and a nominal air-gap induction. An independent calibration can measure the same constant without knowing the field distribution along every wire. Move the pointer through a small controlled angle while measuring its open-circuit voltage with a high-impedance instrument. In the same working interval the voltage is $K(\theta)\dot{\theta}$ up to a polarity choice. Integrating the voltage over the sweep gives $\int_{\theta_1}^{\theta_2} K(\theta)\,d\theta$. If K is constant this is simply $K\Delta\theta$, independent of sweep speed. It is often easier to integrate a recorded voltage pulse accurately than to differentiate the angle trace to obtain instantaneous speed.

For a sweep through $0.0800\,\mathrm{rad}$, suppose the measured voltage integral is $0.401\,\mathrm{mV\,s}$. The generator constant is $5.01\times10^{-3}\,\mathrm{V\,s/rad}$. Independently add a known small torque to the spring and measure its static angle. A torque $32.0\,\mu\mathrm{N\,m}$ rotates the pointer by $0.0400\,\mathrm{rad}$, giving $\kappa = 8.00\times10^{-4}\,\mathrm{N\,m/rad}$. Combining the two measurements predicts a current sensitivity of $6.27\,\mathrm{rad/A}$. Splitting the sweep into smaller equal angular intervals tests whether the measured K depends on angle. Sweeping backwards should reverse the integrated voltage. A voltage offset instead contributes its offset times duration, so repeating at two sweep speeds helps separate it.

A dynamic cross-check uses free decay under two load conditions. Measure the exponential decay rate α_{open} with a high-impedance voltage probe and α_R with a known total resistance in the closed circuit. In the short-electrical-time limit, subtraction of the two damping laws yields

$$K^2 = 2JR(\alpha_R - \alpha_{\mathrm{open}}).$$

With $J = 2.0\times10^{-6}\,\mathrm{kg\,m^2}$, $R = 1.00\,\Omega$, and decay rates 4.0 and $10.25\,\mathrm{s^{-1}}$, this gives

$$K = 0.0050\,\mathrm{N\,m/A}.$$

The method needs two identifiable decay rates and independent inertia. If the loaded response is overdamped, the envelope of two oscillation peaks is no longer available; fit the full two-real-pole response to the measured displacement.

Keep the third dynamical variable in a frequency-response experiment

For a sinusoidal voltage at angular frequency ω the exact linear transduction law follows by eliminating the complex current after transforming both differential equations. The mechanical impedance in angular-displacement form is $\kappa - J\omega^2 + i\omega b$; the winding impedance is $R + i\omega L$. Using phasors with time dependence $e^{i\omega t}$ gives

$$\frac{\Theta}{V} = \frac{K}{(R + i\omega L)(\kappa - J\omega^2 + i\omega b) + i\omega K^2}.$$

At zero frequency the gain is $K/(R\kappa)$ and the phase tends to zero, as the static calibration requires. At a sufficiently high frequency both the electrical and inertial impedances grow. For $L > 0$ the magnitude approaches $K/(LJ\omega^3)$. The reduced model with the current eliminated algebraically falls only as $1/\omega^2$. The change of the asymptotic slope provides an experimental way to distinguish finite inductance from an incorrectly adjusted viscous damping constant. Beyond the working band of a real instrument, elastic modes of the pointer or parasitic capacitance can enter before that asymptote is resolved.

At the nominal undamped frequency $20\,\mathrm{rad/s}$, with $R = 1.0\,\Omega$ and $L = 5.0\,\mathrm{mH}$, the stiffness and inertia terms cancel. The denominator becomes $-\omega^2 Lb + i\omega(Rb + K^2)$, or approximately $-0.000032 + i\,0.000820$ in consistent SI units. Its magnitude gives about $6.09\,\mathrm{rad/V}$. A sinusoid of $1.0\,\mathrm{mV}$ peak produces about $6.09\,\mathrm{mrad}$ peak, whereas the static response to $1.0\,\mathrm{mV}$ is $6.25\,\mathrm{mrad}$. The phases differ radically despite their similar amplitudes: near this frequency the pointer lags by about 92.2°. A gain-only calibration at a single frequency would miss the phase lag.

Change the electrical load and compare two step models

In the live graph the source voltage is chosen anew at each resistance to give a final current of $5.0\,\mathrm{mA}$ after the pointer settles. That convention keeps the final angle common to all curves and isolates the transient response of the load. The full model retains $i, \theta, \dot\theta$; the second curve sets $L\dot i = 0$. Predict first which trace should start flatter. With finite inductance the current initially vanishes and increases at a finite rate. The initial torque and angular acceleration therefore vanish, while the reduced model applies a finite torque immediately. Increasing the inductance makes that distinction easier to see, especially when the electrical response time becomes comparable to the period of mechanical oscillation.

Open the live experiment

Try the calculation

Total resistance (Ω) 1

Winding inductance (mH) 5

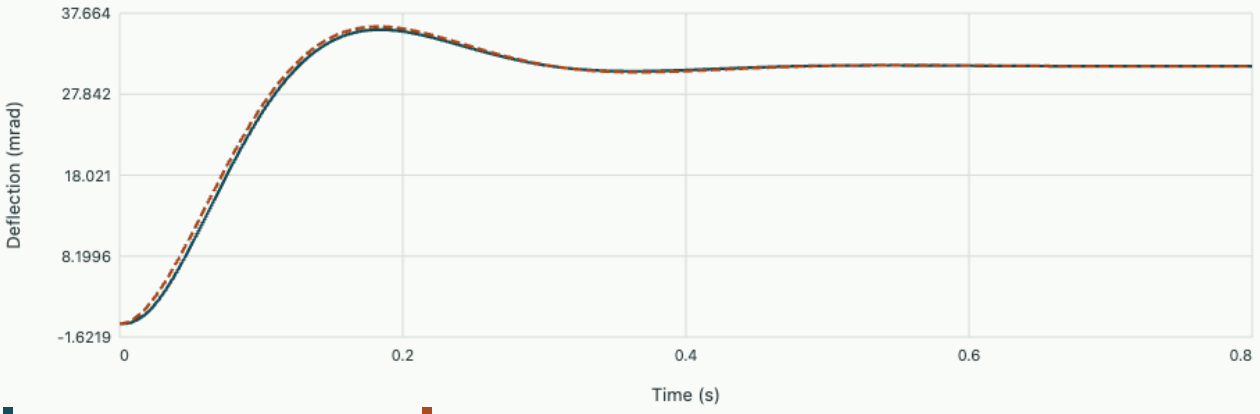

Coupled winding and pointer Short electrical time approximation

The reduced damping ratio is 0.512. The largest deflection in the first 0.80 s is 35.67 mrad. The common static limit is 31.25 mrad.

How could a student change the static range of the instrument without changing its suspension or its torsional stiffness?

▼ **Work through the solution**

For a dc ammeter, connect a calibrated shunt resistance in parallel with the coil, allowing only a known fraction of total current into it. With a coil winding resistance $0.300\,\Omega$ and a $0.0333\,\Omega$ shunt, the coil carries about ten percent of a steady terminal current and the indicated full-scale terminal current increases about tenfold. The total circuit seen by a motional voltage during a pointer oscillation depends on the shunt and source impedance, so the static range multiplier does not by itself give the new damping. For a voltmeter, a series resistance instead sets the current produced by an applied terminal voltage. In both cases record the resistance network whenever reporting a dynamic response.

Estimate the back action on the signal being measured

A galvanometer becomes part of the circuit it observes. Suppose a source with open-circuit voltage $10.0\,\mathrm{mV}$ and internal resistance $2.00\,\Omega$ drives a coil of resistance $0.300\,\Omega$. After settling, the current is $4.35\,\mathrm{mA}$ and the pointer turns by $27.2\,\mathrm{mrad}$. The undisturbed short-circuit current of the source would have been $5.00\,\mathrm{mA}$. Interpreting the indicated value as the current that would flow with a perfect zero-resistance meter underestimates that quantity by about thirteen percent. Measuring the open-circuit voltage instead requires a sufficiently large input resistance, another electrical boundary condition.

During pointer motion the disturbance includes the back emf as well as winding resistance. If the same coil is briefly turning at $0.40\,\mathrm{rad/s}$ it develops a $2.0\,\mathrm{mV}$ back emf. Neglecting inductance for that

estimate, the resulting current is

$$(10.0 - 2.0)\,\mathrm{mV}/2.30\,\Omega = 3.48\,\mathrm{mA}.$$

The deflection therefore contains information about both the source and the pointer's earlier motion. A static calibration alone cannot recover a rapid source waveform. A known source resistance and the two coupled dynamic equations provide a way to estimate the waveform from synchronised angle and current measurements.

Tutorial on calibration and transient identification

A current source produces a static mirror shift of $12.5\,\mathrm{mm}$ on a screen $0.50\,\mathrm{m}$ away. Estimate the current and identify a reversible test for an angular zero offset.

▼ **Work through the solution**

Use $\theta = \frac{1}{2}\arctan(0.0125/0.50) = 0.01250\,\mathrm{rad}$ and $i = \kappa\theta/K = 2.00\,\mathrm{mA}$. Repeat with reversed current of equal magnitude. Half the difference of the two angles cancels a fixed angular zero offset and isolates the response odd in current. A changing temperature during reversal can alter the spring or winding resistance, so alternate the order and record the zero afterwards if the required uncertainty is small.

For an open-circuit free decay the ratio of two successive same-side positive peak angles is 3.60. Their time separation is $0.321\,\mathrm{s}$. Recover the mechanical parameters that can be inferred if J is known.

▼ **Work through the solution**

The logarithmic decrement is $\ln 3.60 = 1.281$. The decay rate is $\alpha = 1.281/0.321 = 3.99\,\mathrm{s}^{-1}$, and the damped angular frequency is

$$2\pi/0.321 = 19.57\,\mathrm{rad/s}.$$

Then $\omega_0 = \sqrt{\omega_d^2 + \alpha^2} = 19.97\,\mathrm{rad/s}$,

$$b = 2J\alpha = 1.60 \times 10^{-5}\,\mathrm{N\,m\,s/rad},$$

$$\kappa = J\omega_0^2 = 7.98 \times 10^{-4}\,\mathrm{N\,m/rad}.$$

This identification assumes viscous damping and a sufficiently high impedance to make the electrical damping negligible.

Explore how motion generates voltage in the induction chapter.

Why an oscillator can move without its packet spreading

Quantum states, dynamics and measurement

Start with the measured mass and curvature of a potential. Factor its Hamiltonian, prove the energy ladder, construct a freely moving Gaussian from number states and find when squeezing or anharmonicity changes that prediction.

Use the equilibrium length and momentum scales

Near a stable minimum a smooth one-dimensional potential has expansion $V(x) = V(0) + m\omega^2 x^2/2 + O(x^3)$ after the origin is shifted to the minimum. Choose the arbitrary zero $V(0) = 0$. The fitted curvature is $m\omega^2$, not ω itself; measuring both the oscillation frequency and restoring slope separately identifies the effective mass. The classical energy ellipse becomes a circle if position and momentum are rescaled consistently. Define $X = \sqrt{m\omega/\hbar}\, x$ and $P = p/\sqrt{m\hbar\omega}$, so $[X, P] = i$ and $H = \hbar\omega(X^2 + P^2)/2$. Since position and momentum fail to commute, multiplying two linear factors must retain their order.

Set $a = (X + iP)/\sqrt{2}$ and $a^\dagger = (X - iP)/\sqrt{2}$. Then

$$a^\dagger a = (X^2 + P^2 + i[X, P])/2 = (X^2 + P^2 - 1)/2.$$

Thus $H = \hbar\omega(N + 1/2)$, $N = a^\dagger a$ and $[a, a^\dagger] = 1$. For every normalised state in the relevant domain $\langle N\rangle = \|a|\psi\rangle\|^2 \geq 0$. The additive half quantum is an energy contribution that survives in a state with vanishing classical means of x, p; discarding the commutator would lose it. Transition frequencies within an ideal ladder measure energy differences, so those frequencies alone cannot determine an absolute zero of energy.

Prove discreteness and construct the ground state

Using the product rule for commutators gives

$$[N, a] = -a,$$
$$[N, a^\dagger] = a^\dagger.$$

If a normalisable energy eigenstate has N eigenvalue ν, application of a either annihilates it or yields an eigenstate of eigenvalue $\nu - 1$ and norm squared ν. Repeated lowering cannot yield a state of negative norm squared. For noninteger nonnegative ν the chain would reach $0 < \nu' < 1$ with nonzero image at a negative eigenvalue. Therefore the chain must terminate at an integer step in an annihilated ground state. This argument uses the bound oscillator's spectrum and states in the ladder operators' domains. Existence and completeness can also be checked by solving the one-dimensional differential equation with decaying boundary conditions.

In coordinate representation $P = -i\, d/dX$, so $a\psi_0 = 0$ reduces to

$$d\psi_0/dX = -X\psi_0.$$

Its square-integrable solution is

$$\psi_0(X) = \pi^{-1/4} e^{-X^2/2}.$$

Normalised excited states follow by $|n\rangle = (a^\dagger)^n |0\rangle / \sqrt{n!}$. Orthogonality follows from the self-adjoint number operator with distinct eigenvalues. The coordinates in metres have ground variance $\sigma_x^2 = \hbar/(2m\omega)$, momentum variance $\sigma_p^2 = m\hbar\omega/2$, and zero symmetrised covariance. The geometric ground-state width is thus fixed by mass and trap stiffness. A semiclassical estimate minimising $\hbar^2/(8m\sigma_x^2) + m\omega^2\sigma_x^2/2$ gives $E_{\min} = \hbar\omega/2$, because the Gaussian saturates the uncertainty inequality used in that estimate.

In a number state both $\langle x\rangle$ and $\langle p\rangle$ vanish. Their fluctuations do not. Substitute $x = \sigma_x(a + a^\dagger)$. Terms $a^2, (a^\dagger)^2$ change the occupation by two and have zero diagonal element, whereas $aa^\dagger$ and $a^\dagger a$ contribute $n + 1$ and n. Hence $\langle x^2\rangle_n = (2n + 1)\sigma_x^2$; similarly $\langle p^2\rangle_n = (2n + 1)\sigma_p^2$. The mean kinetic and potential energies each equal half the total. Measuring a nonzero rms displacement does not imply that the oscillator centre is undergoing a coherent motion.

Find a state whose centre follows the classical trajectory

Search for a normalised eigenstate of a with complex eigenvalue α. It is permissible for this non-Hermitian operator to have complex eigenvalues; they label states rather than directly observable outcomes. Expand $|\alpha\rangle = \sum_n c_n |n\rangle$. Matching every number-state coefficient yields

$$c_{n+1} = \alpha c_n / \sqrt{n + 1}.$$

Using the exponential series to normalise gives

$$|\alpha\rangle = e^{-|\alpha|^2/2} \sum_{n=0}^{\infty} \frac{\alpha^n}{\sqrt{n!}} |n\rangle,$$

$$P(n) = e^{-|\alpha|^2} \frac{|\alpha|^{2n}}{n!}.$$

The mean and variance of occupation are both $|\alpha|^2$. Different coherent states are nonorthogonal: summing the overlap yields

$$|\langle\beta|\alpha\rangle|^2 = e^{-|\alpha-\beta|^2}.$$

At displacement difference one in this dimensionless complex plane the overlap probability is still $e^{-1} = 0.368$. A measurement that distinguishes all such nearby coherent preparations perfectly from one copy would contradict this overlap.

Each coefficient acquires $e^{-i(n+1/2)\omega t}$. Take the common zero-point phase outside the sum, leaving exactly the same expansion with $\alpha(t) = \alpha e^{-i\omega t}$. Hence $\langle x(t)\rangle = 2\sigma_x \operatorname{Re}\alpha(t)$ and $\langle p(t)\rangle = 2\sigma_p \operatorname{Im}\alpha(t)$. The centred operator $a - \alpha$ annihilates the state, so its centred quadrature variances match those of the ground state. The packet moves on the classical phase-space ellipse

without spreading. In a free particle the quadratic momentum phase causes spreading; in the bound oscillator equally spaced energy levels preserve this particular relative-phase structure.

For a vibrational mode with $m = 2.00 \times 10^{-25}$ kg and $\omega = 2\pi \times 100$ kHz, $\sigma_x = 20.5$ nm. Prepare $\alpha = 1.5i$. Initially the average position is zero and the momentum is positive; a quarter period later the centre reaches $3\sigma_x = 61.5$ nm. The mean occupation is 2.25 and the ground probability is 0.1054. This ensemble has a nonzero ground-state probability even though its position oscillation is clearly resolved by repeated measurements. A pure number state of average energy near this value could give similar rms positions but would show no time-dependent centre.

Background · Which measurement distinguishes two oscillators of equal mean energy?

Compare the first excited number state with a coherent state of amplitude $\alpha = 1$. Both have mean occupation one and hence the same mean energy $3\hbar\omega/2$. For a number state the expectation of the lowering operator vanishes because it connects orthogonal levels. For a coherent state its expectation equals α and evolves with the oscillator phase.

$$\langle x(t)\rangle_{\mathrm{coh}} = \sqrt{\frac{2\hbar}{m\omega}}\,\mathrm{Re}(\alpha e^{-i\omega t}),$$

$$\langle x(t)\rangle_{n=1} = 0.$$

Synchronous position measurements on freshly prepared states distinguish the moving centroid from the stationary one. A repeated energy measurement also separates the preparations. The number state always gives one quantum, whereas the coherent state gives a Poisson distribution with mean and variance both equal to one. A mean energy by itself omits both distinctions.

Rotate an uncertainty ellipse and test a nonideal trap

A sudden frequency change provides an experimentally meaningful way to generate a state with unequal quadrature fluctuations. Prepare the ground state at frequency ω_i, then instantaneously change to ω_f. The state in the position representation is continuous through an ideal sudden change. Relative to the final oscillator,

$$\langle X_f^2\rangle = \omega_f/(2\omega_i),$$

$$\langle P_f^2\rangle = \omega_i/(2\omega_f);$$

their product remains $1/4$. Their sum exceeds one unless the two frequencies coincide. Thus the state is a squeezed vacuum for the new trap, with mean occupation $\frac{1}{4}(\omega_f/\omega_i + \omega_i/\omega_f - 2)$. Unlike a coherent displacement its centre remains zero. Measuring a variance as the ellipse rotates distinguishes these preparations even if their average energies match.

For $\omega_f = 2\omega_i$ the mean occupation is 0.125. Since $X_f(t) = X_f(0)\cos\omega_f t + P_f(0)\sin\omega_f t$, variance oscillates between 1 and 0.25 in these units with angular frequency $2\omega_f$. The ground variance for the final trap would be 0.5, so part of the cycle lies below it. Momentum variance rises correspondingly, and at

intermediate angles a nonzero covariance is needed in the uncertainty determinant. Abrupt changes also inject work via the time-dependent Hamiltonian. Energy measured before and after the sudden change need not agree even though the state vector at the switching instant is unchanged.

Real traps eventually depart from exact harmonic confinement. Write a model diagonal spectrum $E_n/\hbar = \omega(n+1/2) + \chi n(n-1)/2$ for weak amplitude-dependent spacings over the occupied range. Coherent-state sums give

$$\langle a(t)\rangle = \alpha e^{-i\omega t}\exp[|\alpha|^2(e^{-i\chi t}-1)].$$

Its magnitude is $|\alpha|\exp[-|\alpha|^2(1-\cos\chi t)]$. The collapse of the centre can occur under strictly unitary evolution while the number probabilities stay fixed. Their phases reassemble at $2\pi/|\chi|$ in this ideal spectrum. Irreversible noise and uncontrolled fluctuations can suppress a measured revival; loss of the mean alone does not diagnose dissipation. A position trace and a number-resolved distribution probe complementary parts of the dynamics.

Factor a measured displacement into force history and oscillator response

A linear force couples to position,

$$H(t) = \hbar\omega(N+1/2) - F(t)x.$$

Even if the force time series is irregular, this driven oscillator is exactly soluble within the harmonic approximation. In the Heisenberg picture use $\dot a = (i/\hbar)[H,a]$. Since $[x,a] = -\sigma_x$, the equation is

$$\dot a = -i\omega a + i\sigma_x F(t)/\hbar.$$

Multiply by $e^{i\omega t}$ and integrate:

$$a(t) = e^{-i\omega t}\left[a(0) + \frac{i\sigma_x}{\hbar}\int_0^t F(t')e^{i\omega t'}dt'\right].$$

A force therefore displaces the rotating oscillator according to one complex Fourier component of its history. Its phase determines which final quadrature changes. The centred operator still evolves as in free oscillation. Thus a known linear drive displaces a ground state into a coherent state without squeezing it. The same formula shifts a thermal state without removing its thermal fluctuations. The statement about pure coherence requires knowing the initial state as well as measuring the final displacement.

Take a constant force F_0 switched on for time T then off. For an initially stationary ground state the final amplitude, measured at switch-off in the original oscillator basis, is $\alpha_F = F_0\sigma_x[1-e^{-i\omega T}]/(\hbar\omega)$. The corresponding mean position is $F_0(1-\cos\omega T)/(m\omega^2)$, agreeing with the classical step response of a mass on a spring. Its excitation number is $4(F_0\sigma_x/\hbar\omega)^2\sin^2(\omega T/2)$. A constant force applied for exactly a full period creates zero residual excitation at switch-off even though the oscillator moved

substantially during the pulse. Motion of the trap centre and persistent excitation after the trap returns must be experimentally distinguished.

For $m = 2.00 \times 10^{-25}$ kg and 100 kHz as above, let $F_0 = 2.00 \times 10^{-21}$ N. Its static equilibrium displacement is

$$F_0/(m\omega^2) = 25.3\,\mathrm{nm}.$$

A half-period pulse leaves the mean at 50.7 nm with zero mean momentum and $|\alpha| = 50.7/(2 \times 20.5) \simeq 1.24$. Its mean added occupation is roughly 1.53. The elastic energy $m\omega^2\langle x\rangle^2/2$ at switch-off matches $\hbar\omega|\alpha|^2$, independently of any counting argument. This check subtracts the unchanged zero-point energy. Using the total energy including zero point in the comparison would incorrectly attribute a half quantum to the drive even when the applied force vanishes.

The sudden impulse limit provides another independent test. Let a short pulse deliver total impulse $J = \int F dt$ over a time much shorter than $1/\omega$. The amplitude increment is approximately $i\sigma_x J/\hbar$ in the appropriate rotating phase. Since $2\sigma_p\sigma_x = \hbar$, the mean momentum changes by J. For a smooth pulse spread around one period the same total impulse can produce a much smaller residual excitation because the force acts at different phases of the oscillator. A force sensor based on final occupation measures the squared magnitude of a windowed resonant integral. Reconstructing a complete time-dependent force from that single energy measurement is generally impossible. Varying the drive start time or measuring both final quadratures gives additional information.

Use operator ordering to predict a phase with zero final displacement

Define the displacement operator $D(\alpha) = \exp(\alpha a^\dagger - \alpha^* a)$. Its generator is anti-Hermitian, so it is unitary. The commutator of $\alpha a^\dagger - \alpha^* a$ with a is a constant. Differentiating $D^\dagger(s\alpha) a D(s\alpha)$ with respect to s and integrating gives

$$D^\dagger(\alpha) a D(\alpha) = a + \alpha.$$

Consequently $D(\alpha)|0\rangle$ is an annihilation eigenstate of eigenvalue α, giving an independent physical construction of the number expansion. The normal-order factorisation $D = e^{-|\alpha|^2/2} e^{\alpha a^\dagger} e^{-\alpha^* a}$ follows from the Baker–Campbell–Hausdorff formula because the relevant commutator is a scalar. Acting on the ground state recovers the Poisson coefficients directly. Omitting the scalar prefactor gives a state with the wrong norm.

Two displacements do not commute as operators despite their effects on the mean phase-space position adding in either order. Their scalar commutator gives

$$D(\alpha) D(\beta) = e^{(\alpha\beta^* - \alpha^*\beta)/2} D(\alpha + \beta).$$

The product around a closed displacement loop is

$$D(\alpha) D(\beta) D(-\alpha) D(-\beta) = e^{\alpha\beta^* - \alpha^*\beta} I.$$

For $\alpha = 1,\ \beta = i/2$ the phase is -1 rad in this written operator order. Reversing the physical order conjugates the phase. The oscillator returns to its initial phase-space position and, apart from this phase, to its initial state. In a single isolated preparation the common phase is invisible. To observe it, place the oscillator interaction under coherent control of one branch of a separate two-level reference, recombine the reference and compare the branch that went around the loop with the branch that did not. Surviving coherence of the reference is essential. The same result can be described as an oriented area in the $\mathrm{Re}\,\alpha, \mathrm{Im}\,\alpha$ plane and ultimately follows from $[x, p] = i\hbar$.

It is useful to trace the actual motion before interpreting a claimed geometric phase. Operators act from right to left on kets, so plotting a particular rectangular loop in time can correspond to the conjugate of a product written left to right. A lab comparison should specify the four pulse phases in chronological order and the ordinary free rotation occurring between them. In the rotating frame the displacement vectors are simple complex increments; in the laboratory frame the oscillator itself continually advances in phase. An uncompensated delay can leave a residual displacement rather than a closed loop. The overlap of that residual displaced ground state with the reference branch is $e^{-|\Delta\alpha|^2/2}$ in amplitude, reducing observed fringe contrast as well as shifting its phase.

Measure displaced parity to distinguish a number state from a mixture

The number parity operator $\Pi = (-1)^N$ gives $+1$ for even and -1 for odd occupation. It implements the coordinate reflection $x \to -x$ for the harmonic oscillator. A position-space Wigner distribution may be sampled by displacing the state and measuring its parity. In the complex phase-space convention used here define $W(\beta) = (2/\pi)\,\mathrm{tr}[D(-\beta)\rho D^\dagger(-\beta)\Pi]$; it integrates to one in $d^2\beta$. At $\beta = 0$ it is just twice the even-minus-odd probability divided by π. Its sign is determined by observable population statistics, but its value at a point is not the probability that a particle occupies a sharp simultaneous position and momentum.

For a coherent input $|\alpha\rangle$, displacement produces $|\alpha - \beta\rangle$ up to a phase. Summing the even-minus-odd Poisson occupations gives $e^{-2|\alpha-\beta|^2}$. Hence $W(\beta) = 2e^{-2|\alpha-\beta|^2}/\pi$, a positive Gaussian. A first excited number state instead has $W(0) = -2/\pi$. Mix that state with ground-state population,

$$\rho = p|1\rangle\langle 1| + (1-p)|0\rangle\langle 0|.$$

Then $W(0) = (2/\pi)(1 - 2p)$, negative only when $p > 1/2$. An observed lack of negativity at one displacement does not imply a Gaussian state or a globally classical description. It may simply mean that the probe is examining a positive region or that losses have mixed the odd preparation with the ground state.

Suppose an experimental detector distinguishes only “zero excitations” from “one or more”. A measured nonzero fraction of 0.80 does not determine parity without further information: all those events might contain one excitation or a substantial even population might be present. Number resolution or a separate calibrated parity mapping is needed. If only ground and first excited population are independently established, an observed $p_1 = 0.70 \pm 0.02$ gives $W(0) = -0.255 \pm 0.025$ in these dimensionless units. Propagating that uncertainty requires the assumption about higher occupations.

Combining a displacement scan with number-resolved or parity-sensitive data therefore tests both the preparation and the adequacy of a finite oscillator basis.

Recover a thermal occupation from two independent observables

For an oscillator in thermal equilibrium at inverse temperature β_T, the occupation probabilities are $P_n = (1-q)q^n$ with $q = e^{-\beta_T \hbar\omega}$. The geometric series gives $\bar{n} = q/(1-q)$ and variance $\bar{n}(\bar{n}+1)$. Unlike a coherent state with the same mean occupation, the number distribution is broader and the free mean displacement is zero. The symmetrised position variance is $(2\bar{n}+1)\sigma_x^2$. A variance measurement alone cannot distinguish a thermal distribution from an incoherent nonthermal mixture with the same mean energy. Resolving more than the variance probes the full probability law.

For example, at $\bar{n} = 2$ thermal equilibrium predicts ground occupation $1/3$, number variance 6 and parity $1/(2\bar{n}+1) = 1/5$. A coherent state with $|\alpha|^2 = 2$ gives ground probability 0.1353, variance 2 and parity $e^{-4} = 0.0183$. A uniform randomisation of the coherent phase removes the mean displacement but leaves these Poisson number statistics unchanged. It can therefore resemble the thermal state on a quadrature average while differing sharply in ground population and parity. A displaced thermal preparation adds a classical centre motion on top of the thermal fluctuations; fitting only its energy would confuse displacement with temperature. Centre, centred variance and at least one independent number statistic make a coherent experimental set of observables for these physically different preparations.

Follow a coherent oscillator state in phase space

Change the magnitude and phase of a coherent amplitude independently. Predict which control changes the mean occupation and which shifts the timing of the position measurement.

Open this experiment online

Try the calculation

Coherent amplitude magnitude **1.3**

Preparation phase (degrees) **30**

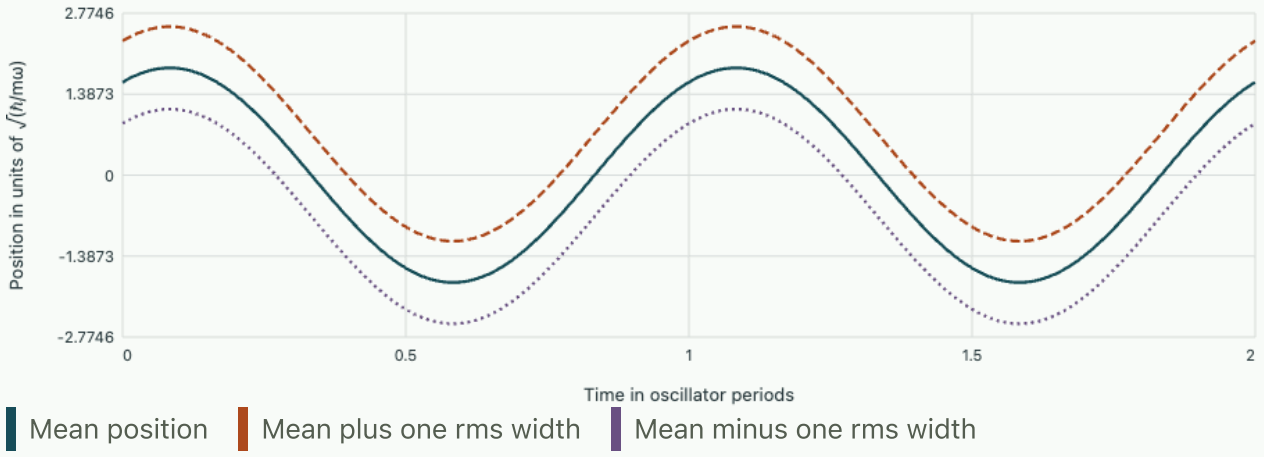

Mean occupation 1.69 quanta, standard deviation 1.3. Ground-state probability 0.18452. Position variance in the plotted units is 1/2.

Recover individual transition probabilities after a sudden trap change

The sudden-frequency experiment predicted mean occupation from the second moments. Number-resolved probabilities provide a stronger test. The initial ground-state wavefunction is even, and changing the trap curvature about the same centre preserves parity. The initial state therefore overlaps only even eigenstates of the final trap. A measured odd population beyond readout uncertainty diagnoses a displaced minimum, parity-breaking drive or imperfect initial preparation. The vanishing of odd occupation is stronger than knowing only the mean and variance of a quadrature.

Write the old annihilator in terms of the new operators,

$$a_i = \cosh r\, a_f - \sinh r\, a_f^\dagger,$$

with $r = \tfrac{1}{2}\ln(\omega_f/\omega_i)$ for this choice of sign. This follows directly by expressing both in the same x, p and comparing coefficients. The relative sign can change under a different convention for defining the squeeze parameter but all probabilities below are invariant. The old vacuum obeys $(a_f - \tanh r\, a_f^\dagger)|0_i\rangle = 0$. In the final number basis $c_n = \langle n_f|0_i\rangle$, the coefficient of $|n\rangle$ gives

$$\sqrt{n+1}\,c_{n+1} = \tanh r \sqrt{n}\, c_{n-1}.$$

The $n = 0$ equation forces $c_1 = 0$, and iteration gives

$$c_{2j} = c_0 \frac{\sqrt{(2j)!}}{2^j j!} (\tanh r)^j,$$

$$c_{2j+1} = 0.$$

To normalise, use the central-binomial series $\sum_j \binom{2j}{j} q^j / 4^j = (1-q)^{-1/2}$ at $q = \tanh^2 r$. Thus

$$|c_0|^2 = 1/\cosh r.$$

A separate coordinate-space check follows by integrating the overlap of two Gaussian ground states, giving $P_0 = 2\sqrt{\omega_i \omega_f}/(\omega_i + \omega_f)$. This agrees with $1/\cosh r$, independently of the operator recursion. Differentiating the normalisation-generating series gives $\bar{n} = \sinh^2 r$, agreeing with the energy inferred from the sudden change of the Hamiltonian.

For a doubling of frequency, $\tanh r = 1/3,\ \cosh r = 3/(2\sqrt{2})$, so

$$P_0 = 0.9428,\ P_2 = P_0/18 = 0.05238,$$

$$P_4 = P_0 (3/8)(1/81) = 0.00436.$$

Higher even levels contain the remaining probability. At a mean excitation of 0.125, a coherent state would instead have $P_1 = 0.1103$. Even imperfect number resolution discriminating odd versus even can strongly distinguish a pure curvature quench from a coherent displacement with equal final energy. A finite switching time can reduce excitation if the oscillator tracks the moving ground state adiabatically. A shift of trap centre during a nominal curvature change adds a displacement and can populate odd levels. Measure the mean and parity along with the energy estimate before inferring a squeeze strength solely from a single occupation number.

Separate temperature from a parity-preserving quench

Before a sudden centred frequency doubling, a calibrated trap has thermal mean occupation 0.10. Predict the fraction of odd-number results after the quench and its final mean occupation. How might an experiment mistakenly interpret the odd results?

▼ **Derive and check the result**

In the initial thermal ensemble parity expectation is

$$1/(2\bar{n}+1) = 1/1.2 = 0.8333.$$

Parity commutes with both centred trap Hamiltonians, and measuring even or odd final occupation measures that same parity operator. The odds fraction is therefore $(1 - 0.8333)/2 = 0.0833$, unchanged by the quench. The final energy fluctuations scale with the initial quadrature variances multiplied by $2\bar{n}+1$, giving $\bar{n}_f + 1/2 = (\bar{n}_i + 1/2)(\omega_f/\omega_i + \omega_i/\omega_f)/2 = 0.75$. Thus $\bar{n}_f = 0.25$. Assuming a perfectly cold initial state might turn the observed odd fraction into a false diagnosis of trap displacement. Measure initial parity and post-quench parity independently to isolate processes that

actually break the symmetry. The increase of mean occupation alongside unchanged parity is the predicted signature of a centred quench.

Tutorial · analyse a state from amplitude and fluctuation data

Test two preparations with the same mean energy

Take a coherent state with $|\alpha|^2 = 3$ and number state $|3\rangle$. Compare energies, number variance, ground probability and the largest possible mean displacement.

▼ **Work through the solution**

Both have $\langle H\rangle = 3.5\hbar\omega$. The coherent number variance is 3 while the number-state variance is zero. Ground probabilities are $e^{-3} = 0.0498$ and zero. By selecting a suitable oscillator phase, the coherent state reaches $2\sqrt{3}\sigma_x$; the number state has zero centre at every time. An energy average alone leaves these preparations indistinguishable. The event of measuring exactly three quanta has probability $e^{-3}3^3/3! = 0.224$ in the coherent case and unity in the number case. Repeated shots allow this comparison without assuming a single shot reveals the input state.

Estimate numerical truncation before trusting a simulated coherent state

Expand a coherent state with $\alpha = 2$ in number states $0, \ldots, 8$. Is the missing probability negligible at a desired accuracy of one part in a thousand?

▼ **Work through the solution**

Generate probabilities successively from $p_0 = e^{-4}$, $p_{n+1} = 4p_n/(n+1)$; summing through 8 gives 0.97864, leaving 0.02136 above the cutoff. Renormalising the retained vector hides this discarded probability from a norm check and distorts quantities weighted by n. Through $n = 11$ the tail is about 0.00092, just below the specified probability tolerance. Energy moments require a separate tail weighted by n; a probability bound alone can be inadequate for them. Vary the cutoff while monitoring both number statistics and the centre motion to separate truncation artefacts from real dephasing.

Infer the coherent displacement and a squeezing test

At a known phase, measurements give

$$\langle x\rangle = 1.2\sigma_x,\ \langle p\rangle = -1.6\sigma_p.$$

Infer the coherent amplitude consistent with those means, then say what must still be measured to confirm a coherent preparation.

▼ **Work through the solution**

The means imply $\mathrm{Re}\,\alpha = 0.60,\ \mathrm{Im}\,\alpha = -0.80$, so $|\alpha| = 1$ and the putative coherent mean occupation is one. They do not fix the variances. A displaced thermal or squeezed state can produce the same means with different fluctuations. Measure the variance along independent quadratures, including a rotated axis to infer covariance. In an ideal normalised state the expectation of the positive operator $(a-\alpha)^\dagger(a-\alpha)$ equals $\langle N\rangle - |\alpha|^2$. If it vanishes exactly, the support is in the kernel of $a-\alpha$, giving the coherent state. With finite uncertainty a near-zero value instead bounds extra excitation in the displaced frame.

Further reading

- Fließbach · Operatorenmethode
- Course experiment · operators and oscillator spectra
- TUM · quantum mechanics, harmonic oscillator and operator formulation

Rotation and finite-amplitude dynamics

Translate an angular-momentum balance between laboratory and body frames. Follow it from impact to gyroscopic motion and distinguish driven nonlinear response from a change of stability.

1. Velocities and accelerations in planar mechanisms
2. Impulse, angular momentum and impact
3. Finite-amplitude oscillations and model validity
4. Steady gyroscopic precession and its two possible rates
5. Why Coulomb damping loses a fixed amplitude each half-cycle
6. When the third harmonic matters more than the fundamental
7. Proving a region of attraction with the energy of a pendulum
8. Finding a turning point without using the load as a coordinate

Velocities and accelerations in planar mechanisms

Machine dynamics

Use the rigid-body velocity and acceleration relations to connect an instantaneously known crank speed to a slider acceleration.

FROM FIRST PRINCIPLES

Differentiate a fixed link vector in a rotating body

For two material points A, B on a rigid planar link, their separation has constant length even while its direction changes. Let $\mathbf{r} = \mathbf{r}_B - \mathbf{r}_A$ and angular velocity vector $\boldsymbol{\omega}$ be perpendicular to the plane. A small rotation by $d\theta$ sweeps a displacement perpendicular to the separation. Dividing by time gives the inertial derivative $\dot{\mathbf{r}} = \boldsymbol{\omega} \times \mathbf{r}$ and hence

$$\mathbf{v}_B = \mathbf{v}_A + \boldsymbol{\omega} \times \mathbf{r}.$$

Differentiate once more using the product rule. Change of angular speed provides the tangential acceleration contribution; change of the separation's direction gives the second cross product.

$$\mathbf{a}_B = \mathbf{a}_A + \boldsymbol{\alpha} \times \mathbf{r} + \boldsymbol{\omega} \times (\boldsymbol{\omega} \times \mathbf{r}).$$

For planar rotation the final term is $-\omega^2 \mathbf{r}$, directed towards A. It remains even when angular speed is constant. These relations concern two fixed points on one rigid body. A slider moving along the rotating link changes the body-relative separation and contributes additional velocity and acceleration terms.

DERIVATION AND APPLICATIONS

Recover planar angular acceleration from two accelerometers

Velocities identify an instantaneous rotation centre, but a time-varying rotation is better characterised by both angular speed and angular acceleration. Mount two aligned accelerometers at points A and B on one rigid planar body. Assume the measured vectors have been expressed in common inertial axes and any gravity contribution cancels in their difference. The separation vector is $\mathbf{r} = \mathbf{r}_B - \mathbf{r}_A$ with fixed length d. Rigid-body kinematics gives

$$\Delta\mathbf{a} = \mathbf{a}_B - \mathbf{a}_A = \alpha\, \mathbf{e}_z \times \mathbf{r} - \omega^2 \mathbf{r}.$$

The two terms point in perpendicular directions. Form the unit vector $\mathbf{e}_r = \mathbf{r}/d$ from A to B and its counterclockwise normal $\mathbf{e}_t = \mathbf{e}_z \times \mathbf{e}_r$. Projecting gives a radial signal proportional to squared angular speed and a tangential signal proportional to signed angular acceleration.

$$\Delta a_r = -d\omega^2,$$
$$\Delta a_t = d\alpha.$$

Thus no knowledge of the translational acceleration of the reference point is needed. An additional tangential relative-velocity measurement supplies the missing sense of rotation because the signed ω enters linearly.

$$|\omega| = \sqrt{-\Delta a_r / d},$$
$$\alpha = \Delta a_t / d,$$
$$\omega = (\mathbf{v}_B - \mathbf{v}_A) \cdot \mathbf{e}_t / d.$$

A positive radial acceleration difference is inconsistent with a rigid pair under the stated conventions. Flexible mounting, sensor misalignment or treating differently oriented sensor components as parallel can all spoil the projection.

WORKED EXAMPLE

Read the motion of a rotating link

At separation 0.200 m the measured acceleration difference is $-3.20\,\mathbf{e}_r + 0.600\,\mathbf{e}_t$ m/s². The link has speed magnitude $\sqrt{3.20/0.200} = 4.00$ rad/s and counterclockwise angular acceleration $0.600/0.200 = 3.00$ rad/s². A measured relative tangential velocity of -0.800 m/s identifies clockwise rotation. Its speed magnitude is decreasing at this instant.

Change the inputs and inspect this calculation below

SECOND APPLICATION

Estimate a sensor spacing from a calibrated turn

A second instrument rotates steadily at 5.00 rad/s and records radial acceleration difference -3.75 m/s². Its effective sensor separation is

$$3.75/25.0 = 0.150\,\mathrm{m}.$$

A later measurement with the same instrument gives tangential difference -0.450 m/s², implying $\alpha = -3.00$ rad/s². This calibration uses steady rotation for the length scale and a distinct transient to determine angular acceleration.

Interactive calculation · Change the inputs of this example

Use the adjustable quantities to test the two worked calculations above. The plot recomputes this derivation's balance or constitutive relation; its numerical readout reports the quantities needed for the forward calculation and the inverse or design question. Keep the fixed assumptions stated in the readout when comparing with the example values.

Open this live calculation

Try the calculation

Sensor separation (m)	0.2
Signed angular speed (rad/s)	-4
Angular acceleration (rad/s²)	3

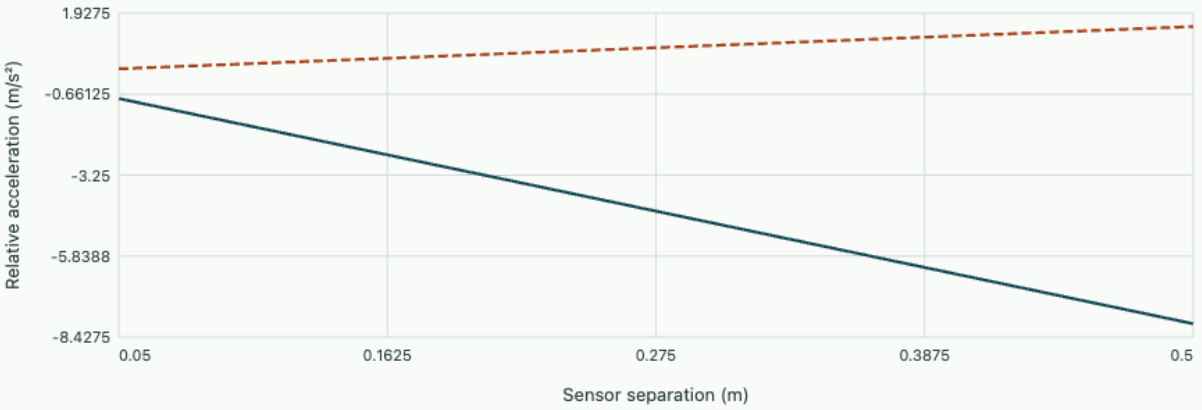

At selected spacing, radial=-3.200 and tangential=0.600 m/s²; relative tangential velocity=-0.800 m/s supplies the rotation sign.

What can change between two points on a link?

The point at which a connecting rod drives a slider moves along a straight line although its other end moves around a crank circle. Writing every trajectory as a function of crank angle is possible, but often only one configuration matters. The rigidity constraint transfers instantaneous velocity and acceleration between points on a link. Choose a fixed inertial frame and use the positive out-of-plane direction for counterclockwise angles. Every vector component below refers to these fixed axes.

Write $r_B = r_A + r_{B/A}$. The vector between two body points keeps its length but changes direction. Its derivative is $\omega \times r_{B/A}$. Differentiating a second time introduces both the changing magnitude of angular velocity and the changing direction of the relative vector:

$$v_B = v_A + \omega \times r_{B/A},$$

$$a_B = a_A + \alpha \times r_{B/A} + \omega \times (\omega \times r_{B/A}).$$

The last term is $-\omega^2 r_{B/A}$ for planar motion. It points along the rod towards A, even when the rod has constant angular speed. Enforce constraints on the actual point B; a slider constrained horizontally has zero vertical velocity and zero vertical acceleration if its guide is straight and fixed.

A crank at its uppermost position

Place crank centre O at the origin and the slider along the positive horizontal axis. The crank length is 50 mm and the connecting rod length is 130 mm. At the configuration considered its pin is $A = (0, 50)\,\mathrm{mm}$ and slider pin $B = (120, 0)\,\mathrm{mm}$, since $120^2 + 50^2 = 130^2$. The crank rotates counterclockwise at constant 20 rad/s. Accordingly $v_A = (-1, 0)\,\mathrm{m/s}$ and $a_A = (0, -20)\,\mathrm{m/s^2}$.

The rod vector from A to B is $(0.120, -0.050)\,\mathrm{m}$. Its relative velocity is $\omega_r(0.050, 0.120)$. The vertical velocity constraint gives $0 = 0 + 0.120\omega_r$, so $\omega_r = 0$ at this instant and $v_B = (-1, 0)\,\mathrm{m/s}$. The rod is instantaneously translating. That description concerns velocity only. A moment later its two ends no longer have the same velocity.

Recover the slider force input

Since $\omega_r = 0$ here, the relative centripetal term for the rod vanishes. The angular-acceleration term gives $0 = -20 + 0.120\alpha_r$, hence $\alpha_r = 166.7\,\mathrm{rad/s^2}$. The slider's horizontal acceleration is

$$a_{Bx} = 0 + 0.050(166.7) = 8.33\,\mathrm{m/s^2}.$$

At this instant the slider is moving to the left while accelerating to the right. A bare slider mass of 3 kg needs a net force of 25.0 N to the right before guide friction or process forces are considered.

A useful independent check follows from the exact geometry $x_B = r\cos\theta + \sqrt{l^2 - r^2\sin^2\theta}$. At $\theta = \pi/2$ the first derivative with respect to angle is $-r$; multiplication by crank speed gives –1 m/s. A numerical second derivative must resolve the curvature of this path. Differentiating noisy measured positions twice can produce a large fictitious force, so comparing observed positions with this geometric constraint is often a better starting point.

Change the drive speed

Repeating the same configuration at twice the constant crank speed doubles every point velocity. Its centripetal terms and the constraint-induced angular acceleration scale with the square of that speed, so the predicted slider acceleration becomes 33.3 m/s². This scaling is one reason mechanism inertia loads can grow rapidly with production rate.

Differentiate a coordinate measured along a rotating guide

The rigid-body formula above assumes that the position vector joining the two points is fixed in their common body. A slider moving along a rotating guide violates that assumption. Introduce a guide-fixed unit vector e_r along the slot and its positive quarter-turn e_θ. At an inertially fixed pivot the slider's position is $r(t)e_r$; the basis changes according to $\dot{e}_r = \omega e_\theta,\ \dot{e}_\theta = -\omega e_r$. Differentiate both the scalar radial position and the changing basis at every step.

$$v = \dot{r}\, e_r + r\omega\, e_\theta,$$

$$a = (\ddot{r} - r\omega^2)e_r + (r\dot{\omega} + 2\dot{r}\omega)e_\theta.$$

The factor two in the transverse contribution has two origins. The outward relative velocity vector rotates with the guide, and the speed of the circumferential transport changes as the slider moves outwards. Each contributes $\dot{r}\omega$. This Coriolis term is an actual part of the acceleration measured in an inertial frame. In a rotating-frame force balance an apparent Coriolis force of opposite sign must be introduced only if the inertial acceleration has been removed from that balance. Counting both would double the effect.

If the guide's pivot itself translates, add its inertial acceleration to the expression. For an instantaneously stationary guide $\omega = 0$ eliminates centripetal and Coriolis terms, but a nonzero angular acceleration can still produce transverse acceleration $r\dot{\omega}$. This distinction parallels the translating rod in the first worked mechanism.

Determine drive and guide reactions on a rotating table

A 2.5 kg carriage slides outwards along a straight radial slot in a horizontal table. At the given instant $r = 0.30\,\mathrm{m}$, $\dot{r} = 0.20\,\mathrm{m/s}$, $\ddot{r} = 0.50\,\mathrm{m/s^2}$, $\omega = 4.0\,\mathrm{rad/s}$ counterclockwise, and $\dot{\omega} = 1.0\,\mathrm{rad/s^2}$. The radial acceleration is $0.50 - 0.30(4)^2 = -4.30\,\mathrm{m/s^2}$ and the transverse acceleration is

$$0.30(1) + 2(0.20)(4) = 1.90\,\mathrm{m/s^2}.$$

A frictionless slot supplies a 4.75 N transverse reaction in the positive rotational direction. The radial actuator must exert a net 10.75 N inward, even though the carriage is moving outwards and accelerating relative to the slot in that direction.

The transverse reaction produces a 1.425 N m moment about the centre. Independently, differentiating the angular momentum $mr^2\omega$ gives

$$m(2r\dot{r}\omega + r^2\dot{\omega}) = 1.425\,\mathrm{N\,m}.$$

A table drive that assumes fixed radius would include only $mr^2\dot{\omega} = 0.225\,\mathrm{N\,m}$, missing most of the required moment in this manoeuvre. Holding angular speed constant would remove this last term but leave the 1.20 N m moment associated with increasing inertia. A torque sensor at the turntable shaft therefore detects radial carriage motion even when no angular acceleration is commanded.

Mechanical power supplies an independent sign check. The rail reaction transmits positive power $4.75(r\omega) = 5.70$ W through the transverse motion at this instant. The inward radial actuator supplies

$-10.75(0.20) = -2.15$ W. Their sum, 3.55 W, equals the instantaneous change of the point mass's translational energy, $m(\dot{r}\,a_r + r\omega a_\theta) = 2.5[0.20(-4.30) + 1.20(1.90)]$. The rail can supply power because it moves transversely with the table even though the contact has no work in the sliding direction.

Construct angular momentum when the rotation axis is not principal

A planar moment of inertia determines one scalar angular momentum. In three dimensions a balanced body can have angular momentum tilted relative to its angular velocity. About its centre of mass a particle at r has velocity $\omega \times r$. Integrate $r \times (\omega \times r)$ over mass and use the vector triple product. The result is

$$H_G = I_G \omega,$$

with tensor $I_G = \int [(r^T r)\mathbf{1} - r r^T]\, dm$. Its x-diagonal element is $\int (y^2 + z^2) dm$ and its xy element is $-\int xy\, dm$. Equal and opposite points cancel their first moments but add their products of inertia. Symmetry about a coordinate plane, rather than symmetry only about the centre, is sufficient to make the associated product vanish.

In a body-fixed basis rotating at ω, the external moment components obey $M_G = I_G \dot{\omega} + \omega \times (I_G \omega)$. This follows from differentiating H_G in an inertial frame: the body basis vectors rotate as well as the components. Even with constant body components of angular velocity, a transverse moment can be required to keep a nonprincipal axis fixed.

Model a compact instrument carrier as two equal 0.50 kg masses at $(0.20, 0.10, 0)$ m and its negative, neglecting the frame mass. Its tensor in kg m² has entries $I_{xx} = 0.010$, $I_{yy} = 0.040$, $I_{zz} = 0.050$, $I_{xy} = -0.020$. At $\omega = (20, 0, 0)$ rad/s, $H_G = (0.20, -0.40, 0)$ kg m²/s. Maintaining that rotation requires $M_G = (0, 0, -8.0)$ N m. There is no offset centre of mass to correct with a single static counterweight. Repositioning the masses to remove the product of inertia, or reorienting the shaft along a principal axis, eliminates this transverse couple in the model. A bearing reaction can reverse the sign convention for the load read by its support. Always state whether the reported moment acts on the rotor or on the frame.

Impulse, angular momentum and impact

Machine dynamics

Find the motion immediately after a short off-centre impact by combining angular impulse with a local restitution condition.

FROM FIRST PRINCIPLES

Close a short collision with impulse and restitution

During a short collision, contact force can be large while the position changes little. Let $g^- = v_1^- - v_2^- > 0$ be the relative approach speed along a fixed impact normal for two freely translating masses. Ignore tangential impulse and external impulses during contact. A compressive contact impulse of magnitude J slows the first mass and speeds the second. Integrating each momentum balance gives

$$v_1^+ = v_1^- - J/m_1,$$
$$v_2^+ = v_2^- + J/m_2.$$

Momentum conservation alone leaves the impulse undetermined. A measured normal coefficient of restitution e supplies the separation speed as a fraction of the approach speed. Substitution then determines the impulse.

$$v_2^+ - v_1^+ = e g^-,$$
$$J = \frac{(1+e)g^-}{1/m_1 + 1/m_2}.$$

For a rigid body struck away from its centre the impulse also changes angular momentum by $\mathbf{r} \times \mathbf{J}$. The normal velocity used in restitution must then be evaluated at the contact point, combining centre translation and rotation. A restitution value is a contact model or measurement, whereas the impulse balances follow directly from mechanics.

Background · Force impulse

$$J = \int F \, dt$$

An impulse changes linear momentum over an event. A coefficient of restitution supplies a separate relative-velocity condition for an impact.

DERIVATION AND APPLICATIONS

Locate the impact point that leaves a pivot without an impulse

A rapid blow on a hinged body can set it rotating while producing zero instantaneous horizontal impulse at the hinge. Model a rigid pendulum initially at rest, with mass m, centre of mass distance a from its frictionless pivot, and moment of inertia I_O about the pivot. Apply a short tangential impulse J at distance b along the same radial line. Neglect the impulse from gravity during contact and take positive velocity along J. Angular impulse about the pivot removes the unknown hinge reaction.

$$I_O\omega^+ = Jb,$$
$$v_G^+ = a\omega^+.$$

Linear impulse along the impact direction includes both J and the unknown hinge impulse H. Substitution of angular speed therefore gives the signed hinge impulse as a function of the impact radius. A reaction in the opposite direction from J corresponds to $H < 0$.

$$mv_G^+ = J + H,$$
$$H = J\left(\frac{mab}{I_O} - 1\right).$$

Set $H = 0$ and use the parallel-axis theorem $I_O = I_G + ma^2$. The resulting radius locates the centre of percussion; it lies beyond the centre of mass for any extended body with $I_G > 0$.

$$b_{\mathrm{cp}} = \frac{I_O}{ma} = a + \frac{I_G}{ma}.$$

This result concerns the net hinge impulse during a short tangential event. Later hinge forces as the body swings need a separate force balance. A finite-duration or oblique impact also requires examining the other force components.

WORKED EXAMPLE

Locate the point on a laboratory pendulum

A uniform slender bar of length 0.900 m and mass 1.50 kg is hinged at one end. Its $a = 0.450$ m and $I_O = mL^2/3 = 0.405$ kg m², giving $b_{\mathrm{cp}} = 0.600$ m. A tangential impulse of 0.300 N s there produces

$$\omega^+ = 0.300(0.600)/0.405 = 0.444\,\mathrm{rad/s}.$$

Its centre momentum is $1.50(0.450)(0.444) = 0.300$ N s, accounting for all of the applied impulse.

Change the inputs and inspect this calculation below

SECOND APPLICATION

Infer inertia from a zero-reaction test

A different hinged fixture has $m = 4.00$ kg and $a = 0.180$ m. An instrumented hinge shows vanishing tangential impulse at $b = 0.320$ m. This gives $I_O = mab = 0.2304$ kg m² and $I_G = 0.1008$ kg m². At $b = 0.160$ m, a 0.500 N s impulse should instead produce $H = 0.500(0.160/0.320 - 1) = -0.250$ N s, a direct sign and calibration check.

Interactive calculation · Change the inputs of this example

Use the adjustable quantities to test the two worked calculations above. The plot recomputes this derivation's balance or constitutive relation; its numerical readout reports the quantities needed for the forward calculation and the inverse or design question. Keep the fixed assumptions stated in the readout when comparing with the example values.

Open this live calculation

Try the calculation

Bar length (m) **0.9**

Impulse (N s) **0.3**

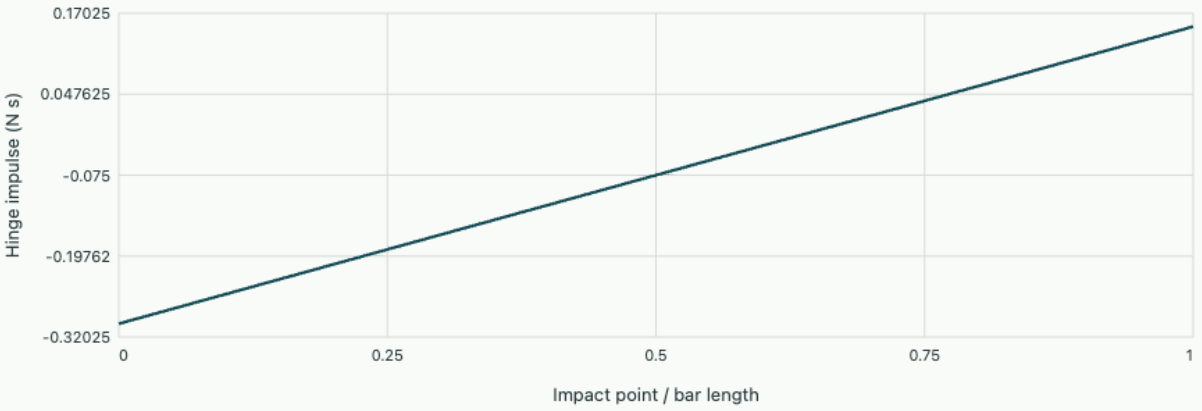

Uniform end-hinged bar

Zero hinge impulse at b=2L/3=0.600 m. For mass1.5 kg the angular-speed jump there is 0.444 rad/s.

Does equal impulse leave equal vibration?

A force hammer and a soft contact pad can deliver the same total impulse in quite different times. The impulse fixes the change of momentum of a free mass. A mounted instrument also feels a spring force

during the contact. The instrument may have already started a substantial fraction of an oscillation while the applied force is still acting, allowing later parts of the pulse to cancel some of the earlier response.

Start an undamped oscillator at rest and apply a force $F(t)$ only between zero and T. Passing a small impulse $F(s)\,ds$ to the oscillator gives a later displacement $F(s)\sin[\omega(t-s)]\,ds/(m\omega)$. Integrating over arrival times for $t > T$ and collecting the coefficients of $\sin\omega t$ and $\cos\omega t$ gives the residual amplitude

$$A = \frac{1}{m\omega}\left|\int_0^T F(s)e^{-i\omega s}\,ds\right|.$$

The relevant measure is the pulse spectrum at the oscillator frequency. Its zero-frequency value is the ordinary impulse. Their difference is negligible when the complex phase changes very little during contact. A wide-band impact model that fits only impulse can otherwise give the wrong residual vibration even when it closely predicts the overall force integral.

Choose a half-sine pulse $F(s) = J\pi\sin(\pi s/T)/(2T)$ with prescribed impulse J. Write the sine as a pair of exponentials, integrate each exponential and take the magnitude. With $r = \omega T$, this produces

$$A/[J/(m\omega)] = \pi^2\left|\cos(r/2)/(\pi^2 - r^2)\right|.$$

At $r = \pi$ the numerator and denominator both vanish. Expanding about π or integrating the sine pulse directly gives the finite limit $\pi/4$. The notebook evaluates a pair of sinc functions to avoid asking the computer to divide zero by zero.

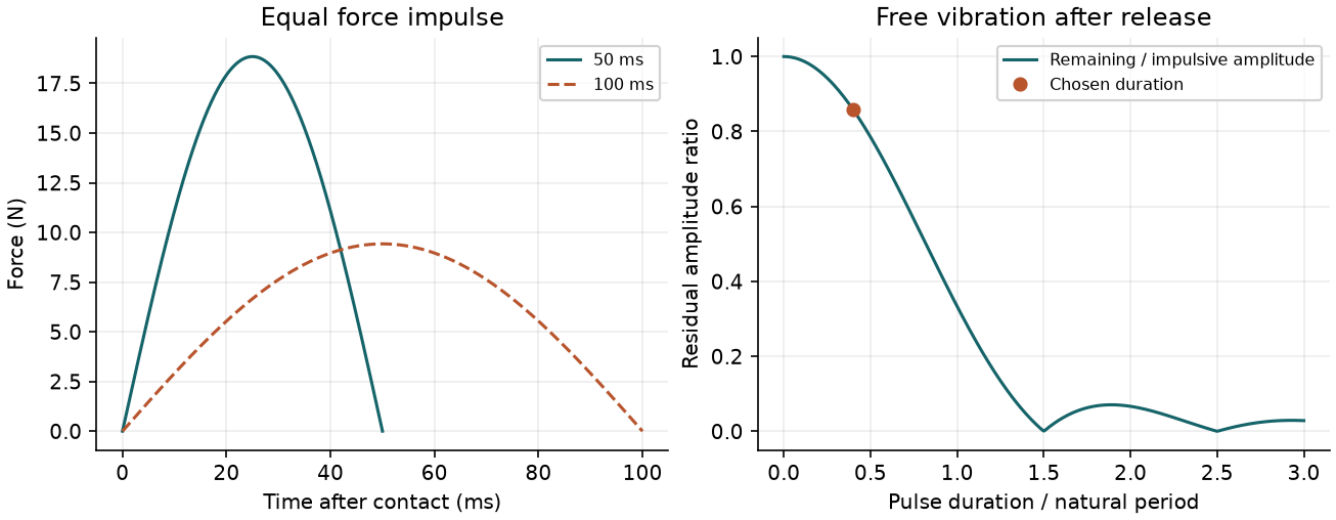

The force integral stays fixed as the pulse broadens. The oscillator weights the individual parts by their arrival phase, so a full cancellation can occur after release.

For a 2 kg instrument with natural frequency 8 Hz and a pulse of 0.6 N s, an instantaneous impulse gives $A = 5.968$ mm. A 50 ms contact occupies 0.4 natural periods and leaves only 5.123 mm. In the notebook, compare the closed result with direct numerical integration of the complex forcing history. Halve the duration while preserving impulse and inspect the approach to the impulsive limit. The force peak must increase to conserve the area.

If an accelerometer is used to check the result, separate the interval during which the hammer is in contact from the ring-down after release. During free vibration the acceleration satisfies $\ddot{x} = -\omega^2 x$, and the measured acceleration amplitude divided by ω^2 gives the residual displacement amplitude. For the 50 ms example this predicts about 12.94 m/s² during the ring-down. During contact the force term $F(t)/m$ also contributes to the acceleration. Applying the same conversion to the largest acceleration in the whole record could therefore assign the forcing pulse to the free vibration. A force transducer identifies the release time independently.

At a duration of 1.5 natural periods, the remaining oscillation of this model vanishes. Does this make such a pulse equivalent to a force that never acted?

▼ **Work through the solution**

At $r = 3\pi$ the cosine numerator is zero and the denominator is finite. Positive parts of the pulse delivered at different phases cancel in the *final* modal state. During contact there is displacement, stored spring energy and a transient force in the support. A specimen containing a second mode will weight the same pulse at another frequency. A cancellation for one mode says little about the maximum support displacement during contact or the other mode’s final amplitude.

Interactive calculation · Half sine force

Vary the notebook inputs and compare both plotted observables. The same equations generate the browser curves and the notebook reference; fixed material, geometry and model assumptions are stated in the readout.

Open this live calculation

Try the calculation

Impulse (N s)	0.6
Natural frequency (Hz)	8
Pulse duration (ms)	50

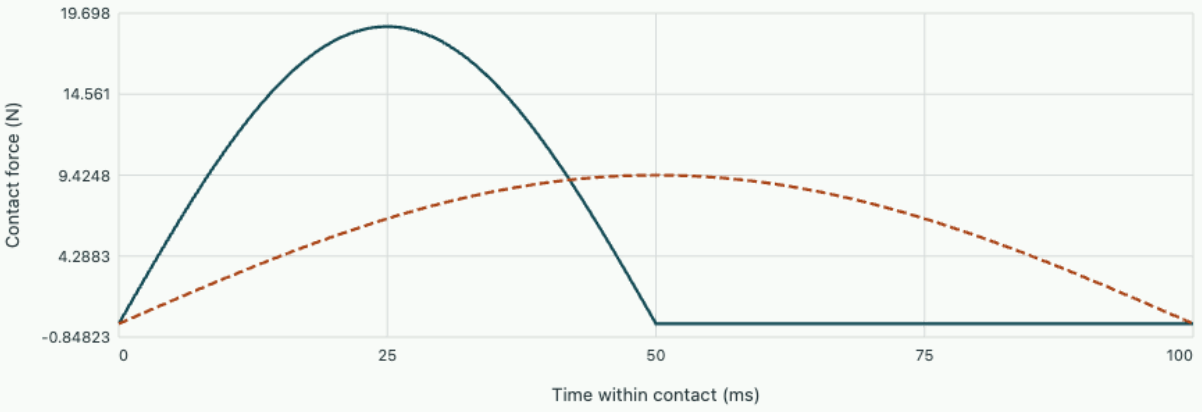

Mass2 kg. Residual amplitude 5.123 mm; instantaneous-impulse limit 5.968 mm. The force integral remains 0.600 N s.

Download the editable notebook for this example

Interactive calculation · Half sine residual

Vary the notebook inputs and compare both plotted observables. The same equations generate the browser curves and the notebook reference; fixed material, geometry and model assumptions are stated in the readout.

Open this live calculation

Try the calculation

Impulse (N s)	0.6
Natural frequency (Hz)	8
Pulse duration (ms)	50

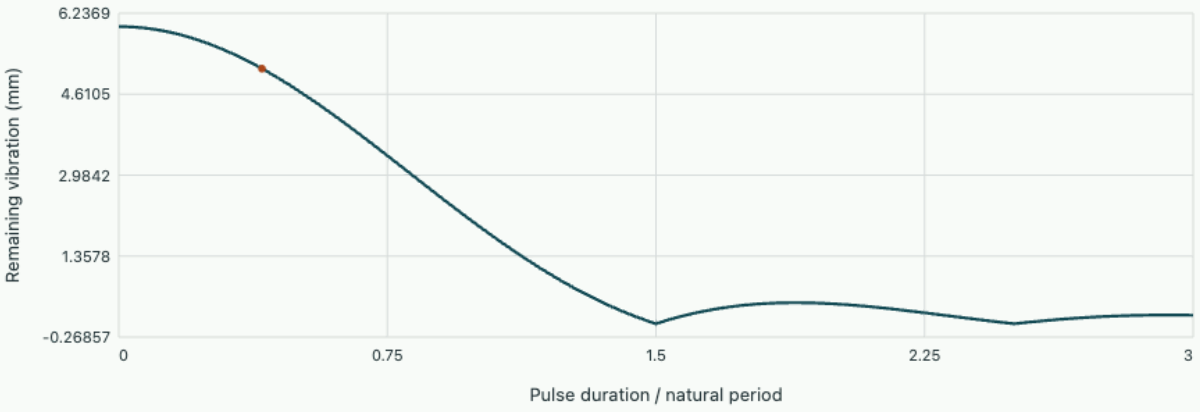

Mass2 kg. Residual amplitude 5.123 mm; instantaneous-impulse limit 5.968 mm. The force integral remains 0.600 N s.

Download the editable notebook for this example

Open editable notebook Download .ipynb

Select a time interval and a reference point

For a short collision, a finite change of velocity occurs over a time in which positions change very little. Integrate Newton's law over that interval. A force that is harmless in an ordinary static calculation can deliver a large impulse if sustained long enough. Conversely, gravity often contributes very little over a millisecond. Compare its estimated impulse $mg\Delta t$ with the contact impulse before neglecting it.

For planar rigid-body motion the impulse–momentum balances about the mass centre G and about an inertially fixed point O are

$$m(v_G^+ - v_G^-) = \sum J,$$
$$H_O^+ - H_O^- = \sum r_{i/O} \times J_i.$$

The superscripts denote states just before and after contact. A hinge can deliver an unknown impulse but exerts no moment impulse about its own centre when modelled as an ideal pin. Choosing that point can eliminate unknowns when calculating angular speed. Kinetic energy is generally lost to deformation, contact vibration and other processes. It cannot supply a conservation equation without an additional elastic-impact assumption.

Apply the contact condition at the points that meet

For a smooth frictionless collision choose the normal from the incoming body towards the target. The separation speed along that normal equals the specified coefficient of restitution e times the approach speed. Evaluate velocities of the actual points in contact; the target's mass-centre speed can be different if the force also rotates it. For a contact point at distance a along a pinned bar and normal perpendicular to the bar, the normal contact velocity immediately after impact is $a\omega^+$.

Take a small slider of mass 1.0 kg moving at 3.0 m/s into a stationary slender uniform bar of mass 3.0 kg, length 0.60 m, pinned at one end. It strikes at $a = 0.40\,\mathrm{m}$, perpendicular to the bar. The bar inertia about the pin is

$$I_O = m_b L^2/3 = 0.360\,\mathrm{kg\,m^2}.$$

Let J be the positive impulse delivered to the bar. The slider exits at $3 - J/1$, and the bar receives angular speed Ja/I_O.

Close the collision and audit its energy

With $e = 0.50$, the restitution condition is $a(Ja/I_O) - (3 - J) = 0.50(3)$, giving $J = 4.5/[1 + 0.4^2/0.36] = 3.115\,\mathrm{N\,s}$. Thus $\omega^+ = 3.46\,\mathrm{rad/s}$ and the slider rebounds slowly at −0.115 m/s. The bar's contact point recedes at 1.385 m/s, exactly 1.50 m/s faster than the slider after separation.

The initial kinetic energy was 4.50 J. The final energy is

$$\tfrac{1}{2}(1)(0.115)^2 + \tfrac{1}{2}(0.360)(3.46)^2 = 2.16\,\mathrm{J}.$$

The energy loss is physically consistent with the specified restitution. The pin impulse need not vanish although its moment impulse vanished. The bar's centre moves at $0.30(3.46) = 1.04\,\mathrm{m/s}$; its linear momentum gain happens to equal about 3.12 N s for this impact position, very close to the contact impulse. Indeed $a = I_O/(m_b L/2) = 0.40\,\mathrm{m}$ is the centre-of-percussion location, for which the ideal transverse pin impulse vanishes exactly.

Determine whether a rough impact sticks or slides

The smooth collision model leaves tangential velocities unaffected. A rough planar impact can also exchange tangential impulse and rotational momentum. Consider a solid disc of radius R striking a fixed horizontal surface at its lowest point. Take horizontal right and vertical up as positive; angular speed is counterclockwise positive. Just before impact let centre velocities be u^-, v^- and angular speed ω^-. The horizontal speed of its contact point is $g_t^- = u^- + R\omega^-$. A rightward tangential impulse J_t produces both a centre velocity increase J_t/m and a positive angular change RJ_t/I_G.

The post-impact contact velocity is $g_t^+ = g_t^- + (1/m + R^2/I_G)J_t$. For the horizontal surface the normal impulse passes through the centre; restitution requires $J_n = -m(1+e)v^-$ for $v^- < 0$. The tangential impulse needed to eliminate slip is

$$J_t^{\text{stick}} = -g_t^- / (1/m + R^2/I_G).$$

Under a simple Coulomb impulse approximation compare this required magnitude with μJ_n. If it lies inside the bound the contact can finish without tangential slip. Otherwise take the limiting friction impulse opposing the pre-impact relative slip. This elementary model assumes no change in slip direction before the limiting impulse is reached, negligible external impulse, and no tangential elastic restitution. Using only the disc centre’s velocity to form the stick condition would miss its rotational compliance.

Compare two surfaces with the same normal restitution

A solid disc has $m = 2.0\,\mathrm{kg}$, $R = 0.10\,\mathrm{m}$,

$$I_G = mR^2/2 = 0.010\,\mathrm{kg\,m^2}.$$

Its centre approaches at $u^- = 3.0,\ v^- = -2.0\,\mathrm{m/s}$, with zero initial spin. For $e = 0.50$, $J_n = 6.0\,\mathrm{N\,s}$ and $v^+ = 1.0\,\mathrm{m/s}$. The inverse tangential effective mass is

$$1/2 + 0.10^2/0.010 = 1.50\,\mathrm{kg^{-1}}.$$

Thus $J_t^{\text{stick}} = -2.0\,\mathrm{N\,s}$ and the friction coefficient needed is at least $2/6 = 0.333$.

On a surface with $\mu = 0.20$, $J_t = -1.2\,\mathrm{N\,s}$, giving $u^+ = 2.4\,\mathrm{m/s}$ and $\omega^+ = -12\,\mathrm{rad/s}$. The contact-point speed remains $2.4 - 1.2 = 1.2\,\mathrm{m/s}$ to the right, consistent with the chosen sliding direction. On a surface with $\mu = 0.50$, the sticking impulse is achievable. It gives $u^+ = 2.0\,\mathrm{m/s}$, $\omega^+ = -20\,\mathrm{rad/s}$, and zero instantaneous tangential contact speed. The disc still leaves the surface vertically because $v^+ = 1.0$. Here sticking means zero relative tangential velocity at separation and does not mean a permanently attached body. The original 13 J of kinetic energy drops to 7.48 J in the sliding case and 7.00 J in the sticking case, consistent with frictional dissipation and a normal restitution below unity.

A high-speed camera that measures only the centre trajectory would determine the change in centre momentum and hence the tangential impulse, provided other horizontal impulses are negligible. Marking the disc edge permits an independent angular check: in the sliding case the ratio $I_G|\Delta\omega|/(Rm|\Delta u|)$ is

$$0.010(12)/[0.10(2)(0.60)] = 1.$$

A substantial measured deviation could indicate an additional contact couple, a second impact point or uncertainty in inertia. Measuring spin is particularly important near the transition to sticking because centre velocity by itself cannot establish that the tangential contact speed has vanished.

A marked rim therefore provides an observable that a centre-tracking experiment alone cannot supply.

Finite-amplitude oscillations and model validity

Machine dynamics

Use conservation of energy and a frequency approximation to quantify when a small-angle pendulum model loses timing accuracy.

FROM FIRST PRINCIPLES

Derive the pendulum period and identify the small-angle assumption

A point mass m suspended on a massless rigid link of length ℓ feels a gravitational torque $-mg\ell\sin\theta$ about the hinge. Assume a stationary pivot and negligible drag. Angular momentum balance gives an exact nonlinear equation. Replacing $\sin\theta$ by θ only for small angles in radians gives a linear oscillator and its predicted period.

$$m\ell^2\ddot{\theta} = -mg\ell\sin\theta,$$

$$T_{\text{small}} = 2\pi\sqrt{\ell/g}.$$

To track finite amplitude, release from rest at angle $A < \pi$ and use mechanical energy conservation. At any intermediate angle, loss of potential energy equals gained rotational kinetic energy.

$$\tfrac{1}{2}m\ell^2\dot{\theta}^2 = mg\ell(\cos\theta - \cos A),$$

$$T = 4\sqrt{\frac{\ell}{2g}}\int_0^A \frac{d\theta}{\sqrt{\cos\theta - \cos A}}.$$

The factor four uses the symmetry of the four quarter cycles. The mass cancels even at large amplitude. The exact restoring torque grows more slowly with deflection than its small-angle approximation, so finite-amplitude swings take longer. Measured variation of period with release angle directly tests the linearisation.

DERIVATION AND APPLICATIONS

Derive the period of an oscillator with purely cubic stiffness

A spring with almost no linear stiffness near equilibrium can have a period set primarily by release amplitude. Consider mass m on a horizontal guide with restoring force $-\beta x^3$ for $\beta > 0$. Ignore damping and assume the fitted force law holds between $-A$ and $+A$. Release from rest at $x = A$. Integrating the force law gives a quartic potential, and conservation of energy provides the speed anywhere on the inward leg.

$$\tfrac{1}{2}m\dot{x}^2 + \tfrac{1}{4}\beta x^4 = \tfrac{1}{4}\beta A^4,$$

$$|\dot{x}| = \sqrt{\frac{\beta}{2m}}\sqrt{A^4 - x^4}.$$

By symmetry the time from an extreme position to the centre is one quarter of a full cycle. Write $dt = |dx|/|\dot{x}|$ and substitute $u = x/A$ in the integral. This isolates the amplitude dependence without guessing a sinusoidal shape.

$$T = \frac{4}{A}\sqrt{\frac{2m}{\beta}}\int_0^1 \frac{du}{\sqrt{1-u^4}}.$$

The dimensionless integral evaluates numerically to 1.31103. Its endpoint singularity is integrable because the speed near the turning point vanishes as the square root of the distance remaining. The resulting period and angular frequency are

$$T = \frac{7.4163}{A}\sqrt{\frac{m}{\beta}},$$

$$\omega = \frac{2\pi}{T} = 0.8472\,A\sqrt{\frac{\beta}{m}}.$$

The positive cubic restores the mass for displacements of either sign, but its tangent stiffness at zero is zero. The full nonlinear dynamics therefore predicts a period diverging with decreasing amplitude. Even a weak residual linear spring would eventually dominate in that limit.

WORKED EXAMPLE

Predict the timing of two releases

Take $m = 0.500$ kg, $\beta = 2.00 \times 10^5$ N/m³ and $A = 20.0$ mm. The predicted period is

$$7.4163\sqrt{0.500/(2.00\times10^5)}/0.0200 = 0.586\,\mathrm{s}.$$

Reducing the release to 10.0 mm doubles the predicted period to 1.17 s. At the larger amplitude the centre-crossing speed is

$$A^2\sqrt{\beta/(2m)} = 0.179\,\mathrm{m/s}.$$

Change the inputs and inspect this calculation below

SECOND APPLICATION

Infer stiffness from a measured period

A second fixture of mass 0.800 kg completes a cycle in 0.750 s after release at 15.0 mm. The implied coefficient is $\beta = m[7.4163/(AT)]^2 = 3.48 \times 10^5$ N/m³. Its predicted restoring-force magnitude at release is

$$\beta A^3 = 1.17\,\mathrm{N}.$$

An independent static force measurement there tests the dynamic estimate without assuming a sinusoidal motion.

Interactive calculation · Change the inputs of this example

Use the adjustable quantities to test the two worked calculations above. The plot recomputes this derivation's balance or constitutive relation; its numerical readout reports the quantities needed for the forward calculation and the inverse or design question. Keep the fixed assumptions stated in the readout when comparing with the example values.

Open this live calculation

Try the calculation

Mass (kg) **0.5**

Cubic force coefficient (kN/m³) **200**

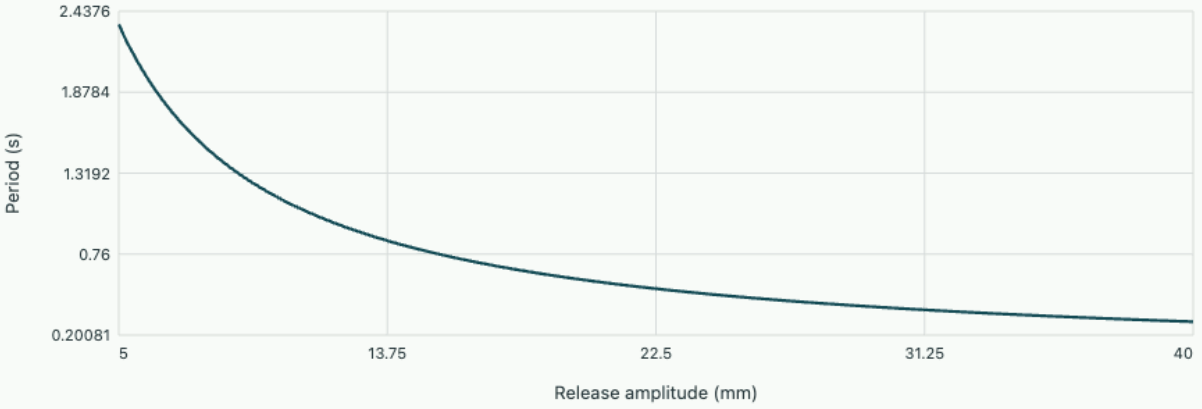

Energy-integral period

At20 mm amplitude, period=0.586 s. This pure cubic spring has no nonzero small-amplitude linear frequency.

Retain the actual restoring moment

A pendulum gives a practical test of a linear model because its length and release angle are easy to set while its period can be measured over many cycles. Approximate the moving body first by a point mass m at distance l from a frictionless pivot. With θ measured from vertically downwards, gravity produces torque $-mgl\sin\theta$. Dividing the rotational balance by ml^2 leaves $\ddot{\theta} + (g/l)\sin\theta = 0$. The linear small-angle frequency $\omega_0 = \sqrt{g/l}$ follows only after replacing $\sin\theta$ by θ in radians.

The leading correction has a definite sign:

$$\sin\theta \simeq \theta - \theta^3/6.$$

At a large positive angle the restoring force magnitude is smaller than the linear extrapolation. The pendulum should take longer to complete its swing. A sign test like this is useful before calculating a period correction.

Derive an integral valid at finite amplitude

For release from rest at amplitude $A < \pi$, conservation of mechanical energy gives

$$\tfrac{1}{2}ml^2\dot{\theta}^2 + mgl(1-\cos\theta) = mgl(1-\cos A).$$

During one quarter of the orbit the angle travels between zero and A. Substitute $\sin(\theta/2) = \sin(A/2)\sin\psi$ into the time integral. Cancelling common square roots gives

$$T = 4\sqrt{l/g}\int_0^{\pi/2} \frac{d\psi}{\sqrt{1 - k^2\sin^2\psi}},$$

$$k = \sin(A/2).$$

For modest amplitudes expand the integrand as $1 + \tfrac{1}{2}k^2\sin^2\psi + \cdots$. The average of $\sin^2\psi$ over the quarter interval is one half. Therefore $T/T_0 \simeq 1 + k^2/4 \simeq 1 + A^2/16$ through second order in amplitude. The oscillation period depends on energy, while in the linear spring model all amplitudes share the same period.

Estimate a measurable timing error

Take $l = 0.80\,\mathrm{m}$, $g = 9.81\,\mathrm{m/s^2}$ and release at $A = 30^\circ = 0.5236\,\mathrm{rad}$. The small-angle period is

$$T_0 = 2\pi\sqrt{0.80/9.81} = 1.794\,\mathrm{s}.$$

The leading correction is 1.71%, giving about 1.825 s. Over ten full oscillations the predicted delay relative to the small-angle model is roughly 0.31 s. Reducing the release angle to 15° reduces the leading relative correction by a factor of four.

A timing series from a damped experimental pendulum may show the period drifting towards T_0 as its amplitude decays. Measuring only the first release angle while averaging many later periods mixes different amplitudes. To test the finite-amplitude law, use consecutive same-direction crossings to measure each local period and estimate its associated amplitude from neighbouring turning points. The correction above is an expansion around zero amplitude. As A approaches the inverted equilibrium, the exact integral grows without bound and a low-order polynomial is no longer an adequate approximation.

Check the scale of the neglected term

Retaining one further term in the integrand gives $1 + \frac{1}{2}k^2\sin^2\psi + \frac{3}{8}k^4\sin^4\psi$. The quarter-interval average of the fourth power of sine is $3/8$, so $T/T_0 \simeq 1 + k^2/4 + 9k^4/64$. At 30° this gives 1.01738, while the leading expansion in amplitude gave 1.01713. The small difference is measurable only if the uncertainty in pendulum length, release angle and crossing times supports the comparison.

Derive an amplitude-dependent resonance relation

A pendulum softens as its amplitude grows because the sine restoring law rises more slowly than its linear tangent. A mechanical flexure can instead harden through geometry. A simple modal model is $m\ddot{x} + c\dot{x} + kx + \beta x^3 = F\cos\omega t$. For positive β the restoring stiffness increases with excursion. Assume one dominant harmonic and take $x \approx A\cos(\omega t - \phi)$. Expanding the cubic gives

$$x^3 = A^3[3\cos(\omega t - \phi) + \cos(3\omega t - 3\phi)]/4.$$

Keeping only the fundamental turns the cubic term into an amplitude-dependent in-phase force.

Balance in-phase and quadrature components against the input, square and add to eliminate ϕ. The first-harmonic amplitude estimate satisfies

$$F^2 = A^2\left[\left(k + \tfrac{3}{4}\beta A^2 - m\omega^2\right)^2 + (c\omega)^2\right].$$

In a lightly damped free motion the same approximation gives a backbone frequency $\omega_b^2 \approx [k + (3/4)\beta A^2]/m$. This is an amplitude-dependent estimate of conservative oscillation frequency, not a new eigenvalue of the linearised equilibrium. At very small amplitude it recovers $\sqrt{k/m}$, while a negative cubic coefficient tilts the relation towards lower frequencies. If the cubic approximation is only a local expansion, do not extrapolate it until it predicts an unphysical loss of global stiffness.

Identify a hardening spring from two release amplitudes

A test component has moving mass 1.0 kg and small-amplitude stiffness 400 N/m. Low-level ring-down gives $\omega_0 = 20\,\mathrm{rad/s}$. At measured oscillation amplitude 20 mm the dominant free frequency is approximately 22 rad/s. Under the weakly nonlinear one-harmonic model,

$\beta \simeq 4m(22^2 - 20^2)/[3(0.020)^2] = 2.80 \times 10^5\,\mathrm{N/m^3}$. At 10 mm the inferred backbone is $\sqrt{400 + 0.75(2.8 \times 10^5)(0.010)^2} = 20.52\,\mathrm{rad/s}$, a direct third reading against which to test the fit.

Now drive near 22 rad/s with viscous coefficient $c = 0.80\,\mathrm{N\,s/m}$. At the 20 mm backbone amplitude the spring and inertia fundamentals cancel, so maintaining this motion takes forcing $F = c\omega A = 0.352\,\mathrm{N}$ in quadrature with displacement. The neglected cubic third-harmonic force amplitude is

$$\beta A^3/4 = 0.56\,\mathrm{N};$$

its displacement effect can nevertheless be small because the oscillator is driven far from its fundamental resonance at 66 rad/s. A separate mode near that frequency would invalidate this simplification. In a forced frequency sweep the amplitude equation can admit several positive roots near resonance. Its algebra does not establish their stability; slow upward and downward sweeps, each with sufficient settling time, can reveal different stable responses and jump transitions.

An initial static measurement tests the sign of the fitted coefficient independently. At a displacement of 20 mm the linear restoring force is

$$400(0.020) = 8.0\,\mathrm{N};$$

the cubic contribution is

$$2.8 \times 10^5 (0.020)^3 = 2.24\,\mathrm{N}.$$

The predicted static force is therefore 10.24 N, and the tangent stiffness is

$$400 + 3(2.8 \times 10^5)(0.020)^2 = 736\,\mathrm{N/m}.$$

This tangent stiffness applies to small vibrations around a held biased equilibrium. Using it directly for an oscillation centred at zero would overestimate the measured amplitude-dependent frequency because the instantaneous stiffness changes during each cycle. Static bias and free oscillation amplitude are physically different tests of the same nonlinear restoring law.

Repeating a decay test around a deliberately shifted equilibrium distinguishes the two experimentally.

Set an amplitude limit for a pendulum-based timing model

For a rigid pendulum released from rest the exact period ratio is $2K(\sin^2(\theta_0/2))/\pi$, where the complete elliptic integral here uses its parameter rather than its modulus. Compare it with the first amplitude correction $1 + \theta_0^2/16$, with angle in radians.

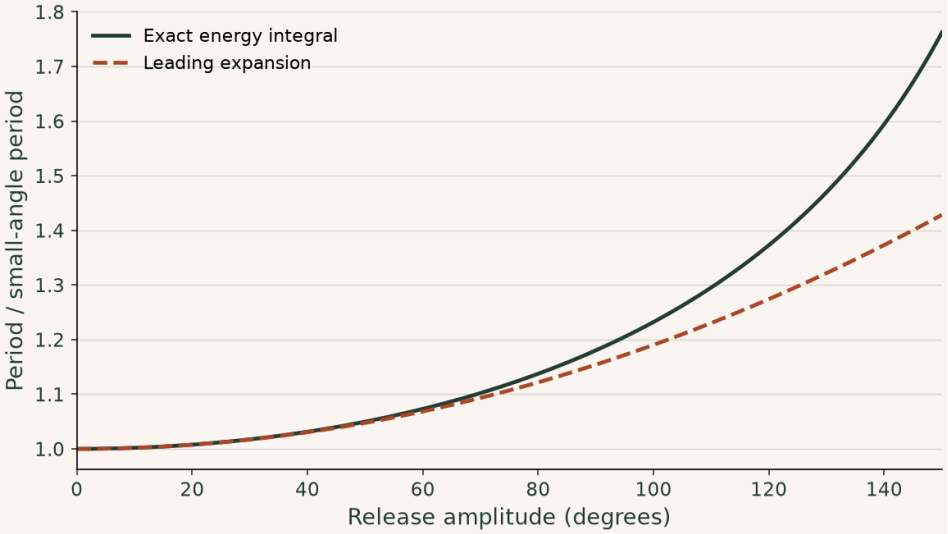

At 90° the exact period is about 1.180 times the linear prediction; the leading expansion gives 1.154. The series is useful at modest amplitudes, but it cannot reproduce the divergence on approach to an upright release.

▶ **Read values from the plot**

Interactive calculation · change the inputs of this example

Increase the maximum release angle and compare the energy integral with the first series correction. Changing length rescales both periods.

The curves below are recalculated from this section's equations in your browser. The fixed reference plot above remains available for comparison.

Open this live calculation

Try the calculation

Maximum release angle (degrees) **150**

Pendulum length (m) **1**

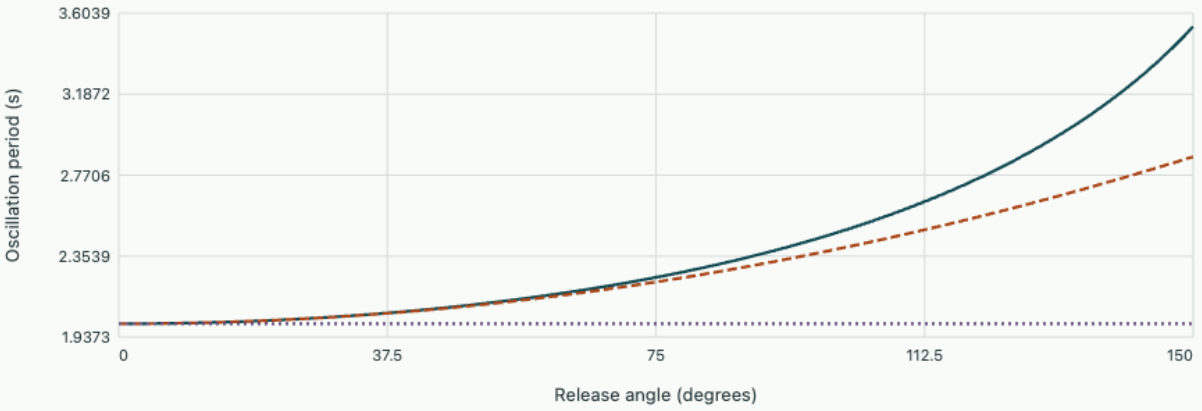

Energy integral via AGM · First amplitude correction · Small-angle limit

At 150° the exact period is 3.535 s, 76.22% above the linear estimate.

Steady gyroscopic precession and its two possible rates

Machine dynamics

A spinning axisymmetric rotor supported at one point can keep a constant tilt under gravity. Predict the rate at which its axis turns, examine the fast-spin approximation and determine when slow steady precession is possible.

Identify the changing direction of angular momentum

Let the centre of mass be a distance l along the symmetry axis from a fixed pivot. The symmetry axis is tilted by θ from the upward vertical. The moment of inertia about that axis is I_3, and about either transverse axis through the pivot it is I_1. Define ω_3 as the total component of angular velocity along the symmetry axis. When the spin angular momentum dominates,

$$\mathbf{H} \simeq I_3 \omega_3 \mathbf{e}_3.$$

Under uniform precession at rate Ω, its tip traces a horizontal circle of radius $I_3\omega_3 \sin\theta$.

$$|\dot{\mathbf{H}}| \simeq \Omega I_3 \omega_3 \sin\theta,$$

$$|\boldsymbol{\tau}_g| = mgl \sin\theta,$$

$$\Omega_{\text{slow}} \simeq \frac{mgl}{I_3\omega_3}.$$

The tilt factors cancel for nonvertical orientations. Gravity changes the direction of angular momentum while doing zero work in a steady precession at fixed height. Reversing the spin changes the direction of slow precession. The support force has zero moment about the pivot.

Keep the angular momentum due to precession

For a regular precession at fixed tilt the transverse angular velocity is the part of $\Omega \mathbf{e}_z$ perpendicular to $\mathbf{e}_3$. Thus $\mathbf{H} = I_1 \Omega \mathbf{e}_z + (I_3\omega_3 - I_1\Omega\cos\theta)\mathbf{e}_3$. The vertical first term is constant. The rotating second term has derivative $\Omega \mathbf{e}_z \times \mathbf{H}$. Equating it to the gravitational torque yields

$$I_1 \cos\theta\, \Omega^2 - I_3\omega_3\Omega + mgl = 0.$$

For $0 < \theta < 90^\circ$ and positive spin, two positive real rates exist only if $D = (I_3\omega_3)^2 - 4I_1 mgl\cos\theta \geq 0$. The smaller root is most accurately evaluated as $2mgl/(I_3\omega_3 + \sqrt{D})$, avoiding subtraction of nearly equal numbers at high spin. The larger root corresponds to a different initial angular velocity. Releasing a rotor without providing an appropriate initial precession generally adds nutation.

A tabletop rotor as its spin slows

Take $m = 0.50$ kg, $l = 0.060$ m, $I_1 = 0.0030$ kg m², $I_3 = 0.0020$ kg m² and $\theta = 60^\circ$. At $\omega_3 = 100$ rad/s the first estimate gives 1.47 rad/s. The quadratic gives 1.49 rad/s for the slow branch and 131.8 rad/s for

the fast branch. The 1% discrepancy in the slow result is consistent with a small transverse angular momentum.

At $\omega_3 = 30$ rad/s the approximation gives 4.91 rad/s and the exact slow rate is 5.72 rad/s. The two rates meet at a spin of roughly 21.0 rad/s. Below this value there is no constant-tilt solution for the prescribed angle and inertias. Plotting the discriminant or using the real branches avoids reporting a fictitious real rate after the branches disappear.

Compare the approximation and exact branch near the minimum admissible spin, then at high spin. Raise the tilt toward a right angle. Predict whether the minimum spin increases or falls before checking the new domain of the curve.

Open this experiment online

Try the calculation

Tilt from vertical (°) **60**

Moment arm (mm) **60**

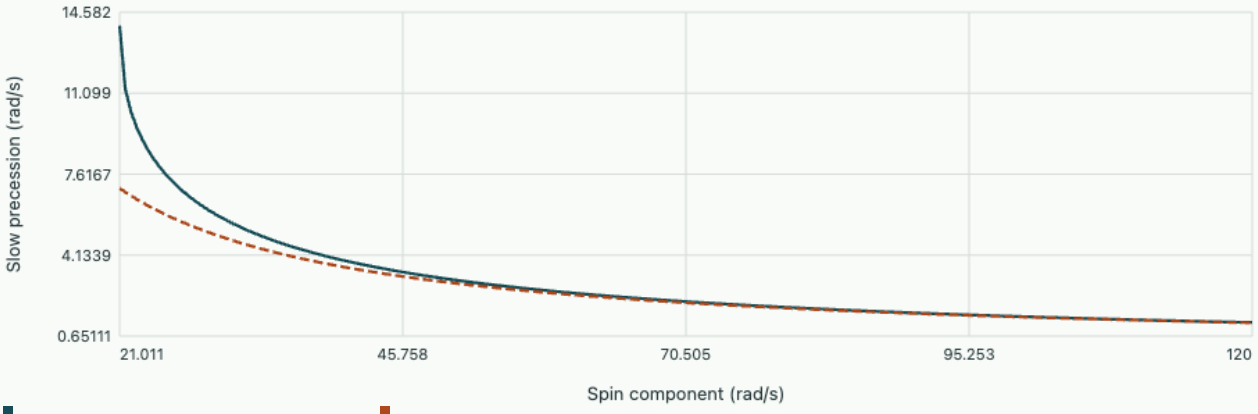

For this tilt the two regular-precession branches first exist at spin 21.0 rad/s. At 100 rad/s the exact slow rate is 1.488 rad/s.

Tutorial · infer a moment arm from observed motion

For the same inertias and mass, measure $\omega_3 = 50$ rad/s, $\Omega = 3.0$ rad/s and $\theta = 60^\circ$. Estimate l from the full relation. Calculate the bias if transverse angular momentum is omitted.

▼ **Show the torque estimate**

The full torque parameter is $mgl = I_3\omega_3\Omega - I_1\cos\theta\,\Omega^2 = 0.300 - 0.0135 = 0.2865$ N m. The arm is

$$l = 0.2865/(0.50 \cdot 9.81) = 58.4\,\mathrm{mm}.$$

Keeping only the first term gives 61.2 mm, overestimating the arm by about 4.7%. Measuring steady precession over several cycles helps distinguish that systematic error from fluctuations caused by nutation.

Further reading · MIT 2.003SC · angular momentum and rotating rigid bodies

Why Coulomb damping loses a fixed amplitude each half-cycle

Machine dynamics

A sliding carriage on a spring can stop away from zero displacement. Determine each turning point without time stepping, then identify the experimentally observable difference between Coulomb and viscous damping.

Write a different equation for each direction of motion

A mass m slides horizontally against a linear spring k. During motion take friction magnitude $F_k > 0$, with force opposing velocity. At rest allow any friction up to the static limit $F_s \geq F_k$. The moving equation is

$$m\ddot{x} + kx = -F_k \operatorname{sgn}(\dot{x}).$$

Release the mass at $x = A > 0$ with zero speed. If $kA \leq F_s$ static friction can hold it there. If $kA > F_s$ it starts moving left. While it moves left, friction points right. Shift the coordinate by $a = F_k/k$ to obtain a homogeneous oscillator:

$$m\ddot{x} + k(x - a) = 0,$$

$$x(t) = a + (A - a)\cos(\omega_n t),$$

$$\omega_n = \sqrt{k/m}.$$

At $t = \pi/\omega_n$ the next turning point is $x_1 = 2a - A$. Test static force balance there before starting another sliding segment. If the mass continues, the sign of friction changes and the next cosine is centred on $-a$. The time for each complete sliding half-cycle is constant despite the decreasing amplitudes. An integration routine that uses only $\operatorname{sgn}(0) = 0$ can generate spurious chatter near the final state.

Recover the amplitude drop from work done by friction

For a full crossing from a positive peak A to a negative peak $-B$, with $A, B > 0$, friction dissipates $F_k(A + B)$. The change in spring energy is $\frac{1}{2}k(A^2 - B^2)$. Cancel the travelled distance to obtain

$$A - B = \frac{2F_k}{k},$$

$$A_j - A_{j+2} = \frac{4F_k}{k}$$

for successive magnitudes on opposite sides and successive positive peaks, respectively, while sliding continues. An ordinary viscous oscillator instead has an approximately fixed ratio between successive positive peaks. A mixed friction-damping experiment can exhibit both effects. An ideal Coulomb model also permits a final equilibrium anywhere in the static-friction band $[-F_s/k, F_s/k]$.

Predict a finite stopping time and reconstruct a friction force

Take $m = 1.0$ kg, $k = 100$ N/m, $F_k = 0.50$ N, $F_s = 0.65$ N and $A = 40$ mm. The shift is 5.0 mm and each sliding half-period is 0.314 s. Starting at +40 mm the successive turns are −30, +20, −10 and 0 mm. The mass sticks at the fourth turn after 1.257 s. A release from +43 mm instead reaches −33, +23, −13 and +3 mm. Since $100(0.003) = 0.30$ N lies below 0.65 N, the residual displacement persists under the assumptions.

Suppose a different test with $k = 200$ N/m shows successive positive peaks of 35, 27 and 19 mm. The 8 mm decrement gives

$$F_k = k(0.008)/4 = 0.40\,\mathrm{N}.$$

A viscous fit would infer logarithmic decrements 0.260 and 0.351 from adjacent pairs. Applying a small constant external force after the final stop can help identify static breakaway independently of the moving-friction estimate.

Compare releases at 40 and 43 mm. Predict the final resting position from the sequence of turning points. Then reduce the release below the static threshold; explain why an initial energy above zero need not imply any motion.

Open this experiment online

Try the calculation

Release displacement (mm) **40**

Sliding friction (N) **0.5**

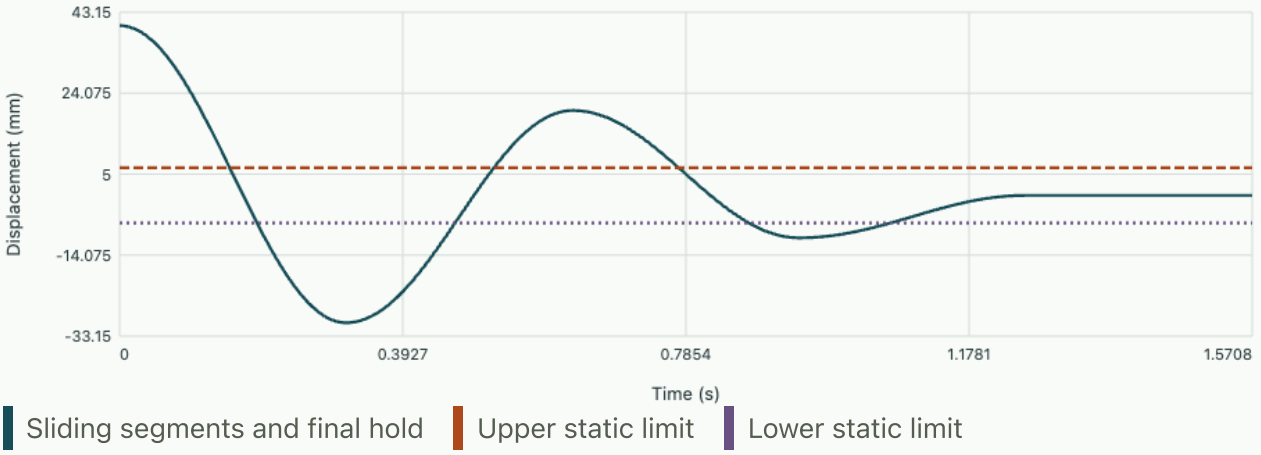

With static friction 1.30 times sliding friction, sticking begins at 1.257 s and 0.00 mm. A full sliding half-cycle lasts 0.314 s.

Tutorial · predict the last turning point even without crossing zero

Use the original mass, stiffness and friction values but release at +8 mm. Does it start, cross zero, and then reverse velocity? Give the final displacement and dissipated energy.

▼ **Follow the event conditions**

The initial spring force 0.80 N exceeds 0.65 N so it moves left. The next turn is

$$2a - A = 10 - 8 = +2\,\mathrm{mm}.$$

It has not crossed zero. At that turn spring force is 0.20 N so it sticks. Friction work is $0.50(0.008 - 0.002) = 0.0030$ J, equal to $\frac{1}{2}(100)(0.008^2 - 0.002^2)$. Blindly subtracting a positive amplitude decrement would have assigned an impossible negative magnitude.

Further reading · University of Alberta, Vibrations and Sound · viscous and Coulomb damping

When the third harmonic matters more than the fundamental

Machine dynamics

A machine applies a short force once per cycle. Its repetition rate looks safely below a structural resonance, but one of its harmonics can lie close to that resonance. Build the forcing spectrum from a pulse and apply a complex response coefficient to each term.

Integrate over the part of the period where force is present

Let an even rectangular force have peak P, period T and on-time dT centred on zero, where $0 < d < 1$. Use an even periodic continuation. Its mean is Pd. Sine coefficients vanish by symmetry. With $\Omega = 2\pi/T$, integrate the cosine terms over the active interval and exploit periodicity:

$$F(t) = Pd + \sum_{n=1}^{\infty} a_n \cos(n\Omega t),$$

$$a_n = \frac{2}{T}\int_{-dT/2}^{dT/2} P\cos(n\Omega t)\,dt = \frac{2P}{n\pi}\sin(n\pi d).$$

The coefficients are signed. A negative coefficient adds a phase reversal; taking its magnitude before summing the time response loses that information. The mean drives a static offset. When nd is an integer, that harmonic vanishes even though the force still has abrupt edges. At a jump the Fourier series converges to the mean of the adjacent values. These details matter when reconstructing force but can have much smaller effects on the filtered displacement.

Solve each harmonic separately and keep phase

For $m\ddot{x} + c\dot{x} + kx = F(t)$ the steady particular solution follows from $H(i\omega) = 1/(k - m\omega^2 + ic\omega)$. Define $\omega_n = \sqrt{k/m}$,

$$\zeta = c/(2\sqrt{km}),$$

$$r_j = j\Omega/\omega_n.$$

The jth response contribution is the real part of $a_j H(ij\Omega)e^{ij\Omega t}$. Thus

$$x(t) = \frac{Pd}{k} + \sum_{j=1}^{\infty} \frac{a_j}{k}\,\frac{(1 - r_j^2)\cos(j\Omega t) + 2\zeta r_j \sin(j\Omega t)}{(1 - r_j^2)^2 + (2\zeta r_j)^2}.$$

Far above resonance each force coefficient is attenuated roughly by another j^{-2} in displacement. Acceleration weights a displacement coefficient by j^2 again, so an adequate displacement truncation can be inadequate for acceleration. Start-up transients are omitted because the expression is the settled periodic response for positive damping.

Compare harmonics before selecting an operating speed

Take $P = 10$ N, $d = 0.25,\ k = 1000$ N/m, natural frequency 12 Hz, damping ratio 0.04, and repetition frequency 4 Hz. The input mean is 2.50 N and $a_1 = 4.50$ N while $a_3 = 1.50$ N. The first harmonic has $r = 1/3$, so its displacement amplitude is about 5.06 mm. The third is exactly resonant and gives

$$1.50/(1000 \cdot 0.08) = 18.8\,\mathrm{mm}.$$

A single harmonic based on the largest force coefficient therefore misses the dominant response.

Choose a new duty $d = 1/3$ while leaving peak force and repetition frequency unchanged. Now $\sin(3\pi d) = 0$, so the resonant third harmonic disappears. The static offset rises from 2.50 to 3.33 mm, and the first two harmonics remain. Holding mean force fixed instead would require rescaling P. A small timing error can reintroduce the third harmonic, especially important when damping is low. Move the duty around one third and compare the full signal with its fundamental-only prediction.

Use 4 Hz and tune the duty as close as the slider allows to one third. Read the residual third harmonic and compare the waveform to the fundamental-only trace. Next shift repetition frequency and distinguish removing the forcing coefficient from moving away from resonance.

Open this experiment online

Try the calculation

Pulse duty fraction **0.25**

Repetition frequency (Hz) **4**

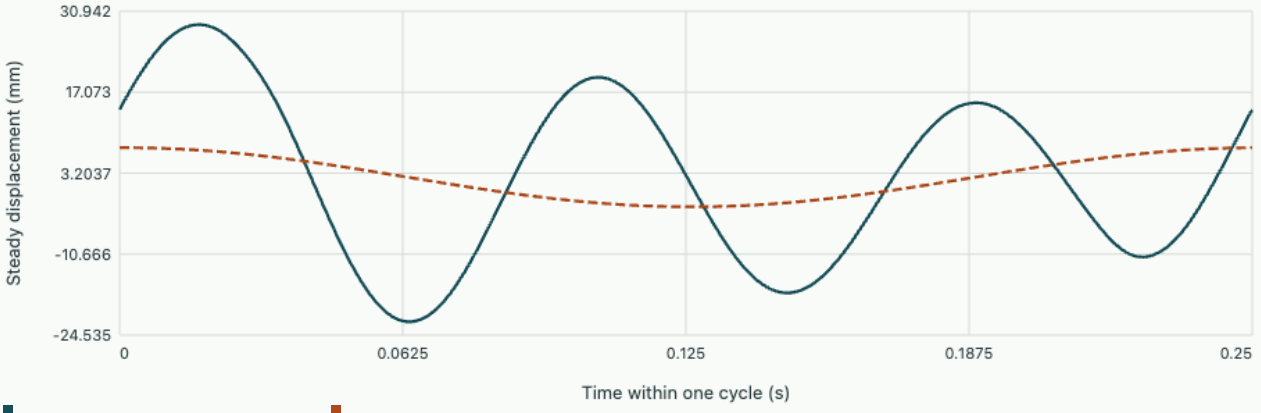

The static offset is 2.50 mm. The third force harmonic is 1.501 N and its displacement amplitude is 18.76 mm at 12.00 Hz.

Tutorial · estimate sensitivity to an on-time error

Near $d = 1/3$ let the duty increase by 0.010 while keeping P fixed. Estimate the newly excited third force harmonic to first order and the resulting displacement near exact resonance. Can this signed contribution

be added directly to the static peak displacement?

▼ **Differentiate the coefficient, then use the transfer function**

From $a_3 = 2P\sin(3\pi d)/(3\pi)$, its derivative is $2P\cos(3\pi d) = -20$ N per unit duty at $d = 1/3$. A change of 0.010 gives about −0.20 N. At resonance the displacement amplitude is

$$0.20/[1000(0.08)] = 2.50\,\text{mm}.$$

The sign sets its phase, and the dynamic transfer adds a quarter-cycle lag at resonance. The largest combined displacement requires summing instantaneous contributions with their correct phases, rather than adding every harmonic magnitude as if their crests coincided.

Further reading · MIT 18.03SC · differential equations with periodic input and resonance

Proving a region of attraction with the energy of a pendulum

Control engineering

Pole locations describe a small neighbourhood of a nonlinear equilibrium. An energy argument can prove that a much larger set of initial conditions converges to the same resting point. Work out the region explicitly and test individual trajectories against its boundary.

Extract a storage function from a torque balance

Measure angle θ from the downward vertical, let $\omega = \dot{\theta}$, and use pivot inertia J and gravitational torque coefficient $K = mgl$. Add viscous damping b and a control torque $u = -k_d\omega$ that opposes motion. The closed dynamics are $J\dot{\omega} = -K\sin\theta - (b + k_d)\omega$. Define a scalar function with units of energy by adding kinetic energy to the integral of the restoring torque from zero angle:

$$V(\theta, \omega) = \frac{1}{2}J\omega^2 + K(1 - \cos\theta),$$

$$\dot{V} = J\omega\dot{\omega} + K\sin\theta\,\omega = -(b + k_d)\omega^2.$$

A positive damping coefficient ensures energy cannot increase. On the branch $-\pi < \theta < \pi$, V is positive away from the hanging rest state and zero there. Its derivative is zero whenever velocity vanishes, including ordinary turning points. To justify eventual convergence we need to establish whether any motion can remain indefinitely in this zero-derivative set.

Distinguish a turning point from an invariant state

At $\omega = 0$ a nonzero $\sin\theta$ produces angular acceleration, taking the trajectory immediately away from zero velocity. Inside the well the only state remaining forever at zero velocity is $(0, 0)$. The upright position sits at potential energy $2K$. Each closed sublevel $V \le c < 2K$ containing the downward rest state is compact and cannot leave the well, because reaching $\theta = \pm\pi$ would cost at least $2K$. LaSalle's invariance principle then establishes asymptotic convergence on that component.

$$|\omega_0| < \sqrt{\frac{2K}{J}(1 + \cos\theta_0)}$$

This expresses the strict sublevel as a speed allowance at each angle. A state outside it can still settle in the same well because damping removes energy before it reaches the top. The inequality is a sufficient certificate that can be tested from an initial measurement. Exactly at the upright rest state no damping torque acts and the system can remain there.

Compare two releases at the same angle

Let $J = 0.20$ kg m², $K = 2.0$ N m and $b + k_d = 0.30$ N m s/rad. At 60° the potential energy is 1.0 J and the certificate allows speeds below $\sqrt{30} = 5.48$ rad/s. At 4 rad/s the total is 2.6 J, safely below the 4 J

barrier. The turning angle cannot exceed $\arccos(1 - 2.6/2) = 107.5^\circ$ in magnitude. Positive damping reduces the actual maximum further.

At 6 rad/s the initial energy is 4.6 J, outside that guarantee. The instantaneous dissipation is $0.30(6)^2 = 10.8$ W, so dissipation before any top crossing may be substantial. Integrate the equation with the same initial angle and compare the true energy trace with the barrier. Moving the damping slider changes the rate of energy loss, while the sublevel calculated from J and K remains fixed.

Raise the starting speed until the initial energy just exceeds the barrier. Compare a damped run with a zero-damping run. Use the two traces to distinguish a guaranteed sublevel from energy actually removed during a particular trajectory.

Open this experiment online

Try the calculation

Initial angular speed (rad/s) **4**

Total viscous damping (N m s/rad) **0.3**

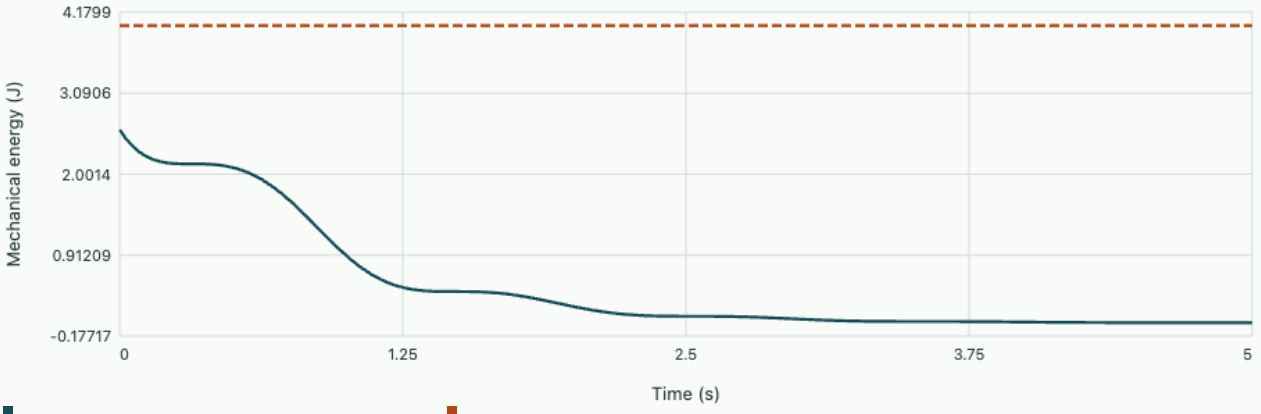

The 60° release starts at 2.600 J and has 0.003 J after 5 s. Its starting sublevel stays inside the initial well.

Tutorial · design an admissible release speed

At 120° with the same parameters, choose a speed ensuring the trajectory remains below 90% of the barrier. What changes in the proof if the velocity gain cancels the physical damping exactly?

▼ **Show the energy budget**

The potential energy is

$$2(1 - \cos 120^\circ) = 3.0\,\mathrm{J}.$$

The target maximum total energy is 3.6 J, leaving 0.6 J of kinetic energy. Thus $|\omega_0| \le \sqrt{2(0.6)/0.20} = 2.45$ rad/s to the quoted precision. When $b + k_d = 0$, energy is constant. The sublevel remains invariant, but whole undamped orbits now lie in the zero-derivative set, so convergence to rest no longer follows.

Further reading · Åström and Murray, Feedback Systems · chapter 5, Lyapunov stability

Finding a turning point without using the load as a coordinate

Nonlinear equations

Use tangent geometry to continue across a fold, and distinguish branch sensitivity from an ill-posed choice of variable in an equilibrium computation.

Two equilibria share one control value

Use the scaled normal form $F(x, p) = x^2 + p = 0$. The equilibrium curve is $p = -x^2$. At $p = -0.01$ two displacements, $x = \pm 0.1$, give the same load. Direct continuation in p uses $dx/dp = -F_p/F_x = -1/(2x)$. The derivative diverges at the fold. Plotting p against x, however, produces a smooth curve there.

> **Background · Backward error**
>
> $$F(\hat{x}) + \delta F = 0$$
>
> Specify how perturbations in data or equations are measured. A tiny perturbation making the computed value exact can coexist with a large solution error near a fold.

Add a geometric condition

At a known point $y_0 = (x_0, p_0)$, let t be a unit tangent perpendicular to $(2x_0, 1)$. A predictor $y_* = y_0 + \Delta s\, t$ lies on the tangent. Correct it by solving $F(x, p) = 0$ together with $t \cdot (y - y_*) = 0$, which confines corrections to a line normal to the old tangent. At the fold the Jacobian of this pair is

$$J = \begin{pmatrix} 0 & 1 \\ t_x & t_p \end{pmatrix}, \qquad \det J = -t_x.$$

With the tangent aligned with the displacement axis, t_x is nonzero. The pair remains locally invertible where load control alone fails. This is a change in the computation's coordinate, not removal of the physical multiple equilibria at a fixed load.

A step that crosses the maximum

Start at $x_0 = -0.1, p_0 = -0.01$ with increasing x, so $t = (1, 0.2)/\sqrt{1.04}$. A step of length 0.2 predicts $x_* \simeq 0.0961, p_* \simeq 0.0292$, which is off the curve and has positive load. The correction line satisfies

$$x + 0.2p = x_* + 0.2p_*.$$

Substitute $p = -x^2$ to obtain $x - 0.2x^2 \simeq 0.1020$. The nearby root is about 0.1041 and the corrected load about −0.0108. Both endpoints have negative load despite crossing the maximum.

Test the predictor before trusting it

Choose the starting displacement and step length. Plot the tangent segment, the original curve and the selected nearby intersection of the correction line with the curve. A large step makes the tangent less faithful. The correction must stay on the intended local branch.

Open this experiment online

Try the calculation

Starting displacement **-0.1**

Tangent step length **0.2**

Predictor (0.096116, 0.029223). Nearby corrected point (0.10413, -0.010843).

Tutorial on the experimental meaning

At $p = -0.01$, a pressure measurement has uncertainty 0.001. Estimate its local displacement uncertainty and compare it near $p = -0.0001$.

▼ **Worked solution**

At $|x| = 0.1$, $|dx/dp| = 5$ and the linear estimate is 0.005. At $|x| = 0.01$, the formal factor is 50. The same pressure error now exceeds the distance to the fold, so the local linear approximation itself loses validity.

If the continuation algorithm traces both sides smoothly, are both equilibria dynamically stable?

▼ **Worked solution**

A static residual gives equilibrium locations. Stability requires the linearisation of a specified evolution law or a second variation of the appropriate energy. Smooth numerical traversal gives no such certificate.

From discrete coordinates to a continuum

Follow two coupled coordinates into a chain and a rod. Compare wave and beam dispersion, derive the role of the mass matrix and use an energy quotient to estimate a frequency.

1. Coupled oscillators and normal coordinates
2. Modal participation and absorber tuning
3. How a longitudinal pulse reflects from a change in rod section
4. Why the frequencies of a bending beam are not equally spaced
5. Estimating a cantilever frequency from energy
6. Weak forms and finite elements
7. Wave speeds and numerical dispersion
8. Why two finite-element wave solvers propagate the same mode at different speeds
9. Vibrations of monoatomic and diatomic chains
10. Rotational and vibrational populations in a molecular gas

Coupled oscillators and normal coordinates

Machine dynamics

Derive and interpret the two modes of a coupled machine, then decide which mode an applied load can excite.

FROM FIRST PRINCIPLES

Find natural modes from the free force balance

For small motions of a conservative system with several coordinates, linear inertia forces are represented by a positive-definite mass matrix M and linear restoring forces by a symmetric stiffness matrix K. Collect the free balance and try a motion in which the coordinate amplitudes stay in one fixed ratio as each oscillates at frequency ω.

$$M\ddot{\mathbf{x}} + K\mathbf{x} = 0,$$
$$\mathbf{x} = \boldsymbol{\phi}\cos(\omega t) \implies (K - \omega^2 M)\boldsymbol{\phi} = 0.$$

A nonzero shape $\boldsymbol{\phi}$ can solve these homogeneous equations only when the coefficient matrix is singular. The determinant condition gives candidate squared frequencies, and the nullspace at each frequency gives a mode shape up to scale.

$$\det(K - \omega^2 M) = 0,$$
$$K\boldsymbol{\phi}_j = \omega_j^2 M\boldsymbol{\phi}_j.$$

For identical masses linked by a spring, a common translation leaves that link unstretched and an opposite motion stretches it from both ends. This observation identifies common and differential shapes even before evaluating the determinant. Initial displacement and velocity select their amplitudes; the eigenproblem identifies the motions the structure can support.

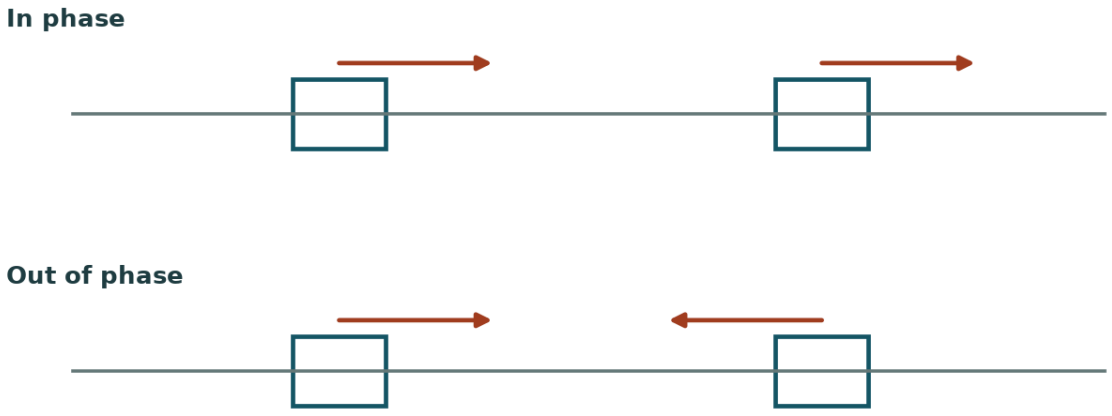

Which spring deforms in each mode?
Assume equal end springs k, equal masses m and a central coupling spring k^c. A common displacement leaves the coupling spring at its original length. In the lower drawing each mass moves a distance x towards the other, compressing the central spring by 2x. Half a cycle later the same spring extends by 2x. The ratios of restoring force to displacement are k and k + $2k^c$, giving squared frequencies k/m and (k + $2k^c$)/m.

DERIVATION AND APPLICATIONS

Quantify the splitting of two weakly coupled modes

When two machines have the same uncoupled natural frequency, adding a weak connecting spring splits that frequency into two. Consider identical sliders of mass m each attached to ground by stiffness k and linked to each other by stiffness k_c. Neglect damping and choose displacements in the same direction from equilibrium. The coupling spring responds only to the displacement difference. Adding and subtracting the two force balances therefore gives separate equations for $s = (x_1 + x_2)/2$ and $d = (x_1 - x_2)/2$.

$$m\ddot{s} + ks = 0,$$

$$m\ddot{d} + (k + 2k_c)d = 0.$$

Release slider one at A and slider two at zero, both from rest. The two modal coordinates then both start at $A/2$. Write $\omega_s = \sqrt{k/m}$ and $\omega_d = \sqrt{(k + 2k_c)/m}$ and combine their solutions.

$$x_1 = \tfrac{A}{2}(\cos\omega_s t + \cos\omega_d t),$$

$$x_2 = \tfrac{A}{2}(\cos\omega_s t - \cos\omega_d t).$$

Introduce $\bar{\omega} = (\omega_s + \omega_d)/2$ and $\Delta\omega = \omega_d - \omega_s$. The sum-to-product identities separate the fast motion from slow modulation. When the split is small, the modulation resembles a repeated transfer of motion between the sliders.

$$x_1 = A\cos(\bar{\omega}t)\cos(\Delta\omega t/2),$$
$$x_2 = A\sin(\bar{\omega}t)\sin(\Delta\omega t/2).$$

The first minimum of the slider-one displacement envelope occurs at $t = \pi/\Delta\omega$. Its instantaneous velocity there need not vanish because the envelope itself is changing. The envelope timing remains identifiable from repeated peaks at weak coupling.

WORKED EXAMPLE

Time the exchange of motion

For $m = 1.00$ kg, $k = 100$ N/m and $k_c = 10.5$ N/m, the two frequencies are 10.0 and 11.0 rad/s. The first envelope minimum appears at 3.14 s and the first full recovery of its magnitude at 6.28 s. Releasing the first slider by 8.00 mm sets both modal initial amplitudes to 4.00 mm. Releasing both sliders together instead excites only the slower common motion.

Change the inputs and inspect this calculation below

SECOND APPLICATION

Estimate coupling from a beat measurement

A second pair has mass 2.00 kg per slider and measured lower frequency 25.0 rad/s. Consecutive magnitude maxima of one slider's envelope occur 5.00 s apart. Thus

$$\Delta\omega = 2\pi/5.00 = 1.257\,\mathrm{rad/s},$$
$$k_c = m[(25 + 1.257)^2 - 25^2]/2 = 64.4\,\mathrm{N/m}.$$

The independently inferred grounding stiffness is $m\omega_s^2 = 1250$ N/m, making the connector about 5.2 percent as stiff.

Interactive calculation · Change the inputs of this example

Use the adjustable quantities to test the two worked calculations above. The plot recomputes this derivation's balance or constitutive relation; its numerical readout reports the quantities needed for the forward calculation and the inverse or design question. Keep the fixed assumptions stated in the readout when comparing with the example values.

Open this live calculation

Try the calculation

Coupling stiffness (N/m) **10.5**

Initial release (mm) **8**

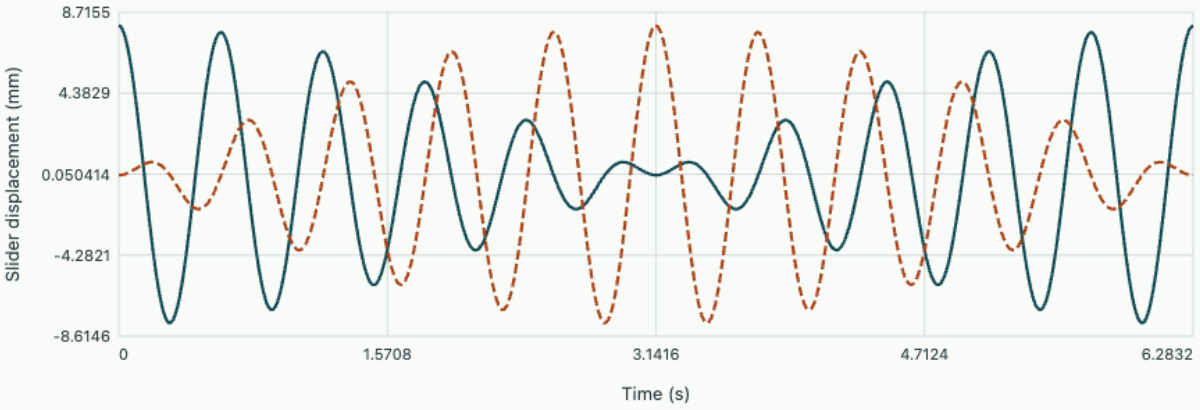

Frequencies 10.000 and 11.000 rad/s; first envelope minimum at 3.142 s. Equal masses1 kg; grounded stiffness100 N/m.

Two masses allow two independent shapes

Two identical instruments sit on separate spring mounts and are connected by a flexible link. Pull both by the same amount and the link keeps its natural length. Pull them in opposite directions and the link stretches twice as much as either displacement. The two tests reveal distinct restoring mechanisms. A model with one equivalent spring and the sum of both masses would discard one of them.

Let x_1, x_2 be horizontal displacements from equilibrium. Each mass is m, each ground spring has stiffness k, and the coupling spring has stiffness k_c. With light springs, small displacements and no damping, the kinetic energy is $m(\dot{x}_1^2 + \dot{x}_2^2)/2$ and the elastic energy is $k(x_1^2 + x_2^2)/2 + k_c(x_1 - x_2)^2/2$. The coupling energy contains the difference of displacements because it is the extension between its ends.

Separate space from time

Taking the derivative of elastic energy with respect to each coordinate gives $m\ddot{x}_1 + (k + k_c)x_1 - k_c x_2 = 0$ and the symmetric second equation. Look for $\mathbf{x} = \boldsymbol{\phi}\cos\omega t$. Nonzero modal shapes solve $(\mathbf{K} - \omega^2\mathbf{M})\boldsymbol{\phi} = 0$. For this pair the determinant equation is

$$(k + k_c - m\omega^2)^2 - k_c^2 = 0.$$

Taking both signs of the square root gives

$$\omega_1^2 = k/m,$$

$$\omega_2^2 = (k + 2k_c)/m.$$

Substitution back yields shapes proportional to $(1, 1)$ and $(1, -1)$. For the first, the connector transmits no incremental force. For the second, the connector acts strongly. Reversing both signs of a plotted eigenvector or multiplying it by a nonzero number describes the same physical mode.

Predict a release test at both instruments

Take $m = 5.0$ kg, $k = 2000$ N/m and $k_c = 1500$ N/m. The two angular frequencies are 20.0 and 31.62 rad/s, or 3.18 and 5.03 Hz. Pull only the first instrument 4.0 mm and release from rest. The initial displacement vector equals $2(1, 1) + 2(1, -1)$ mm. Each modal amplitude starts at its corresponding value with zero initial velocity. Hence

$$x_1(t) = 2\cos(20t) + 2\cos(31.62t),$$

$$x_2(t) = 2\cos(20t) - 2\cos(31.62t)$$

in millimetres. At zero time the second displacement vanishes while the connector exerts 6.0 N on its mass. Its initial acceleration is 1.2 m/s² toward the first instrument’s displacement. This apparent transfer of motion needs neither forcing nor damping: modal displacements add and cancel differently at the two observation points.

Distinguish available modes from visible modes

Define average and relative coordinates $q_s = (x_1 + x_2)/2$ and $q_a = (x_1 - x_2)/2$. Adding or subtracting the original equations decouples them. Equal external forces excite only q_s; equal and opposite forces excite only q_a. Taking the signal $(x_1 + x_2)/2$ likewise hides the antisymmetric mode. A missing spectral peak can therefore reveal the symmetry of a load or sensor arrangement, even though the corresponding eigenmode still exists.

If the two masses differ, the simple sum and difference cease to diagonalise the equations. The general route is to form the physical mass and stiffness matrices and solve the symmetric generalised eigenproblem. Distinct modes of an undamped conservative system are orthogonal with respect to mass,

$\boldsymbol{\phi}_i^T \mathbf{M} \boldsymbol{\phi}_j = 0$. This weighted orthogonality is what permits a measured motion or distributed load to be projected into separate modal coordinates.

Predict which mode responds to adding rotary inertia

For a unit mode shape ϕ, the quotient $\omega^2 = \phi^T K \phi / (\phi^T M \phi)$ compares stored elastic energy with inertia. Increasing inertia at a coordinate matters most when that coordinate has appreciable motion in the mode. A frame with three tip coordinates offers a way to check this reasoning beyond the symmetric two-mass illustration.

Compare two changes to the same frame: double only the tip mass from 200 to 400 kg, then restore it and double only the tip rotary inertia from 60 to 120 kg m². Predict whether either change can raise a natural frequency for the same stiffness and compute the fractional shift of the third mode in each case. Use the negligible-member-mass row throughout. Check the frame frequency measurements.

Derive bounce and pitch modes of a supported machine

A long machine supported on two mounts can translate and rotate as a nearly rigid body even if there is negligible frame bending. Let the mass centre move vertically by z and rotate by small angle θ, with positive rotation raising a point to the right. Vertical spring deflections relative to ground are $z - a\theta$ on the left and $z + b\theta$ on the right. Measure displacements from static equilibrium. The kinetic energy is $(m\dot{z}^2 + I_G\dot{\theta}^2)/2$, and the spring energy is $[k_L(z - a\theta)^2 + k_R(z + b\theta)^2]/2$.

Differentiating potential energy gives stiffness terms $K_{zz} = k_L + k_R,\ K_{\theta\theta} = k_L a^2 + k_R b^2,\ K_{z\theta} = -k_L a + k_R b$. The mass matrix is diagonal because translation was measured at the centre of mass. A vertical translation produces a moment whenever the weighted mount locations fail to balance, and a pure rotation then also produces a vertical force by reciprocity. If $k_L a = k_R b$ the modes are pure translation and pure pitch. Equal spring rates alone do not guarantee decoupling when the lever arms differ.

For free motion solve $(K - \omega^2 M)\phi = 0$. In mixed coordinates, metres and radians label different displacement entries, so a numerical component ratio needs units or a stated length scale. Measured vertical motions at two actual sensor locations provide an unambiguous observable mode shape.

Separate a heaving mode from a rocking mode

Let $m = 200$ kg, $I_G = 40\,\mathrm{kg\,m^2}$, $a = b = 0.50$ m and mount rates $k_L = 30000,\ k_R = 50000\,\mathrm{N/m}$. The stiffness entries are 80000 N/m, 20000 N m/rad and 10000 N in the mixed term. Setting the determinant to zero gives $(80000 - 200\lambda)(20000 - 40\lambda) - 10000^2 = 0$ with $\lambda = \omega^2$. Dividing through by 8000 yields

$$\lambda^2 - 900\lambda + 187500 = 0.$$

The squared frequencies are 327.5 and 572.5 s⁻², giving 2.88 and 3.81 Hz.

For the lower mode the first row implies

$$\theta/z = -(80000 - 200 \times 327.5)/10000 = -1.45\,\mathrm{rad/m}.$$

If mass-centre motion has 1 mm amplitude, the mount-point displacements are 1.725 and 0.275 mm, in phase but strongly unequal. The higher mode gives $\theta/z = +3.45\,\mathrm{rad/m}$, so the left point now moves oppositely to the right. An accelerometer placed close to a mode's nodal point can scarcely detect it although that mode remains physically present. For the low mode the vertical node lies about $1/1.45 = 0.69$ m to the right of the centre, beyond the right mount. Two well-separated measurement points make the rotational contribution identifiable.

A static load experiment can identify the stiffness coupling before a modal test. Apply a known vertical force F at the centre and no external moment. The pitch-equilibrium equation gives $\theta = -K_{z\theta}z/K_{\theta\theta} = -0.50z$ rad per metre for these mounts. Substitution into the vertical balance leaves effective static stiffness $80000 - 10000^2/20000 = 75000\,\mathrm{N/m}$. Under 150 N centre load, predicted motion is 2.00 mm and pitch −0.0010 rad, giving left and right mount readings of 2.50 and 1.50 mm. A centre gauge alone would only indicate an apparent softening, while the unequal pair exposes the rotational coupling that later appears in the two mode shapes.

Find a sensor position that can see a mode

Use the first three bending modes of an ideal simply supported uniform beam as a continuous analogue of coupled oscillators. A local displacement transducer reports a modal coordinate multiplied by the signed shape at the measurement location.

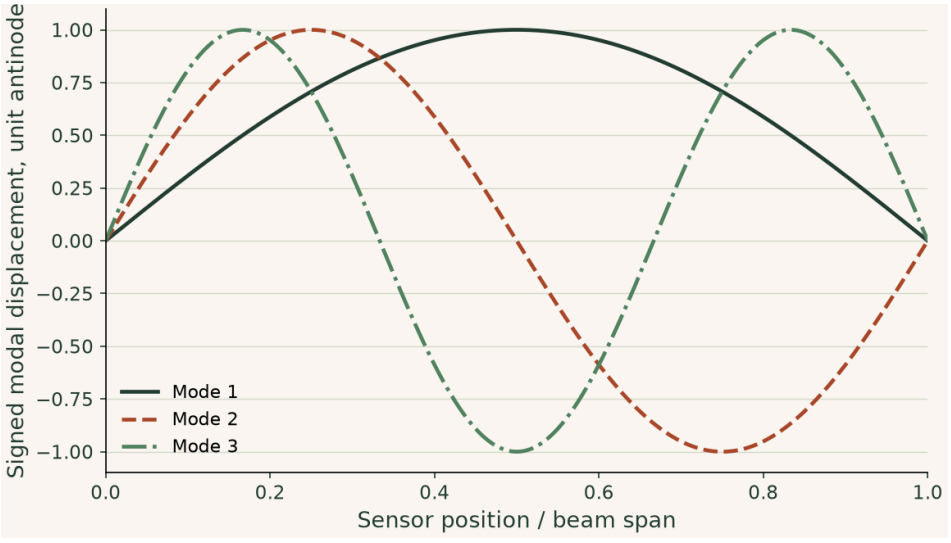

A midspan sensor misses the second mode even if excitation and damping would produce a large second modal coordinate. At one third span the third mode is invisible. Several sensor locations help distinguish a missing mode from a measurement node.

▶ **Read values from the plot**

Interactive calculation · change the inputs of this example

Move the sensor to a node and then change mode number. A zero local reading does not imply a stationary beam.

The curves below are recalculated from this section's equations in your browser. The fixed reference plot above remains available for comparison.

Open this live calculation

Try the calculation

Mode number	2
Sensor position / span	0.5
Modal amplitude (mm)	2

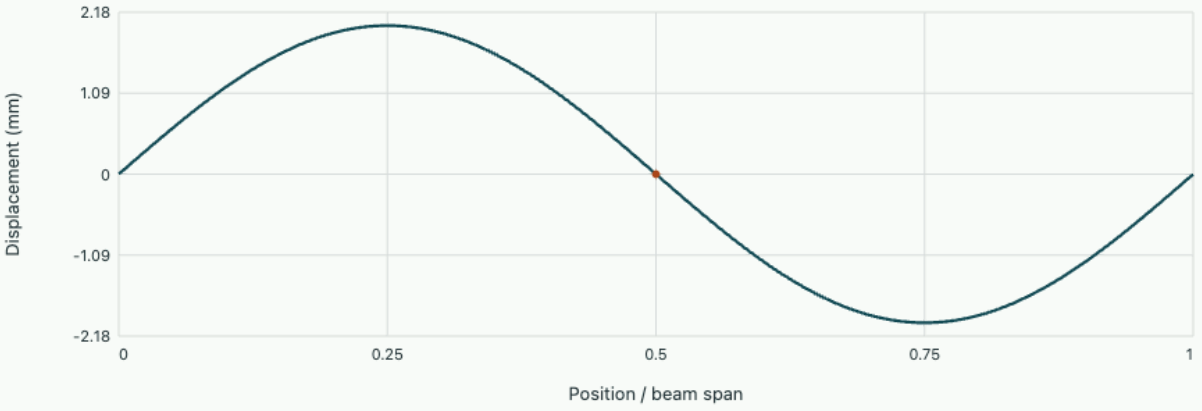

Selected mode Sensor reading

The sensor reads 0.000 mm. Mode 2 has 1 internal displacement nodes. A zero reading can conceal nonzero modal energy.

Modal participation and absorber tuning

Machine dynamics

Project external forcing onto vibration modes and determine when a vibration absorber suppresses displacement at a selected frequency.

FROM FIRST PRINCIPLES

Project a physical force onto a vibration mode

For small undamped motions a structure obeys $M\ddot{\mathbf{x}} + K\mathbf{x} = \mathbf{f}(t)$ with symmetric mass and stiffness matrices. Its normal modes satisfy

$$K\boldsymbol{\phi}_j = \omega_j^2 M\boldsymbol{\phi}_j.$$

Expand displacement in these mode shapes, using time-dependent coefficients q_j. Premultiply the result by the transpose of one mode.

$$\mathbf{x} = \sum_j \boldsymbol{\phi}_j q_j,$$

$$\sum_j (\boldsymbol{\phi}_i^{\mathsf{T}} M\boldsymbol{\phi}_j\, \ddot{q}_j + \boldsymbol{\phi}_i^{\mathsf{T}} K\boldsymbol{\phi}_j\, q_j) = \boldsymbol{\phi}_i^{\mathsf{T}}\mathbf{f}.$$

For distinct frequencies, symmetry makes different modes orthogonal under both matrices. The corresponding off-diagonal products vanish, leaving a separate scalar oscillator for the selected mode.

$$m_i\ddot{q}_i + m_i\omega_i^2 q_i = Q_i(t),$$

$$m_i = \boldsymbol{\phi}_i^{\mathsf{T}} M\boldsymbol{\phi}_i,$$

$$Q_i = \boldsymbol{\phi}_i^{\mathsf{T}}\mathbf{f}.$$

The force projection has a direct interpretation as work per unit modal displacement. A symmetric load can have zero projection onto an antisymmetric mode despite a large total force. The displacement at a particular sensor is obtained only after adding its components from all excited modes.

Background · Modal participation

$$Q_j = \phi_j^{\mathsf{T}} f$$

A mode is excited according to its overlap with the force. Always state how its mode vector and modal mass were normalised.

DERIVATION AND APPLICATIONS

Determine how a point force appears in collocated modal measurements

The displacement measured at the force location can have a zero between two structural resonances. Consider an undamped linear structure with two relevant modes, distinct natural frequencies $\omega_1 < \omega_2$ and modal masses $m_j > 0$. Apply a harmonic point force of complex amplitude F at coordinate a and measure displacement at the same coordinate. For modal shape component $\phi_j(a)$, the generalised force is $\phi_j(a)F$, and reconstruction at the sensor supplies a second factor of that component.

$$q_j = \frac{\phi_j(a)F}{m_j(\omega_j^2 - \omega^2)},$$

$$H_{aa} = \frac{x_a}{F} = \frac{A_1}{\omega_1^2 - \omega^2} + \frac{A_2}{\omega_2^2 - \omega^2},$$

$$A_j = \frac{\phi_j(a)^2}{m_j}.$$

The residues A_j are positive when both modes are visible. Between the two poles the first denominator is negative and the second positive. Set the sum to zero and multiply through by both denominators to find the antiresonance.

$$A_1(\omega_2^2 - \omega_z^2) + A_2(\omega_1^2 - \omega_z^2) = 0,$$

$$\omega_z^2 = \frac{A_1\omega_2^2 + A_2\omega_1^2}{A_1 + A_2}.$$

A zero in the measured displacement can therefore result from cancellation of two finite modal displacements. Its position also reveals their relative participation without requiring the absolute force calibration.

$$\frac{A_1}{A_2} = \frac{\omega_z^2 - \omega_1^2}{\omega_2^2 - \omega_z^2}.$$

Separated force and response locations can give signed residues and change the interlacing. With damping a finite minimum commonly replaces the exact zero, so using its frequency as an exact antiresonance is an approximation.

WORKED EXAMPLE

Predict the dip of a two-mode stage

For $\omega_1 = 10.0$ rad/s, $\omega_2 = 20.0$ rad/s and $A_1 = 2A_2$, the squared zero frequency is $(2 \times 400 + 100)/3 = 300$ s⁻², hence $\omega_z = 17.3$ rad/s. At that frequency the first contribution is

$2A_2/(100-300) = -0.0100A_2$ and the second is

$$A_2/(400-300) = +0.0100A_2.$$

The sensor is stationary while both modes respond.

Change the inputs and inspect this calculation below

SECOND APPLICATION

Recover a relative participation from a measured minimum

A different collocated test gives resonances at 30.0 and 50.0 Hz and a negligible-damping minimum at 40.0 Hz. Ratios of squared angular frequencies can equally be expressed through squared frequencies in hertz. The residue ratio is

$$(40^2 - 30^2)/(50^2 - 40^2) = 7/9 = 0.778.$$

With equal modal masses the first shape magnitude at the force point is $\sqrt{7/9} = 0.882$ of the second.

Interactive calculation · Change the inputs of this example

Use the adjustable quantities to test the two worked calculations above. The plot recomputes this derivation's balance or constitutive relation; its numerical readout reports the quantities needed for the forward calculation and the inverse or design question. Keep the fixed assumptions stated in the readout when comparing with the example values.

Open this live calculation

Try the calculation

First modal participation / second	2
First natural frequency (rad/s)	10
Second natural frequency (rad/s)	20

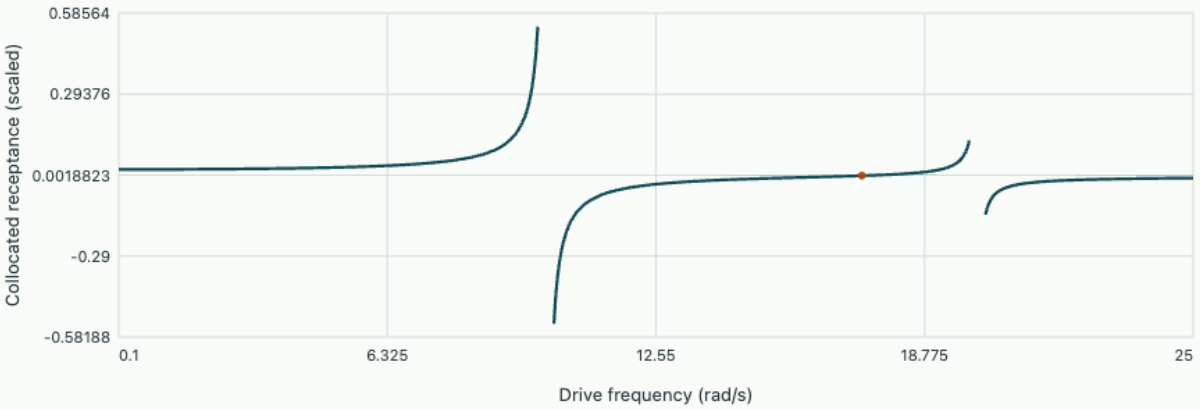

Two undamped modal terms Antiresonance

The cancellation lies at 17.321 rad/s between the two poles. Small neighbourhoods of the undamped poles are omitted from the curve.

Recover motion from mode amplitudes

Knowing a structure's natural frequencies does not yet tell you which frequencies a particular actuator will excite. For a linear undamped system write $M\ddot{x} + Kx = f(t)$ and let ϕ_j be a real mode shape solving $K\phi_j = \omega_j^2 M\phi_j$. Assume a complete set of independent modes and expand the displacement $x = \sum_j \phi_j q_j$. Multiplying the equation by ϕ_i^T uses mass and stiffness orthogonality to remove other modal coordinates.

$$m_i\ddot{q}_i + k_i q_i = \phi_i^T f(t),$$

$$m_i = \phi_i^T M \phi_i,$$

$$k_i = \omega_i^2 m_i.$$

Multiplying a mode shape by a constant changes the numerical modal mass and generalised force, while the reconstructed physical motion remains invariant. Thus a tabulated mode shape needs its normalisation if it is used to compute a physical response. A forcing pattern whose projection vanishes excites none of that mode from rest, even if the excitation frequency equals its natural frequency.

Select a mode by choosing the actuator pattern

Suppose two identical masses 2 kg each have mode shapes $(1, 1)$ and $(1, -1)$, with frequencies 10 and 20 rad/s. Both modal masses are 4 kg. A 12 N harmonic force on the first mass projects 12 N onto each mode in this normalisation. At a forcing frequency of 5 rad/s the undamped steady modal amplitudes are

$$12/[4(10^2 - 5^2)] = 0.0400\,\mathrm{m},$$

$$12/[4(20^2 - 5^2)] = 0.00800\,\mathrm{m}.$$

Recombination gives first and second physical amplitudes 0.0480 and 0.0320 m.

Now distribute the same total force as 6 N on each mass in phase. The first projection stays 12 N and the second becomes $6 - 6 = 0$. The masses now both move 0.0400 m. Relocating or phasing actuators can therefore change observed vibration without changing any mass, spring or natural frequency.

Cause the primary displacement to vanish

Attach an auxiliary mass m_a by spring k_a to a primary mass m_p grounded by spring k_p. A harmonic force of amplitude F acts on the primary mass. Seek displacement amplitudes X_p, X_a. The absorber equation is

$$-k_a X_p + (k_a - m_a\omega^2) X_a = 0.$$

At $\omega^2 = k_a/m_a$ this enforces $X_p = 0$. The primary equation then gives

$$X_a = -F/k_a.$$

The absorber's spring force balances the excitation while the primary mass is stationary in this ideal steady response.

For $m_a = 0.50\,\mathrm{kg}$, a measured forcing frequency of 20 Hz requires

$$k_a = m_a(2\pi 20)^2 = 7896\,\mathrm{N/m}.$$

An 8 N forcing amplitude gives absorber travel amplitude 1.01 mm. The two coupled resonances bracket this tuned antiresonance; startup or a change of shaft speed can pass through them. Damping limits the resonant peaks but generally prevents the exact cancellation obtained from these undamped equations.

OneSimulation · How can two resonant modes cancel the primary displacement?

Apply a sinusoidal force to a 5 kg primary mass supported by a 500 N/m spring. An attached 0.5 kg absorber connects through a 50 N/m spring. At the undamped tuning frequency the absorber equation forces the primary displacement to zero. The full coupled system still has two distinct natural frequencies. With mass-normalised modes and the force and displacement at coordinate 1, the receptance is

$$\frac{X_1}{F_1} = \sum_j \frac{\phi_{1j}^2}{\omega_j^2 - \omega^2 + 2i\zeta_j\omega_j\omega}.$$

OneSimulation obtains the eigenpairs from the mass-scaled stiffness. The eigenfrequencies are 1.36 and 1.86 Hz. Between these frequencies the two undamped real contributions have opposite signs. They cancel at 1.59 Hz. The code checks this zero and independently verifies the static compliance. Increase the common modal damping ratio and inspect the notch: losses shift the modal phases, so the exact zero becomes a finite minimum.

```
"""A force on the primary mass excites two modes of a tuned absorber."""
import matplotlib.pyplot as plt
import numpy as np
from onesim.numerics.linear.matrices.dense_linear_algebra import symmetric_eigensystem

mass = np.array([5., 0.5])  # kg, primary and absorber
support, spring = 500., 50.  # N/m, support and connecting spring
stiffness = np.array([[support+spring, -spring], [-spring, spring]])
scale = np.diag(1/np.sqrt(mass))
omega2, shapes = symmetric_eigensystem(scale @ stiffness @ scale)
modes = scale @ shapes
residues = modes[0]**2      # applied force and measured motion both at mass 1
tuned = np.sqrt(spring/mass[1])
assert abs(np.sum(residues/(omega2 - tuned**2))) < 1e-12
assert np.isclose(np.sum(residues/omega2), 1/support)

frequency = np.linspace(1.0, 2.3, 600)  # Hz
omega = 2*np.pi*frequency[:, None]
fig, ax = plt.subplots(figsize=(7, 4), constrained_layout=True)
for damping, colour in [(0.005, "#19596a"), (0.04, "#a5442e")]:
    denominator = omega2 - omega**2 + 2j*damping*np.sqrt(omega2)*omega
    response = np.sum(residues / denominator, axis=1)
    ax.semilogy(frequency, 1000*abs(response), color=colour,
                label=f"Both modal damping ratios {100*damping:g}%")

ax.axvline(tuned/(2*np.pi), color="0.5", linestyle=":", label="Undamped cancellation")
ax.set(xlabel="Excitation frequency (Hz)", ylabel="Primary displacement / force (mm/N)")
ax.legend(fontsize=8)
fig.savefig("machine-dynamics.png", dpi=170)
```

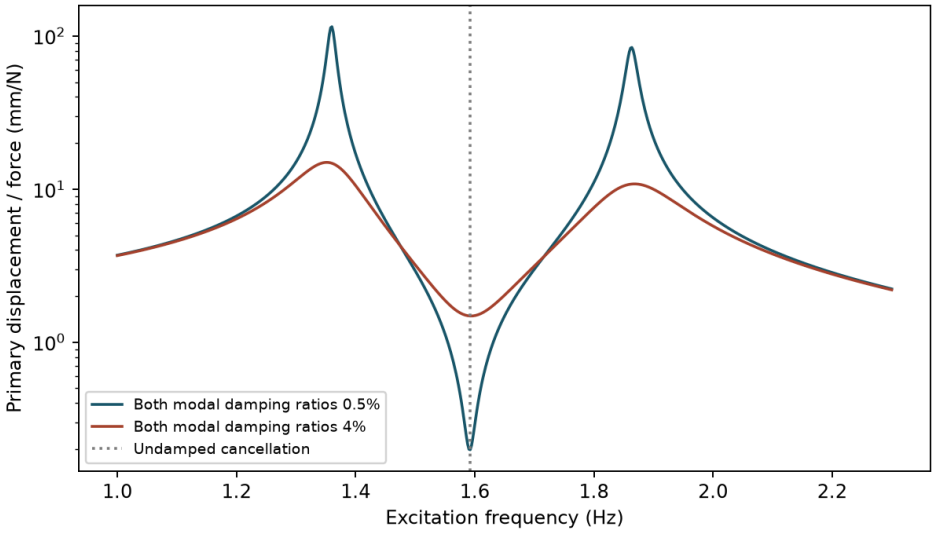

A low reading at the primary mass can coexist with substantial absorber motion. The plotted response and static-limit check both refer to the force application point.

Download the Python example

Change the inputs of this exact example and compare the recalculated curves with the recorded OneSimulation output above. The browser evaluates the stated analytical or modal reference.

Open this live calculation

Try the calculation

Common modal damping ratio	**0.02**
Absorber mass (kg)	**0.5**
Absorber spring (N/m)	**50**

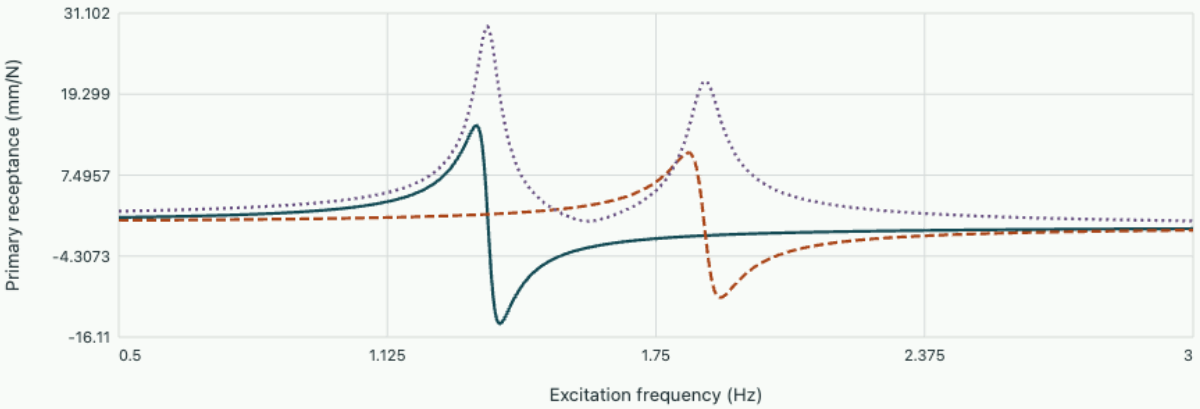

Natural frequencies 1.360, 1.863 Hz. At undamped tuning 1.592 Hz, receptance is 0.77774 mm/N. Static compliance 2.000 mm/N. A common modal damping ratio modifies each modal phase; it is distinct from a physical dashpot attached only to the absorber.

Choose where to observe cancellation

At the tuned absorber frequency a sensor on the primary reports zero ideal steady displacement, while a sensor on the attached mass records finite motion. A force transducer between the bodies measures the full applied excitation in the opposing phase. Moving the sensor can therefore turn the same test from an apparent null into a readily measurable response, without altering the underlying eigenfrequencies.

Project a spatially distributed load onto a flexible member

A beam or string has motion distributed along its length. Its modal forcing is determined by a spatial integral, analogous to the vector dot product for discrete coordinates. For a taut uniform string of length L, linear density μ and constant tension H, small transverse displacement $w(x,t)$ obeys $\mu w_{tt} - H w_{xx} = p(x,t)$. The tension term follows from the difference in vertical tension components on a short segment. Assume both ends fixed in displacement and neglect bending stiffness, damping and the change of tension caused by stretching. The modes are $\phi_n = \sin(n\pi x/L)$, with frequencies $\omega_n = (n\pi/L)\sqrt{H/\mu}$.

Expand $w = \sum \phi_n q_n$, multiply by ϕ_j and integrate over the length. The mass integral is

$$m_j = \mu \int_0^L \phi_j^2 dx = \mu L/2.$$

Integration by parts of the tension term gives the modal stiffness $k_j = m_j \omega_j^2$, with the fixed-end boundary terms vanishing. The modal input becomes

$$Q_j = \int_0^L p \phi_j dx.$$

Under a uniform harmonic load amplitude p_0,

$$Q_j = \frac{p_0 L}{j\pi}[1 - (-1)^j].$$

Even modes have zero generalised force because their positive and negative portions cancel exactly. A point load at x_0 instead yields

$$Q_j = F \phi_j(x_0).$$

Moving an actuator or changing a load footprint can thus suppress a resonance by symmetry without changing the material, tension or natural frequency.

Estimate a cable’s displacement from its first few modes

A laboratory cable spans 2.0 m under 200 N tension and has linear density 0.50 kg/m. Its wave speed is $20\,\mathrm{m/s}$, so $f_1 = 20/(2L) = 5.0\,\mathrm{Hz}$ and $m_j = 0.50\,\mathrm{kg}$. Apply a distributed harmonic pressure-equivalent line load $p_0 = 0.40\,\mathrm{N/m}$ at 2.0 Hz. For mode one, $Q_1 = 2(0.40)(2)/\pi = 0.509\,\mathrm{N}$, and its dynamic stiffness is

$$0.50[(2\pi 5)^2 - (2\pi 2)^2] = 414.5\,\mathrm{N/m}.$$

Its modal amplitude is 1.23 mm.

The third mode has $Q_3 = 0.170\,\mathrm{N}$, $f_3 = 15$ Hz and amplitude $0.170/\{0.50[(2\pi 15)^2 - (2\pi 2)^2]\} = 0.0390\,\mathrm{mm}$. At the midpoint $\phi_1 = +1$ while $\phi_3 = -1$, so the two-term prediction is approximately 1.19 mm. The next odd mode contributes with the opposite sign again, but is far stiffer at this drive frequency. In the static limit an independent check follows from the parabolic string solution $w(L/2) = p_0 L^2/(8H) = 1.00\,\mathrm{mm}$. If a strong measured response appears at the symmetric load’s even-mode resonance, investigate load asymmetry, asymmetric support stiffness or a disturbed initial condition before assigning a nonzero ideal modal projection.

The spatial convergence pattern can be estimated before adding many terms. For odd mode number n well above the forcing frequency, the uniform-load projection decreases as $1/n$ while modal stiffness increases as n^2. Each displacement contribution therefore decreases roughly as $1/n^3$. A point actuator at midspan instead gives modal projections of essentially alternating constant magnitude for odd modes, producing only a $1/n^2$ displacement decay. Hence a truncation that accurately predicts the response to a distributed flow load can be less accurate for an impulsive local tap. Strain or slope predictions may require still more terms because a spatial derivative introduces an additional factor of mode number. Choose the retained modes for the actual load and observed quantity.

The uniform cable problem admits an independent harmonic calculation without modal truncation. Set $w(x,t) = W(x)\cos \Omega t$. The governing equation gives

$$W'' + \kappa^2 W = -p_0/H,$$

$$\kappa = \Omega\sqrt{\mu/H}.$$

Symmetry about midspan and fixed ends select $W(x) = [p_0/(\mu\Omega^2)]\{\cos[\kappa(x - L/2)]/\cos(\kappa L/2) - 1\}$, provided the denominator is nonzero. For the test above $\kappa L/2 = 0.6283$ and $W(L/2) = 0.40[1/\cos(0.6283) - 1]/[0.50(2\pi 2)^2] = 1.196\,\mathrm{mm}$. This direct boundary-value result confirms both the signs and the scale of the first two odd-modal contributions.

As the excitation approaches the first natural frequency, $\kappa L/2$ approaches $\pi/2$ and the undamped steady expression becomes singular. An actual time record may instead show progressively growing amplitude before damping or geometric effects intervene. At very low frequency expand $\sec q \simeq 1 + q^2/2$; substituting $q = \Omega L\sqrt{\mu/H}/2$ recovers the static midpoint displacement without subtracting two nearly equal numerical values. The modal and spatial calculations thus furnish independent checks in the static, off-resonant and resonant limits.

What happens to the notch of a tuned absorber?

Attach an absorber of mass 0.10 times the primary mass, tuned to the primary's undamped frequency. Include 2.5% primary damping. Solve the complex two-mass force balance for primary displacement under harmonic forcing; the absorber spring and dashpot act on relative motion.

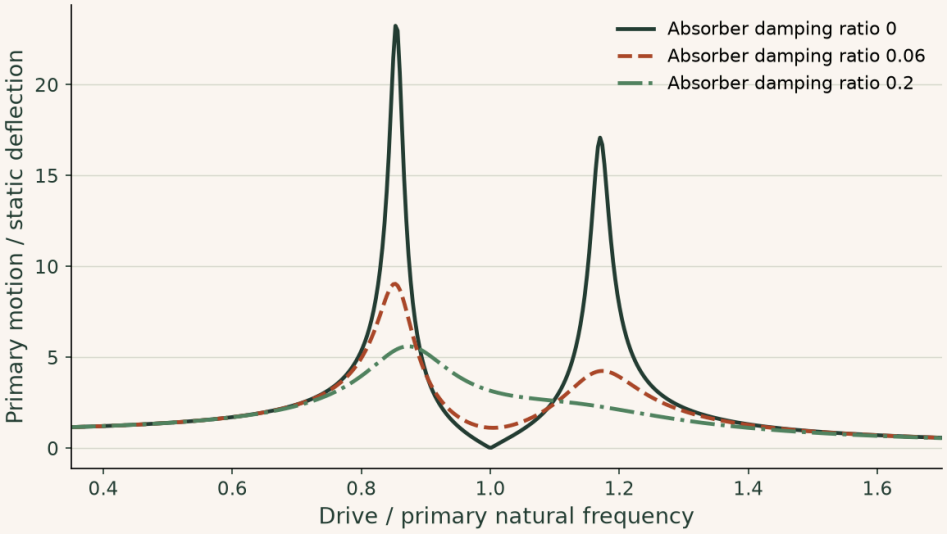

Without absorber damping the primary displacement vanishes at the tuned frequency, with response peaks on both sides. Absorber damping fills the notch and changes those adjacent peaks. An installation with variable drive speed must check the entire band.

▶ **Read values from the plot**

Interactive calculation · change the inputs of this example

Detune the absorber, then add damping. Compare the cancellation notch with both adjacent peaks.

The curves below are recalculated from this section's equations in your browser. The fixed reference plot above remains available for comparison.

Open this live calculation

Try the calculation

Absorber / primary mass	**0.1**
Absorber damping ratio	**0.06**
Absorber / primary frequency	**1**

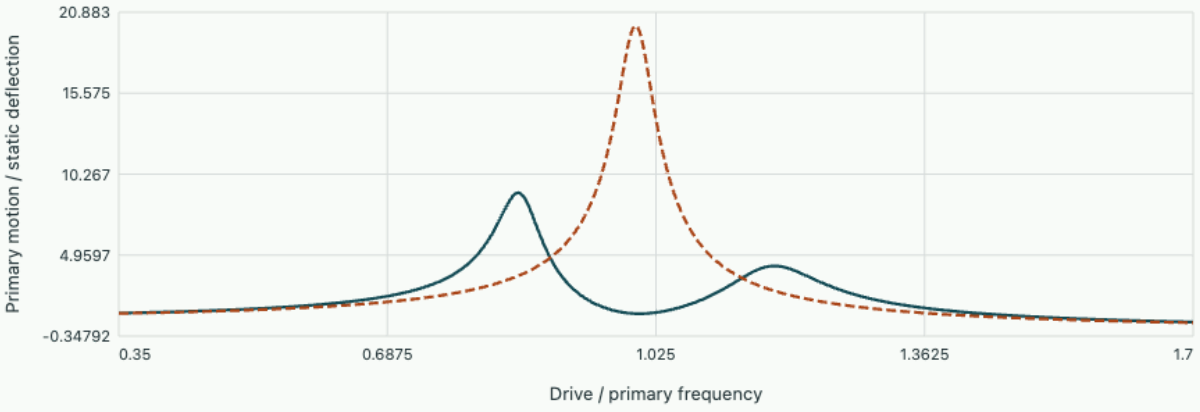

At the primary natural frequency, amplification is 1.125. A damped or mistuned absorber fills the exact undamped cancellation notch.

How a longitudinal pulse reflects from a change in rod section

Machine dynamics

A tap on one end of a rod reaches a receiver after a finite delay. Two rods joined end to end can even return a pulse before the receiver sees a far-end reflection. Derive propagation speed and distinguish the displacement amplitude from the energy carried by a pulse.

From the cut force to a travelling disturbance

Measure the small axial displacement $u(x,t)$ from a stress-free reference. In a slender homogeneous rod of area A, tensile force is

$$N = EAu_x.$$

A slice of length dx and mass $\rho A\,dx$ accelerates because its right and left forces differ by $N_x dx$. For constant properties, cancelling A gives

$$\rho A u_{tt} = (EAu_x)_x,$$

$$u_{tt} = c^2 u_{xx},$$

$$c = \sqrt{E/\rho}.$$

Either $u = f(x - ct)$ or $u = g(x + ct)$ satisfies this equation by differentiation. Curves of constant phase move right or left with speed c. Long-wavelength assumptions suppress lateral inertia and radial modes. Rod area cancels from wave speed but remains in the force carried at given particle velocity. For a right-moving pulse $v = u_t = -cu_x$, so tensile force $N = -Zv$, with mechanical impedance $Z = \rho Ac = EA/c$. The sign reverses for a left-moving wave.

Match velocity and force at a bonded junction

Let amplitudes I, R and T denote incident, reflected and transmitted particle velocity at the junction. A massless, perfectly bonded interface requires equal velocities and transmitted force. Apply the preceding sign convention separately to each travelling direction. The two equations determine two unknowns.

$$I + R = T,$$

$$-Z_1 I + Z_1 R = -Z_2 T,$$

$$\frac{R}{I} = \frac{Z_1 - Z_2}{Z_1 + Z_2},$$

$$\frac{T}{I} = \frac{2Z_1}{Z_1 + Z_2}.$$

The instantaneous power transported to the right is $-Nv = Zv^2$ for a single right-moving wave. For the same pulse shape the reflected energy fraction is $(R/I)^2$ and the transmitted fraction is

$(Z_2/Z_1)(T/I)^2$. They sum to one. A transmitted velocity amplitude exceeding the incident amplitude can thus be compatible with conservation of energy.

A stepped rod and a pulse-echo observation

Join two aluminium rods of areas 80 and 160 mm², $E = 70$ GPa and $\rho = 2700$ kg/m³. Both have $c = 5092$ m/s, but the second impedance is twice the first. An incident velocity of 0.30 m/s produces a reflected −0.10 m/s and a transmitted 0.20 m/s. The reflected pulse carries one ninth of the energy. Reversing the experiment makes the reflection positive and the transmitted velocity 0.40 m/s for the same incident amplitude. The two energy fractions are unchanged on reversal.

A receiver at the tap detects a reflected pulse 0.40 ms after launch, before any far-end reflection contaminates it. The return path covers the distance twice, so the inferred junction is $c(0.00040)/2 = 1.02$ m away. Measure pulse velocity rather than strain when comparing the signs to the plot. Incident tensile force has sign opposite incident velocity with the convention used here.

Keep the incoming pulse fixed and change the area ratio from 2 to 0.5. Determine which velocity component reverses sign and compare reflected energy fractions. Explain the difference by writing power balance for the two experiments.

Open this experiment online

Try the calculation

Second / first section area **2**

Incident peak velocity (m/s) **0.3**

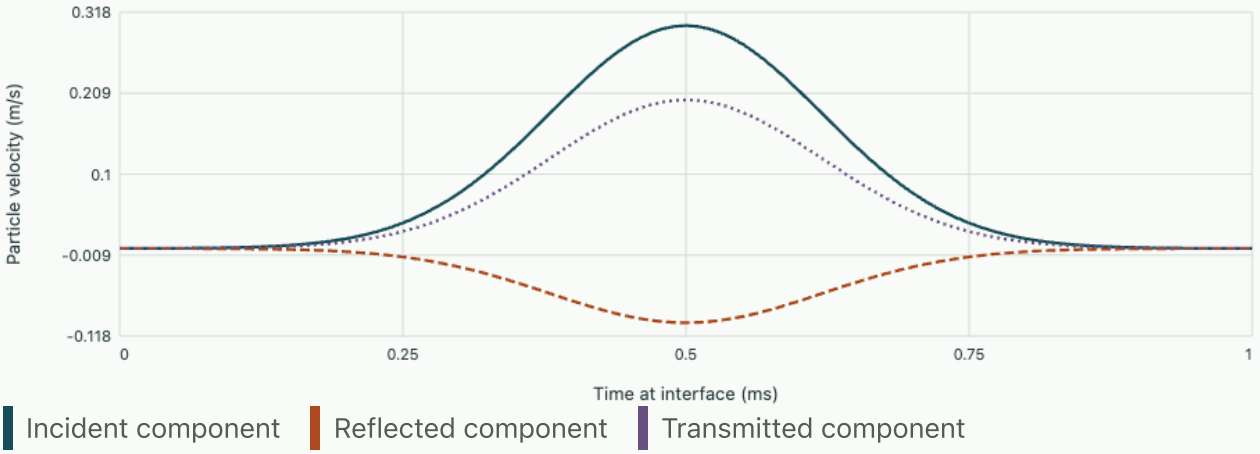

Peak reflected velocity is -0.100 m/s and transmission is 0.200 m/s. The reflection carries 11.1% of the incident energy.

Tutorial · infer a second cross-section

On a uniform material an isolated junction returns 25% of the incident velocity amplitude with the same sign. Infer the area ratio and transmitted energy fraction. How could an energy-only measurement leave the geometry ambiguous?

▼ **Show the inverse relation**

Let $z = Z_2/Z_1 = A_2/A_1$. Then $0.25 = (1 - z)/(1 + z)$, so $z = 0.60$. The transmitted velocity is $1.25I$. Its energy fraction is

$$0.60(1.25)^2 = 0.9375.$$

Measuring only the reflected energy gives 0.0625 and loses the sign of the amplitude. A thickening by a factor $1/0.60$ would give the same energy reflection and the opposite sign in the velocity trace.

Further reading · Bower, Applied Mechanics of Solids · solutions to problems involving vibrations and wave propagation

Why the frequencies of a bending beam are not equally spaced

Machine dynamics

A distributed beam can bend into infinitely many shapes. Derive the relation between wavelength and oscillation frequency, then compare the measured response of a beam with the mode family predicted by its supports.

Combine transverse force, moment and curvature

Take a straight uniform beam with small transverse deflection $w(x,t)$, density ρ, area A and second moment of area I about the bending axis. Euler–Bernoulli kinematics keeps cross-sections perpendicular to the centreline. The bending resistance is proportional to curvature EIw_{xx}. For a load-free part of the beam the gradient of moment supplies shear and the gradient of shear accelerates the mass. With restoring forces opposing deflection, the resulting equation is

$$\rho A\, w_{tt} + EI\, w_{xxxx} = 0.$$

The fourth spatial derivative calls for four boundary conditions. At a simple support the displacement vanishes and the bending moment is zero, hence

$$w = w_{xx} = 0.$$

A clamp instead fixes displacement and slope. Interchanging a pin and a clamp changes the allowed shape family even if the span and material remain fixed.

Obtain the simply supported series

Try $w = W\sin(kx)\cos(\omega t)$. Two spatial derivatives bring down $-k^2$, and four give $+k^4$. Substitution balances the inertia and stiffness terms. The conditions at x=0 hold for every k in this sine family. At x=L the sine must vanish, yielding

$$\omega^2 = \frac{EI}{\rho A}k^4,$$

$$k_n = \frac{n\pi}{L},$$

$$f_n = \frac{n^2\pi}{2L^2}\sqrt{\frac{EI}{\rho A}}.$$

A long travelling sinusoid has phase velocity $\omega/k = k\sqrt{EI/(\rho A)}$. The group velocity $d\omega/dk$ is twice that value in this model. A localized pulse contains many wavelengths, which can therefore separate as it propagates. Predictions at wavelengths near the thickness require accounting for rotary inertia and shear deformation.

Choose sensor positions as carefully as the frequency range

Use a 1 m steel strip 20 mm wide and 4 mm thick with $E = 200$ GPa and $\rho = 7800$ kg/m³. For bending about the thin direction $I = bh^3/12$ and $I/A = h^2/12$. The first three simply supported frequencies are roughly 9.18, 36.7 and 82.7 Hz. Doubling the width alone doubles stiffness and mass together and leaves these frequencies unchanged. Doubling thickness doubles each frequency. Shortening the span by 20% increases all three by $1/0.8^2 = 1.56$.

At the centre a displacement pickup sees $\sin(n\pi/2)$. It sees the first mode at its antinode and misses the second mode entirely. At the quarter point it sees that second mode strongly. An absent spectral peak can therefore result from excitation or sensing at a node. Move the measuring point before adjusting a fitted damping value to explain its absence.

Find a common node of the first and third modes and a location that suppresses the second mode alone. Change the thickness and then the span. Use the resulting frequencies to test whether each scaling is linear or quadratic.

Open this experiment online

Try the calculation

Span (m) 1

Thickness (mm) 4

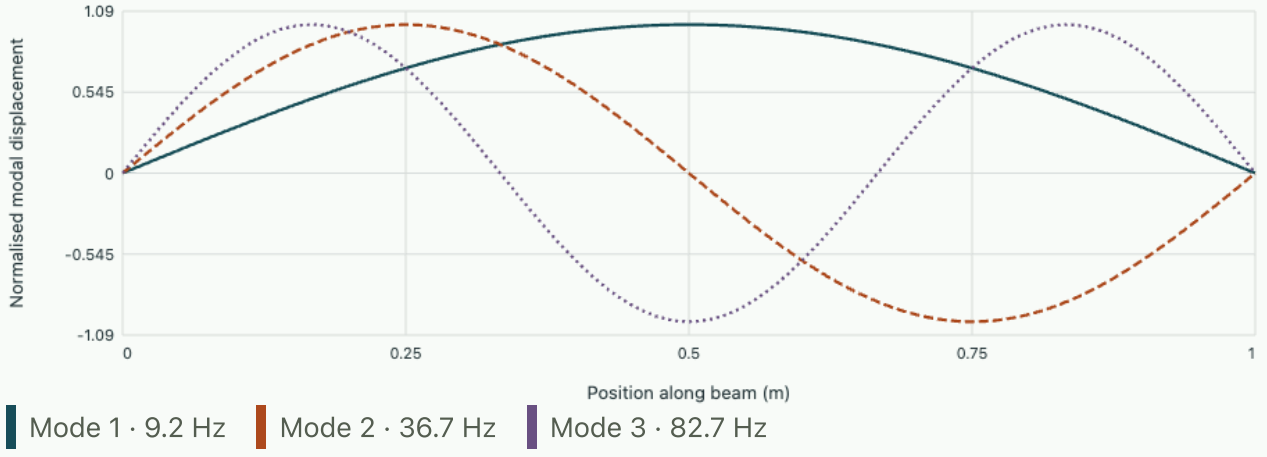

At midspan the second mode has a displacement node. The three frequencies are 9.18, 36.74, 82.66 Hz.

A related OneSimulation calculation

For a frame whose geometry and end payload preclude the simply supported sine family, compare the first three computed modes after changing the tip mass. Test whether all frequencies scale by the same factor.

Compare frame modes with OneSimulation

Tutorial · distinguish distributed bending from a tensioned string

A simply supported specimen has prominent peaks at 12 Hz and 108 Hz with the receiver at midspan. Infer which bending modes these could be and predict the frequency and receiver location for the missing mode. What would the third-to-first frequency ratio be for an ideal string?

▼ **Show the mode test**

The ratio $108/12 = 9$ agrees with n^2 for $n = 3$. The second bending mode should lie near $4(12) = 48$ Hz. Measure at one quarter span and excite away from its nodes. An ideal uniform string has $\omega = ck$ and a third-to-first ratio of 3. Checking both the midspan node and the shifted pickup spectrum distinguishes these models more effectively than a single peak.

Further reading · MIT 2.003SC · lecture 27 on vibration of continuous structures

Estimating a cantilever frequency from energy

Machine dynamics

A clamped beam carries a small sensor at its tip. Its precise mode shape is unknown. Use the static deflection shape to approximate the fundamental frequency and see why concentrating a small mass at the tip has a large effect.

Choose a displacement field that respects the support

Write $w(x,t) = q(t)\phi(s)$ with $s = x/L$, taking q as tip displacement. Choose the shape from a uniform cantilever under a static transverse tip force. The bending moment varies linearly from root to tip. Integrating curvature twice with $w(0) = w'(0) = 0$, then normalizing at $s = 1$, gives

$$\phi = s^2(3 - s)/2.$$

The shape satisfies both essential clamp conditions. Its free-tip shear need not match the exact unloaded vibration mode. The energy formulation can use such admissible trial shapes.

Background · Rayleigh quotient

$$R(u) = u^{\mathsf{T}} K u / (u^{\mathsf{T}} M u)$$

For symmetric stiffness and positive mass this estimates squared angular frequency. A kinematically admissible displacement is required for a useful structural estimate.

Compute effective stiffness and mass from the same field

The strain energy density of a slender beam in bending is $\frac{1}{2} EI w_{xx}^2$. Its translational kinetic energy is $\frac{1}{2}\rho A w_t^2$ per unit length. Changing variables from x to s introduces different powers of L into the two integrals. Include a point mass M at the tip, neglecting its rotary inertia.

$$U = \frac{EIq^2}{2L^3} \int_0^1 (\phi'')^2 \, ds,$$

$$K = \frac{\dot{q}^2}{2} \left[\rho A L \int_0^1 \phi^2 \, ds + M \right].$$

Since $\phi'' = 3(1 - s)$, the stiffness integral is 3. Squaring $s^2(3 - s)/2$ and integrating $(9s^4 - 6s^5 + s^6)/4$ gives $33/140$. The Euler–Lagrange equation for q is consequently a single oscillator equation with

$$\omega_R^2 = \frac{3EI/L^3}{(33/140)\rho A L + M}.$$

For M=0 this gives the dimensionless coefficient $\sqrt{140/11} = 3.5675$. Solving the exact unloaded cantilever condition $\cosh\beta\cos\beta = -1$ gives

$$\beta_1^2 = 3.5160.$$

The estimate is high by about 1.5%. The Rayleigh minimum principle explains that direction of error for conservative systems with admissible trial shapes. Restricting motion to a single shape restricts the set over which the energy quotient can attain its minimum.

Choose a sensor after estimating its dynamic effect

Take $EI = 10$ N m², $L = 0.50$ m and total beam mass 0.40 kg. The tip stiffness is 240 N/m and the distributed effective mass is only 0.0943 kg. The estimate gives 8.03 Hz without a sensor and 6.49 Hz with a 0.05 kg tip sensor. The sensor weighs one eighth of the beam, yet it has over half the effective mass associated with the chosen tip coordinate.

Place the same sensor at half-span instead. There $\phi(0.5) = 0.3125$. Its kinetic energy contributes $M\phi(0.5)^2 = 0.00488$ kg to the effective mass, so the estimate rises to 7.83 Hz. The sensor measures a smaller local motion as it perturbs the frequency less. Compare that trade-off at different attachment positions with the plot.

Move along the position axis with a fixed sensor mass. Identify the interval in which frequency is most sensitive to changing attachment position. Double the sensor mass and check whether the change in frequency doubles at the tip.

Open this experiment online

Try the calculation

Attached mass (kg) **0.05**

Bending rigidity (N m²) **10**

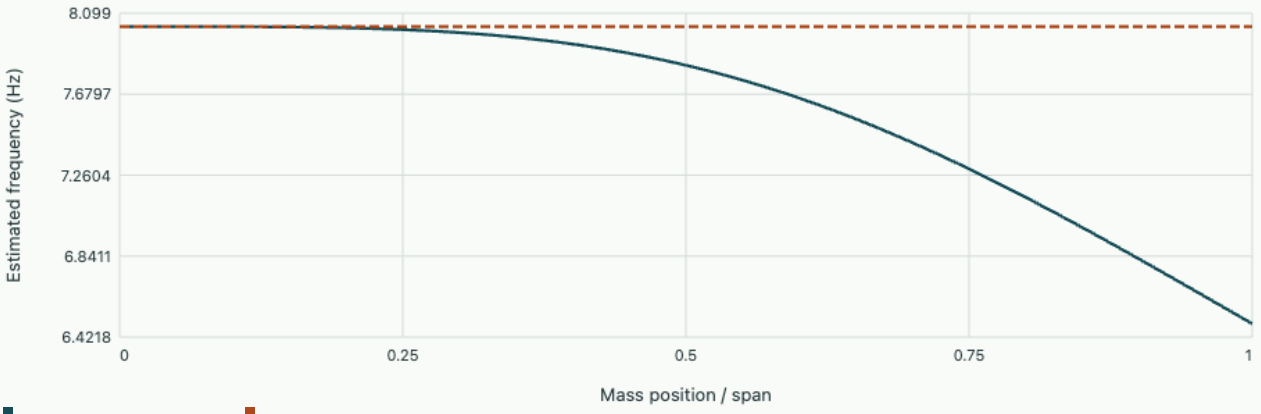

The estimate is 6.49 Hz with the sensor at the tip and 7.83 Hz at half-span. The bare-beam estimate is 8.03 Hz.

A related OneSimulation calculation

The course frame model has several modes and an independently variable payload rotary inertia. Compare a pure translation-mass change with a rotary-inertia change; the scalar point-mass estimate above addresses the first mechanism.

Open the OneSimulation frame eigenvalue experiment

Tutorial · estimate an unknown attached mass

The same bare beam is fitted with a small tip part and resonates at 6.0 Hz. Estimate the attached mass. Give one reason the inferred mass could differ from a scale reading even when the frequency measurement is accurate.

▼ **Show the mass estimate**

The required effective mass is

$$240/(2\pi \cdot 6)^2 = 0.1689\,\mathrm{kg}.$$

Subtract 0.0943 kg for the beam to obtain about 0.0746 kg. Clamp compliance would reduce the effective stiffness and frequency, which this fit would interpret as extra tip mass. The trial shape and omission of rotary inertia also limit the estimate for a part with appreciable extent.

Further reading · Bower, Applied Mechanics of Solids · Rayleigh–Ritz methods

Weak forms and finite elements

Numerical partial differential equations

Derive a variational statement by integration by parts, assemble element matrices for a one-dimensional rod and explain what the Galerkin solution minimises.

FROM FIRST PRINCIPLES

Obtain the weak diffusion problem by moving one derivative

For a stationary diffusion problem $-\nabla \cdot (k\nabla u) = f$, suppose temperature is prescribed on part of the boundary and the outward flux $q_n = -k\nabla u \cdot \mathbf{n}$ on the remainder. A classical second derivative may not exist across a material interface. Instead multiply the conservative equation by a smooth test function v that vanishes where u is prescribed. The divergence theorem moves one derivative from the flux onto v:

$$\int_\Omega k\nabla u \cdot \nabla v \, d\Omega = \int_\Omega f v \, d\Omega - \int_{\Gamma_N} v q_n \, d\Gamma.$$

Approximate u with continuous element shape functions N_j that are differentiable inside each element. Choose each allowable shape function as the test function. Linearity then yields element contributions

$$K_{ij}^{(e)} = \int_e k\nabla N_i \cdot \nabla N_j \, d\Omega,$$

$$f_i^{(e)} = \int_e f N_i \, d\Omega.$$

Neighbouring elements contribute to the same global unknown at a shared node. Adding their contributions enforces weak equilibrium. The flux sign in the boundary term follows from an outward-positive definition; switching to prescribed inward heat supply reverses that sign in the load vector.

Background · Weak form

$$\int k\nabla u \cdot \nabla v \, dV = \int f v \, dV + \text{boundary terms}$$

Integration by parts lowers the derivative requirement. Essential and natural boundary data enter the discrete system differently.

DERIVATION AND APPLICATIONS

How a Robin boundary enters both the stiffness matrix and the

load

A convecting boundary couples an unknown surface temperature to an ambient temperature. Unlike a prescribed heat source it contributes to both sides of the assembled equations. Consider steady diffusion $-\nabla \cdot (k \nabla T) = s$ in a two-dimensional region of unit thickness, with $k > 0$. On a straight boundary segment impose the empirical film law $-k \nabla T \cdot \mathbf{n} = h(T - T_\infty)$ using the outward normal. Multiply the field equation by a test function v vanishing on prescribed-temperature boundaries, integrate, and apply the divergence theorem:

$$\int_\Omega k \nabla v \cdot \nabla T \, dA - \int_{\partial\Omega} v k \nabla T \cdot \mathbf{n} \, ds = \int_\Omega v s \, dA.$$

Substitution on the film boundary Γ places the unknown surface term on the left and the ambient contribution on the right:

$$\int_\Omega k \nabla v \cdot \nabla T \, dA + \int_\Gamma h v T \, ds = \int_\Omega v s \, dA + \int_\Gamma h v T_\infty \, ds$$

with any other natural boundary terms added separately. To assemble one linear edge of length ℓ, use edge functions $N_1 = 1 - \xi$, $N_2 = \xi$, $\xi \in [0, 1]$. Insert the nodal interpolation for T and choose each N_i as test function. Constant h, T_∞ give

$$K_\Gamma = \frac{h \ell}{6} \begin{pmatrix} 2 & 1 \\ 1 & 2 \end{pmatrix}, \qquad f_\Gamma = \frac{h \ell T_\infty}{2} \begin{pmatrix} 1 \\ 1 \end{pmatrix}.$$

The off-diagonal term is present because both nodes influence temperature across the same edge. In the limit $h = 0$ the boundary is insulated. A very large film coefficient constrains the temperature toward ambient but can introduce a large stiffness contrast.

WORKED EXAMPLE

Assemble a convecting edge by hand

Use a one-metre out-of-plane thickness, $\ell = 0.300$ m, $h = 20.0$ W/(m² K) and $T_\infty = 290$ K. Then K_Γ has diagonals 2.00 W/K and off-diagonals 1.00 W/K. The load is $(870, 870)$ W. At nodal temperatures 300 and 310 K the film residual $K_\Gamma T - f_\Gamma$ is $(40, 50)$ W. The sum 90 W agrees with $h \ell [(300 + 310)/2 - 290]$.

SECOND APPLICATION

Test a constant solution before using the boundary routine

Set both temperatures to 290 K, the ambient value. Each row has sum 3.00 W/K, so every residual is $3(290) - 870 = 0$. If the code includes the ambient load but forgets the matrix, it predicts 1740 W of heating at thermal equilibrium. This constant-field patch test detects sign errors and omission of the surface matrix independently of the volume mesh.

Reduce the differentiability required by equilibrium

A rod is fixed at $x = 0$, pushed by a distributed load f and by an end force t at $x = L$. Axial displacement u satisfies $-(EAu')' = f$, $u(0) = 0$ and $EAu'(L) = t$. The product EA is positive. A trial profile assembled from linear pieces has jumps in its derivative, so differentiating it twice pointwise is unsuitable. Instead multiply the strong equation by a test displacement v vanishing at the fixed end and integrate by parts once.

The resulting equation is

$$\int_0^L EA\, u'v'\, dx = \int_0^L fv\, dx + tv(L).$$

Only first derivatives are required. The fixed displacement is imposed directly on trial and test spaces; the end traction appears in the load functional. This clarifies why prescribing both force and displacement independently at the same end can overconstrain a second-order problem. The test functions represent allowable virtual displacements, and the integral identity expresses equality of internal and external virtual work.

Background · Why can the derivative jump while the displacement stays continuous?

At a bonded interface with no concentrated force, displacement and axial force are continuous. If EA jumps, the strain u' can jump inversely even though the product EAu' is continuous. For a continuous piecewise linear displacement, the weak first derivative is the ordinary piecewise constant slope. The squared-gradient energy is therefore finite.

A displacement jump is different. Replacing a jump of size d by a straight ramp over width δ costs strain energy $EAd^2/(2\delta)$ for constant positive stiffness, which diverges as the ramp shrinks. A standard conforming displacement space encodes this distinction. If the mechanics really allow slip, the interface needs its own model and a space which permits the two traces to differ.

Assemble one element and connect it to its neighbour

On an element from x_i to x_{i+1} of length h, use shape functions $N_1 = 1 - s,\ N_2 = s$ with $s = (x - x_i)/h$. Their physical derivatives are $-1/h,\ 1/h$. For constant EA, integrating products $EAN_a'N_b'$ gives the matrix $(EA/h)\left(\begin{smallmatrix} 1 & -1 \\ -1 & 1 \end{smallmatrix}\right)$. A constant distributed load contributes $fh(1,1)^T/2$. Summing element contributions for a shared global node enforces balance there without prescribing the internal traction manually.

Take $L = 1,\ EA = 1,\ f = 2,\ t = 0$ in consistent units and use two equal elements. After eliminating the fixed displacement, the stiffness matrix is $\left(\begin{smallmatrix} 4 & -2 \\ -2 & 2 \end{smallmatrix}\right)$ and the load is $(1, 0.5)^T$. Solving gives

$$u(0.5) = 0.75,\ u(1) = 1.$$

The exact solution is $2x - x^2$ and agrees at both nodes. Inside the first element at $x = 0.25$, the linear interpolant gives 0.375, whereas the exact value is 0.4375. Nodal agreement can coexist with a substantial interior error.

Assemble a physical triangle from a reference element

A line element has one length scale. A triangle can stretch, rotate and shear, so the element area alone cannot determine its diffusion matrix. Start with the reference vertices $(0,0), (1,0), (0,1)$ and the linear shape functions $1 - \xi - \eta, \xi, \eta$. Send the reference triangle to a physical cell with vertices P_0, P_1, P_2 by $x = P_0 + J(\xi, \eta)^T$, where the columns of J are $P_1 - P_0$ and $P_2 - P_0$. For a nondegenerate triangle, the chain rule and area transformation give

$$\nabla_x N_i = J^{-T} \nabla_{\xi,\eta} \widehat{N}_i,$$

$$dx\, dy = |\det J|\, d\xi\, d\eta.$$

To see why the inverse transpose occurs, take an arbitrary displacement $d\widehat{x}$. Both gradients must describe the same change in a shape function. Thus $(\nabla_x N_i)^T J\, d\widehat{x} = (\nabla \widehat{N}_i)^T d\widehat{x}$ for every such displacement. For unit isotropic conductivity, the transformed gradients are constant and the physical stiffness entries reduce to

$$K_{ij} = |T| \nabla N_i \cdot \nabla N_j,$$

with $|T| = |\det J|/2$. A constant cell load f contributes $f|T|/3$ at each vertex because each linear shape function has mean $1/3$.

A sheared cell and an exact affine-field check

Take $P_0 = (0,0), P_1 = (2,0), P_2 = (1,1)$. The columns of J are $(2,0)$ and $(1,1)$, so the cell area is 1. Applying J^{-T} to the three reference gradients gives $(-1/2, -1/2), (1/2, -1/2), (0,1)$. Their dot products and the load $f = 3$ yield

$$K = \begin{pmatrix} 1/2 & 0 & -1/2 \\ 0 & 1/2 & -1/2 \\ -1/2 & -1/2 & 1 \end{pmatrix}, \qquad b = (1,1,1)^T.$$

Every row sums to zero because a constant field has zero gradient. For a more discriminating test use $u = x + 2y$, with vertex values $U = (0,2,3)^T$. Weighting the three gradients by these values gives $(1,2)$. The physical integral of its squared gradient equals $1(1^2 + 2^2) = 5$, and direct multiplication gives $U^T K U = 5$. A transposed mapping error can pass the constant test and fail this second one.

Identify the energy that is best approximated

Let $a(u,v)=\int EA\,u'v'$ and denote the external work by $\ell(v)$. The discrete solution u_h satisfies $a(u_h,v_h)=\ell(v_h)$ for every test function from its finite-dimensional space. The continuous solution satisfies the same equation for every such test, so $a(u-u_h,v_h)=0$. This Galerkin orthogonality means the error is perpendicular to the trial space in the energy inner product. For any other admissible discrete w_h, write $u-w_h=(u-u_h)+(u_h-w_h)$ and expand its squared energy norm. The cross term vanishes and $\|u-w_h\|_a^2=\|u-u_h\|_a^2+\|u_h-w_h\|_a^2$.

Thus the conforming Galerkin solution is the best energy approximation in its space for this symmetric linear problem and exact integration. The statement concerns a specific norm and model. It does not guarantee pointwise optimal stresses or carry unchanged into nonsymmetric transport problems. In the rod example the computed strain is constant on each element, replacing a linearly varying exact strain. Refinement improves this derivative field even when a table of nodal displacements already looks exact.

Recover a support reaction

The reaction at a prescribed-displacement node is hidden if one inspects only the reduced interior system. Assemble all element internal forces Ku_h before discarding constrained rows, then subtract the full external load vector. The entries at free degrees of freedom should be near zero; the entry at a prescribed degree of freedom gives the reaction in the chosen sign convention.

In the uniformly loaded rod, the first element strain is

$$(0.75-0)/0.5=1.5.$$

Its internal nodal force at the left is -1.5, while the first node receives an external distributed-load share of $+0.5$. Their difference -2 is the support reaction. It balances the total applied load $2\cdot 1=2$. Looking only at the derivative in the first element would have reported magnitude 1.5, missing that load share. A reaction from assembled balance and a stress recovered by pointwise differentiation are related but distinct quantities on a finite mesh.

Obtain actual norm errors from the Galerkin property

For $-u''=f$ on the unit interval with homogeneous Dirichlet values, the elementary energy inner product is $a(u,v)=\int u'v'$. Let I_hu be the continuous piecewise-linear interpolant of a sufficiently smooth exact solution at mesh nodes. On each element its slope is the average of u'. Every linear finite-element test function v_h has constant derivative on that element. Consequently

$$\int_E (u-I_hu)'v_h'=v_h'[u-I_hu]_{\partial E}=0.$$

Summing proves global energy orthogonality.

The Galerkin solution satisfies the same orthogonality, and positive definiteness gives uniqueness. Thus $u_h = I_h u$ in this one-dimensional, constant-coefficient problem with exactly integrated load and matching boundary values. Nodal errors vanish, although the field and derivative between nodes can still be inaccurate. Variable coefficients inside an element generally destroy the simple telescoping argument because the factor multiplying v_h' is no longer constant. The result also should not be transferred to multidimensional triangulations without proof.

Compare nodal, field and flux accuracy for one solution

Choose $u = x(1 - x)$, so $f = 2$. On an element starting at a write $s = x - a \in [0, h]$. Subtract the straight interpolant from the parabola to get $u - u_h = s(h - s)$, vanishing at both nodes and attaining $h^2/4$ at the element centre. Its derivative is $h - 2s$; the exact and numerical slopes agree at the midpoint but differ by magnitude h at each endpoint taken from that element. Testing only the midpoint slope or the nodal values would entirely conceal these other discrepancies.

Compute the squared energy error on this element:

$$\int_0^h (h - 2s)^2 ds = h^3/3.$$

With $1/h$ equal elements, the global energy error is $h/\sqrt{3}$. Similarly the element squared field error is $\int_0^h s^2(h - s)^2 ds = h^5/30$, giving global L^2 error $h^2/\sqrt{30}$. For $h = 1/4$, the two errors are approximately 0.14434 and 0.01141; the maximum field error is 0.015625. Halving the mesh width halves the energy error but divides the field error by four. All these measurements concern the very same numerical solution whose nodal error is exactly zero.

For a physical diffusion flux with constant conductivity one, flux error equals minus derivative error. A cell-averaged flux test is also special here: the numerical slope equals the exact average slope on each element for the same reason used in the proof. To verify local flux resolution, compare at more than a midpoint or a cell average and retain the measure used for convergence. A reported order is a statement about an observable and a norm as well as a finite-element space.

These formulas also identify a misleading manufactured test: if an automated comparison stores only nodal differences, the estimated order is undefined because both coarse and fine errors vanish. Adding independently evaluated quadrature points inside elements exposes the field error immediately. To check a flux implementation, use a quadrature rule capable of resolving the squared linear derivative error; a one-point midpoint rule would again report zero despite the nonzero exact energy norm.

Distribute a moving point source in a weak form

A one-dimensional Poisson problem has a concentrated source $Q\delta(x - a)$. Its weak load against a linear hat function is $Q\phi_i(a)$, so the two adjacent degrees of freedom share it in proportion to their shape functions.

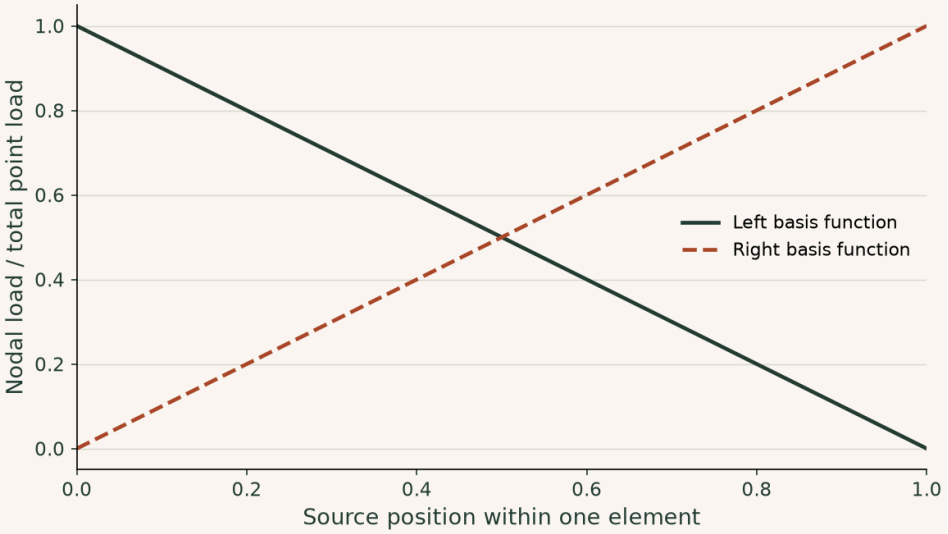

At 30% of the element length the split is 70% left, 30% right. The loads sum to Q and reproduce the correct first moment. Placing the whole source at the nearest node preserves total load but jumps abruptly at mid-element.

▶ **Read values from the plot**

Change parameters · Distribute a moving point source in a weak form

Change one input at a time and compare the recalculated curves with the argument above. The browser evaluates this small model locally; the accompanying numerical values state its assumptions and reference checks. Reset restores the reference inputs, and the data can be downloaded as CSV.

Open this calculation with adjustable inputs

Try the calculation

Source strength Q **1**

Selected element coordinate a/h **0.3**

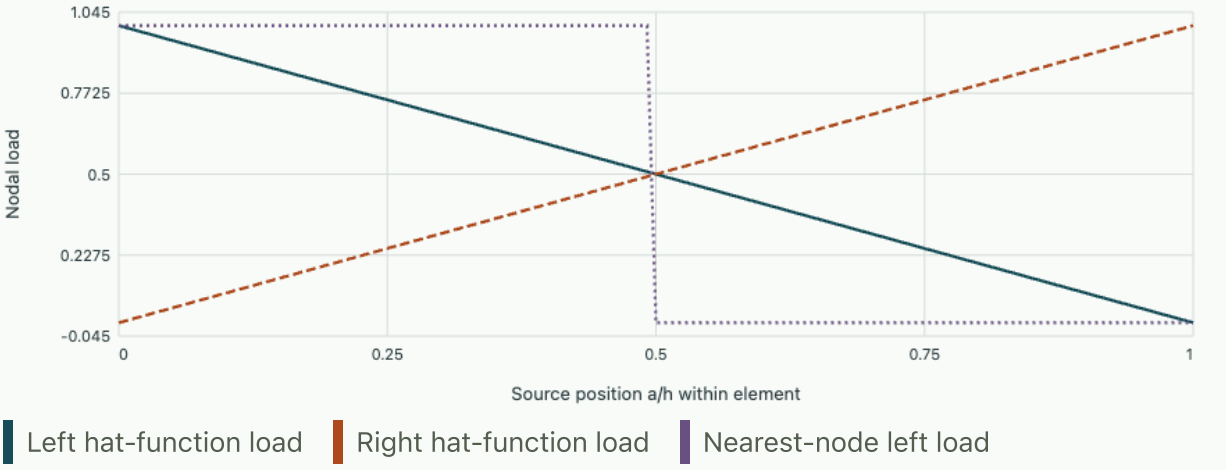

Selected loads 0.7 and 0.3 sum to Q = 1 and reproduce the source first moment. Nearest-node placement preserves only the total.

Wave speeds and numerical dispersion

Numerical partial differential equations

Derive the leapfrog dispersion relation, use the Courant condition to distinguish boundedness from accurate travel time and initialise a standing-wave calculation consistently.

FROM FIRST PRINCIPLES

Derive the numerical wave dispersion relation by advancing a single mode

Consider a one-dimensional homogeneous wave with speed c, uniform spatial grid h and time increment Δt. Centred second differences approximate both accelerations and spatial curvatures using the values on either side of their evaluation point. The governing equation $u_{tt} = c^2 u_{xx}$ becomes

$$u_j^{n+1} - 2u_j^n + u_j^{n-1} = C^2(u_{j+1}^n - 2u_j^n + u_{j-1}^n),$$
$$C = c\Delta t/h.$$

To determine what the grid does to one travelling component, insert $u_j^n = e^{i(kjh - \omega n \Delta t)}$ and divide by the value at (j, n). In both directions the pair of opposite phases combines to a cosine. Using $2 - 2\cos z = 4\sin^2(z/2)$ then gives

$$\sin^2(\omega \Delta t/2) = C^2 \sin^2(kh/2).$$

Long wavelengths recover $\omega \simeq c|k|$. Short waves can propagate at a different phase speed even in a perfectly homogeneous physical medium. Requiring a real ω for every resolved k gives $C \leq 1$. This derivation concerns interior grid modes; domain boundaries can introduce reflected waves as a separate numerical effect.

DERIVATION AND APPLICATIONS

Derive a conserved energy for the centred wave update

A time-stepping method can support a numerical travelling wave while transporting its phase at a slightly incorrect speed. For a second diagnostic, ask whether total discrete vibration energy remains bounded. Consider a uniform one-dimensional periodic grid for $u_{tt} = c^2 u_{xx}$, unit mass density and no forcing. Denote the forward spatial difference by D and the half-step velocity by $v^{n+1/2} = (u^{n+1} - u^n)/\Delta t$. Summation by parts on this grid gives $\langle v, D^{\mathsf{T}} D u \rangle = \langle Dv, Du \rangle$ using the grid inner product. The centred step can be written

$$v^{n+1/2} - v^{n-1/2} = -c^2 \Delta t D^{\mathsf{T}} D u^n.$$

Take the inner product with $(v^{n+1/2}+v^{n-1/2})/2$. The left side becomes a difference of two kinetic energies. On the right use $\Delta t(v^{n+1/2}+v^{n-1/2}) = u^{n+1}-u^{n-1}$ and move D to the other factor:

$$E^{n+1/2} = E^{n-1/2},$$
$$E^{n+1/2} = \tfrac{1}{2}\|v^{n+1/2}\|^2 + \tfrac{1}{2}c^2\langle Du^{n+1}, Du^n\rangle.$$

The potential term couples consecutive time levels. Writing it in terms of the midpoint displacement $\bar{u} = (u^{n+1}+u^n)/2$ identifies when the invariant bounds the solution:

$$E^{n+1/2} = \tfrac{1}{2}\|v\|^2 - \tfrac{1}{8}c^2\Delta t^2\|Dv\|^2 + \tfrac{1}{2}c^2\|D\bar{u}\|^2.$$

Since $\|Dv\| \le 2\|v\|/\Delta x$, the kinetic part is bounded below by $(1-C^2)\|v\|^2/2$, with $C = c\Delta t/\Delta x$. The invariant controls nonconstant waves for $C < 1$. An exact but indefinite conservation law alone would not guarantee a bounded numerical solution.

WORKED EXAMPLE

Read a timestep from a material and grid

Take $c = 100$ m/s, $\Delta x = 0.0500$ m and $\Delta t = 0.400$ ms. Then $C = 0.800$ and the bound preserves at least $1 - C^2 = 0.360$ of the usual half-step kinetic term even in the worst spatial mode. The customary limiting step from this argument is 0.500 ms.

SECOND APPLICATION

Show why equality of successive energies can mislead

Take the alternating grid mode for which $\|Dv\| = 2\|v\|/\Delta x$, and choose adjacent displacements whose midpoint is zero. At $C = 1.20$ the invariant for this state is

$$E = (1-1.44)\|v\|^2/2 = -0.220\|v\|^2.$$

Negative energy here is a property of the numerical quadratic form. A solver can preserve it exactly and still exhibit amplitude growth.

Distinguish transport of phase from transport of energy

A taut string with small transverse displacements and fixed tension obeys $u_{tt} = c^2u_{xx}$. The physical speed c is independent of wavelength in this ideal one-dimensional model. A discrete solver can transport long waves at nearly the correct speed while short waves arrive late. In a pulse comprising many wavelengths, this artificial dependence on frequency distorts its shape even in a stable computation. A phase comparison at a probe provides information beyond monitoring maximum amplitude.

Use centred second differences in both time and space, with $C = c\Delta t/h$. Solving explicitly for the new level gives

$$u_i^{n+1} = 2u_i^n - u_i^{n-1} + C^2(u_{i-1}^n - 2u_i^n + u_{i+1}^n).$$

To initialise, expand $u(\Delta t) = u(0) + \Delta t\, v(0) + (\Delta t)^2 c^2 u_{xx}(0)/2 + \cdots$. Replacing $u_{xx}(0)$ by the same spatial difference gives a first level consistent with the initial velocity and acceleration. Simply copying the starting displacement to level one can introduce a spurious launch velocity.

Derive the discrete dispersion relation

Take a travelling mode $u_i^n = \exp[\mathrm{i}(i\theta - n\omega_h \Delta t)]$ with spatial phase $\theta = kh$. Inserting it makes the temporal second difference proportional to $-4\sin^2(\omega_h \Delta t/2)$ and the spatial second difference proportional to $-4\sin^2(\theta/2)$. Thus on the positive-frequency branch

$$\sin(\omega_h \Delta t/2) = C \sin(kh/2).$$

A real ω_h exists for all resolvable real spatial phases only when $C \le 1$. If $C > 1$, the shortest wave makes the right-hand side exceed one; a temporal amplification root then lies outside the unit circle. Even when stable, the ratio of numerical to physical phase speed is $2\arcsin[C\sin(\theta/2)]/(C\theta)$. A fine spatial sample makes θ small and the ratio tends to one. At $C = 1$ the ideal uniform one-dimensional interior stencil reproduces the wave phase on the resolved branch. Boundaries, material transitions and multiple dimensions require separate analysis.

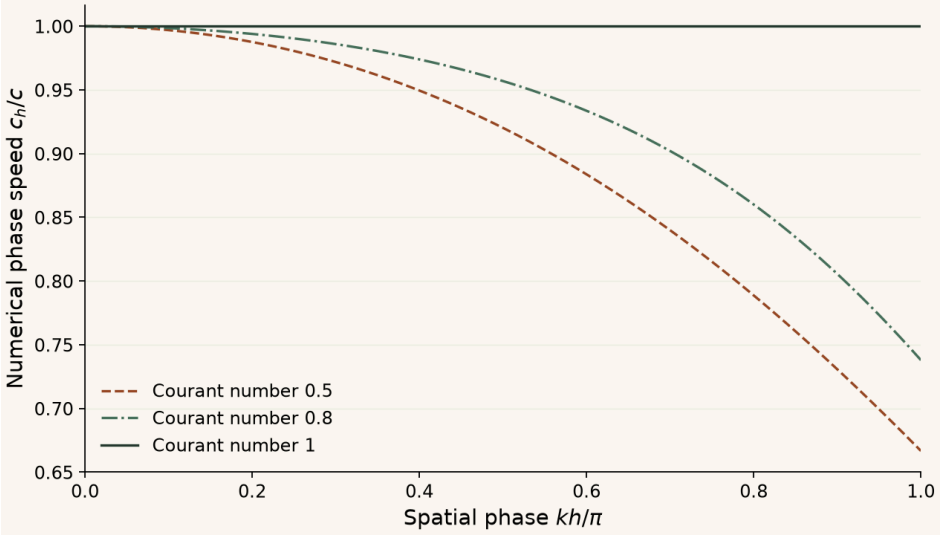

Centred one-dimensional wave discretisation. A short wave remains stable for the illustrated Courant numbers while accumulating substantial phase error in two of the runs.

Estimate a travel-time error

Take $C = 0.5$ and four points per wavelength, so $\theta = \pi/2$. Then

$$\omega_h \Delta t = 2 \arcsin[0.5 \sin(\pi/4)] = 0.72273 \,\mathrm{rad}.$$

The physical advance is

$$C\theta = \pi/4 = 0.78540 \,\mathrm{rad}.$$

The numerical phase speed is about 0.920 of the true speed. After ten physical periods, its accumulated phase is about 9.20 cycles. A stable solution can therefore be nearly one oscillation behind while retaining a visually plausible amplitude.

Group velocity is $d\omega_h/dk$, obtained by differentiating the dispersion relation. On this branch $v_g/c = \cos(\theta/2)/\sqrt{1 - C^2 \sin^2(\theta/2)}$, about 0.756 in the four-point example. A narrow-band packet's envelope and an individual crest then propagate at different numerical speeds. When interpreting a probe trace, say whether the reported arrival corresponds to a crest, an envelope or a threshold. Repeat the calculation at additional points per wavelength using the same Courant number to isolate spatial-phase improvement from changes in the time integration.

Interpret the grid's travelling domain of dependence

In one explicit wave step, a node uses only itself and its two nearest neighbours. After n steps its numerical domain of dependence extends at most n grid cells to either side. The continuous wave at the same time can depend on initial data a distance $cn\Delta t$ away. For convergence that physical domain must fit inside the numerical one, giving $c\Delta t \le h$. This reproduces the Courant condition from geometry without inserting a Fourier mode. It is a necessary information-speed test; by itself it does not establish stability or accuracy of an arbitrary scheme.

As an example, with $c = 340$ m/s and $h = 0.01$ m, the step bound is about 29.4 microseconds. A 20 microsecond step satisfies it but need not give an accurate answer for a mode represented by only three or four points per wavelength. Time-of-flight information and wavelength resolution are related to different discretisation choices. Document both when comparing two wave calculations.

Derive a reflected wave from a discrete outgoing condition

For a one-dimensional wave travelling right at speed c, the outgoing continuum condition is $u_t + c u_x = 0$ at the right boundary. It annihilates an exact right-travelling waveform. A numerical boundary update using forward time and backward space gives

$$u_N^{n+1} = (1 - C) u_N^n + C u_{N-1}^n,$$

where $C = c\Delta t/h$. A wave satisfying the interior discrete dispersion relation need not satisfy this one-sided relation. Even when the continuum boundary is perfectly absorbing, a mismatch of discrete phase relations can send energy back into the computational domain.

Let $z = e^{-i\omega\Delta t}$, with the incident and reflected grid waves represented by $e^{i\theta(j-N)}z^n$ and $Re^{-i\theta(j-N)}z^n$. At the boundary their sum is $1 + R$ times z^n. Substitution in the outgoing update and grouping incident and reflected terms gives

$$R = -\frac{z - 1 + C - Ce^{-i\theta}}{z - 1 + C - Ce^{i\theta}}.$$

This amplitude ratio assumes a homogeneous grid, a propagating frequency and distinct incident and reflected branches. It compares each wave at the boundary itself. Signals measured farther inward acquire additional phase and travel-time factors and can interfere if both arrive in the same observation window.

Calculate a reflection generated by numerical mismatch

Use the centred wave scheme with $C = 1/2$ and grid angle $\theta = \pi/2$, four cells per wavelength. The interior relation gives $\sin(\omega\Delta t/2) = (1/2)\sin(\pi/4) = 1/(2\sqrt{2})$, hence $z = 0.75 - i\sqrt{7}/4$. The incident mismatch in the numerator is $0.25 - i(\sqrt{7}/4 - 0.5)$; the reflected denominator is $0.25 - i(\sqrt{7}/4 + 0.5)$. Squaring the magnitudes gives $(3 - \sqrt{7})/4$ and $(3 + \sqrt{7})/4$, respectively. Therefore $|R| = \sqrt{(3 - \sqrt{7})/(3 + \sqrt{7})} \approx 0.2505$. Roughly one quarter of the incident amplitude is reflected solely by this discrete boundary treatment.

For incident and reflected branches on the same symmetric grid, their group-speed magnitudes match. The corresponding reflected energy fraction is $|R|^2 \approx 0.0627$, about six percent. That is small enough for a short experiment to appear satisfactory until the pulse returns to a sensor. Testing only the incident travel time would miss this boundary error. Compare a time window before reflection with the expected window for the return journey.

At $C = 1$ and $0 < \theta < \pi$, the right-moving interior root is $z = e^{-i\theta}$. The numerator vanishes exactly and the boundary update transmits that branch without reflection. This exact compatibility is special to this one-dimensional grid, this step size and this outgoing condition. Varying the propagation angle in two dimensions, changing an interface spacing or using a higher-order interior stencil changes the phase relation that the boundary operator needs to match.

There is a practical way to isolate this reflection in a pulse computation. Record incident and outgoing velocity or flux at the same interior sensor, and choose the duration so that the reflected signal arrives after the incident pulse has passed. Normalise amplitudes in the same physical variable, and avoid dividing a pressure peak by a displacement peak. A broadband pulse contains many values of the grid angle, so its returned waveform can change shape even when each monochromatic component obeys the calculated reflection coefficient.

Change parameters · Wave speeds and numerical dispersion

Change one input at a time and compare the recalculated curves with the argument above. The browser evaluates this small model locally; the accompanying numerical values state its assumptions and reference checks. Reset restores the reference inputs, and the data can be downloaded as CSV.

Open this calculation with adjustable inputs

Try the calculation

Courant number ν **0.5**

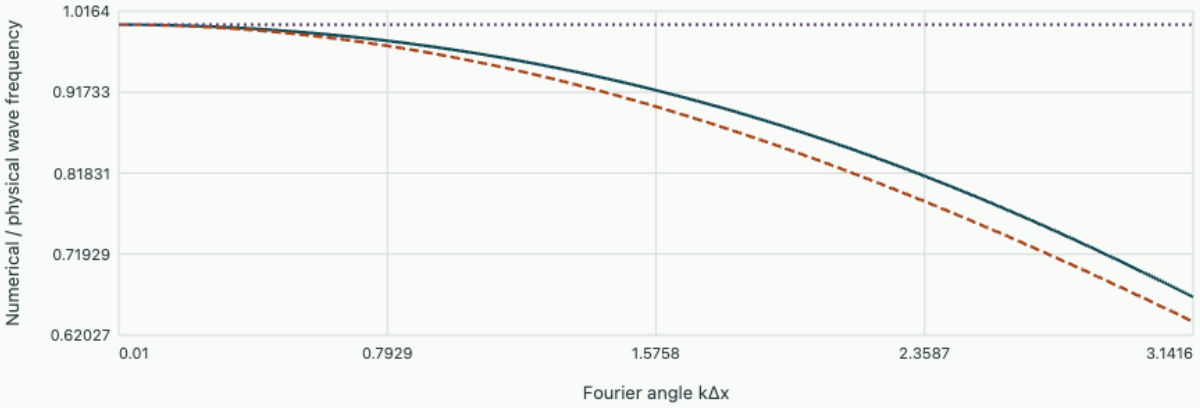

The formula follows sin(ωh/2) = ν sin(kΔx/2). At ν = 1, this one-dimensional constant-speed scheme has exact resolved-mode phase propagation.

Why two finite-element wave solvers propagate the same mode at different speeds

Numerical partial differential equations

Build the element mass matrix by integrating shape functions and track the effect of diagonal lumping on the wave spectrum.

From a continuum wave to nodal masses

For $u_{tt} = c^2 u_{xx}$, multiply by a test function and integrate by parts. On a periodic line the boundary contributions cancel. A piecewise-linear element of width h uses shape functions $1-\xi, \xi$, with $\xi \in [0,1]$. Integrating products of shape functions gives

$$M_e = (h/6)\begin{pmatrix} 2 & 1 \\ 1 & 2 \end{pmatrix}.$$

Integrating derivative products gives

$$K_e = (c^2/h)\begin{pmatrix} 1 & -1 \\ -1 & 1 \end{pmatrix}.$$

Row-sum lumping replaces each mass row by its sum on the corresponding diagonal, $h/2$. This preserves the mass associated with a uniform velocity but changes the response to a velocity that varies within an element.

Background · Numerical dispersion

$$c_{\mathrm{ph,h}} = \omega_h(k)/k$$

A discretised wave can retain its amplitude and still propagate at the wrong speed. Compare phase and group errors over the actual resolved wavelengths.

Diagonalise the assembled periodic problem

A periodic nodal mode has $u_j = e^{ij\theta}$. Each neighbour contributes $e^{\pm i\theta}$ relative to node j. Thus K multiplies by $2c^2(1-\cos\theta)/h$, consistent M by $h(2+\cos\theta)/3$, and lumped M by h. Dividing stiffness by mass gives the discrete squared frequency. Relative to the exact frequency $c\theta/h$,

$$\frac{\omega_L}{c\theta/h} = \frac{2\sin(\theta/2)}{\theta},$$

$$\frac{\omega_C}{c\theta/h} = \frac{2\sin(\theta/2)}{\theta}\sqrt{\frac{3}{2+\cos\theta}}.$$

Both tend to one for long waves; the leading quadratic errors have opposite signs. This is a spatial effect, present even with exact time integration.

Two wavelengths in one mesh

At four cells per wavelength $\theta = \pi/2$. The lumped ratio is $2\sqrt{2}/\pi \approx 0.9003$; the consistent ratio is about 1.1027. One wave solver lags by roughly ten per cent and the other leads by roughly ten per cent. At eight cells per wavelength the ratios move much closer to one, but repeated propagation over many wavelengths can still accumulate visible phase error.

At the shortest grid mode $\theta = \pi$, the consistent frequency is $\sqrt{12}c/h$ and the lumped frequency $2c/h$. A central-difference time integrator stable for $h_t\omega \le 2$ therefore requires a smaller step for the consistent mass. Accuracy at one wavelength and stability at the grid scale are different design criteria.

Open this experiment online

Try the calculation

Cells per selected wavelength **8**

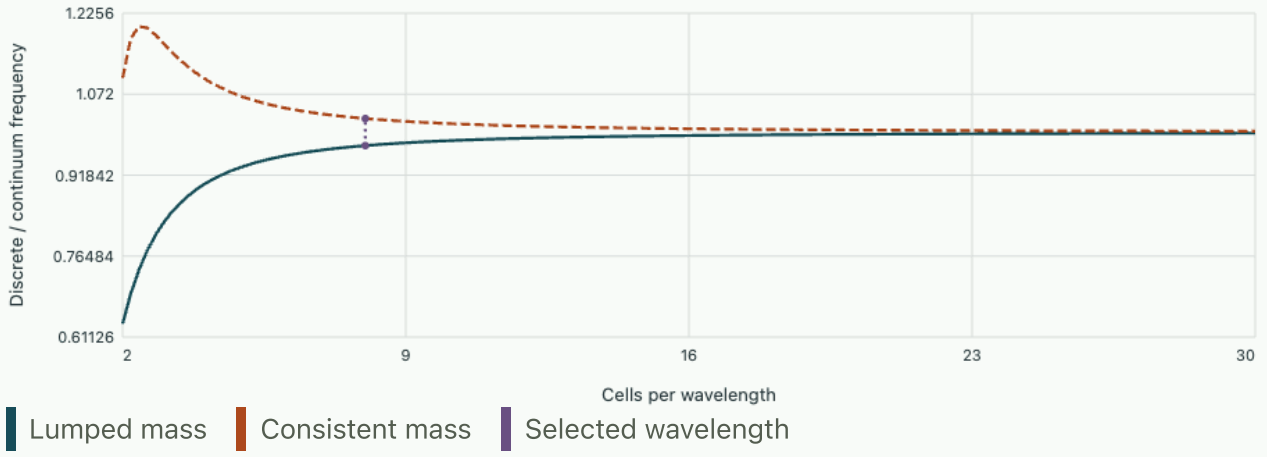

At 8 cells per wavelength the lumped ratio is 0.9745 and the consistent ratio 1.0259.

Tutorial on interpreting a convergence test

Which mass gives the exact kinetic energy for a linear velocity varying from v to $-v$ on one element?

▼ **Worked solution**

The continuum energy with unit density is $hv^2/6$. The consistent matrix reproduces it by exact integration. The lumped kinetic energy is $hv^2/2$, because it assigns both end masses the full endpoint speed.

How would you isolate spatial dispersion from time stepping in a measurement of a cavity eigenfrequency?

▼ **Worked solution**

Solve the generalised eigenproblem $Kq = \omega^2 Mq$ directly for increasingly fine meshes or converge time steps on each fixed mesh. Then compare with the continuum frequency and report both h and the time tolerance.

Vibrations of monoatomic and diatomic chains

Condensed matter and band theory

Derive normal modes from a local force law and identify the physical motion behind the acoustic and optical branches.

FROM FIRST PRINCIPLES

Turn a local spring law into a phonon dispersion relation

Consider identical atoms of mass m spaced by a along a chain. Write u_j for the displacement from the equilibrium position of atom j. For small changes of bond length, expand the bond energy to second order about its minimum. Its first derivative vanishes and its positive second derivative K is the measured bond stiffness. The bond on the right pulls with force $K(u_{j+1} - u_j)$; the left bond contributes $K(u_{j-1} - u_j)$. Newton's law gives

$$m\ddot{u}_j = K(u_{j+1} - 2u_j + u_{j-1}).$$

Translation of a normal mode by one site can change its phase but not its shape. Insert $u_j = Ue^{i(kja-\omega t)}$, divide by the common amplitude, and simplify:

$$-m\omega^2 = K(e^{ika} + e^{-ika} - 2) = -4K\sin^2(ka/2),$$

$$\omega = 2\sqrt{K/m}\,|\sin(ka/2)|.$$

For wavelengths much larger than a,

$$\sin(ka/2) \simeq ka/2.$$

The slope gives the sound speed $a\sqrt{K/m}$. At $k = 0$ all atoms move together and no bond stretches, which explains the zero frequency. More than one atom per primitive cell permits internal relative motion even at $k = 0$, the ingredient needed for an optical branch.

DERIVATION AND APPLICATIONS

Count the modes that crowd against a chain's band edge

Why can a narrow frequency bin near the top of a vibration band contain a substantial share of all modes? Take a monoatomic chain of N equal masses m with one longitudinal displacement each. Impose periodic ends and use identical harmonic nearest-neighbour springs of stiffness K with spacing a. The frequency on the positive half of the first zone rises monotonically to $\omega_m = 2\sqrt{K/m}$. Inverting that branch gives the wavevector bounding the states below a trial frequency,

$$k(\omega) = \frac{2}{a}\arcsin\left(\frac{\omega}{\omega_m}\right), \qquad 0 \le \omega \le \omega_m.$$

Allowed wavevectors are spaced by $2\pi/(Na)$. Counting the interval of width $2k(\omega)$ includes both propagation directions. In a large chain the fractional count and its derivative per atom are therefore

$$F(\omega) = \frac{2k(\omega)}{2\pi/(Na)}\frac{1}{N} = \frac{2}{\pi}\arcsin\left(\frac{\omega}{\omega_m}\right),$$

$$g(\omega) = \frac{dF}{d\omega} = \frac{2}{\pi\omega_m\sqrt{1-(\omega/\omega_m)^2}}.$$

Here $g\,d\omega$ is a fraction of the modes. The normalization follows from $F(\omega_m) = 1$, as required by the count of independent displacements. Near the edge the slope of the dispersion tends to zero, so evenly spaced wavevectors map into progressively smaller frequency intervals. This causes an integrable singularity in the continuum density. A finite spectrometer bin always contains a finite count. A measured spectrum can also weight modes differently through a probe's coupling to atomic motion.

WORKED EXAMPLE

Count modes within the upper tenth of the band

Change the inputs and investigate this derivation.

For $N = 10{,}000$, the interval between $0.9\omega_m$ and the upper edge contains $N[1 - (2/\pi)\arcsin(0.9)] \simeq 2871$ modes, allowing a mode or two for endpoints. A uniform distribution in frequency would give 1000. A nearly stationary wave packet near the upper edge and a large number of modes per unit frequency have the same origin in the small group velocity.

SECOND APPLICATION

Use the spectral median to infer a spring stiffness

Change the inputs and investigate this derivation.

An ideal chain with atomic mass $5.00 \times 10^{-26}\,\mathrm{kg}$ has half of its longitudinal modes below an ordinary frequency of $4.00\,\mathrm{THz}$. Setting $F = 1/2$ gives

$$\omega_{1/2}/\omega_m = \sin(\pi/4).$$

The upper frequency is $5.66\,\mathrm{THz}$, and $K = m(2\pi f_m)^2/4 = 15.8\,\mathrm{N/m}$. The frequency ratio is unchanged by conversion to angular frequency, but the final stiffness requires that conversion.

Try it · Chain count

Vary the physical parameters in the derived relation. Use the units and assumptions in the readout to connect the curves to the two worked examples. A parameter study can test the forward prediction; the same relation can then be inverted to infer a parameter from a measurement.

Open this live calculation

Try the calculation

Selected fraction of band-edge frequency **0.9**

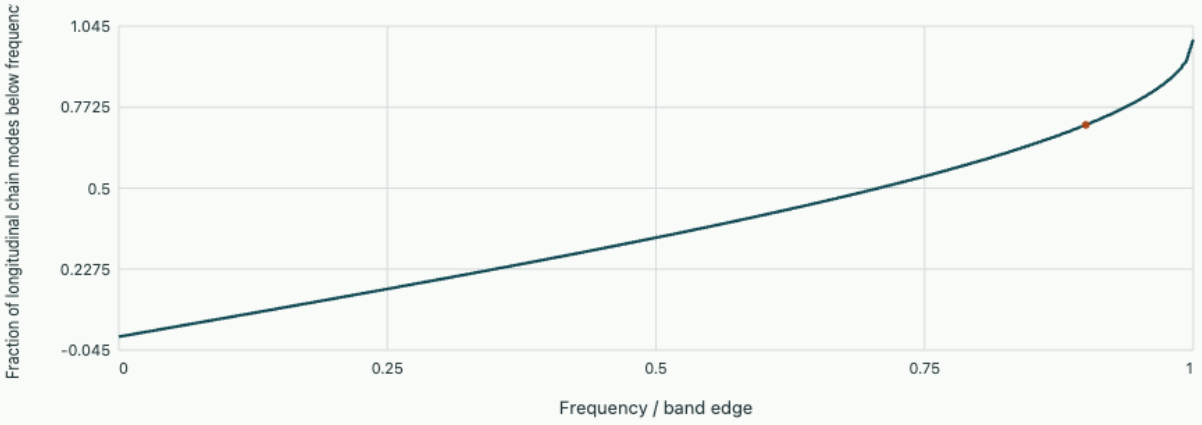

Uniform wavevector count Selected cutoff

Fraction above selected cutoff 0.28713. The spectral median is ωmax/√2; mode density diverges integrably at the band edge.

From bond extension to a travelling displacement

Let atoms of mass m on a line be coupled by springs of stiffness K, spaced a apart. The spring to the right pulls site n by $K(u_{n+1}-u_n)$; the left contributes $K(u_{n-1}-u_n)$. A uniform shift produces no force. Translation symmetry suggests $u_n = u e^{i(kna-\omega t)}$. Substitution gives

$$\omega^2(k) = \frac{2K}{m}(1-\cos ka) = \frac{4K}{m}\sin^2(ka/2).$$

The sound speed at long wavelength is $a\sqrt{K/m}$, consistent with a continuum rod whose one-dimensional stiffness is Ka and whose mass per length is m/a. At $k=\pi/a$ neighbouring atoms move in opposition and the slope of the dispersion vanishes. A wave packet made of nearby k's moves with the group velocity $d\omega/dk$, which can differ greatly from the phase velocity ω/k near the boundary.

Background · Why must one vibration have exactly zero frequency?

Give every atom the same displacement. If the potential energy depends only on separations, no bond changes length and no atom experiences a restoring force. Differentiate the force with respect to this uniform translation. For one displacement direction the resulting row-sum condition on the force constants is

$$\sum_j K_{ij} = 0,$$

$$D\,(\sqrt{m_1}, \ldots, \sqrt{m_N})^T = 0,$$

$$D = M^{-1/2} K M^{-1/2}.$$

With unequal masses the translational eigenvector is uniform in physical displacement, while its mass-weighted components vary. A nonzero frequency at zero wavevector may reveal missing neighbour interactions in a numerical model. A real spring to a substrate also breaks translation symmetry and produces a physical gap. The boundary conditions decide which explanation is plausible.

Introduce an internal coordinate

Place masses m, M alternately, with spacing $a/2$ between neighbours and cell period a. Let their displacements in cell n be Ue^{ikna} and Ve^{ikna} times the same time factor. The two force balances contain sums of neighbouring amplitudes. For example the A mass sees B in cell n and in cell $n-1$, giving $m\omega^2 U = 2KU - K(1 + e^{-ika})V$. Exchanging the masses and conjugating the phase gives the second row. Requiring a nonzero solution yields

$$mM\omega^4 - 2K(m+M)\omega^2 + 4K^2 \sin^2(ka/2) = 0.$$

There are two nonnegative solutions for ω^2 per k. With N cells under periodic boundary conditions this gives $2N$ longitudinal modes, exactly matching the number of independent displacements. At $k = 0$ the lower branch has $U = V$ and zero frequency. For the upper branch the centre of mass stays fixed, $mU + MV = 0$, with $\omega^2 = 2K(1/m + 1/M)$. An electric field can excite some optical modes in polar crystals; the branch name alone does not guarantee optical activity.

A gap and a sound speed answer different questions

At the zone boundary $1 + e^{ika} = 0$, so the sublattices decouple. If $M = 4m$, the two edge frequencies are $\sqrt{K/(2m)}$ and $\sqrt{2K/m}$, a factor of two apart. When the masses become identical the two folded branches meet, recovering the original monoatomic chain in a doubled cell. An apparent branch boundary created by plotting in a smaller zone need not be a physical frequency gap.

Expand the determinant for small k on the lower branch. Since ω^2 scales as k^2, discard the term of order k^4. This gives

$$v_s = a\sqrt{K/[2(m+M)]}.$$

The two springs in a cell act in series for long waves, while both masses contribute to inertia. The sound speed alone determines a stiffness-to-mass ratio; measuring the upper branch supplies independent information about the internal motion.

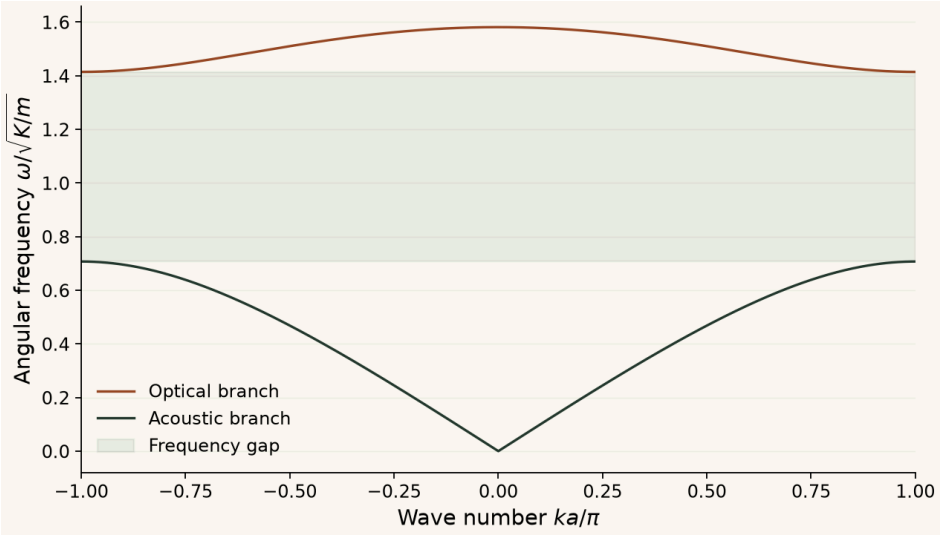

For a four-to-one mass ratio the zone-edge frequencies differ by a factor of two. The shaded interval contains no longitudinal normal mode of the infinite chain.

Try it · Diatomic

Change the inputs and compare the recalculated curves with the preceding derivation and baseline figure. The axes give the units; the numerical readout states the model assumptions and any limiting cases. Reset the inputs to return to the reference setting.

Open this live calculation

Try the calculation

Heavy / light mass 4

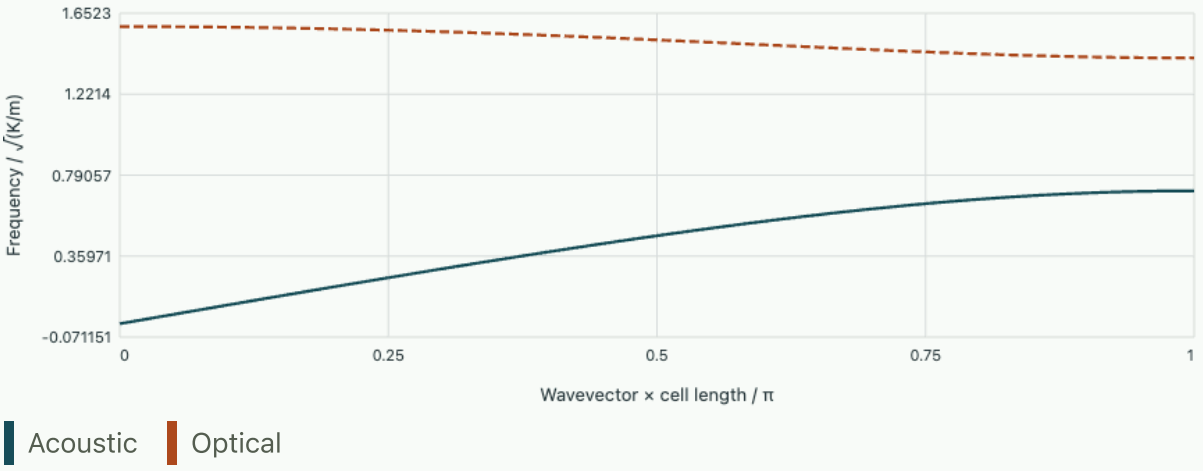

Zone-edge frequencies 0.70711 and 1.4142. The gap closes at equal masses.

Convert a mode count into thermal predictions

Quantisation assigns a harmonic mode levels $\hbar\omega(j+1/2)$. The thermal part of its mean energy is $\hbar\omega/[\exp(\hbar\omega/k_BT)-1]$. Low-temperature excitations thus select long-wavelength acoustic modes while high-frequency optical modes remain scarcely populated. Counting states in a three-dimensional sphere gives a low-frequency density proportional to ω^2 for linear branches. Rescaling the energy integral by $\hbar\omega/k_BT$ gives thermal energy proportional to T^4 and heat capacity proportional to T^3. Dimensionality and linear dispersion are essential assumptions behind that power.

Count thermally generated vacancies

A mode calculation for a perfect crystal starts with one atom on every site. Heating a real sample can leave some atoms at a surface or reservoir and some lattice sites empty. How large should that defect population be even at thermal equilibrium? Consider N equivalent sites and n_v independent vacancies. At fixed temperature and pressure let g_f be the Gibbs cost of making one vacancy and transferring its

atom to the reservoir. It may contain local vibrational contributions. We count the separate entropy of choosing the missing sites explicitly.

There are $W = N!/[n_v!(N-n_v)!]$ such arrangements. With $x = n_v/N$ and macroscopic occupations, Stirling's formula gives

$$\frac{G - G_0}{N} = x g_f + k_B T\,[x \ln x + (1-x)\ln(1-x)].$$

Minimizing with respect to x gives

$$g_f + k_B T \ln[x/(1-x)] = 0.$$

The second derivative is positive. Thus $x = 1/(1 + e^{g_f/(k_B T)})$. For positive $g_f \gg k_B T$ there are few vacancies and $x \simeq e^{-g_f/(k_B T)}$. Each vacancy costs energy, but at tiny x the number of possible positions grows fast enough to favour a nonzero population. A finite microscopic specimen can still contain zero vacancies at a given instant.

Take $g_f = 0.800\,\mathrm{eV}$ as constant over the chosen range and $k_B = 8.6173 \times 10^{-5}\,\mathrm{eV/K}$. At $900\,\mathrm{K}$, $k_B T = 0.07756\,\mathrm{eV}$ and $x = 3.31 \times 10^{-5}$. A region with 10^{15} sites contains an expected 3.31×10^{10} empty sites. At $600\,\mathrm{K}$ the equilibrium fraction drops to 1.91×10^{-7}. Rapid cooling may leave an excess because vacancies must migrate to sinks before the concentration relaxes. The formation free energy in this calculation sets an equilibrium population. A migration barrier would enter the time to attain it.

A light substitution can localize a vibration

An infinite monatomic chain has a continuous vibration band, while a single altered atom can support a vibration spatially concentrated near one site. Let identical springs of stiffness K connect masses m on a chain of spacing a, except the central mass at site zero is M. Seek a symmetric localized solution with alternating neighbouring amplitudes $u_n = A(-q)^{|n|}e^{-i\omega t}$ for $0 < q < 1$. Alternation is motivated by the top of the perfect-chain band where adjacent atoms oscillate out of phase. Exponential decay supplies the localization.

At any ordinary site away from the impurity, the equation $-m\omega^2 u_n = K(u_{n+1} + u_{n-1} - 2u_n)$ gives

$$m\omega^2 = K(2 + q + q^{-1}).$$

Since $q + q^{-1} > 2$, this frequency lies above the perfect-chain band edge $\omega_{\max} = 2\sqrt{K/m}$. At site zero both neighbours have displacement $-qu_0$, giving $M\omega^2 = 2K(1+q)$. Eliminating ω and cancelling $1+q$ yields

$$q = \frac{M}{2m - M},$$

$$\omega^2 = \frac{K}{m}(2 + q + q^{-1}).$$

The physical condition $0 < q < 1$ requires a lighter central mass $0 < M < m$. A heavy isotope can still scatter travelling waves or produce resonant response within the band. This ansatz predicts no exponentially localized symmetric mode above the band for the heavier substitution. Its absence follows from the admissible decay factor rather than an assumption that a heavy impurity cannot move.

Predict a localized spectral peak

Take host atomic mass $m = 4.00 \times 10^{-26}$ kg, spring stiffness $K = 40.0$ N/m, lattice spacing $a = 0.300$ nm and impurity $M = m/2$. The host upper angular frequency is

$$2\sqrt{40.0/(4.00 \times 10^{-26})} = 6.32 \times 10^{13}\,\mathrm{rad/s}.$$

For the impurity $q = 1/3$, so $\omega^2 = (16/3)K/m$, giving $\omega = 7.30 \times 10^{13}$ rad/s or $f = 11.6$ THz. The ordinary chain ends near 10.1 THz.

The neighbour amplitude is minus one third of the central amplitude, and the second neighbour has plus one ninth. Expressing the absolute envelope as $e^{-|n|a/\xi}$ gives localization length $\xi = a/\ln 3 = 0.273$ nm. As M approaches m from below, q approaches one, localization length diverges and the extra frequency merges with the band edge. A finite-chain calculation should therefore vary chain length before claiming that a very weak impurity mode is spatially localized: a box shorter than its decay length cannot separate that broad tail from a standing host mode.

Spatially resolved displacement data can provide two independent estimates of impurity mass. Invert the decay-factor relation to obtain $M/m = 2q/(1+q)$ from neighbouring displacement amplitudes. Separately insert the measured localized frequency and the same host force constant in the central equation of motion. Agreement tests the assumption that the impurity changes only inertia. A substituted atom may also change the two neighbouring springs: in that case the observed frequency and decay factor can no longer be fitted by altering mass alone. This inversion distinguishes an isotope-like substitution from a stronger local bonding perturbation.

A weak second impurity far away perturbs the localized mode only through its exponentially small tail. Bringing two such impurities within a few decay lengths allows the modes to mix and split in frequency, offering another test of their spatial localization.

Rotational and vibrational populations in a molecular gas

Statistical mechanics from microscopic counting to material response

A pressure thermometer and a calorimeter do not count molecular degrees of freedom in the same way. A dilute diatomic gas can retain nearly ideal pressure while its heat capacity changes appreciably as discrete internal levels become populated. Build the molecular partition function, derive the rotor and oscillator contributions, and infer temperatures from line populations without treating spectral intensity as a direct state count.

When a molecule's partition function factorises

Assume a dilute gas of stable diatomic molecules with weak interparticle interactions. Approximate one molecule's Hamiltonian by independent translational, rotational, vibrational and electronic parts. This requires a bond sufficiently stiff that rotation does not greatly alter vibrational energy and a temperature well below electronic excitations or dissociation when the electronic factor is treated as constant. If energies add and allowed states form a product, Boltzmann factors multiply. Thus $q = q_{\mathrm{tr}} q_{\mathrm{rot}} q_{\mathrm{vib}} q_{\mathrm{el}}$, $Z_N \simeq q^N / N!$ in the dilute classical translational regime. The logarithm converts this product into additive free energies, energies and heat capacities.

The translational factor V/λ_T^3 provides the volume derivative and hence ideal pressure $N k_B T / V$. A volume-independent internal factor changes neither that derivative nor the associated translational equation of state. It does change entropy, chemical potential and calorimetry. The molar heat capacities satisfy $C_p - C_V = R$ for a fixed-composition ideal gas, even when both vary strongly with temperature. Dissociation, chemical equilibration or significant intermolecular interactions can change the conclusion for the measured sample.

One danger is double-counting states. Angular momentum orientations belong to rotational degeneracy, oscillator quanta to vibration, electronic spin and nuclear exchange symmetry may constrain one another. A constant electronic degeneracy contributes an additive entropy $N k_B \log g$ but no internal energy or heat capacity at fixed level energies. A large heat capacity is evidence for energetically separated states becoming populated, not just for a large number of exactly degenerate states.

Derive the quantum rigid-rotor contribution

For a molecule of moment of inertia I about its centre of mass, rotational Hamiltonian is $\hat{L}^2/(2I)$. Angular momentum eigenvalues are $\hbar^2 J(J+1)$, with $2J+1$ projections at fixed $J = 0, 1, \ldots$. Define rotational temperature $\theta_r = \hbar^2/(2Ik_B)$. For distinguishable nuclei and a common nuclear spin factor omitted, the rotational sum and populations are

$$q_r = \sum_{J=0}^{\infty} (2J+1) e^{-\theta_r J(J+1)/T},$$

$$p_J = (2J+1) e^{-\theta_r J(J+1)/T} / q_r.$$

At high temperature the populated range contains many adjacent J values. Replacing the sum with an integral and substituting $u = J(J+1)$ gives

$$q_r \simeq T/\theta_r.$$

Hence $U_r \simeq Nk_BT$, $C_{V,r} \simeq Nk_B$, the classical result for two independent rotational kinetic energies of a linear object. At low temperature only $J = 0$ and $J = 1$ matter. Their degeneracies and gap $2k_B\theta_r$ give $q_r \simeq 1 + 3e^{-2\theta_r/T}$ and an exponentially vanishing heat capacity. Keeping the degeneracy three is essential for both its magnitude and the temperature of its turn-on.

For an illustrative heteronuclear rotor with $\theta_r = 85$ K, direct summation at 20 K gives $q_r = 1.00061$ and $C_{V,r} = 0.0440k_B$ per molecule. At 90 K the corresponding values are 1.471 and 1.063. At 300 K the heat capacity is 1.002. A small overshoot above the classical rotational value is possible during the crossover. A model that simply switches from zero to one classical degree contribution at $T = \theta_r$ misses the entire smooth population redistribution and cannot predict line ratios.

The most populated J need not be zero, despite increasing energies, because the projection multiplicity increases with J. Viewing the numerator as a smooth function of J gives $J_{\mathrm{peak}} \simeq [\sqrt{2T/\theta_r} - 1]/2$, to be checked against neighbouring integer values. The estimate is unreliable if it predicts only one or two populated levels. Computing a short discrete sum costs little and reveals its own truncation error through the final omitted weights.

Derive oscillator energy and heat capacity from a geometric series

Near its bond-length minimum approximate the interaction by a spring. With reduced mass m_r and angular vibration frequency ω_v, quantum energies are $E_n = \hbar\omega_v(n + 1/2)$. Define $\theta_v = \hbar\omega_v/k_B$. Summing the resulting geometric series and differentiating gives

$$q_v = \frac{e^{-\theta_v/(2T)}}{1 - e^{-\theta_v/T}},$$

$$\frac{U_v}{N} = k_B\theta_v\left(\frac{1}{2} + \frac{1}{e^{\theta_v/T} - 1}\right),$$

$$\frac{C_{V,v}}{Nk_B} = \frac{x^2e^{-x}}{(1 - e^{-x})^2},$$

$$x = \theta_v/T.$$

The zero-point term contributes energy but no heat capacity at fixed frequency. For $x \ll 1$ the heat capacity approaches k_B per independent vibrational mode, comprising kinetic and potential contributions. For $x \gg 1$ excitation is too costly and the heat capacity behaves as $k_Bx^2e^{-x}$. A molecule can still vibrate quantum mechanically in its ground state while contributing virtually no vibrational heat capacity. A calorimeter measures sensitivity of mean energy to temperature and need not see the ground-state motion.

Take $\theta_v = 3000$ K. At $T = 300$ K the vibrational contribution is only $0.00454k_B$, while at 1200 K it reaches $0.609k_B$. Combining with the earlier rotor gives molar C_V approximately $2.507R$ at 300 K and $3.109R$ at 1200 K, assuming stable composition and frozen electronic structure. For acoustic measurements the ideal adiabatic ratio $\gamma = (C_V + R)/C_V$ then decreases from about 1.399 to 1.322.

An acoustic drive faster than vibrational relaxation can measure a frequency-dependent effective ratio because internal populations fail to remain equilibrated through a compression cycle.

Compare this single oscillator with the frequency distribution in the lattice heat-capacity plot

Nuclear exchange and the symmetry number

For a homonuclear molecule, rotating its classical orientation by half a turn end for end does not create a second distinct arrangement. In a high-temperature rotational count a symmetry number two therefore divides the distinguishable-nuclei rotor partition function once the compatible spin states are accounted for. Since this factor is constant with temperature it shifts entropy and chemical potential, but not the classical rotational energy or heat capacity. At low temperature it is important to treat actual quantum parity, not divide every level by two.

A homonuclear diatomic rotational wavefunction acquires a factor $(-1)^J$ under exchange of nuclei. The complete state also includes nuclear spin, electronic and vibrational parts. For ordinary molecular hydrogen in its electronic and vibrational ground state the protons are spin-half fermions. Antisymmetry pairs even J with the single antisymmetric spin singlet and odd J with the three symmetric triplet spin states. In true spin-conversion equilibrium the rotor sum uses weights one or three in addition to $2J+1$. At temperatures large compared with rotational spacing, even and odd J sectors have nearly equal rotational sums and the equilibrium odd-to-even population ratio approaches three.

Conversion between spin species can be slow. A rapidly cooled sample may preserve its prepared fractions rather than attain spin equilibrium. Then compute separate parity-restricted partition functions for fixed species numbers, and average their thermal observables with the frozen proportions. Allowing the total odd fraction to relax yields a different heat capacity, including the energy liberated by conversion. Two experiments on chemically identical hydrogen can consequently report different heating curves because their preparation constrains different internal sectors.

Use intensities only after accounting for the instrument

An absorption line originating from level J has a strength depending on more than its population. Transition moment, polarisation, transition frequency, stimulated emission correction, instrument response and path length can all enter. Suppose line strengths and detector factors have been divided out to yield quantities proportional to level populations N_J. Then a straight-line fit of $\log[N_J/(2J+1)]$ against $J(J+1)$ has slope $-\theta_r/T$ for the simple heteronuclear model. Its intercept depends on total particle number, partition function and residual instrumental gain.

For $\theta_r = 10$ K, a measured corrected ratio $N_2/N_0 = 2.00$ implies $2 = 5e^{-60/T}$ and $T = 65.5$ K. Omitting the factor of five would make an upper population larger than the lower one appear incompatible with positive temperature. The inferred temperature assumes the rotational populations are equilibrated at one temperature; an optically pumped or rapidly expanding sample may have different rotational and translational distributions.

A plot over several J values can test whether one slope is adequate. Curvature may come from centrifugal distortion, line saturation, unresolved overlap, multiple temperatures or a wrong nuclear-spin

degeneracy. Alternating residuals for even and odd J indicate a different physical problem from a smooth quadratic residual against $J(J+1)$. Repeat with lower optical depth to isolate saturation, and use independently measured transition frequencies to fix level energies before fitting populations.

Recover molecular translation separately from internal structure

In a low-density molecular beam, the translational speed distribution is often easier to measure than the internal populations. For an equilibrium gas leaving a small opening into vacuum, the molecular flux is weighted by the normal velocity. Fast molecules reach and cross the aperture more frequently, so the distribution of speeds in the beam differs from the Maxwell speed distribution inside the reservoir. The mean translational energy of molecules in an effusive beam is $2k_B T$, whereas the bulk mean is $3k_B T/2$. This selectivity occurs even when rotational and vibrational populations remain canonical.

To derive the difference, start with the bulk velocity density proportional to $e^{-mv^2/(2k_B T)}$. Write the outward normal speed as $v\cos\theta$, integrate over the outward hemisphere and include the velocity-space shell factor $v^2 dv$. The resulting beam speed density is proportional to $v^3 e^{-mv^2/(2k_B T)} dv$, while the original bulk speed density has v^2. Taking a ratio of Gaussian moments gives the stated energy. Comparing a beam energy to the wrong bulk prefactor would yield a temperature one third too high.

If the aperture is small compared with the mean free path and transition-detection efficiency is independent of speed after correction, internal state probabilities factor out of this flux weighting. A rotational population ratio can then report the reservoir temperature while the observed mean translational energy follows the effusive weighting. In a dense nozzle undergoing many collisions, expansion can cool translation and rotation differently. An inferred rotational and translational temperature disagreement is therefore not automatically bad calibration; first identify whether the beam is effusive, collisionally expanding or selectively detected.

As a bench example, a beam mean translational energy of 0.060 eV corresponds to approximately 348 K under effusion, using $k_B = 8.6173 \times 10^{-5}$ eV/K. Treating it as the bulk mean would give about 464 K. Compare against a population ratio from two corrected lines spanning $80k_B$ kelvin and equal degeneracies. At the two temperatures the predicted ratios are about 0.795 and 0.842. Resolving this difference demands a relative line calibration appreciably better than six percent even though the two erroneous temperature interpretations differ by more than one hundred kelvin.

An isotope mixture reveals which spectral changes affect entropy

Compare two isotopic forms with the same approximate electronic potential surface. Bond force constant and equilibrium bond length then remain nearly unchanged while reduced nuclear mass changes. The harmonic vibrational frequency scales as $m_r^{-1/2}$, while the rotational temperature scales as m_r^{-1}. Consequently vibration and rotation respond differently to the same isotope substitution. Their shifts can jointly test whether two sets of spectral features genuinely belong to the same molecular carrier.

Suppose the reduced mass rises by a factor 1.21. A vibrational line at 2000 inverse centimetres moves approximately to 1818 inverse centimetres, and a rotational constant initially 2.00 inverse centimetres moves to 1.65 inverse centimetres. The vibrational characteristic temperature follows from $hc\tilde{\nu}/k_B$,

about 1.4388 K per inverse centimetre. At room temperature the two vibrational gaps still greatly exceed thermal energy, so the vibrational heat capacity can remain small even though the spectral isotope shift is easy to resolve.

The zero-point energies nevertheless differ. For this vibrational example their difference is $hc(2000 - 1818)/2$ per molecule, corresponding to about 131 kelvin in thermal units or 1.09 kJ/mol. Such offsets cancel within a fixed-species heat-capacity derivative but can matter to comparisons of chemical equilibrium or isotopic exchange. An analysis that discards all constant energy offsets independently in each molecular species can corrupt a reaction free energy unless it restores a consistent reference across reactants and products.

For a thermal entropy contribution from this one oscillator use $S_v = k_B[(n+1)\log(n+1) - n\log n]$ with $n = 1/(e^x - 1)$. This follows by inserting U_v and $\log q_v$ into $S = k_B \log q + U/T$; the zero-point contributions cancel exactly. Thus the measured isotope shift can change vibrational entropy via occupancy even while the zero-point offset itself contributes no entropy. It is helpful to evaluate all three quantities—energy difference, entropy difference and heat-capacity difference—rather than presume that a line shift must have the same thermodynamic role in each.

An internal relaxation time appears in frequency-dependent calorimetry

The equilibrium partition function assumes internal mode populations re-equilibrate on times short compared with the measurement. Model one slower internal degree by an internal energy U_s relaxing toward its equilibrium value at the instantaneous translational temperature T, with $\dot{U}_s = [U_{s,\mathrm{eq}}(T) - U_s]/\tau_s$. For a small oscillation around T_0,

$$\delta U_{s,\mathrm{eq}} = C_s \delta T.$$

In the $e^{-i\omega t}$ convention, the complex internal heat capacity and the total measured capacity including an instantaneous background C_f are

$$C^*(\omega) = C_f + \frac{C_s}{1 - i\omega\tau_s}.$$

At low frequency the capacity is $C_f + C_s$. At high frequency the slow internal energy cannot follow and the apparent in-phase capacity approaches C_f. Its out-of-phase component peaks at $\omega\tau_s = 1$, where real and imaginary increments equal $C_s/2$. The structure resembles dielectric relaxation because both arise from one relaxing state variable driven by a controlled sinusoid. It follows here from an explicit energy-exchange model and its assumptions.

Take a molar fast contribution $2.50R$, slow equilibrium contribution $0.60R$ and relaxation time 2 ms. The full equilibrium value is $3.10R$. At about 79.6 Hz the real measured capacity is $2.80R$ and the imaginary increment magnitude $0.30R$. A heat pulse much shorter than two milliseconds initially raises the temperature as if the capacity were close to $2.50R$, then energy flows into the internal mode. A slow calorimetric ramp can be perfectly consistent with a faster acoustic measurement that infers a smaller active capacity.

A sample container connected to a thermal bath produces its own complex temperature response even if molecular populations are always equilibrated. Disentangle those effects by calibrating the empty cell or an inert reference gas across the same frequency range, changing pressure to alter collision-mediated internal-relaxation time, and checking the predicted equilibrium limit from independently known level spacings. A mechanical resonance in the apparatus can be separated by varying cell geometry while keeping gas composition fixed. Fitting one imaginary peak to a molecular relaxation model without these controls does not uniquely determine the microscopic relaxation time.

How a line ratio and a calorimeter constrain degeneracies differently

Two groups report a low-energy excited manifold with dimensionless population ratio $r = N_1/N_0$ at two temperatures. A single ratio determines only $r = (g_1/g_0)e^{-\Delta/(k_B T)}$, so changing the assigned degeneracy changes the inferred gap. Taking the log ratio at two known temperatures removes a common degeneracy factor. The slope of $\log r$ against $1/T$ is minus the gap in kelvin, and the intercept is the log degeneracy ratio if the line-strength calibration and equilibrium assumptions hold.

For illustrative values $r = 0.300$ at 100 K and $r = 0.949$ at 200 K, the log change is approximately 1.152. Dividing by the inverse-temperature change magnitude 0.005 per kelvin gives $\Delta/k_B \simeq 230$ K. Inserting the first ratio gives $g_1/g_0 \simeq 3.00$. The same two-manifold model predicts a dimensionless heat capacity $x^2 r/(1+r)^2$ per molecule. At 100 K it is about 0.94, a separate calorimetric prediction independent of the absolute number of detected photons.

A third temperature materially improves the test. An unseen nearby manifold or a line strength that changes with instrumental settings may fit two exact population ratios but produce curvature and excess heat capacity elsewhere. Spectroscopy resolves ordered energy differences while calorimetry sums energy variances over all accessible states. Their combination offers more information than adding further precision to one population measurement under the same ambiguous degeneracy assumption.

Compress a gas without pretending its heat capacity stays constant

A reversible adiabatic compression is often summarised by a fixed exponent γ. That power law assumes temperature-independent heat capacities along the path. Molecular populations give a direct case where the exponent changes. For an ideal gas at fixed composition,

$$dS = C_V(T)\,dT/T + N k_B\,dV/V.$$

Along a reversible adiabatic path set the sum to zero and integrate. The volume ratio is determined by an integral of measured or calculated $C_V(T)/T$, not by a universal constant exponent across every temperature.

As an illustrative calculation approximate translation and fully active rotation by $C_V = 2.5 N k_B$ plus one harmonic vibrational mode with $\theta_v = 3000$ K. Heating from 300 to 1200 K at constant entropy gives a

volume contraction factor from the fast degrees alone of $4^{2.5} = 32$. The vibrational entropy difference adds another factor $e^{\Delta S_v/(N k_B)}$. At 300 K the oscillator entropy is only about $0.00050 k_B$, while at 1200 K it is about $0.309 k_B$. The combined estimate requires $V_i/V_f \simeq 43.6$, a substantially larger compression than the frozen-vibration approximation predicts.

This comparison assumes ideal gas throughout and no dissociation, conditions to be checked in a real large compression. It nevertheless identifies the mechanism: part of the compression work goes into levels that were effectively inactive initially. Using the final high-temperature heat capacity across the whole path would err in the opposite direction by assigning that energy storage to the low-temperature portion as well. The entropy integral correctly weights each temperature interval by its actual internal population response.

A numerically stable solution can avoid differentiating noisy calorimetry. Integrate the entropy increment from tabulated heat capacities in the log-temperature variable. Compare an adaptive integral with a refined straightforward grid, paying particular attention to the rotational or vibrational crossover scale. Alternatively compute endpoint entropies from partition functions when an independently justified spectral model exists. Agreement between calorimetric integration and spectroscopy-derived endpoint entropy checks both assignments without demanding exact agreement of noisy pointwise derivatives.

Experimental pressure also checks the endpoint calculation independently. After equilibration, the ideal equation of state predicts $p_f/p_i = (T_f/T_i)(V_i/V_f)$, approximately 174 for this idealised path. Finite heat leakage or a pressure-dependent nonideality can change that value. A rapid adiabatic compression can be irreversible even if little heat leaves the chamber, and then the measured entropy can increase. Distinguish a reversible reference calculation from an actual rapid piston protocol before using a mismatch to infer missing molecular levels.

An independent isotropic acoustic test at a fixed initial temperature infers γ from the small-amplitude sound speed $c_s^2 = \gamma R T/M$, where M is molar mass. At fixed molecular mass a decrease of γ from 1.40 to 1.32 at the same temperature would lower sound speed by the square root of their ratio, roughly three percent. That comparison must truly hold temperature fixed: the large direct thermal dependence of sound speed can easily exceed the internal-mode effect. Frequency-resolved acoustics can see part of a vibrational mode freeze dynamically while equilibrium spectroscopy still predicts its population. Record both phase velocity and acoustic attenuation if the aim is to identify a relaxation time. Across the relaxation band, dispersion without the corresponding dissipative response should prompt a check of transducer phase calibration and acoustic boundary conditions.

Read the rotational level spacing from thermal energy storage

Sum the discrete levels of a linear rotor and compare the heat capacity with equipartition as temperature rises.

Open this experiment online

Try the calculation

Rotational temperature θrot (K) 8

Chosen gas temperature (K) 20

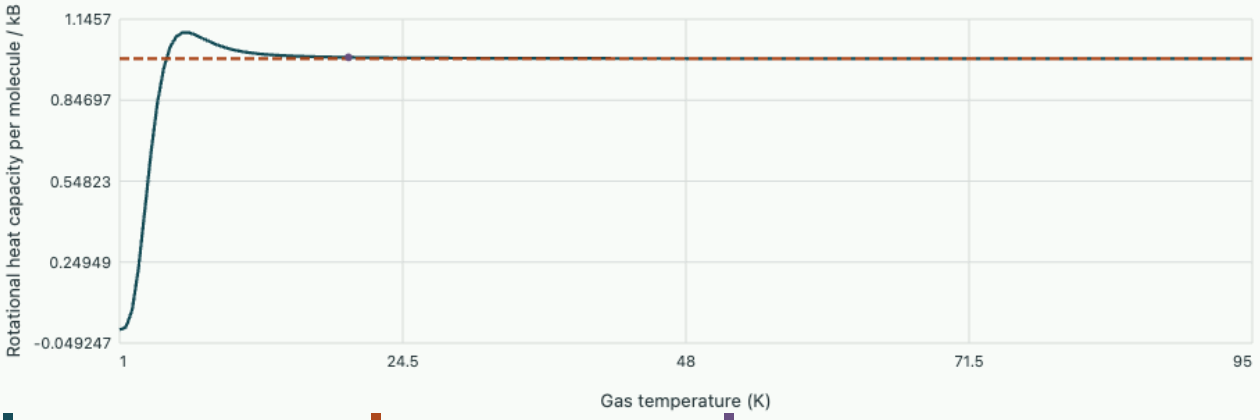

Heteronuclear rigid rotor | Two quadratic rotations | Selected temperature

First excited rotational level has E_1/k_B = 16 K. At the selected temperature C_{rot}/k_B = 1.0051. Vibrational and translational contributions are excluded.

Tutorial · Identify a rotor inertia from spectral spacing

For a heteronuclear linear rotor the lowest pure rotational transition has ordinary frequency 120 GHz. Infer θ_r, the moment of inertia and the expected $J = 1$ to $J = 0$ population ratio at 10 K. How could an isotope substitution test the interpretation?

▼ **Use the transition gap and keep angular and ordinary frequency distinct**

The gap is $2k_B\theta_r = h\nu$, so $\theta_r = 2.88$ K and $I = \hbar^2/(2k_B\theta_r) = 1.40 \times 10^{-46}$ kg square metres. The population ratio is

$$3e^{-5.76/10} = 1.69.$$

The upper manifold contains more molecules even though each of its levels has lower individual Boltzmann weight. Increasing reduced mass at nearly fixed bond length increases I, reducing the transition frequency approximately inversely with reduced mass. A vibrational frequency from the same spring would scale instead with inverse square root of reduced mass.

Tutorial · Infer an excitation temperature from calorimetry

A gas of linear molecules has molar $C_V = 2.91R$ at a temperature where translation and rotation contribute $2.50R$. Neglect electronic excitation and estimate the characteristic temperature of a single

harmonic vibration in units of measurement temperature. Would a measured C_p be usable unchanged?

▼ **Invert the oscillator contribution and verify its feasible range**

The remaining $0.41R$ lies between zero and the one-mode classical limit R. Solve $x^2e^{-x}/(1-e^{-x})^2 = 0.41$ on positive x. At 3.0 it is 0.496 and at 3.5 it is 0.393, placing the root near 3.41. Thus θ_v is about 3.41 times measurement temperature. Use several temperatures to verify the characteristic value and frozen-composition model. For ideal gas at fixed composition, subtract R from C_p before applying this constant-volume balance. Latent processes, reaction and internal relaxation would require an extended model.

Tutorial · Distinguish equilibrium hydrogen from a frozen spin mixture

At low temperature only $J = 0$ in the even sector and $J = 1$ in the odd sector contribute. Use $\theta_r = 85$ K and $T = 30$ K. Estimate the equilibrium odd fraction and compare the energy stored in a sample frozen at a three-quarter odd fraction, measured relative to the common lowest even state.

▼ **Normalise both sectors and identify the energy released on conversion**

The relative weight of $J = 1$ is $3(2J+1)e^{-170/30} = 0.0311$; the even ground state has weight one. The equilibrium odd fraction is approximately 0.0302. A frozen sample at odd fraction 0.75 stores about $0.75(170)k_B = 127.5k_B$ kelvin of rotational energy per molecule, versus about $5.1k_B$ kelvin for equilibrium. The excess expressed per mole is roughly $R(122.4\,\mathrm{K}) = 1.02$ kJ/mol.

The frozen low-temperature heat capacity can be small even while substantial energy remains trapped in the odd sector. A calorimeter monitoring a slowly converting sample measures time-dependent heat release, not simply the derivative of a stationary restricted partition function. Measure the spin fraction independently or vary equilibration time before comparing its heat curve with an equilibrium prediction.

Cambridge Statistical Physics · molecular partition functions and internal degrees of freedom

Hamiltonian motion viewed in other coordinates and frames

Test phase-space area in a numerical orbit, track an observer change, then compare a relativistic worldline with a semiclassical quantisation condition.

1. Energy and geometric integration
2. Störmer–Verlet and a discrete invariant
3. Implicit midpoint, reversibility and the phase of an oscillator
4. What different observers measure
5. Relativistic particle dynamics and the field tensor
6. Semiclassical quantization
7. A phase accumulated by slowly turning a magnetic field
8. A magnetic orbit that spirals outward in a perfect vacuum
9. How a turning point supplies the missing semiclassical phase
10. Ensembles, thermodynamic potentials and measurable curvature
11. Master equations, detailed balance and probability currents

Energy and geometric integration

Numerical ordinary differential equations

Compare three time updates on a conservative oscillator and explain why a method can have small short-term state error yet distort an orbit over many periods.

FROM FIRST PRINCIPLES

Build an oscillator update out of two area-preserving shears

Take one undamped oscillator of mass $m > 0$ and stiffness $k > 0$. Its canonical position q and momentum p satisfy

$$\dot{q} = p/m,$$
$$\dot{p} = -kq.$$

Exact trajectories run along energy ellipses and preserve phase-plane area. If both slopes are taken at the left endpoint, the update and its area factor are

$$\begin{pmatrix} q_{n+1} \\ p_{n+1} \end{pmatrix} = \begin{pmatrix} 1 & h/m \\ -hk & 1 \end{pmatrix} \begin{pmatrix} q_n \\ p_n \end{pmatrix}, \qquad \det = 1 + h^2 k/m.$$

A positive factor greater than one at each step makes the numerical orbit spiral outward. Instead update the momentum at fixed position, then move the position using that new momentum. Both operations are shears:

$$p_{n+1} = p_n - hkq_n,$$
$$q_{n+1} = q_n + hp_{n+1}/m.$$

The product matrix has diagonal entries $1 - h^2k/m$ and 1, with off-diagonal product $-h^2k/m$, giving determinant one. Its eigenvalues form a conjugate pair on the unit circle when $|2 - h^2k/m| < 2$. This calculation explains the bounded oscillatory behaviour for $0 < h\sqrt{k/m} < 2$. Preserving area alone would also allow one real mode to grow while another shrinks. It does not establish either stability or exact conservation of the original energy.

Background · Symplectic map

$$(D\Phi)^{\mathsf{T}} J (D\Phi) = J$$

This is preservation of the canonical symplectic form. It provides control of long-time structure without guaranteeing that every trajectory has the exact phase.

DERIVATION AND APPLICATIONS

Which quadratic energy does symplectic Euler preserve?

An undamped linear oscillator conserves the physical sum of kinetic and potential energy. A geometric time integrator may conserve a nearby quadratic form instead. Take $q'' = -\omega^2 q$ with constant ω and unit mass. Scale velocity by setting $u = \dot{q}/\omega$ so that both variables have units of length, and write $z = h\omega$. Use the kick-then-drift version of symplectic Euler. Its step is two triangular shears:

$$u' = u - zq,$$
$$q' = q + zu' = (1 - z^2)q + zu.$$

To find a preserved quantity, test a quadratic form $I = q^2 + u^2 + \alpha qu$. The changes of the ordinary sum and the product follow directly by multiplication and collection:

$$q'^2 + u'^2 - q^2 - u^2 = z(q'u' - qu),$$
$$I' - I = (z + \alpha)(q'u' - qu).$$

Choosing $\alpha = -z$ cancels the entire change at every step. Completing the square identifies the range where the invariant confines trajectories to closed ellipses:

$$I = q^2 + u^2 - zqu = (u - zq/2)^2 + (1 - z^2/4)q^2.$$

For $|z| < 2$ the form is positive definite. The physical energy is proportional to $q^2 + u^2$ and can oscillate, but the invariant bounds it. As $h \to 0$ the tilted ellipse approaches the exact energy circle. At the endpoint $|z| = 2$ the quadratic form ceases to bound both variables; preservation of an indefinite form alone does not guarantee stable trajectories.

WORKED EXAMPLE

Follow a moderate step exactly

Take $\omega = 2.00$ s⁻¹, $h = 0.250$ s, $q = 1.00$ m and $u = 0$. Then $z = 0.500$, $u' = -0.500$ m and $q' = 0.750$ m. The ordinary sum falls from 1.00 to 0.8125 m². But $I' = 0.8125 - 0.500(0.750)(-0.500) = 1.00$ m². A plot restricted to physical energy at one time could mistake the discrepancy for damping.

SECOND APPLICATION

Diagnose a seemingly exact conservation test outside stability

Choose $z = 2.50$ and the same initial $(q, u) = (1, 0)$. One step gives $(-5.25, -2.50)$. The ordinary sum is 33.8125, whereas the cross term is $2.50(13.125) = 32.8125$, so $I' = 1$. The invariant remains exact while the amplitude grows. Testing positivity of the conserved quadratic form therefore supplies information absent from a conservation-only check.

Choose the diagnostic before choosing the method

A mass on an ideal spring with unit mass and stiffness obeys $\dot{q} = p,\ \dot{p} = -q$. The state moves on circles with conserved energy $H = (q^2 + p^2)/2$. At short times a state norm measures trajectory error, but over many periods there are independent questions about amplitude, phase and energy. A time-stepping method that systematically increases the orbit radius can produce an artificial runaway even on this simplest stable physical system.

Forward Euler updates $q_{n+1} = q_n + hp_n,\ p_{n+1} = p_n - hq_n$. Square and add: the cross terms cancel, leaving $H_{n+1} = (1 + h^2)H_n$. The phase space area factor of the update matrix is its determinant $1 + h^2$, also greater than one. Backward Euler instead contracts energy by $1/(1 + h^2)$. The second method is stable in the sense of bounded states, but it removes mechanical energy from an undamped model. The sign of drift explains much more here than a solitary endpoint comparison.

Update momentum before position

The momentum-first symplectic Euler scheme sets $p_{n+1} = p_n - hq_n$ and $q_{n+1} = q_n + hp_{n+1}$. Its update matrix in (q, p) has rows $(1 - h^2, h)$ and $(-h, 1)$. Its determinant is one and trace is $2 - h^2$. For $0 < h < 2$, the two eigenvalues are a complex conjugate pair of unit magnitude because their product is one and the trace lies strictly between –2 and 2. The resulting numerical frequency satisfies

$$2\cos\theta = 2 - h^2.$$

Thus phase error still accumulates even if the amplitudes remain bounded.

Direct substitution also verifies an exact discrete invariant $\tilde{H} = (q^2 + p^2 - hqp)/2$. For $h < 2$ the corresponding quadratic form is positive definite, so constant $\tilde{H}$ confines the state to an ellipse. The exact physical energy can fluctuate around its initial level as the point moves around that ellipse. Area preservation alone would not guarantee this behaviour: for $h > 2$ the determinant remains one but real reciprocal eigenvalues permit growth. The eigenvalue and invariant calculations supply the missing qualification.

Check a long-time forecast with numbers

Start at $(q, p) = (1, 0)$ with $h = 0.1$. Forward Euler gives $(1, -0.1)$ and $H = 0.505$ after one step. After 100 steps the exact multiplicative law predicts

$$H = 0.5(1.01)^{100} = 1.3524.$$

Symplectic Euler instead gives $(0.99, -0.1)$, $H = 0.49505$, but $\tilde{H} = 0.5$ again. The first step alone might suggest that the second scheme dissipates energy. The invariant predicts that the decrease cannot continue monotonically over many periods.

Implicit midpoint, $(y_{n+1} - y_n)/h = J(y_n + y_{n+1})/2$ with the skew-symmetric oscillator matrix J, preserves the exact quadratic energy. Dot both sides with the midpoint state. The left side is proportional

to $H_{n+1} - H_n$ and the right side is zero by skew symmetry. Its rotations need not accumulate the exact physical phase, since the rotation angle per step is $2\arctan(h/2)$. A meaningful long-time study therefore records measured period, energy range and reversibility alongside any state error after a specified number of cycles.

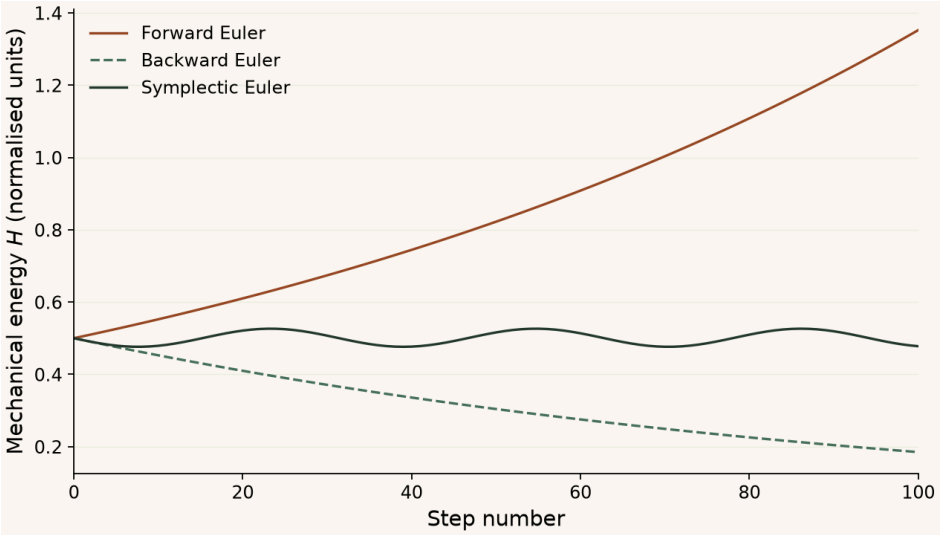

An ideal oscillator sampled with step 0.1. Checking only the first few updates obscures the systematic growth or decay visible after 100 steps.

Test an algorithm by reversing the clock

A method is time symmetric if taking a step of length h and then a step of length $-h$ restores the starting state, up to arithmetic and solve tolerance. For the midpoint update, exchanging the old and new values leaves their average unchanged and changes both sides of the difference equation consistently. This gives exact reversibility for an accurately solved implicit step. For forward Euler on the oscillator, the product of the forward and backward matrices is $(1 + h^2)I$, so reversal actually scales the state.

At $h = 0.1$, the simple reversal from $(1, 0)$ therefore returns $(1.01, 0)$ for forward Euler, making the failure visible in one pair of steps. This diagnostic is useful only for a reversible underlying evolution paired with its time-reversed integration law. A dissipative or dissipatively constrained physical system has different requirements. Reversibility, energy preservation and phase accuracy probe separate mathematical properties, each with a different operational test.

Test a flow map on a small cell of phase space

For canonical coordinates $z = (q, p)$, a differentiable Hamiltonian update $z_+ = \Psi(z)$ is symplectic when its Jacobian $D\Psi$ preserves the matrix $J = \left(\begin{smallmatrix} 0 & 1 \\ -1 & 0 \end{smallmatrix}\right)$ through $D\Psi^T J D\Psi = J$. Direct multiplication shows that for any real two-by-two matrix M, $M^T J M = (\det M) J$. Thus in one degree of freedom symplecticity is equivalent to preserving oriented area. A small rectangle of nearby initial conditions should map to a region of the same signed area even when its sides stretch or tilt.

For more than one degree of freedom, preserving ordinary volume is necessary but no longer sufficient. A map may stretch one canonical (q, p) plane and compress another by the reciprocal factor. Its full determinant remains one while the area pairing in each plane changes. Energy is a further, independent diagnostic: an area-preserving map can move individual points among nearby energy contours. The determinant calculation tests a geometric property of the map across neighbouring trajectories, rather than just the energy at one chosen state.

Compare the phase volume of an oscillator ensemble

For $q' = p,\ p' = -q$ with unit frequency, forward Euler gives $M = \left(\begin{smallmatrix} 1 & h \\ -h & 1 \end{smallmatrix}\right)$, of determinant $1 + h^2$. Backward Euler gives $(I - hA)^{-1}$, where A has off-diagonal entries $1, -1$, so its determinant is $1/(1 + h^2)$. A kick followed by a drift gives the symplectic Euler matrix with rows $(1 - h^2, h)$ and $(-h, 1)$, whose determinant is exactly one. These facts hold for every input rectangle, so they can be checked by integrating its corners rather than relying on a single solution.

Choose $h = 0.2$ and an initial ensemble occupying a rectangle of area 0.01 in normalised phase coordinates. After 25 steps forward Euler predicts area $0.01(1.04)^{25} \approx 0.02666$. Backward Euler gives $0.01/(1.04)^{25} \approx 0.00375$. Symplectic Euler preserves 0.01. Repeated steps compound even a four percent per-step area change into a substantial distortion. For the oscillator all three approximate individual paths can initially look plausible, so this ensemble diagnostic reveals information inaccessible in a short plot of one coordinate.

As a counterexample in four dimensions, scale the first pair of coordinates by $(2, 1)$ and the second pair by $(1/2, 1)$. The volume multiplier is one, but the first canonical area doubles while the second halves. A full symplecticity test must check $M^T J M - J$ using the correctly ordered canonical coordinate pairs. An algorithm preserving volume in an arbitrary collection of engineering state units is not automatically qualified for long-time Hamiltonian integration.

Area preservation also survives composing individual canonical shears: the determinants multiply and every shear has determinant one. This explains why reversing the order of a kick and a drift changes the phase error but preserves the two-dimensional area test. The two compositions may therefore produce different numeric positions while agreeing precisely on one geometric invariant. A useful verification suite includes both ensemble area and a trajectory observable with a known time dependence.

Change parameters · Energy and geometric integration

Change one input at a time and compare the recalculated curves with the argument above. The browser evaluates this small model locally; the accompanying numerical values state its assumptions and reference checks. Reset restores the reference inputs, and the data can be downloaded as CSV.

Open this calculation with adjustable inputs

Try the calculation

Time step h (ω = 1) **0.5**

Number of forward steps **20**

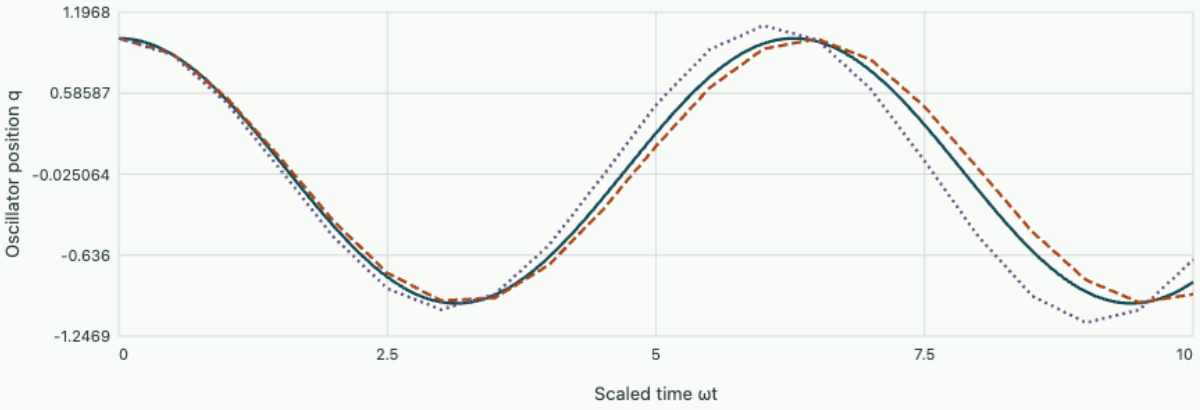

Implicit midpoint phase lag 0.2009 rad. Forward-backward distance from the start is 8.951e-16 for implicit midpoint and 0.3635 for explicit midpoint.

Störmer–Verlet and a discrete invariant

Numerical ordinary differential equations

Derive the leapfrog update, identify its oscillatory stability interval and quantify the difference between bounded energy and correct phase.

FROM FIRST PRINCIPLES

Derive a reversible position update from Newton's law

For a force that depends only on position, $m\ddot{q} = F(q)$, the acceleration can be evaluated at a stored position without an implicit solve. Expand the exact position one step forward and one step backward about the same time t_n. The odd derivatives reverse sign and cancel when the expansions are added:

$$q(t_n + h) + q(t_n - h) = 2q(t_n) + h^2\ddot{q}(t_n) + O(h^4).$$

Replace acceleration by force divided by mass and solve for the forward position. The resulting relation is unchanged if the labels $n + 1$ and $n - 1$ are exchanged:

$$q_{n+1} = 2q_n - q_{n-1} + \frac{h^2}{m}F(q_n).$$

Introduce the staggered momentum $p_{n-1/2} = m(q_n - q_{n-1})/h$. The same algebra becomes an impulse followed by a drift,

$$p_{n+1/2} = p_{n-1/2} + hF(q_n),$$
$$q_{n+1} = q_n + hp_{n+1/2}/m.$$

A specified momentum at $t = 0$ starts the first half step with $p_{1/2} = p_0 + hF(q_0)/2$. For smooth forces the method has second-order position accuracy. It is important to distinguish the staggered momentum from momentum at the stored position time when checking energy.

DERIVATION AND APPLICATIONS

Why a stable Verlet trajectory can arrive at the wrong time

Long-term energy behaviour is important in reversible mechanics, but phase error can dominate a timing measurement. Consider the velocity-independent linear oscillator $q'' = -\omega^2 q$. Use a uniform step h, an accurately initialized first point and the position recurrence obtained by eliminating the half-step momenta in Verlet. Write $z = h\omega$:

$$q_{n+1} - 2q_n + q_{n-1} = -z^2 q_n.$$

Assume a discrete mode $q_n = e^{in\vartheta}$. Divide by the mode value at n and combine the two exponentials. The angle advanced per step obeys

$$2\cos\vartheta - 2 = -z^2,$$
$$\sin(\vartheta/2) = z/2.$$

For $0 < z < 2$ choose the branch continuous with the exact oscillation at small h. The discrete angular frequency and its expansion are

$$\widetilde{\omega} = \frac{2}{h}\arcsin(z/2) = \omega\left[1 + \frac{z^2}{24} + O(z^4)\right].$$

The numerical oscillator runs slightly fast even though its amplitude can remain bounded indefinitely. Its phase lead grows approximately linearly with elapsed time at fixed step. Above $z = 2$ the dispersion relation permits no real phase angle, signaling a separate stability failure. The formula concerns time discretization alone; incorrect initial half-step velocities can add an initial phase offset.

WORKED EXAMPLE

Estimate a ten-period timing error

For $\omega = 5.00$ rad/s and $h = 0.100$ s, $z = 0.500$ and $\widetilde{\omega} = 20\arcsin(0.250) = 5.054$ rad/s. Ten true periods last 12.57 s. Over that duration the numerical phase gains about $(5.054 - 5.00)(12.57) \simeq 0.674$ rad. The estimated time at which the numerical oscillator completes its tenth period is $20\pi/5.054 = 12.43$ s, about 0.13 s too soon.

SECOND APPLICATION

Select a step from a phase requirement

Suppose 100 periods should accumulate less than 0.100 rad of phase error. The leading estimate gives $2\pi(100)z^2/24 < 0.100$, so $z < 0.0618$. For $\omega = 5.00$ rad/s this means $h < 0.0124$ s. A choice based only on the stability requirement $h < 0.400$ s would be far too coarse. Halving a small step should reduce the accumulated phase error by approximately four at fixed physical duration.

Position and momentum at staggered times

For unit mass and a time-independent potential $V(q)$, the equations are

$$q' = p,\; p' = -V'(q).$$

Treat the potential force over a half step, drift with the updated momentum for a full step, then use the new position for the last half kick. This yields

$$p_{n+1/2} = p_n - \tfrac{h}{2} V'(q_n),$$
$$q_{n+1} = q_n + h p_{n+1/2},$$
$$p_{n+1} = p_{n+1/2} - \tfrac{h}{2} V'(q_{n+1}).$$

Successive half kicks at the same position share a force evaluation. Reversing the sign of h exactly undoes the steps in reverse order, in exact arithmetic. Subtracting consecutive position increments gives

$$q_{n+1} - 2q_n + q_{n-1} = -h^2 V'(q_n).$$

The starting position and velocity must initialise the very first half step correctly; using the full velocity as the half-step velocity injects an initial phase error.

The oscillator has an exactly computable modified energy

For $V = \omega^2 q^2/2$ define $z = h\omega$. The position coefficient of q_n after one step is

$$a = 1 - z^2/2;$$

the momentum coefficient of q_n is $-h\omega^2(1 - z^2/4)$. The full map has equal diagonal entries a and off-diagonal entries $h, -hc$ with $c = \omega^2(1 - z^2/4)$. Since $a^2 + h^2 c = 1$, expanding squares shows $p_{n+1}^2 + c q_{n+1}^2 = p_n^2 + c q_n^2$.

When $0 < z < 2$, $c > 0$ and level sets of this invariant are bounded ellipses. The eigenvalues are $e^{\pm i\theta}$ with $\cos\theta = a$. Beyond two, one real eigenvalue has magnitude greater than one and trajectories generically grow. At exactly two the invariant loses control of position and a repeated eigenvalue can cause linear growth. An apparently bounded run starting from specially chosen data at the threshold cannot certify stability for arbitrary perturbations.

Follow a step and its timing

For $\omega = 1, h = 1, q_0 = 1, p_0 = 0$, the half kick gives -0.5, the drift gives $q_1 = 0.5$, and the final half kick gives $p_1 = -0.75$. The physical energy decreases from 0.5 to 0.40625 in this first step. The modified energy $(p^2 + 0.75q^2)/2$ equals 0.375 at both points. The discrete phase is $\theta = \pi/3$, so the computed trajectory returns after six steps. The true oscillator returns after $2\pi \approx 6.283$ seconds. A stable trajectory with a bounded energy error can therefore accumulate a large timing error over many cycles.

For small z, expanding $\theta = 2\arcsin(z/2)$ gives

$$\theta = z + z^3/24 + O(z^5).$$

At a fixed final time the accumulated phase error is therefore second order in h. A period estimate and an energy trace probe different aspects of long-time integration and should be reported separately.

Why the initial velocity test matters

A test with only the initial position nonzero may conceal the borderline instability at $h\omega = 2$. At that boundary the update is

$$q_{n+1} = -q_n + hp_n,\ p_{n+1} = -p_n.$$

For $p_0 = 0$ the positions merely alternate sign forever. With $q_0 = 0$ and $p_0 = 1$, however, explicit iteration gives

$$p_n = (-1)^n,$$

$$q_n = (-1)^{n-1} nh.$$

The position magnitude grows linearly. A stability test must account for all independent starting directions or small perturbations of the chosen one, especially when an eigenvalue of modulus one is repeated.

Prove conservation of angular momentum by individual substeps

For a particle of constant mass in a radial potential $V(\|q\|)$, the force is parallel to the position vector. Its angular momentum is $L = q \times p$. During a kick of duration τ, momentum changes by $\tau F(q)$ at fixed position, so the change in L is

$$\tau q \times F(q) = 0.$$

During a drift, position changes by $\tau p/m$ at fixed momentum, giving change $(\tau/m)p \times p = 0$. The full kick–drift–kick map therefore preserves angular momentum exactly in arithmetic without rounding, for any step length for which these evaluations are defined.

The proof uses radial force and the relationship between velocity and momentum. An external noncentral force exerts a physical torque, while a coordinate-dependent mass matrix changes the drift subflow. Under either modification the two zero cross products need rechecking. The argument also gives no bound on energy or phase. Exact conservation of angular momentum constrains orbital geometry but leaves freedom to move from the correct energy level onto a nearby one or to return to a point on the orbit at the wrong time.

Compare three diagnostics on an elliptical oscillator trajectory

Use unit mass and two-dimensional potential $V = (x^2 + y^2)/2$. Start at $q = (1, 0)$, $p = (0, 2)$, so $L = 2$ and physical energy is

$$E = (1 + 4)/2 = 2.5.$$

At step $h = 0.5$, the first half kick gives

$$p_{1/2} = (-0.25, 2).$$

The drift leads to $q_1 = (0.875, 1)$. The last half kick subtracts $0.25 q_1$, giving $p_1 = (-0.46875, 1.75)$. The resulting planar angular momentum is $0.875(1.75) - 1(-0.46875) = 2$, exactly as proved.

Calculate energy separately. The squared position is $0.875^2 + 1 = 1.765625$, and the squared momentum is

$$0.46875^2 + 1.75^2 = 3.2822265625.$$

Hence the physical energy after this step is 2.52392578125, about 0.96 percent above the initial value. The exact continuous position at this time is $(\cos 0.5, 2 \sin 0.5) \approx (0.87758, 0.95885)$, so the position error is concentrated in the second coordinate. Angular momentum, physical energy and the individual trajectory coordinates expose three distinct properties of the same update.

Because the harmonic force is separable by coordinate, the modified invariant from the scalar oscillator adds across the two directions: $[\|p\|^2 + (1 - h^2/4)\|q\|^2]/2$ is constant. Substitution gives 2.46875 at both steps, independently checking the arithmetic. For a general radial potential this particular quadratic modified invariant no longer follows, while the angular momentum proof remains valid. A conservation claim should identify the symmetry responsible rather than assuming every observed invariant survives a change of potential.

If there were a small constant transverse force, the physical change in angular momentum would be the time integral of $q \times F_{\text{ext}}$. A better diagnostic would subtract the accumulated applied torque from the measured change in L, rather than demand that L remain fixed. This distinction also guards against a subtle implementation error: zeroing a real torque to improve a conservation plot would change the physical problem and could hide a significant trajectory bias.

Measuring the signed torque makes its direction as well as its magnitude available for this balance check.

Estimate the phase error of a stable Verlet orbit

Eliminate momentum from velocity Verlet for the harmonic oscillator. A discrete sinusoid obeys $\cos\theta = 1 - (h\omega)^2/2$. Its angular frequency is θ/h; divide by ω before comparing steps.

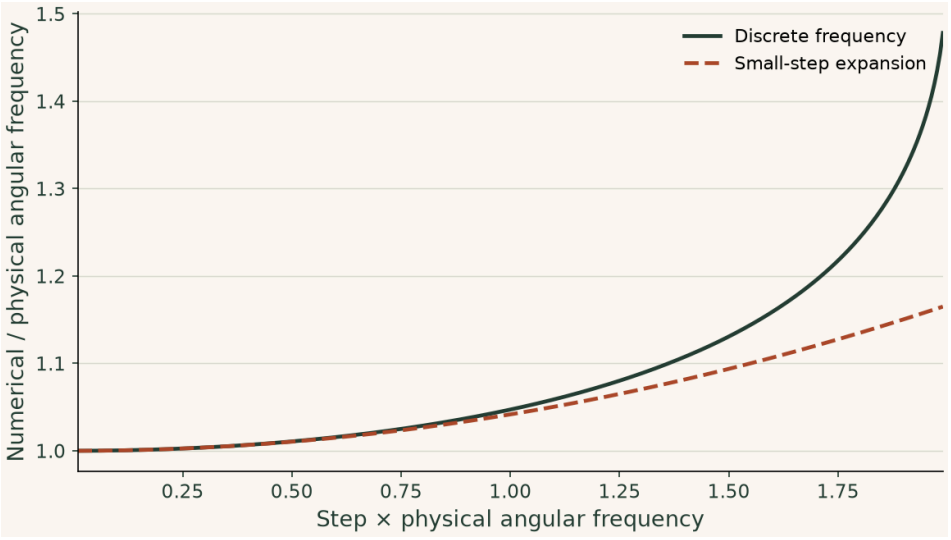

At hω = 1 the numerical frequency exceeds the true one by about 4.72%. The scheme can maintain a bounded orbit yet acquire a substantial phase error after many cycles. The chart stops below the stability boundary at two.

▶ **Read values from the plot**

Change parameters · Estimate the phase error of a stable Verlet orbit

Change one input at a time and compare the recalculated curves with the argument above. The browser evaluates this small model locally; the accompanying numerical values state its assumptions and reference checks. Reset restores the reference inputs, and the data can be downloaded as CSV.

Open this calculation with adjustable inputs

Try the calculation

Selected hω **1**

Physical cycles **10**

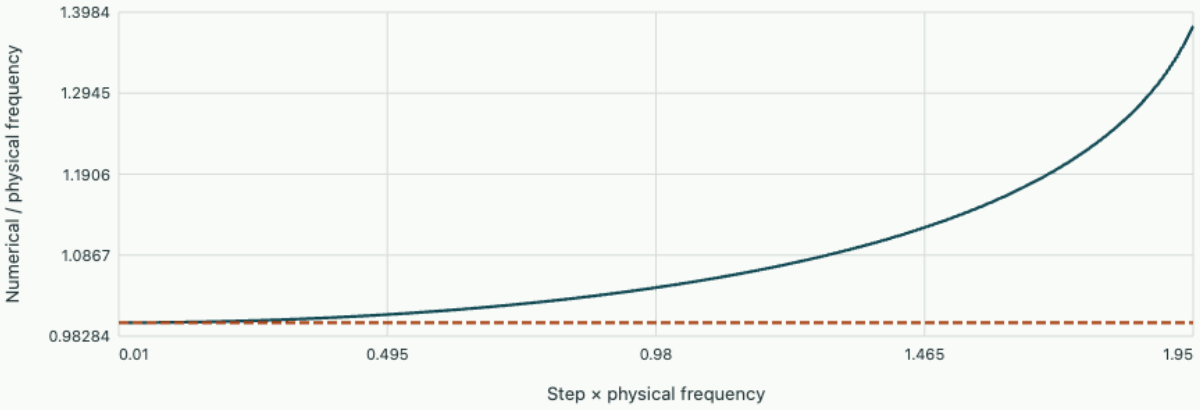

Selected frequency ratio 1.0472; phase lead after 10 exact cycles is 2.9655 rad. The stability boundary is hω = 2.

Implicit midpoint, reversibility and the phase of an oscillator

Numerical ordinary differential equations

Imagine integrating a mechanical trajectory forward, saving only its end state and then running the same method backward. Recovering the start is a stronger demand than obtaining a plausibly small one-step error. Even exact recovery does not guarantee that an oscillation peaked at the correct time.

Build a method from a centred difference

Integrate $y' = f(t, y)$ over an interval of length h. Midpoint quadrature approximates the integral by h times its integrand at $t_n + h/2$. The arithmetic mean of the unknown endpoint states approximates the exact midpoint state up to order h^2 on a smooth trajectory. Using this mean as the derivative's state argument gives

$$y_{n+1} - y_n = h f(t_n + h/2, (y_n + y_{n+1})/2).$$

Errors from midpoint quadrature and from evaluating f at the approximate midpoint both contribute $O(h^3)$ locally, giving global order two on a fixed interval under the usual regularity and stability conditions. In general the unknown appears inside f, so an implicit equation must be solved. If f is Lipschitz with constant L_f, direct fixed-point iteration contracts when $|h|L_f/2 < 1$. Newton iteration can converge over a wider range. Neither a failed nonlinear solve nor loose tolerances inherit the exact algebraic properties of the method.

Exchange y_n, y_{n+1} and replace h by $-h$. The left side changes sign, the arithmetic midpoint is identical and the midpoint time is identical if the reverse step starts at t_{n+1}. Thus, on the same locally unique solution branch,

$$\Phi_{-h} = \Phi_h^{-1}.$$

A round trip using variable steps must repeat the accepted steps in reverse order. Independently choosing a new adaptive mesh on the way back need not retrace the states.

Solve the step for a harmonic oscillator

Write $q' = \omega p,\ p' = -\omega q$, with scaled momentum p in the same units as q, and $z = q + ip$. The ODE becomes

$$z' = -i\omega z.$$

Solving the linear midpoint equation gives the scalar multiplier

$$M(u) = \frac{1 - iu/2}{1 + iu/2} = \exp[-2i \arctan(u/2)],$$

$$u = \omega h.$$

Its numerator and denominator are complex conjugates. Hence it preserves $q^2 + p^2$, proportional to the oscillator energy, exactly in real arithmetic. For any radius or step size $M(-u)M(u) = 1$. The rotation per step is

$$\theta = 2\arctan(u/2) = u - u^3/12 + O(u^5).$$

The numerical phase lags by $u - \theta$ per step. After N steps the accumulated lag is $N(u - \theta)$, increasing linearly in elapsed time even while the energy remains exactly constant.

Compare explicit midpoint Runge–Kutta. A half Euler predictor leads to

$$M_{\mathrm{RK2}} = 1 - iu - u^2/2.$$

It also has order two, but $|M_{\mathrm{RK2}}|^2 = 1 + u^4/4$. The amplitude grows slowly at every nonzero step. A forward and reverse pair multiplies the starting amplitude by $1 + u^4/4$. In a conservative problem these two second-order procedures can produce visibly different long records.

Inspect the return and the lag separately

With $\omega = 1$, $h = 0.5$, $N = 20$, exact accumulation is 10 radians. Midpoint gives $40\arctan(0.25) = 9.7991$ radians, a lag of 0.2009 radians. The explicit round trip multiplies the radius by $(1 + 0.5^4/4)^{20} \simeq 1.364$. The implicit round trip returns the original radius and phase to roundoff. Run both updates below. Compare results at equal elapsed time by halving h and doubling N. The phase error should drop by about a factor of four. The graph uses computed steps for the methods and a more finely sampled exact reference.

Open this experiment online

Try the calculation

Time step h (ω = 1) **0.5**

Number of forward steps **20**

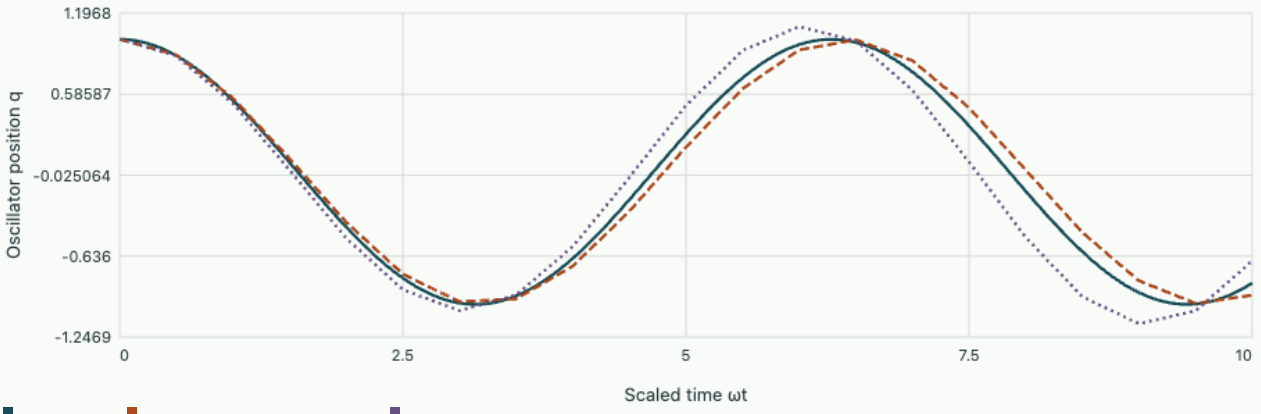

Implicit midpoint phase lag 0.2009 rad. Forward-backward distance from the start is 8.951e-16 for implicit midpoint and 0.3635 for explicit midpoint.

Tutorial on designing an accuracy criterion

A solver preserves the harmonic energy exactly over a simulation of 100 time units with $\omega = 1$. A measurement also requires phase error below 0.01 radians. Use the leading midpoint error to estimate an admissible step. How would you verify it?

▼ **Work through the solution**

The accumulated phase error is approximately $T\omega^3 h^2/12$. Solving $100h^2/12 < 0.01$ gives $h < 0.0346$. Verify at a chosen integer step count using $T - 2N\arctan[T/(2N)]$, or by convergence against a refined trajectory that measures the phase continuously. Energy alone has zero error for all these steps, so it cannot certify the phase target.

Further reading · Hairer's TUM geometric numerical integration course, symmetric methods.

What different observers measure

Waves, radiation and relativity

A moving observer carries clocks, rulers and a calibrated test charge. A statement about the electric field must specify which observer held that test charge at rest. In this chapter we derive how different measurements can agree on the force law and yet assign different electric fields, magnetic fields and charge densities to the same physical apparatus. A current-carrying wire and a light pulse will provide independent checks.

Events, synchronisation and directed boosts

Use two inertial coordinate systems with aligned axes. The primed origin moves at speed v in the positive laboratory x direction. Choose coincident origins when both clocks read zero and synchronise distant clocks in each frame by light signals. Homogeneity makes the transformation linear. The worldline of the primed origin requires

$$x' = A(x - vt).$$

A light ray moving along either axial direction must still obey $x' = \pm ct'$. Substituting its two possible worldlines into the linear map fixes the relative coefficients of x and t in t'. Reversing the transformation by changing the sign of v fixes the remaining scale.

$$x' = \gamma(x - vt),$$
$$t' = \gamma(t - vx/c^2),$$
$$y' = y,$$
$$z' = z,$$
$$\gamma = (1 - v^2/c^2)^{-1/2}.$$

The squared interval $c^2\Delta t^2 - |\Delta \mathbf{r}|^2$ is unchanged, a direct algebra check that detects a surprising number of sign choices. Two sparks separated by 3.0 m along a laboratory bench and simultaneous on laboratory clocks have $\Delta t' = -7.51$ ns for $v = 0.60c$, if the second event is at larger x. Their ordering in this frame is consistent with their spacelike separation. Events joined by a light signal are null-separated and retain their order under this boost.

Length measurements need two simultaneous endpoint readings in the chosen frame. A bar at rest in the lab and parallel to the axis has length L/γ in the primed frame. Substituting the simultaneous laboratory endpoint events into the boost instead gives γL, but their primed times differ. This distinction reappears when we count charge per unit length in a moving wire. The result of that count depends on the spacetime slice used to perform it.

A current is a rate of charge crossing a surface

Begin with a single population of particles, each carrying charge q, whose proper number density is n_0. Their counting volume is Lorentz-contracted only along their motion. The lab assigns density $n = \gamma_u n_0$

and current density $qn\mathbf{u}$. Both are components of $j^\mu = qn_0 u^\mu$, where $u^\mu = \gamma_u(c, \mathbf{u})$ is the four-velocity. Independent species can be superposed. A total four-current can consequently be spacelike even though every material particle moves more slowly than light.

$$\rho' = \gamma(\rho - vJ_x/c^2),$$

$$J'_x = \gamma(J_x - v\rho),$$

$$J'_y = J_y,$$

$$J'_z = J_z.$$

The usual continuity law becomes $\partial_\mu j^\mu = 0$ with $\partial_0 = c^{-1}\partial_t$. Transformation of the derivative and of the current cancels exactly in this contraction. An isolated finite charge distribution has an observer-independent total charge if each observer integrates through a complete spacelike slice. One way to see this is to connect the two slices by a large timelike enclosing wall. Four-dimensional flux conservation sets the difference between the two charge integrals equal to the current crossing the wall. For a wall outside all the charge trajectories that last contribution vanishes.

For a charge-neutral straight wire carrying conventional current $I = 2.0$ A along $+x$, a frame moving parallel to the wire at $0.20c$ assigns line density $\lambda' = -\gamma v I/c^2 = -1.36$ nC/m. Transverse cross-section is unchanged. There is no requirement that electrons themselves travel at $0.20c$. Both the mobile and immobile species contribute to the transformed density. The ideal wire is infinitely long, so one cannot integrate its transformed charge density out to infinity and apply the finite isolated system argument.

Obtaining field components from measured forces

Place a test charge at rest at an event in the primed frame. In the lab it has velocity $v\mathbf{e}_x$ and force $q(\mathbf{E} + \mathbf{v} \times \mathbf{B})$. To transform the force, transform the corresponding momentum change. For a small transverse kick, $dp'_y = dp_y$ while $dt' = dt/\gamma$ on the test charge's path. Thus $F'_y = \gamma F_y$ and similarly for z. For the parallel component use $dp'_x = \gamma(dp_x - v\,d\mathcal{E}/c^2)$ and $d\mathcal{E}/dt = vF_x$. The result is

$$F'_x = F_x.$$

Dividing by q gives the electric field. Requiring the same force law for charges moving transversely, or transforming the magnetic flux measured by a moving loop, gives the magnetic field.

$$\mathbf{E}'_\parallel = \mathbf{E}_\parallel,$$

$$\mathbf{B}'_\parallel = \mathbf{B}_\parallel,$$

$$\mathbf{E}'_\perp = \gamma(\mathbf{E} + \mathbf{v} \times \mathbf{B})_\perp,$$

$$\mathbf{B}'_\perp = \gamma(\mathbf{B} - \mathbf{v} \times \mathbf{E}/c^2)_\perp.$$

Imagine a uniform $+y$ electric field of 90.0 kV/m and a $+z$ magnetic field with $cB = 150$ kV/m. For a boost along $+x$, the y component of $\mathbf{v} \times \mathbf{B}$ is negative. At $\beta = 0.60$ the electric field vanishes. The

remaining magnetic field has $cB' = 1.25(150 - 54) = 120$ kV/m or 0.400 mT. A particle comoving with that frame feels no force at that event. A different particle moving across the magnetic field can still curve.

Vary the observer speed and compare the electric and magnetic field invariants

Compare two force measurements near an ideal wire

Return to the 2.0 A wire and put the observation point 1.0 cm along $+y$. Ampère's law gives $B_z = \mu_0 I/(2\pi r) = 40.0$ microtesla. The lab radial electric field is zero in this idealised symmetric model. A positive test charge moving along $+x$ at $0.20c$ experiences an inward magnetic force per unit charge of 2.40 kV/m. In its momentary rest frame the wire's negative line charge produces an inward radial electric field. The field from Gauss's law is $|\lambda'|/(2\pi\epsilon_0 r) = 2.45$ kV/m. The difference in the reported transverse forces is precisely the factor $\gamma = 1.0206$ derived from the momentum kick.

There is no contradiction between a field with zero laboratory divergence outside the wire and a different electric field in the primed frame. The charge density at the wire itself also transforms. If the laboratory wire carries a real driving surface charge and a return conductor, add their fields and charges before transforming. A claimed measurement of this ideal result without specifying the return path and electrostatic shielding needs a separate model for those additional fields.

When can a field be made purely electric or magnetic?

Direct substitution in the transverse transformation leaves the scalars $B^2 - E^2/c^2$ and $\mathbf{E}\cdot\mathbf{B}$ unchanged. The first is a difference, so retain its sign. If the second is nonzero, no observer sees either field vanish. If the fields are orthogonal and $E < cB$, choose $\mathbf{v} = \mathbf{E}\times\mathbf{B}/B^2$. The vector identity for $(\mathbf{E}\times\mathbf{B})\times\mathbf{B}$ cancels $\mathbf{E}$, and the required speed is below c. With $E > cB$, choosing $c^2\mathbf{E}\times\mathbf{B}/E^2$ instead cancels $\mathbf{B}$.

When both invariants vanish one must still distinguish a field identically zero from a nonzero null field. A vacuum travelling plane wave satisfies $E = cB$ and orthogonality everywhere. The advertised boost would then require speed c. An observer can lower its measured frequency and amplitude continuously by following the wave at increasing speed but can never transform away its nonzero field. A superposition of waves need not be null. A standing wave has positions and times where only one of the fields is present.

Phase matching across inertial frames

Every observer agrees on whether a particular spacetime event is a crest. The phase $\mathbf{k}\cdot\mathbf{r} - \omega t$ therefore labels the same event in each frame. Substituting the inverse coordinate transformation gives the transformation of frequency and wavevector. For vacuum propagation at laboratory angle θ to the boost, divide the transformed longitudinal wavenumber by the transformed magnitude.

$$\omega' = \gamma\omega(1 - \beta\cos\theta),$$

$$\cos\theta' = \frac{\cos\theta - \beta}{1 - \beta\cos\theta}.$$

An observer chasing a collinear 600 nm light wave at $0.60c$ sees half its frequency and a wavelength of 1200 nm. A beam entering at 90° to the boost appears at $\cos\theta' = -0.60$ and frequency 1.25ω. Asking for a transverse Doppler shift without saying in whose frame the angle is a right angle leaves the problem under-specified. A detector counts phase fronts crossing its own trajectory and its own clock sets the elapsed time.

A boosted light beam also transports momentum

Frequency alone does not specify the energy measured by a moving detector. Its collecting surface and clock must be assigned to an observer. For a monochromatic collimated beam in vacuum, one route is to transform both fields and calculate their new Poynting vector. Another route is to transform the stress-energy tensor, whose energy density, momentum density and momentum flux describe the same field together. This second route shows explicitly which measured quantity is being transformed and extends to superposed beams with zero mean momentum in one frame.

For a right-moving plane wave along x, the energy density is $u = S_x/c$, momentum density is u/c and normal momentum flux is u. In coordinates with $x^0 = ct$, the relevant block has $T^{00} = T^{01} = T^{10} = T^{11} = u$. Boost both indices using the same Lorentz matrix as for coordinates. The transformed energy density follows directly:

$$T'^{00} = \gamma^2(T^{00} - 2\beta T^{01} + \beta^2 T^{11}) = \gamma^2(1-\beta)^2 u.$$

The frequency Doppler factor enters twice. One factor corresponds to lower energy per photon and one to the changed number per unit volume. For a finite pulse, its length at a common primed time grows for an observer following it, so the total energy changes by only one Doppler factor. Volumes measured between equal-time spatial endpoints must be computed on the appropriate observer's simultaneity slice, just as for a moving rod.

Now superpose two equal-intensity mutually incoherent plane waves in opposite axial directions. In the laboratory $T^{01} = 0$, while $T^{11} = T^{00} = u$ for the combined radiation. An observer moving at $0.60c$ obtains $u' = \gamma^2(1+\beta^2)u = 2.125u$, with net flux $S'_x = -2\gamma^2\beta\,cu = -1.875\,cu$. The counterpropagating beam that the observer meets head-on is blueshifted, while the other is redshifted. Energy density remains greater than the magnitude of momentum density times c, as required for a superposition of distinct propagation directions. This check fails if one transforms a zero Poynting vector as though it were the spatial component of a four-vector with no stress information.

The direction-independent radiation field in an ideal cavity has $T^{ii} = u/3$ for each spatial axis in its rest frame rather than $T^{11} = u$. The one-third comes from averaging n_i^2 over a sphere. The moving observer then sees $u' = \gamma^2 u(1 + \beta^2/3)$ and a net longitudinal flux. At $\beta = 0.60$ the energy-density factor is 1.75. An isotropic thermal field becomes directionally distorted; assigning one Doppler factor to the whole sky would give neither the correct integrated energy density nor its directional spectrum.

A moving parallel-plate capacitor tests surface sources

Choose large parallel conducting plates at $z = \pm d/2$ carrying opposite uniform surface densities $\pm\sigma$. Ignore edge effects in the central region. In the lab the field between them has magnitude $E_0 = \sigma/\epsilon_0$ and there is no magnetic field. A frame boosted along $+x$ sees both plates move at $-v$. Their areas contract along x, so their surface charge magnitudes become $\gamma\sigma$; their equal and opposite surface currents point in opposite senses. Use Gauss's law and the magnetic jump condition on each sheet to reconstruct the transformed fields. The current sheets reinforce magnetically between the plates and cancel outside, just as electric sheets of opposite charge do electrostatically.

For laboratory electric field along $+z$, the moving observer has $E'_z = \gamma E_0$ and $B'_y = +\gamma v E_0/c^2$. Cross the primed plate velocity $-v\mathbf{e}_x$ with this magnetic field to find a force along $-z$ on a positive surface charge, partly cancelling the enhanced electric attraction towards the opposite plate. When finding the force on a sheet, use the fields of the other sheet or the arithmetic mean of the two limiting fields. Substituting the total interior field without removing the self contribution would double the result.

At $E_0 = 2.00$ MV/m and $\beta = 0.60$, the primed interior field is 2.50 MV/m and its magnetic field 5.00 mT. Per positive surface charge the transverse attraction from the opposite sheet has magnitude $\gamma E_0(1-\beta^2)/2 = E_0/(2\gamma)$. This is 0.800 MV/m, compared with 1.00 MV/m in the laboratory. The transformation factor is inverse γ because the charge in this example is at rest in the original laboratory; the earlier force derivation placed the test charge at rest in the primed frame. Interchanging those initial conditions without changing the time conversion reverses the factor.

Multiplying the primed force per charge by the larger surface density $\gamma\sigma$ restores the same force per transverse plate area in this tangential boost. The cancellation supplies a local cross-check among length contraction, field transformation and mechanical force. A complete calculation of the total energy or momentum of an accelerated finite capacitor must also account for stresses in its supports and for the fields near its edges. Taking the uniform central field times a transformed volume is adequate for a local comparison, but does not by itself describe that whole closed mechanical system.

Test a field transformation with an invariant

Change observer speed, compare the separately transformed fields and inspect the invariant combination. Agree on the event before comparing measurements.

Open this experiment online

Try the calculation

Electric field E (kV/m) **90**

Magnetic field cB (kV/m) **150**

Observer speed β **0.6**

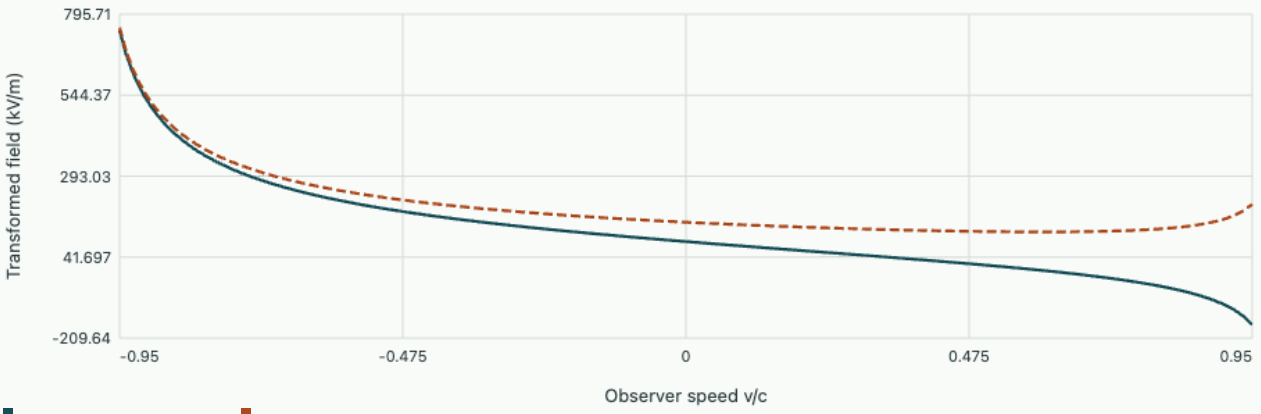

At the selected speed E′ = 0 kV/m and cB′ = 120 kV/m. E′² − c²B′² = -14400 (kV/m)².

Worked observer problem · a null of one component does not imply a vanishing field

At one event a laboratory finds $\mathbf{E} = (30, 40, 0)$ kV/m and $c\mathbf{B} = (0, 0, 50)$ kV/m. Another laboratory reports that it can remove the magnetic field by boosting along the direction of $\mathbf{E} \times \mathbf{B}$. Test the claim and predict the fields for a boost of speed $0.80c$ along this direction. Does the local measurement establish that this is an infinite plane wave?

▼ **Evaluate the invariants and transform the transverse field**

The electric and scaled magnetic fields both have magnitude 50 kV/m and are perpendicular. Both quadratic Lorentz invariants vanish, while the fields themselves are nonzero. With $\mathbf{v}$ along $\mathbf{E} \times \mathbf{B}$, both field vectors are perpendicular to the boost. The cross terms reduce their magnitudes by a common factor $\gamma(1 - \beta) = 1/3$ for this speed, so $E' = cB' = 16.7$ kV/m. Their directions in this transverse configuration are unchanged. No subluminal boost removes either nonzero field, as follows also by applying the inverse transformation to an alleged zero field.

A pulse at one point can have these local field values, as can the field near a suitable superposition at a particular event. A local tensor and its invariants contain no information about all the field derivatives elsewhere. To establish a plane-wave model measure spatial phase across transverse probes, verify the propagation relation at separated stations and bound amplitude variation over the required observation region. Infinity is an idealisation established only to a scale specified by the experiment.

As an error check, compare the measured difference $E^2 - c^2B^2$ with the propagated uncertainties of both meters. Small nonzero estimated differences near a null may be statistically insignificant, while a systematic alignment error in $\mathbf{E} \cdot \mathbf{B}$ can obscure orthogonality. Classifying a field as electric-dominated or magnetic-dominated from a difference of nearly equal large squares requires an uncertainty budget. The exact mathematical classification and the experimental confidence in assigning it answer different questions.

Recover a source direction from two clocks and a known speed

Two perfectly synchronised receivers travel with equal speed in opposite directions along the laboratory axis. They sample the same monochromatic plane wave. Their measured frequencies are proportional to $1 - \beta\cos\theta$ and $1 + \beta\cos\theta$, with a common Lorentz factor. Taking their difference divided by their sum determines $\beta\cos\theta$ without prior knowledge of emitted frequency. Their sum then fixes that frequency once the speed is calibrated. The construction combines two observer assignments rather than treating a transverse Doppler correction as an unknown empirical shift.

For speeds of half the speed of light and a measured frequency ratio of three to two, with the receiver travelling toward negative x recording the higher value, the inferred cosine is 0.40. If their average measured frequency is 600 THz, the emitted laboratory frequency is about 520 THz. A second direction on the opposite side of the boost axis has the same cosine, so the two receivers alone cannot determine the full incoming unit vector.

A third receiver with a nonparallel velocity supplies another directional projection. Detector clocks must be calibrated in their respective rest frames and each must see the same stable source frequency. If the source itself chirps between noncoincident measurements, that chirp can imitate an angular shift. Using overlapping signals and comparing phase histories addresses this limitation more directly than quoting only two peak frequencies.

Tutorial · Infer charge and current from two observers

A uniform channel carries an unknown lab line charge λ and current I along its axis. Observers moving at $+0.30c$ and $-0.30c$ measure line densities 1.0 and 3.0 nC/m respectively. Recover the laboratory quantities. Can a third observer travel alongside this current so that the measured current vanishes?

▼ Recover the two independent quantities and classify the current

Adding the readings gives $2\gamma\lambda = 4.0$ nC/m, so $\lambda = 1.908$ nC/m. Subtraction gives $2\gamma\beta I/c = 2.0$ nC/m and hence $I = 0.953$ A. Reinsert both signs in the original equations as a check. The speed needed to cancel the current would be $I/\lambda = 5.00 \times 10^8$ m/s. It exceeds the speed of light. The current four-vector is spacelike since $I^2 > (c\lambda)^2$.

A frame with zero line charge can instead move at $v = c^2\lambda/I = 0.600c$. A spacelike total current is possible for superposed charge carriers of opposite sign. The calculation would rule out a model

consisting solely of one sign of carriers all propagating with a common subluminal drift velocity. It does not rule out the measured pair of densities.

Tutorial · What does a moving pulse detector count?

A 10.0 ns rectangular-envelope light pulse moves in $+x$ in vacuum. A detector moves along the same direction at $0.60c$. Compute the interval between its encounters with the leading and trailing edges using laboratory kinematics, then its own clock. Predict its measured peak intensity and fluence relative to a stationary detector for a broad collimated beam.

▼ **Track the two crossing events and transform the flux**

The pulse is $c(10.0\,\mathrm{ns})$ long in the lab. Its back approaches the moving detector at coordinate closing speed $c - v = 0.40c$, so the two events occur 25.0 ns apart in laboratory time. Both events lie on the detector worldline, so its proper interval is 20.0 ns. This agrees with the inverse Doppler factor of two. A pulse of enough cycles to define a carrier now has half the frequency and twice its envelope duration.

For a transverse plane wave the field amplitude transforms as $\gamma(1 - \beta) = 0.50$ times the laboratory value. The primed Poynting flux is therefore one quarter as large. Integrating over twice the proper duration gives one half the original energy per unit transverse area. The cross section perpendicular to the boost is unchanged. Photons are registered with half their laboratory energy and the same total number if the beam is entirely collected, an independent check on the fluence result.

Cambridge Electromagnetism · electromagnetism and relativity

Relativistic particle dynamics and the field tensor

Waves, radiation and relativity

A circular track measures momentum per charge. A clock following the particle registers proper time, and a detector records how much kinetic energy it has gained. We will put these observations in one dynamical equation, solve that equation in uniform fields and exhibit a numerical pusher that can get the energy right while its orbit phase slowly slips.

What the track, clock and calorimeter measure

Consider a particle of invariant mass m, signed charge q and ordinary velocity $\mathbf{v}$. Inertial observers agree on the proper time between neighbouring events on its timelike worldline,

$$d\tau = dt\sqrt{1 - v^2/c^2}.$$

Adopt coordinates $x^\mu = (ct, x, y, z)$ and metric $g = \mathrm{diag}(1, -1, -1, -1)$. Dividing the displacement by proper time produces a vector of fixed Minkowski norm. Multiplying it by invariant mass gives four-momentum.

$$u^\mu = \gamma(c, \mathbf{v}),$$
$$p^\mu = m u^\mu = (\mathcal{E}/c, \mathbf{p}),$$
$$\mathcal{E}^2 - c^2|\mathbf{p}|^2 = m^2 c^4.$$

Energy includes the rest term. Momentum is $\gamma m \mathbf{v}$. Differentiating the last equation on a trajectory gives

$$d\mathcal{E}/dt = \mathbf{v} \cdot d\mathbf{p}/dt.$$

This identity replaces the nonrelativistic step of dotting $m\mathbf{a}$ with velocity. A magnetic field can rotate momentum with fixed magnitude and energy, whereas an electric field can change energy by doing work.

Suppose an electron begins at rest and gains 10.0 keV of kinetic energy across an electrostatic potential difference in vacuum. Its rest energy is 511 keV, giving $\gamma = 1.01957$ and $v/c = \sqrt{1 - 1/\gamma^2} = 0.1950$. The nonrelativistic estimate is 0.1978. In a modest energy measurement the discrepancy could lie below the experimental spread. For a precise orbit calculation the 1.96 percent change in relativistic cyclotron period is measurable independently of that discrepancy in speed.

A linear map that produces the Lorentz force

Seek a local equation linear in field and four-velocity and covariant under boosts. For the energy component to give $q\mathbf{E} \cdot \mathbf{v}$, and for the spatial components to give the electric force and the oriented cross product, construct the antisymmetric field tensor. With the stated metric and $\epsilon^{123} = 1$, set

$$F^{0i} = -E_i/c,$$

$$F^{i0} = E_i/c,$$

$$F^{ij} = -\epsilon^{ijk} B_k,$$

$$\frac{dp^\mu}{d\tau} = qF^{\mu\nu} u_\nu.$$

Lowering the index on u reverses the signs of its spatial components. The spatial product becomes $q\gamma(\mathbf{E} + \mathbf{v} \times \mathbf{B})$, and division by γ converts the proper-time derivative to $d\mathbf{p}/dt$. The time component similarly yields

$$d\mathcal{E}/dt = q\mathbf{E} \cdot \mathbf{v}.$$

Contract the force with u_μ. The symmetric product $u_\mu u_\nu$ annihilates the antisymmetric tensor, which proves that the evolution preserves the mass shell.

To recover Maxwell's kinematic constraints from potentials, put $A^\mu = (\phi/c, \mathbf{A})$ and $F^{\mu\nu} = \partial^\mu A^\nu - \partial^\nu A^\mu$. Then $F^{0i} = (\partial_t A_i + \partial_i \phi)/c = -E_i/c$, while the spatial-spatial components are the magnetic curl. Adding a four-gradient to A^μ leaves the tensor unchanged because ordinary derivatives commute. The particle action $S = -mc^2 \int d\tau - q \int A_\mu dx^\mu$ gives the same force after integrating variations by parts with fixed endpoints. Gauge changes add only an endpoint term to this action. A trajectory measured with local forces cannot distinguish such potential representatives.

Compare the potentials and field-based description in the field-tensor chapter

Constant force, variable coordinate acceleration

Put a particle initially at rest in a uniform static electric field along x. Let $a_0 = qE/m$ be signed. Integration of $dp_x/dt = qE$ gives $p_x = ma_0 t$, so the speed tends to c even while momentum increases linearly. Proper-time evolution is simplest in terms of rapidity η, where $u^0 = c\cosh\eta$, $u^x = c\sinh\eta$. The two tensor equations imply $d\eta/d\tau = a_0/c$.

$$t = \frac{c}{a_0}\sinh(a_0\tau/c),$$

$$x = \frac{c^2}{a_0}\{\cosh(a_0\tau/c) - 1\},$$

$$\frac{dv_x}{dt} = \frac{a_0}{\gamma^3}.$$

The initial time and position are zero. The work $qEx = mc^2(\cosh\eta - 1)$ equals kinetic energy, which checks both the integration constant and the dimensional factor in the displacement. For an electron use the direction of the electric force as positive to simplify signs. At 20.0 kV/m it gains 1.0 keV in 5.0 cm. The energy gain follows from the static potential even though the speed does not grow exactly as the square root of distance. The field region must last long enough for the particle to cross it and fringe fields can alter the entry trajectory.

Compare momentum, coordinate time and proper time in the charged-worldline experiment

Helical motion, radius and period

A uniform magnetic field along z keeps p_z, energy and $|\mathbf{p}_\perp|$ fixed. Write $p_x + ip_y$ as a complex number. The Lorentz force reduces to a first-order rotation equation and a single time integration gives the corresponding position. With positive B, positive charges starting along $+x$ initially turn towards $-y$.

$$\frac{d}{dt}(p_x + ip_y) = -i\frac{qB}{\gamma m}(p_x + ip_y),$$

$$R = \frac{p_\perp}{|q|B},$$

$$T = \frac{2\pi\gamma m}{|q|B}.$$

The helical pitch is $v_z T$. Radius gives transverse momentum and a calibrated period gives total energy through γ. A track seen only in projection along the field gives no direct evidence that longitudinal momentum vanishes. A second view or a timing measurement can resolve this ambiguity.

At 10.0 keV the electron has $pc = \sqrt{K(K + 2mc^2)} = 101.6$ keV. With entry perpendicular to a 2.0 mT field its radius is 0.169 m and its period 18.2 ns. Doubling the field halves both radius and period at fixed injection energy. Doubling momentum at fixed field doubles radius but changes period by the ratio of Lorentz factors. These are different tests of a track calibration. A beam with a spread of energies will dephase relative to a narrow timing gate even when every single particle remains in a perfectly uniform field.

A drift frame gives an exact crossed-field solution

For constant crossed fields with $E < cB$, transform to the frame moving at $\mathbf{v}_d = \mathbf{E} \times \mathbf{B}/B^2$. There $E' = 0$ and $B' = \sqrt{B^2 - E^2/c^2}$; calculate the transformed initial momentum and integrate a helix. Transform two successive equal-phase events back to the lab. Their perpendicular displacement in the electric-free frame is zero. If the motion has no component parallel to $\mathbf{B}$, the entire displacement there is zero, and the average lab cycle velocity is exactly $\mathbf{v}_d$. The detailed lab trace need not be circular and the instantaneous lab energy may oscillate.

Take $E = 30.0$ kV/m along y and $B = 0.50$ mT along z. The drift is along $+x$ at 6.00×10^7 m/s. A particle injected at that velocity crosses the uniform fields on a straight line because the forces cancel. An initially stationary positive particle instead begins by accelerating along $+y$. These observations can use the same field with different injected particles. If E exceeds cB, this electric-free frame is unavailable. Transform to a magnetic-free frame and integrate electric acceleration instead.

Continuous rotation and a discrete experiment

A naive forward step $\mathbf{p}_{n+1} = \mathbf{p}_n + q\Delta t\, \mathbf{v}_n \times \mathbf{B}$ adds a vector perpendicular to the previous momentum. Its squared norm increases by the squared magnitude of that kick. The apparent heating will persist in perfectly static uniform magnetic fields. For a purely magnetic update, evaluate the direction using the mean of old and new momenta. At fixed γ, the resulting implicit two-dimensional linear map can be solved algebraically and is an exact rotation by a modified angle.

$$\delta = 2\arctan\left(\frac{\omega_c \Delta t}{2}\right),$$

$$\omega_c = \frac{qB}{\gamma m}.$$

The sign of rotation follows the earlier complex equation. Dotting the update with the mean momentum gives zero change in squared norm, which verifies the energy property even for relatively large time steps. A common electromagnetic pusher surrounds the magnetic rotation by two electric half-kicks. In spatially varying fields, specify at what time and position each field is sampled, and check spatial interpolation and time convergence. For ultrarelativistic nearly cancelling electric and magnetic fields, preserving rotation in a pure field alone does not ensure cancellation is represented accurately.

Solve the constant tensor without transforming every time step

When uniform electric and magnetic fields are constant in spacetime, the Lorentz equation is a linear constant-coefficient equation for four-velocity as a function of proper time. Nonlinearity in ordinary time hides that simple structure, because the rate at which proper time accumulates changes along the orbit. Define the mixed tensor $M^{\mu}{}_{\nu} = (q/m)F^{\mu\alpha}g_{\alpha\nu}$. In a uniform field it does not vary along the trajectory. A formal solution is then

$$u(\tau) = e^{M\tau}u(0),$$

$$x(\tau) - x(0) = \int_0^{\tau} e^{Ms}u(0)\, ds.$$

The coordinate formula is written as an integral since M can be singular, as it is in a purely magnetic field. Blindly replacing this integral by $M^{-1}(e^{M\tau} - I)$ fails in exactly such simple cases. A power series for the integral or a block matrix exponential treats zero eigenvalues without an artificial inverse. Antisymmetry of the tensor implies $M^{\mathsf{T}}g + gM = 0$. Differentiating $e^{M^{\mathsf{T}}\tau}ge^{M\tau}$ shows that it stays equal to g, making preservation of $u^{\mu}u_{\mu} = c^2$ a structural property of the exact mapping.

For parallel constant fields along z, the matrix decomposes into a boost in the ct, z subspace and a rotation in x, y. Write $\alpha = qE/(mc)$, $\Omega = qB/m$, and denote the initial four-velocity components by u_0^{μ}. The proper-time solution is

$$u^0 = u_0^0 \cosh \alpha\tau + u_0^z \sinh \alpha\tau,$$
$$u^z = u_0^z \cosh \alpha\tau + u_0^0 \sinh \alpha\tau,$$
$$u^x + iu^y = (u_0^x + iu_0^y)e^{-i\Omega\tau}.$$

The longitudinal and transverse operations commute because they act in different subspaces. In lab time the transverse rotation slows as the electric field increases energy, although the proper-time rotation frequency stays constant. A particle therefore traces a helix whose transverse radius $p_\perp/(|q|B)$ is fixed while the pitch evolves. A single measured turn time without a tagged position in the accelerating region is insufficient for an energy reconstruction.

As a numerical test use an electron, quoting magnitudes, with $B = 1.0$ mT, $E = 10.0$ kV/m and initial purely transverse speed $0.10c$. One magnetic turn takes 35.72 ns in proper time and accumulates electric rapidity magnitude $|\alpha|\tau \simeq 0.2096$. The final Lorentz factor is $\gamma_i \cosh(0.2096) = 1.0272$, giving final kinetic energy about 13.9 keV, compared with 2.57 keV initially. The lab-time turn duration is $\gamma_i \sinh(|\alpha|\tau)/|\alpha| \simeq 36.2$ ns. Reversing the electric field changes the direction of the axial displacement but leaves final energy and turn duration unchanged for this initially transverse particle. Reversing the initial longitudinal velocity would generally break that energy symmetry.

Infer uncertainty and test units in a momentum reconstruction

A track fitter commonly reports field, radius, pitch, time and a fitted covariance matrix. The dynamical relation turns these observed quantities into momentum. Let L_z denote a signed pitch per turn. With known signed direction of circulation and calibrated absolute field magnitude,

$$|\mathbf{p}| = |q|B\sqrt{R^2 + (L_z/2\pi)^2}.$$

For small errors, logarithmic differentiation gives weights for fractional radius and pitch errors:

$$d\log p = d\log B + w_R\, d\log R + w_L\, d\log |L_z|,$$
$$w_R = \frac{R^2}{R^2 + (L_z/2\pi)^2},$$
$$w_L = 1 - w_R.$$

For $R = 0.20$ m and $L_z = 0.30$ m the radius accounts for 94.6 percent of the squared transverse-plus-longitudinal geometric factor. Independent relative uncertainties of 0.20 percent in field, 0.50 percent in radius and 2.0 percent in pitch yield about 0.525 percent uncertainty in total momentum. A common detector scale controlling both radius and pitch would enter with correlated signs and should not be counted as two independent errors. When the pitch tends to zero, use the original derivatives with respect to L_z; a reported fractional error on a quantity consistent with zero is ill defined.

Differentiating $K = \sqrt{m^2c^4 + p^2c^2} - mc^2$ gives

$$d\log K = (\gamma + 1)d\log p/\gamma.$$

The coefficient approaches two at low energy and one at very high energy. At the approximately 3.70 keV energy of the tutorial the above momentum error would imply about a 1.05 percent energy error. A kinetic-energy estimate from a small difference of nearly equal numbers can also lose numerical precision at much lower energies. Rationalise it as $K = p^2c^2/(\sqrt{m^2c^4 + p^2c^2} + mc^2)$ when working near rest.

Several independent checks use this reconstruction without assuming the track fitter is correct. The turn time inferred from the fitted γ can be compared with a separate timing channel. Reverse the magnetic field to reverse the direction of curvature while keeping the speed and energy approximately fixed. Translate the beam within a mapped uniform field and look for changing fitted radius that correlates with position, an indication of geometric or field-map bias. Finally plot the residual of the magnetic force law separately for transverse magnitude and angle. A time integrator may conserve momentum magnitude for symmetry reasons even when its field interpolation biases the phase or shifts the guiding centre systematically.

Advance a charge using relativistic momentum

Increase the impulse while following speed, energy and proper time. Identify the range where a Newtonian momentum update becomes inaccurate.

Open this experiment online

Try the calculation

Electric field magnitude (kV/m) **100**

Lab time for a reading (ns) **17**

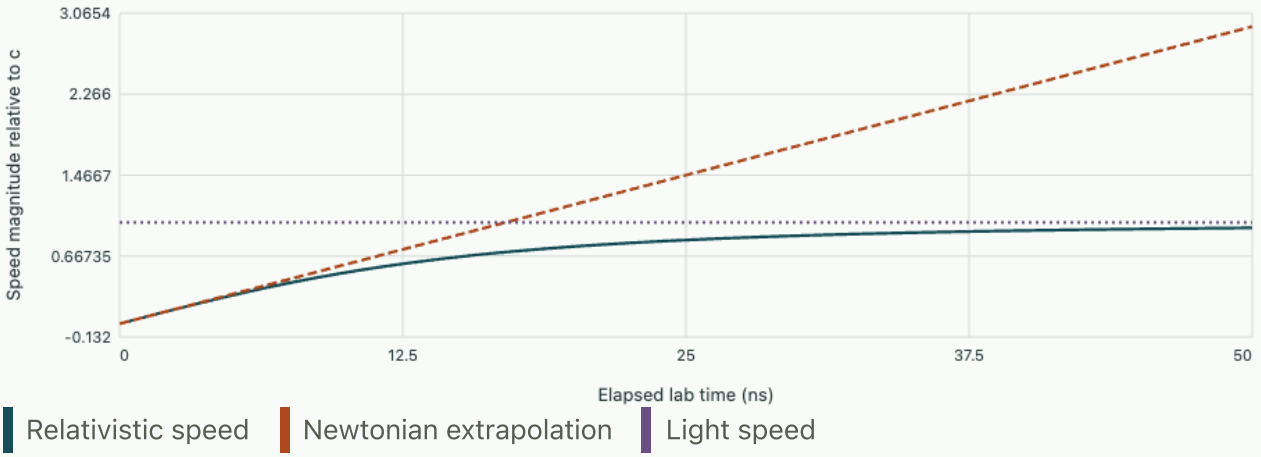

At 17 ns laboratory time the electron speed is 0.706 c. Its clock has advanced 15 ns and it has gained 211 keV.

Worked timing problem · infer an accelerating voltage without a radius

A tagged electron bunch completes ten nearly circular turns in a calibrated 5.0 mT magnetic field. Two time stamps indicate an elapsed 73.0 ns. The field is perpendicular to the orbit. Assuming complete turns and negligible electrical work during the timed interval, estimate the injection energy. What timing precision would distinguish a one-percent change in that energy?

▼ **Use the relativistic period sensitivity rather than the energy fraction directly**

The nonrelativistic turn period is

$$2\pi m/(eB) = 7.145\,\mathrm{ns}.$$

The measured period is 7.30 ns, giving $\gamma \simeq 1.0217$ and $K = (\gamma - 1)mc^2 \simeq 11.1$ keV. The relative energy sensitivity is much larger than the relative period change when γ is close to one. A one-percent change in K corresponds to $\Delta\gamma \simeq 2.17 \times 10^{-4}$, or relative period change 2.12×10^{-4}. Over the ten turns this gives approximately 15.5 ps.

To resolve that change spectroscopically, uncertainties in the elapsed time and field scale must together be significantly smaller than the equivalent change. A constant pickup cable delay cancels if the same electronics register both ends of the interval, while a drift of its timebase scale does not. Timing over more turns improves the total accumulated signal but also increases exposure to field inhomogeneity, energy loss and dephasing among particles with different injection energies. A narrower timing histogram does not automatically eliminate a systematic field calibration.

Finally verify the integer turn count independently. Missing a pickup crossing would cause a much larger change in inferred energy than the desired resolution. The measured wave packet may broaden so strongly that later crossings overlap. Recording the full pickup waveform and tracking ordered crossings, along with an independent rough radius estimate, can constrain the turn assignment before fitting the small relativistic shift. A perfect circular image with no time labels cannot supply that missing count.

Why momentum and kinetic energy do not gain fixed fractions together

In an electrostatic accelerating gap, the kinetic energy increment for a particle passing between two equipotential surfaces is its charge times the potential drop, regardless of injection energy. This statement follows by integrating the Lorentz power law over the actual path. A magnetic guiding field can alter the path and transit time while doing no direct work. A time-dependent electric field, a missed equipotential endpoint or appreciable radiation changes the simple inference and must be addressed separately.

For an electron entering with 10 keV and acquiring an additional 10 keV, kinetic energy doubles. Its initial momentum times c is about 101.6 keV and its final value about 144.4 keV. The radius in the same subsequent perpendicular magnetic field increases by a factor approximately 1.42. Doubling the radius

would instead require doubling momentum, which demands a substantially greater energy increment at this low initial energy. Comparing radii before and after a known voltage supplies an independent check on the sign and magnitude of a particle's charge-to-mass model.

A measured energy gain below the nominal voltage does not by itself diagnose radiation. The potential actually traversed, finite angular acceptance, entrance or exit fringe fields, collision losses and biases in reconstructing longitudinal momentum can all matter. Repeat with reversed field polarity or several injection energies and compare the kinetic-energy difference rather than the two radii directly.

Tutorial · Reconstruct a track with two measurements

A particle known to be an electron or positron crosses a uniform $+z$ field of 1.0 mT. The projected radius is 0.200 m and the pitch magnitude is 0.300 m. Recover the transverse and longitudinal momentum, energy and period. What else must the detector record to determine the sign of charge?

▼ **Reconstruct both momentum components**

The transverse momentum is $|q|BR = 3.20 \times 10^{-23}$ kg m/s. During a cycle the parallel displacement is $p_z T/(\gamma m) = 2\pi p_z/(|q|B)$, so $|p_z| = 7.65 \times 10^{-24}$ kg m/s. The quadrature total is 3.29×10^{-23} kg m/s, yielding $p/(mc) = 0.1206$, $\gamma = 1.00724$, and approximately 3.70 keV kinetic energy. The period is about 36.0 ns.

Neither radius nor pitch magnitude carries the signed circulation. Record the direction of traversal relative to the calibrated direction of magnetic field. Reversing both charge and the direction of traversal yields the same unlabelled transverse ring. If timing or two ordered detectors supply a direction, the sign follows from the first Lorentz kick.

Tutorial · Can a constant-energy circle be trusted?

A pusher uses 20 uniform steps per exact cyclotron period in a uniform magnetic field. It reproduces initial kinetic energy to machine precision for 50 turns. Estimate the phase drift from the midpoint rotation formula. Design a refinement diagnostic that distinguishes a time-discretisation bias from a field calibration error.

▼ **Compare the exact and discrete angles**

The exact unsigned angle per step is

$$h = 2\pi/20 = 0.31416.$$

The discrete one is

$$2\arctan(h/2) = 0.31161.$$

The accumulated deficit over 1,000 steps is about 2.55 rad, roughly 0.41 turn. The method can keep every track point on a closed momentum circle yet miss the pickup electrode by a large fraction of a revolution. Coordinate radius may depend on how positions were staggered, so perform the angular comparison on momentum first.

Double the number of steps at fixed physical end time and take the difference in unwrapped phases. The leading angular error $h^3/12$ per step becomes a quadratic global error, so halving the step should reduce it by about four. A calibration error in $qB/(\gamma m)$ persists under time refinement. Track both the expected frequency and the convergence of the time series; comparing the coordinates at a single late time can confuse complete turns with near agreement.

Cambridge Electromagnetism · four-vectors, fields and charged matter

Semiclassical quantization

Quantum mechanics

Use a local wavelength to construct the quantization rule for a smooth well and recognize where that construction breaks down.

FROM FIRST PRINCIPLES

Build the semiclassical phase and the turning-point condition

In a classically allowed interval define $p(x) = \sqrt{2m[E - V(x)]} > 0$ and seek a one-dimensional stationary wave $\psi = A(x)e^{iS(x)/\hbar}$. Assume p varies little over a local wavelength. Substitute into the Schrödinger equation and separate terms by powers of $\hbar$. The leading real and next imaginary balances give

$$(S')^2 = p^2,$$

$$2A'S' + AS'' = 0 \quad \Longrightarrow \quad A^2 S' = \text{constant}.$$

Thus the phase increment is $\int p\,dx/\hbar$ and the travelling-wave amplitude varies as $p^{-1/2}$. This approximation fails where $p = 0$. Near each smooth simple turning point the potential is locally linear; the decaying exterior Airy solution matches an interior sine with phase shift $\pi/4$. The waves entering from the left and right must describe the same standing wave. Combining the two end phases gives

$$\int_{x_-}^{x_+} p(x)\,dx = \pi\hbar(n + \tfrac{1}{2}),$$

$$n = 0, 1, \ldots.$$

The offset comes from the two soft turning points. A hard wall imposes its own node condition and changes the quantization offset. The construction becomes more reliable when the state samples many local wavelengths inside the well.

DERIVATION AND APPLICATIONS

Read a quantum level spacing from a classical clock

The semiclassical quantization rule uses the area swept in phase space. Its change with energy also carries information about time. Consider a smooth one-dimensional binding potential with two simple turning points $x_\pm(E)$, mass m, and many accessible levels. Write the half-cycle action using the positive momentum branch $p(x, E) = \sqrt{2m[E - V(x)]}$:

$$I(E) = \int_{x_-}^{x_+} p(x, E)\,dx,$$

$$I(E_n) \simeq \pi\hbar(n + \tfrac{1}{2}).$$

The endpoints move with energy, but their boundary contributions when differentiating the integral contain $p(x_\pm) = 0$. Inside the well $\partial_E p = m/p$. Its divergence near a simple turning point behaves as an inverse square root and is integrable. Using $p/m = \dot{x}$ on the forward leg now gives

$$\frac{dI}{dE} = \int_{x_-}^{x_+} \frac{m}{p(x,E)}\,dx = \int_{x_-}^{x_+} \frac{dx}{\dot{x}} = \frac{T_{\mathrm{cl}}(E)}{2}.$$

Two neighbouring quantized actions differ by $\pi\hbar$. If the classical period varies little over a level spacing, linearizing the action about one level leads to

$$E_{n+1} - E_n \simeq \frac{2\pi\hbar}{T_{\mathrm{cl}}(E_n)} = \frac{h}{T_{\mathrm{cl}}(E_n)}.$$

Thus a densely spaced part of the spectrum is associated with a long classical excursion. For a harmonic well the period is constant and the result is exactly the known spacing; near a separatrix the rapidly varying period makes a one-step linearization less reliable. Only the period of a complete return to the starting phase-space point belongs in this relation.

WORKED EXAMPLE

Estimate a frequency from adjacent lines

Change the inputs and investigate this derivation.

Consider an approximately harmonic vibrational well with nearby levels separated by 2.50 meV. With $h = 4.136$ meV ps, the inferred classical period is 1.65 ps and the ordinary oscillation frequency is 0.604 THz. A transit from the left turning point to the right should take about 0.827 ps. Equating this one-way transit with the period would overestimate the energy spacing by two.

SECOND APPLICATION

Predict the scaling change for a quartic well

Change the inputs and investigate this derivation.

In $V(x) = \lambda x^4$ the turning point is $x_t = (E/\lambda)^{1/4}$. Substituting $x = x_t u$ into $T_{\mathrm{cl}} = 2\int_{-x_t}^{x_t} m\,dx/p$ leaves an energy-independent integral and gives

$$T_{\mathrm{cl}} \propto E^{-1/4}.$$

Therefore local level spacing grows as $E^{1/4}$. At sixteen times the energy a spacing of 0.180 meV should become about 0.360 meV, assuming both regions contain enough levels for semiclassical counting. The quadratic trap would show no comparable growth.

Try it · Power law spacing

Vary the physical parameters in the derived relation. Use the units and assumptions in the readout to connect the curves to the two worked examples. A parameter study can test the forward prediction; the same relation can then be inverted to infer a parameter from a measurement.

Open this live calculation

Try the calculation

Potential exponent p in |x|^p

4

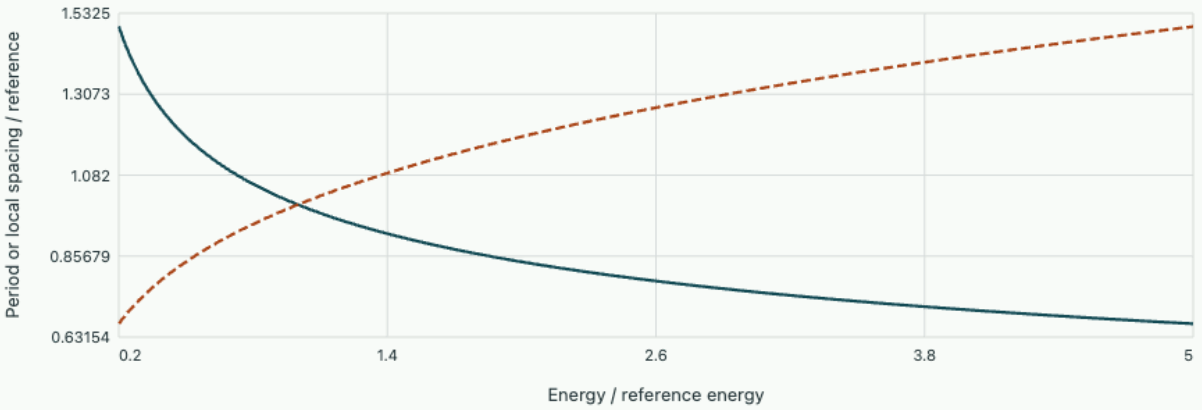

Classical period Semiclassical spacing

The action scales as E^(1/2+1/p). Differentiation gives T∝E^(1/p−1/2) and ΔE≈h/T. This local-spacing estimate improves for high quantum numbers.

A locally oscillating solution

Consider one-dimensional bound motion of mass m in a smoothly varying potential. In allowed regions the stationary equation is $\psi'' + p(x)^2\psi/\hbar^2 = 0$ with $p = \sqrt{2m(E-V)}$. If the potential changes little over a local wavelength, a small interval resembles a free-particle region. Accumulating its local phase produces the action integral $\int p\,dx/\hbar$. Yet a wave with changing local momentum must also change amplitude in order to conserve current.

Substitute $\psi = A(x)\exp[iS(x)/\hbar]$. The leading real terms give

$$S'^2 = p^2.$$

The next imaginary terms give $2A'S' + AS'' = 0$, or $(A^2S')' = 0$. Therefore each travelling contribution has amplitude proportional to $1/\sqrt{p}$. Equivalently a classical particle dwells longer where it

is slow, and the smoothed semiclassical probability mirrors this dwell time. The neglected derivative terms are small away from turning points when $\hbar|p'| \ll p^2$.

Match through a turning point

At an ordinary turning point $V(x_t) = E$ with nonzero slope, the local wavelength diverges and the previous criterion fails. Linearizing V there gives the Airy equation. Its decaying forbidden-side solution continues to an oscillatory allowed-side standing wave with a phase offset of $\pi/4$. Matching decaying exterior tails on both sides of a well bounded by two such turning points imposes

$$\int_{x_-}^{x_+} p(x)\,dx = \pi\hbar(n + \tfrac{1}{2}),$$

$$n = 0, 1, 2, \ldots.$$

The offset encodes the two smooth reflections. An infinite hard wall instead imposes a node directly and has a different reflection phase. Applying this rule unchanged to a hard box would count its levels incorrectly. For slowly varying barriers the forbidden action also controls exponential attenuation, but the two-turning-point integral above determines the energies of a classically allowed well.

A trap with measurable spacings

For $V = m\omega^2 x^2/2$ let $x_t = \sqrt{2E/(m\omega^2)}$. Put $x = x_t \sin u$ in the action integral. The integrand becomes $(2E/\omega)\cos^2 u\,du$ between $-\pi/2$ and $\pi/2$, yielding $\pi E/\omega$. The rule gives $E_n = \hbar\omega(n + 1/2)$, exceptionally exact even for the oscillator’s lowest levels.

For a mechanical trap at frequency 100 kHz, $E_4 = 4.5hf = 2.98 \times 10^{-28}$ J, equivalent to 21.6 µK on division by k_B. The spacing is hf or 4.80 µK. These temperatures express energy units; no equilibrium ensemble was assumed. As a transfer test consider $V = gx^4$. Rescaling $x = (E/g)^{1/4} y$ makes the action proportional to $E^{3/4}$. Quantization gives $E_n \propto (n + 1/2)^{4/3}$, so successive spacings grow with excitation. At sufficiently high level number the action changes slowly over a wavelength, making the predicted trend more trustworthy than a low-level numerical prefactor.

An independent check on the energy spacing follows by differentiating the action with respect to energy. The integrand vanishes at the turning points, so their moving endpoints add no first-order term. Inside the integral $\partial p/\partial E = m/p = 1/v$. Consequently the derivative of the one-way action is the time for the classical particle to travel from one turning point to the other. Adjacent quantum levels at high excitation then have separation approximately h divided by the full classical period. Measuring a variation of level spacing with excitation is therefore also probing the dependence of the classical orbit period on energy.

Estimate tunnelling between two bound wells

A nearly symmetric double well can have pairs of quantum states concentrated mainly in classically separate regions. For one such pair take approximately orthogonal localized states $|L\rangle, |R\rangle$ with equal

isolated energy E_0 and a small real tunnelling matrix element $-J$. The sign of either localized basis state can be chosen so $J > 0$. The two-level Hamiltonian has symmetric and antisymmetric eigenstates with energies $E_0 - J$ and $E_0 + J$, respectively. A local preparation $|L\rangle$ is a superposition of both and acquires a relative phase at rate $2J/\hbar$.

On evolution the probability to be in the other well is $P_R(t) = \sin^2(Jt/\hbar)$. The first complete transfer occurs at $t_{\mathrm{tr}} = \pi\hbar/(2J) = h/(2\Delta E)$ with $\Delta E = 2J$. In a high smooth barrier the localized wave tails overlap weakly. A semiclassical estimate gives

$$J \simeq J_0 e^{-\mathcal{S}/\hbar},$$

with $\mathcal{S} = \int_{x_1}^{x_2} \sqrt{2m[V(x) - E_0]}\, dx$ between inner turning points. This is an amplitude action. The through-barrier transmission probability of a scattering experiment instead contains twice that exponent. Confusing the two quantities gives an incorrect predicted change in the oscillation time.

Predict how a gate changes a tunnelling period

Suppose a symmetric electron double well shows a spectroscopic splitting $\Delta E = 40.0$ μeV. Its predicted first full transfer time is

$$h/(2\Delta E) = 51.7\,\mathrm{ps}.$$

Use the measured splitting to eliminate the unknown semiclassical prefactor. A gate modification adds a nearly flat forbidden segment of width 0.300 nm where $V - E_0 = 0.150$ eV and otherwise changes the wells negligibly. Using $\hbar^2/(2m_e) = 0.0381$ eV nm² gives decay wavenumber $\kappa = \sqrt{0.150/0.0381} = 1.98$ nm⁻¹. The added dimensionless action is 0.595.

If the prefactor and individual well frequencies remain similar, the new splitting is $40.0 e^{-0.595} = 22.1$ μeV, and transfer time rises to 93.6 ps. Doubling the width change multiplies the splitting by the square of the original ratio, not by twice the original ratio. These estimates concern coherent dynamics before energy relaxation or phase noise destroys the relative phase.

A gate can also shift the two well bottoms differently. With detuning δ the splitting is $\sqrt{\delta^2 + 4J^2}$, while maximum transfer falls to $4J^2/(\delta^2 + 4J^2)$. A larger measured splitting can therefore accompany poorer population transfer if symmetry is lost. Comparing spectroscopy and time-resolved populations distinguishes a changed tunnel coupling from an unintended potential offset.

The small tunnel coupling also sets a time criterion for disorder: a fluctuating left–right offset comparable with the splitting can produce substantial changes in both transfer amplitude and oscillation frequency. A static distribution of offsets across repeated preparations can wash out ensemble oscillations even when each individual preparation evolves coherently. Repeating the experiment after compensating the measured detuning separates this ensemble averaging from intrinsic energy relaxation. The semiclassical action comparison is most reliable when the two localized levels remain nearly resonant throughout the modification and no higher intrawell level enters the same small energy window.

Independent measurements of the individual well minima supply a practical detuning calibration.

A phase accumulated by slowly turning a magnetic field

Quantum mechanics

A spin aligned with a slowly rotating field returns to its original measurement probabilities after one loop. Derive the additional phase that becomes observable when that path interferes with a reference path.

Separate following the state from acquiring a phase

Let a spin one-half have $H = -(\hbar\omega_0/2)\,\mathbf{n}(t)\cdot\boldsymbol{\sigma}$, with $\mathbf{n}$ a unit vector and constant $\omega_0 > 0$. The two instantaneous energies are separated by $\hbar\omega_0$. Prepare the lower-energy state and rotate $\mathbf{n}$ on a smooth path. If the rate of change of its eigenvector is small compared with the gap in angular-frequency units, transitions to the upper state are small. Following one eigenstate still allows a time-dependent complex phase.

Write $|\psi(t)\rangle = e^{i\alpha(t)}|n(t)\rangle$, substitute in the time-dependent Schrödinger equation and project onto $\langle n|$. Normalization makes $\langle n|\dot{n}\rangle$ imaginary. Consequently

$$\dot{\alpha} = -E_n/\hbar + i\langle n|\dot{n}\rangle.$$

The first contribution accumulates in proportion to elapsed time. The integral of the second depends on the path of the instantaneous eigenvector. The splitting into pieces changes with the arbitrary phase used to define $|n(t)\rangle$; after a closed loop the geometric phase in a single-valued gauge is invariant modulo 2π.

Evaluate a circle on the sphere of directions

Represent the aligned spin by the column $(\cos(\theta/2), e^{i\phi}\sin(\theta/2))^T$. Its mean spin points along the polar angles θ, ϕ. Hold θ fixed and increase ϕ by one revolution. Only the lower component contributes to the derivative. Its coefficient is its occupation weight:

$$i\langle n|\partial_\phi n\rangle = -\sin^2(\theta/2),$$

$$\gamma = -2\pi\sin^2(\theta/2) = -\pi(1-\cos\theta).$$

The solid angle enclosed by the latitude is $2\pi(1-\cos\theta)$, found by integrating $\sin\theta'\,d\theta'\,d\phi$ over the cap. The aligned spin accumulates minus half this angle. Reversing traversal changes its sign. As the cone closes to a point, the result vanishes continuously. Around the equator the result is $-\pi$.

Predict an interference fringe

Split a coherent preparation into two equal-amplitude paths and arrange the reference so the dynamical phases match. If only the signal path gains γ, an ideal balanced recombiner gives the bright-port probability $P = (1+\cos\gamma)/2$ for zero additional reference phase. The overall phase of one isolated spin would never produce this signal. The reference path supplies a phase comparison.

For $\theta = 60^\circ$, the solid angle is π, the geometric phase is $-\pi/2$, and $P = 1/2$. For a circuit of the equator the same port becomes dark. Reversing the 60° loop still gives one-half at zero reference phase. Introduce a known reference shift χ: the probability becomes $[1 + \cos(\chi + \gamma)]/2$ in the chosen convention. Choosing $\chi = \pi/2$ changes the two directions of traversal into full and zero probability, revealing the sign.

Scan the reference phase

Set the cone angle, then vary the reference phase. The horizontal axis scans the cone angle and the marker value is returned in the readout. A source with finite path coherence would reduce the modulation depth, whereas unmatched dynamical phases would shift the fringe.

Open this experiment online

Try the calculation

Cone angle (degrees) **60**

Reference phase (degrees) **0**

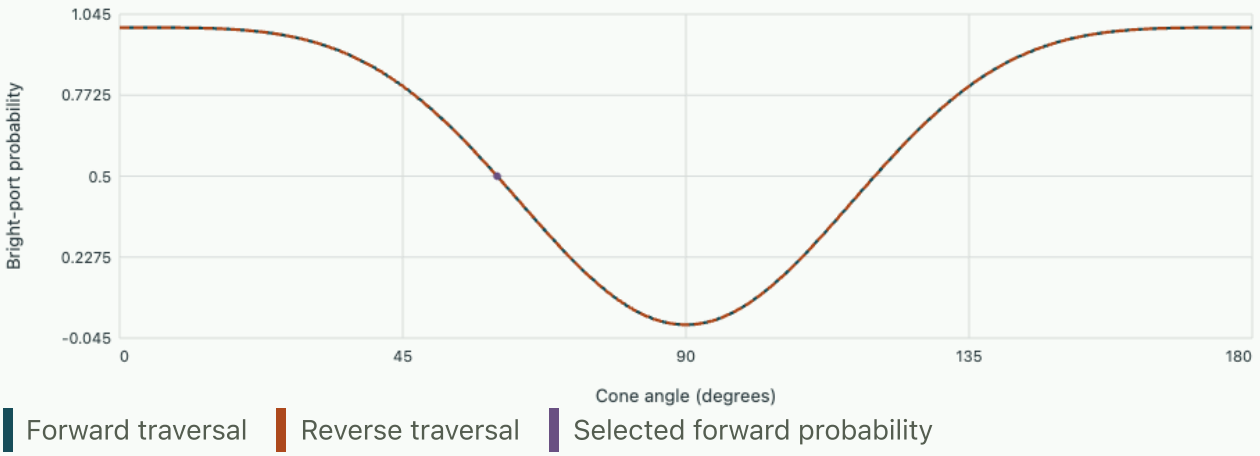

Forward geometric phase -0.5π radians. Forward port probability 0.5, reverse 0.5.

Tutorial on the following condition

A cone has angle 60°. At what rate scale does uniform azimuthal rotation stop being reliably adiabatic, and why can a change in loop duration alter a real experiment?

▼ **Work through the solution**

The off-diagonal eigenstate derivative has magnitude $|\dot{\phi}| \sin\theta/2$, so one requires $|\dot{\phi}| \sin\theta/(2\omega_0) \ll 1$. Increasing duration reduces that coupling but also changes the dynamical phase and can permit

decoherence. An interferometer must control both even when the ideal geometric phase has no dependence on duration.

Keep the cone angle at 60° but make two complete positive circuits before recombination. What probability appears at the bright port with zero reference phase? Would performing one forward and one reverse circuit give the same result?

▼ Work through the solution

Each positive traversal contributes $-\pi/2$. Two give $-\pi$, hence zero bright-port probability. A positive and negative traversal instead add to zero, giving unit probability when dynamical phases are matched. These outcomes test orientation and addition of the geometric phase over consecutive cycles.

Estimate the sensitivity to a cone-angle calibration error at 60°. Express the first-order phase error for one angular degree.

▼ Work through the solution

Differentiating in radians gives

$$d\gamma/d\theta = -\pi \sin\theta.$$

Multiplication by $\pi/180$ yields -0.0475 radians of phase error per added degree at 60°. At a port fringe extremum the intensity change from this small phase error begins quadratically. Near a half-bright fringe it appears linearly and is easier to detect.

Further reading · Tong, Topics in Quantum Mechanics, adiabatic theorem and Berry phase.

A magnetic orbit that spirals outward in a perfect vacuum

Numerical field laboratory

Track a charged particle in a prescribed uniform field, derive a rotation update and separate numerical energy growth from a real magnetic force.

Use the work law before solving the trajectory

A nonrelativistic charged particle of mass m and charge q moves perpendicular to a uniform, time-independent magnetic field $B\hat{\mathbf{z}}$. There is no electric field and the dilute test particles do not affect the applied field. The Lorentz force gives $\dot{v}_x = \omega v_y,\ \dot{v}_y = -\omega v_x$ for $\omega = qB/m$. Dotting with $\mathbf{v}$ gives zero, so the speed should stay constant. This property holds for either sign of the charge; the direction of rotation changes. It is a better initial test of a trajectory solver than how circular a short segment looks on screen.

Define $J(v_x, v_y) = (v_y, -v_x)$, so $J^T = -J$ and $J^2 = -I$. The exact velocity over a time step h is $[\cos(\omega h)I + \sin(\omega h)J]\mathbf{v}$. Integration in time gives a circular orbit of radius $v_\perp/|\omega|$ once the guiding centre is chosen. A magnetic field alone bends a trajectory without changing its kinetic energy; a slowly growing orbit radius at fixed B and fixed initial speed demands an explanation.

Why forward Euler adds energy at every step

Euler gives $\mathbf{v}_+ = (I + dJ)\mathbf{v}$ with $d = \omega h$. Squaring the norm eliminates the cross term because $v^T J v = 0$, leaving $\|\mathbf{v}_+\|^2 = (1 + d^2)\|\mathbf{v}\|^2$. No nonzero step has exact unit gain. A geometric picture makes the bias tangible: a tangent step leaves the initial velocity circle on its outside, whatever the point of departure.

After N steps the speed factor is $(1 + d^2)^{N/2}$. With 24 steps per physical orbit, $d = 2\pi/24 \simeq 0.2618$, so a full orbit multiplies speed by roughly 2.2. At shorter times or smaller steps this can resemble weak physical acceleration. Reducing h at fixed physical duration reduces the growth. Testing one step at fixed count, rather than comparing over a fixed physical interval, underestimates the cumulative error.

Solve a centred magnetic step exactly

Use the time-centred velocity in the Lorentz force:

$$\mathbf{v}_+ - \mathbf{v} = dJ(\mathbf{v}_+ + \mathbf{v})/2.$$

Premultiply by the transpose of $\mathbf{v}_+ + \mathbf{v}$. The left side is the difference of squared speeds and the right side vanishes, so the update preserves speed for every d in exact arithmetic. Rearranging yields a two-dimensional linear solve; using $J^2 = -I$ turns it into a rotation,

$$\mathbf{v}_+ = \frac{1 - t^2}{1 + t^2}\mathbf{v} + \frac{2t}{1 + t^2}J\mathbf{v},$$

$$t = d/2.$$

These coefficients are $\cos\alpha$ and $\sin\alpha$ for $\alpha = 2\arctan(d/2)$. This is the magnetic rotation used in the nonrelativistic Boris integrator. For simultaneous electric fields, the usual split step adds two half electric impulses around the magnetic rotation. The current experiment isolates the magnetic part; it makes no claim about a nonuniform electric field or the accuracy of interpolation from a field mesh to particles.

Open the live experiment

Try the calculation

Steps per exact orbit **24**

Number of orbits **4**

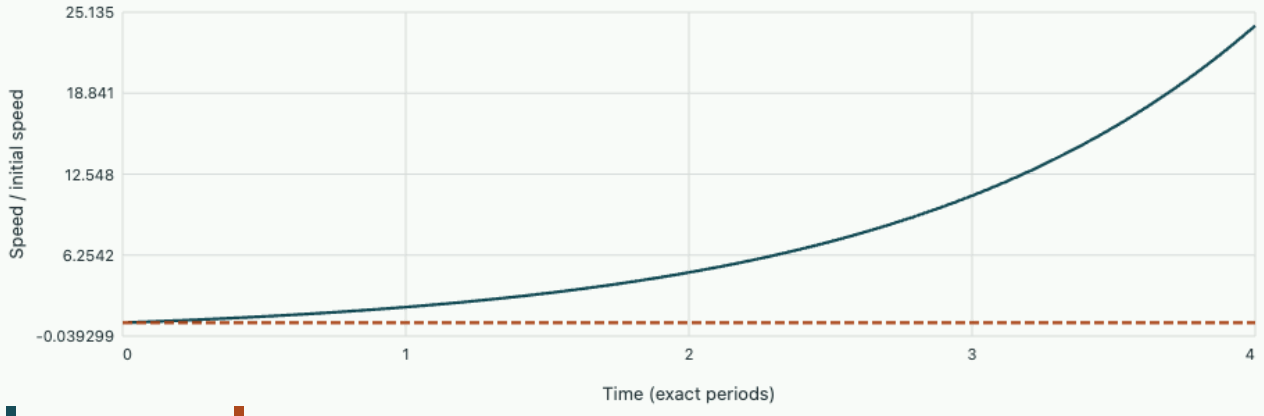

After 4 orbit(s), Euler speed 24.096, rotation speed 1. Rotation still lags the exact phase by 8.1411°.

Speed conservation does not fix arrival time

At small d,

$$\alpha = d - d^3/12 + O(d^5).$$

A speed-preserving orbit lags in gyrophase, even when its energy plot stays perfectly flat. After four true orbits at 24 steps per orbit the predicted lag is about 8.14 degrees. The browser advances the Euler and rotation velocities and reports both norm and lag. The y-axis rescales to fit both curves, so a sharply growing Euler error can flatten the appearance of the well-behaved curve. Inspect numerical values as well as the picture.

Suppose an optical pickup observes the time at which a dilute ion tracer first crosses a known line of sight after several orbits. A phase error can be an important measurement error even when the speed is exact. To use the trajectory as a reference, refine the step until the crossing time changes by less than the experimental timing resolution. If the required integration spans many revolutions, a uniform field permits exact substeps. In realistic fields one can retain a structure-preserving rotation while resolving spatial variation independently.

A separate diagnostic is time reversal. Starting from the final velocity and applying the rotation with $-d$ exactly inverts a centred step, up to rounding. Forward Euler with $-d$ after $+d$ gives

$$(I - dJ)(I + dJ) = (1 + d^2)I.$$

A forward/backward test detects the lost reversibility without knowing a single experimental constant.

Tutorial

Given an orbit with 48 steps per period, estimate the gyrophase error after ten periods using the leading asymptotic term.

▼ **Work through the solution**

There are 480 steps with $d = 2\pi/48$. The accumulated lag is about $480d^3/12 \simeq 0.0897$ rad, or 5.14 degrees. Doubling the number of steps per period reduces the leading accumulated error fourfold.

A computation preserves speed but reverses the sign of its orbit relative to observation. Would the magnetic work test detect the error?

▼ **Work through the solution**

Both field signs give zero work. Check a signed initial acceleration component $a_y = -qBv_x/m$ for a positive initial v_x, or observe the oriented trajectory. A scalar invariant cannot detect all vector-sign errors.

What changes in the relativistic case with appreciable kinetic energy?

▼ **Work through the solution**

Evolve momentum $\mathbf{p} = \gamma m\mathbf{v}$ and infer velocity from momentum. In a uniform magnetic field without electric work γ stays constant, and the orbital frequency is reduced to $|q|B/(\gamma m)$. An energy-preserving nonrelativistic integration at the wrong frequency would still give the wrong measured period.

How a turning point supplies the missing semiclassical phase

Quantum states, dynamics and measurement

Far from a turning point the wavelength follows the classical momentum. At the turning point that approximation becomes singular. Derive the Airy connection, quantise a smooth well, distinguish a hard wall and estimate a tunnelling exponent with a defensible error check.

Expand the action before interpreting a local wavelength

For a stationary one-dimensional state with smooth potential $V(x)$, write $\psi = e^{iS(x)/\hbar}$. Substitution into Schrödinger's equation gives

$$S'^2 - i\hbar S'' = 2m(E - V) = p^2(x).$$

Expand $S = S_0 + (\hbar/i)S_1 + \cdots$. The leading terms give $S_0' = \pm p$ and $S_1' = -p'/(2p)$ in an allowed region where $p > 0$. Thus travelling waves have form $Cp^{-1/2}\exp[\pm i\int^x p\,dx/\hbar]$. The amplitude factor is physically essential: for a single such branch the current to leading order is $\pm|C|^2/m$, independent of x, as required for steady flux in a real potential. A constant amplitude with variable wavenumber would predict current piling up in a stationary region.

A local condition for this expansion is $\hbar|p'|/p^2 \ll 1$ together with control over higher derivatives on the wavelength scale. Away from a barrier the phase can remain accurate even if absolute amplitude normalisation must be fixed globally. Where $E < V$, define $\kappa = \sqrt{2m(V - E)}$ with units of momentum. The local solutions become $\kappa^{-1/2}\exp[\pm\int \kappa\,dx/\hbar]$. A single real decaying branch carries zero probability current by itself. Stationary tunnelling flux through a finite barrier involves a complex combination satisfying both exterior matching conditions, even though the leading size of transmission can often be inferred from the decaying exponential.

Resolve the apparent divergence near a simple turning point

Let x_t satisfy

$$V(x_t) = E,$$

with slope $F = V'(x_t) > 0$. Linearise $V - E \simeq F(x - x_t)$. The local Schrödinger equation becomes

$$\psi'' = (2mF/\hbar^2)(x - x_t)\psi.$$

Introduce length $\ell = (\hbar^2/(2mF))^{1/3}$ and $\xi = (x - x_t)/\ell$, leaving $d^2\psi/d\xi^2 = \xi\psi$. Its two independent solutions are Ai and Bi. On the positive side $\mathrm{Ai}(\xi)$ decays, whereas $\mathrm{Bi}(\xi)$ grows. A bound state extending into a semi-infinite forbidden region selects the former. At $\xi = 0$ the Airy function is finite; the apparent divergence $p^{-1/2}$ came from extending the outer approximation beyond its range.

The asymptotic forms for $s > 0$ large are

$$\mathrm{Ai}(s) \sim \frac{e^{-2s^{3/2}/3}}{2\sqrt{\pi}\, s^{1/4}}, \qquad \mathrm{Ai}(-s) \sim \frac{\sin(2s^{3/2}/3 + \pi/4)}{\sqrt{\pi}\, s^{1/4}}.$$

For a linear slope, $2s^{3/2}/3$ equals $|\int_{x_t}^{x} p\, dx|/\hbar$ on the allowed side or $\int_{x_t}^{x} \kappa\, dx/\hbar$ on the forbidden side. Matching in an interval where $|x - x_t| \gg \ell$ but the potential remains effectively linear gives the connection from a decaying tail of coefficient C to $2C\, p^{-1/2} \sin[\hbar^{-1} \int_{x}^{x_t} p\, dx + \pi/4]$. The coefficient two and phase $\pi/4$ both come from the same local solution. A turning point with zero slope, a sharp step or two turning points closer than their Airy lengths requires a different local treatment.

Join two decaying tails to a standing wave

For a smooth well with two well-separated simple turning points x_1, x_2, the left tail matches to $\sin[\hbar^{-1} \int_{x_1}^{x} p\, dx + \pi/4]$. The right tail matches to $\sin[\hbar^{-1} \int_{x}^{x_2} p\, dx + \pi/4]$. Their zeros and logarithmic derivatives must coincide throughout the overlap, up to an overall sign. The sum of the two phase arguments is the full one-way action divided by $\hbar$ plus $\pi/2$, which must be an integer multiple of π. Taking $n \geq 0$ gives

$$\int_{x_1}^{x_2} p(x, E_n)\, dx = \pi\hbar(n + 1/2).$$

For a harmonic oscillator the turning point magnitude is $a = \sqrt{2E/(m\omega^2)}$ and $p = m\omega\sqrt{a^2 - x^2}$. The action is the area of a semicircle times $m\omega$, equal to $\pi E/\omega$. The rule reproduces $E_n = \hbar\omega(n + 1/2)$ exactly for this special spectrum, even though its outer WKB wavefunction is still inaccurate near each turning point and globally for low quantum number. Equality of a spectral result does not imply equality of spatial densities or agreement of all observables.

Different boundaries change the phase budget. Take a hard wall at $x = 0$ and a linearly rising potential Fx for $x > 0$. The solution decaying to the right is $\mathrm{Ai}[(x - E/F)/\ell]$. Its exact energies follow from $\mathrm{Ai}(-E/F\ell) = 0$. The wall imposes a node without an Airy phase at the left. Setting the right-matched standing wave to zero at the wall gives

$$\int_{0}^{E/F} p\, dx = \pi\hbar(n + 3/4).$$

Thus $E/(F\ell) \simeq [3\pi(n + 3/4)/2]^{2/3}$. For $n = 0$ this is about 2.320 versus the first exact zero 2.338; with $n = 4$ the approximation is about 7.94. Replacing the wall by a second smooth turning point would instead introduce an erroneous half offset.

Separate a credible exponential estimate from its prefactor

For a barrier with two simple turning points x_a, x_b, a large forbidden action $I = \int_{x_a}^{x_b} \kappa\, dx/\hbar$ suppresses the transmitted flux approximately as $T \simeq e^{-2I}$, up to prefactors and corrections that depend on

geometry and matching. For a triangular forbidden region with height $V_0 - E = \Delta$ at $x = 0$ falling as $\Delta - Fx$ to zero at Δ/F, its action is $I = 2\sqrt{2m}\Delta^{3/2}/(3\hbar F)$. A discontinuous incident-side boundary may affect the prefactor substantially. It does not justify assigning a second smooth-turning-point phase to the discontinuity. For a rectangular barrier the exact thick-barrier prefactor is $16E(V_0 - E)/V_0^2$ times the decaying exponential at equal exterior potentials. It can exceed one while total transmission remains small.

Suppose two measurements change only the forbidden width of a flat barrier from d to $d + \Delta d$, keeping both interfaces and asymptotic energies the same. In the thick limit the ratio $T(d + \Delta d)/T(d) \simeq e^{-2\kappa \Delta d/\hbar}$ cancels the common prefactor. If $\kappa/\hbar = 2.0\,\mathrm{nm}^{-1}$ and $\Delta d = 0.50$ nm, this ratio is

$$e^{-2} = 0.1353.$$

An offset error in barrier width that leaves this ratio unchanged can still cause a large error in absolute transmission. Near the top two turning points can merge, I becomes small, and the raw exponential lacks a unitary connection to the over-barrier reflection regime. Use a suitable uniform approximation or a direct scattering solution there.

Predict a high-energy spectrum without a closed-form wavefunction

Consider a pure quartic trap $V(x) = \lambda x^4$ with $\lambda > 0$. Classical turning points lie at $x = \pm a,\ a = (E/\lambda)^{1/4}$. Unlike the harmonic oscillator its period changes with energy, so its levels cannot be equally spaced. The semiclassical action can be evaluated once in dimensionless coordinates and then rescaled to any m, λ, E:

$$A(E) = \int_{-a}^{a} \sqrt{2m(E - \lambda x^4)}\, dx = 2\sqrt{2m}\, \lambda^{-1/4} E^{3/4} I_4,$$

$$I_4 = \int_0^1 \sqrt{1 - y^4}\, dy.$$

With $s = y^4$,

$$I_4 = \frac{1}{4} B(1/4, 3/2) \simeq 0.8740.$$

Quantising $A(E_n) = \pi\hbar(n + 1/2)$ predicts $E_n \simeq [\pi\hbar(n + 1/2)\lambda^{1/4}/(2\sqrt{2m} I_4)]^{4/3}$. The dependence $E \propto n^{4/3}$ and the dimensional factor $\hbar^{4/3}\lambda^{1/3}m^{-2/3}$ can be checked independently from scaling the full Schrödinger equation. That dimensional argument does not supply the coefficient or the half-integer offset. The action and boundary phases supply the additional physics.

Choose units such that $H = -d^2/dx^2 + x^4$. Then $2m = \hbar = 1$ in the scaled equation, and the leading energies are $[\pi(n + 1/2)/(2I_4)]^{4/3}$. For $n = 0$ this gives about 0.868, below the accurately computed ground value around 1.060. An independent variational Gaussian $\psi = (\beta/\pi)^{1/4} e^{-\beta x^2/2}$ has energy

$\beta/2 + 3/(4\beta^2)$, minimised at $\beta^3 = 3$ and giving 1.082. Its proximity to the true ground energy has a different status: the Gaussian energy is an upper bound by the variational principle, while leading WKB provides no universal bound for this potential. Using agreement between two approximate numbers as proof of a rigorous interval would require actual lower and upper estimates.

At larger n the period relation provides an additional prediction. Since $A \propto E^{3/4}$,

$$T_{\mathrm{cl}} = 2\,dA/dE \propto E^{-1/4};$$

the frequency increases at larger amplitude, and the local spacing should grow as $E^{1/4}$. Numerically compute a handful of high levels with a direct finite-difference or spectral Hamiltonian, then plot $E_n^{3/4}$ against $n + 1/2$. A nearly linear trend is a more sensitive diagnostic of the predicted law than comparing a single apparent power from a log plot at low n. Increase domain size and basis cutoff independently. A truncation that confines high-energy tails can falsely steepen the spacing, while a coarse grid can flatten the kinetic-energy dispersion. Both errors become more visible for rapidly oscillating states.

Relate a barrier action to a coherent population oscillation

Take two identical minima separated by a smooth barrier. At energies below the barrier top but above each isolated-well ground, there are two classically allowed intervals and a central forbidden region. If the barrier is sufficiently opaque, construct approximate localised states $|L\rangle, |R\rangle$ with equal one-well energy E_0. In their span the simplest symmetric Hamiltonian is $H = E_0 I - J(|L\rangle\langle R| + |R\rangle\langle L|)$ with $J > 0$ in a suitable phase convention. The even and odd combinations have energies $E_0 - J, E_0 + J$. The tunnel splitting is $2J$, set to leading exponential order by the overlap of amplitudes through the central forbidden interval.

A single under-barrier wavefunction amplitude carries e^{-I},

$$I = \int \kappa dx/\hbar.$$

For an open barrier the transmission probability is proportional to e^{-2I}. For a symmetric double-well splitting the relevant quantity is a coherent off-diagonal energy amplitude, so its leading exponential is $J \propto e^{-I}$, times a prefactor involving the oscillation scales and matching in the two wells. Confusing these exponents can lead to a severe error when using a calculated spatial barrier to predict a coherent tunnel frequency. The exact prefactor depends on the potential and turning-point normalisations. A direct symmetric numerical eigenproblem giving the difference of two nearly equal energies requires enough precision to resolve an exponentially small splitting.

Prepare $|L\rangle$ at time zero. Its evolution under the two-state Hamiltonian gives

$$P_R(t) = \sin^2(Jt/\hbar);$$

the first full transfer time is $\pi\hbar/(2J)$. If the observed energy splitting expressed as ordinary frequency is $2J/h = 20$ Hz, the first transfer occurs at 25 ms. Changing only the barrier action by $+0.70$ at fixed prefactor multiplies the splitting by $e^{-0.70} = 0.497$ and approximately doubles the transfer time. An

open-barrier transmission experiment over the same change instead sees factor $e^{-1.4} = 0.247$. Both tests depend exponentially on barrier shape but interrogate different quantities.

Now add a calibrated tilt $\epsilon = E_L - E_R$. The 2×2 Hamiltonian after trace subtraction is $(\epsilon/2)\sigma_z - J\sigma_x$, and the maximum transfer falls to $4J^2/(\epsilon^2 + 4J^2)$. At $\epsilon = 2J$ it is one half while the oscillation angular frequency increases from $2J/\hbar$ to $2\sqrt{2}J/\hbar$. A loss of transfer contrast need not be environmental decoherence; static tilt alone yields this combination of increased frequency and reduced amplitude. Measuring both quantities and reversing the tilt tests the two-level model. If a higher intrawell level lies within the tilt or excitation range, a single tunnelling doublet no longer spans the relevant motion and a larger basis is required.

Understand the angular correction at a radial turning point

In three dimensions the reduced radial equation on $r > 0$ has a centrifugal term $\hbar^2 l(l+1)/(2mr^2)$. Applying the flat-coordinate WKB rule directly to this equation can give incorrect phases at its singular endpoint, especially for low l. A way to see the appropriate angular correction without guessing is to set $r = r_0 e^x$, mapping the half-line to all real x, and write $u(r) = e^{x/2} w(x)$. The arbitrary reference r_0 keeps the logarithm dimensionless. Since $d/dr = r^{-1} d/dx$, differentiating twice yields

$$\frac{d^2u}{dr^2} = \frac{e^{x/2}}{r^2}\left(w'' - \frac{1}{4}w\right).$$

The resulting equation for w has squared local action momentum in x proportional to $2mr^2(E - V) - \hbar^2(l + 1/2)^2$. Thus returning its action $\int p_x dx$ to r uses $l(l+1) \to (l+1/2)^2$ in the radial semiclassical momentum. This is the Langer correction. It does not change the exact angular eigenvalue $L^2 = \hbar^2 l(l+1)$; it accounts for the coordinate transformation and endpoint behaviour of the semiclassical representation. Confusing those statements would alter the exact radial equation to repair an approximate integration rule.

An instructive check is the isotropic oscillator. For $V = m\omega^2 r^2/2$ and effective classical angular momentum $L = (l + 1/2)\hbar$, the radial action over its two roots is

$$A_r = (\pi/2)(E/\omega - L).$$

One can obtain this without an explicit contour integral by noting that radial motion repeats at twice the Cartesian frequency, so

$$dA_r/dE = \pi/(2\omega).$$

Fix the integration constant at the circular-orbit threshold $E = \omega L$, where the two radial turning points meet and $A_r = 0$. Quantising $A_r = \pi\hbar(n_r + 1/2)$ gives $E = \hbar\omega(2n_r + l + 3/2)$, matching the exact three-dimensional oscillator spectrum. For $l = 0$ the naive uncorrected centrifugal term has no inner turning point; transferring a generic two-smooth-turning-point formula into that half-line problem without reconsidering its origin is especially unsafe.

Calculate an exponentially small transmission without subtracting nearly equal numbers

In a classically forbidden interval the local solution contains a growing and a decaying branch. In a long interval numerical transfer matrices can contain elements as large as e^{I}, while the quantity sought is as small as e^{-2I}. Straight propagation of a decaying boundary condition in the unstable direction can contaminate it with a tiny growing roundoff component which eventually dominates. A plot matching the expected slope over the first few decay lengths gives no guarantee that a final tiny flux is accurate. Numerically stable alternatives include propagating a logarithmic derivative with controlled handling of its poles, matching independently normalised left and right solutions, or composing scattering matrices for short slices while retaining decaying propagation factors.

For a square barrier the exact transmission at $E < V_0$ in equal exterior regions is $T = [1 + V_0^2 \sinh^2(\kappa d/\hbar)/(4E(V_0 - E))]^{-1}$. With $E = V_0/2$ this simplifies to $\operatorname{sech}^2 I$. At $I = 20$ its value is approximately $4e^{-40} = 1.70 \times 10^{-17}$. Computing $T = 1 - R$ in ordinary double precision can give exactly zero since the reflection probability rounds to one. Compute transmitted amplitude or its logarithm directly and compare $\log T \simeq \log 4 - 2I$. At a moderate I, where both currents are accurately representable, independently verify $R + T = 1$. Moving the benchmarking point across the barrier-opacity range tests both the physical approximation and the floating-point representation of the desired observable.

Resolve a wave through a classical turning point

Vary the physical length scale in a locally linear potential. Compare the numerical Airy solution and the two semiclassical branches near and away from the turn.

Open this experiment online

Try the calculation

Turning-point length (nm) **0.8**

Turning-point position (nm) **0.4**

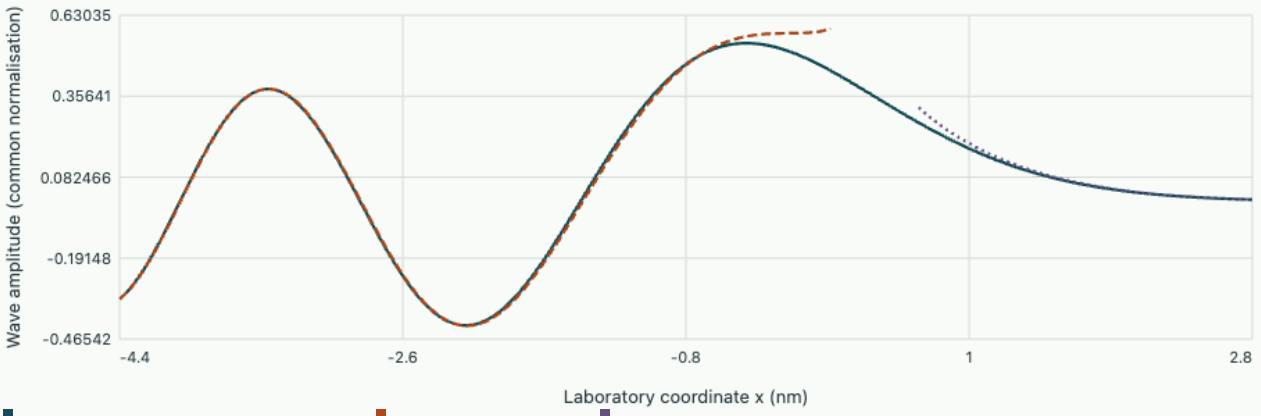

Numerically integrated Ai | Allowed WKB | Forbidden WKB

The turn at 0.4 nm has finite Ai value 0.35503. The characteristic transition length is 0.8 nm; the asymptotic curves omit the nearest 0.35 lengths.

Connect semiclassical action to counting states in phase space

The action quantisation rule can also be read as a statement about the number of energy levels below a chosen energy. In a one-dimensional smooth confining well the classically accessible region in (x, p) has area $\Omega(E) = \int dx \int_{-p(x)}^{p(x)} dp = 2A(E)$. Roughly one stationary state fits per phase-space area $2\pi\hbar$, with an endpoint correction from the turning-point phases. The smoothed density of states follows by differentiating $\bar{N}(E) \simeq \Omega(E)/(2\pi\hbar)$, giving $\bar{\rho}(E) = T_{\mathrm{cl}}/(2\pi\hbar)$. This counts levels after smoothing over individual spacing; the exact count is a staircase and its derivative a sum of delta functions. A formula for a smooth density cannot predict each state in a near-degenerate doublet without additional phase and tunnelling information.

For a particle in a two-dimensional rigid rectangular region, apply the same counting idea in four-dimensional phase space. With area $\mathcal{A} = L_x L_y$, accessible momentum disk $p_x^2 + p_y^2 < 2mE$, the scalar smoothed count is $\bar{N}(E) \simeq \mathcal{A}\pi(2mE)/(2\pi\hbar)^2 = \mathcal{A}mE/(2\pi\hbar^2)$. Its derivative is a constant, unlike the $E^{-1/2}$ free one-dimensional density and the $\sqrt{E}$ three-dimensional density. This leading area law can be checked by directly counting positive integer lattice points satisfying $(n_x\pi/L_x)^2 + (n_y\pi/L_y)^2 < k^2$ in a Dirichlet rectangle. It works after smoothing when many modes fit in the domain and makes no assumption that the rectangular shape itself models all possible billiards.

A more sensitive check accounts for the excluded axes in that first-quadrant lattice count. For a Dirichlet rectangle subtract half of the positive-axis contributions at each boundary of the quadrant. In terms of perimeter $\mathcal{P} = 2(L_x + L_y)$, the resulting first two terms are $\bar{N}(k) \simeq \mathcal{A}k^2/(4\pi) - \mathcal{P}k/(4\pi) + O(1)$ after appropriate smoothing, with fluctuations from discrete modes beyond this local expansion. Neumann boundaries reverse the sign of the perimeter term because modes constant along one

coordinate are admitted. Area alone determines the bulk growth, whereas boundary condition affects the next correction. The finite corner term and spectral fluctuations require more care than assigning one universal integer offset to every billiard.

The distinction between smoothing and exact prediction also explains why counting every computed eigenvalue only up to an arbitrarily sharp threshold can produce apparent convergence jumps as the mesh improves. If a true eigenvalue lies near the threshold, a small numerical shift changes an integer count by one. Compare a range of cumulative counts, track nearby eigenvalue residuals and study the smoothed density with a bandwidth large enough to include several levels but small compared with the energy scale of interest. Repeating for two geometries of equal area and different perimeter tests actual geometric information beyond an overall energy scale.

Measure the boundary correction in a square cavity

A scalar mode calculation uses a square of side 10.0 length units and reports all Dirichlet modes with $k < 5.00$ inverse length units. Find the leading area estimate, add the perimeter correction, and compare with a direct lattice-point count.

▼ **Derive and check the result**

The area contribution is $100(25)/(4\pi) = 198.94$; the perimeter subtraction is $40(5)/(4\pi) = 15.92$, giving a smoothed estimate 183.03 before corner and oscillatory terms. The exact count uses positive integers n_x, n_y satisfying $n_x^2 + n_y^2 < (50/\pi)^2 \simeq 253.30$. For each $n_x = 1, \ldots, 15$, count $n_y \le \lfloor \sqrt{253.30 - n_x^2} \rfloor$ and sum. The values are $15, 15, 15, 15, 15, 14, 14, 13, 13, 12, 11, 10, 9, 7, 5$, giving 183. Agreement at this threshold is close, while the leading area term alone is about sixteen high. Nearby thresholds can have different residual fluctuations, so the close integer agreement at this one wave number should not be treated as an exact two-term counting rule. The same calculation on a different aspect ratio at fixed area would change both the perimeter and the lattice pattern.

Measure a reflection phase separately from the travel action

In a one-dimensional cavity a quantisation condition can be written as a round-trip phase budget. Let an allowed region accumulate one-way phase $\theta(E)$ and let reflections at its left and right bounding regions have phase shifts $\phi_L(E), \phi_R(E)$ for unit-modulus reflection. A self-reproducing wave requires

$$2\theta(E) + \phi_L(E) + \phi_R(E) = 2\pi n,$$

with an integer depending on the chosen phase origin. A rigid Dirichlet wall reflects with amplitude -1; a smooth decaying turning point contributes a different reflection phase that the Airy matching fixed. Adding 2π to one reflection phase simply relabels the integer, but an energy-dependent boundary phase alters the spacing and cannot be removed by a constant relabelling.

A useful boundary that can be solved without approximation is a finite step $V = 0$ for $x < 0$, $V = V_0 > E$ for $x > 0$. With incident wave e^{ikx}, reflected amplitude re^{-ikx} and exterior evanescent $te^{-\kappa x}$, where k, κ here are inverse lengths, continuity of the value and derivative gives

$$1 + r = t,\ ik(1 - r) = -\kappa t.$$

Solving yields

$$r = (k - i\kappa)/(k + i\kappa).$$

Its magnitude is one and its phase can be written $-2\arctan(\kappa/k)$. As V_0 tends to infinity with E fixed, the phase tends to $-\pi$, giving the rigid-wall limit. Just below the step threshold it approaches zero. Two mirrors with equally complete reflection can therefore produce different cavity eigenfrequencies.

Near the rigid-wall limit expand $r \simeq -e^{2ik/\kappa}$. To leading order the exterior behaves like a rigid reflecting plane displaced a penetration length $1/\kappa$ beyond the interface. For a deep symmetric finite well of width L, the phase condition approximately replaces L by $L + 2/\kappa(E)$. This shift lowers levels relative to a rigid well of the same geometric width. It is only an approximation because penetration depends on energy. Matching logarithmic derivatives independently on the two sides is preferable near threshold or when the barrier shape varies over the penetration length.

Infer a boundary penetration from a measured free spectral interval

A long one-dimensional cavity with identical deep finite barriers has a measured low-mode wavenumber interval 2% smaller than π/L. Under the constant penetration approximation infer $1/\kappa$ relative to L and identify a check on the approximation.

▼ **Derive and check the result**

Set $\pi/(L + 2/\kappa) = 0.98\pi/L$. Then $2/\kappa L = 1/0.98 - 1 = 0.0204$, or a penetration distance $1/\kappa = 0.0102L$ at each wall. For $L = 100$ nm this is about 1.02 nm. Measure several successive intervals to see whether one penetration length describes them. An increasing penetration with energy changes the reflection-phase derivative and therefore the spacing; the physical group delay then contains travel time in the allowed region plus boundary delay. A geometrically longer rigid cavity would produce a similar single interval but a different energy dependence, so an isolated observation does not uniquely identify the cause.

Tutorial · determine what a semiclassical estimate can certify

Recover the period and level spacing from an action curve

For $A(E) = \int_{x_1}^{x_2} p\,dx$ in a smooth bound well, derive dA/dE and infer the local energy spacing. Apply it to a 100 kHz oscillator and express spacing in both joules and electronvolts.

▼ **Work through the solution**

The endpoint derivative terms vanish because $p = 0$ at both ends. Inside, $\partial p/\partial E = m/p = 1/v$, so dA/dE equals the classical one-way travel time $T_{\mathrm{cl}}/2$. From the quantisation rule increasing n by one gives local spacing $\Delta E \simeq 2\pi\hbar/T_{\mathrm{cl}} = h f_{\mathrm{cl}}$. At 100 kHz this is 6.626×10^{-29} J or 4.136×10^{-10} eV. In an anharmonic potential the classical period generally depends on energy; use the local slope or integrate between adjacent solutions rather than assuming a universal ladder spacing.

Check whether the Airy overlap interval exists

For a model atom with mass 1.44×10^{-25} kg let $F = 1.0 \times 10^{-21}$ N at the turning point. Find the Airy length. If $|V''| = 1.0 \times 10^{-16}\,\mathrm{N/m}$, estimate the relative quadratic correction at 5ℓ.

▼ **Work through the solution**

The length is $(\hbar^2/2mF)^{1/3} \simeq 3.38 \times 10^{-8}$ m. The ratio of quadratic potential term to linear term at 5ℓ is $|V''|5\ell/(2F) \simeq 0.00845$. Thus several Airy lengths can fit in a region with small curvature correction for these numbers. The parameter $|x - x_t|/\ell = 5$ should still be checked against the desired asymptotic precision; the result supports an overlap interval but does not guarantee a prescribed decimal accuracy. Bringing a second turning point within a few such lengths changes the matching problem qualitatively.

Compare a triangular action with a rectangular shortcut

A linearly falling barrier has initial forbidden wavenumber $\kappa_0/\hbar = 3.0\,\mathrm{nm}^{-1}$ and width $d = 2.0$ nm. Compare its exponential estimate with that of a rectangle using initial height throughout. What would a rectangle at the average potential height predict?

▼ **Work through the solution**

For the triangle, $\kappa(x) = \kappa_0\sqrt{1 - x/d}$, so $I = (2/3)(\kappa_0/\hbar)d = 4.0$, giving $e^{-8} = 3.35 \times 10^{-4}$. The initial-height rectangle gives $I = 6$ or $e^{-12} = 6.14 \times 10^{-6}$. Averaging the potential height first gives wavenumber $\kappa_0/\sqrt{2}$, $I = 4.24$ and $e^{-8.49} \simeq 2.06 \times 10^{-4}$. The action averages the square root of the local energy gap, not the gap itself. Agreement in mean barrier height is insufficient for predicting an exponential observable. Exact matching or a direct numerical probability current would be needed to determine the prefactor.

Further reading

- Fließbach · Näherungsmethoden
- Cambridge · WKB, Airy matching and semiclassical quantisation
- Course investigation · semiclassical quantisation and tunnel splitting

Ensembles, thermodynamic potentials and measurable curvature

Statistical mechanics from microscopic counting to material response

A sample sealed inside an insulated container, a sample weakly coupled to a temperature bath and a surface exchanging particles with a reservoir need different probability laws. Derive the three laws from one composite-system count. Then use the curvature of their generating functions to predict noise, response and parameter uncertainty without assuming that microscopic quantities take their mean values in every run.

Expand the reservoir count rather than postulating a probability

Let a small system occupy a microstate i of energy E_i while a weakly coupled reservoir holds the remainder of a fixed total energy. The composite system is isolated. Conditional on i, the number of compatible reservoir states is $\Omega_R(E_{\text{total}} - E_i)$. This weight is the same for degenerate system microstates of equal energy. For a macroscopic reservoir, expand its entropy about an appropriate reference energy. The first derivative is $1/T$, and its second derivative at fixed other extensive parameters is $-1/(T^2 C_R)$.

$$S_R(E_R - \epsilon) = S_R(E_R) - \frac{\epsilon}{T} - \frac{\epsilon^2}{2T^2 C_R} + \cdots.$$

Exponentiating and taking the limit where the quadratic and further corrections are negligible yields $p_i = e^{-\beta E_i}/Z$, $\beta = 1/(k_B T)$, and $Z = \sum_i e^{-\beta E_i}$. A constant shift in all system energies multiplies both numerator and partition sum by the same factor. Relative probabilities are therefore independent of energy-zero convention. If a calculation sums over energy values rather than microstates, insert their degeneracies explicitly. These two equivalent ways of counting should never be applied simultaneously.

The derivation assumes weak coupling so that assigning energies separately makes sense, and a reservoir whose temperature does not respond significantly to typical exchanges. A small heat capacity in the bath can suppress sample fluctuations even at the same mean temperature. The relevant test concerns excursions explored by the sample, not simply whether the bath contains more particles. Near a transition or in an engineered small reservoir a canonical distribution may need a measurable correction.

Compare sample-energy fluctuations for finite and effectively infinite heat reservoirs

Differentiate the normalisation to obtain energy and its variance

Differentiate $\log Z$ with respect to β at fixed energy levels. The first derivative yields minus mean energy. A second derivative gives the mean square minus the squared mean. Changing differentiation from β to temperature gives the equilibrium heat capacity:

$$\langle E \rangle = -\partial_\beta \log Z,$$

$$\operatorname{var}(E) = \partial_\beta^2 \log Z = k_B T^2 C_V.$$

This proves nonnegative canonical heat capacity for a temperature-independent Hamiltonian. If the model Hamiltonian contains parameters that themselves vary with temperature after other degrees of freedom have been eliminated, the derivative also acts on those parameters. Inserting measured effective levels into the simple identity without that dependence need not reproduce the calorimetric capacity.

A two-level system has energies zero and Δ, with upper probability $p = 1/(1 + e^{\beta\Delta})$ for equal degeneracies. Its variance is $\Delta^2 p(1-p)$ and $C/k_B = (\beta\Delta)^2 p(1-p)$. At $\Delta/k_B T = 2$, $p = 0.1192$ and $C = 0.420 k_B$. In one thousand independent copies the expected upper count is 119 and its standard deviation about 10.2. An actual count of 130 is unremarkable. An experiment resolving only one sample at one time cannot identify the variance from its energy alone.

Higher derivatives of $\log Z$ generate cumulants. A Gaussian approximation discards cumulants beyond the second. For a small two-level population near low occupancy the histogram is skewed and the approximation can yield artificial negative occupancies. An exactly binomial count or a direct discrete partition sum handles this elementary case without assuming that the central-limit regime has arrived. Sample-to-sample correlations can also prevent variances from scaling as the sum of independent variances.

Why the Helmholtz free energy knows the same equilibrium as entropy

Group the canonical sum by energy. A shell with entropy $S(E)$ has weight proportional to $e^{S(E)/k_B - \beta E}$. For a macroscopic system with a dominant smooth interior maximum this exponent is stationary at $(\partial S/\partial E)_{V,N} = 1/T$. The leading free energy $-k_B T \log Z$ is then the minimum of $E - TS(E)$; the width of the peak gives the energy fluctuations. The exact finite-system integral is a Laplace transform. Replacing it by its stationary contribution is an approximation, often called the Legendre-transform limit.

An equivalent variational argument works for finite discrete states without a saddle point. Choose arbitrary trial probabilities q_i, their mean energy $U[q]$ and Shannon entropy $S[q] = -k_B \sum_i q_i \log q_i$. Subtract the canonical free energy and insert the canonical weights. Algebra gives

$$U[q] - TS[q] - F = k_B T \sum_i q_i \log(q_i/p_i) \geq 0.$$

The final inequality follows from convexity of the logarithmic divergence and becomes an equality only for the canonical distribution on the permitted support. For an isolated system one instead maximises entropy subject to its prepared energy constraint. Helmholtz free-energy minimisation at fixed temperature is thus a consequence of reservoir exchange and normalisation, not an additional force sending every microstate to the lowest energy. At finite temperature high-multiplicity excited states can dominate the equilibrium probability.

Now include volume work in the fundamental differential $dU = TdS - pdV + \mu dN$. Product differentiation gives $dF = -SdT - pdV + \mu dN$, $dG = -SdT + Vdp + \mu dN$, and $d\Omega = -SdT - pdV - Nd\mu$ for $\Omega = F - \mu N$. A potential's natural variables specify which gradient directly returns an observable. From $F(T, V, N)$ one obtains

$$p = -(\partial F/\partial V)_{T,N},$$
$$S = -(\partial F/\partial T)_{V,N};$$

their cross derivatives agree if the potential is smooth. At phase boundaries use phase branches and appropriate coexistence conditions instead of differentiating through a kink as if it were smooth.

Let the reservoir exchange particles as well as energy

With both exchanges allowed, expand reservoir entropy in E and N. Its differential includes $-\mu_R dN_R/T$. A system microstate with E, N therefore acquires weight $e^{-\beta(E-\mu N)}$. Summing normalises the grand canonical distribution. At fixed temperature and volume, derivatives with respect to $\beta\mu$ give mean particle number and number variance. In a homogeneous equilibrium region with suitable thermodynamic limit, $\Omega = -pV$.

$$\Xi = \sum_N e^{\beta\mu N} Z_N,$$
$$\langle N\rangle = \partial_{\beta\mu} \log \Xi,$$
$$\mathrm{var}(N) = k_B T \left(\frac{\partial \langle N\rangle}{\partial \mu}\right)_{T,V}.$$

A surface of M independent adsorption sites, each empty or holding one particle with binding energy $-\epsilon$, has $\Xi = [1 + e^{\beta(\mu+\epsilon)}]^M$. Its occupancy fraction is logistic and its variance $Mf(1-f)$. At $M = 400$ and half coverage, the mean occupancy is 200 with standard deviation 10. The slope with respect to chemical potential is largest there. Near saturation, a small number variance and an apparently quiet detector indicate poor sensitivity to further increases of μ, not necessarily high precision in inferring μ.

Compare the adsorption response slope with the independently predicted number variance

The grand formula links number fluctuations to isothermal compressibility in a bulk one-component fluid. Write $n = \langle N\rangle/V$ and use $dp = n\,d\mu$ at constant T. Then $(\partial n/\partial \mu)_T = n^2 \kappa_T$ and $\mathrm{var}\,N/\langle N\rangle = n k_B T \kappa_T$. A dilute classical ideal gas gives unity. These fluctuations refer to a region exchanging particles. If an observer counts all particles of a strictly sealed closed box, the number variance is zero even though its compressibility is not. The boundary condition of the measurement is part of the formula.

Infer a temperature and explain when it is identifiable

The logarithm of a measured population ratio is linear in β for nondegenerate known levels. With enough independent samples one can estimate temperature either from this ratio or by matching measured energy to its canonical expectation. If all observed states have nearly the same energy, changing β barely changes their probabilities. The available temperature information then becomes small, regardless of detector precision.

For independent canonical draws, differentiating a single log probability gives

$$\partial_\beta \log p_i = -(E_i - \langle E \rangle).$$

Its squared expectation is energy variance, the Fisher information per observation about inverse temperature. At n_s independent draws information adds. Equality between response and noise reappears as a statistical bound on temperature estimation. A long record with correlation time comparable to its length may contain few independent draws despite a large sample count. Recording more frequently without extending the observation window need not improve a temperature estimate.

A pressure reservoir selects enthalpy-weighted volume fluctuations

An isothermal piston in contact with a pressure reservoir supplies a fourth ensemble closely related to the first three. A configuration at volume V costs external work $p_{\mathrm{ext}}V$ in addition to its microscopic system energy. At fixed T, N, p_{ext}, integrate the canonical configurational partition over possible piston positions with weighting $e^{-\beta p_{\mathrm{ext}} V}$. For an ideal gas in a cylinder of fixed cross-sectional area the piston coordinate is proportional to V, so its geometric measure is a constant times dV. Mechanical kinetic factors independent of V cancel from its normalised distribution.

For $Z_N(V) \propto V^N$, the probability density for volume is proportional to $V^N e^{-\beta p_{\mathrm{ext}} V}$ on the positive real axis. Normalisation uses $\int_0^\infty V^N e^{-aV} dV = N!/a^{N+1}$. The maximum, mean and variance are

$$V_{\mathrm{mode}} = \frac{N}{\beta p_{\mathrm{ext}}},$$

$$\langle V \rangle = \frac{N+1}{\beta p_{\mathrm{ext}}},$$

$$\mathrm{var}(V) = \frac{N+1}{(\beta p_{\mathrm{ext}})^2}.$$

The finite-N offset between mode and mean comes from the skewed piston-volume distribution. The most likely volume obeys the usual ideal gas law evaluated using N, while the exact mean differs in this simple piston model. At $N = 99$ the difference is about one percent and relative volume fluctuations are ten percent. At thermodynamic sizes the fractional difference vanishes. When calibrating nanoscale pressure from a histogram, a mean, a peak and a mean of reciprocal volume should therefore not be treated as interchangeable.

Check the force equilibrium directly. The instantaneous gas pressure conditional on V is Nk_BT/V. The gamma distribution has $\langle 1/V \rangle = \beta p_{\mathrm{ext}}/N$, so its mean gas pressure equals the imposed external pressure exactly. Substituting the mean volume into the nonlinear pressure formula instead gives $Np_{\mathrm{ext}}/(N+1)$. This calculation illustrates a general statistical rule: mechanical balance concerns the mean actual force, not necessarily that force evaluated at the mean position.

If the piston lies horizontally and dry static friction is appreciable, configurations can remain stuck with nonzero force imbalance. A distribution fitted to the equilibrium piston formula would then return apparent biases in pressure or particle number. Reverse the pressure change and vary waiting times to

expose hysteresis, or remove the mechanical sticking before interpreting volume fluctuations as an equilibrium susceptibility.

A matrix of fluctuations controls coupled responses

Many experiments permit exchange of more than one extensive quantity. Write a general ensemble with natural control parameters θ_a and weights proportional to $e^{\sum_a \theta_a X_a}$, with a fixed set of microscopic state values X_a. The first derivatives of the log normalisation give their means and the second derivatives give the full covariance matrix. Off-diagonal entries describe coupled responses. For the grand canonical ensemble choose $\theta_1 = -\beta$, $\theta_2 = \beta\mu$, $X_1 = E$, $X_2 = N$. One must keep the other natural parameter fixed while taking a partial derivative in this form.

A covariance matrix is positive semidefinite because the variance of any linear combination of the X_a is nonnegative. Consequently $\mathrm{var}(E)\mathrm{var}(N) \geq \mathrm{cov}(E,N)^2$. A measured matrix violating this inequality cannot describe these two observables on the same equilibrium sample space. Possible causes include mixing variances and covariances from different sample preparations, subtracting a poorly estimated instrumental background or an inconsistent energy reference when counting particles.

Suppose a volume exchanges particles each carrying a fixed energy e_0 plus other thermal energy. If the system energy reference shifts by a per particle, new energy is

$$E' = E + aN.$$

Its covariance with N changes by $a\,\mathrm{var}(N)$, although no physical heat changed. A useful combination for isolating fluctuations uncorrelated with particle transport is $E - bN$, with $b = \mathrm{cov}(E,N)/\mathrm{var}(N)$. Minimising the variance with respect to b gives residual variance $\mathrm{var}(E) - \mathrm{cov}(E,N)^2/\mathrm{var}(N)$, invariant under this reference shift. In a general nonlinear conditional distribution that residual is a best linear prediction variance, not automatically the exact variance conditional on a fixed integer N.

For a unit-normalised example, suppose energy variance is $25\epsilon^2$, number variance is 4 and their covariance is 8ϵ. The best linear energy increment per exchanged particle is 2ϵ, and the residual energy variance is $9\epsilon^2$. Replacing energy by $E - 3\epsilon N$ changes the covariance to -4ϵ, but recalculating the residual returns the same value. A data-analysis code can use this reference-invariance as a check on both numerical units and susceptibility derivatives.

The same covariance structure controls simultaneous inference. If two state observables are nearly proportional over all sampled configurations, the log-likelihood curvature has a nearly zero eigenvalue. The individual fields conjugate to them are then hard to determine even if one linear combination is tightly constrained. Preparing the system in a region with different accessible states or adding an independent observable can resolve the degeneracy. Increasing the sampling rate on exactly the same narrow manifold cannot create a missing independent direction.

When the maximum-probability replacement loses a phase

The passage from a Laplace transform to a Legendre transform assumes one dominant smooth contribution or handles multiple branches explicitly. Near a first-order transition two energy ranges can have comparable canonical weights. Replacing the energy distribution by a single Gaussian around its mean then produces a state that may be relatively improbable, lying in the trough between two peaks. The finite partition sum remains smooth, but its derivatives can vary rapidly over a narrowing range of temperature.

In a simple two-phase approximation take branch partition contributions proportional to $e^{-\beta F_1(T)}$ and $e^{-\beta F_2(T)}$. Their ratio is $e^{-\beta(F_2-F_1)}$. At coexistence the leading bulk free-energy densities agree. If their entropy densities differ, then a small temperature change produces an extensive branch free-energy difference proportional to volume times that temperature shift. The equal-weight finite-size window therefore narrows inversely with volume in this simplest picture. Interfacial states, boundaries and phase degeneracy can shift detailed crossing locations.

Consider an energy histogram with equal phase probabilities and sharply peaked branch energies differing by total ΔE. The mixture variance includes $p(1-p)(\Delta E)^2 = (\Delta E)^2/4$ in addition to within-phase fluctuations. As ΔE is extensive this gives an extensive heat-capacity peak per particle in a finite coexistence window, much larger than the smooth single-phase contribution. This does not imply an infinite heat capacity throughout an interval of bulk temperature. The peak becomes higher and narrower and encodes latent heat in the thermodynamic limit.

An experimental or simulated time series can undersample one branch when interfacial barriers make switching rare. Estimating the variance from one branch then yields a completely different apparent heat capacity from a record containing a few switches. Compare heating and cooling preparations, identify branch-specific energy distributions and establish a reproducible equilibrium weight ratio before treating the union as a canonical histogram. In a macroscopic sample, calorimetric latent heat often provides a more reliable bulk quantity than a noisy attempt to observe whole-sample switching.

Use one equilibrium histogram to predict a nearby temperature

If a canonical run at inverse temperature β_0 samples energies E_i, a nearby expectation at β_1 can be expressed as a ratio of weighted averages with factors $w_i = e^{-(\beta_1-\beta_0)E_i}$. Multiplying numerator and denominator by the same constant allows one to subtract a reference energy to maintain numerical precision. Mathematically the ratio is exact when the original distribution covers every important configuration. Finite data can render an exact identity practically useless outside its overlap window.

For an approximately Gaussian energy histogram of standard deviation σ_E, reweighting shifts its influential energy region by roughly $-(\beta_1-\beta_0)\sigma_E^2$. Expressed in original standard deviations the shift is $|\beta_1-\beta_0|\sigma_E$. A value of 0.3 stays near the observed centre; a value of five asks for configurations five original widths away. At the latter value a smooth computed curve can be governed almost entirely by one observation at the extreme edge of the histogram.

Inspect the effective weight count $(\sum_i w_i)^2/\sum_i w_i^2$ alongside the raw record length. This statistic does not account for time correlation or prove that missing configurations are irrelevant, but a collapse to a handful of weights is a clear failure of overlap. Simulate or measure directly at a second temperature

displaced toward the target and compare its actual histogram with the reweighted prediction. This connects the formal equivalence of ensemble descriptions to a concrete question of measurement coverage and uncertainty.

A finite-spin thermodynamic cycle tests mixed derivatives

Consider independent two-state magnetic moments with energies $\mp\mu B$ in a prescribed induction B. Ignore interactions and orbital response. Per moment the canonical sum is $2\cosh x$, $x = \mu B/(k_B T)$. Its Helmholtz free energy is $-k_B T \log(2\cosh x)$ and the average magnetic moment is

$$m = -\partial F/\partial B = \mu \tanh x.$$

The entropy follows from $-\partial F/\partial T$, yielding $S/k_B = \log(2\cosh x) - x\tanh x$. These component equations define an exactly soluble controlled system in which thermal and magnetic responses are coupled.

Equality of the mixed free-energy derivatives predicts

$$(\partial S/\partial B)_T = (\partial m/\partial T)_B.$$

Both are negative for positive field in this model. Increasing field at fixed temperature aligns spins and reduces their entropy. If the spin system is instead isolated reversibly, its entropy is constant, which requires x constant away from singular limiting cases. Reducing field then reduces temperature in proportion to field. This is the ideal paramagnetic demagnetisation argument, derived here from the canonical weights rather than an empirical cooling rule.

For an idealised system prepared at 3.0 K and 1.5 T, reducing the field quasistatically to 0.50 T under thermally isolated conditions gives 1.0 K. Its mean alignment fraction stays constant even as the Zeeman gap shrinks. A real specimen includes lattice heat capacity, residual interactions and inevitable heat leakage. If the lattice remains equilibrated with the moments, the total entropy includes both subsystems and the simple proportional temperature drop is modified. If spin–lattice exchange is too slow, a single temperature may fail to describe both during the field ramp.

A numerical test can use a rectangular loop in the T, B plane. Evaluate the change in F along one path using the integral of $-S\,dT - m\,dB$, then return along the other path. At successively finer quadrature the closed integral should approach zero. By contrast heat and magnetic work evaluated separately generally have nonzero loop integrals and cancel only in their appropriate state-function combination. A nonzero free-energy residual that does not shrink under refinement points toward a sign error, an inconsistent field-energy convention or different energy references on the two paths.

Finally use the weak-field limit to estimate experimental sensitivity. There $m \simeq \mu^2 B/(k_B T)$, so a thermometer inferred from magnetisation is sensitive to both the magnetic-field scale and the independent number of active moments. Saturation measurements can calibrate their total number, while a field reversal removes a constant magnetometer offset. A mixed-derivative test based on independently measured calorimetry and magnetisation is more discriminating than fitting a temperature parameter to a single magnetic trace that already assumed the predicted population law.

The spin example also gives a direct thermal-noise measurement of susceptibility. For one moment the variance of its projection is $\mu^2[1-\tanh^2 x]$, and differentiating mean moment with respect to induction gives exactly this variance divided by thermal energy. At $x=1$, magnetisation is 0.762 of saturation and variance is $0.420\mu^2$. For a thousand independent moments the total rms fluctuation is about 20.5μ, even though their mean total moment is about 762μ. An instrument averaging over many reversals may see the mean accurately and suppress the variance; replaying the same averaging operation on a simulated equilibrium time series makes the comparison meaningful. A direct susceptibility inferred from a very large field modulation would instead sample the curved magnetisation over a finite interval. Use a small symmetric modulation and verify its amplitude scaling to compare with the local fluctuation slope.

Count the configurations of two finite reservoirs

Change the reservoir size and compare the observed energy histogram with a canonical ensemble at the same mean.

Open this experiment online

Try the calculation

Reservoir modes **8**

Excitation quanta **24**

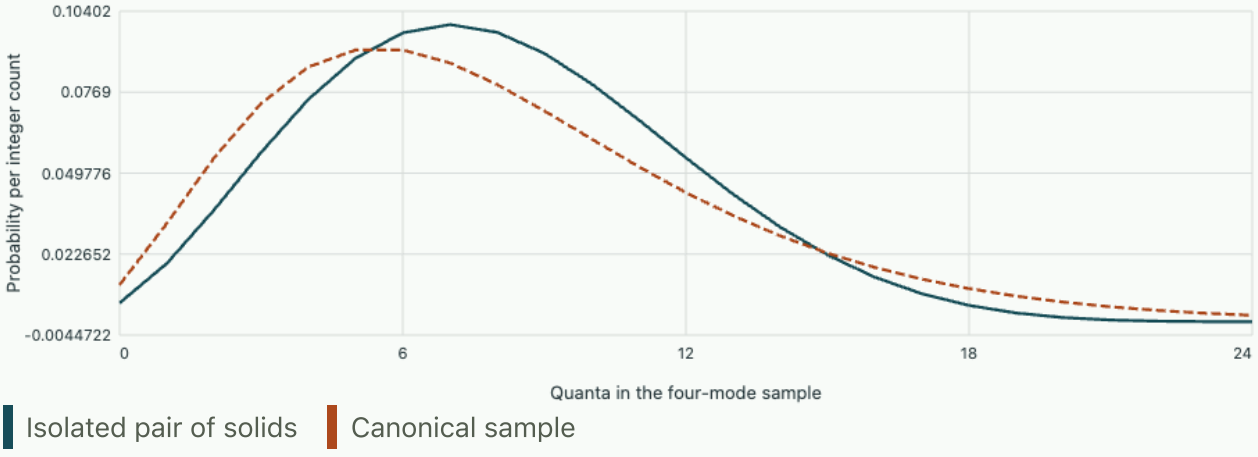

Mean 8 quanta; closed-pair variance 14.769. Canonical variance 24.

Tutorial · Can a finite bath explain unusually quiet energy data?

A sample has canonical heat capacity $60k_B$ at the mean temperature. Contact with a small reservoir reduces the measured equilibrium energy variance to three quarters of its canonical value. Approximate both entropies quadratically near their common equilibrium and infer the bath heat capacity. What other measurement could mimic the reduction?

▼ **Add the two inverse susceptibilities and check the observation**

The joint log probability has curvature $-[1/C_s + 1/C_R]/(k_B T^2)$. Hence the effective variance is $k_B T^2 C_s C_R/(C_s + C_R)$. Dividing by $k_B T^2 C_s$ and setting the ratio to $3/4$ gives

$$C_R = 3C_s = 180 k_B.$$

The temperature at maximum probability still agrees for bath and sample at leading order. The suppressed fluctuations reflect their shared total-energy constraint.

Finite temporal averaging of a fast energy signal can also suppress measured variance. Vary detector bandwidth and check convergence of the measured area, then repeat with a different independently estimated reservoir capacity. A corrected variance scaling with the harmonic combination supports the finite-bath interpretation. A single reduced number cannot distinguish thermodynamic curvature from the detector response.

Tutorial · Determine a volume response from temperature data

For a fixed amount of a smooth single-phase material near one operating point, the thermal expansion coefficient is α, the isothermal compressibility is κ_T and the volume is V. Derive $C_p - C_V$ from a Maxwell relation. Evaluate it for $T = 300$ K, molar volume 1.0×10^{-5} cubic metres, $\alpha = 6.0 \times 10^{-5}$ per kelvin and $\kappa_T = 1.0 \times 10^{-11}$ per pascal.

▼ **Eliminate the unmeasured mixed entropy derivative**

Write $dS = (C_V/T)dT + (\partial p/\partial T)_V dV$, using the Helmholtz mixed derivative. On the constant-pressure path $dV = \alpha V dT$. Holding volume fixed in $dV/V = \alpha dT - \kappa_T dp$ gives

$$(\partial p/\partial T)_V = \alpha/\kappa_T.$$

Therefore $C_p - C_V = TV\alpha^2/\kappa_T = 1.08$ J per mole kelvin. Positive isothermal compressibility and positive temperature imply the difference is nonnegative even for negative expansion coefficient.

Tutorial · Infer two unknowns from occupancy measurements

At two distinct temperatures a set of dilute independent adsorption sites gives coverages 0.20 and 0.60. Why can these two readings fail to identify binding energy if the reservoir chemical potentials are not independently known? Express the unknown combination and suggest an experiment that would determine the binding energy.

▼ **Write an equation for each observation before counting parameters**

The log odds satisfy

$$\log[f/(1-f)] = (\mu + \epsilon)/(k_B T).$$

The measured log odds are minus 1.386 and plus 0.405. They determine the value of $\mu + \epsilon$ in each run multiplied by its known inverse thermal energy. With two unrelated reservoir potentials there are three unknown dimensional quantities and only two equations. Increasing coverage precision cannot resolve that degeneracy.

A separately calibrated reservoir supplies $\mu(T, p)$ relative to a consistent energy reference. Then several pressures at one temperature verify the model and several temperatures can test a constant binding energy against an additional binding entropy or site degeneracy. A reported equilibrium constant alone can always absorb a reference-state shift; the reference reservoir and site standard state are part of a physically interpretable adsorption energy.

Cambridge Statistical Physics · canonical and grand canonical ensembles

Master equations, detailed balance and probability currents

Statistical mechanics from microscopic counting to material response

A two-state detector can switch at random while displaying reproducible occupation fractions and relaxation times. A three-state detector can maintain exactly constant occupancies while carrying a persistent directed current. Derive the probability dynamics, infer transition rates from timed records and decide what a stationary histogram can and cannot reveal about equilibrium.

From short-time transition probabilities to a generator

Take discrete states i resolved by an instrument. In a short time dt, conditional on current state i, let the probability of one transition $i \to j$ be $w_{ij}dt + o(dt)$. The probability of remaining in i is one minus the sum of departures to this order. Assume time-independent rates and the Markov property, meaning the conditional law of future transitions is determined by the current state. Sum gains and losses to derive

$$\dot{p}_i = \sum_{j \neq i} (p_j w_{ji} - p_i w_{ij}),$$

$$\sum_i \dot{p}_i = 0.$$

Each gain in one state is a loss in another, so total probability is conserved. In a column-vector convention $\dot{\mathbf{p}} = L\mathbf{p}$, off-diagonal entry $L_{ij} = w_{ji}$ and columns sum to zero. In a row-vector convention transpose the matrix. This is not cosmetic in a numerical calculation: using a matrix assembled for column probabilities while evolving rows can lose normalisation or give an incorrect stationary distribution.

For a given state the exit rate is

$$r_i = \sum_{j \neq i} w_{ij}.$$

Its survival probability obeys $\dot{S}_i = -r_i S_i$, so $S_i(t) = e^{-r_i t}$. Conditional on exiting, the destination has probability w_{ij}/r_i. This permits direct event-driven simulation: draw an exponential waiting time, choose a destination with these probabilities, advance the clock and repeat. Sampling one transition per arbitrary fixed time step generally distorts waiting-time statistics unless a controlled approximation or exact finite-time propagator is used.

Determine two rates from one occupancy and one time

For a two-state system name the rates $a = w_{01}$, $b = w_{10}$. Eliminating $p_0 = 1 - p_1$ gives

$$\dot{p}_1 = a - (a + b)p_1.$$

Its stationary value $p_* = a/(a + b)$ is independent of the common rate scale, and deviations decay with time constant $\tau = 1/(a + b)$. Thus one stationary fraction gives a ratio, one relaxation time gives a sum, and the two together identify both rates.

A location sensor records an upper-state fraction 0.30 and relaxation time 0.20 seconds. Then $a = 1.50$ and $b = 3.50$ per second. Mean waiting times are $1/a = 0.667$ s in the lower state and $1/b = 0.286$ s in the upper one. Neither equals the population relaxation time of 0.20 s. A transition rate inferred by taking the reciprocal of the average of these two waiting times estimates a different quantity.

Define the indicator $X = 1$ in state one and zero otherwise. Conditional probabilities from the same linear solution give

$$\langle [X(t) - p_*][X(0) - p_*] \rangle = p_*(1 - p_*)e^{-|t|/\tau}.$$

Consequently a normalised equilibrium autocorrelation determines τ without needing a deliberate preparation away from stationarity. A bandlimited detector may miss short visits, reducing counts and distorting waiting-time distributions even if the mean occupation looks plausible. Compare time sampling with both exit times as well as the relaxation time, or model the measured signal with an explicit observation process.

Detailed balance is stronger than stationarity

Let π_i denote a stationary distribution. The net probability current on an oriented edge is $J_{ij} = p_i w_{ij} - p_j w_{ji}$. Stationarity requires only that currents sum to zero at each vertex. Detailed balance requires $\pi_i w_{ij} = \pi_j w_{ji}$ on every edge individually. For a system in equilibrium with one heat bath, with states even under time reversal and energies E_i, thermal rates satisfy $w_{ij}/w_{ji} = e^{-\beta(E_j - E_i)}$ for nondegenerate states. If states collect multiple microstates, degeneracies or coarse-grained free energies enter their equilibrium weights.

For the previous two-state process at equilibrium with equal state degeneracies, $p_*/(1 - p_*) = 3/7$ implies

$$(E_1 - E_0)/(k_B T) = \log(7/3) = 0.847.$$

Multiplying both rates by ten preserves the energy inference and speeds relaxation tenfold. Thermodynamic weights therefore do not determine the kinetic barrier. A physical sample may change its rate scale with solvent viscosity or transition geometry without changing the equilibrium ratio.

A convenient test on a connected graph with reciprocal edges is the product of rate ratios around each closed cycle. With detailed balance all stationary factors telescope to one. Conversely, if the product is one on every independent loop, consistent state weights can be reconstructed from any reference state by integrating ratios along a path. Path independence makes these weights a detailed-balance stationary distribution after normalisation. A missing reverse edge or unobserved channel requires additional care; a detector that cannot resolve two routes can hide directed currents.

A steady nonequilibrium system with the same state histogram

Consider three equally named sites arranged in a ring, with clockwise rate k_+ and anticlockwise rate k_- on every link. Symmetry gives stationary occupation $1/3$ at each site for all positive rates. Each oriented

clockwise edge carries current $J = (k_+ - k_-)/3$. The cycle affinity in dimensionless units is $\mathcal{A} = \log[(k_+/k_-)^3]$. For $k_+ = 4$, $k_- = 1$ per second, each edge transports net probability one per second, and $\mathcal{A} = 3\log 4 = 4.159$. A perfectly flat histogram conceals the directed operation.

For Markov jumps with resolved reversible edges and their conventional time reversals, the total stochastic entropy production rate is

$$\dot{S}_{\mathrm{tot}} = \frac{k_B}{2}\sum_{ij}(p_i w_{ij} - p_j w_{ji}) \log \frac{p_i w_{ij}}{p_j w_{ji}} \geq 0.$$

Each term is nonnegative under the product $(x - y)\log(x/y)$; the factor of one half prevents counting both directions separately. For the stationary ring this gives $k_B J \mathcal{A} = 4.159 k_B$ per second. An actual heat dissipation rate needs a physical local detailed-balance model identifying environments, work and entropy flows. A collection of counted transitions without that calibration can still yield evidence for broken time-reversal symmetry at its level of resolution.

Stationary Shannon entropy $-k_B \sum p_i \log p_i$ is constant in this ring. The positive total entropy production is compatible with that constancy because an environment sustains the directed current and carries compensating entropy. Equating production with just the derivative of stationary state entropy would predict zero for every driven stationary process.

Why a distribution relaxes toward a stationary law

For a finite irreducible time-independent chain let $\pi_i > 0$ be its unique stationary distribution. The relative entropy $D(p\|\pi) = \sum p_i \log(p_i/\pi_i)$ is nonnegative. To see its contraction over a finite observation interval, write the propagated probability as a stochastic mixture of earlier probabilities and apply the log-sum inequality to each output state. Summing gives

$$D(Pp\|P\pi) \leq D(p\|\pi).$$

Since $P\pi = \pi$, the relative entropy to stationarity cannot grow.

For a detailed-balance chain, substituting the master equation into this derivative gives $-k_B dD/dt = \dot{S}_{\mathrm{tot}}$ in the simple closed heat-bath model. For a driven chain the system may remain at π with constant relative entropy while producing positive steady entropy. Relaxation toward stationarity and dissipation required to maintain that stationary state are distinct measurable quantities.

Compare relaxation inferred from a time trace with the thermodynamic irreversibility experiment

Infer generator entries from residence times

An ideal continuously observed Markov record contains successive states and dwell lengths. Let T_i be accumulated time in state i and N_{ij} the number of resolved $i \to j$ jumps. Its log likelihood contains $\sum_{ij} N_{ij} \log w_{ij} - \sum_i T_i \sum_{j \neq i} w_{ij}$. Differentiation gives

$$\widehat{w}_{ij} = N_{ij}/T_i.$$

Dividing by total experiment time instead estimates the gross stationary flux $\pi_i w_{ij}$, not a conditional transition rate.

For a nearly stationary two-state record with $T_0 = 70$ s, $T_1 = 30$ s and 105 transitions in each direction the estimates are 1.50 and 3.50 per second. Counting uncertainty for each reasonably large Poisson-like count is roughly the inverse square root of the count in relative terms; precise interval estimates condition correctly on exposures and the observation process. Equality of opposite transition counts in a long two-state record is essentially forced by alternation. It cannot by itself establish a thermal energy gap or exclude multiple hidden driven pathways.

Turn a barrier diagram into two independently measurable rates

A thermally activated transition between two metastable configurations often has a forward rate $a = \nu_A e^{-(G^\ddagger - G_A)/(k_B T)}$ and reverse rate $b = \nu_B e^{-(G^\ddagger - G_B)/(k_B T)}$, where $G^\ddagger$ denotes a dividing-surface barrier under a chosen model. If the same transition-state construction applies in both directions with consistent partition factors, their ratio reproduces the equilibrium free-energy difference. The overall barrier controls how rapidly equilibrium is approached. Changing a barrier while leaving both wells unchanged can alter both kinetics by many orders of magnitude without changing stationary occupancy.

As an illustration let the higher-energy state cost $2k_B T$, and put a transition configuration $10k_B T$ above the lower state. With a common attempt rate of 10^6 per second, the upward rate is 45.4 per second and the downward rate 335 per second. The stationary upper fraction is approximately 0.119 and the relaxation time 2.63 ms. Lower the barrier by $2k_B T$ without changing the two state energies. Both rates increase by $e^2 = 7.39$, while occupancy is unchanged. A detector recording only the equilibrium level histogram could miss the intervention entirely.

For a temperature scan, a straight line in the log rate against inverse temperature is evidence for an approximately constant activation energy and prefactor over that interval. A free-energy barrier includes entropic as well as enthalpic contributions; its numerical value can vary with temperature even if the microscopic potential does not. A change of dominant pathway can bend the apparent Arrhenius plot. Measure forward and reverse rates independently, then compare their ratio with an independently determined equilibrium population. A barrier fit explaining one rate but violating the equilibrium ratio usually indicates inconsistent state definitions, missed short visits or an unmodelled pathway.

A useful control is a weak static bias that lowers one well relative to the other. The equilibrium log-odds shift measures the difference between the state couplings to the bias. The individual log-rate shifts additionally report the related dividing-surface response. If the state-occupation ratio moves as expected but only one rate changes appreciably, the effective transition configuration may be much closer in bias response to the other state. Such statements depend on the activated single-path interpretation; the response slopes themselves are more directly observed than an inferred barrier shape.

Use uniformisation to propagate a generator without negative probabilities

The formal finite-time propagator of a time-independent jump process is $P(t) = e^{Lt}$. A forward Euler update $p(t + \Delta t) = (I + L\Delta t)p(t)$ conserves total probability if the generator is assembled correctly, but a large step can yield negative diagonal probabilities. An exact algebraic representation starts with a rate q at least as large as every total exit rate. Then $K = I + L/q$ is a stochastic matrix in the same column convention. Write $L = q(K - I)$; since K and the identity commute,

$$e^{Lt} = e^{-qt} \sum_{n=0}^{\infty} \frac{(qt)^n}{n!} K^n.$$

This can be read as drawing a Poisson number of opportunities at rate q, followed by n transitions of K. At a lightly connected state some opportunities become self transitions. The construction leaves real waiting-time statistics correct while eliminating negative transition probabilities. Its truncation error in total probability is bounded by the omitted Poisson tail because every matrix power is stochastic.

For a two-state model with rates two and six per second choose $q = 6$ per second. Starting in the lower state, the first opportunity after some waiting time moves upward with probability one third and otherwise does nothing. In the upper state the next opportunity moves downward with probability one. At 0.25 s the Poisson mean is 1.5. Retaining terms through order eight leaves a tail below 3×10^{-5}. Compare the resulting upper probability against $(2/8)[1 - e^{-8(0.25)}] = 0.2162$. A small discrepancy due solely to truncation should shrink with the computable tail probability.

The representation also suggests a measured-data sanity check. A fitted generator with negative off-diagonal rates cannot yield a valid K at any positive q. A snapshot transition matrix can itself be nonnegative and stochastic but need not arise from a time-homogeneous continuous-time generator. In the two-state case its nontrivial eigenvalue must be $e^{-(a+b)t} > 0$. A measured negative eigenvalue rules out that simple generator model under perfect sampling, though finite counts and hidden periodic driving can distort empirical estimates. Taking a matrix logarithm blindly may return complex or negative rates rather than a physical kinetic explanation.

Population relaxation and a first-arrival experiment answer different questions

A first-passage measurement stops its clock when a target is first reached, even if that target would subsequently be left many times. To calculate its mean, treat the target as absorbing. For any other state i, wait on average $1/r_i$, then add the mean remaining time from the next state weighted by its conditional transition probability. The backward equations are

$$-1 = \sum_j w_{ij}(t_j - t_i),$$

with $t_{\mathrm{target}} = 0$. Their solution depends on possible returns before the first successful passage. It generally differs from an inverse equilibrium occupation or from a slowest relaxation time.

Consider a three-site linear chain $0 \leftrightarrow 1 \leftrightarrow 2$ with equal rate k on each adjacent directed edge, starting at zero and stopping at two. From zero one must reach one after mean $1/k$. From one the mean wait is $1/(2k)$, then there is probability one half of returning to zero and one half of finishing. Solving $t_0 = 1/k + t_1$, $t_1 = 1/(2k) + t_0/2$ gives

$$t_0 = 3/k.$$

Ignoring returns would yield $1.5/k$, exactly half the correct first-passage mean.

The unmodified closed chain has equal stationary weights, but that fact alone says nothing about the numerical value of $3/k$. Speeding every link by ten leaves occupancies unchanged and reduces passage times tenfold. A detector that registers only visits longer than a threshold makes a brief first arrival invisible and can report even longer apparent passage times. Calibrate detector dead time and distinguish entrance to the target from persistence within it.

For a larger network, solve the sparse backward linear system and compare against many event-driven paths. Check boundary initial conditions by starting simulations exactly at the absorbing target: the first-passage time must then be zero under that convention. Some experiments instead ask for a first return after leaving, which requires a different initial condition. A zero-lag event in one definition is a physically different measurement in the other.

Estimate a cycle affinity with finite counting statistics

A clockwise ring trajectory contains gross counts in both directions on each edge. Estimating each conditional rate as count divided by origin-state exposure, the product of clockwise-to-anticlockwise rates around a complete closed loop cancels the exposures. The estimated cycle affinity is the sum of log forward counts minus log reverse counts, assuming every required count is nonzero and rates were stationary during the record. This is a useful cross-check independent of how the total time was partitioned among states.

If all three edges register roughly 120 clockwise and 80 anticlockwise events, the estimated affinity is

$$3 \log(1.5) = 1.216.$$

For large independent Poisson-like gross counts the approximate variance of this log product is $3(1/120 + 1/80) = 0.0625$, giving standard error 0.25 as a first estimate. Actual path constraints couple counts; uncertainty can be assessed from independent records or a complete stochastic likelihood. The point estimate alone does not tell whether an observed directionality is statistically distinguishable from zero.

One missing reverse event makes the unregularised logarithm infinite, but a finite record cannot establish an infinite physical affinity. Report a confidence bound based on the exposure and upper limit on the unseen reverse rate. Extend the acquisition or change sampling speed to exclude missed short-lived reverse states. Numerical addition of an arbitrary count can help regularise a plotting routine but is not a substitute for a specified prior or measurement model when claiming physical entropy production.

A driven occupation loop can carry charge without changing concentrations

Place three sites in a cycle and drive their transition rates by two controls, for example energies and barriers. Even if each instantaneous frozen generator satisfies detailed balance with a well-defined equilibrium distribution, the physical occupations need not equal that moving equilibrium distribution at each moment. A slow lag can produce a small edge current at every instant and a finite integrated current over a cycle. The current through an edge is time-integrated transfer; it can be nonzero while all occupations return to their initial values after a complete drive period.

A simple piecewise illustration avoids subtleties of adiabatic geometric pumping. In stage one, connect only sites zero and one while strongly favouring one. In stage two connect only one and two while favouring two. In stage three connect only two and zero while favouring zero. Begin with nearly all probability at zero and wait long enough for each enabled pair to relax. Almost the entire population travels once around the loop per cycle. No site accumulates probability over repeated complete cycles, but each edge registers about one forward crossing net per cycle. External control changes the energy and barrier landscape and supplies the required work.

If each programmed transfer succeeds with probability 0.95, it is tempting to announce a current of 0.95^3 per cycle. This is the probability of one fully successful trajectory starting on the prescribed site in a simplified no-return preparation, not generally the long-run edge current of a periodically driven ensemble. Failed transfers leave probability on other sites in later stages. The correct periodic distribution is the unit-eigenvalue vector of the product of the three finite-time propagators. Compute edge currents during each stage using its evolving occupations and integrate, then compare a complete cycle after transients have decayed.

This construction supplies a statistical check on experimental counting. Over a complete cycle the integrated net inflow at a site equals its change in occupancy probability. In a periodically stationary state that change is zero, so all three consistently oriented integrated edge currents must agree. A disagreement between measured edges can reveal a missed transition channel, a start-up transient or incorrect gating. Agreement does not prove absence of drive or detailed balance. A torque-free stationary ring and a three-stage external pump can share nearly the same time-averaged site histogram yet differ clearly in time-resolved edge currents.

Finally compare the work and heat bookkeeping with the master-equation entropy-production expression. During an external change of a site's energy without a transition, the state's energy changes by work. During a transition at frozen controls, assigning heat requires the energy difference and the relevant bath. Lumping an entire driven cycle into a single time-averaged generator can conceal those distinctions and underestimate dissipation.

The ordered protocol can also be run backwards. If the three stages are reversed while preparations are equilibrated in each corresponding periodic state, the preferential current direction should reverse in the ideal transfer picture. A fixed instrumental preference for counting neighbouring sites in one direction would not generally reverse. This distinguishes controlled transport from a direction-dependent detection efficiency. Do not confuse this observed current reversal with exact microscopic time reversal of each individual stochastic trajectory: the reversed experiment has its own ensemble of random jumps. Comparing path probabilities, rather than pairing individual paths as though their noise histories were

reproducible, is the appropriate starting point for entropy-production and fluctuation-relation tests. The distinction becomes particularly visible when a stage transfers almost all the probability in one direction while a few rare trajectories travel against the applied protocol.

Distinguish stationarity from detailed balance

Keep the three populations identical while varying the directed transition rates. Identify the observable that reveals time-reversal asymmetry.

Open this experiment online

Try the calculation

Clockwise bias **0.5**

Total jump rate (s⁻¹) **8**

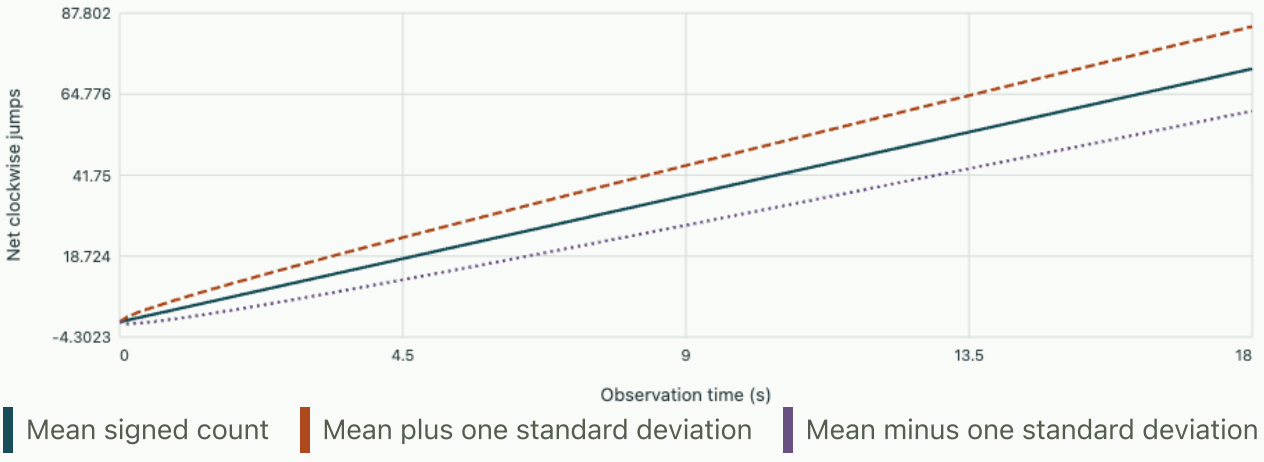

Every stationary population is 1/3. Net clockwise edge current 1.3333 s⁻¹. Entropy production 4.3944 kB/s.

Tutorial · Recover a generator from snapshots rather than full events

At sampling interval 0.10 s, a two-state record yields $P_{01} = 0.12$ and $P_{10} = 0.28$. Infer the continuous-time rates, and compare with directly dividing each transition probability by 0.10 s.

▼ **Use the exact finite-interval propagator**

The exact transition probabilities are $P_{01} = p_*[1 - e^{-(a+b)\Delta t}]$ and $P_{10} = (1 - p_*)[1 - e^{-(a+b)\Delta t}]$. Their sum is 0.40, so $a + b = -\log(0.60)/0.10 = 5.108$ per second. The stationary upper fraction is

$$0.12/0.40 = 0.30.$$

Thus $a = 1.532$ and $b = 3.576$ per second. Dividing by the interval gives only 1.2 and 2.8 because return transitions inside a sampling interval can erase evidence of the intermediate visit.

Tutorial · Can measured rates arise from one equilibrium potential?

For a three-state triangle suppose clockwise to counterclockwise conditional rate ratios are 2, 3 and 0.25 around the three distinct edges. Could these be equilibrium weights in a common bath? If a single uncertain ratio were corrected, what would it have to be on the third link?

▼ **Apply the closed-loop consistency condition**

The product is $2 \cdot 3 \cdot 0.25 = 1.5$, giving nonzero loop affinity $\log 1.5 = 0.405$. No consistent detailed-balance set of three state weights exists for these exact ratios. The third ratio would have to be $1/6$, giving a telescoping unit product. If counts are noisy, propagate uncertainty in the log ratios or compare a constrained detailed-balance likelihood against an unconstrained model. A value barely inconsistent with unity within one sparse record is not enough to establish driving.

Tutorial · Detect a hidden state with the same observed level

A detector reports two visible levels, but its lower level combines two unresolved substates. The measured lower-state survival probability is $0.5e^{-t} + 0.5e^{-9t}$ with time in seconds. Calculate the initial hazard and its long-time limit. Can a two-state Markov fit reproduce both?

▼ **Differentiate survival before interpreting the tail**

The hazard is minus the derivative of $\log S$. At zero time it is the initial weighted mean of rates, 5 per second. At long times the rapidly departing component has almost disappeared and the hazard tends to 1 per second. A single Markov exit rate would give a constant hazard for all dwell ages. The observed model cannot reproduce both limits with one rate.

A changing apparent hazard may also result from limited detector temporal resolution or variable preparation of the substates. Repeat with shorter acquisition intervals and condition the dwell distribution on the preceding visible transition or an independent preparation marker. A fitted sum of exponentials identifies a need for a richer observation or state model; it does not uniquely identify microscopic structures absent in the measurements.

Cambridge Kinetic Theory · stochastic processes and approach to equilibrium

Applied study

Use energy and angular momentum to find the turning points and period of an orbit.

What fixes an orbit?

An object at the same distance from Earth can follow a circle, a long ellipse or a path that escapes. Position sets the gravitational acceleration. The initial velocity distinguishes those trajectories. Begin in an inertial frame centred on a spherical Earth, and neglect atmospheric drag, other bodies and the motion of Earth in response to the much smaller satellite. With $\mu = GM$, Newton's law reads $\ddot{\mathbf{r}} = -\mu\mathbf{r}/r^3$. Everything that follows concerns motion outside Earth.

Crossing this equation with $\mathbf{r}$ shows that the specific angular momentum $\mathbf{h} = \mathbf{r} \times \dot{\mathbf{r}}$ is constant. The orbit lies in the plane perpendicular to $\mathbf{h}$. In polar coordinates $h = r^2\dot{\theta}$, so the area swept per second is $h/2$. An object must move faster around the centre when it is closer to it.

Read the turning points from the energy

Take the scalar product of Newton's equation with velocity. The derivative of $v^2/2$ equals the negative derivative of $-\mu/r$, so the specific energy $\mathcal{E} = v^2/2 - \mu/r$ is constant. Substituting the angular momentum for tangential speed gives a one-dimensional radial balance

$$\mathcal{E} = \frac{\dot{r}^2}{2} + U_{\text{eff}}(r),$$

$$U_{\text{eff}}(r) = \frac{h^2}{2r^2} - \frac{\mu}{r}.$$

Only radii with $\mathcal{E} \geq U_{\text{eff}}$ can be reached. At the minimum of U_{eff} a circular orbit is possible. A bound eccentric orbit has two turning radii r_p, r_a. At each, $\dot{r} = 0$, so both are roots of $2\mathcal{E}r^2 + 2\mu r - h^2 = 0$. Their sum fixes $\mathcal{E} = -\mu/(2a)$, with $a = (r_p + r_a)/2$. Substitution into the energy gives the speed at any point, $v^2 = \mu(2/r - 1/a)$.

Recover the shape and the clock

Set $u = 1/r$ and use $d/dt = hu^2 d/d\theta$ in the radial force equation $\ddot{r} - r\dot{\theta}^2 = -\mu/r^2$. This gives

$$u'' + u = \mu/h^2,$$

with primes denoting angle derivatives. Choosing $\theta = 0$ at closest approach yields

$$r = (h^2/\mu)/(1 + e\cos\theta).$$

For $0 < e < 1$ the shape is an ellipse, with $e = (r_a - r_p)/(r_a + r_p)$ and semiminor axis $b = a\sqrt{1 - e^2}$.

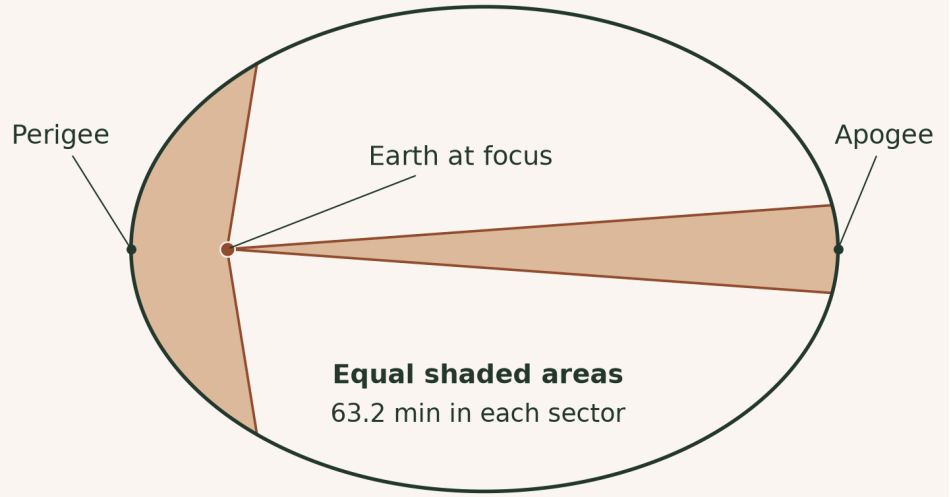

Each shaded sector sweeps out one tenth of the ellipse in one tenth of a period. The satellite follows a longer arc near perigee in the same 63.2 minutes. Earth is marked by its centre.

An ellipse encloses area $\pi a b$. Divide that area by $h/2$ and use $h^2 = \mu a(1-e^2)$ to obtain $T = 2\pi\sqrt{a^3/\mu}$. Eccentricity redistributes the time spent along the path. At a given semimajor axis it leaves the full period unchanged. Angular momentum also constrains a rotating body about its own centre. Torque-free rigid-body motion.

From force components to Lagrange's equation

A constrained system often has fewer independent coordinates than Cartesian components. Consider a bead of mass m on a light rigid rod of length ℓ, moving in a vertical plane. The pivot fixes the radius. Its force is perpendicular to the allowed displacement, so the angle θ measured from the downward vertical suffices. The kinetic and gravitational energies are $K = m\ell^2\dot\theta^2/2$ and $U = mg\ell(1-\cos\theta)$.

For conservative forces with ideal constraints, varying the action $\int (K-U)\,dt$ with fixed endpoints gives $d(\partial\mathcal{L}/\partial\dot q)/dt = \partial\mathcal{L}/\partial q$ for each independent coordinate q, with $\mathcal{L} = K - U$. For the rod this yields

$$m\ell^2\ddot\theta = -mg\ell\sin\theta.$$

Close to the stable minimum $U \simeq mg\ell\theta^2/2$, and the motion oscillates with period $2\pi\sqrt{\ell/g}$. For $\ell = 1.00$ m and $g = 9.81$ m/s², the period is 2.01 s.

The same curvature test works for a near-circular orbit. Expand the specific effective potential at $r_c = h^2/\mu$. Its positive curvature is $U_{\mathrm{eff}}''(r_c) = \mu/r_c^3$, so a small radial displacement oscillates at $\sqrt{\mu/r_c^3}$. The period of this small radial motion agrees with the circular orbital period obtained from the area law. Both a pendulum and a nearly circular orbit reveal a restoring force through the curvature of an energy minimum.

An ellipse from two distances

Take $\mu = 3.9860 \times 10^{14}$ m³/s², $r_p = 6628.137$ km and $r_a = 42164$ km, all radii measured from the centre. The semimajor axis is 24396.1 km and $e = 0.7283$. The speed equation at closest approach gives 10.195 km/s. The product $r_p v_p = r_a v_a$ then gives 1.603 km/s at the far end. Using a in metres in the period formula gives 37 922 s, about 10.534 hours.

Exercises on speed and timing

1. Compare two bound orbits

A circle and an ellipse have the same semimajor axis a. The ellipse has $e = 0.6$. Compare their periods and find the ratio of the highest to the lowest speed in the ellipse.

▼ **Compare the two orbits**

The periods agree because T depends only on a and μ. At the turning points the velocity is tangent. Therefore

$$v_p / v_a = r_a / r_p = (1 + e)/(1 - e) = 4.$$

Equal periods are compatible with very different local speeds.

---

2. Find the escape threshold

At radius r, compare the circular speed with the minimum speed needed to reach arbitrarily large radius. Assume an initially tangential velocity.

▼ **Derive the speed ratio**

For the circle, radial acceleration requires

$$v_c^2 / r = \mu / r^2.$$

Escape at threshold arrives at infinity with zero speed, so $\mathcal{E} = 0$ and $v_e = \sqrt{2\mu / r} = \sqrt{2}\, v_c$. At a speed just below this threshold, energy is negative and there is still a finite outer turning point.

ONESIMULATION LABORATORY

Measure a period from an orbit

Compare recorded OneSimulation runs on this page. To test your own inputs, download the notebook and model files and run the model in an activated OneSimulation environment.

The orbit notebook integrates Cartesian position and velocity. Its upwards crossings of $y = 0$ measure successive revolutions. Run the supplied time-step study, reading the measured period and maximum radius from the 15 s run. Reset the orbital parameters to their original values before each change. Model equations and worked orbit.

1. **Baseline.** Use the supplied closest and farthest radii. Check the crossing period against 10.534 h and the largest radius against 42 164 km. Compare the largest relative energy error at steps of 30 and 15 s.
2. **Bring the outer turning point closer.** Set `apogee = 26.560e6` m, keeping the original perigee. Run from the orbital parameters onward so the initial velocity updates. Predict 5.909 h and a maximum radius of 26 560 km.
3. **Raise the inner turning point.** Restore the original apogee and set `perigee = earth_radius + 2000e3`. The predicted period becomes 11.106 h while the outer radius stays 42 164 km. Check both periods within 0.1% and both maximum radii within 1 km. Record which quantity distinguishes these orbits even when their maximum radius is identical.

Orbits measured from the 15 s trajectory

Perigee altitude / apogee radius (km)	Crossing period (s)	Maximum radius (km)
250 / 42 164	37921.96	42164.00
250 / 26 560	21273.57	26560.00
2000 / 42 164	39980.33	42164.00

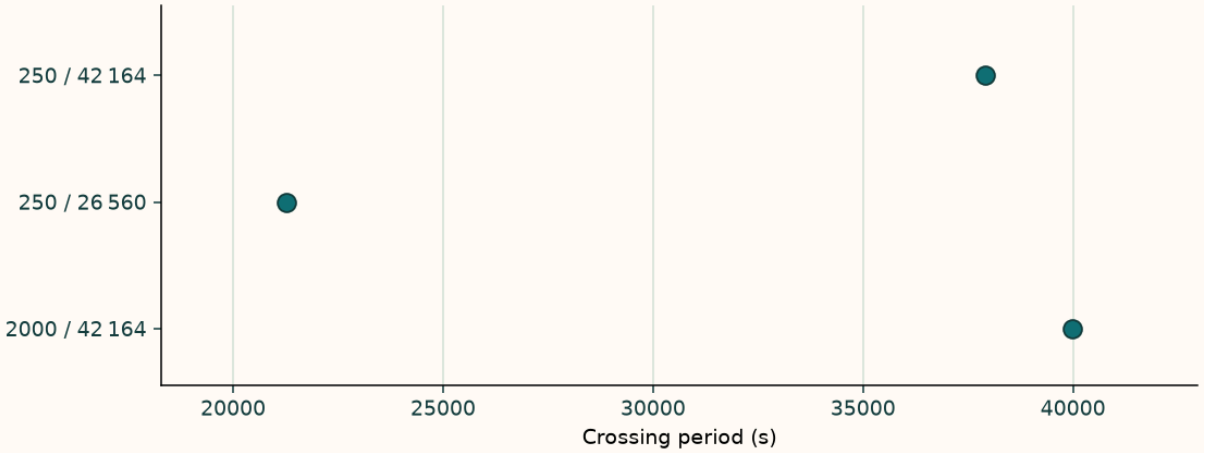

At fixed perigee the lower apogee shortens the measured period from 10.53 to 5.91 hours. At fixed apogee, raising the perigee lengthens the period.

Download experiment files (ZIP)

Extract the files together and open `spacecraft_kepler_orbit.ipynb` in a local OneSimulation environment.

Try it · The transfer-orbit clock

Start with the same 250 km perigee altitude and 42164 km apogee radius as the OneSimulation orbit. Lower the apogee to 26560 km, then restore it and raise the perigee altitude to 2000 km: compare all three periods with the table. This analytical Kepler curve checks the numerical integration; it does not simulate timestep error.

Open the corresponding OneSimulation notebook, code and output

Open this live calculation

Try the calculation

Perigee altitude above Earth (km) **250**

Apogee radius from Earth centre (km) **42164**

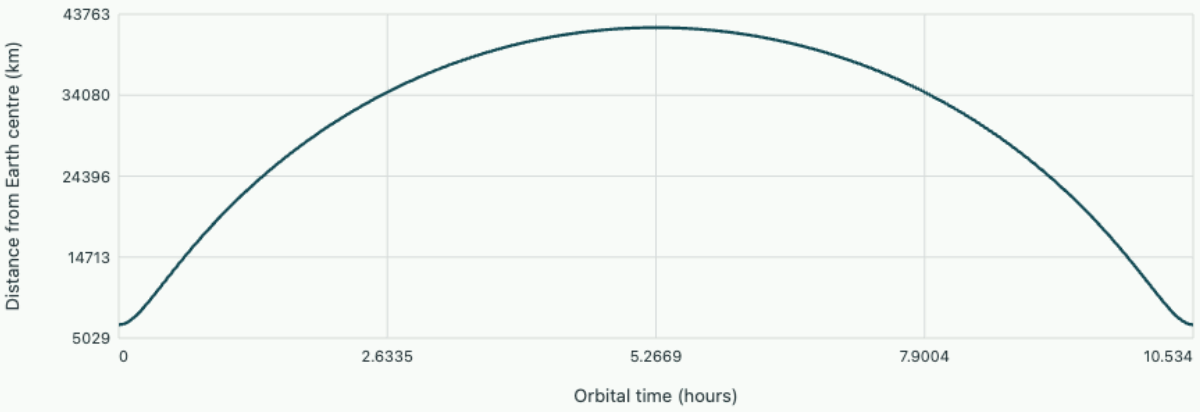

Analytical Kepler ellipse

Period 37921.96 s (10.534 hours); eccentricity 0.72831. Perigee/apogee radii 6628.137 / 42164 km. Analytical central-gravity reference with Earth radius 6378.137 km and μ = 398600.4418 km³/s²; the OneSimulation notebook separately checks integration and crossing-time errors.

Problem sheet 4 · Reconstruct an orbit from its clock

Notation and assumptions

Read each defining equation with its assumptions and units, then follow the link to the argument that gives the equation its meaning.

Action

$$S = \int_{t_1}^{t_2} L(q, \dot{q}, t)\, dt$$

Compare nearby admissible paths with the specified endpoint data. Stationarity gives a local equation of motion. In SI the action has units of joule seconds.

Derivation · Constraints and Lagrange’s equations

Action variable

$$J = (2\pi)^{-1} \oint p\, dq$$

This area measure is defined for a closed cycle. It can change strongly near a separatrix even under a slow parameter variation.

Derivation · Read a period from the area enclosed by an orbit

Differential cross-section

$$d\sigma/d\Omega = (b/\sin\theta)|db/d\theta|$$

For an axially symmetric single-valued scattering branch this converts incoming area to outgoing solid angle. Sum contributions if more than one impact parameter gives the same angle.

Derivation · Impact parameters and scattering cross-sections

Generalised momentum

$$p_i = \partial L/\partial \dot{q}_i$$

Its units depend on the coordinate. Conjugacy to an angle gives an angular momentum. Conservation requires the associated coordinate to be cyclic in the chosen Lagrangian.

Derivation · Hamiltonian motion in phase space

Normal frequency

$$\det(K - \omega^2 M) = 0$$

Small oscillations around a force-balanced configuration give this generalised eigenproblem. The ordinary frequency in hertz is the angular frequency divided by two pi.

Derivation · Normal modes and energy exchange

Reduced mass

$$\mu = m_1 m_2 / (m_1 + m_2)$$

The relative coordinate of an isolated two-body system carries this inertia. The centre-of-mass motion remains a separate degree of freedom.

Derivation · Two-body motion and binary masses

Further reading

- Follow the passage from the action principle to conserved momenta in chapter 2, then revisit the free top in chapter 3 in its body-fixed frame. David Tong · Classical Dynamics

Compare specific topics with the university sources